

https://dspace.org/

Contribution to Gauteng atmospheric emissions characterization and source identification using conditional probability function modelling

Singo, Shonisani Norman

2020
https://hdl.handle.net/10539/31296

Downloaded from a DSpace repository. https://dspace.org/



CONTRIBUTION TO GAUTENG ATMOSPHERIC EMISSIONS CHARACTERIZATION AND SOURCE IDENTIFICATION USING CONDITIONAL PROBABILITY FUNCTION MODELLING

by

Shonisani Norman Singo

A thesis submitted to the Faculty Engineering and The Built Environment, University of The Witwatersrand, in fulfilment of the requirements for the degree of Doctor of Philosophy in Chemical Engineering

2020

DECLARATION

I declare that Contribution to Gauteng Atmospheric Emissions Characterization and Source Identification Using Conditional Probability Function Modelling is my own work and that all the sources that I have used or quoted have been indicated and acknowledged by means of complete references. It has not been submitted before for any degree or examination in any other university.

_____

Mr. Shonisani Norman Singo
(1814779)

ABSTRACT

More than 50 percent (50%) of Gauteng Province areas has been declared by the South African government as an air quality priority area due to poor ambient air quality. The Gauteng province has highest number of industrial activities registered on the National Atmospheric Emission Inventory System (NAEIS) of South Africa which account more than 40% percent of South African Air Quality listed activities (www.saaelip.environment.gov.za). Gauteng ambient monitoring stations measured numerous sources of air emissions, including chemical plants, manufacturing, mining activities and domestic fuel burning, both resulting in heavy air emissions. Gauteng ambient monitoring stations was installed with the aim of monitoring local area sources within Gauteng region. The problem of residential air pollution is mostly related to dense communities of low-income such as townships. The study explores sources of pollution affecting Gauteng province, South Africa. The goal of this study was to assess and determine significant emission sources that affect the province by investigating ambient concentration correlation parameters, pollution roses, and probability modelling functions using Openair software package for air pollution analysis based on the R statistical package. The investigation focused on the following contaminants: sulphur dioxide, nitrogen dioxide, ozone and PM_{10} (particulate matter in which 50% of particles have an aerodynamic diameter of less than 10 μm). Hourly data were used to formulate probability functions for defining and characterizing secret or unknown sources of pollution. In addition, K-clustering algorithm analysis technique has been employed to provide effective graphical meaning for sources in characterizing the classes and source identification. The analysis disclosed major and minor sources. Problematic directional emission sources were identified for PM_{10},ozone, sulfur dioxide and nitrogen dioxide.

The K-clustering algorithm analysis technique was used to provide effective graphical meaning for sources in class characterization and source identification. This study provides baseline information for a comprehensive understanding of the current pollution levels and possible sources within Gauteng province, South Africa.

ACKNOWLEDGEMENT

I wish to express enormous appreciation to my supervisor Professor Jean Mulopo for his patience and guidance given to me in making the thesis successful. His way of welcoming me in his office and his inputs made a big difference in my career.

I would also like to thank the people who have given me their time and help with the information, through mails, interviews and calls. I would like to send a special thanks to my parents and siblings for their tireless support. The following individuals added value to this research study Mr. Mpho Nekhwalivhe, Mr. Jacob Legadima and Ms. Kefiloe Sekhu. I would like to thank to the Department of Environmental, Forestry and Fisheries, South African Weather Service, City of Ekurhuleni, City of Johannesburg, City of Tshwane, Sedibeng District Municipality and West Rand District Municipality for the positive contribution to my studies and providing ambient monitoring data used on this thesis. Lastly, I would like to thank Gauteng Department of Economics Development, Agriculture and Environment especially Air Quality Management Directorate and ICT Support and Information Systems Directorate towards completion of a Doctor of Philosophy degree in the Chemical Engineering at the University of the Witwatersrand, Johannesburg.

TABLE OF CONTENTS

DECLARATION II

ABSTRACT III

ACKNOWLEDGEMENT IV

TABLE OF CONTENTS V

LIST OF TABLE VII

LIST OF FIGURES VIII

ACRONYMS XV

1. CHAPTER 1: INTRODUCTION 1

1.1 BACKGROUND 1
1.2 RESEARCH OBJECTIVES AND PROBLEM STATEMENT OF THE STUDY 3
1.2.1 Research Objectives 3
1.2.2. Problem Statement of the Study 4

2. CHAPTER 2: LITERATURE REVIEW 6

2.1 SULFUR DIOXIDE 8
2.2 NITROGEN DIOXIDE 13
2.3 PARTICULATE MATTER (PM_{10} AND $PM_{2,5}$) 17
2.4 OZONE 23
2.5 SOURCES OF EMISSIONS WITHIN GAUTENG PROVINCE IN SOUTH AFRICA 28
2.6 AIR QUALITY MODELLING USING OPEN-AIR 32
2.7 THE DEVELOPMENT OF SOURCE-RECEPTOR RELATIONSHIPS 32
2.8 SOURCE IDENTIFICATION USING CONDITIONAL PROBABILITY FUNCTION MODELLING 36

3. CHAPTER 3: RESEARCH METHODOLOGY 39

3.1 INTRODUCTION 39
3.2 AREA OF THE STUDY AND DATA COLLECTION 39
3.3 METHODOLOGIES 42
3.3.1 Method 1: Investigation of correlation coefficient, r. 42
3.3.2 Method 2: Investigation of pollution roses 42
3.3.3 Method 3: Investigation of pollution sources using the bivariate polar plot at receptor. 43
3.3.4 Method 4: Identification of similar characteristics sources using k-means clustering method. 45
3.4 USING R TO ANALYSE AIR POLLUTION MONITORING DATA 47
3.4.1 Data preparation 47
3.4.2 Data into R 47

4. CHAPTER 4: RESULTS AND DISCUSSIONS 49

4.1 INTRODUCTION 49
4.2 CORRELATIONS 49
4.2.1 Correlation for Ozone at Gauteng ambient monitoring stations 49
4.2.2 Correlation for sulfur dioxide at Gauteng ambient monitoring stations 52
4.2.3 Correlation for nitrogen oxides at Gauteng ambient monitoring stations. 52
4.3.4 Correlation for PM_{10} at Gauteng ambient monitoring stations 55
4.3.5 Gauteng ambient monitoring station with ambient correlation parameters 57
4.2 POLLUTION ROSE ANALYSIS AT AMBIENT MONITORING STATIONS. 87
4.3 BIVARIATE POLAR PLOT AT RECEPTOR AND EMISSION INVENTORY FACILITIES WITHIN GAUTENG PROVINCE. 153
4.4 CONDITIONAL PROBABILITY FUNCTION PLOT (K-MEANS CLUSTERING) AT GAUTENG PROVINCE. 238

4.5. Summary of the results and discussions Chapter 312
4.5.1 Correlations 312
4.5.2 Pollution Rose 313
4.5.3 Bivariate Polar Plot at receptor and Emission Inventory Facilities within Gauteng Province. 316
4.5.4 Conditional Probability Function Plot (K-Means Clustering) at Gauteng Province. 317
5. CHAPTER 5: CONCLUSION AND RECOMMENDATIONS 319
6. REFERENCES 320
7. APPENDIX - GAUTENG AMBIENT AIR QUALITY DATA SUMMARY 328

LIST OF TABLE

TABLE 2.1: NATIONAL AMBIENT AIR QUALITY STANDARDS FOR SULFUR DIOXIDE (SO_2) 9
TABLE 2.2: NATIONAL AMBIENT AIR QUALITY STANDARDS FOR NITROGEN DIOXIDE (NO_2) 13
TABLE 2.3: NATIONAL AMBIENT AIR QUALITY STANDARDS FOR PARTICULATE MATTER LESS THAN 10 μM DIAMETER (PM_{10}) 18
TABLE 2.4: NATIONAL AMBIENT AIR QUALITY STANDARDS FOR OZONE (O_3) 23
TABLE 2.5: SELF-PROPELLED VEHICLE POPULATION PER VEHICLE CLASS- OCTOBER/NOVEMBER 2019 30
TABLE 2.6: LIST OF AIRPORTS IN GAUTENG PROVINCE, SOUTH AFRICA 31
TABLE 2.7: GAUTENG AMBIENT MONITORING STATIONS AND ASSOCIATED MONITORING SOURCES 35
TABLE 3.1: GAUTENG AMBIENT MONITORING STATIONS AND MEASURED PARAMETERS 41

LIST OF FIGURES

FIGURE 1.1: AIR QUALITY PRIORITY AREAS WITHIN AND AROUND GAUTENG PROVINCE 5
FIGURE 2.1: SO_2 DAILY LIMIT FOR THE CITY OF EKURHULENI. RESULTS FROM THE CITY OF EKURHULENI FOR SULFUR DIOXIDE IN PARTS PER BILLION. 10
FIGURE 2.2:SO_2 DAILY LIMIT FOR THE CITY OF TSHWANE 11
FIGURE 2.3:SO_2 DAILY LIMIT FOR THE COJ, SEDIBENG AND WEST RAND DISTRICT MUNICIPALITY. 12
FIGURE 2.4: NO_2 HOURLY LIMIT FOR THE COJ AND WEST RAND DISTRICT MUNICIPALITY 14
FIGURE 2.5:NO_2 HOURLY LIMIT FOR THE CITY OF EKURHULENI 15
FIGURE 2.6:NO_2 HOURLY LIMIT FOR THE CITY OF TSHWANE 16
FIGURE 2.7:PM_{10} DAILY LIMIT FOR THE COJ 19
FIGURE 2.8:PM_{10} DAILY LIMIT FOR THE CITY OF TSHWANE 20
FIGURE 2.9:PM_{10} DAILY LIMIT FOR THE CITY OF EKURHULENI 21
FIGURE 2.10:PM_{10} DAILY LIMIT FOR SEDIBENG AND WEST RAND DISTRICT MUNICIPALITY 22
FIGURE 2.11: OZONE 8 HOURS RUNNING FOR THE COJ AND WEST RAND DISTRICT MUNICIPALITY 24
FIGURE 2.12: OZONE 8 HOURS RUNNING FOR THE CITY OF TSHWANE AND SEDIBENG DISTRICT MUNICIPALITY 25
FIGURE 2.13: OZONE 8 HOURS RUNNING FOR THE CITY OF EKURHULENI FOR THE OZONE AMBIENT CONCENTRATION IN PARTS PER BILLION IN 8 HOURLY AVERAGE 26
FIGURE 2.14:NO_2 HOURLY LIMIT FOR THE CITY OF EKURHULENI FOR NITROGEN DIOXIDE IN PARTS PER BILLION 27
FIGURE 2.15: DISTRIBUTION OF GAUTENG AMBIENT MONITORING STATION IN RELATION TO INDUSTRIES EMISSION INVENTORY 34
FIGURE 2.16: K-MEANS MOVES THE CENTROIDS TOWARDS THE ACTUAL CLUSTER CENTRES 37
FIGURE 3.1: FLOWCHART OF K-MEANS CLUSTERING 46
FIGURE 4.1:CORRELATIONS OF OZONE TO GAUTENG AMBIENT MONITORING STATIONS 51
FIGURE 4.2:CORRELATIONS OF SULFUR DIOXIDE TO GAUTENG AMBIENT MONITORING STATIONS 53
FIGURE 4.3:CORRELATIONS OF NITROGEN OXIDES TO GAUTENG AMBIENT MONITORING STATIONS 54
FIGURE 4.4: CORRELATIONS OF PM_{10} TO GAUTENG AMBIENT MONITORING STATIONS 56
FIGURE 4.5: GERMISTON AMBIENT MONITORING STATION PARAMETERS CORRELATIONS 58
FIGURE 4.6: BEDFORDVIEW AMBIENT MONITORING STATION PARAMETERS CORRELATIONS 59
FIGURE 4.7: THOKOZA AMBIENT MONITORING STATION PARAMETERS CORRELATION 60
FIGURE 4.8: BUCCLEUCH AMBIENT MONITORING STATION PARAMETERS CORRELATIONS 61
FIGURE 4.9: DAVIDSONVILLE AMBIENT MONITORING STATION PARAMETERS CORRELATIONS 62
FIGURE 4.10: DELTA PARK AMBIENT MONITORING STATION PARAMETERS CORRELATIONS 63
FIGURE 4.11: DIEPSLOOT AMBIENT MONITORING STATION PARAMETERS CORRELATIONS 64
FIGURE 4.12: EKANDUSTRIA AMBIENT MONITORING STATION PARAMETERS CORRELATIONS 65
FIGURE 4.13: ETWATWA AMBIENT MONITORING STATION PARAMETERS CORRELATIONS 66
FIGURE 4.14: JABULANI AMBIENT MONITORING STATION PARAMETERS CORRELATIONS 67
FIGURE 4.15: IVORY PARK AMBIENT MONITORING STATION PARAMETERS CORRELATIONS 68
FIGURE 4.16: MAMELODI AMBIENT MONITORING STATION PARAMETERS CORRELATIONS 69
FIGURE 4.17: MEYERTON AMBIENT MONITORING STATION PARAMETERS CORRELATIONS 70
FIGURE 4.18: MOGALE CITY AMBIENT MONITORING STATION PARAMETERS CORRELATIONS 71
FIGURE 4.19: NEWTOWN AMBIENT MONITORING STATION PARAMETERS CORRELATIONS 72
FIGURE 4.20: OLIFANSFONTEIN AMBIENT MONITORING STATION PARAMETERS CORRELATIONS 73
FIGURE 4.21: ORANGE FARM AMBIENT MONITORING STATION PARAMETERS CORRELATIONS 74
FIGURE 4.22: PRETORIA WEST AMBIENT MONITORING STATION PARAMETERS CORRELATIONS 75
FIGURE 4.23: ROSSLYN AMBIENT MONITORING STATION PARAMETERS CORRELATIONS 76
FIGURE 4.24: SPRINGS AMBIENT MONITORING STATION PARAMETERS CORRELATIONS 77
FIGURE 4.25: TSAKANE AMBIENT MONITORING STATION PARAMETERS CORRELATIONS 78
FIGURE 4.26: VANDERBIJLPARK AMBIENT MONITORING STATION PARAMETERS CORRELATIONS 79
FIGURE 4.27: WATVILLE AMBIENT MONITORING STATION PARAMETERS CORRELATIONS 80
FIGURE 4.28: POLLUTION ROSES AT THE ALEXANDRA AMBIENT MONITORING STATION AND GAUTENG EMISSION INVENTORY FACILITIES 88
FIGURE 4.29: POLLUTION ROSES AT THE BEDFORDVIEW AMBIENT MONITORING STATION AND GAUTENG EMISSION INVENTORY FACILITIES 89

FIGURE 4.30: POLLUTION ROSES AT THE BEDFORDVIEW AMBIENT MONITORING STATION AND GAUTENG EMISSION INVENTORY FACILITIES 90
FIGURE 4.31: POLLUTION ROSES AT THE BEDFORDVIEW AMBIENT MONITORING STATION AND GAUTENG EMISSION INVENTORY FACILITIES 91
FIGURE 4.32: POLLUTION ROSES AT THE BEDFORDVIEW AMBIENT MONITORING STATION AND GAUTENG EMISSION INVENTORY FACILITIES 92
FIGURE 4.33: POLLUTION ROSES AT THE BODIBENG AMBIENT MONITORING STATION AND GAUTENG EMISSION INVENTORY FACILITIES . 93
FIGURE 4.34: POLLUTION ROSES AT THE BOOYSENS AMBIENT MONITORING STATION AND GAUTENG EMISSION INVENTORY FACILITIES . 94
FIGURE 4.35: POLLUTION ROSES AT THE BOOYSENS AMBIENT MONITORING STATION AND GAUTENG EMISSION INVENTORY FACILITIES 95
FIGURE 4.36: POLLUTION ROSES AT THE BUCCLEUCH AMBIENT MONITORING STATION AND GAUTENG EMISSION INVENTORY FACILITIES 96
FIGURE 4.37: POLLUTION ROSES AT THE BUCCLEUCH AMBIENT MONITORING STATION AND GAUTENG EMISSION INVENTORY FACILITIES 97
FIGURE 4.38: POLLUTION ROSES AT THE DAVIDSONVILLE AMBIENT MONITORING STATION AND GAUTENG EMISSION INVENTORY FACILITIES 98
FIGURE 4.39: POLLUTION ROSES AT THE DELTA AMBIENT MONITORING STATION AND GAUTENG EMISSION INVENTORY FACILITIES 99
FIGURE 4.40: POLLUTION ROSES AT THE DIEPSLOOT AMBIENT MONITORING STATION AND GAUTENG EMISSION INVENTORY FACILITIES 100
FIGURE 4.41: POLLUTION ROSES AT THE EKANDUSTRIA AMBIENT MONITORING STATION AND GAUTENG EMISSION INVENTORY FACILITIES 101
FIGURE 4.42: POLLUTION ROSES AT THE EKANDUSTRIA AMBIENT MONITORING STATION AND GAUTENG EMISSION INVENTORY FACILITIES 102
FIGURE 4.43: POLLUTION ROSES AT THE ETWATWA AMBIENT MONITORING STATION AND GAUTENG EMISSION INVENTORY FACILITIES 103
FIGURE 4.44: POLLUTION ROSES AT THE GERMISTON AMBIENT MONITORING STATION AND GAUTENG EMISSION INVENTORY FACILITIES 104
FIGURE 4.45: POLLUTION ROSES AT THE GERMISTON AMBIENT MONITORING STATION AND GAUTENG EMISSION INVENTORY FACILITIES 105
FIGURE 4.46: POLLUTION ROSES AT THE GERMISTON AMBIENT MONITORING STATION AND GAUTENG EMISSION INVENTORY FACILITIES 106
FIGURE 4.47: POLLUTION ROSES AT THE IVORY PARK AMBIENT MONITORING STATION AND GAUTENG EMISSION INVENTORY FACILITIES 107
FIGURE 4.48: POLLUTION ROSES AT THE JABAVU AMBIENT MONITORING STATION AND GAUTENG EMISSION INVENTORY FACILITIES ... 108
FIGURE 4.49: POLLUTION ROSES AT THE LEONDALE AMBIENT MONITORING STATION AND GAUTENG EMISSION INVENTORY FACILITIES 109
FIGURE 4.50: POLLUTION ROSES AT THE MAMELODI AMBIENT MONITORING STATION AND GAUTENG EMISSION INVENTORY FACILITIES 110
FIGURE 4.51: POLLUTION ROSES AT THE MAMELODI AMBIENT MONITORING STATION AND GAUTENG EMISSION INVENTORY FACILITIES 111
FIGURE 4.52: POLLUTION ROSES AT THE MEYERTON AMBIENT MONITORING STATION AND GAUTENG EMISSION INVENTORY FACILITIES 112
FIGURE 4.53: POLLUTION ROSES AT THE MOGALE CITY AMBIENT MONITORING STATION AND GAUTENG EMISSION INVENTORY FACILITIES 113
FIGURE 4.54: POLLUTION ROSES AT THE MOGALE CITY AMBIENT MONITORING STATION AND GAUTENG 114
FIGURE 4.55: POLLUTION ROSES AT THE NEWTOWN AMBIENT MONITORING STATION AND GAUTENG EMISSION INVENTORY FACILITIES 115
FIGURE 4.56: POLLUTION ROSES AT THE OLIEVENHOUTBOSCH AMBIENT MONITORING STATION AND GAUTENG EMISSION INVENTORY FACILITIES 116
FIGURE 4.57: POLLUTION ROSES AT THE OLIEVENHOUTBOSCH AMBIENT MONITORING STATION AND GAUTENG EMISSION INVENTORY FACILITIES 117
FIGURE 4.58: POLLUTION ROSES AT THE ORANGE FARM AMBIENT MONITORING STATION AND GAUTENG EMISSION INVENTORY FACILITIES 118
FIGURE 4.59: POLLUTION ROSES AT THE PRETORIA WEST AMBIENT MONITORING STATION AND GAUTENG EMISSION INVENTORY FACILITIES 119
FIGURE 4.60: POLLUTION ROSES AT THE PRETORIA WEST AMBIENT MONITORING STATION AND GAUTENG EMISSION INVENTORY FACILITIES 120

FIGURE 4.61: POLLUTION ROSES AT THE RANDFONTEIN AMBIENT MONITORING STATION AND GAUTENG EMISSION INVENTORY FACILITIES 121
FIGURE 4.62: POLLUTION ROSES AT THE ROSSLYN AMBIENT MONITORING STATION AND GAUTENG EMISSION INVENTORY FACILITIES . 122
FIGURE 4.63: POLLUTION ROSES AT THE SPRINGS AMBIENT MONITORING STATION AND GAUTENG EMISSION INVENTORY FACILITIES .. 123
FIGURE 4.64: POLLUTION ROSES AT THE SPRINGS AMBIENT MONITORING STATION AND GAUTENG EMISSION INVENTORY FACILITIES .. 124
FIGURE 4.65: POLLUTION ROSES AT THE TEMBISA AMBIENT MONITORING STATION AND GAUTENG EMISSION INVENTORY FACILITIES . 125
FIGURE 4.66: POLLUTION ROSES AT THE THOKOZA AMBIENT MONITORING STATION AND GAUTENG EMISSION INVENTORY FACILITIES 126
FIGURE 4.67: POLLUTION ROSES AT THE TSAKANE AMBIENT MONITORING STATION AND GAUTENG EMISSION INVENTORY FACILITIES . 127
FIGURE 4.68: POLLUTION ROSES AT THE TSAKANE AMBIENT MONITORING STATION AND GAUTENG EMISSION INVENTORY FACILITIES . 128
FIGURE 4.69: POLLUTION ROSES AT THE TSHWANE MARKET AMBIENT MONITORING STATION AND GAUTENG EMISSION INVENTORY FACILITIES 129
FIGURE 4.70: POLLUTION ROSES AT THE VANDERBIJLPARK AMBIENT MONITORING STATION AND GAUTENG EMISSION INVENTORY FACILITIES 130
FIGURE 4.71: POLLUTION ROSES AT THE WATTVILLE AMBIENT MONITORING STATION AND GAUTENG EMISSION INVENTORY FACILITIES 131
FIGURE 4.72: POLLUTION ROSES AT THE WATTVILLE AMBIENT MONITORING STATION AND GAUTENG EMISSION INVENTORY FACILITIES 132
FIGURE 4.73: POLLUTION ROSES AT THE WATTVILLE AMBIENT MONITORING STATION AND GAUTENG EMISSION INVENTORY FACILITIES 133
FIGURE 4.74: BIVARIATE POLAR PLOT AT THE ALEXANDRA AMBIENT MONITORING STATIONS AND EMISSION INVENTORY FACILITIES IN GAUTENG PROVINCE 155
FIGURE 4.75: BIVARIATE POLAR PLOT AT THE BEDFORDVIEW AMBIENT MONITORING STATIONS AND EMISSION INVENTORY FACILITIES IN GAUTENG PROVINCE 156
FIGURE 4.76: BIVARIATE POLAR PLOT AT THE BEDFORDVIEW AMBIENT MONITORING STATIONS AND EMISSION INVENTORY FACILITIES IN GAUTENG PROVINCE 157
FIGURE 4.77: BIVARIATE POLAR PLOT AT THE BEDFORDVIEW AMBIENT MONITORING STATIONS AND EMISSION INVENTORY FACILITIES IN GAUTENG PROVINCE 158
FIGURE 4.78: BIVARIATE POLAR PLOT AT THE BEDFORDVIEW AMBIENT MONITORING STATIONS AND EMISSION INVENTORY FACILITIES IN GAUTENG PROVINCE 159
FIGURE 4.79: BIVARIATE POLAR PLOT AT THE BODIBENG AMBIENT MONITORING STATIONS AND EMISSION INVENTORY FACILITIES IN GAUTENG PROVINCE 160
FIGURE 4.80: BIVARIATE POLAR PLOT AT THE BODIBENG AMBIENT MONITORING STATIONS AND EMISSION INVENTORY FACILITIES IN GAUTENG PROVINCE 161
FIGURE 4.81 : BIVARIATE POLAR PLOT AT THE BOOYSENS AMBIENT MONITORING STATIONS AND EMISSION INVENTORY FACILITIES IN GAUTENG PROVINCE 162
FIGURE 4.82: BIVARIATE POLAR PLOT AT THE BOOYSENS AMBIENT MONITORING STATIONS AND EMISSION INVENTORY FACILITIES IN GAUTENG PROVINCE 163
FIGURE 4.83: BIVARIATE POLAR PLOT AT THE BOOYSENS AMBIENT MONITORING STATIONS AND EMISSION INVENTORY FACILITIES IN GAUTENG PROVINCE 164
FIGURE 4.84: BIVARIATE POLAR PLOT AT BUCCLUECH AMBIENT MONITORING STATIONS AND EMISSION INVENTORY FACILITIES IN GAUTENG PROVINCE 165
FIGURE 4.85: BIVARIATE POLAR PLOT AT BUCCLUECH AMBIENT MONITORING STATIONS AND EMISSION INVENTORY FACILITIES IN GAUTENG PROVINCE 166
FIGURE 4.86: BIVARIATE POLAR PLOT AT THE DAVIDSONVILLE AMBIENT MONITORING STATIONS AND EMISSION INVENTORY FACILITIES IN GAUTENG PROVINCE 167
FIGURE 4.87: BIVARIATE POLAR PLOT AT THE DELTA PARK AMBIENT MONITORING STATIONS AND EMISSION INVENTORY FACILITIES IN GAUTENG PROVINCE 168
FIGURE 4.88: BIVARIATE POLAR PLOT AT THE DIEPSLOOT AMBIENT MONITORING STATIONS AND EMISSION INVENTORY FACILITIES IN GAUTENG PROVINCE 169
FIGURE 4.89: BIVARIATE POLAR PLOT AT THE DIEPSLOOT AMBIENT MONITORING STATIONS AND EMISSION INVENTORY FACILITIES IN GAUTENG PROVINCE 170
FIGURE 4.90: BIVARIATE POLAR PLOT AT THE EKANDUSTRIA AMBIENT MONITORING STATIONS AND EMISSION INVENTORY FACILITIES IN GAUTENG PROVINCE 171

Figure 4.91: Bivariate polar plot at the Ekandustria Ambient Monitoring Stations and Emission Inventory Facilities in Gauteng Province 172
Figure 4.92: Bivariate polar plot at the Etwatwa Ambient Monitoring Stations and Emission Inventory Facilities in Gauteng Province 173
Figure 4.93: Bivariate polar plot at the Etwatwa Ambient Monitoring Stations and Emission Inventory Facilities in Gauteng Province 174
Figure 4.94: Bivariate polar plot at the Germiston Ambient Monitoring Stations and Emission Inventory Facilities in Gauteng Province 175
Figure 4.95: Bivariate polar plot at the Ivory Park Ambient Monitoring Stations and Emission Inventory Facilities in Gauteng Province 176
Figure 4.96: Bivariate polar plot at the Ivory Park Ambient Monitoring Stations and Emission Inventory Facilities in Gauteng Province 177
Figure 4.97: Bivariate polar plot at the Jabavu Ambient Monitoring Stations and Emission Inventory Facilities in Gauteng Province 178
Figure 4.98: Bivariate polar plot at the Jabavu Ambient Monitoring Stations and Emission Inventory Facilities in Gauteng Province 179
Figure 4.99: Bivariate polar plot at the Leondale Ambient Monitoring Stations and Emission Inventory Facilities in Gauteng Province 180
Figure 4.100: Bivariate polar plot at the Leondale Ambient Monitoring Stations and Emission Inventory Facilities in Gauteng Province 181
Figure 4.101: Bivariate polar plot at the Leondale Ambient Monitoring Stations and Emission Inventory Facilities in Gauteng Province 182
Figure 4.102: Bivariate polar plot at the Mamelodi Ambient Monitoring Stations and Emission Inventory Facilities in Gauteng Province 183
Figure 4.103: Bivariate polar plot at the Mamelodi Ambient Monitoring Stations and Emission Inventory Facilities in Gauteng Province 184
Figure 4.104: Bivariate polar plot at the Meyerton Ambient Monitoring Stations and Emission Inventory Facilities in Gauteng Province 185
Figure 4.105: Bivariate polar plot at the Meyerton Ambient Monitoring Stations and Emission Inventory Facilities in Gauteng Province 186
Figure 4.106: Bivariate polar plot at the Mogale City Ambient Monitoring Stations and Emission Inventory Facilities in Gauteng Province 187
Figure 4.107: Bivariate polar plot at the Mogale City Ambient Monitoring Stations and Emission Inventory Facilities in Gauteng Province 188
Figure 4.108: Bivariate polar plot at the Newtown Ambient Monitoring Stations and Emission Inventory Facilities in Gauteng Province 189
Figure 4.109: Bivariate polar plot at the Newtown Ambient Monitoring Stations and Emission Inventory Facilities in Gauteng Province 190
Figure 4.110: Bivariate polar plot at the Newtown Ambient Monitoring Stations and Emission Inventory Facilities in Gauteng Province 191
Figure 4.111: Bivariate polar plot at the Olievenhoutbosch Ambient Monitoring Stations and Emission Inventory Facilities in Gauteng Province 192
Figure 4.112: Bivariate polar plot at the Olievenhoutbosch Ambient Monitoring Stations and Emission Inventory Facilities in Gauteng Province 193
Figure 4.113: Bivariate polar plot at the Orange Farm Ambient Monitoring Stations and Emission Inventory Facilities in Gauteng Province 194
Figure 4.114: Bivariate polar plot at the Pretoria West Ambient Monitoring Stations and Emission Inventory Facilities in Gauteng Province 195
Figure 4.115: Bivariate polar plot at the Pretoria West Ambient Monitoring Stations and Emission Inventory Facilities in Gauteng Province 196
Figure 4.116: Bivariate polar plot at the Pretoria West Ambient Monitoring Stations and Emission Inventory Facilities in Gauteng Province 197

Figure 4.117: Bivariate polar plot at the Randfontein Ambient Monitoring Stations and Emission Inventory Facilities in Gauteng Province 198
Figure 4.118: Bivariate polar plot at the Rosslyn Ambient Monitoring Stations and Emission Inventory Facilities in Gauteng Province 199
Figure 4.119: Bivariate polar plot at the Rosslyn Ambient Monitoring Stations and Emission Inventory Facilities in Gauteng Province 200
Figure 4.120: Bivariate polar plot at the Rosslyn Ambient Monitoring Stations and Emission Inventory Facilities in Gauteng Province 201
Figure 4.121: Bivariate polar plot at the Rosslyn Ambient Monitoring Stations and Emission Inventory Facilities in Gauteng Province 202
Figure 4.122: Bivariate polar plot at the Springs Ambient Monitoring Stations and Emission Inventory Facilities in Gauteng Province 203
Figure 4.123: Bivariate polar plot at the Springs Ambient Monitoring Stations and Emission Inventory Facilities in Gauteng Province 204
Figure 4.124: Bivariate polar plot at the Springs Ambient Monitoring Stations and Emission Inventory Facilities in Gauteng Province 205
Figure 4.125: Bivariate polar plot at the Tembisa Ambient Monitoring Stations and Emission Inventory Facilities in Gauteng Province 206
Figure 4.126: Bivariate polar plot at the Tembisa Ambient Monitoring Stations and Emission Inventory Facilities in Gauteng Province 207
Figure 4.127: Bivariate polar plot at the Thokoza Ambient Monitoring Stations and Emission Inventory Facilities in Gauteng Province 208
Figure 4.128: Bivariate polar plot at the Thokoza Ambient Monitoring Stations and Emission Inventory Facilities in Gauteng Province 209
Figure 4.129: Bivariate polar plot at the Tsakane Ambient Monitoring Stations and Emission Inventory Facilities in Gauteng Province 210
Figure 4.130: Bivariate polar plot at the Tsakane Ambient Monitoring Stations and Emission Inventory Facilities in Gauteng Province 211
Figure 4.131: Bivariate polar plot at the Tsakane Ambient Monitoring Stations and Emission Inventory Facilities in Gauteng Province 212
Figure 4.132: Bivariate polar plot at the Tshwane Market Mobile Ambient Monitoring Stations and Emission Inventory Facilities in Gauteng Province 213
Figure 4.133: Bivariate polar plot at the Tshwane Market Mobile Ambient Monitoring Stations and Emission Inventory Facilities in Gauteng Province 214
Figure 4.134: Bivariate polar plot at the Vanderbijlpark Ambient Monitoring Stations and Emission Inventory Facilities in Gauteng Province 215
Figure 4.135: Bivariate polar plot at the Wattville Ambient Monitoring Stations and Emission Inventory Facilities in Gauteng Province 216
Figure 4.136: Bivariate polar plot at the Wattville Ambient Monitoring Stations and Emission Inventory Facilities in Gauteng Province 217
Figure 4.137: Conditional Probability Function Plot (K-Means Clustering) at the Alexandra 239
Figure 4.138: Conditional Probability Function Plot (K-Means Clustering) at the Bedfordview 240
Figure 4.139: Conditional Probability Function Plot (K-Means Clustering) at the Bedfordview 241
Figure 4.140: Conditional Probability Function Plot (K-Means Clustering) at the Bedfordview 242
Figure 4.141: Conditional Probability Function Plot (K-Means Clustering) at the Bedfordview 243
Figure 4.142: Conditional Probability Function Plot (K-Means Clustering) at the Bodibeng 244
Figure 4.143: Conditional Probability Function Plot (K-Means Clustering) at the Bodibeng 245
Figure 4.144: Conditional Probability Function Plot (K-Means Clustering) at the Booysens 246
Figure 4.145: Conditional Probability Function Plot (K-Means Clustering) at the Booysens 247
Figure 4.146: Conditional Probability Function Plot (K-Means Clustering) at the Buccleuch 248
Figure 4.147: Conditional Probability Function Plot (K-Means Clustering) at the Buccleuch 249
Figure 4.148: Conditional Probability Function Plot (K-Means Clustering) at the Davidsonville 250
Figure 4.149: Conditional Probability Function Plot (K-Means Clustering) at the Delta Park 251

Figure 4.150: Conditional Probability Function Plot (K-Means Clustering) at the Diepsloot 252
Figure 4.151: Conditional Probability Function Plot (K-Means Clustering) at the Ekandustria 253
Figure 4.152: Conditional Probability Function Plot (K-Means Clustering) at the Ekandustria 254
Figure 4.153: Conditional Probability Function Plot (K-Means Clustering) at the Etwatwa 255
Figure 4.154: Conditional Probability Function Plot (K-Means Clustering) at the Etwatwa 256
Figure 4.155: Conditional Probability Function Plot (K-Means Clustering) at the Germiston 257
Figure 4.156: Conditional Probability Function Plot (K-Means Clustering) at the Germiston 258
Figure 4.157: Conditional Probability Function Plot (K-Means Clustering) at Ivory 259
Figure 4.158: Conditional Probability Function Plot (K-Means Clustering) at the Jabavu 260
Figure 4.159: Conditional Probability Function Plot (K-Means Clustering) at the Jabavu 261
Figure 4.160: Conditional Probability Function Plot (K-Means Clustering) at the Leondale 262
Figure 4.161: Conditional Probability Function Plot (K-Means Clustering) at the Leondale 263
Figure 4.162: Conditional Probability Function Plot (K-Means Clustering) at the Mamelodi 264
Figure 4.163: Conditional Probability Function Plot (K-Means Clustering) at the Mamelodi 265
Figure 4.164: Conditional Probability Function Plot (K-Means Clustering) at the Meyerton 266
Figure 4.165: Conditional Probability Function Plot (K-Means Clustering) at the Meyerton 267
Figure 4.166: Conditional Probability Function Plot (K-Means Clustering) at the Mogale City 268
Figure 4.167: Conditional Probability Function Plot (K-Means Clustering) at the Mogale City 269
Figure 4.168: Conditional Probability Function Plot (K-Means Clustering) at the Newtown 270
Figure 4.169: Conditional Probability Function Plot (K-Means Clustering) at the Newtown 271
Figure 4.170: Conditional Probability Function Plot (K-Means Clustering) at the Olievenhoutbosch 272
Figure 4.171: Conditional Probability Function Plot (K-Means Clustering) at the Olievenhoutbosch 273
Figure 4.172: Conditional Probability Function Plot (K-Means Clustering) at the Orange Farm 274
Figure 4.173: Conditional Probability Function Plot (K-Means Clustering) at the Orange Farm 275
Figure 4.174: Conditional Probability Function Plot (K-Means Clustering) at the Pretoria West 276
Figure 4.175: Conditional Probability Function Plot (K-Means Clustering) at the Pretoria West 277
Figure 4.176: Conditional Probability Function Plot (K-Means Clustering) at the Pretoria West 278
Figure 4.177: Conditional Probability Function Plot (K-Means Clustering) at the Randfontein 279
Figure 4.178: Conditional Probability Function Plot (K-Means Clustering) at the Randfontein 280
Figure 4.179: Conditional Probability Function Plot (K-Means Clustering) at the Rosslyn 281
Figure 4.180: Conditional Probability Function Plot (K-Means Clustering) at the Rosslyn 282
Figure 4.181: Conditional Probability Function Plot (K-Means Clustering) at the Tembisa 283
Figure 4.182: Conditional Probability Function Plot (K-Means Clustering) at the Tembisa 284
Figure 4.183: Conditional Probability Function Plot (K-Means Clustering) at the Tembisa 285
Figure 4.184: Conditional Probability Function Plot (K-Means Clustering) at the Thokoza 286
Figure 4.185: Conditional Probability Function Plot (K-Means Clustering) at the Thokoza 287
Figure 4.186: Conditional Probability Function Plot (K-Means Clustering) at the Tsakane 288
Figure 4.187: Conditional Probability Function Plot (K-Means Clustering) at the Tsakane 289
Figure 4.188: Conditional Probability Function Plot (K-Means Clustering) at the Tsakane 290
Figure 4.189: Conditional Probability Function Plot (K-Means Clustering) at the Tsakane 291
Figure 4.190: Conditional Probability Function Plot (K-Means Clustering) at the Vanderbijlpark 292
Figure 4.191: Conditional Probability Function Plot (K-Means Clustering) at the Vanderbijlpark 293
Figure 4.192: Conditional Probability Function Plot (K-Means Clustering) at the Wattville 294
Figure 4.193: Conditional Probability Function Plot (K-Means Clustering) at the Wattville 295
Figure 7.1: Alexandra ambient air quality data summary 328
Figure 7.2: Bedfordview ambient air quality data summary 329
Figure 7.3: Booysens ambient air quality data summary 330
Figure 7.4: Buccleuch ambient air quality data summary 331
Figure 7.5: Delta Park ambient air quality data summary 332
Figure 7.6: Diepsloot ambient air quality data summary 333
Figure 7.7: Ekandustria ambient air quality data summary 334
Figure 7.8: Etwatwa ambient air quality data summary 335
Figure 7.9: Germiston ambient air quality data summary 336

FIGURE 7.10: IVORY PARK AMBIENT AIR QUALITY DATA SUMMARY 337
FIGURE 7.11: LEONDALE AMBIENT AIR QUALITY DATA SUMMARY 338
FIGURE 7.12: MAMELODI AMBIENT AIR QUALITY DATA SUMMARY 339
FIGURE 7.13: MEYERTON AMBIENT AIR QUALITY DATA SUMMARY 340
FIGURE 7.14: NEWTOWN AMBIENT AIR QUALITY DATA SUMMARY 341
FIGURE 7.15: OLIFANSFONTEIN AMBIENT AIR QUALITY DATA SUMMARY 342
FIGURE 7.16: ORANGE FARM AMBIENT AIR QUALITY DATA SUMMARY 343
FIGURE 7.17: PRETORIA WEST AMBIENT AIR QUALITY DATA SUMMARY 344
FIGURE 7.18: RANDFONTEIN AMBIENT AIR QUALITY DATA SUMMARY 345
FIGURE 7.19: ROSSLYN AMBIENT AIR QUALITY DATA SUMMARY 346
FIGURE 7.20: SPRINGS AMBIENT AIR QUALITY DATA SUMMARY 347
FIGURE 7.21: TEMBISA AMBIENT AIR QUALITY DATA SUMMARY 348
FIGURE 7.22: THOKOZA AMBIENT AIR QUALITY DATA SUMMARY 349
FIGURE 7.23: TSAKANE AMBIENT AIR QUALITY DATA SUMMARY 350
FIGURE 7.24: VANDERBIJLPARK AMBIENT AIR QUALITY DATA SUMMARY (2017 -2018) 351
FIGURE 7.25: WATVILLE AMBIENT AIR QUALITY DATA SUMMARY 352

ACRONYMS

C_6H_6	Benzene
CBPF	Conditional Bivariate Probability Function
CO	Carbon Monoxide
CoJ	City of Johannesburg
CoE	City of Ekurhuleni
CSV	Comma Separated Value
CoT	City of Tshwane
DEFF	Department of Environmental Forestry and Fisheries
GAM	Generalized Additive Model
GDEDAE	Gauteng Department of Economic Development ,Agricultural and Environment
GDP	Gross Domestic Product
HPA	Highveld Priority Area
HUM	Relative Humidity
NAEIS	National Atmospheric Emission Inventory System
NEMAQA	National Environmental Management: Air Quality Act 39 of 2004 as amended
NO	Nitric Oxide
NO_2	Nitrogen Dioxide
NO_x	Nitrogen Oxides
O_3	Ozone
ppb	parts per billion
PM_{10}	Particulate Matter of aerodynamic diameter less than equal to 10 micrograms
$PM_{2.5}$	Particulate Matter of aerodynamic diameter less than equal to 2 comma 5 micrograms
PRESS	Pressure
SA	South Africa
SAAQIS	South African Air Quality Information System
SAWS	South African Weather Service
SDM	Sedibeng District Municipality
SO_2	Sulfur Dioxide
SOL	Solar Radiation
$\mu g/m^3$	Micrograms per cubic meter
TEMP	Temperature
TOL	Toluene

UV	Ultraviolet
VOC	Volatile organic compounds
VTAPA	Vaal Triangle Air-Shed Priority Area
WHO	World Health Organization
WPA	Waterberg Bojanala Priority Area
WIND	Wind Direction
WINDS	Wind Speed
WRDM	West Rand District Municipality

1. CHAPTER 1: INTRODUCTION

1.1 Background

The province of Gauteng is not only the wealthiest province in South Africa (CDP, 2014), it is also its economic hub, accounting for 36 percent of the country's Gross Domestic Product (GDP) and 10% of the African continent's GDP. Approximately 40.6% of South Africa's manufacturing industry is carried out within this province even though it covers only about 1.5% of the South African geographical area. Gauteng Province has also the largest population in South Africa (Mushongera et al.,2017 & Retief et al.,2011). The intense industrial activities within the province (depending upon their processes, inputs, and outputs) release various pollutants into the atmosphere (Panichev et al., 2019 & Nkosi et al.,2017). These industries include among other metallurgical industries, mineral processing, organic chemical, inorganic chemicals, storage of petroleum, small boiler and thermal treatment of hazardous waste and general waste operations.

The Gauteng Province currently has 380 identified mine residue areas of which the majority are gold-mining residues (Kamunda et al.,2016) and are sources of dust pollution, especially during secondary reclamation of the tailings that entails the removal of protective layers of vegetation for the duration of the reclamation project. The Gauteng Province also experiences a high-energy demand and motorization due to a combination of factors i.e. rapid population growth, industrialization, and relatively high living standard. Gauteng Province has the largest number of vehicles in South Africa accounted for 37.76% followed by Western Cape and KwaZulu Natal provinces at 16.21% and 13.74% respectively (Statistics-eNatis, 2019). It has the largest amount of vehicles in South Africa and in 2014, the City of Johannesburg (CoJ) was ranked fifth as the world's most polluted city in terms of particulate matter emissions. Emissions considered for this sector include those from all vehicles travelling in the CoJ (for the 1km resolution domain) and Gauteng (for the 3km resolution domain) roads i.e. private passenger, commercial passenger, public transport and freight (Chiloane et al.,2017).

The concentration of air pollution in a given environment depends on both the amount of pollution produced and the rate at which pollutants disperse (Carslaw and Beevers, 2013). In areas where the wind is very strong, pollution is dispersed whereas in areas where there is little or no wind, air pollution accumulates and concentrations can be quite high. Local factors such as topography (hills

and mountains), proximity to the coast, building height and time of the year all affect local wind conditions and can play a role in increasing air pollution levels. Wind direction together with wind speed can be highly effective at discriminating different emission sources (Carslaw and Beevers, 2013). Ambient air quality is defined as the physical and chemical measurements of pollutant concentrations in the atmosphere to which the general population is exposed. In most developing countries, ambient air quality is reported to have deteriorated seriously, especially in urban areas, exposing populations to pollutant levels above the recommended limits (Coker & Kizito,2018). In South Africa; ambient air quality monitoring stations have been commissioned throughout the Gauteng Province in order to measure and evaluate the ambient air quality levels. Gauteng Province has a total of 34 ambient air quality monitoring stations of which 29 and 5 are respectively owned by municipalities and the national Department of Environmental Affairs. The majority of these monitoring stations are situated within 3 metropolitan areas namely the Ekurhuleni Metro, CoJ and City of Tshwane, with a smaller number in Vaal Triangle, Airshed Priority Area, and West Rand District Municipalities. The Gauteng Province state of air report for the period of 1st November 2016 to 30 June 2017 has shown that the concentration of Particulate Matters of diameter less than 10 $\mu g/m^3$ (PM_{10}) exceeded the daily average of 75 $\mu g/m^3$ across the province whereas sulfur dioxide also exceeded the daily average of 125 ($\mu g/m^3$) in both the City of Ekurhuleni and Sedibeng Municipality District which have been identified as priority areas.

On a global stage, in 2014, 92 percent of the world's population lived in locations where the World Health Organization (WHO) air quality guidelines were not adhered to (WHO, 2016). In 2012, there were an estimated 3 million premature deaths worldwide caused by air pollution in urban and rural areas (WHO, 2013). By reducing levels of air pollution, countries can reduce the burden of disease caused by stroke, heart disease, lung cancer and chronic or acute respiratory diseases such as asthma. It is worth noting that ambient air quality standards of the WHO (SO_2= 20 $\mu g/m^3$ on average for a 24 hours period and PM_{10}=20 $\mu g/m^3$ on average per year) is stricter compared to the South African standards (SO_2= 125 $\mu g/m^3$ on average for a 24 hours period and PM_{10}=40 $\mu g/m^3$ on average per year).

Over the years, South Africa has gradually strived to ensure improved air quality, while promoting high industrialization: Various air quality management instruments have been developed including environmental legislation, emissions inventories, dispersion modelling and concentration inventories, revision of ambient air quality limits, proactive planning by local authorities and

sector-specific controls. The government's national policy on integrated pollution and waste management were set out in the year 2000 with the vision and objectives outlined in the white paper on integrated pollution and waste management in South Africa. Further attention was given to the shift in policy and legislative direction since the promulgation of the National Environment Management Air Quality Act 39 of 2004. Further attention was also drawn towards national and international legislation and how it affected the decisions of air quality management mandatory functions within the spheres of government, particularly in the last decade (DEA,2013). The national framework for air quality management in South Africa were promulgated in 2012. Regulations regarding air dispersion modelling with series of mathematical simulations were promulgated in 2014.

However, very few air quality modelling studies have been conducted by/for the Gauteng Province. Air dispersion modelling within South Africa is mainly performed by industrial companies and governmental authorities and to some extent by research councils. Industrial companies are usually required to conduct dispersion modelling for regulatory purposes to ensure that their emissions are below standard concentrations. The current air quality monitoring policies are mainly based on compliance with set limit values for various key pollutants as defined by the national directives and measured on fixed sites (Chen et al.,2017). While this strategy may be effective for pollutants with homogeneous concentrations on a large geographic scale, it does not allow for assessing the population exposure to pollutants with high spatial variability such as ultrafine particles. Moreover, the current regulations do not include the monitoring of directly exploitable parameters in terms of the health impact of air pollution or emission sources although the above information remains essential for the development of adequate public policies for better control of air quality. Therefore, there is a need to conduct an in-depth air quality study within the Gauteng Province.

1.2 Research Objectives and Problem Statement of the Study

1.2.1 Research Objectives

The main aim of this study was to Investigate emission sources and emissions characterization through probability function.: The specific objectives are:

i) develop source-receptor relationships using correlation matrix air quality function
ii) Investigating pollution rose at receptor
iii) Investigating bivariate polar plot at receptor
iv) Determining conditional probability modelling
v) K-means clustering for similar and different groups

Ambient monitoring station data will be used to validate the model before the recommendation of preventive interventions.

1.2.2. Problem Statement of the Study

More than 50% of Gauteng industrial areas have been declared by the national Environmental Affairs ministry as an air quality priority area (refer to figure 1.1 below) due to poor ambient air quality and this despite the fact that not all sources of air pollution are accounted for during air quality management planning. This implies that the way ahead may be extremely difficult in terms of reducing high levels pollutants in the Gauteng atmosphere. It was, therefore, the objective of this study to assess hidden significant sources of emission within and at the boundary of the Gauteng Province of Gauteng using probability functions modelling in order to help identify sources that are causing exceedance to ambient air quality standards. We believe that the modelling approach may add value to the current work done by the province such as emission inventory by i) building valid source-receptor relationships of the available emission inventory, ii) providing a meaningful link of pollutant emissions versus concentrations changes, iii) linking ambient pollutants concentrations and unknown or unquantified sources. It is expected that the outcomes of this research project may help identify significant pollutant sources within and around the province, provide support for effective reduction strategies and ultimately assist the province in complying with the national ambient air quality standards.

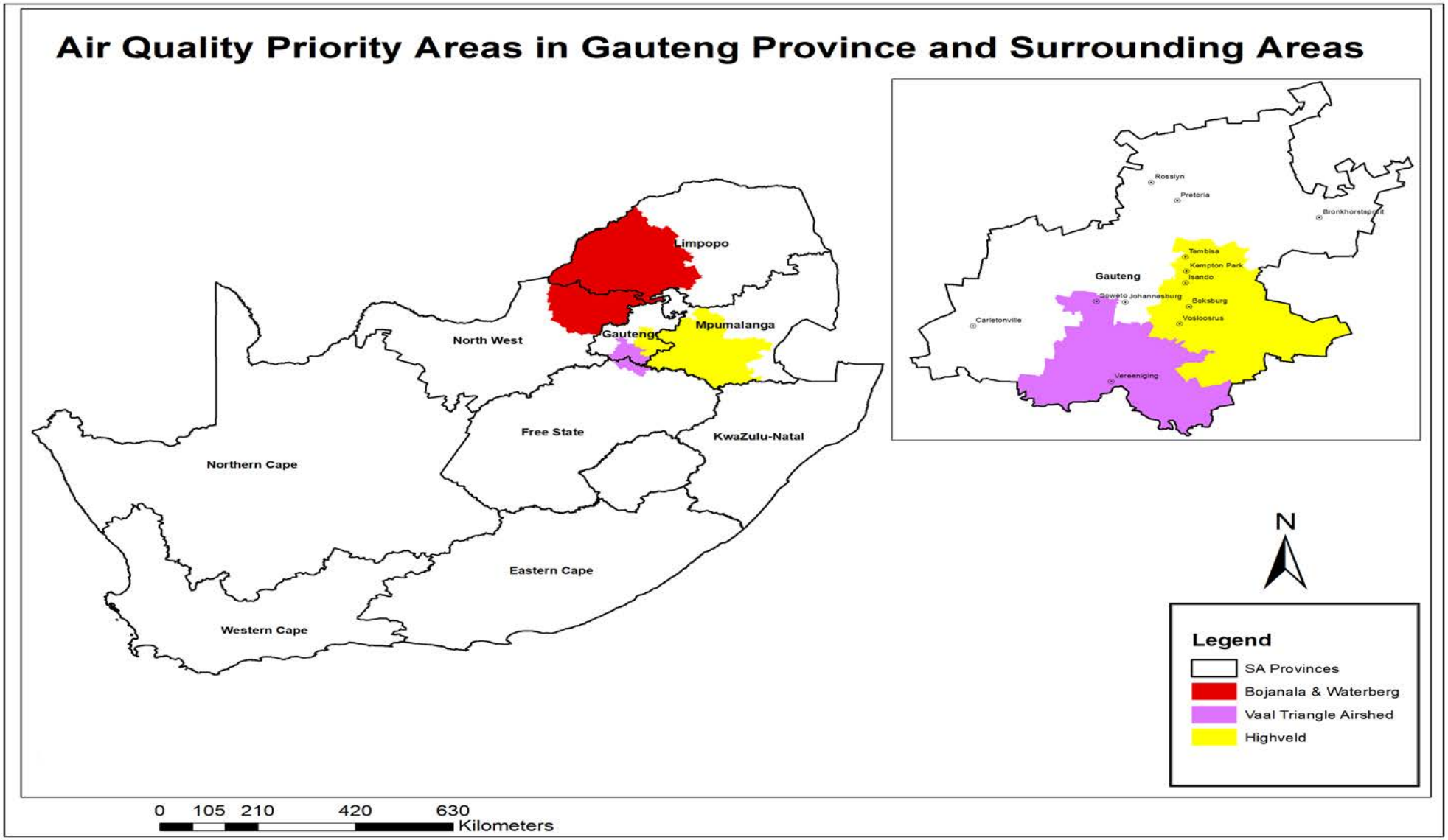

Figure 1.1: Air Quality Priority Areas within and around Gauteng Province

2. CHAPTER 2: LITERATURE REVIEW

The Gauteng Province is one of the provinces with a high standard of living in South Africa. Gauteng is the economic hub of South Africa, accounting for 36 % of the country's GDP and 10 percent of the African continent's GDP. Approximately 40.6 % of South Africa's manufacturing industry is carried out within this province. Gauteng has the largest population in South Africa and covers only 18178 kilo square meters which are 1.5 % of the South African geographical area. There are no doubts that these intense economic activities have created noticeable air quality challenges for the province. In this regard, various air quality management instruments have been developed over the years that include environmental legislation, emissions inventories, and dispersion modelling and concentration inventories. The government's national policy on integrated pollution and waste management were set out in the year 2000 with the vision and objectives outlined on the white paper on integrated pollution and waste management in South Africa (Deat, 2000). The national framework for air quality management in the Republic of South Africa were promulgated in 2012. Regulations regarding air dispersion modelling with series of mathematical simulations were promulgated in 2014.

The current air quality monitoring policies are mainly based on compliance with set limit values for various key pollutants defined by the national directives (PDA, 2016), measured on fixed sites, the number and spatial distribution of which are defined. While this strategy may be effective for pollutants with homogeneous concentrations on a large geographic scale, it does not allow for assessing the population's exposure to pollutants with high spatial variability such as ultrafine particles. Moreover, the current regulations do not include the monitoring of directly exploitable parameters in terms of the health impact of air pollution or emission sources. However, this information is essential for the development of adequate public policies for better control of air quality, therefore there is a need to conduct an in-depth air quality study within the Gauteng region, specifically within a modelling framework. Ambient air quality is defined as the physical and chemical measurements of pollutant concentrations in the atmosphere to which the general population is exposed. In most developing countries, ambient air quality is reported to have deteriorated seriously, especially in urban areas, exposing populations to pollutant levels above the recommended limits (Coker and Kizito,2018). Ozone, nitrogen dioxide, sulfur dioxide and Particulate Matters are currently problematic pollutants in Gauteng because they present a health

risk with annual average concentrations relatively high and sometimes higher than the national recommended standards. In general, pollutants can be classified in 2 categories: primary and secondary pollutants. The primary pollutants, such as sulfur dioxide, nitrogen oxides (NOx) are directly emitted by sources of emission (road traffic, industries, the buildings, etc). The secondary pollutants, the secondary ozone (O_3) and particles, are formed by photochemistry or chemical reaction from the primary education pollutants (Haskins et al.,2019). The nature and the quantity of primary pollutants emitted by various sources of emission are generally indexed in various emissions inventories. Ambient air quality monitoring stations have been commissioned throughout the Gauteng Province in order to measure and evaluate the ambient air quality levels. Gauteng Province has a total of 34 ambient air quality monitoring stations, 29 and 5 are owned by municipalities and the Department of Environmental Affairs respectively. The majority of the monitoring stations are situated within the 3 metropolitan areas (i.e. CoE, CoJ and CoT), with a smaller number in Vaal Triangle, Airshed Priority Area, and West Rand District Municipalities. Gauteng Province state of air report for the period of 1st November 2016 to 30 June 2017, showed that PM_{10} is exceeding the daily average of 75 $\mu g/m^3$ across the province. Sulfur dioxide is exceeded by the daily average of 125 $\mu g/m^3$ at CoE and SMD, which are within the priority areas. Ozone is not exceeding the 120 $\mu g/m^3$, but the results in most of the stations show that the ozone might be a problematic pollutant in the near future across the province.

The WHO air quality guidelines assess the health effects of air pollution and provide threshold values beyond which it is detrimental. In 2014, 92 percent of the world's population lived in locations where the WHO air quality guidelines were not respected. In 2013, there were an estimated 3 million premature deaths worldwide caused by air pollution in urban and rural areas (WHO, 2013). Air pollution represents a major environmental risk to health. By reducing levels of air pollution, countries can reduce the burden of disease caused by stroke, heart disease, lung cancer and chronic or acute respiratory diseases such as asthma (Schraufnagel et al.,2019). Ambient air quality standard for sulfur dioxide of the WHO is stricter compared to the South African one that is 20 and 125 $\mu g/m^3$ respectively on average for the period of 24 hours. Particulate Matter (PM) for the WHO is stricter than South Africa air quality ambient standard of 20 and 40 $\mu g/m^3$ respectively on average per year. Ozone for WHO is stricter compared to the South African ambient air quality standard of 100 and 120 $\mu g/m^3$, respectively for an average of 8 hours running.

On average the WHO air quality guidelines are stricter than the South African national ambient quality standards.

The study will assess gathered results against the national ambient air quality standards for sulfur dioxide, nitrogen dioxide, ozone and PM_{10} within 2 districts i.e. Sedibeng and West Rand District Municipality and 3 metros, which are the City of Ekurhuleni, Johannesburg and Tshwane.

2.1 Sulfur Dioxide

Sulfur dioxide generally results from natural and manmade sources. Sulfur dioxide is found in the gas phase and is colourless. Sulfur dioxide is a compound of sulfur and oxygen molecules that predominantly occurs at lower atmosphere. Man-made activities include combustion for energy production and heating purposes. Sulfur dioxide also results from burning of fossil fuel in industrial process (such as smelters and power generation), emissions from engine exhaust (such as vehicle and aircraft) and, domestic fuel burning. Sulfur dioxide is used extensively in various industrial processes such petroleum refining, chemical preparation and solvent extraction, pulp-making. The food industries use sulfur dioxide during preparation and preservation of food due to its ability to prevent bacteria growth and browning of fruit (Joradol et al.,2019). Sulfur dioxide is one of the criteria pollutants in terms the WHO and the South African National Environmental Management Air Quality Act 39 of 2004 as amended. In figure 2.1, ten ambient monitoring stations were considered for sulfur dioxide data collection within the City of Ekurhuleni. The ambient monitoring stations were for domestic fuel burning (8 stations), industrial (1 station) and traffic sources (1 station).

Table 2.1 below shows the national ambient air quality standards for sulfur dioxide at different averaging period of 10 minutes, one hour, daily and yearly.

Table 2.1: National Ambient Air Quality Standards for Sulfur dioxide (SO_2)

Averaging Period	Concentration	Frequency of Exceedance
10 minutes	500 µg/m^3 (191 ppb)	526
1 hour	350 µg/m^3 (134 ppb)	88
24 hours	125 µg/m^3 (48 ppb)	4
1 year	50 µg/m^3 (19 ppb)	0

NB: The reference method for the analysis of sulfur dioxide is ISO 6767

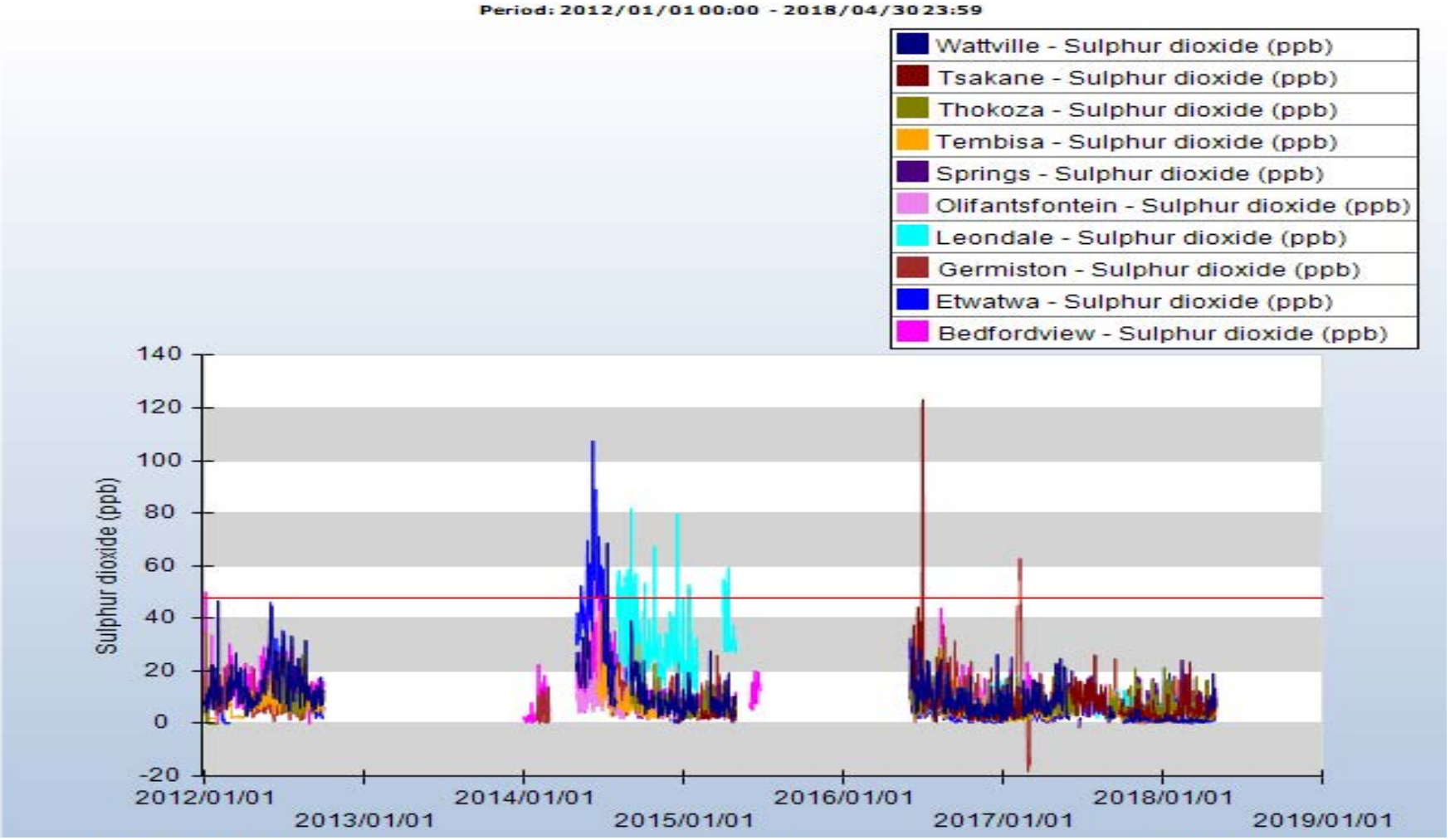

Figure 2.1: SO_2 daily limit for the City of Ekurhuleni. Results from the City of Ekurhuleni for Sulfur dioxide in parts per billion.

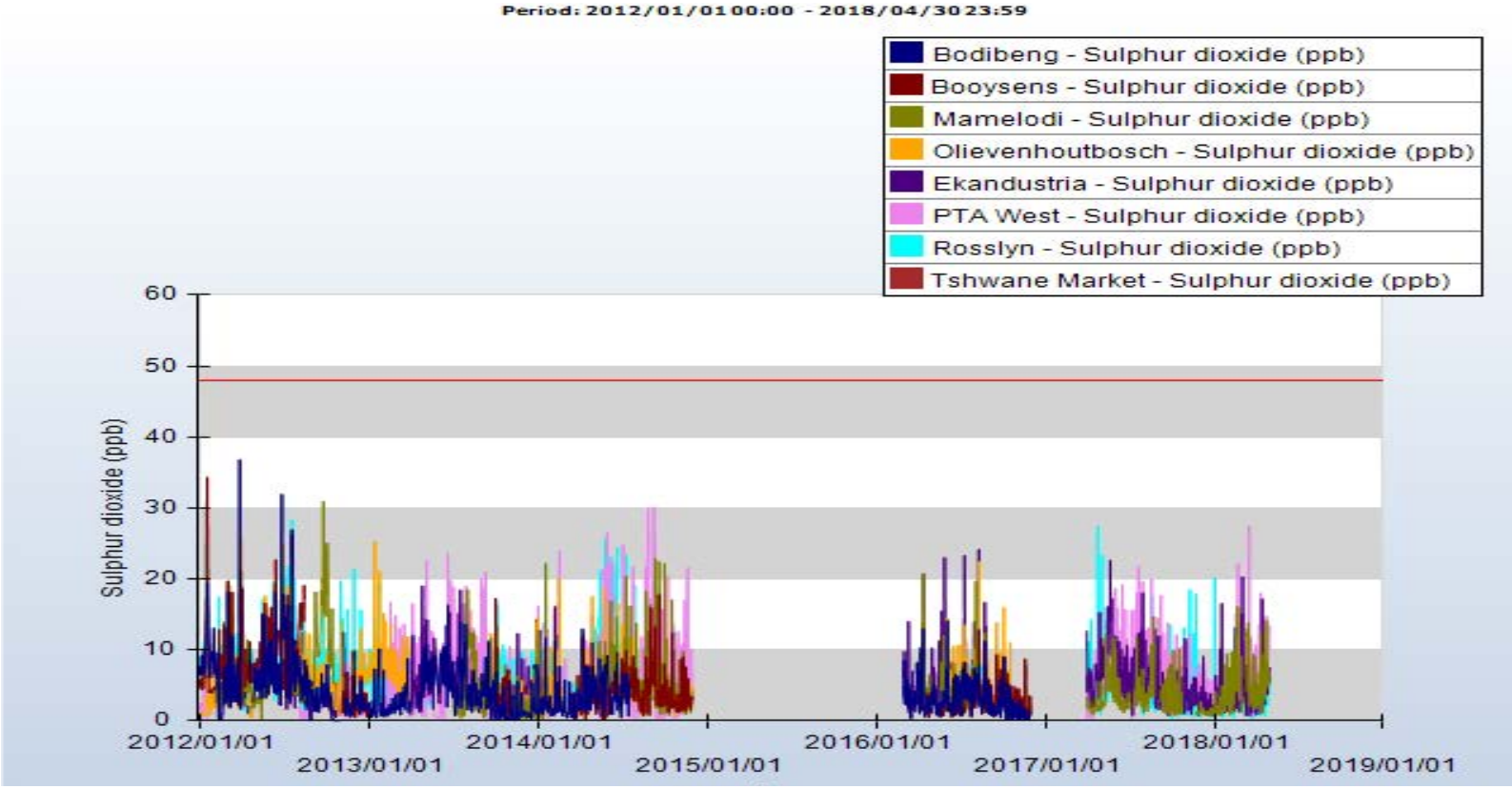

Figure 2.2:SO_2 daily limit for the City of Tshwane

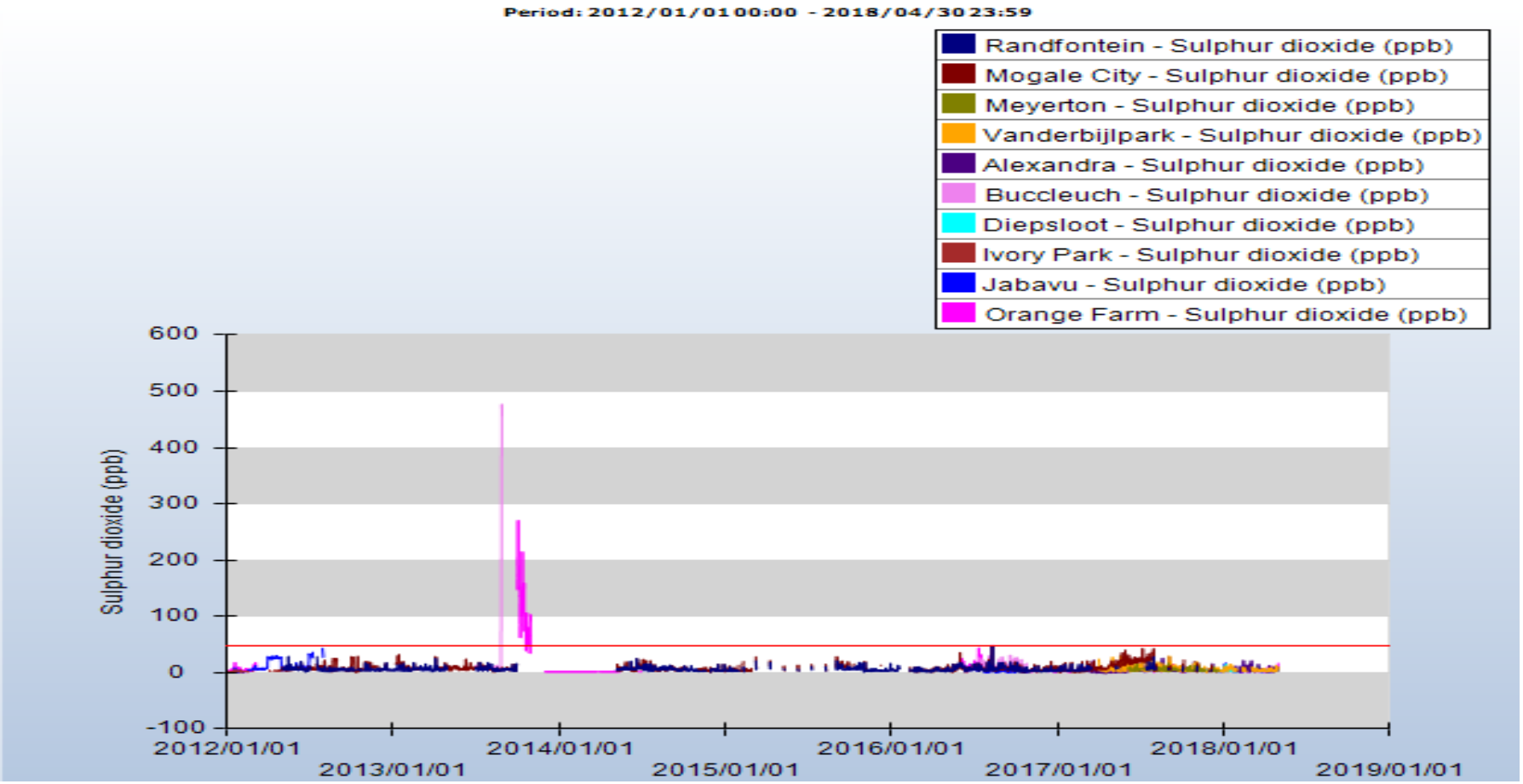

Figure 2.3:SO_2 daily limit for the CoJ, Sedibeng and West Rand District Municipality.

2.2 Nitrogen Dioxide

The nitrogen dioxide (NO_2) is frequently associated with nitrogen monoxide (NO). The sum of these 2 pollutants is indicated by nitrogen oxides (NOx). They are mainly emitted as nitrogen monoxide by fossil combustions at high temperature (Patel et al.,2019). In the atmosphere, in contact with oxygen, NO oxidizes to NO_2 and although the NO_x are often studied together, only NO_2 is harmful to human health and is thus regarded as one of the principal problematic pollutants. Oxides of nitrogen are very small in size and can penetrate deeply into lungs which caused different disease such as bronchitis, emphysema and asthma (Falcon-Rodriguez.,2016). Particles of nitrite can reduce the visibility by blocking the transmission of light. Table 2.2 below shows the national ambient air quality standards for nitrogen dioxide for one hour and yearly averaging period at one hundred and 6 and 20-one ambient concentrations parts per billion respectively. Nitrogen dioxide standards will be presented in terms of hourly average with 88 frequency of exceedance.

Table 2.2: National Ambient Air Quality Standards for Nitrogen Dioxide (NO_2)

Averaging Period	Concentration	Frequency of Exceedance
1 hour	200 $\mu g/m^3$ (106 ppb)	88
1 year	40 $\mu g/m^3$ (21 ppb)	0

NB: The reference method for the analysis of nitrogen dioxide is ISO 7996

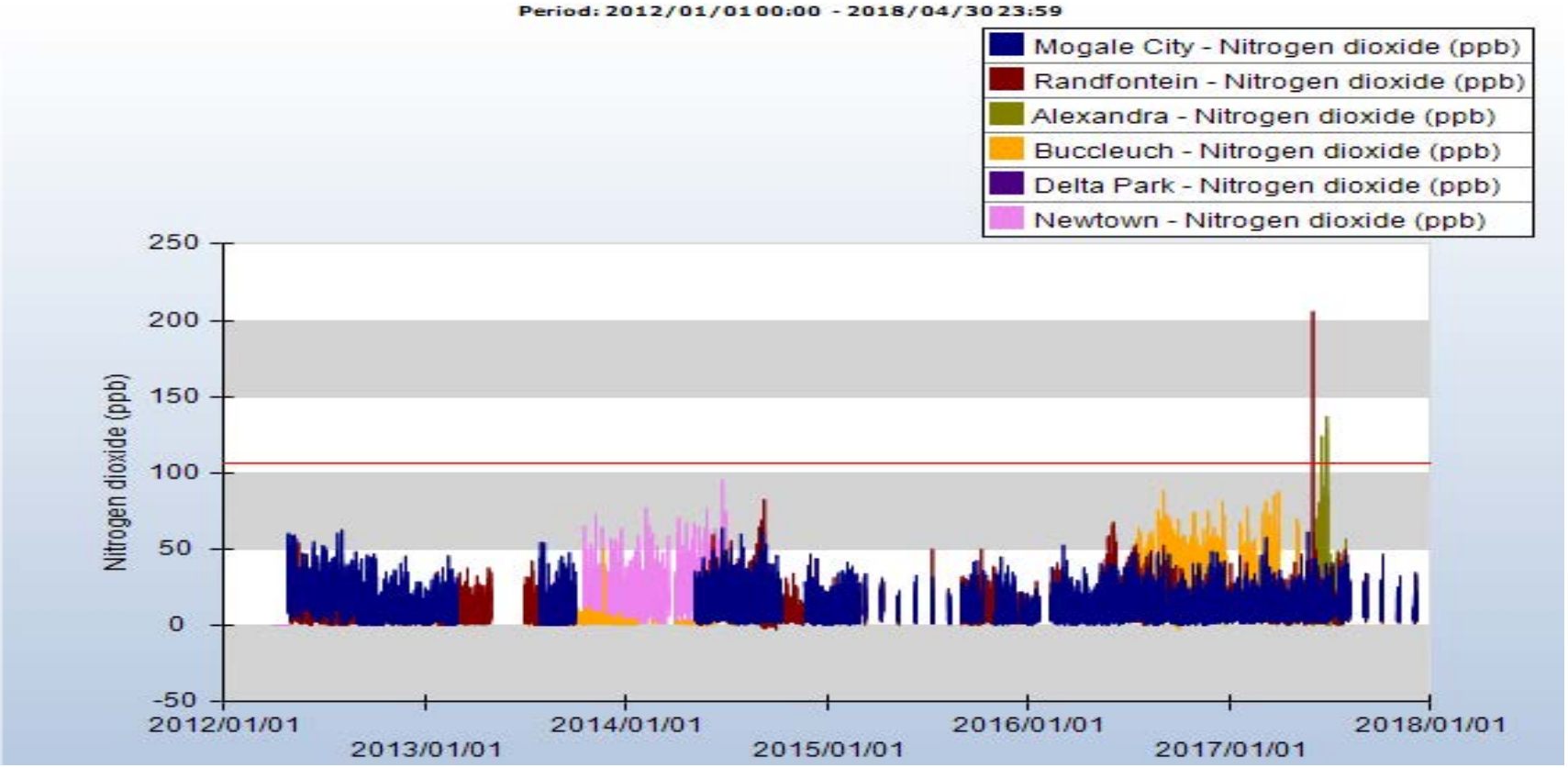

Figure 2.4: NO_2 hourly limit for the CoJ and West Rand District Municipality

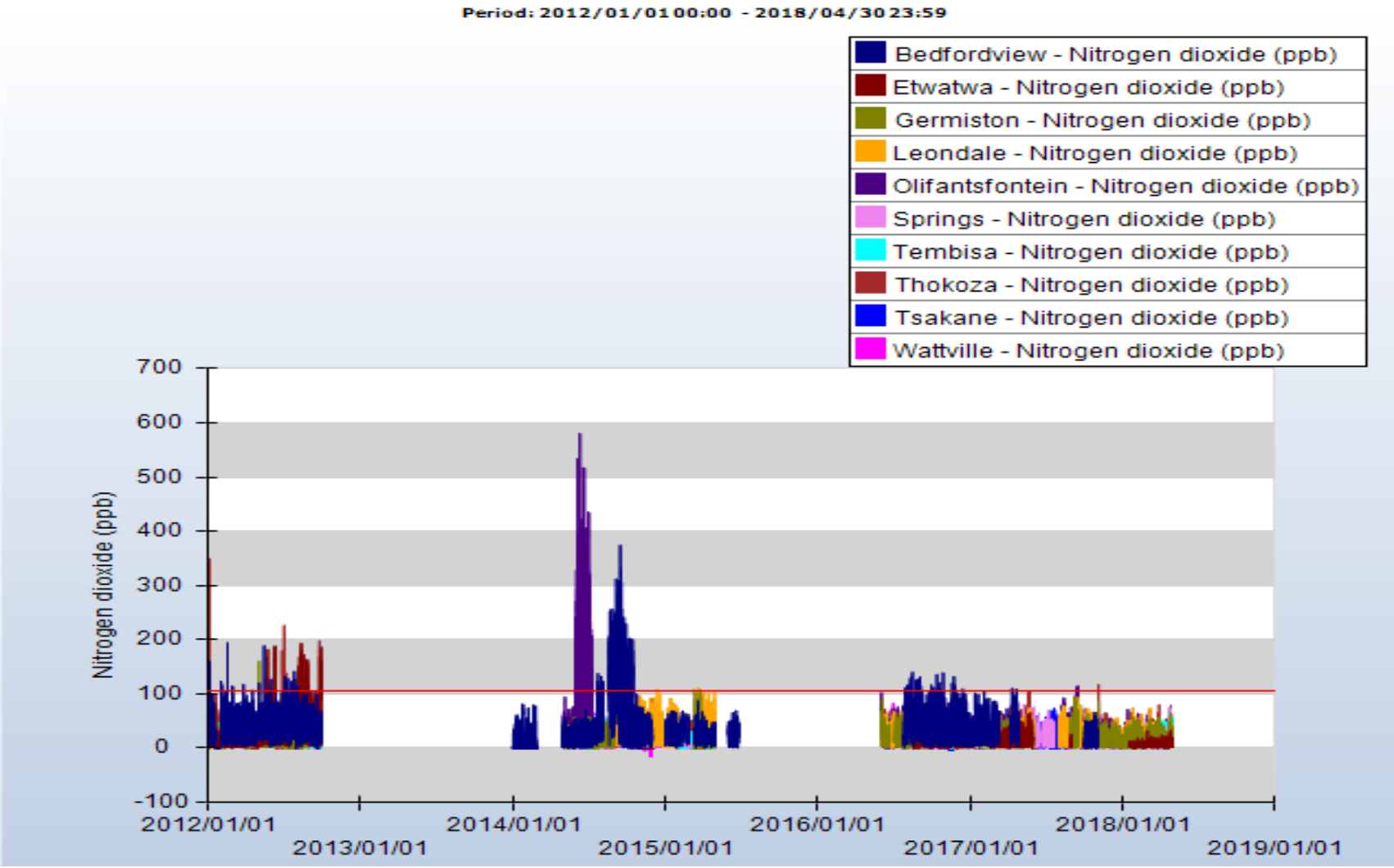

Figure 2.5:NO_2 hourly limit for the City of Ekurhuleni

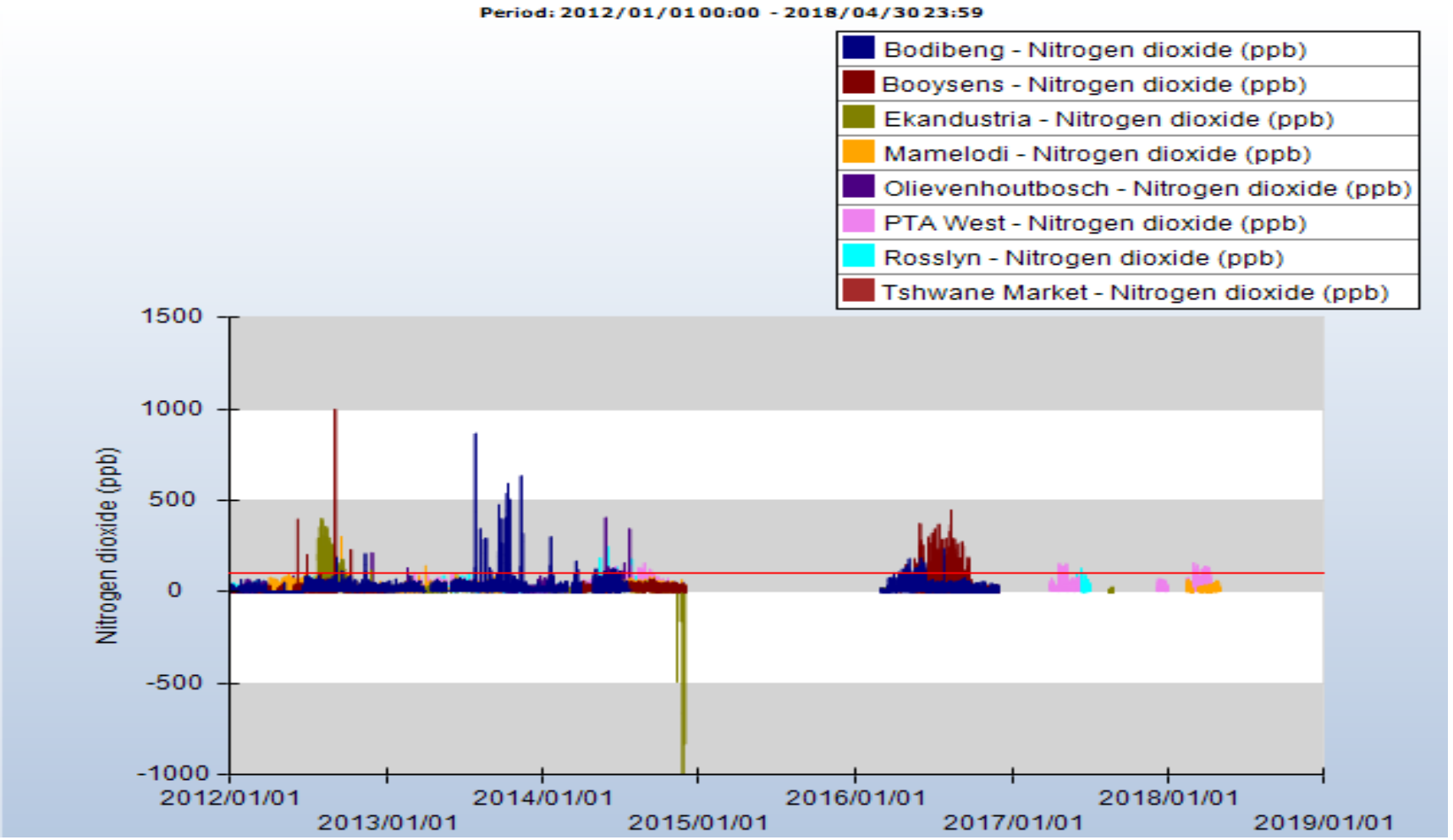

Figure 2.6:NO_2 hourly limit for the City of Tshwane

2.3 Particulate Matter (PM_{10} and $PM_{2,5}$)

The term "particulate" indicated a solid mixture and/or liquid present in a gas mixture. Particulate pollution is much more complex than gaseous pollutants such as the NO_2 and O_3 because it does not refer a well-defined chemical entity but rather to a heterogeneous mixture of solid and fluids elements whose size and chemical composition many evolves dynamically from a diverse source of emissions (Li et al.,2019).

Particulate pollutions are measured by the concentration in mass of the PM_{10} and $PM_{2,5}$ (Kalaiarasan et al.,2018). The PM_{10} and the $PM_{2,5}$ are particles of average aerodynamic diameter lower than 10 μm and 2,5 μm respectively. The particles having a diameter between 2,5 and 10 μm are known as "coarse" and those with a diameter lower than 2,5 μm are known as "fines". Many researchers have argued that particle sizes measurement is not probably the most relevant indicator to characterize the particles because it does not take into account their chemical composition (Horváth et al, 2017).

Particles present in ambient air can be characterize as "primary" or "secondary. This aspect makes the characterization of the secondary particles very complex and their effects on health will differ according to their sizes but also according to their chemical composition (Lehner et al.,2019). The primary particles are directly emitted in the atmosphere by natural sources (marine or biogenic) and by anthropic sources (road transport, manufacturing industry, residential-tertiary sector, agriculture, conversion energy).

"Secondary" particles are particles formed in the atmosphere by complex chemical processes, and may lead to the formation of chemical precursors such as oxides of sulfur, nitrogen, ammonia and organic compounds. The chemical composition of these particles is thus very variable and may vary spatially, temporally and according to the size of the particles. This aspect makes the characterization of the secondary particles very complex and their effects on health will differ according to their sizes but also according to their chemical composition (Lehner et al., 2019).

Table 2.3: National Ambient Air Quality Standards for particulate matter less than 10 μm diameter (PM_{10})

Averaging Period	Concentration	Frequency of Exceedance
24 hours	75 $\mu g/m^3$	4
1 year	40 $\mu g/m^3$	0

NB: The reference method for the analysis of the particulate matter fraction of suspended particulate matter is EN 12341

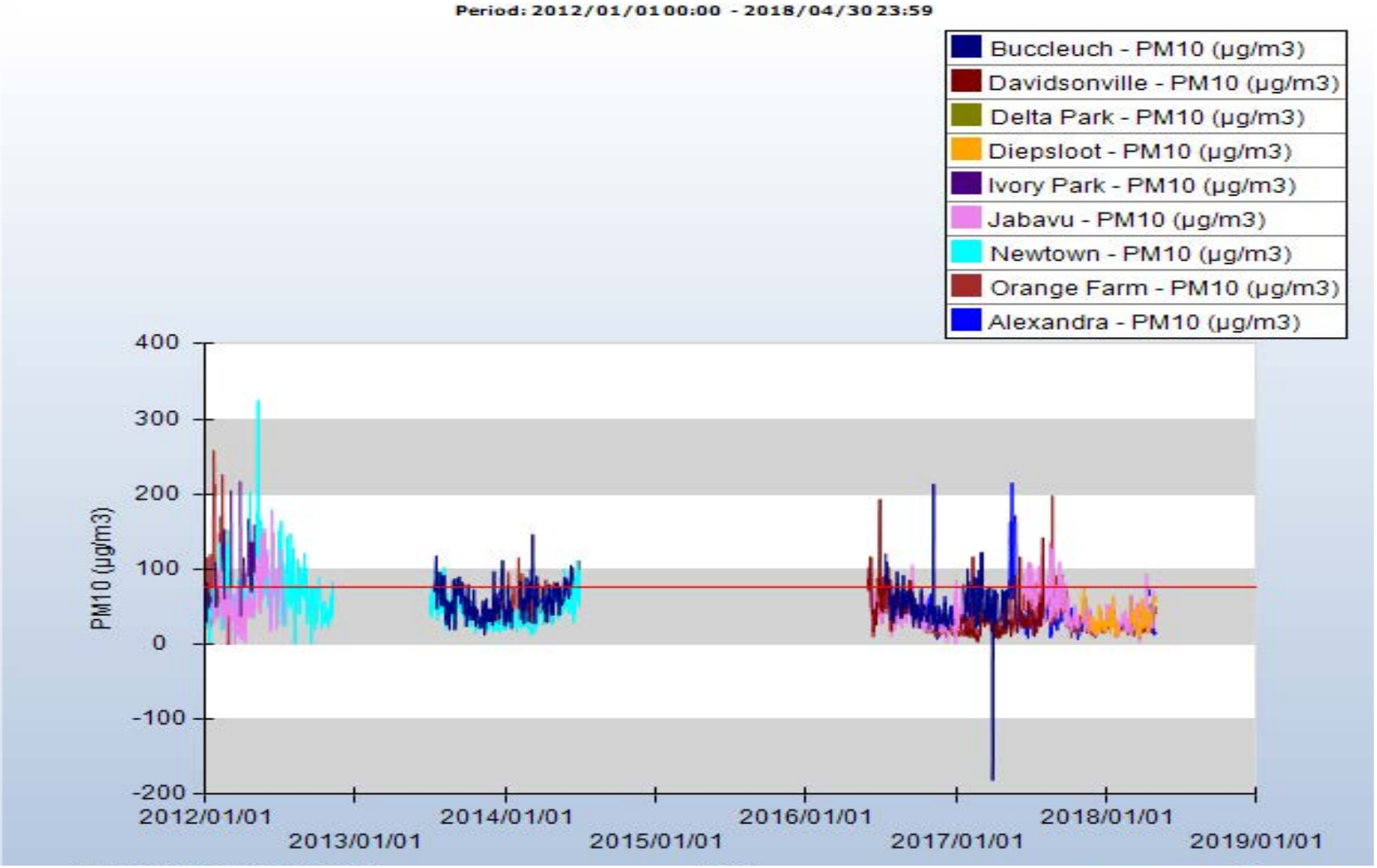

Figure 2.7:PM_{10} daily limit for the CoJ

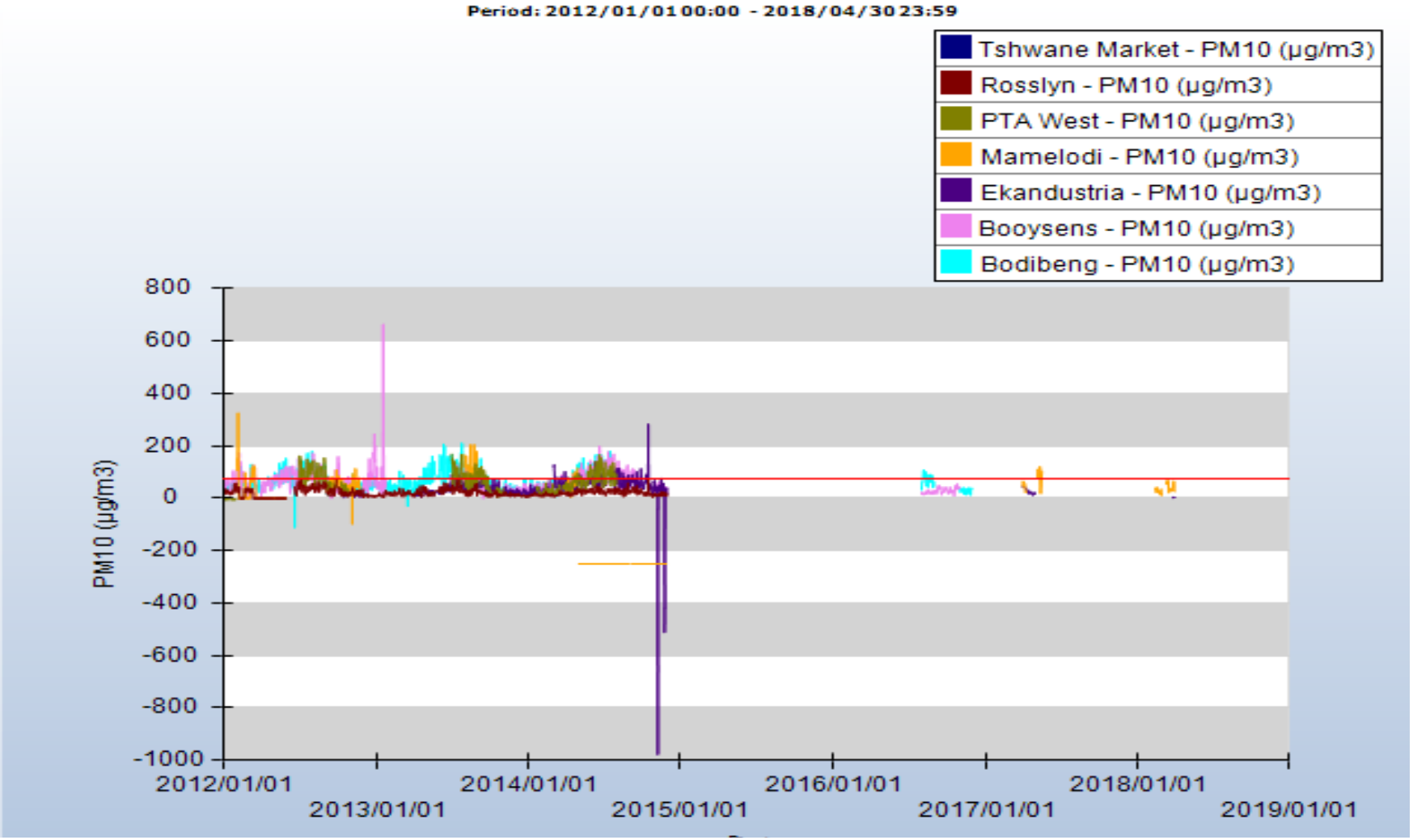

Figure 2.8:PM_{10} daily limit for the City of Tshwane

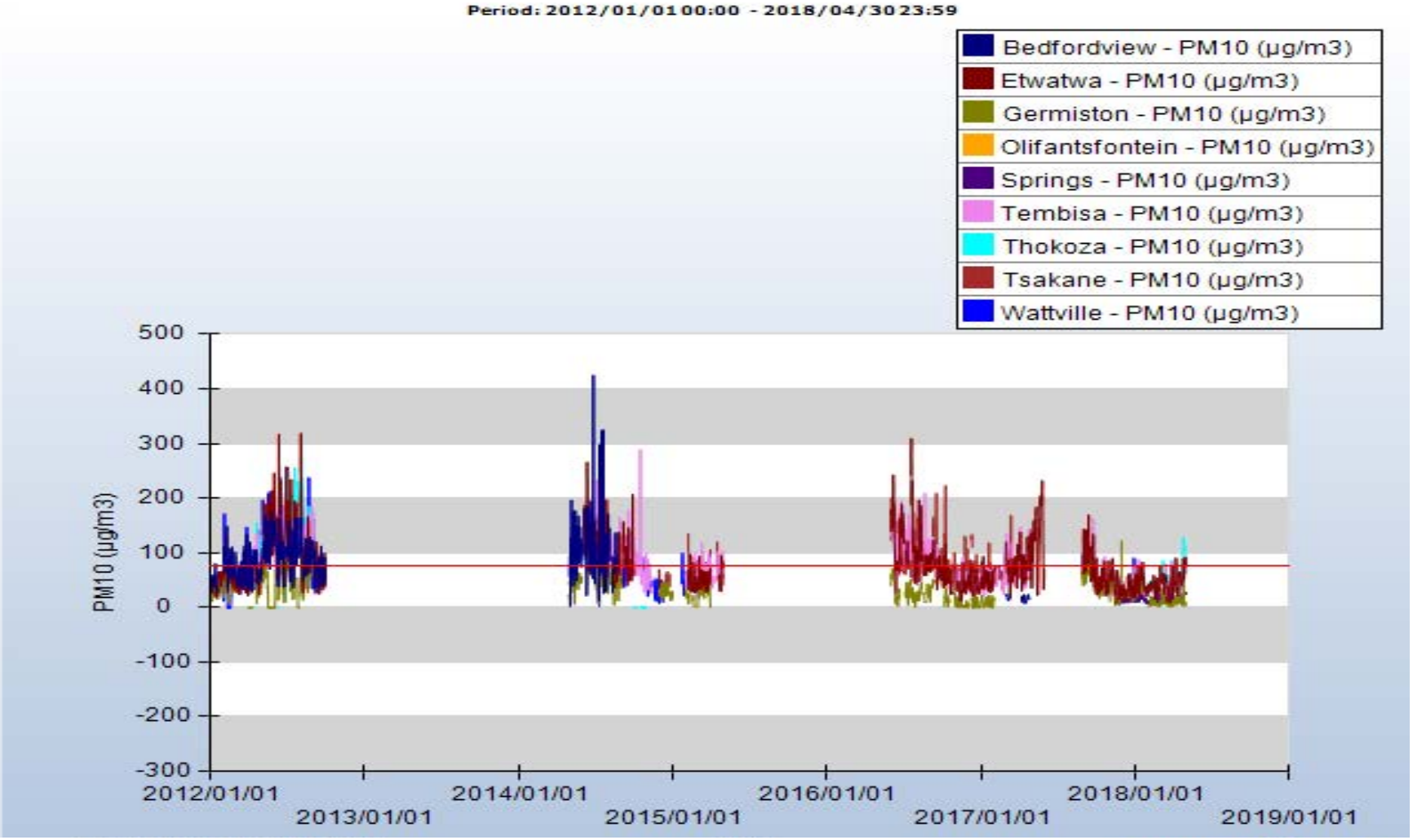

Figure 2.9:PM_{10} daily limit for the City of Ekurhuleni

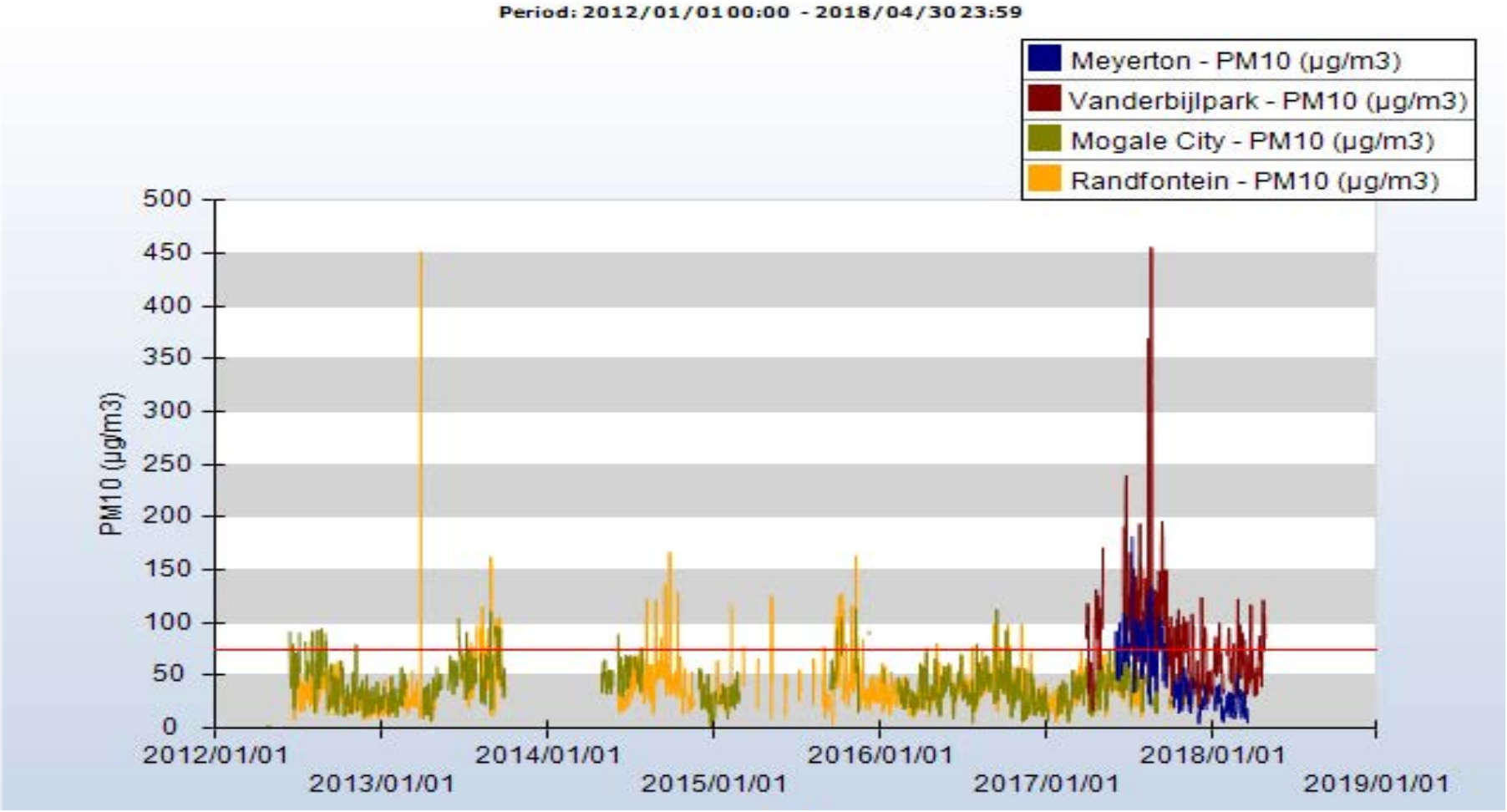

Figure 2.10:PM_{10} daily limit for Sedibeng and West Rand District Municipality

2.4 Ozone

Tropospheric ozone is a secondary pollutant. On local scales, ozone is formed by photochemical oxidation of NOx and volatile organic compounds (VOC) (organic compounds) and HOx radicals. To a lesser extent, the carbon monoxide (CO) and methane (CH_4) can also be the source of O_3. The principal formation of ozone is always done in the presence of NOx thought a complexity of chemical reactions can intervene in the formation of ozone (Greenslade, 2019). NO_2 is dissociated under the effect of solar radiation (below 420 Nm wavelength) which gives nitric oxide and oxygen. The atomic oxygen reacts with the dioxygen to form ozone.

High level of ozone pollutant is the serious concern to the living organism because ozone pollutant can irritate the respiratory tract and eyes(Ghorani-Azam et al,2016). High exposure to the ozone pollutants may lead to coughing, chest tightness and wheezing amongst sensitive human being. Multi occurrence of ozone for several months may cause permanent lung damage (USEPA, 2010a). Table 2.4 below shows the national ambient air quality standards for ozone at the averaging period of 8 hours running average at 61 parts per billion.

Table 2.4: National Ambient Air Quality Standards for Ozone (O_3)

Averaging Period	Concentration	Frequency of Exceedance
8 hours(running)	120 µg/m^3 (61 ppb)	11

NB: The reference method for the analysis of the analysis of Ozone shall be UV photometric method as described in ISO 13964

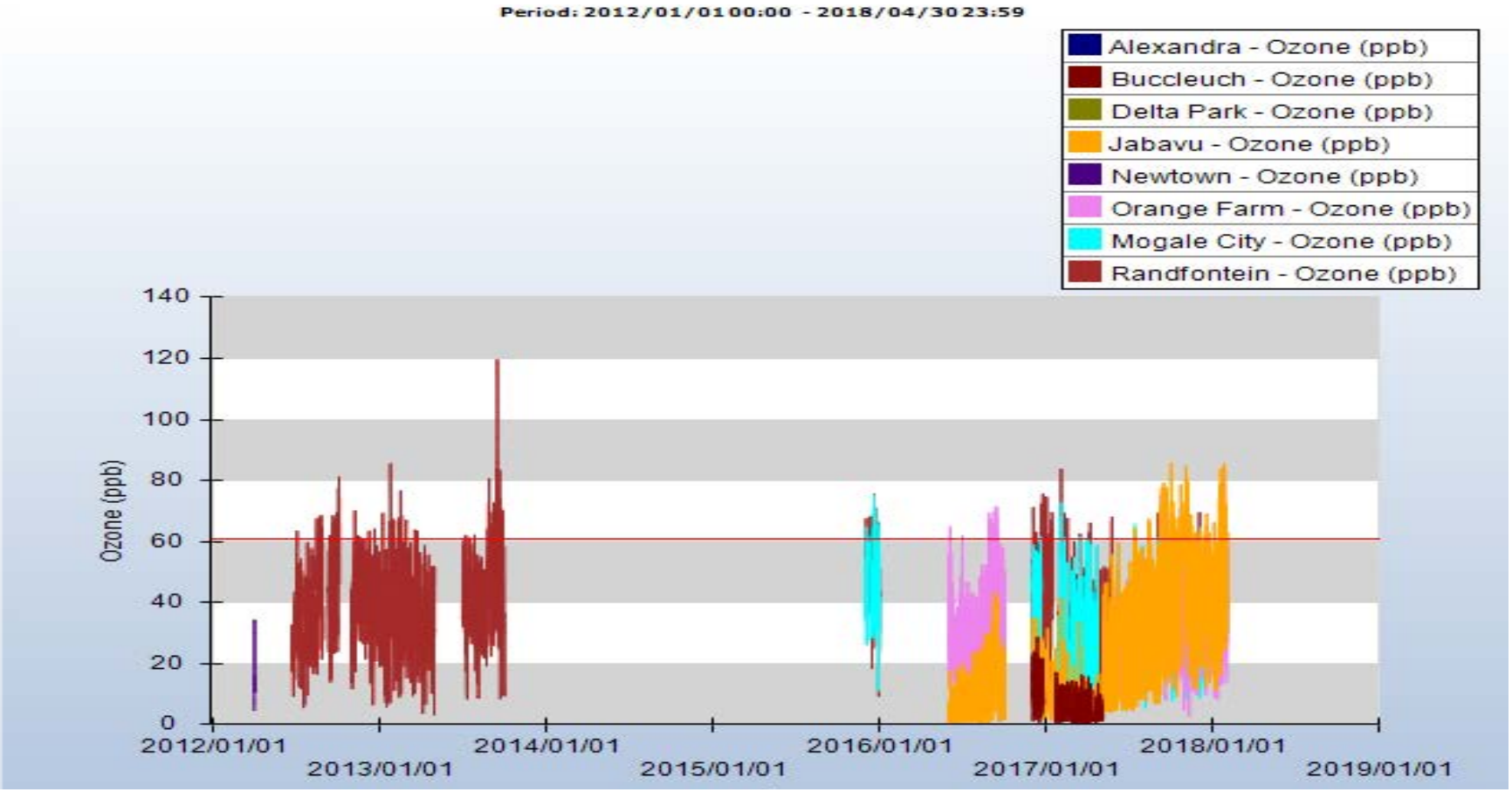

Figure 2.11: Ozone 8 hours running for the CoJ and West Rand District Municipality

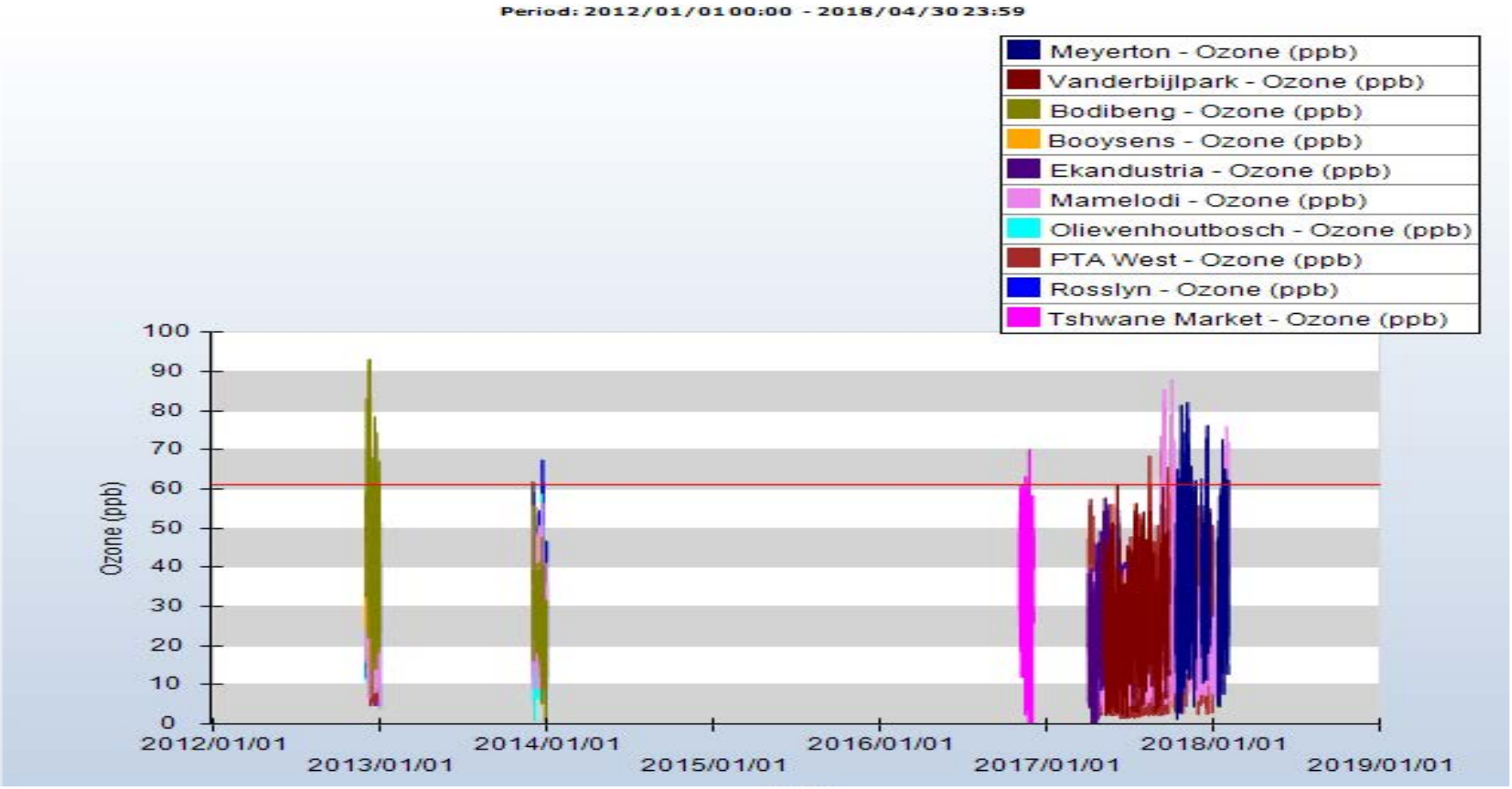

Figure 2.12: Ozone 8 hours running for the City of Tshwane and Sedibeng District Municipality

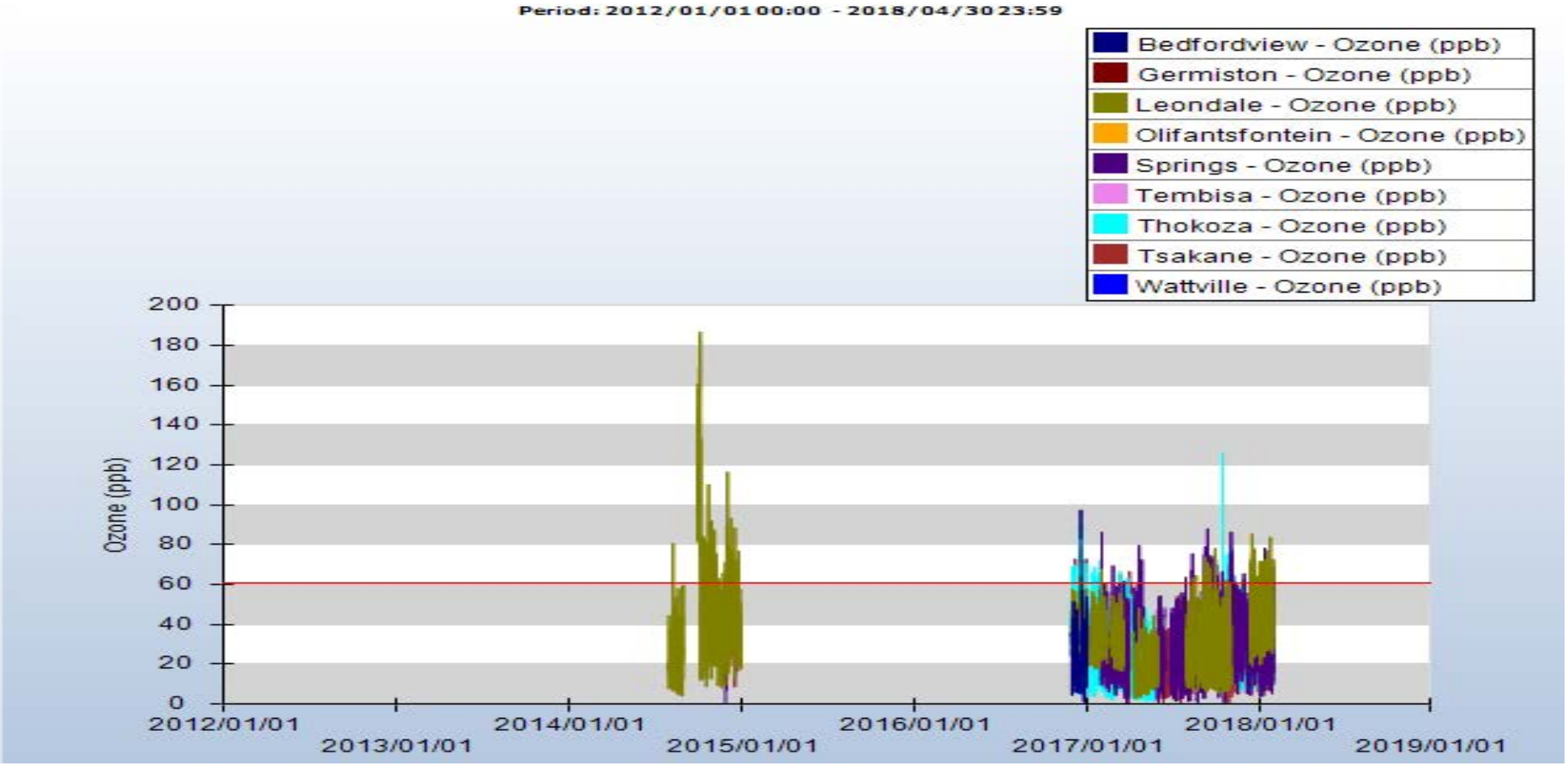

Figure 2.13: Ozone 8 hours running for the City of Ekurhuleni for the Ozone ambient concentration in parts per billion in 8 hourly average

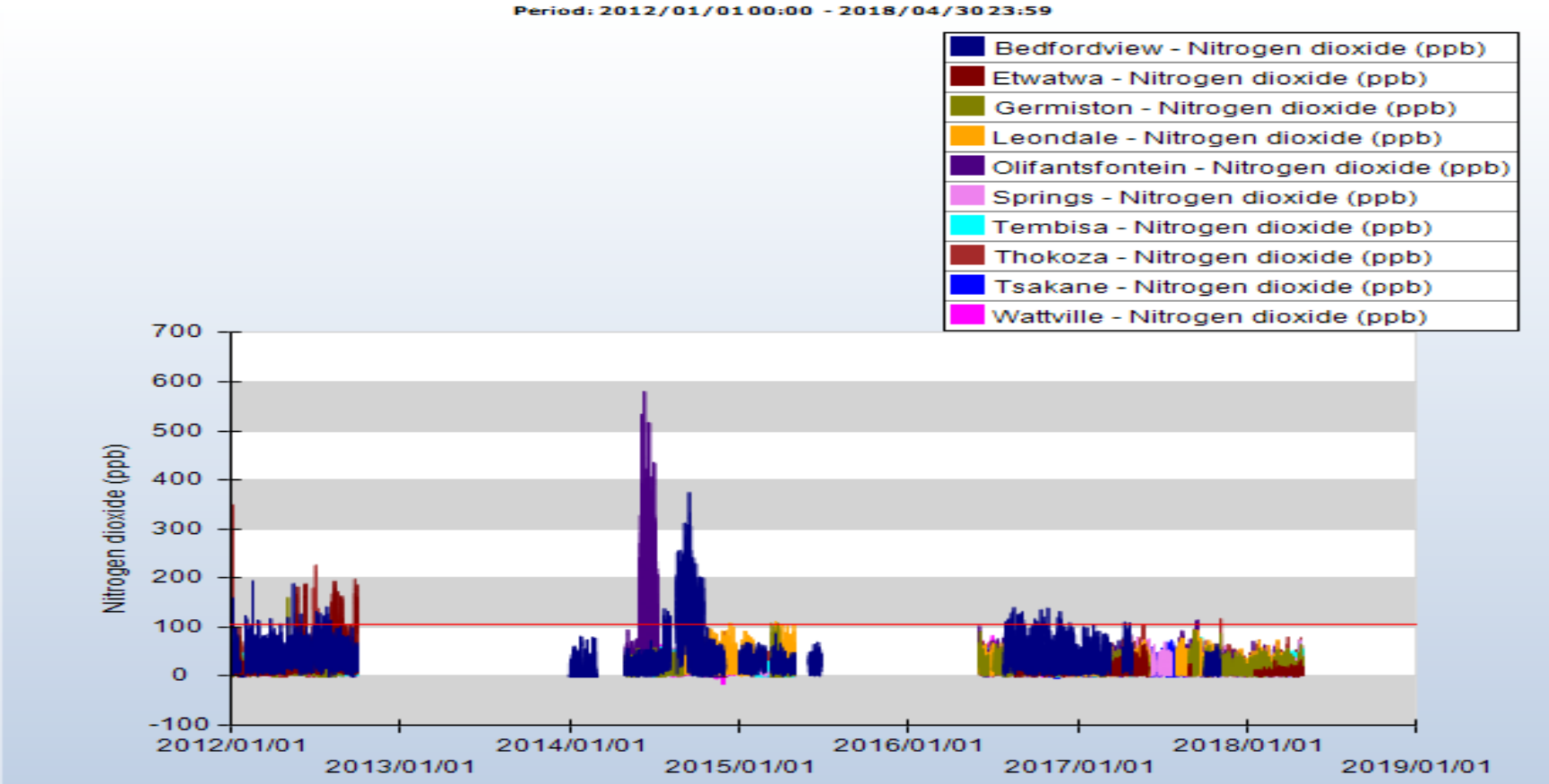

Figure 2.14:NO_2 hourly limit for the City of Ekurhuleni for Nitrogen dioxide in parts per billion

2.5 Sources of emissions within Gauteng Province in South Africa

The recent South African most forms of air pollution are because of human activities and include fossil fuel burning (coal, oil and natural gas in industrial processes), electricity generation, vehicle emissions, aircraft emissions, domestic fuel burning, and the use of household materials that contain persistent organic pollutants, biomass burning and waste incineration. In South Africa, the industry is a major consumer of energy and depends mainly on fossil fuels, especially coal. The industrial/mining sector remains also a major consumer of electricity nationally (Inglesi-Lotz and Blignaut, 2011). The largest industrial consumer of electricity is the industry sector, followed by the iron and steel, Chemical and Petroleum, and non-ferrous metals industries (Wang and Zhao, 2017). Air pollution is a major concern especially heavy industrial development areas such as the Vaal Triangle Airshed Priority Area,) and the Highveld Priority Area (HPA) (Altieri and Keen,2019). Gauteng Province has the highest percentages of facilities on the national atmospheric emission inventory system followed by Kwazulu-Natal province. South Africa has 1396 facilities on the national atmospheric emission inventory system of which Gauteng, Kwazulu-Natal and Western Cape have the highest number of facilities registered at 387, 243 and 173 respectively. At municipal level, the Ekurhuleni Metropolitan Municipality has the largest number of facilities in the country compare to any other municipality in the country followed by the City of Tshwane (CoT) and City of Johannesburg (CoJ) with (https://saaelip.environment.gov.za, 23 May 2019). Moreover, Gauteng currently has 380 identified mine residue areas of which the majority are gold-mining residues (GDARD, 2009). Many of these mine residue areas are sources of dust pollution, especially during secondary reclamation of the tailings that entails removal of protective layers of vegetation for the duration of the reclamation project. Industries situated throughout the province include metallurgical industries, mineral processing, organic chemical, inorganic chemicals, storage of petroleum, small boiler and thermal treatment of hazardous waste and general waste operations among others. Industrial activities depending upon their processes, inputs and outputs release various pollutants into the atmosphere.

According to the Gauteng State of Environment Report (GDARD, 2011), Iron and steel processes are the most common industrial operation within the province, followed by ceramic processes, waste incineration, power generation and cement and lead processing. Industrial activities and coal-fired power stations contribute to sulfur dioxide, particulates and oxides of nitrogen that are

significant sources of emissions specifically in highly industrialized areas such as Ekurhuleni Metropolitan Municipal and the Vaal Triangle (SOER, 2004). The data above give a baseline for the understanding of emission sources distributions within the province but not necessarily help in identifying the cause nor the sources of the poor ambient air quality. It is, therefore, one of the objectives of this work to detail specific points area and line that are causing exceedance to the national ambient standards within the Gauteng Province.

Recent evidences have shown that domestic fuel burning presented the most significant source of respiratory hospital admissions and premature hospitalities in Gauteng (GDACE, 2009) and that the main pollutants of concern associated with domestic fuel burning are fine particulates (PM_{10}) and sulfur dioxide. A further study in the Soweto township indicated that domestic coal combustion contributed to approximately 70% of the ambient total particulate matter PM_{10} load (Annegarn et.al.,1998) and in the Vaal Triangle it was found that domestic coal combustion contributed on average 37% to the atmospheric PM_{10} load, and that this value rose to 65% during winter periods (Engelbrecht et.al., 1998). Gauteng is also known for mine tailings dams that may be the sources of blown dust in the province.

Spatial and temporal study of gaseous pollutant in the Highveld by Lourens et al. (Lourens et.al., 2011) indicated that nitrogen dioxide and Sulfur dioxide levels were higher at sites situated in or near industrialized areas. Their results further showed that sites that have higher Sulfur dioxide and nitrogen dioxide concentrations exhibit the lowest ozone levels, while higher ozone concentration coincided with lower Sulfur dioxide and nitrogen dioxide levels (Lourens et.al., 2011). Mdluli et al. (Mdluli et al, 2005) assessed air quality in selected townships and the potential implications for local communities. Their study showed that air pollution exposure results in numerous health problems in the general population with the effects more pronounced among the elderly and the young. Health impacts associated with air pollution in the Vaal Triangle were estimated already at about R289 million per annum 20 years ago (Scorgie et al.,2003).

Gauteng has the largest number of vehicles in South Africa as shown in Table 2.5 (Statistics-eNatis, 2019). Vehicle exhaust emissions have been identified as a growing concern in South Africa. Gauteng Province has the largest number of vehicles in South Africa accounted for 37.76% followed by Western Cape and KwaZulu Natal provinces at 16.21% and 13.74% respectively (Statistics-eNatis, 2019).

Table 2.5: Self-propelled vehicle population per vehicle class- October/November 2019

Vehicle Class	Gauteng Province
Motor cars and station wagon	3 123 446
Minibuses	131 372
Buses, bus train, minibuses	20 469
Motorcycles, quadracycles, tricycles	139 529
LDV's, panel vans, other light load vehicles' GVM<=3500kg	854 918
Trucks (Heavy load vehicles GVM.3500kg)	139 529
Other self-propelled vehicles	36 397
Total self-propelled vehicles	4 446 341
Gauteng Province over South Africa	38,76%

(Statistics-eNatis, 2019)

The Gauteng Province also boasts number active airports as shown in Table 2.6 below.

Table 2.6: List of Airports in Gauteng Province, South Africa

List of Airports in Gauteng Province			
Airport Name	**City Served**	**Coordinates**	**Elevation(ft)**
O.R. Tambo International Airport	Johannesburg/Kempton Park	26 08'01"S and 28 14'32"E	5,558
Krugersdorp Airport	Krugersdorp	26 04'54"S and 27 43'32"E	5,499
Rand Airport	Germiston	26 14'31"S and 28 09'05"E	5,483
Springs Airport	Springs	26 14'54"S and 28 23'51"E	5,34
Grand Central Airport	Johannesburg/Midrand	25 59'13"S and 28 08'26"E	5,325
Brakpan Airport	Brakpan	26 14'17"S and 28 18'21"E	5,3
AFB Waterkloof	Pretoria	25 49'40"S and 28 13'15"E	4,94
Vereeniging Airport	Vereeniging	26 34'12"S and 27 57'36"E	4,846
AFB Swartkop (Zwartkop)	Pretoria	25 48'35"S and 28 09'53"E	4,78
Lanseria International Airport	Johannesburg/Randburg	25 56'23"S and 27 55'29"E	4,517
Wonderboom Airport	Pretoria	25 39'13"S and 28 13'27"E	4,095
Heidelberg Airport	Heidelberg	26 30'30"S and 28 23'30"E	

2.6 Air Quality Modelling using Open-air

Open-air modelling has been developed by Insightful Corporation under the free Software Foundation's for General Public License. The package can be downloaded from http://www.openair-project.org. The tool can analyse big data in a form of computer programs that predict temporary and spatial various pollutants accurately. The R project is statistical computation language which improves air quality data analyses. Then air quality data to be analysed can be inputted from computer files or imported from a monitoring station (Carslaw and Ropkins, 2012). The application of open-air model for air quality monitoring analyses is still scarce though, some researches have used open-air for analysis (Agustine et al., 2017; Carslaw et al.,2006; Carslaw and Beevers, 2013; Szulecka et al.,2017).

2.7 The Development of Source-receptor Relationships

Recent population trends in South Africa have seen a migration from rural to urban areas, which has resulted in a population explosion in most urban cities. Due to the low income of unskilled workers within the Gauteng Province and the increase of electricity tariffs, many households utilise coal, Wood and paraffin for cooking and heating purposes, which undoubtedly lead to high levels of toxic pollutants such as particulate matter (PM), nitrogen dioxide (NO_2), sulfur dioxide (SO_2) and VOCs.

Gauteng is SA most populous province despite that its geographical area covers only 1.5 % of the South African land mass. The Gauteng province is densely populated and urbanized, and accounts for 33 % of the country's GDP. It is the economic heart of Africa, chipping in an impressive 10 % to the continent's GDP. The province is situated in the Highveld of South Africa, situated on a high-altitude plateau of extensive grasslands about 1500 meters above sea level. The Witwatersrand, a ridge mostly formed from quartzite, conglomerates and shale that runs in an East-West direction through Gauteng, is famous for being the source of 40 % of all the gold ever mined from the Earth. The Gauteng Province has a total of 34 ambient air quality-monitoring stations. The majority of the monitoring stations are situated within the 3 metropolitan areas (i.e. CoE, CoJ and CoT), with a smaller number in Vaal Triangle, Airshed Priority Area and WRDM as shown in Figure 2.15.

In this work, Gauteng Atmospheric Emission Inventory data were gathered from the national atmospheric emission inventory system (NAEIS) (www.saaqis.org.za). Emission sources included on the atmospheric emission inventory are listed activities industries in terms of NEMAQA, Section 21(heavy industries), Section 23 (Controlled Emitters such as small boilers and temporary asphalt plants), mining & quarries and non-industrial activities.

Table 2.7 below shows the different Gauteng ambient monitoring stations and the associated monitoring sources.

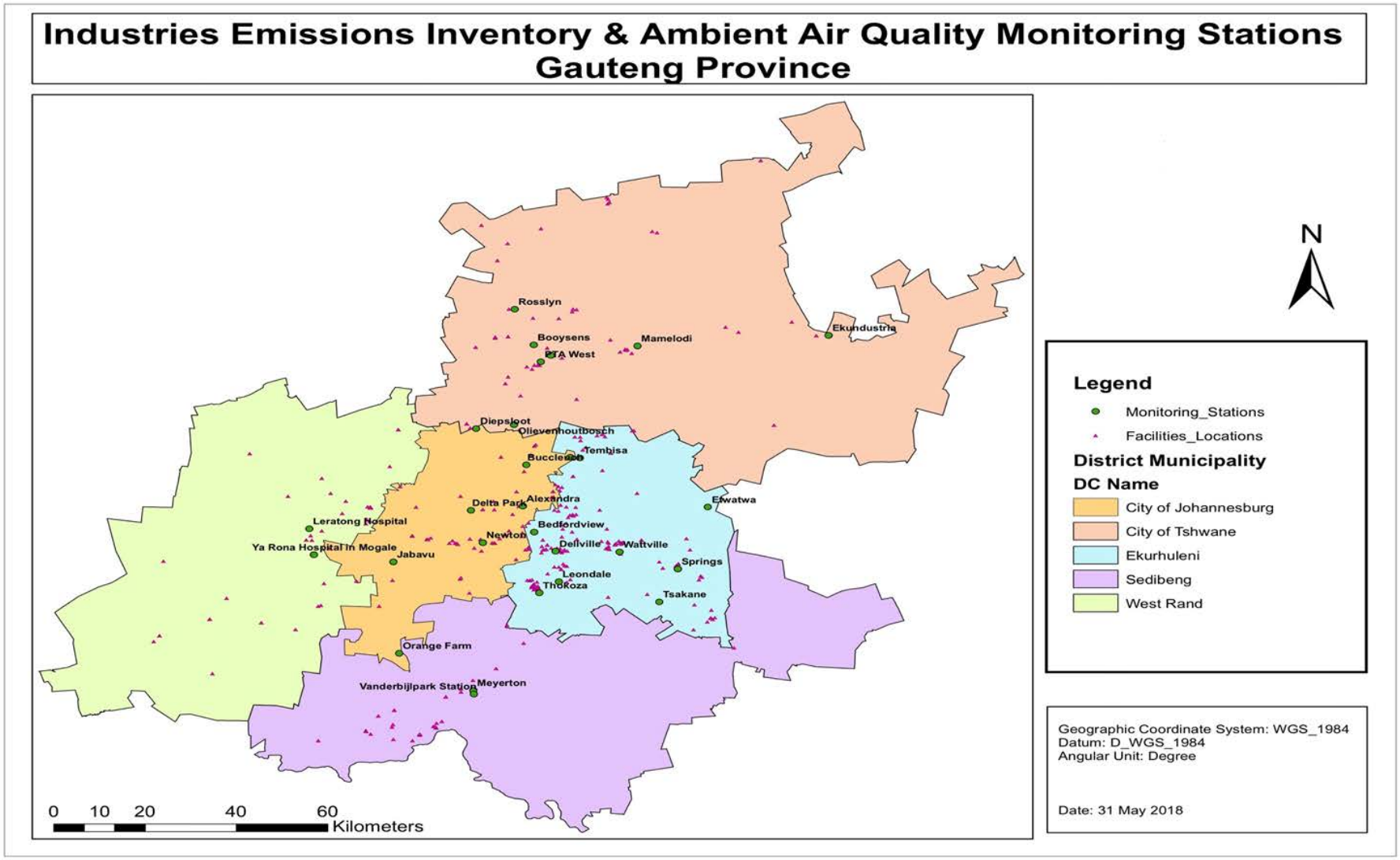

Figure 2.15: Distribution of Gauteng ambient monitoring station in relation to industries Emission inventory

Table 2.7: Gauteng ambient monitoring stations and associated monitoring sources

Licensing Authority	Ambient Air Quality Monitoring Station	Domestic	Industrial	Traffic	Background Information
CoE	Bedfordview	×	×	√	×
	Etwatwa	√	×	×	×
	Germiston	√	×	×	×
	Tembisa	√	×	×	×
	Thokoza	√	×	×	×
	Watville	×	√	×	×
	Springs	√	×	×	×
	Tsakane	√	×	×	×
	Olifantsfontein	×	√	×	×
	Leondale	√	×	×	×
CoJ	Alexandra	√	×	×	×
	Buccleuch	×	×	√	×
	Delta Park	√	×	×	×
	Jabavu	√	×	×	×
	Newtown (M1/M2 Interchange)	×	×	√	×
	Orange Farm	√	×	×	×
	Diepsloot	√	×	×	×
	Ivory Park	√	×	×	×
	Davidsonville (Mobile)	√	×	×	×
CoT	Pretoria West	×	√	×	×
	Rosslyn	×	√	×	×
	Mamelodi	√	×	×	×
	Booysens	×	√	×	×
	Tshwane Market (Mobile)	×	×	√	×
	Olievenhoutbosch Clinic	√	×	×	×
	Bodibeng	√	×	×	×
	Ekandustria	×	√	×	×
	Hammarskraal	√	×	×	×
SDM	Vanderbijlpark	×	√	×	×
	Meyerton	×	√	×	×
WRDM	Mogale, Krugersdorp	×	×	×	√
	Leratong, Randfontein	×	×	×	√

Pollutant roses are diagrams that show how air pollution depends on wind direction (Cosemans and Kretzschmar, 2002). In this study, pollution roses are used in the investigations of relationship directional sources for sulfur dioxide, nitrogen dioxide, ozone and PM of less than 10 $\mu g/m^3$ from 31 ambient monitoring within Gauteng. Pollution roses give valuable information on the location of the most important pollutant sources that affect the monitoring site. Pollution roses are used to calculate the average concentrations of a pollutant at a receptor from multiple emission sources over a period of time as a function of wind direction (Mc Naught and Wilkinson, 2012). Location of emission sources and ambient monitoring stations as per Figure 2.15, will be helpful to determine areas of concern. The pollution roses will be able to indicate concentration level and direction of origin.

2.8 Source Identification using Conditional Probability Function Modelling

Clustering is a division of data into groups of similar objects. Each group is called a cluster which consists of objects that are similar amongst themselves and dissimilar compared to object of other groups (Kassambara, 2017). The k-means algorithm used were developed by Hartigan and Wong (1979). Clusters are defined as areas of higher density within the data space compared to other regions. The drawback with these methods is that they expect some kind of density guide or parameters to detect cluster borders (Cluster analysis, 2019). Bivariate polar plot features can be identified and group using k-means clustering approach (Carslaw and Beevers,2013). Figure 2.16 below indicated centroid location before (on the left) and after (on the right) one k-means iteration.

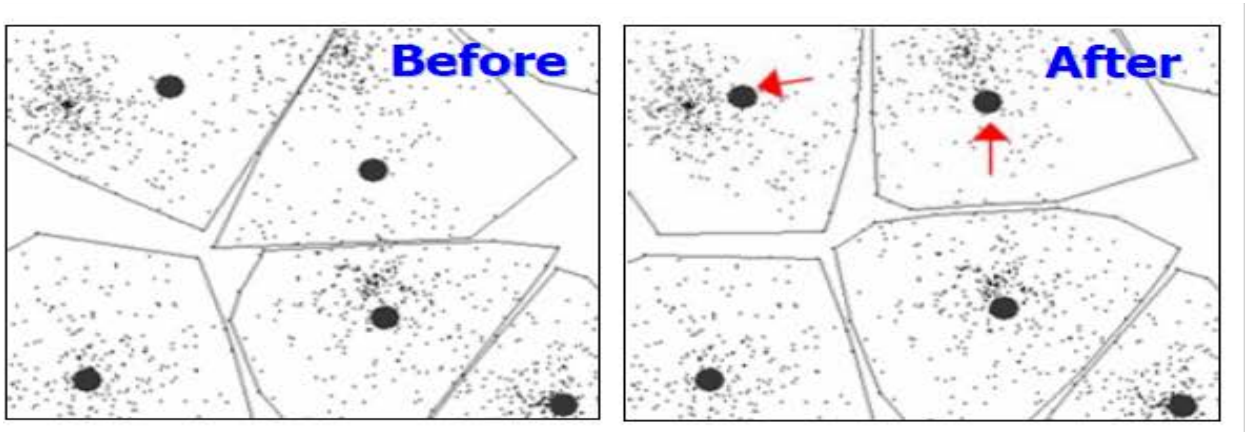

Figure 2.16: K-means moves the centroids towards the actual cluster centres

The main purpose of grouping data is to identify records in the original time series data. k-means clustering proceeds as follows: i) k points are randomly chosen from the space represented by initial group centroids, ii) each object is assigned to the group that has the closest centroid, iii) when all objects have been assigned, the positions of the k centroids is recalculated. The previous 2 steps are repeated until the centroid no longer move. Central to the idea of clustering data is the distances of similar or dissimilarity between points. It is important to compare the points of the cluster which is separated by the small distances relative to the distance between the clusters (Strauss and von Maltitz,2017). The Conditional Probability Function method is effective for providing directional information concerning major sources (Uria-Tellaetxe and Carslaw, 2014; Vedantham et al., 2014). Bae et al. (2011) used a Conditional Probability Function technique to help identify the directionality of sources contributing to observed pollutant concentrations at a rural site in a New York State. It has been shown that considering the wind speed and direction dependence of pollutant concentrations, Conditional Probability Function technique can yield better information concerning dominant source types (Carslaw et al., 2006). Malby et al. (2013) reported diverse approaches that have also been also used to identify dominant sources using non-parametric statistical analysis. Henry et al. (2009) developed a non-parametric wind regression

approach to identify and quantify the impact of possible source regions of pollutants as defined by wind direction sectors. They were able to quantify the contribution of different emission sources and demonstrate that some large sources, such as a steel mill, made only minor contributions of PM2.5 concentrations (Zheng et al,2019).

Kim and Hopke (2004) compared the Conditional Probability Function approach with the non-parametric regression approach for fine particle concentrations in the United States of America. They found that the Conditional Probability Function and non-parametric regression methods both worked well in identifying known local point sources. However, the Conditional Probability Function approach were easier to calculate compared with the non-parametric regression approach. Their results provided broad, dominant source directions in both cases.

This research study will investigate probability function to identify and characterize emission sources from the receptor location in the Gauteng Province. The goal is to identify sources that are contributing to ambient air quality and are causing continuous exceedance to the national ambient air quality standards.

3. CHAPTER 3: RESEARCH METHODOLOGY

3.1 Introduction

The aim of this study was to assess sources of air pollution in Gauteng Province by investigating correlation, pollution roses, conditional probability and probabilities of conditional functional modelling and k-means clustering. This chapter provides an overview of the research methodology and approach used in order to achieve the research objectives. The research methodology was selected based on the research problem statement and a preview of previous studies helped to identify an effective methodology for answering the research questions. The ambient monitoring data and emission inventory were collected. Previous studies were used, reports, records and information from the relevant authorities within the Gauteng Province. The approach used consisted of developing relationship, investigate pollution sources and clustering of similar data. This study focused on the spatial and exceedance analysis using open-air R 'package' in order to understand the air quality situation within the Gauteng Province.

3.2 Area of the study and data collection

This study is primarily based on data obtained from ambient air quality monitoring stations situated in Gauteng Province, which are reported to South African Weather Services (SAWS) and South African Air Quality Information System (SAAQIS). For the 6 years and 5 months period, the environmental quality monitoring data used were from 1 January 2012 to 30 first April 2018. The data parameters include concentrations of $PM_{2.5}$, PM_{10}, NO_2, SO_2 and O_3. Environmental monitoring data also includes meteorological data parameters such as wind speed, wind direction, humidity, pressure, solar radiation and ambient temperature. The data used for the study were on an hourly average. Thirty-one environmental monitoring stations data were used for this study. Out of 34 ambient air quality monitoring stations, 29 are owned by municipalities and 5 quality monitoring are owned by the Department of Environmental Affairs. The majority of the monitoring stations are situated within the 3 metropolitan areas (i.e. City of Ekurhuleni, City of Johannesburg and City of Tshwane), with a smaller number in Vaal Triangle, Airshed Priority

Area and West Rand District Municipalities. Data collection dated first January 2012 to 30 April 2018.

Gauteng Atmospheric Emission Inventory data were also gathered from national atmospheric emission inventory system dated thirty April 2019. Emission sources included on the atmospheric emission inventory are listed activities industries in terms of NEMAQA, Section 21(heavy industries), Section 23 (Controlled Emitters such as small boilers and temporary asphalt plants), mining & quarries and non-industrial activities. 3 hundred and ninety-6 facilities were registered on the Gauteng Atmospheric Emission Inventory data dated the thirty first (31st) of March 2019.

The development of correlation is a useful measure for air pollutants and the determination of the relationship of parameters within a single station i.e. the relationship between ozone, sulfur, nitrogen and particulate matter of less than 10 $\mu g/m^3$ diameter. Correlation has been used in this study to develop a relationship between sources that emit from the same or different sources that undergo similar chemical and physical transformations in the atmosphere. The data were used to formulate probability functions to identify and characterize hidden or unknown emission sources within and at the Gauteng Province boundary using probability function modelling to help identify sources that result in excess of ambient air quality standards.

Clustering helps us to detect and classify similar relationships within the data set with the future classified. The study disclosed major and minor sources in the received environment. Knowing the availability of pollutant analyser and meteorological ambient monitoring data at the Gauteng ambient monitoring station will be important in the creation of the link between ambient station data. Table 3.1, below, shows the equipment at the ambient monitoring station at the Gauteng ambient monitoring station, but the ambient monitoring equipment may vary depending on the need and the financial budget for the maintenance and upgrade of the station. Specific contaminants are dependent on the sources around the receiving area.

Table 3.1: Gauteng ambient monitoring stations and measured parameters

Municipality	Site	PM_{10}	$PM_{2.5}$	CO	NO	NO_2	NO_x	O_3	SO_2	TOL	C_6H_6	Rain	TEMP	SOL	HUM	PRESS	WIND	WINDS
CoE	Bedfordview	√	√	√	√	√	√	√	√	√	√	x	x	x	√	x	√	√
	Etwatwa	√	x	√	√	√	√	x	√	√	√	√	x	x	√	√	√	√
	Germiston	√	x	√	√	√	x	√	√	√	√	x	x	x	x	x	√	√
	Tembisa	√	x	√	√	√	√	√	√	√	√	√	x	x	√	x	√	√
	Thokoza	√	x	√	√	√	√	√	√	x	x	x	√	x	√	x	√	√
	Watville	X	x	√	√	√	√	x	√	√	√	x	x	x	x	x	√	√
	Springs	X	x	x	x	x	x	x	x	x	x	x	√	x	x	x	√	√
	Tsakane	√	x	√	√	√	√	√	√	√	√	√	x	√	√	x	√	√
	Olifantsfontein	√	x	√	√	x	√	x	√	√	√	x	x	√	√	√	√	√
	Leondale	X	x	x	√	√	x	√	√	√	√	x	√	√	√	√	√	√
CoJ	Alexandra	√	√	x	x	√	x	x	√	x	x	√	x	√	√	√	√	√
	Buccleuch	√	√	√	√	√	√	√	√	x	x	√	x	√	√	√	√	√
	Delta Park	X	x	x	x	x	x	√	x	x	x	√	x	√	√	√	√	√
	Jabavu	√	x	x	x	x	x	√	√	x	x	√	√	√	√	√	√	√
	Newtown	√	x	√	√	√	√	√	x	x	x	√	√	√	x	x	√	√
	Orange Farm	√	x	x	x	x	x	√	√	x	x	√	√	√	√	√	√	√
	Diepsloot	√	x	x	x	x	x	x	√	x	x	√	x	x	√	√	√	√
	Ivory Park	√	x	x	x	x	x	x	√	x	x	√	√	x	√	√	√	√
	Davidsonville	√	x	x	x	x	x	x	x	x	x	x	√	√	√	x	√	√
CoT	Pretoria West	√	x	√	√	√	√	√	√	√	√	√	√	√	x	√	√	√
	Rosslyn	√	x	√	√	√	√	√	√	x	x	√	√	√	√	√	√	√
	Mamelodi	√	√	√	√	√	√	√	√	x	x	√	√	√	√	√	√	√
	Booysens	√	x	√	√	√	√	√	√	√	√	√	x	x	√	x	√	√
	Olievenhoutbosch	√	x	√	√	√	√	√	√	x	x	√	√	√	√	x	√	√
	Bodibeng	√	x	√	√	√	√	x	√	x	x	√	√	√	√	√	√	√
	Ekandustria	√	x	√	√	√	√	√	√	x	x	√	x	√	√	√	√	√
SDM	Vanderbijlpark	√	x	X	x	x	x	√	√	x	x	√	√	x	√	√	√	√
	Meyerton	X	x	√	√	√	√	x	√	√	√	√	x	x	√	√	√	√
WRDM	Mogale, Krugersdorp	√	√	√	√	√	√	√	√	√	√	√	x	√	√	√	√	√
	Leratong, Randfontein	√	x	√	√	√	√	√	√	x	x	x	x	√	√	√	√	√

3.3 Methodologies

The following methodology was used in the analysis of correlation of pollutants at different receptors which are affecting Gauteng ambient monitoring station. The study uses pollution rose polar coordinates plots to provide a useful graphical technique which provides directional information on sources. Ambient concentration, wind direction together with wind speed can be highly effective at discriminating different emission sources affecting the ambient station. The study investigated using k-means clustering to discriminates of similarity or dissimilarity between the features which can be identified and grouped.

3.3.1 Method 1: Investigation of correlation coefficient, r.

The (Pearson) correlation coefficient is a measure of the strength of the linear relationship between 2 variables. If there was perfect linear relationship with positive slope between the 2 variables, r = 1. If there is a perfect linear relationship with negative slope between the 2 variables r = −1. A correlation coefficient of 0 (0) means that there was no linear relationship between the variables refer to equation 3.1 below.

$$r_{xy} = \frac{\sum(x_i - \bar{x})\,(y_i - \bar{y})}{\sqrt{\sum(x_i - \bar{x})^2 \sum(y_i - \bar{y})^2}} \qquad [3.1]$$

3.3.2 Method 2: Investigation of pollution roses

Pollution rose is defined as variation of wind rose that is useful for considering pollutant concentrations by wind direction and percentage time the concentration in a particular range. The variation of wind speed and wind direction on different time was assessed using the wind rose function. The wind rose function gives concentration levels, percentage time the concentration in particular range, wind direction mean and % of calm. At the selected ambient monitoring station $PM_{10}(\mu g/m^3)$, sulfur dioxide (ppb), nitrogen dioxide (ppb) and ozone (ppb).

Pollution roses are polar diagrams that display air pollution depending on wind direction. If an ambient air quality monitoring station was markedly influenced by a source of the pollutant measured, the pollution rose shows a peak towards the local source. The construction of a pollution rose was easy when the wind direction and the concentrations of pollutants are averaged over one hour and therefore the data used in this analysis are at hourly averages. The pollution roses were determined according to the equation 3.2 below:

$$C_{dd} = \frac{\sum_{j=1,n} p_j f_{dd,j} \alpha_j}{\sum_{j=1,n} f_{dd,j}\, \alpha_j} \qquad [3.2]$$

where C_{dd} was the average concentration for wind sector dd, n was the number of days in the period for which the rose was constructed, p_j was the measured concentration on day j, $f_{dd,\,j}$ was the frequency that the wind came from sector dd and α_j was some weight function based on the persistency of the wind vector during day j refer to equation 3.3.

$$\sum_{dd=1,ndd} c_{dd} f_{dd,j} = p_j \sum_{dd=1,ndd} f_{dd,j} \qquad [3.3]$$

Where $\sum_{dd=1,ndd} f_{dd,j}$ was the sum of frequencies of the wind direction over the ndd different bins during day j, i usually returns values for the concentrations c_{dd}that, for successive wind direction bins, oscillate between large positive values and large negative values.

3.3.3 Method 3: Investigation of pollution sources using the bivariate polar plot at receptor.

Concentration of a species varies to specific degree at the certain area, influenced by wind speed and wind direction in a polar coordinate. Wind direction together with wind speed can be highly effective at discriminating different emission sources. By using polar coordinates, the plots provide a useful graphical technique which can provide directional information on sources. Bivariate polar plots are constructed in the following way. First, wind speed, wind direction and concentration data are partitioned into wind speed-direction ‘bins’ and the mean concentration calculated for each bin.

Binning the data in this way is not strictly necessary but acts as an effective data reduction technique without effecting fidelity of the plot itself. Furthermore, because of the inherent wind direction variability in the atmosphere, data from several weeks, months or years typically used to construct a bivariate polar plot tends to be diffuse and does not vary abruptly with either wind direction or speed. The wind components, u and v are calculated:

$$u = \bar{u}.sin\left(\frac{2\pi}{\theta}\right), v = \bar{u}.sin\left(\frac{2\pi}{\theta}\right) \quad [3.4]$$

With u was the mean hourly wind speed and ū was the mean wind direction in degrees with 90 degrees as being from the East. The calculations above provide a u, v, concentration (C) surface. While it would be possible to work with this surface data directly a better approach was to model the surface to describe the concentration as a function of the wind components u and v to extract real source features rather than noise. A flexible framework for fitting a surface is to use a Generalized Additive Model (GAM) e.g. (Wood, 2006). The GAM can be expressed as shown in Equation 7:

$$\sqrt{C_i} = \beta_o + s(u_i, v_i) + \epsilon_i \quad [3.5]$$

Where Ci is the ith pollutant concentration, β_o was the overall mean of the response, $s(u_i, v_i)$ was the isotropic smooth function of ith value of covariate u and v, and ϵ_i was the ith residual. A penalized regression spline was used to model the surface as described by Wood (2003). Note that Ci was square root transformed as the transformation generally produces better model diagnostics e.g. normally distributed residuals. Moreover, the smooth function used is isotropic because u and v are on the same scales. The isotropic smooth avoids the potential difficulty of smoothing 2 variables on different scales e.g. wind speed and direction, which introduces further complexities.

Finally, conditional bivariate probability functions polar plots showing how species concentration vary jointly with wind speed and wind direction in polar coordinates will be formulated for all activities listed or not impacting ambient air quality in order to identify pollutants that cause exceedance as per equation 3.6 below.

$$CBPF_{\Delta\theta,\Delta_u} = \frac{m_{\Delta\theta,\Delta_u} I_{C \geq x}}{n_{\Delta\theta}} \quad [3.6]$$

Where $m_{\Delta\theta,\Delta_u}$ was the number of samples in the wind sector $\Delta\theta$ with wind speed interval Δ_u having concentration C greater than a threshold value x, $n_{\Delta\theta}$ was the total number of samples in that wind direction-speed interval

3.3.4 Method 4: Identification of similar characteristics sources using k-means clustering method.

K-means clustering is one method in which bivariate polar plot features can be identified and grouped. The main purpose of grouping data in this way is to identify records in the original time series data by cluster to enable post-processing to better understand potential source characteristics. Figure 3.1 display k-means flowchart of k-means clustering below.

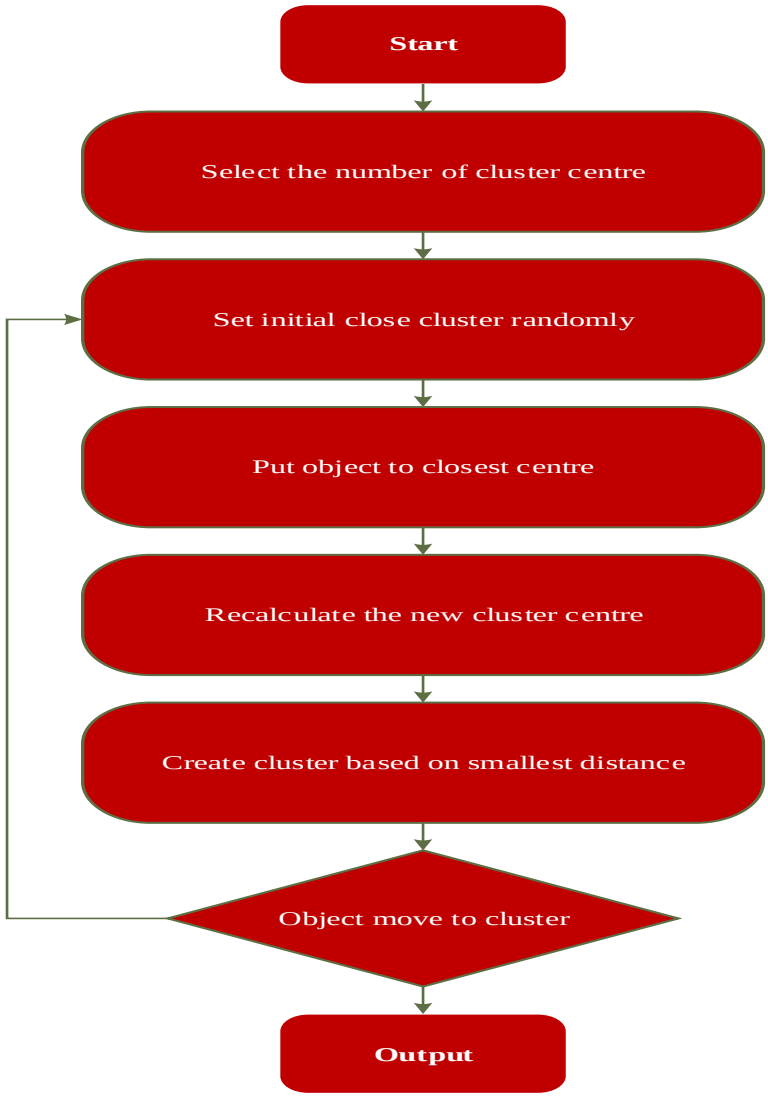

Figure 3.1: Flowchart of K-means clustering

Central to the idea of clustering data is the concept of distance i.e. some measure of similarity or dissimilarity between points. Clusters should be comprised of points separated by small distances relative to the distance between the clusters. The similarity of concentrations shown in Figure 3.1 was determined by 3 variables: the u and v wind components and the concentration, C. All 3 variables are equally important in characterizing the concentration location information, but they exist on different scales i.e. a wind speed-direction measure and a concentration. Let X = fxig; i = 1; n be a set of n points to be clustered into K clusters, C =fck; k = 1;Kg. The basic k-means algorithm for K clusters was obtained by minimising:

$$\sum_{k=1}^{k} \sum_{x1 \in_{ck}} \| X_i - \mu_k \|^2 \quad [3.7]$$

Where $\| X_i - \mu_k \|^2$ was a chosen distance measure, μ_k was the mean of cluster ck. The distance measure is defined as the Euclidean distance:

$$d_{x,y} = \left(\sum_{j=1}^{n} (x_j - x_j)^2 \right)^{1/2} \quad [3.8]$$

Where n represents number of features as defined by Euclidean distance ($d_{x,y}$). Where **x** and **y** are 2 J-dimensional vectors, which have been standardised by subtracting the mean and dividing by the standard deviation. In the current case j was of length 3 i.e. the wind components u and v and the concentration C, each of which is standardised.

$$x_j = \left(\frac{x_j - \bar{x}}{\sigma_x} \right) \quad [3.9]$$

These sources could include major point sources that are far from receptor and minor sources that are difficult to detect. In order to propose relevant reductions strategy for poor air quality in the Gauteng Province, source identification need to be prioritized and clearly defined.

3.4 Using R to analyse air pollution monitoring data

3.4.1 Data preparation

More effort should be in making sure that data are correct before start analyzing them. When using R, it is advisable to have variable names with no spaces. It is also more convenient to keep variable names in lower case because is more difficult to type in capital letters. It is also convenient to keep your variables names simple because one requires to refer to them lots. Also, we find it is a good idea to keep everything in lower case letters, again because they are quicker to type.

3.4.2 Data into R

Ambient monitoring station data should be converted to comma-separated value (csv) format. Once the file is on csv turns to be easy to read and used by R software. The file contains a

column representing dates/times in the format dd/mm/yyyy HH:MM, which is very common in data sets of monitoring data. To read the file in, type or better still copy and paste this directly into R. This reads the file into something called a (data. Frame), which is the most common way in which R stores data (others include vectors, matrices and arrays).

```
mydata <- read.csv(file.choose(), header = TRUE)
mydata$date <- as.POSIXct(strptime(mydata$date, format = "%d/%m/%Y %H:%M", tz = "GMT"))
```

Another way of getting data into R if you are interested in having a quick look at data is to read data directly from the clipboard. If you are using Excel you can copy some data (which may or may not include column headers; better if it does) and read it into R easily by: mydata <- read.delim("clipboard", header = TRUE).When R read the csv file is automatically assign missing data the value NA. In this case it is necessary to deal with dates and times and two functions are used to convert the date to something recognized as such by R. The function (**strptime**) tells R what format the data are in case day/month/year hour: minute. The openair package will automatically do these conversions if the data are in a format dd/mm/yyyy HH:MM.

4. CHAPTER 4: RESULTS AND DISCUSSIONS

4.1 Introduction

This study investigated the correlation for ozone, sulfur dioxide, nitrogen dioxide and PM_{10} pollutants amongst Gauteng ambient monitoring stations. Study investigated correlations of the above parameters in order to determine sources of similar pollutant. The study looked at pollution roses of the selected pollutants PM_{10}, SO_2, NO_2 and O_3. Results for the bivariate polar plot displayed how ambient concentrations varies with the wind speed and wind direction in polar coordinates. Wind speed and wind direction can be highly effective at identifying different sources. Features were grouped and identified using k-means clustering to identify records in the original time series data by cluster in order to allow post-processing.

4.2 Correlations

For use in polar plots, the correlation statistic implemented were the weighted Pearson correlation coefficient (r) (Canty and Ripley, 2016).

4.2.1 Correlation for Ozone at Gauteng ambient monitoring stations

In order to determine common variables and behaviour in a specific area, it is important to investigate the relationship between 2 areas of similar pollutant. It is therefore imperative to determine the relationship to the ambient concentration, wind speed and direction of the particular receptor. Most analysts preferred rating scales because the results reflect the relationship in the real world (Babchishin et al.,2016). Ozone activity in the Gauteng ambient monitoring station results showed that much of the relationship rating is very low in both positive and negative relationships. The highest positive ozone correlation was found of 59% medium positive relationship at Mogale City and Buccleuch, and that is unusual since the 2 stations were designed to track background information and traffic respectively.

Meyerton and Thokoza ambient ozone concentrations showed similar moderate positive correlation pathways as these stations were designed to monitor industrial and domestic fuel activities with different characteristics. The Orange Farm and Pretoria West stations had moderate positive relationships, and focused on domestic fuel combustion and industrial activities. Jabavu and Pretoria West also showed a moderate positive relationship, and were designed for monitoring domestic and industrial activities. Jabavu and Orange Farm were both built to control domestic fuel activities, so that a positive relationship is assumed to be good to very strong due to similar characteristics.

The Newtown and Buccleuch ambient monitoring stations had no relationship with the ozone behaviour as both ambient monitoring stations are situated in the City of Johannesburg and are designed to monitor emissions from traffic activities. Springs and Buccleuch showed that there is no relationship between the 2 ambient monitoring stations and that the sources which could be monitored are not the same as those focused on domestic and traffic activities. Mamelodi and Meyerton ambient station displayed no relationship and this could be attributed to the facts that the sources monitored are different (domestic versus industrial activities). Vanderbijlpark had a positive correlation with Thokoza, Meyerton while Buccleuch had a moderate correlation strength. (Figure 4.1).

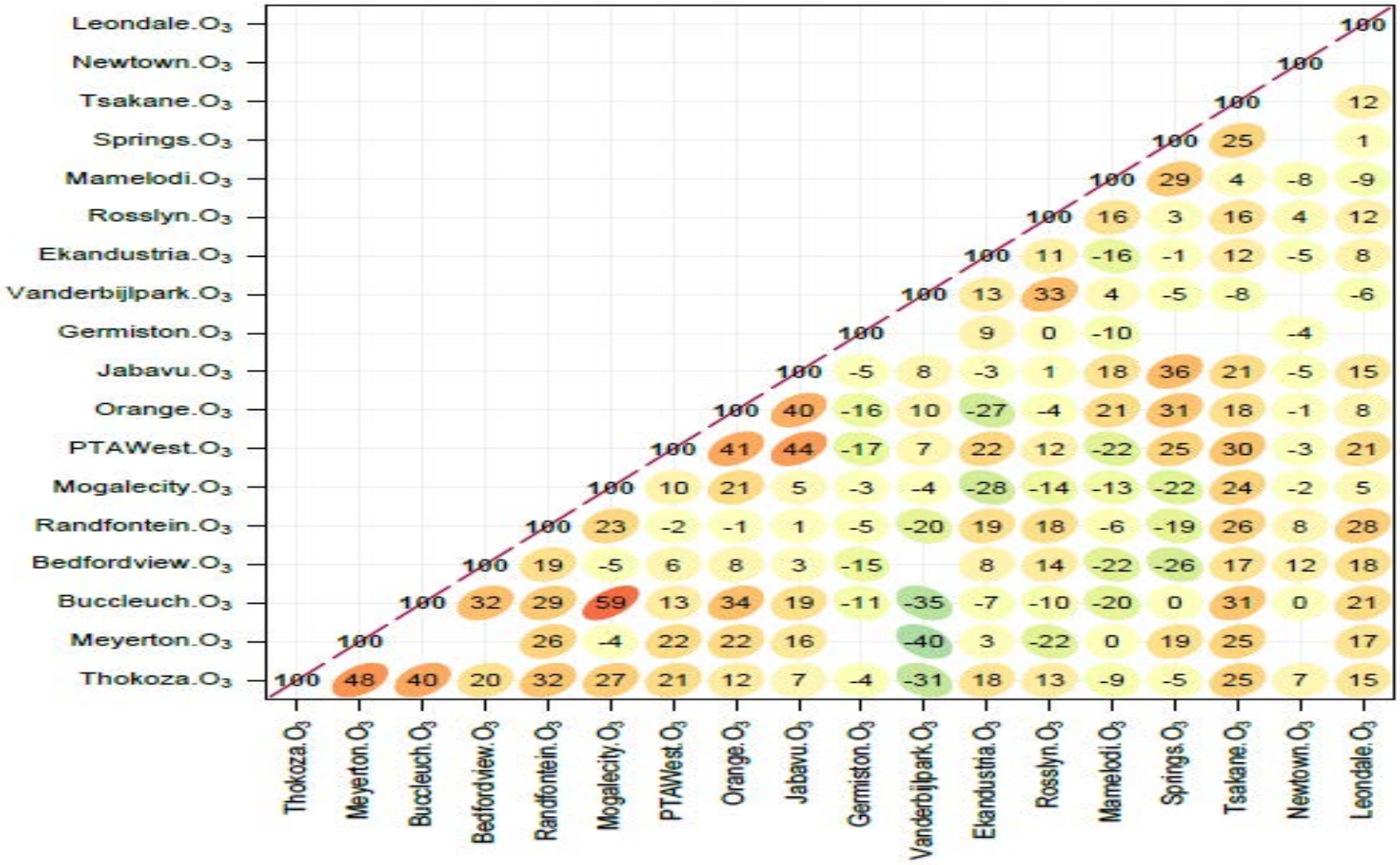

Figure 4.1:Correlations of Ozone to Gauteng Ambient Monitoring Stations

4.2.2 Correlation for sulfur dioxide at Gauteng ambient monitoring stations

Using Evans (1996) guide, it was found that there were several positive correlations in the City of Johannesburg at domestic fuel burning on moderate. Jabavu and Diepsloot showed strong moderate correlations from domestic coal burning activities. Jabavu and Diepsloot displayed strong moderate correlations from domestic fuel burning activities. As shown in Figure 4.2, Thokoza and Mogale City shoved varying sulfur dioxide concentrations with no likelihood of either increasing or decreasing indicating that there is no connection between 2 variables. Germiston and Meyerton sulfur dioxide hade the highest negative correlation at a weak range.

4.2.3 Correlation for nitrogen oxides at Gauteng ambient monitoring stations

Nitrogen oxides pollutant was also assessed. The highest ranging correlation for nitrogen oxides was moderate between the Newtown and Olifansfontein ambient monitoring stations. Randfontein and Buccleuch ambient monitoring stations which main purpose is background information and traffic activities were expected not to have nitrogen oxides correlation (Figure 4.3).

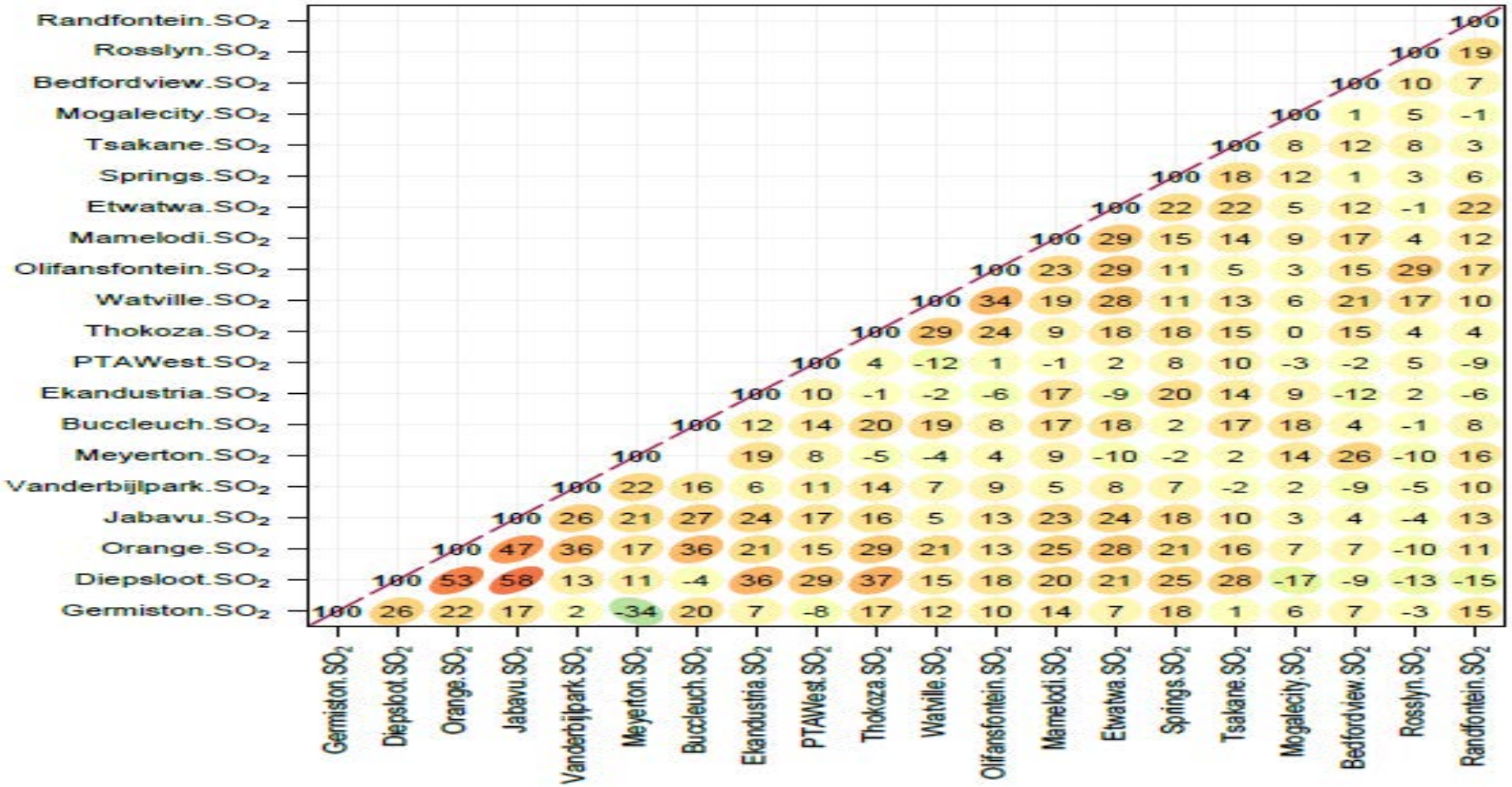

Figure 4.2:Correlations of sulfur dioxide to Gauteng ambient Monitoring Stations

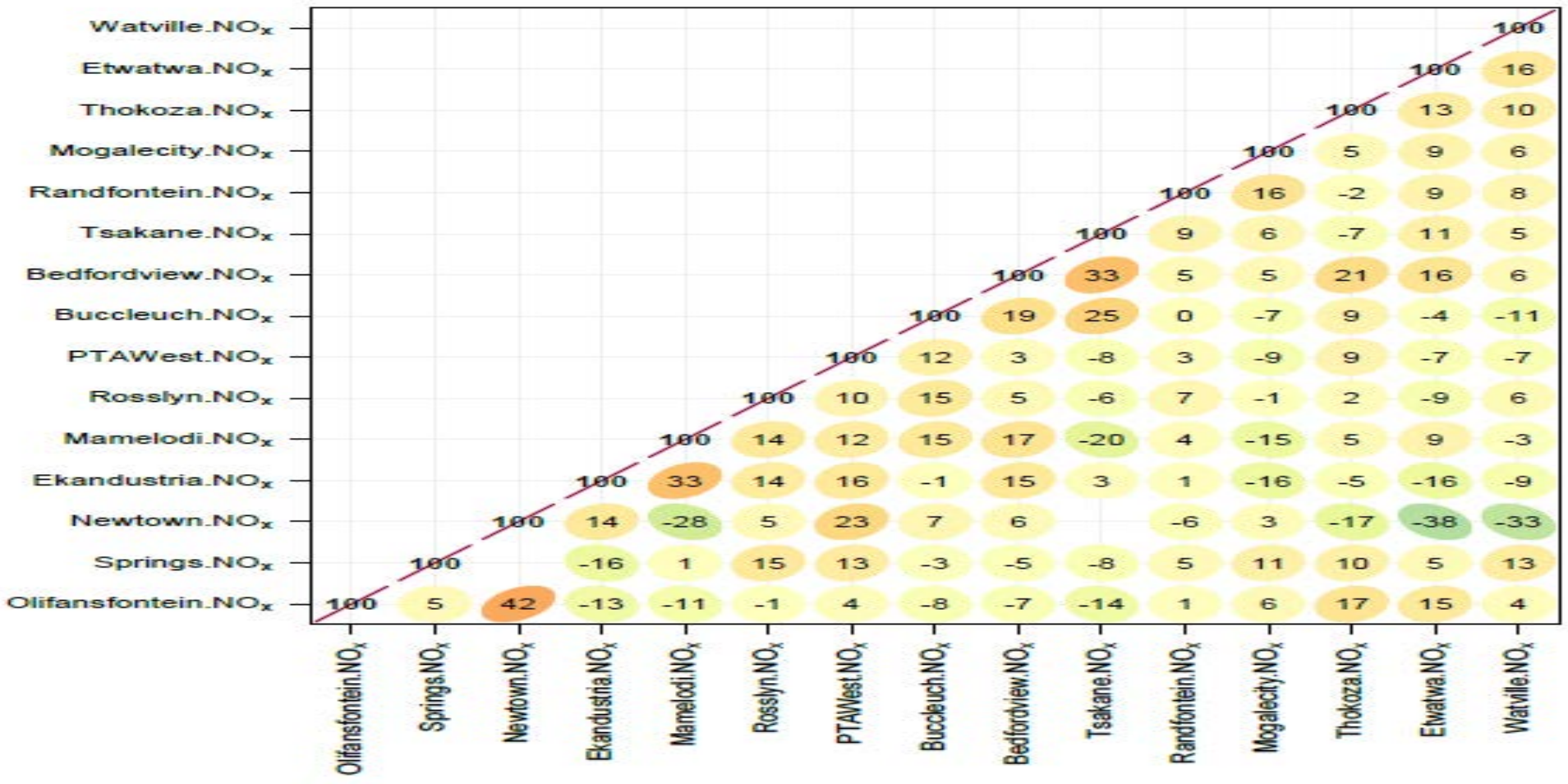

Figure 4.3:Correlations of Nitrogen Oxides to Gauteng ambient Monitoring Stations

4.3.4 Correlation for PM_{10} at Gauteng ambient monitoring stations

PM_{10} had 6 highest positive moderate rating correlation strengths. The ambient PM_{10} concentrations for Thokoza and Spring had the highest correlations with moderate strength as shown in Figure 4.4 as both stations monitor domestic fuel burning. The Diepkloof ambient monitoring stations can be either Thokoza, Jabavu or Etwatwa with a positive correlation of moderate rating, and this is justifiable since all ambient stations track similar activities (domestic fuel burning activities). Bedfordview and Thokoza had a higher tolerance of positive correlation based in the City of Ekurhuleni. Finally, Newtown and Buccleuch, both of which aim to monitor emissions from traffic activities, showed positive correlation.

Pretoria West ambient PM_{10} results had no correlation with Etwatwa PM_{10} ambient concentration. Randfontein PM_{10} atmospheric concentrations did not have a correlation with Mamelodi ambient monitoring station which purpose is to provide background information and domestic fuel burning activity. The PM_{10} results of the Davidsonville ambient station and Etwatwa had no correlation probably because both ambient monitoring stations are designed to monitor domestic fuel burning activity. Newtown and Jabavu, stations owned by the City of Johannesburg were primarily intended to monitor traffic and domestic fuel combustion respectively and did not show a correlation between the two concentrations of PM_{10} as shown in Figure 4.4. The lowest correlation was noticed between Davidsonville and Diepsloot, which had the lowest negative correlation at a low rating, as shown in Figure 4.4 below.

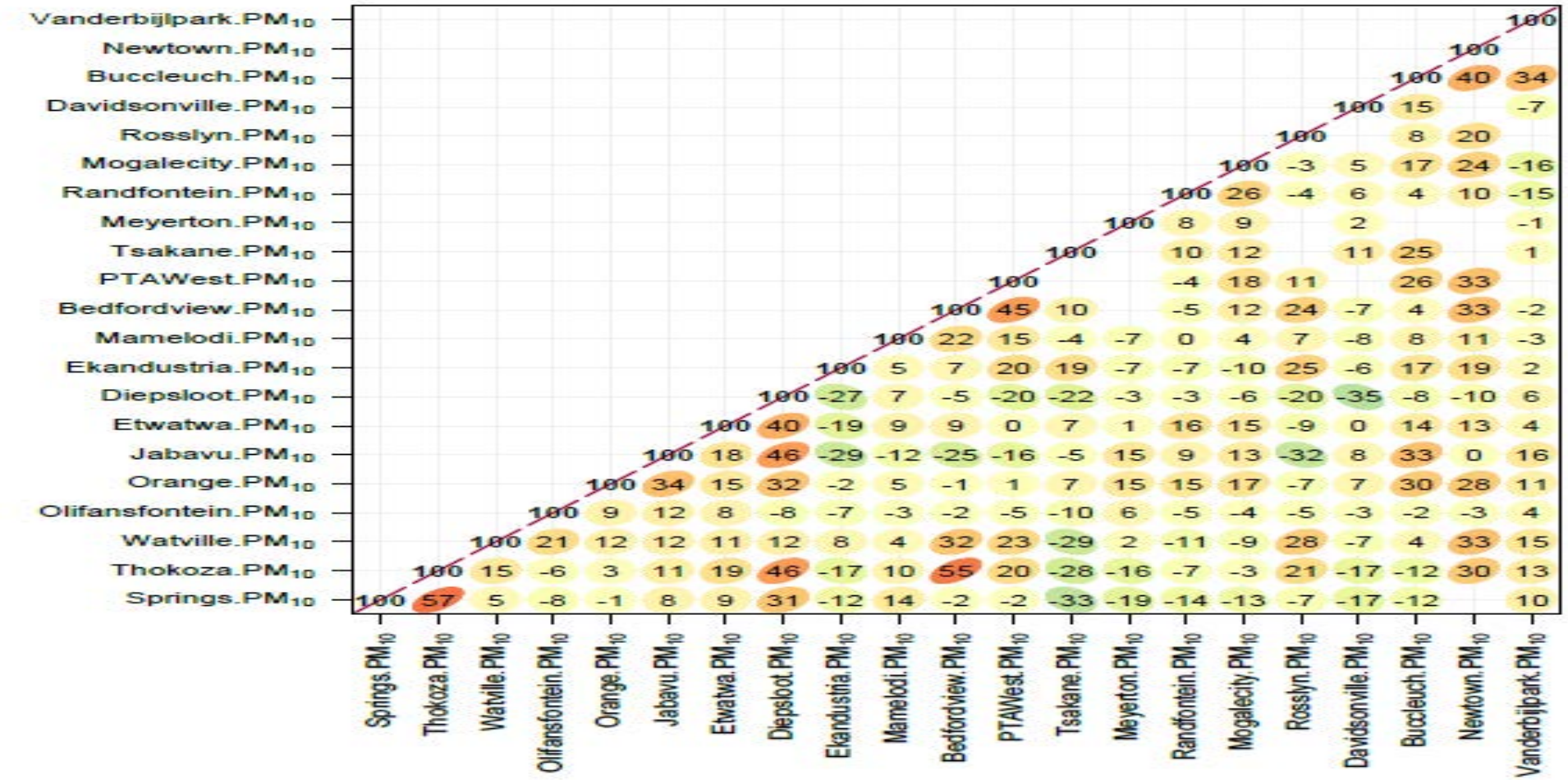

Figure 4.4: Correlations of PM_{10} to Gauteng ambient Monitoring Stations

4.3.5 Gauteng ambient monitoring station with ambient correlation parameters

Figure 4.5 to Figure 4.27 present correlation results for specific ambient monitoring stations. Evans guide were used for the correlation assessment (Evans, 1996). Requirements of environmental monitoring include benzene, toluene, carbon monoxide, nitric oxide, nitrogen dioxide, nitrogen oxides, ozone, sulfur dioxide, PM_{10} and $PM_{2.5}$, ambient temperature, air pressure, wind speed, wind direction, relative humidity and solar radiation.

It was important to investigate the correlation between the Germiston ambient station parameters provided by the Gauteng ambient monitoring station and the Evans rating (Evans, 1996). The idea was to investigate how the different results interrelate at the Germiston Environmental Monitoring Station. It was found that wind speed and wind direction parameters have a strong positive correlation as shown in Figure 4.5. There is a moderate positive correlation for nitrogen oxide parameters of either sulfur dioxide or PM_{10} concentrations. Thermometer reading shows a moderate positive correlation. There is a moderate positive correlation between nitrogen monoxide and SO_2, PM_{10}, NO_2 or CO concentrations. Ozone concentrations are negatively correlated with wind direction. The concentration of toluene shows very poor negative associations with SO_2, NO_2, NO, O_3 and temperature readings.

Bedfordview ambient monitoring station parameters correlations are in Figure 4.6 and results showed that toluene concentration had a very strong positive correlation with benzene concentrations, which may indicate the same source of volatile organic compound storage or production activities in Bedfordview. The concentration of nitrogen oxides at the Bedfordview atmospheric monitoring station showed a strong moderate association with either nitrogen dioxide or carbon monoxide concentrations. The concentration of nitrogen monoxide had a strong, moderate association. Wind direction reading showed no correlation to carbon monoxide concentrations. $PM_{2.5}$ showed a very weak negative correlation with either NO or NOx. Concentrations of $PM_{2.5}$ indicated a weak negative correlation with either CO or PM_{10} concentrations.

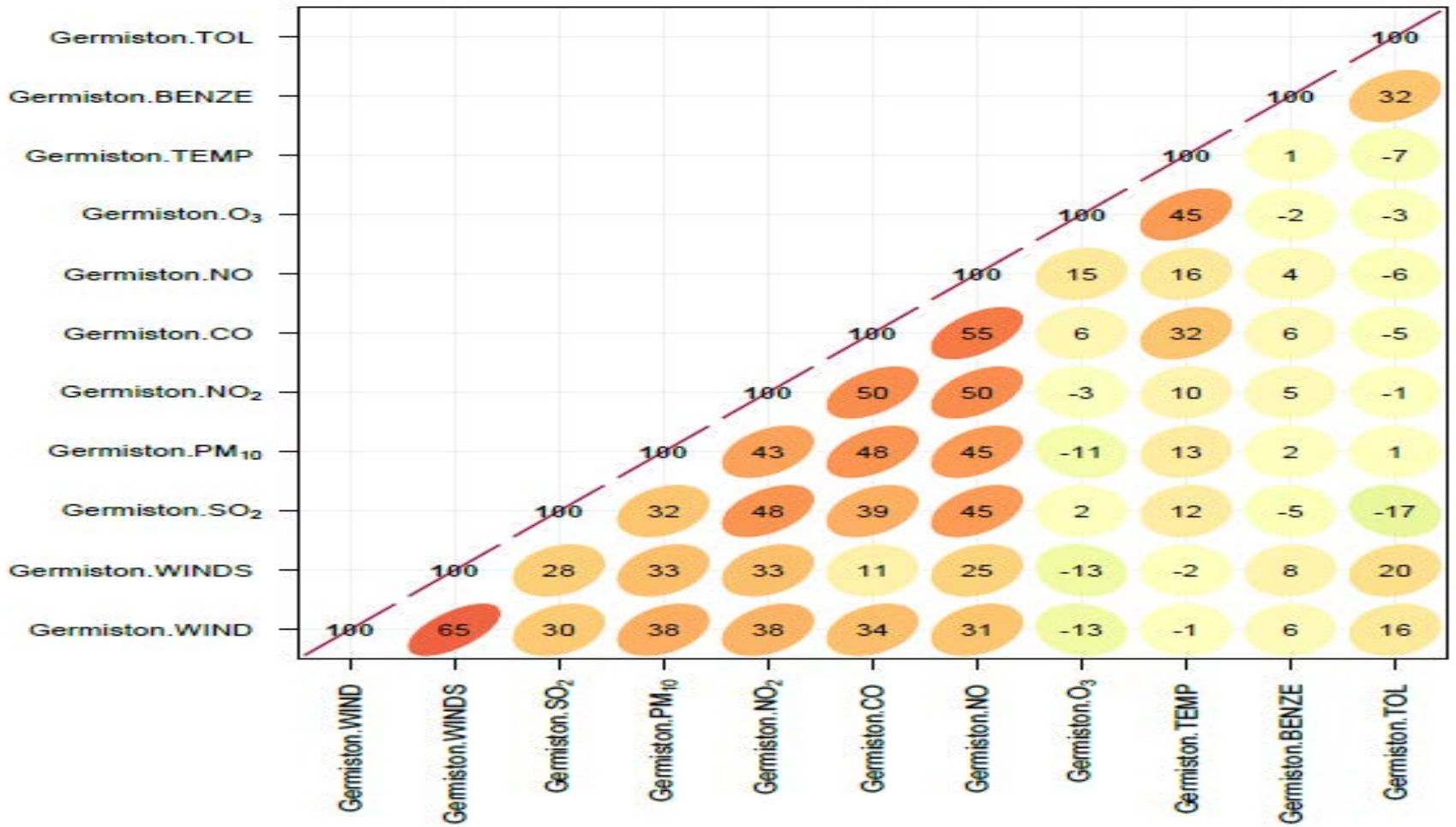

Figure 4.5: Germiston Ambient Monitoring Station parameters correlations

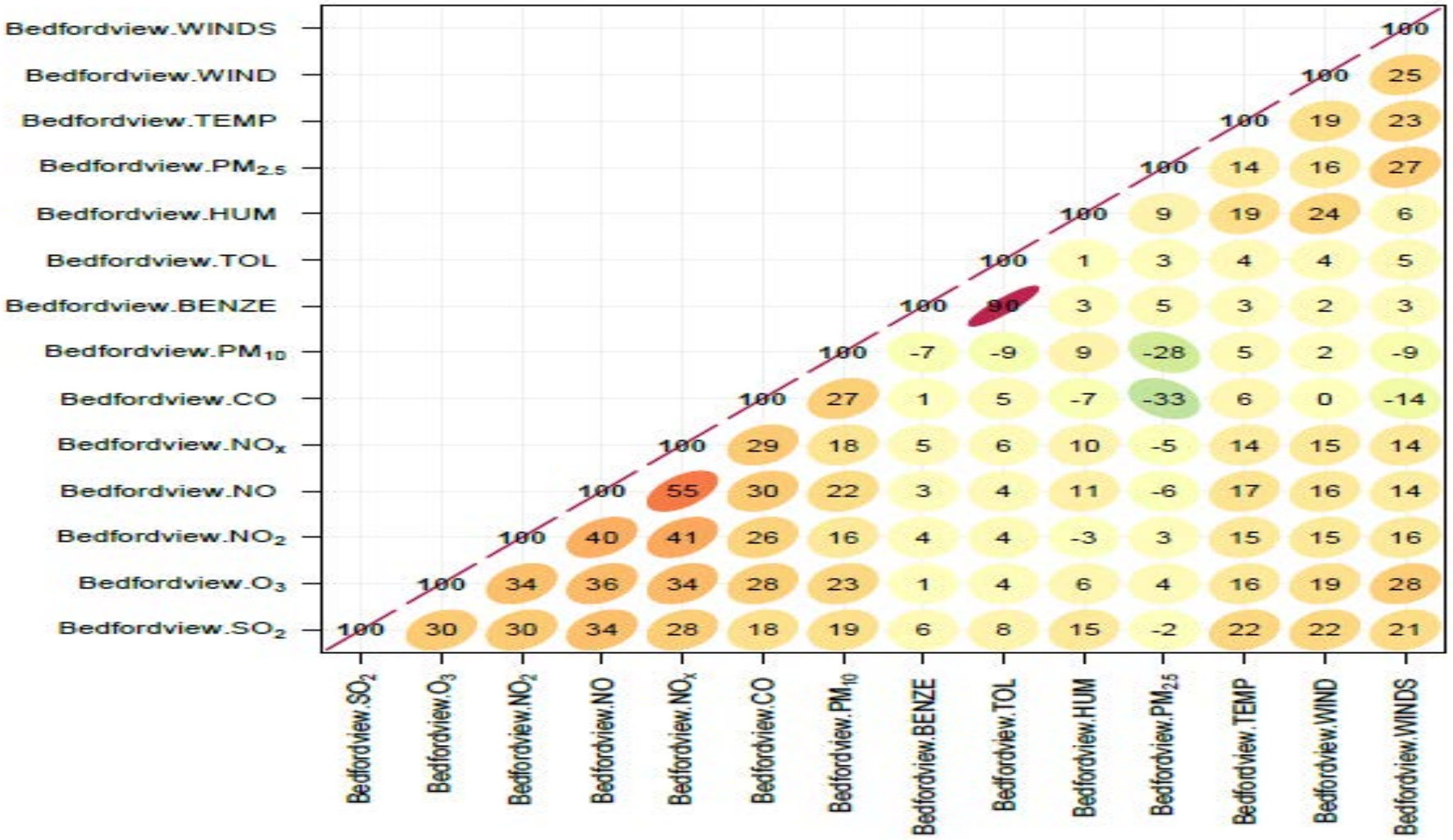

Figure 4.6: Bedfordview Ambient Monitoring Station parameters correlations

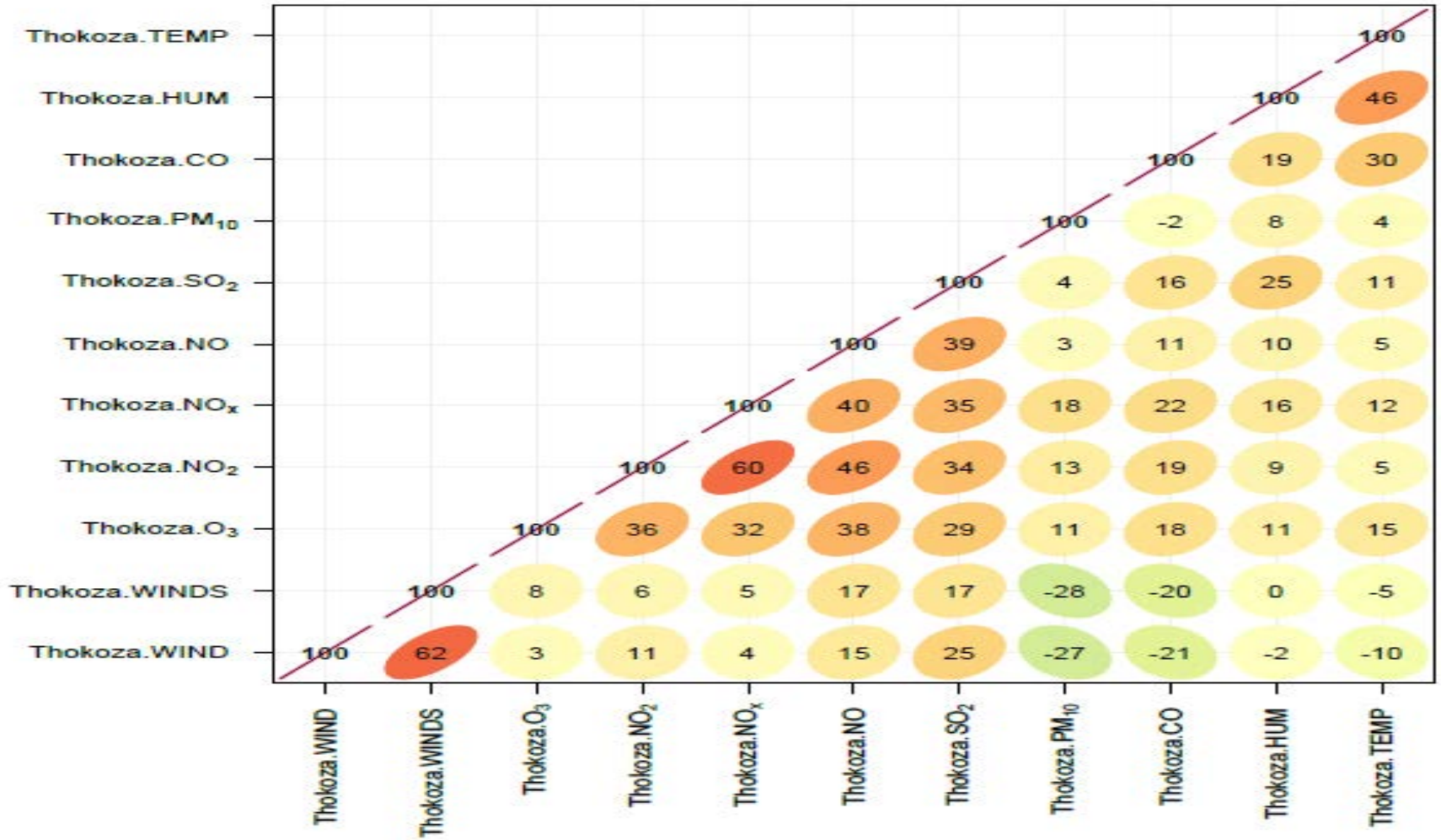

Figure 4.7: Thokoza Ambient Monitoring Station parameters correlation

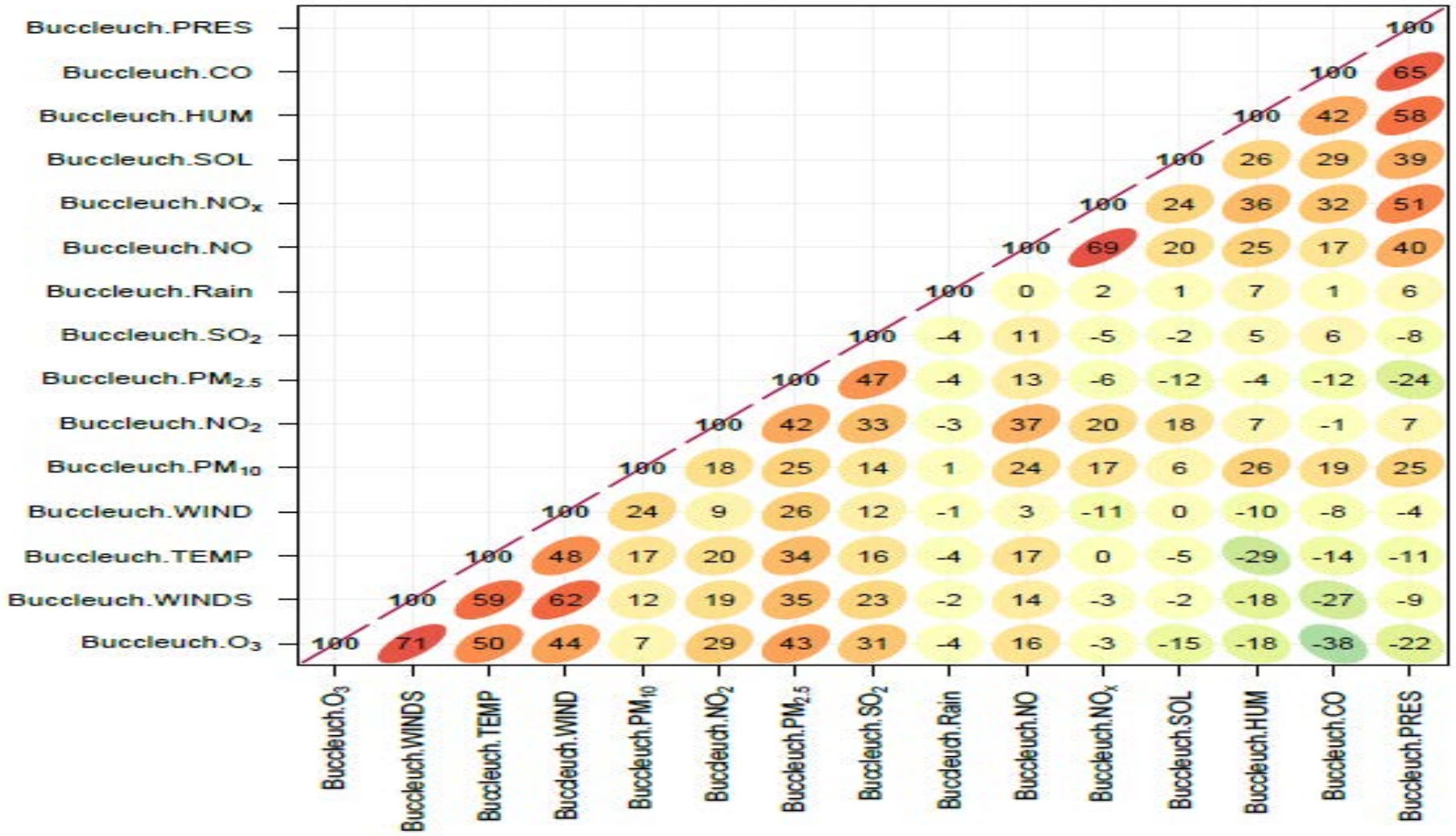

Figure 4.8: Buccleuch Ambient Monitoring Station parameters correlations

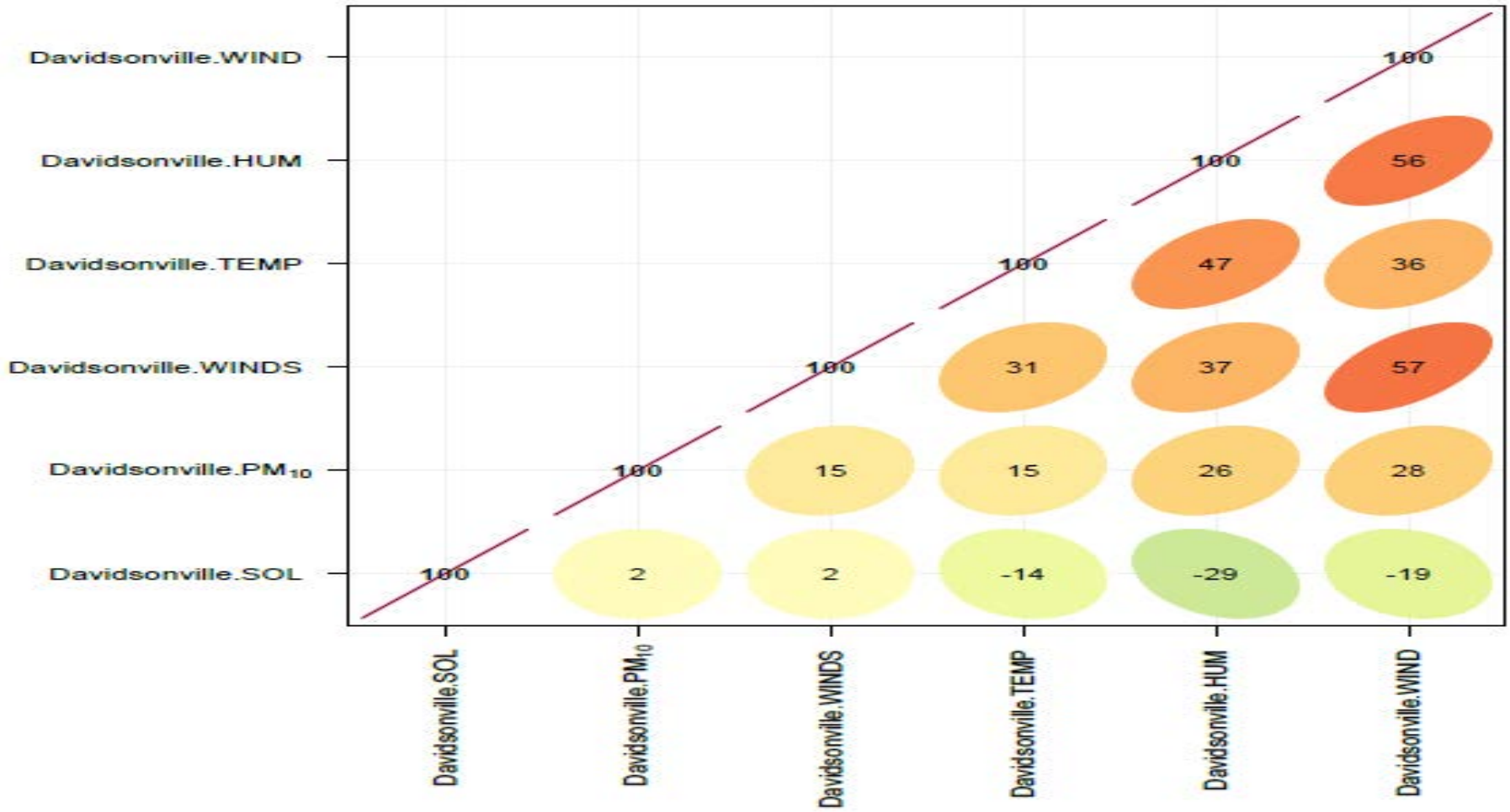

Figure 4.9: Davidsonville Ambient Monitoring Station parameters correlations

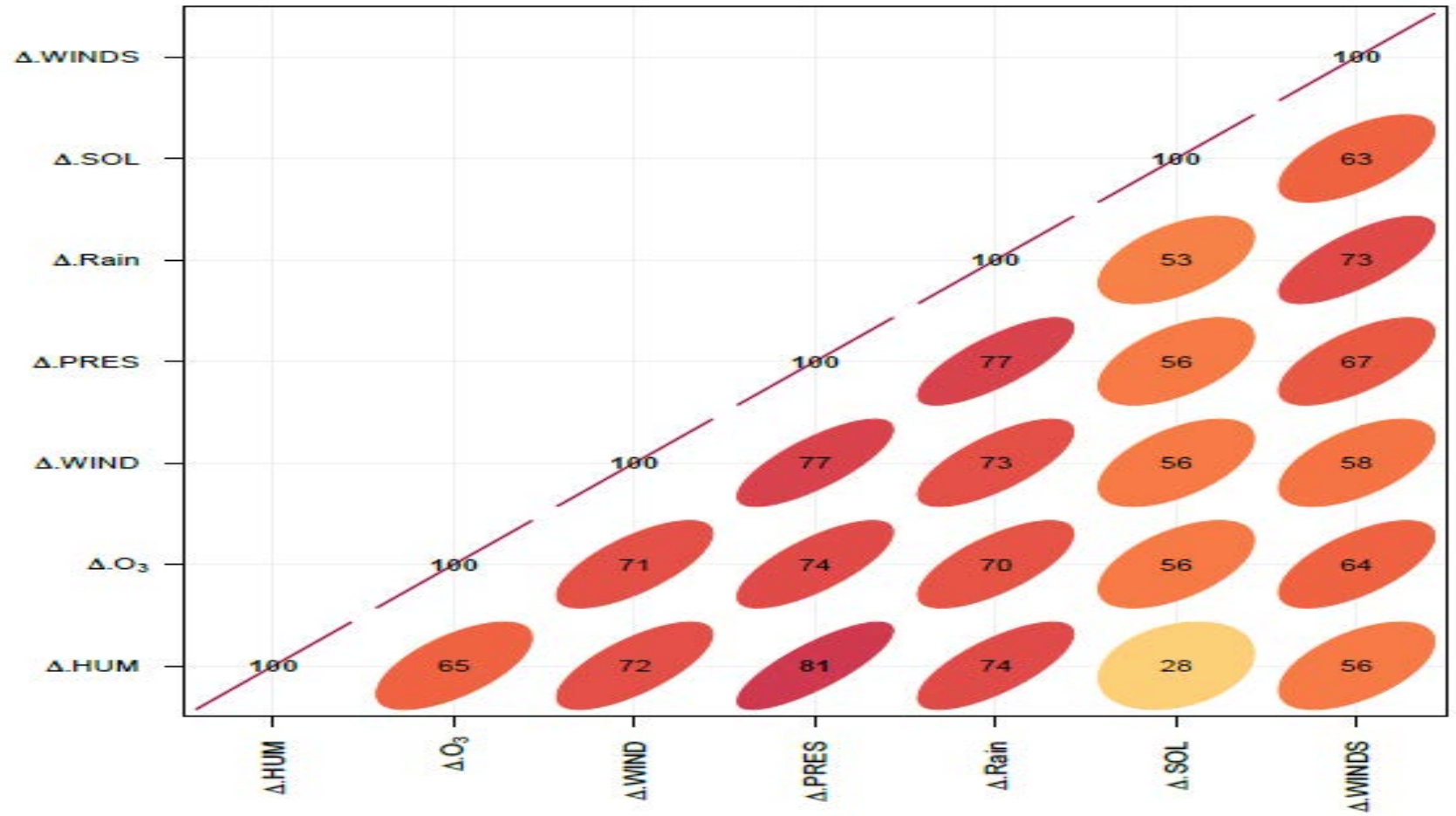

Figure 4.10: Delta Park ambient Monitoring Station parameters correlations

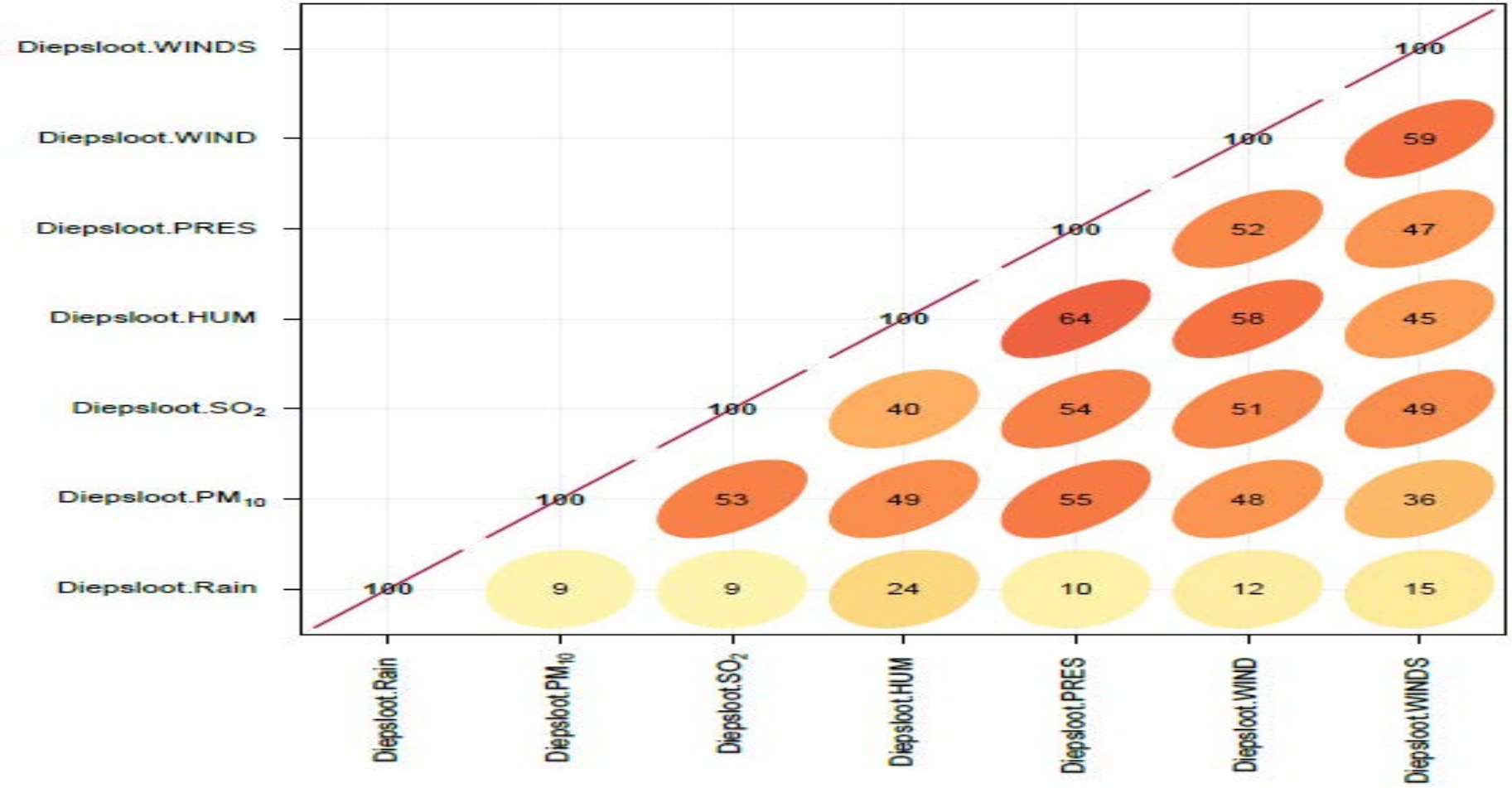

Figure 4.11: Diepsloot Ambient Monitoring Station parameters correlations

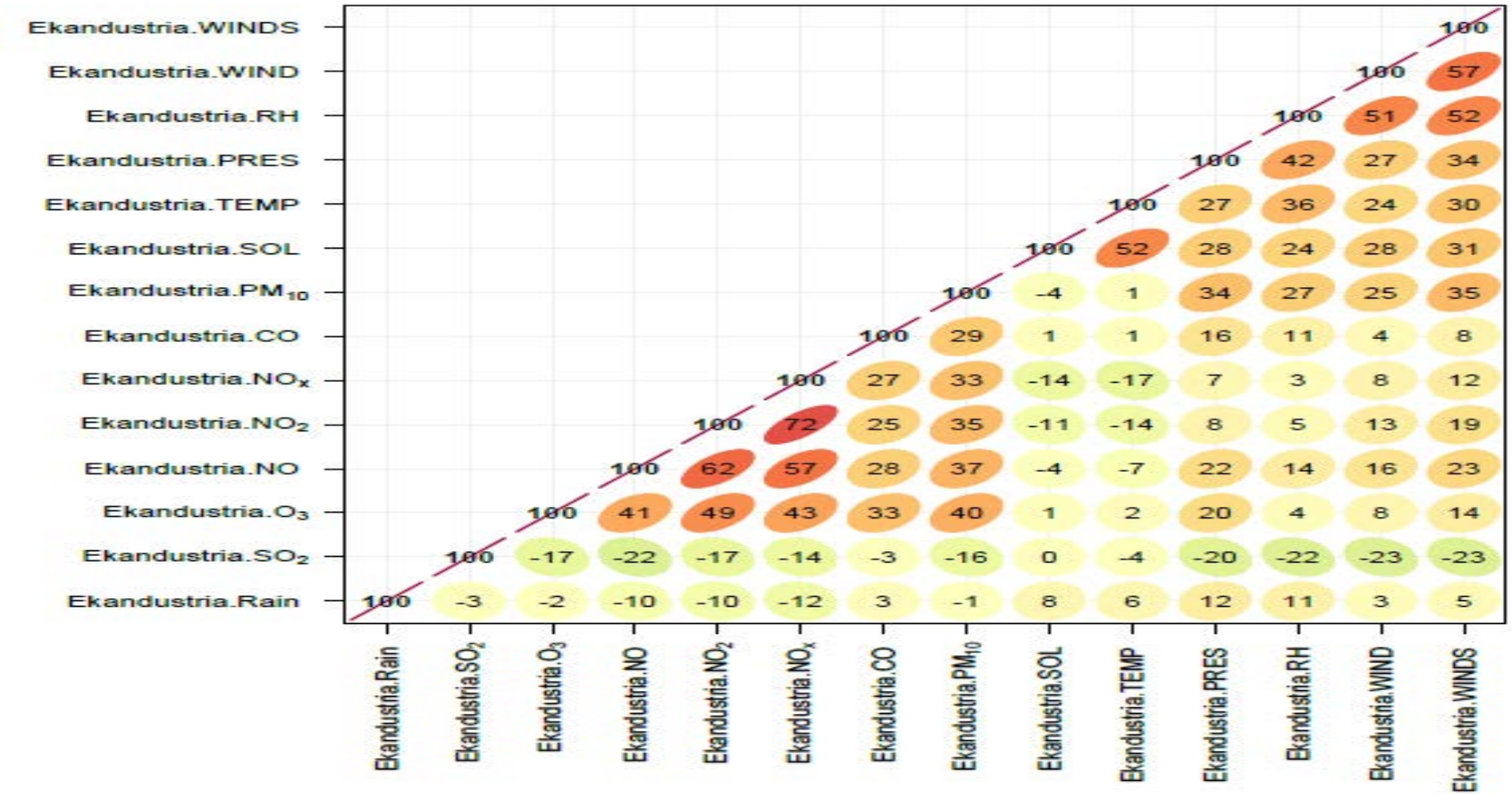

Figure 4.12: Ekandustria Ambient Monitoring Station parameters correlations

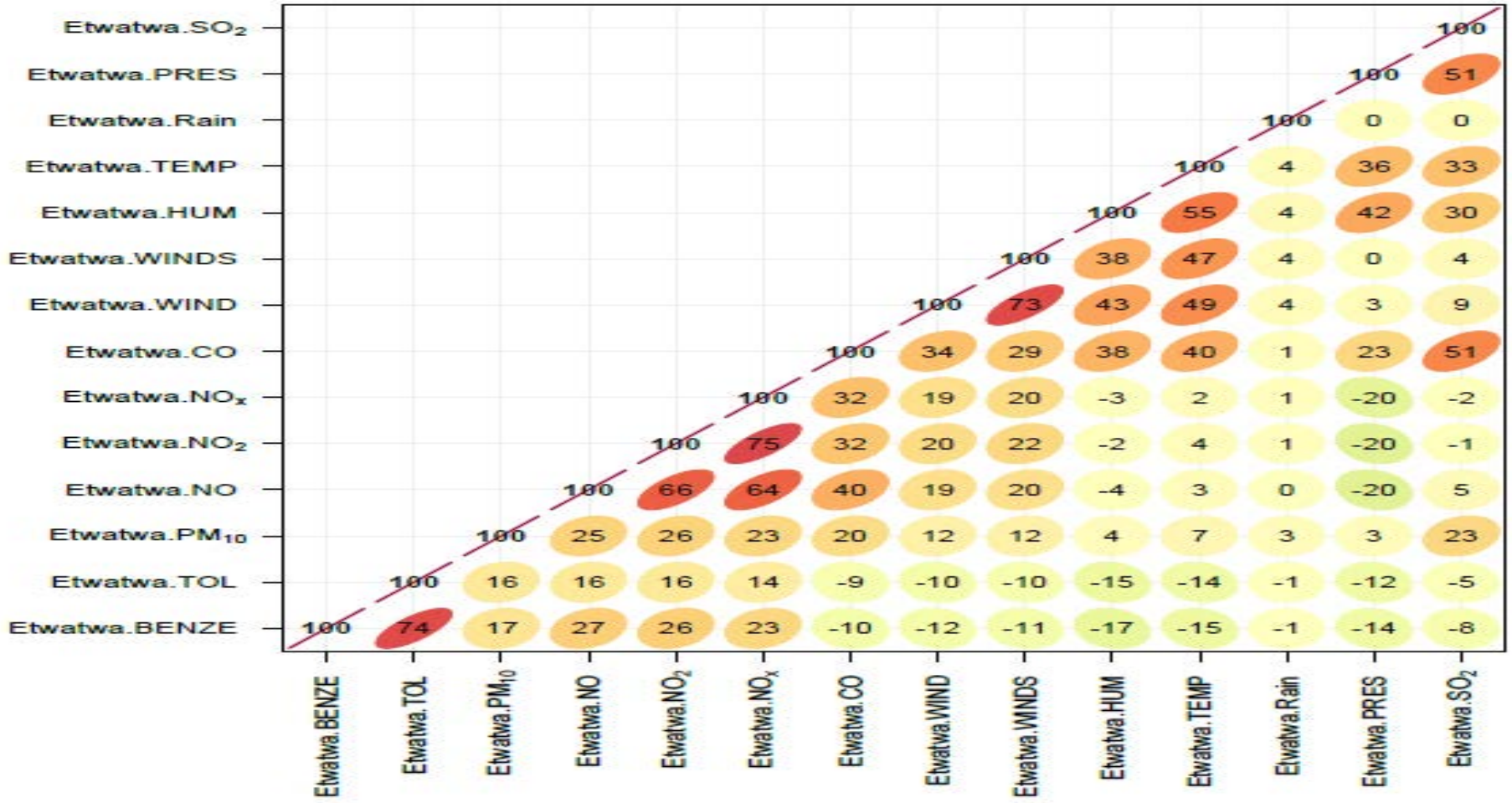

Figure 4.13: Etwatwa Ambient Monitoring Station parameters correlations

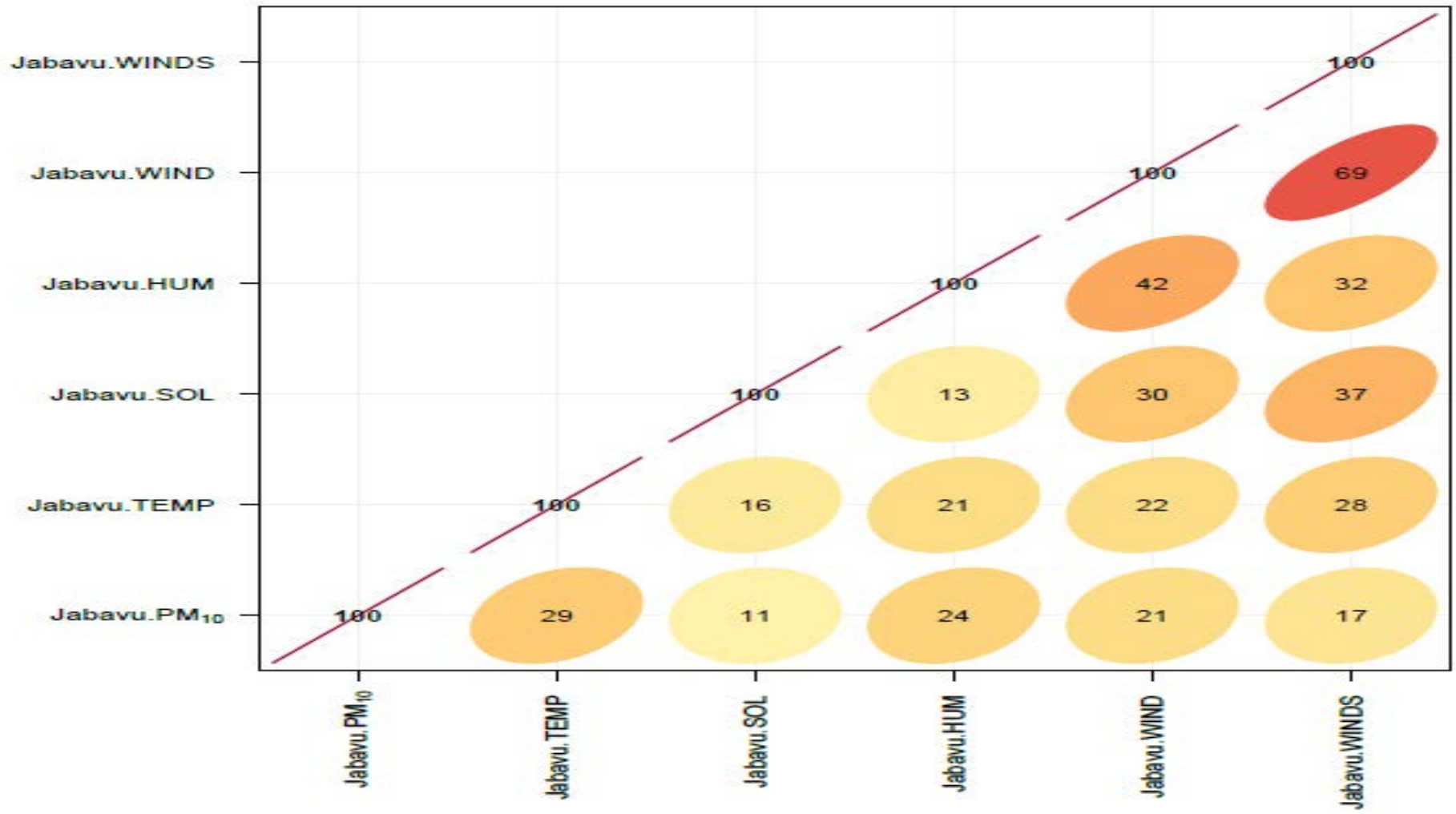

Figure 4.14: Jabulani Ambient Monitoring Station parameters correlations

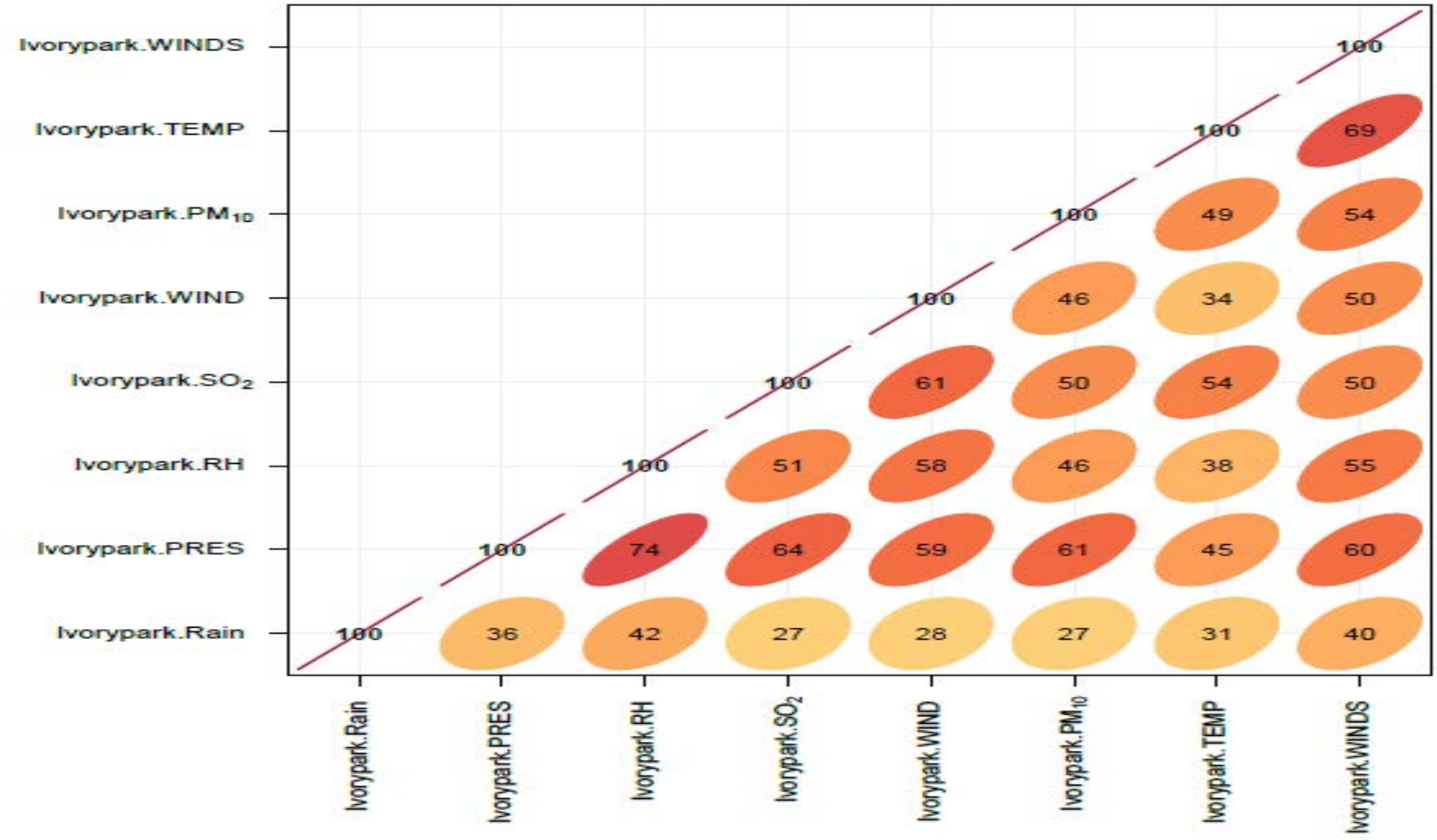

Figure 4.15: Ivory park Ambient Monitoring Station parameters correlations

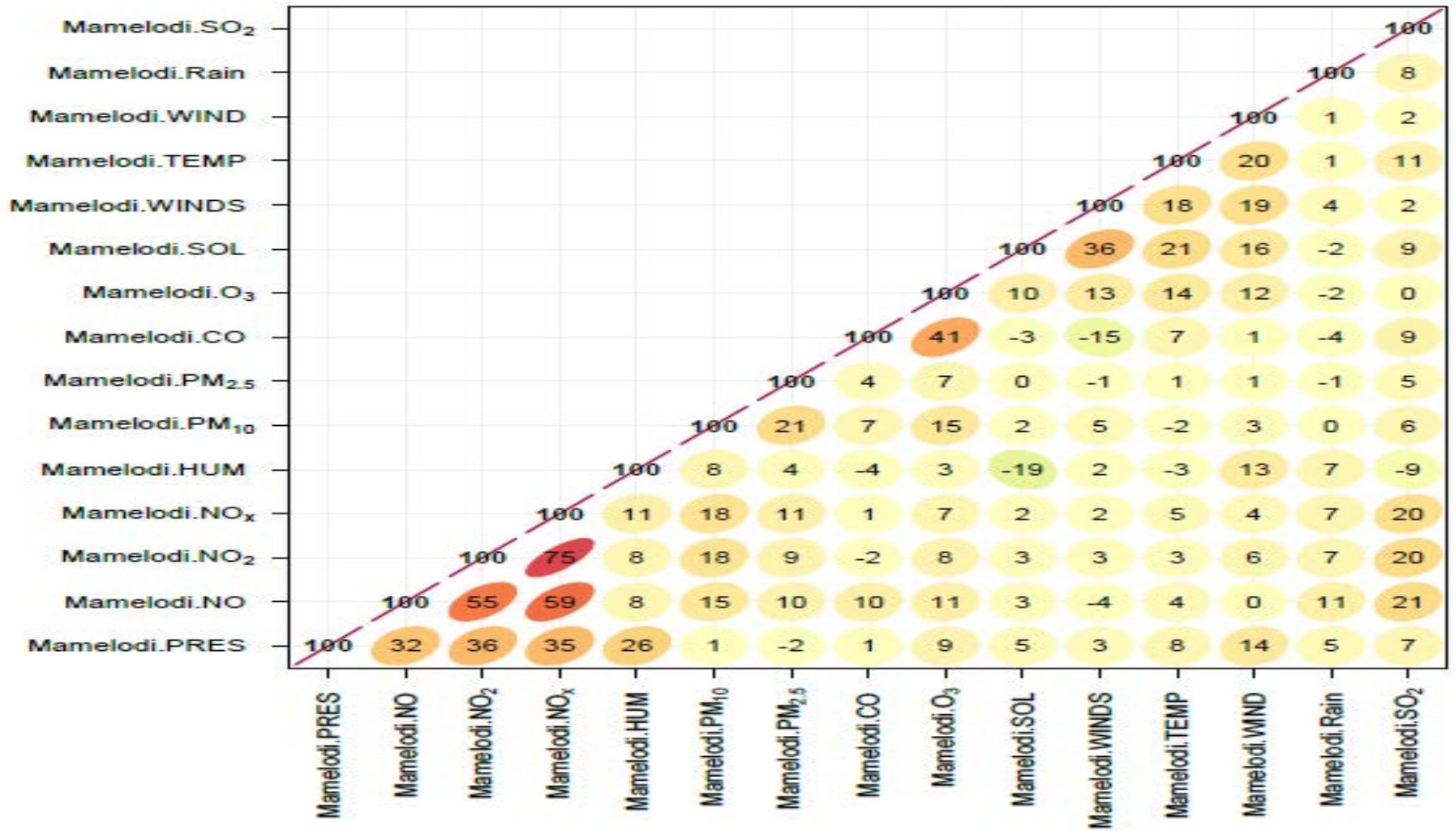

Figure 4.16: Mamelodi Ambient Monitoring Station parameters correlations

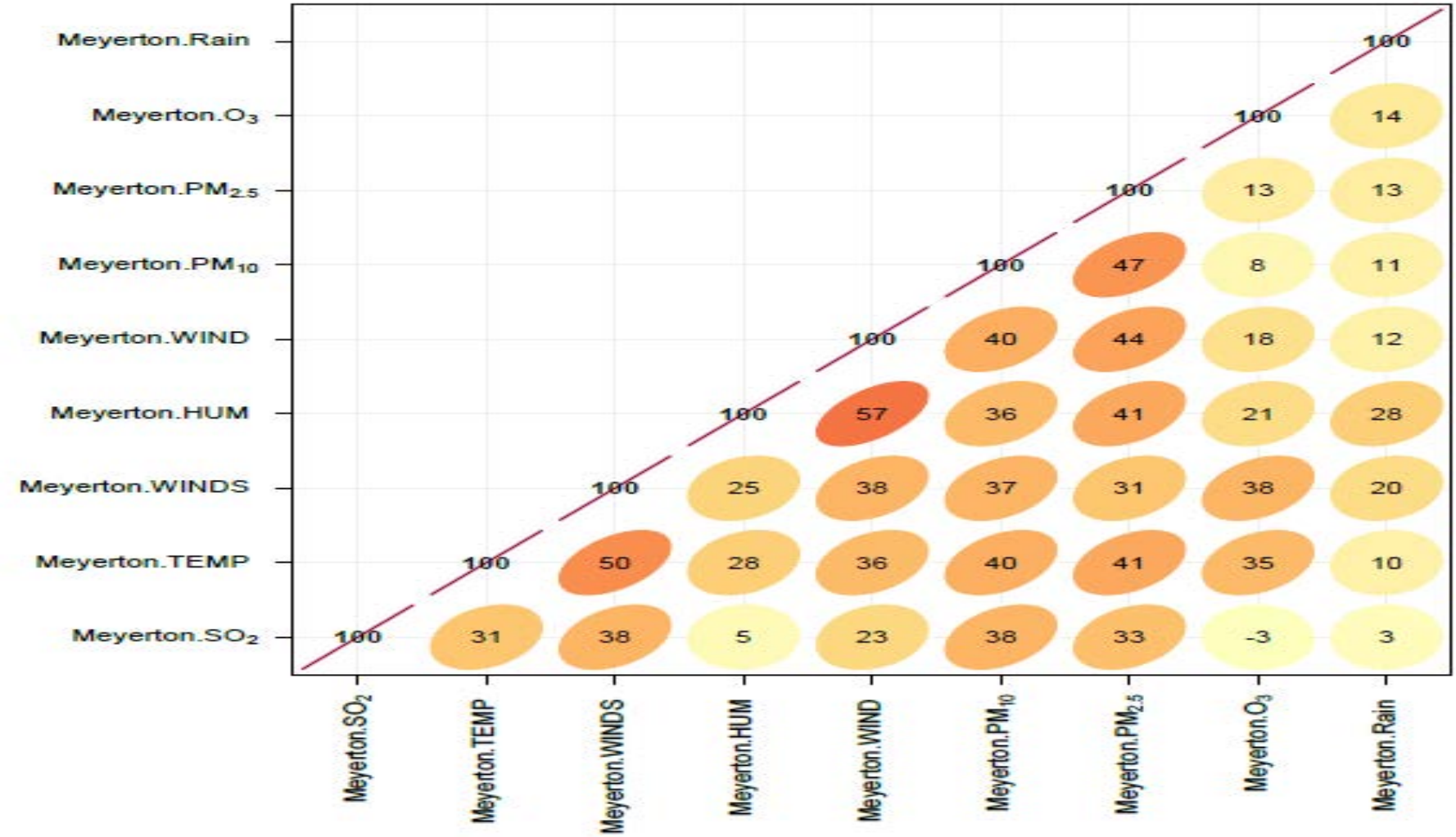

Figure 4.17: Meyerton Ambient Monitoring Station parameters correlations

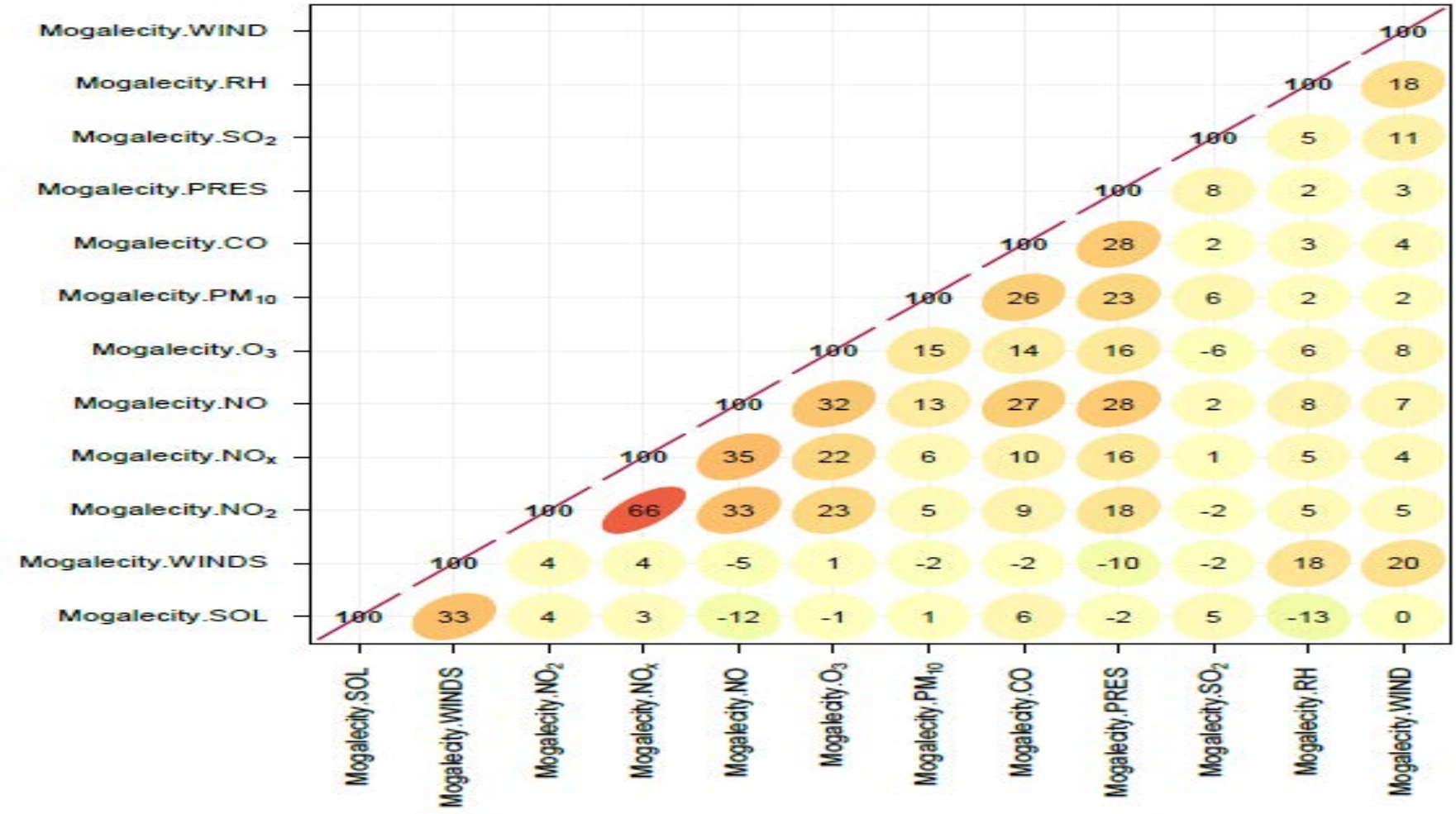

Figure 4.18: Mogale City Ambient Monitoring Station parameters correlations

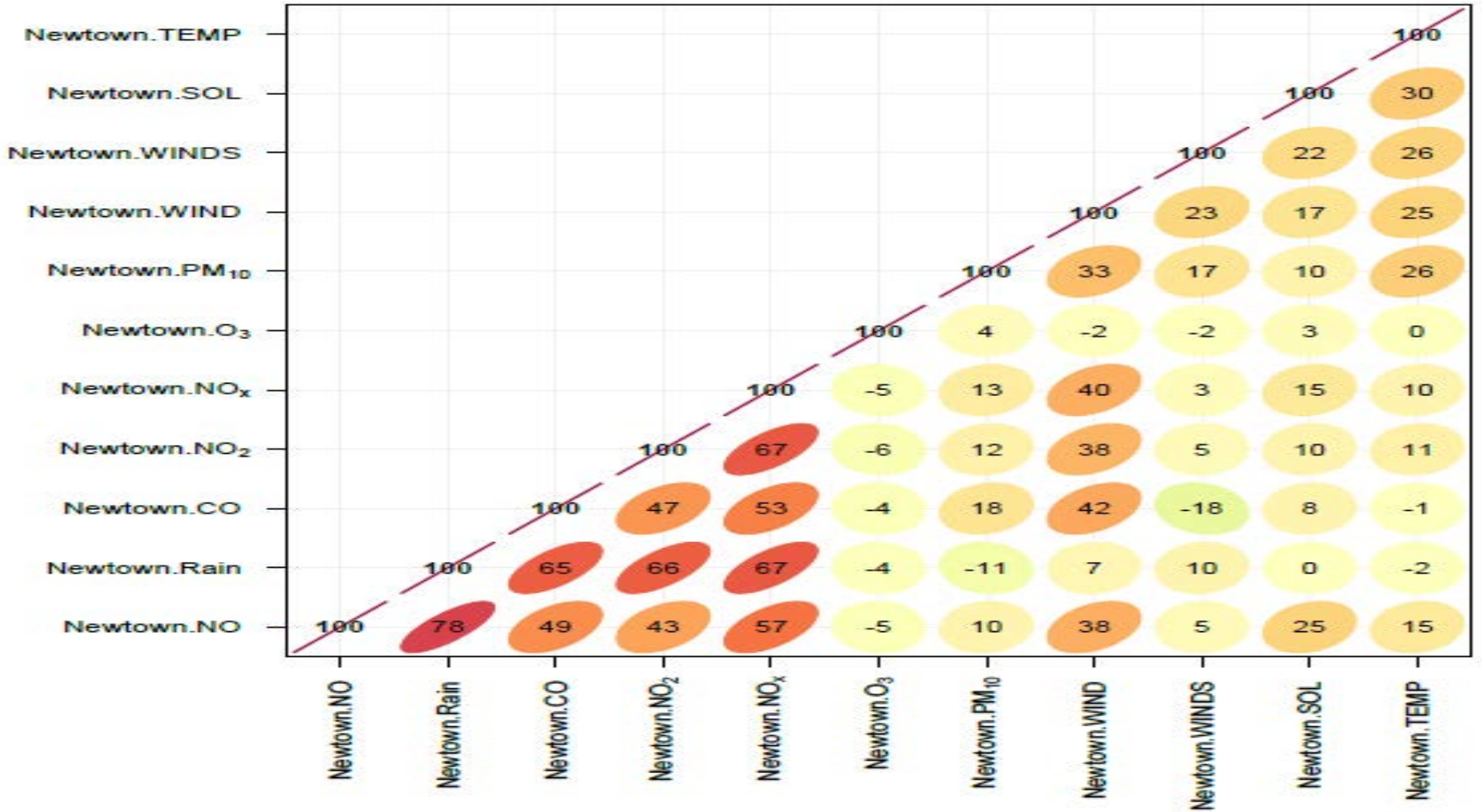

Figure 4.19: Newtown Ambient Monitoring Station parameters correlations

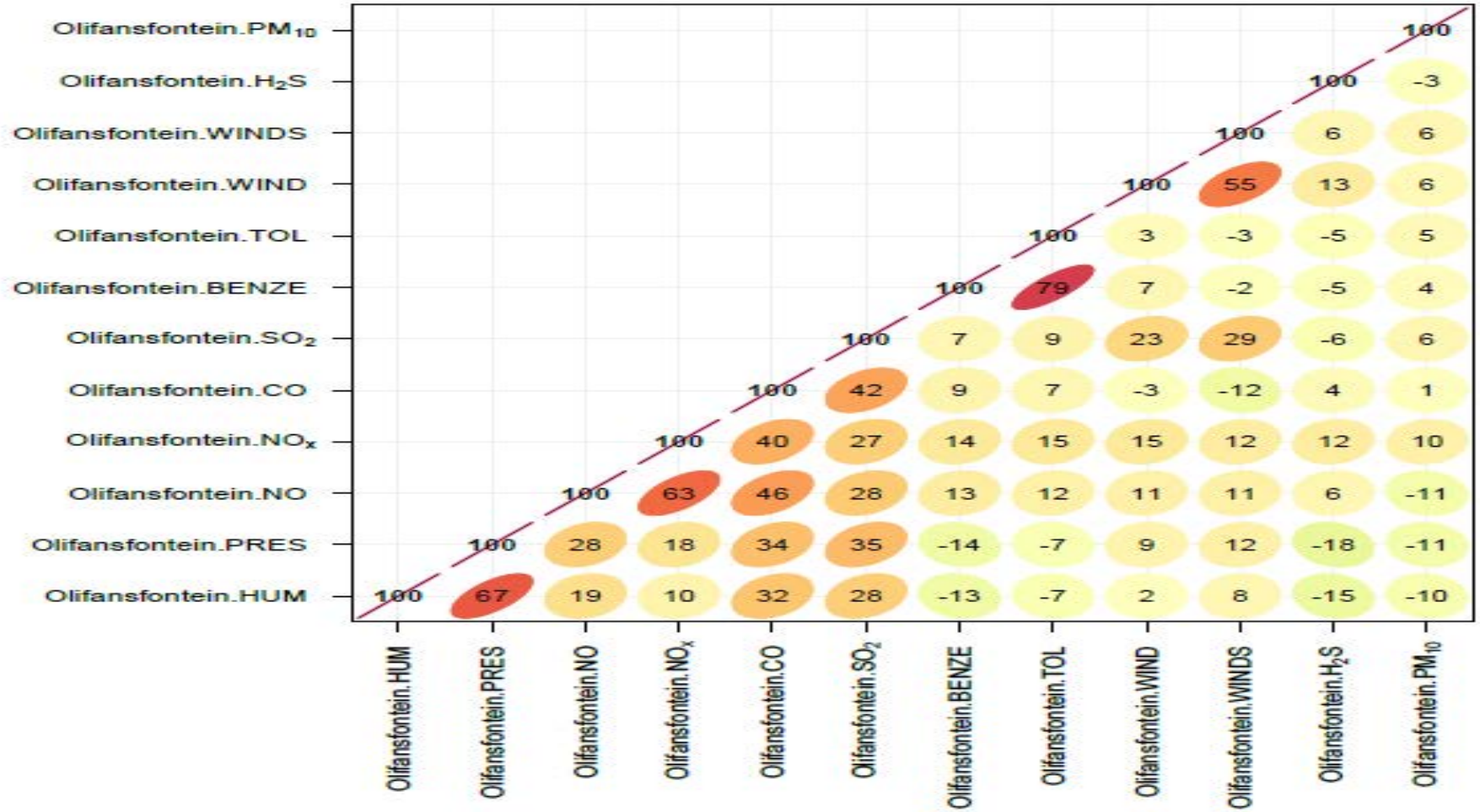

Figure 4.20: Olifansfontein Ambient Monitoring Station parameters correlations

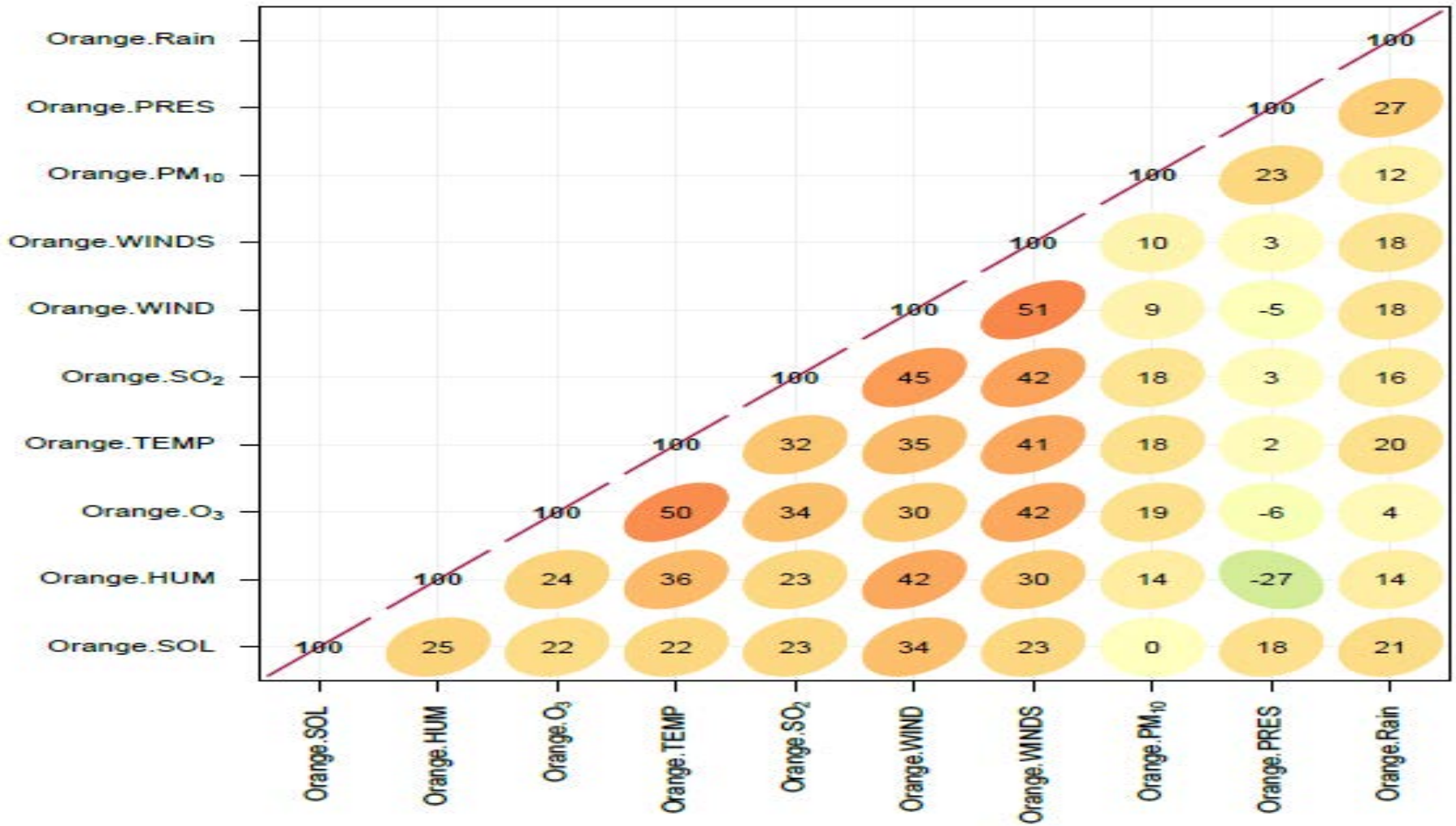

Figure 4.21: Orange Farm Ambient Monitoring Station parameters correlations

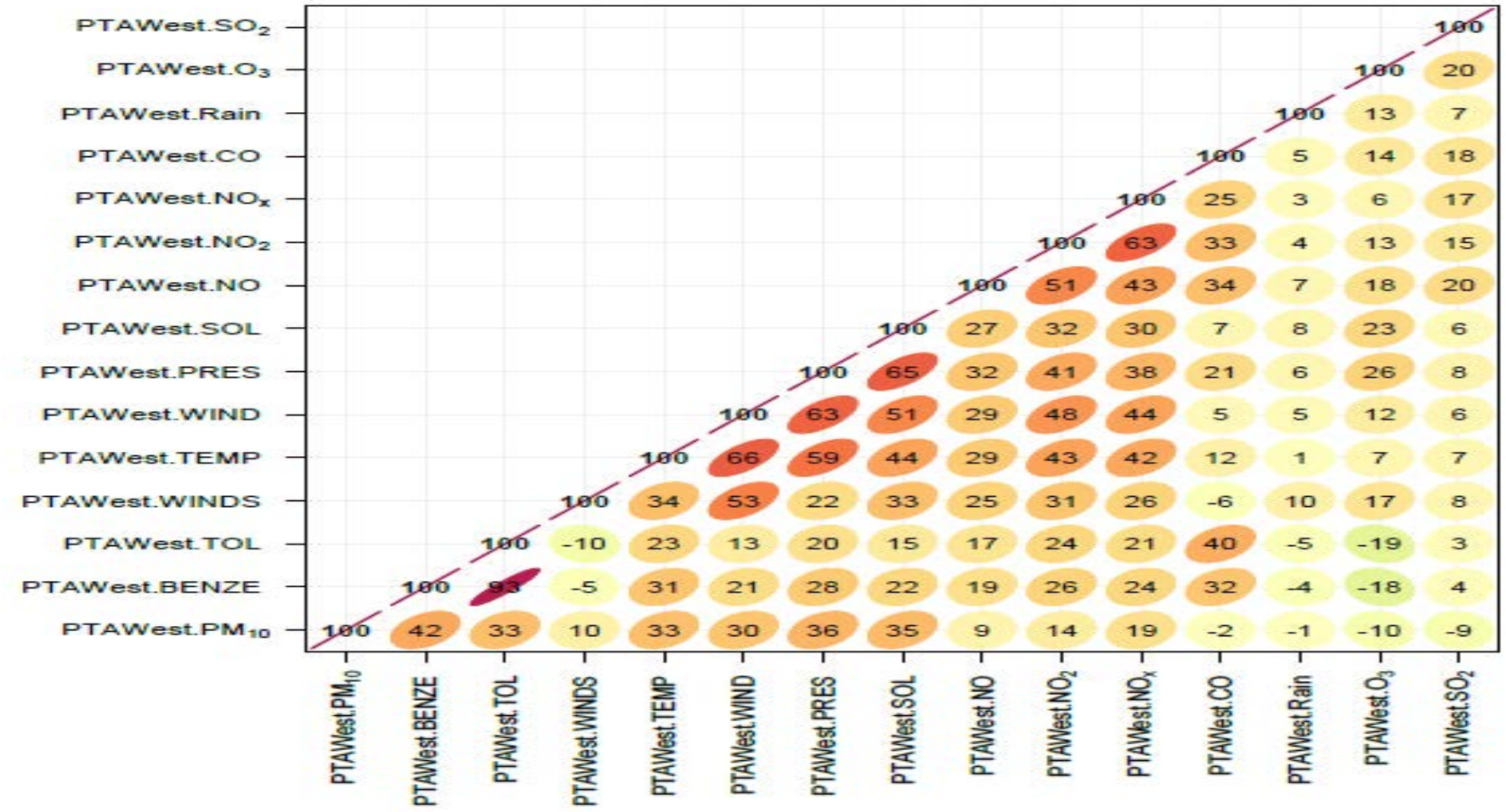

Figure 4.22: Pretoria West Ambient Monitoring Station parameters correlations

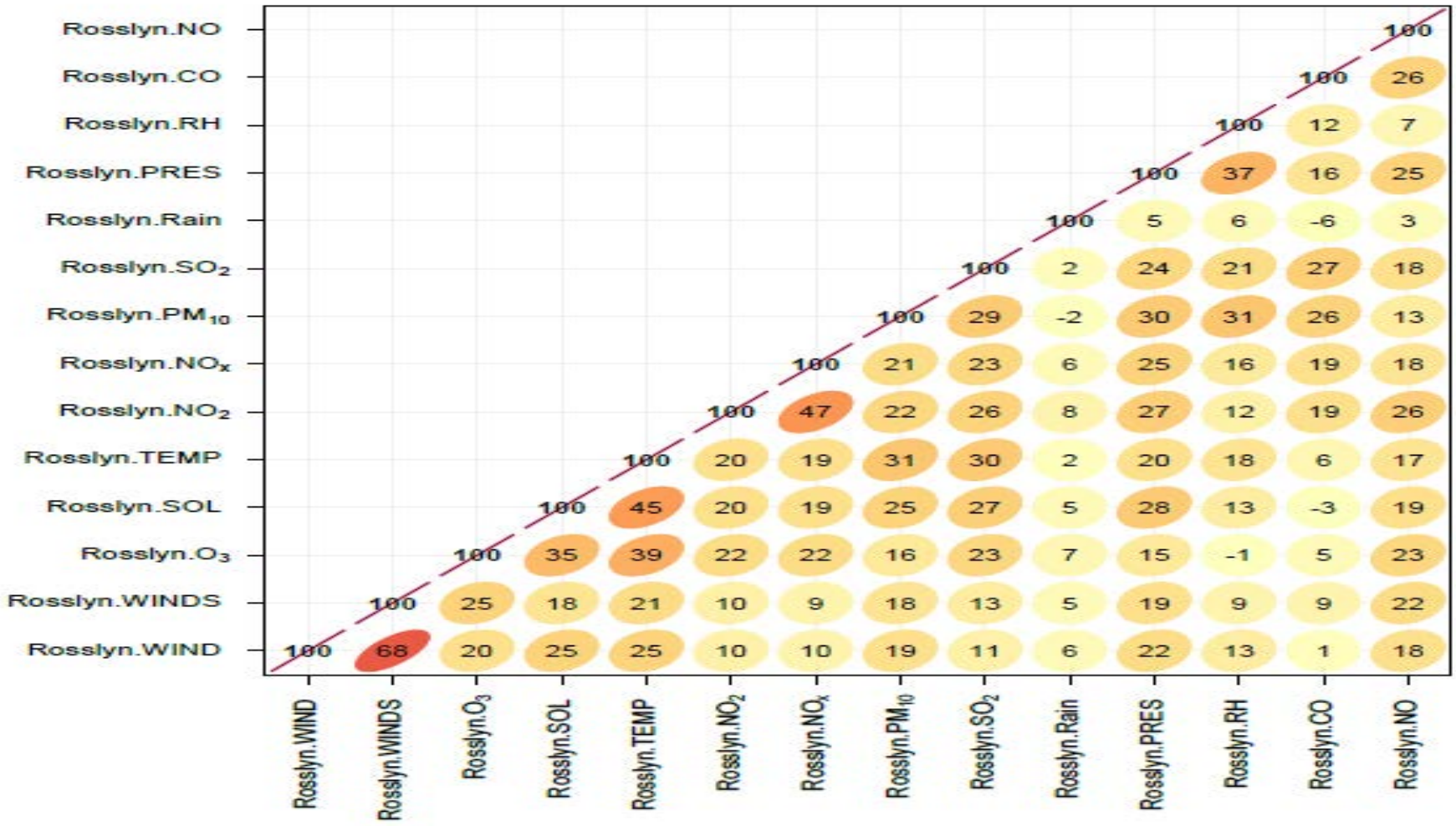

Figure 4.23: Rosslyn Ambient Monitoring Station parameters correlations

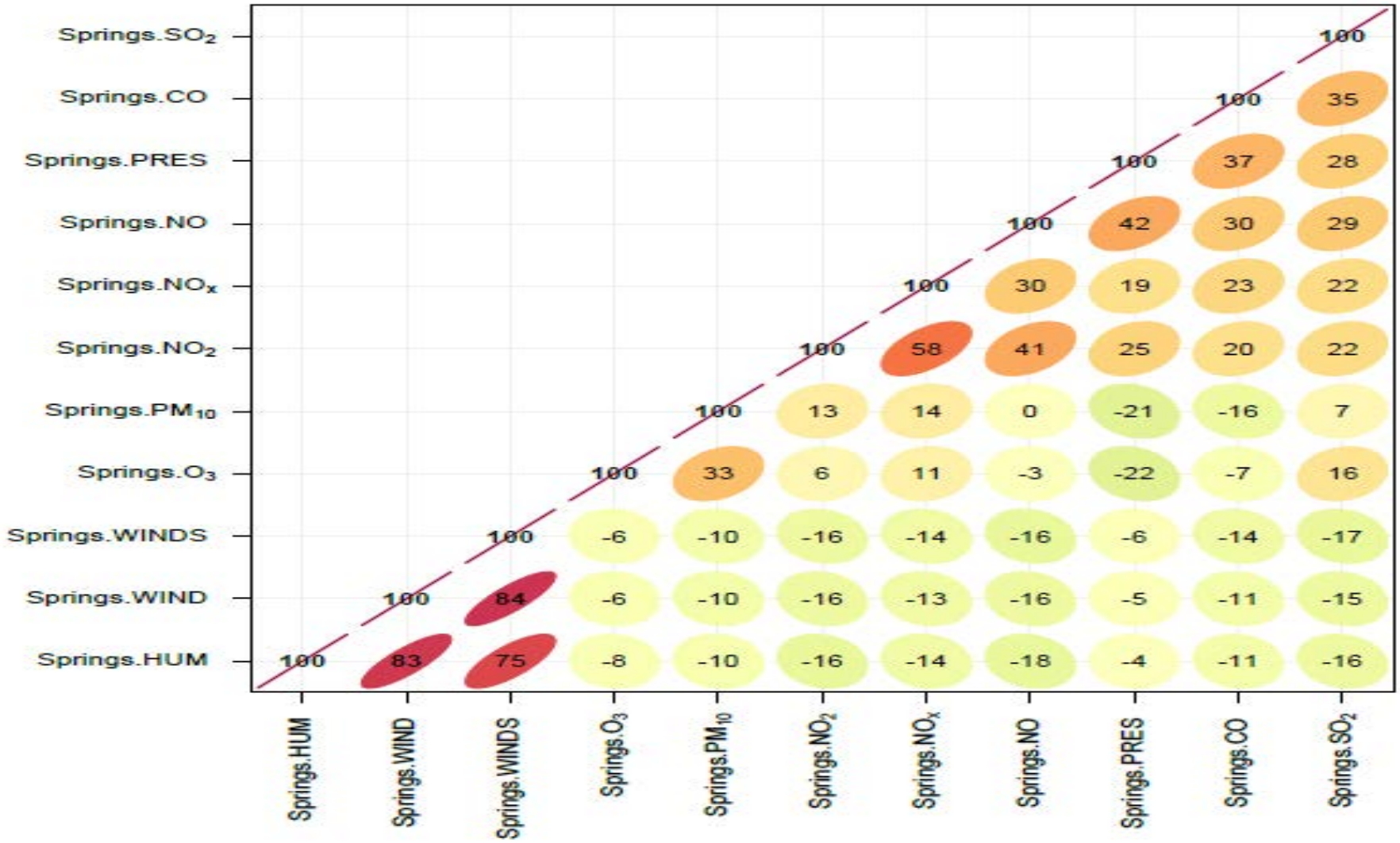

Figure 4.24: Springs Ambient Monitoring Station parameters correlations

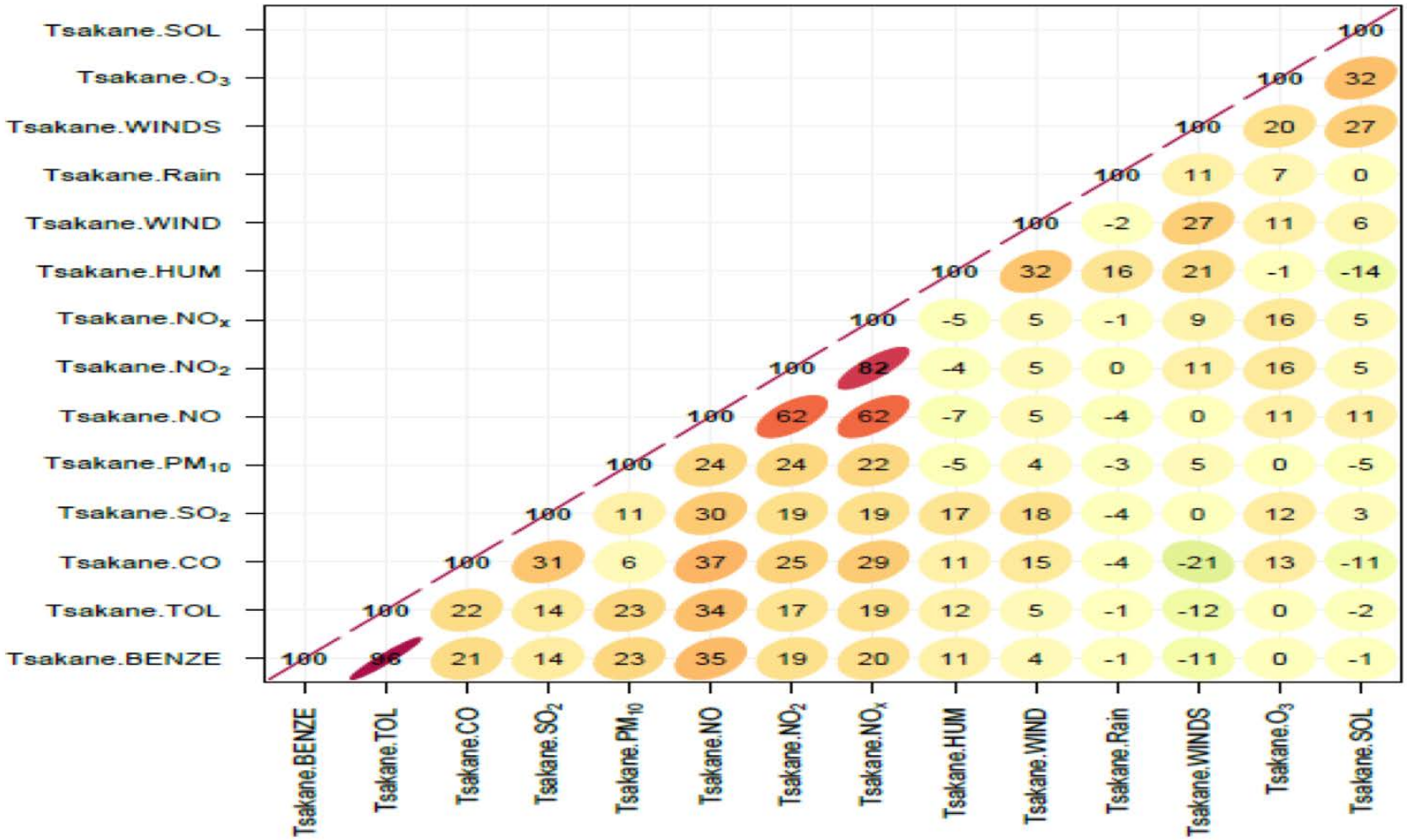

Figure 4.25: Tsakane Ambient Monitoring Station parameters correlations

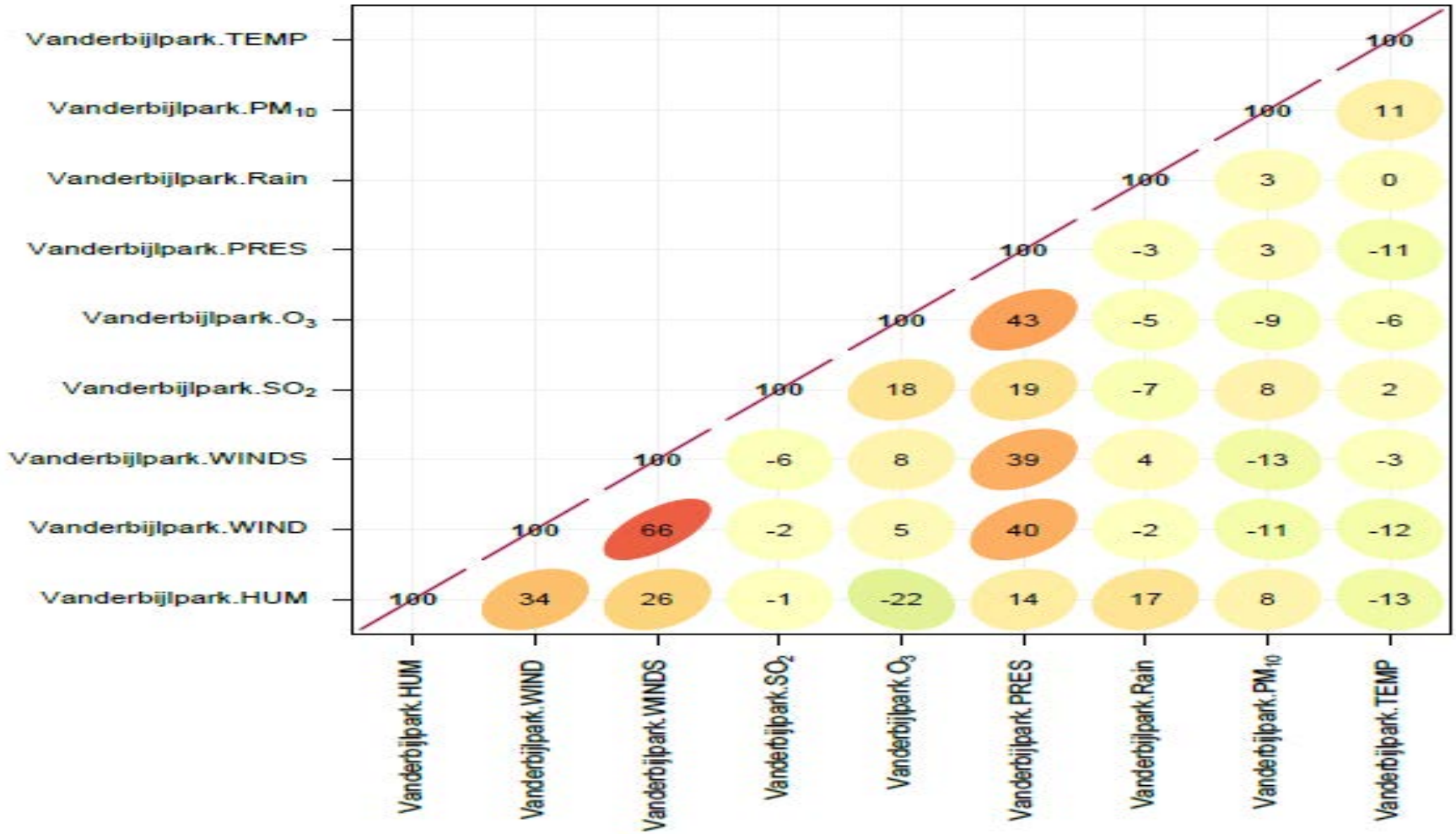

Figure 4.26: Vanderbijlpark Ambient Monitoring Station parameters correlations

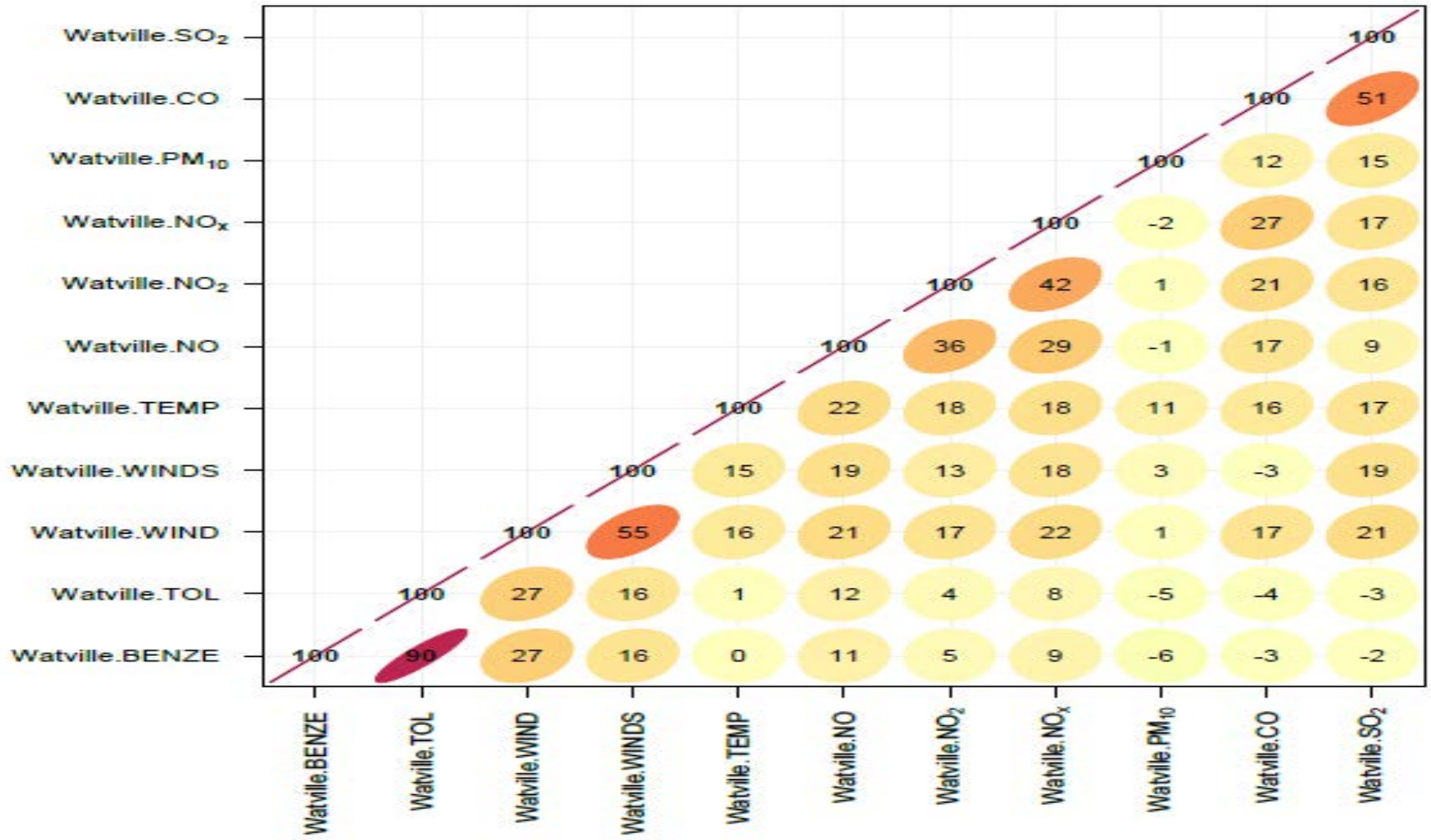

Figure 4.27: Watville Ambient Monitoring Station parameters correlations

Figure 4.7 showed a strong positive correlation between wind speed and wind direction at the Thokoza ambient monitoring station. Nitrogen oxides had a strong positive correlation with the concentration of nitrogen dioxide. Nitrogen Monoxide concentrations had a moderate positive correlation with either nitrogen oxides or nitrogen dioxide oxides. The ambient temperature displayed a strong moderate association. The PM_{10} concentration displayed a weak negative correlation with either wind speed or wind direction.

Wind speed and ozone contaminants in Figure 4.8 showed a strong positive correlation at the Buccleuch atmospheric monitoring station. Wind speed had shown a strong positive association with wind speed. Nitrogen oxides and nitrogen monoxide showed a strong positive correlation at the Buccleuch ambient monitoring station. The concentration of carbon monoxide showed a strong positive correlation with the ambient pressure. The ambient pressure showed a moderately strong positive correlation with either NO, NOx or relative humidity. There was no correlation between rain and nitrogen monoxide results. Nitrogen Oxides and ambient temperature had no tendency either to increase or decrease. Carbon monoxide had a negative correlation with either ozone, ambient temperature, wind speed or direction.

The findings of the Davidsonville ambient monitoring station in Figure 4.9 showed a strong positive correlation between wind speed and relative humidity. Relative humidity had a strong, moderate correlation to ambient temperature. Solar radiation had a negative correlation with either ambient temperature, relative humidity or wind direction. Wind speed had a poor positive correlation to either ambient temperature or relative humidity at the Davidsonville ambient monitoring station.

Figure 4.10 indicated that most of the data in Delta Park had a strong positive correlation. Ozone concentrations had a strong positive correlation and relative humidity. Wind direction had a strong positive association between relative humidity and ozone concentrations. Ambient pressure had a strong positive correlation with either relative humidity, ozone pollutant or wind direction. Rain at the Delta Park had a strong positive correlation between relative humidity, ozone, wind direction and ambient pressure. Solar radiation had a strong positive correlation between heat, atmospheric pressure, wind direction, relative humidity or ozone pollutant. Wind speed had a strong positive correlation between the

ozone pollutant, solar radiation, rain or ambient pressure. Wind speed showed a strong positive correlation with wind direction or relative humidity.

At the Diepsloot ambient monitoring station in Figure 4.11, the ratio between ambient pressure and relative humidity is the highest. Sulfur dioxide concentrations had a moderate positive PM_{10} correlation in the Diepsloot Region. Relative humidity and atmospheric pressure had a strong, moderate association between PM10 and SO_2 concentrations. Wind speed shows a strong positive correlation with either SO_2 or relative humidity

Ekandustria ozone pollutants had a moderate positive correlation with nitrogen monoxide in Figure 4.12. Nitrogen dioxide had a strong positive interaction with nitrogen monoxide. Ozone had a positive correlation with nitrogen dioxide. Nitrogen oxides had a strong positive correlation with nitrogen dioxide. Nitrogen Oxides had a moderate positive correlation between nitrogen monoxide and ozone ambient concentrations. PM_{10} showed ae moderate intensity of the correlation. The ambient temperature showed a moderate positive correlation with the solar radiation. Relative humidity at the Ekandustria showed a strong positive correlation between ambient pressure and wind direction. Wind speed indicated a strong positive correlation between relative humidity and wind direction.

At the Etwatwa ambient monitoring station in Figure 4.13, toluene concentrations showed a strong positive correlation with the benzene concentration. Nitrogen dioxide pollutants exhibited a strong positive correlation with nitrogen monoxide. Nitrogen oxide had a strong positive correlation with nitrogen monoxide or nitrogen dioxide. Carbon monoxide had a moderately positive correlation with nitrogen monoxide. Wind velocity had a strong positive correlation with wind direction. The relative humidity at the ambient monitoring station showed a moderate positive correlation with the wind direction. The ambient temperature showed a moderate positive correlation between carbon monoxide, wind direction, wind speed or relative humidity. The atmospheric pressure displayed a strong positive correlation with relative humidity. Sulfur dioxide showed a positive, moderate correlation with either carbon monoxide or ambient pressure. Rain and nitrogen monoxide had no correlation between 2 variables at the Etwatwa.

Wind speed and wind direction at the Jabulani ambient monitoring station are shown in Figure 4.14. The results showed a strong positive correlation. Relative humidity had a

moderate positive correlation with the direction of the wind. Most of the correlations had low positive correlations at the Jabulani ambient monitoring station.

The relative humidity of the Ivory Park had a strong positive correlation with the ambient pressure. Sulfur dioxide had a strong positive correlation with ambient pressure. Wind direction with sulfur dioxide concentration showed a strong positive correlation. There was a strong positive PM_{10} correlation and the atmospheric pressure is shown in Figure 4.15. Wind speed showed a strong positive correlation between ambient pressure and ambient temperature. The ambient temperature showed a moderate positive correlation with either ambient pressure or relative humidity around Ivory Park. PM_{10} had a strong positive correlation with either relative humidity, sulfur dioxide or wind direction. Wind direction had a strong intermediate correlation with either ambient pressure or relative humidity. The relative humidity had a strong positive correlation with the rainfall. Sulfur dioxide had a strong positive correlation with relative humidity.

The Mamelodi atmospheric monitoring station in Figure 4.16 showed a strong positive correlation only with nitrogen dioxide and nitrogen oxide. Nitrogen Monoxide had a moderate positive correlation with either nitrogen oxide or nitrogen dioxide. Ozone pollutants had a strong positive carbon monoxide correlation. Concentrations of sulfur dioxide did not show a tendency to increase or decrease with concentrations of ozone. No link between nitrogen oxides and Mamelodi atmospheric rain monitoring. Wind direction and nitrogen monoxide did not show a correlation between 2 variables. $PM_{2.5}$ and solar radiation did not show a correlation between the two variables. The highest negative correlation was between solar radiation and relative humidity in Mamelodi.

Results in Figure 4.17 of the Meyerton ambient monitoring station showed either positive or negative correlations. $PM_{2.5}$ had a mild association with either relative humidity, wind direction or PM_{10}. PM_{10} had a moderate positive correlation with either the ambient temperature or the wind direction. Wind direction and relative humidity showed a strong moderate correlation. Wind speed had a positive, moderate correlation with ambient temperature. Ozone concentrations showed a very weak negative correlation with sulfur dioxide.

A strong positive correlation of nitrogen dioxide and nitrogen oxides was observed at the Mogale City atmospheric monitoring station in Figure 4.18. There was no correlation

between wind direction and trends in solar radiation data. Negative very weak correlation was found between wind speed with either nitrogen monoxide, PM_{10}, carbon monoxide, ambient pressure or sulfur dioxide. Solar radiation had a very low negative correlation, with carbon monoxide, ozone, atmospheric pressure or relative humidity.

In Figure 4.19, the Newtown Environmental Monitoring Station showed a strong positive correlation between the amount of precipitation received and the concentration of nitrogen monoxide. The station was designed to monitor traffic emissions from roads such as the M1 and M2 exchanges in the City of Johannesburg. Carbon monoxide had a positive correlation with the recorded rainfall. Rain recorded at the Newtown ambient monitoring station had a strong presence of either nitrogen dioxide or nitrogen oxides. Nitrogen oxides had a positive correlation with nitrogen dioxide. Wind direction showed a moderate correlation between carbon monoxide and nitrogen oxides. Nitrogen oxides had a positive, moderate correlation between nitrogen monoxide and carbon monoxide. Nitrogen dioxide had a strong, moderate association between nitrogen monoxide and carbon monoxide. Carbon monoxide had a moderate positive correlation with nitrogen monoxide. The results in Figure 4.19 showed no correlation between recorded rainfall and solar radiation. There was no correlation between the ambient temperature and the ozone concentration. Ozone concentrations displayed a very poor negative correlation between nitrogen monoxide, heat, carbon monoxide, nitrogen dioxide or nitrogen oxides at the Newtown atmospheric monitoring station.

In Figure 4.20, the positive correlation between ambient pressures and relative humidity were found at the Olifansfontein ambient monitoring station. Nitrogen monoxide showed a strong positive association with nitrogen oxides. The most positive correlation was observed at atmospheric concentrations of toluene and benzene, which could suggest related sources. There was a strong positive correlation between wind speed and wind direction at Olifansfontein. Sulfur dioxide concentrations displayed a strong positive correlation with carbon monoxide. Carbon monoxide showed a moderate positive correlation between nitrogen monoxide and nitrogen oxides. Highest negative very low correlation was found between hydrogen sulphide, with either relative humidity or atmospheric pressure.

The Orange Farm Environmental Monitoring Station is situated in the City of Johannesburg and is designed to monitor emissions from fuel domestic activities. In Figure 4.21, the ambient temperature showed a moderate positive ambient correlation with the

ambient ozone concentrations recorded at the Orange Farm. Wind speed showed a strong moderate association, with ozone, sulfur dioxide concentrations, ambient temperature or wind direction. The wind direction showed a moderate positive correlation between relative humidity and ambient sulfur dioxide concentrations. PM_{10} at the Orange Farm showed no correlation with the solar radiation analysis at the Orange Farm. Ambient pressure indicated a negative correlation between relative humidity, ozone concentrations or wind direction at the Orange Farm.

Pretoria West Environmental Monitoring Station is situated in Tshwane City and the station is designed to track industrial activities. In Figure 4.22, toluene test indicated a very strong positive reading of benzene. Wind direction showed a strong positive correlation with an ambient temperature of 25ºC. Wind direction showed a strong positive correlation with ambient pressure. At the ambient pressure, there was a strong positive correlation with the direction of the wind. Positive strong correlation with solar radiation was observed at ambient pressure. The concentration of nitrogen dioxide showed a strong positive correlation with nitrogen oxides. Nitrogen oxides showed a positive correlation between ambient temperature, wind direction or nitrogen monoxide. Solar radiation had either positive, moderate wind direction or ambient temperature. Carbon monoxide showed a positive, moderate correlation with the concentration of toluene. The atmospheric pressure displayed a strong moderate correlation with the ambient temperature. Wind speed had a positive, moderate correlation with wind direction. The concentration of ozone had a very weak negative correlation, either PM_{10}, C_6H_6 or C_7H_8.

Rosslyn Environmental Monitoring Station is situated in Tshwane City and is intended to track industrial activities. In Figure 4.23, wind speed had a strong tendency to increase in the direction of the wind. Solar radiation showed a moderate positive correlation with the ambient temperature. Nitrogen dioxide had a strong positive correlation with nitrogen oxides. Carbon monoxide had a very poor negative correlation between either solar radiation or rain.

The results of the Springs ambient monitoring station in Figure 4.24 showed a very strong positive correlation with relative humidity. Wind speed showed a positive, strong correlation between relative humidity and wind direction. Nitrogen dioxide had a positive, moderate correlation between nitrogen oxides and nitrogen monoxide. Nitrogen monoxide had a strong, moderate association with ambient pressure. The ambient pressure showed a poor

negative correlation between ozone and PM_{10}. The air pressure displayed a very poor negative correlation, including relative humidity, wind speed or wind direction. The concentration of sulfur dioxide had a very weak correlation, either relative humidity, wind speed or wind direction.

Nitrogen oxides at the Tsakane displayed a very strong positive association with nitrogen dioxide at the Tsakane. Nitrogen monoxide showed a strong positive correlation between nitrogen dioxide and nitrogen oxides. There was a very strong positive correlation between the concentration of toluene and benzene. Ozone concentration shows no correlation between PM10, C_6H_6 or C_7H_8. Wind speed indicated no correlation between sulfur dioxide or nitrogen monoxide. Rain had no association with nitrogen dioxide. The solar radiation showed no connection with the rain reported at the Tsakane ambient station. There was a very weak negative relationship between rain, either CO, C_6H_6 or C_7H_8.Solar radiation had a very weak negative correlation, either CO, C_6H_6 or C_7H_8, as shown in Figure 4.25.

In Figure 4.26, the wind speed at the Vanderbijlpark showed a strong positive correlation with the wind direction. The air pressure showed a strong moderate association between wind speed and ozone concentration. Sulfur dioxide had a very weak negative correlation, either relative humidity, wind speed or wind direction. The ambient temperature displayed a negative correlation between relative humidity, wind speed or wind direction.

In Figure 4.27, the Watville Toluene concentrations showed a very strong positive correlation with the benzene concentration. Wind speed had a moderate positive correlation with wind direction. Nitrogen oxides had a strong, moderate correlation with nitrogen dioxide. Sulfur dioxide had a strong positive carbon monoxide correlation. The ambient temperature had no association with the concentration of benzene. The correlation of toluene and benzene was very low, with either PM_{10}, CO or SO_2.

4.2 Pollution Rose Analysis at ambient monitoring stations.

The results of pollution rose analysis at various Gauteng ambient monitoring stations are presented in Figure 4.28-Figure 4.73 below. The Figures below displayed pollution roses for PM_{10}, sulfur dioxide, nitrogen dioxide and ozone. Pollution rose in Figure 4.28 indicated the concentration of PM_{10} at the Alexandra station showing the wind in North and North-East directions. The North and North-East wind direction displayed an atmospheric concentration rate of 10-20 $\mu g/m^3$. The North bin has a longer range compared to the North-East basket. 60-400 $\mu g/m^3$ was found to be between 20 and 25%, while the same concentration range for the North-East bin is between 15 and 20%.

In Figure 4.29, the findings showed an increase in NO_2 concentrations at the Bedfordview, where the South and Southwest wind directions predominated at 12 and 11%, respectively, of the count level. 11% of the wind count were centred in the Northern regions with a high correlation of nitrogen dioxide. This means that the frequency was equal to 36.6 and the calm of 0.2%. The smallest level of count by wind direction was situated in the South-East of the Bedfordview ambient monitoring stations.

In Figure 4.30, Pollution increased in Bedfordview i.e. PM_{10} pollution increased from 6 to 8 % Southwest and from 6 to 8 % South. The average and mean atmospheric concentrations for PM_{10} at the Bedfordview ambient monitoring stations were 499.95 and 87.154 $\mu g/m^3$, respectively. At ambient concentrations of 0 to 50 $\mu g/m^3$, strong pollution increased from Southwest. In Figure 4.31, sulfur dioxide emission showed similar trends to nitrogen dioxide. Northern regions had an 8 % frequency of wind counts followed by Northwest and North-East regions with a 4 % frequency of wind counts. North-West varied by wind speed below 2% of the level. At 4 % in the South-East, the maximum atmospheric concentration was between 25 and 361.67 parts per billion. There was a high range of concentration distribution in the Southern bins.

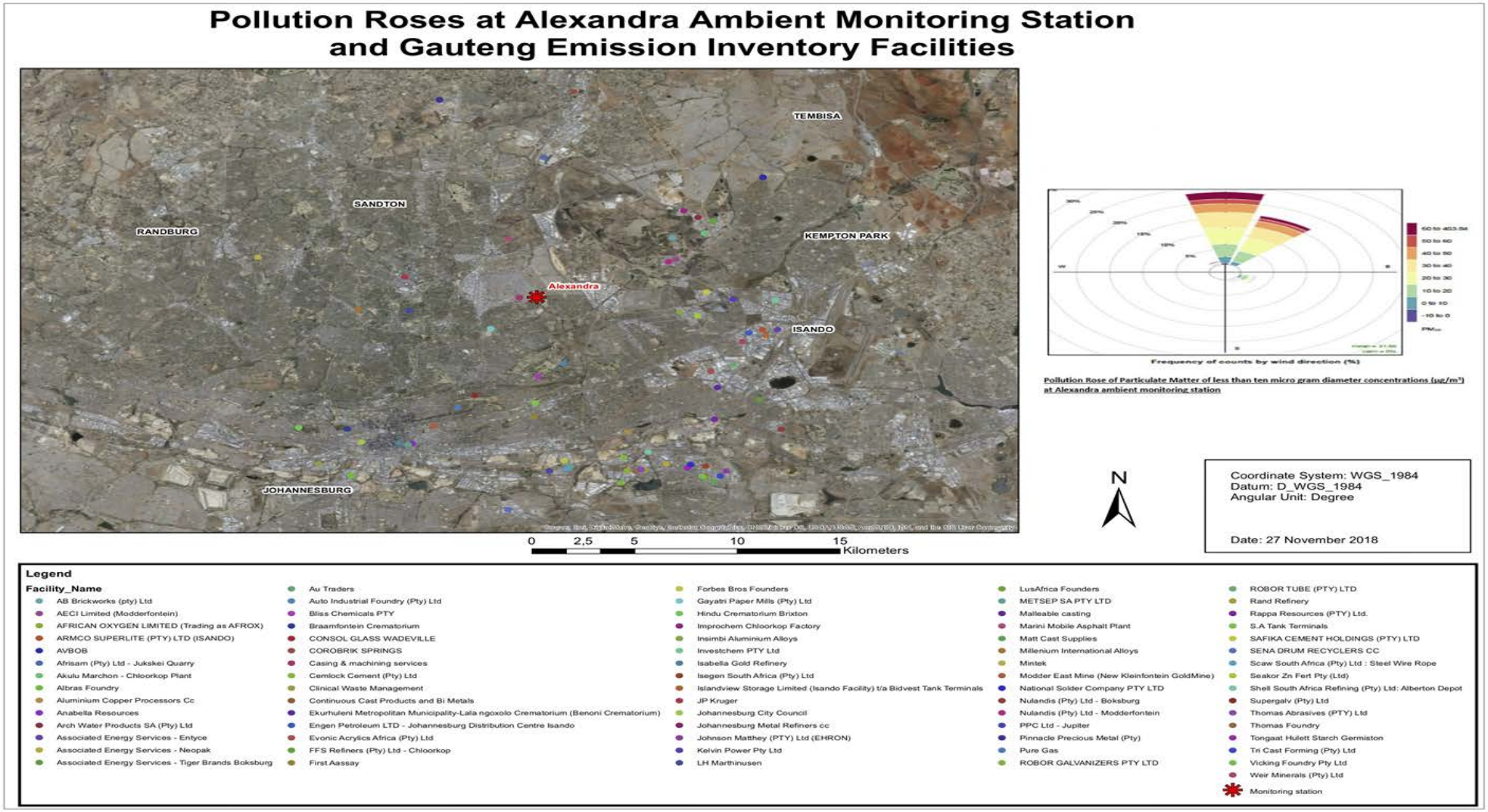

Figure 4.28: Pollution Roses at the Alexandra Ambient Monitoring Station and Gauteng Emission Inventory Facilities

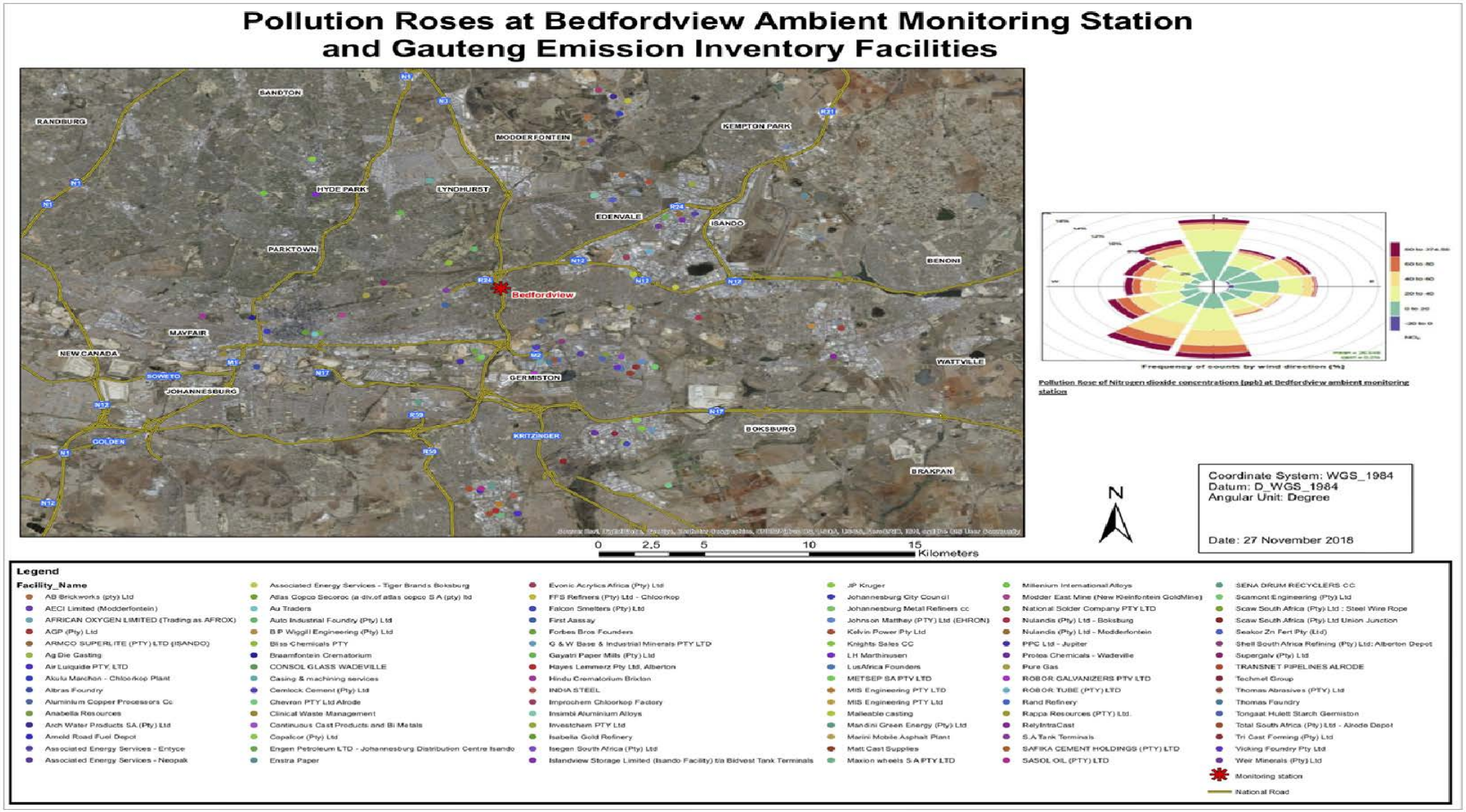

Figure 4.29: Pollution Roses at the Bedfordview Ambient Monitoring Station and Gauteng Emission Inventory Facilities

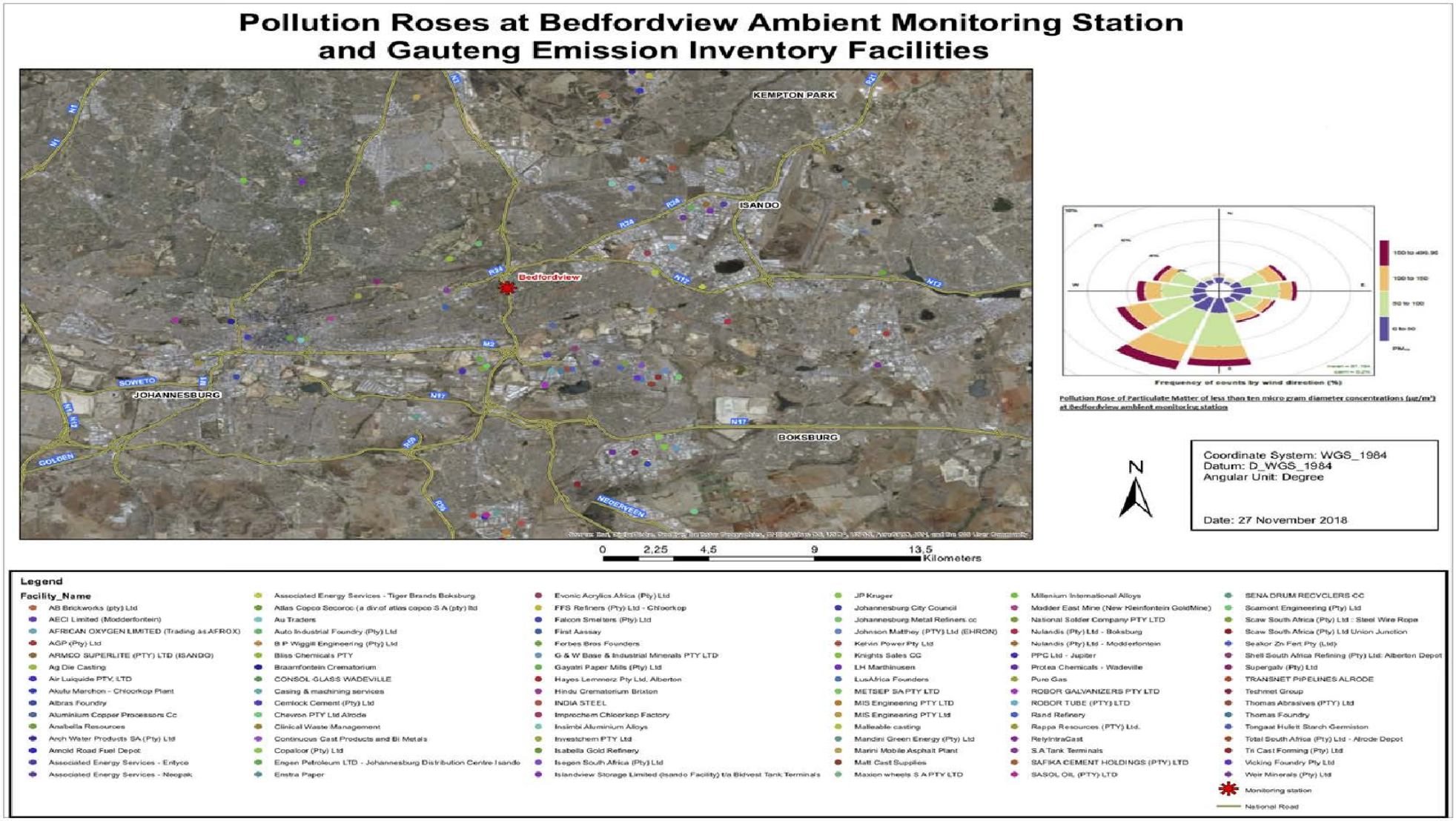

Figure 4.30: Pollution Roses at the Bedfordview Ambient Monitoring Station and Gauteng Emission Inventory Facilities

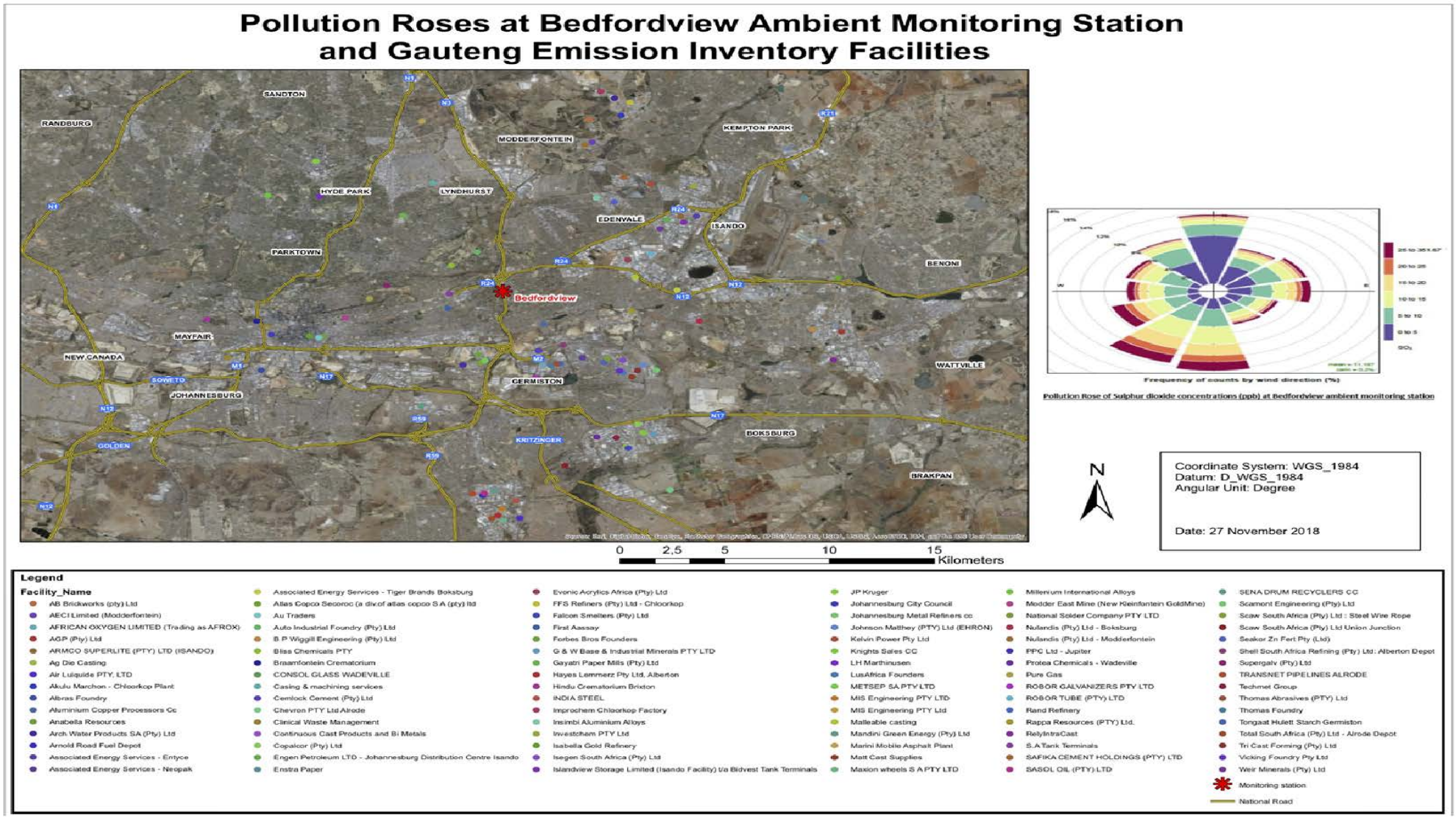

Figure 4.31: Pollution Roses at the Bedfordview Ambient Monitoring Station and Gauteng Emission Inventory Facilities

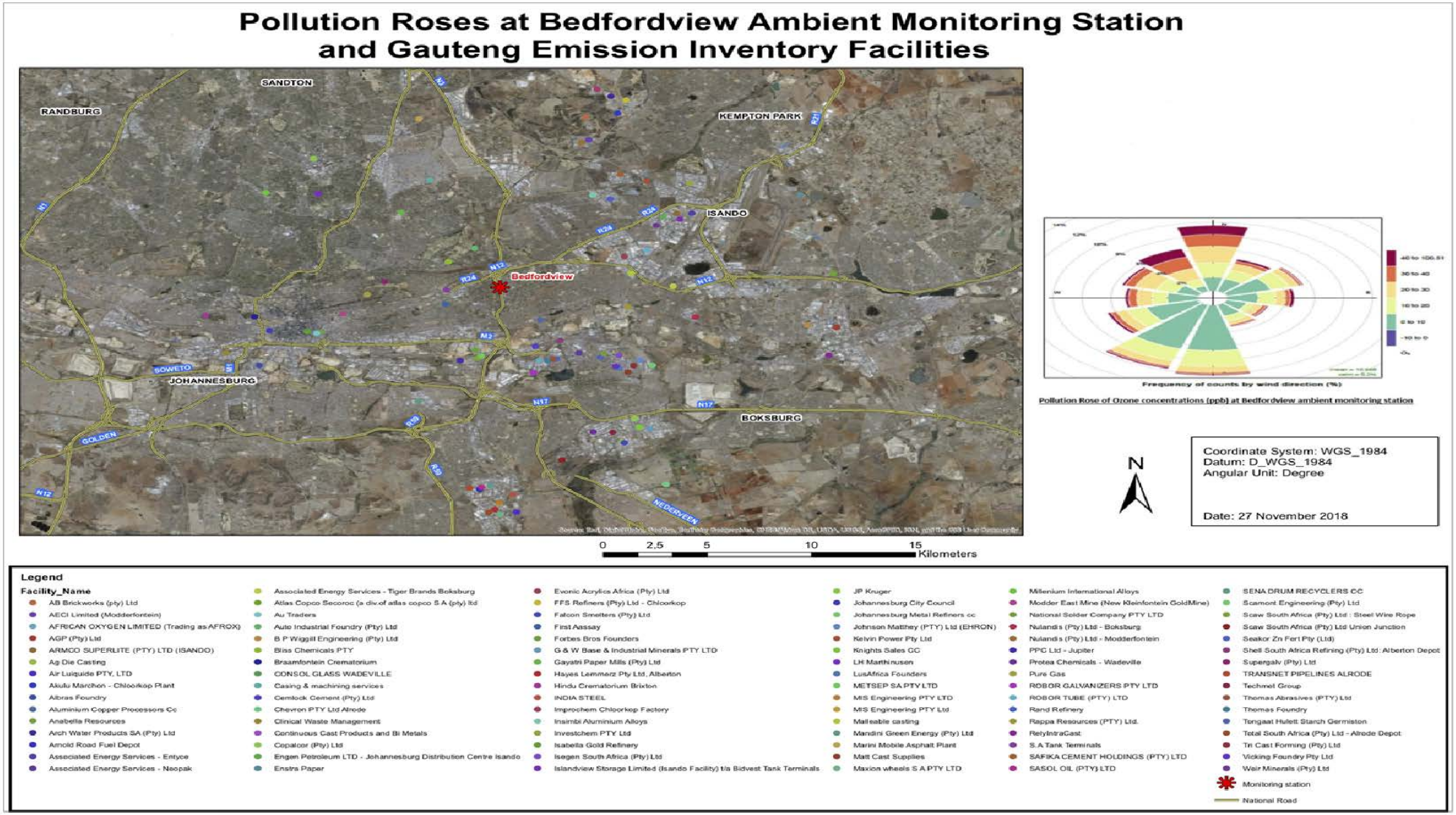

Figure 4.32: Pollution Roses at the Bedfordview Ambient Monitoring Station and Gauteng Emission Inventory Facilities

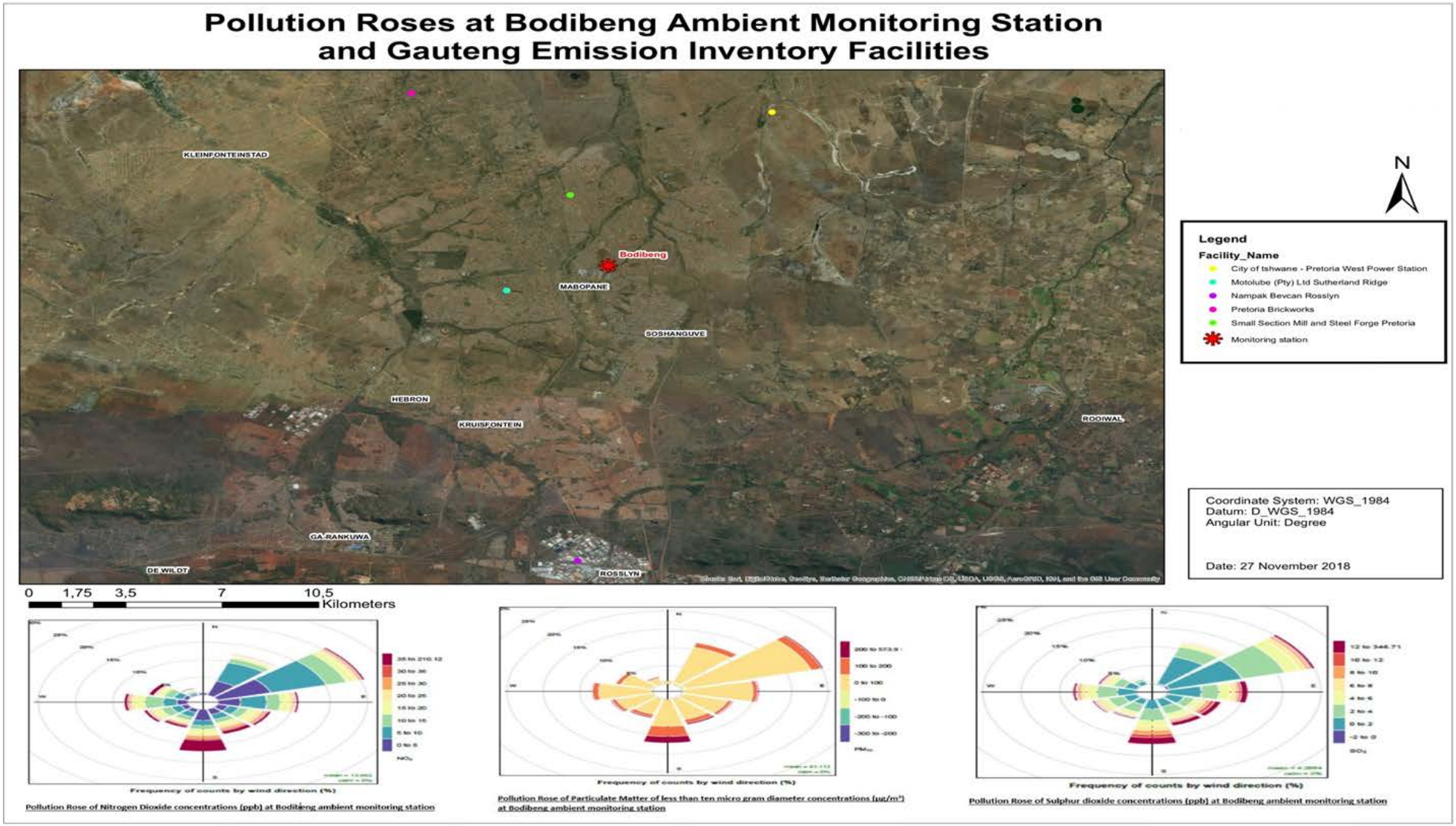

Figure 4.33: Pollution Roses at the Bodibeng Ambient Monitoring Station and Gauteng Emission Inventory Facilities

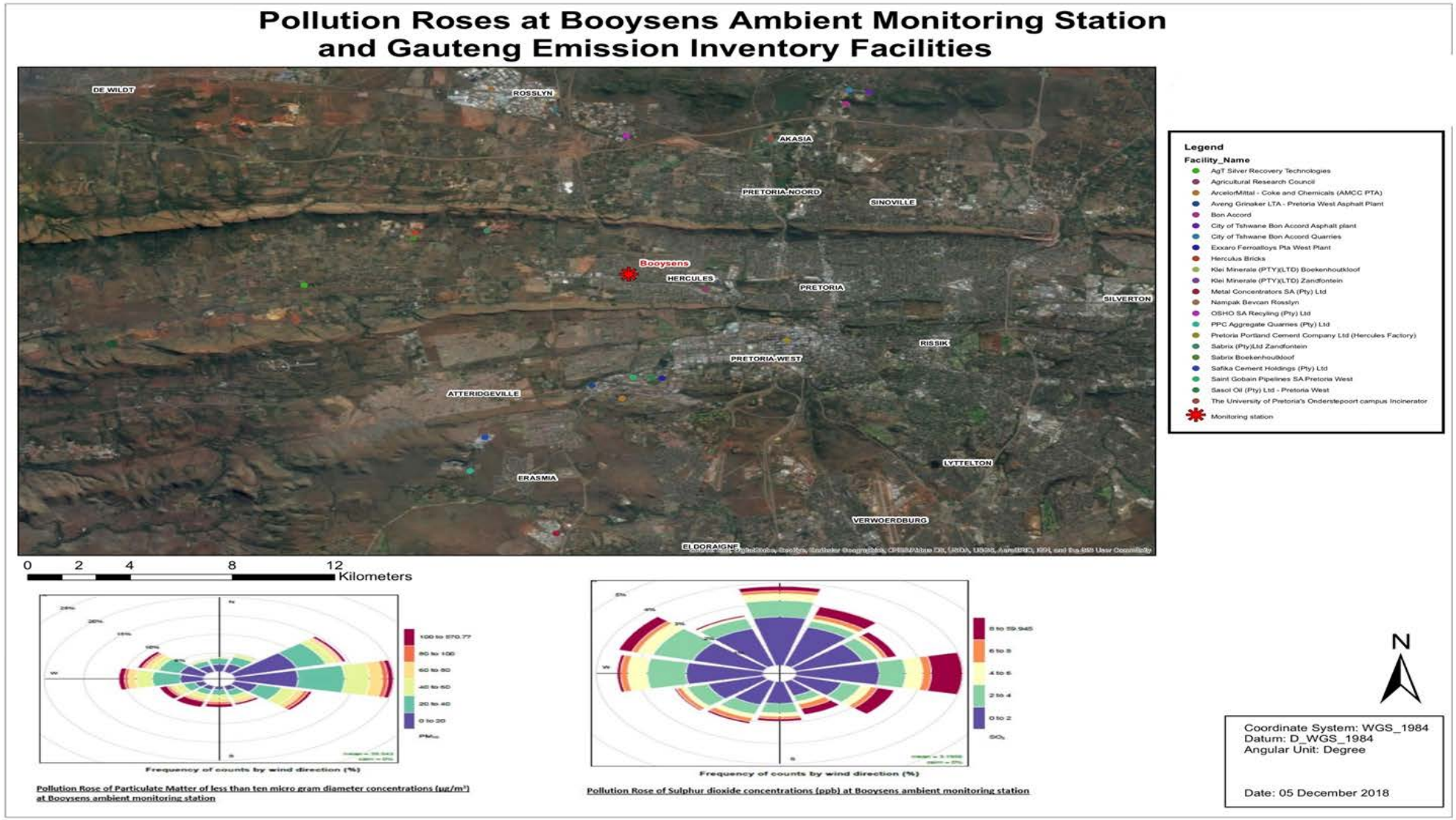

Figure 4.34: Pollution Roses at the Booysens Ambient Monitoring Station and Gauteng Emission Inventory Facilities

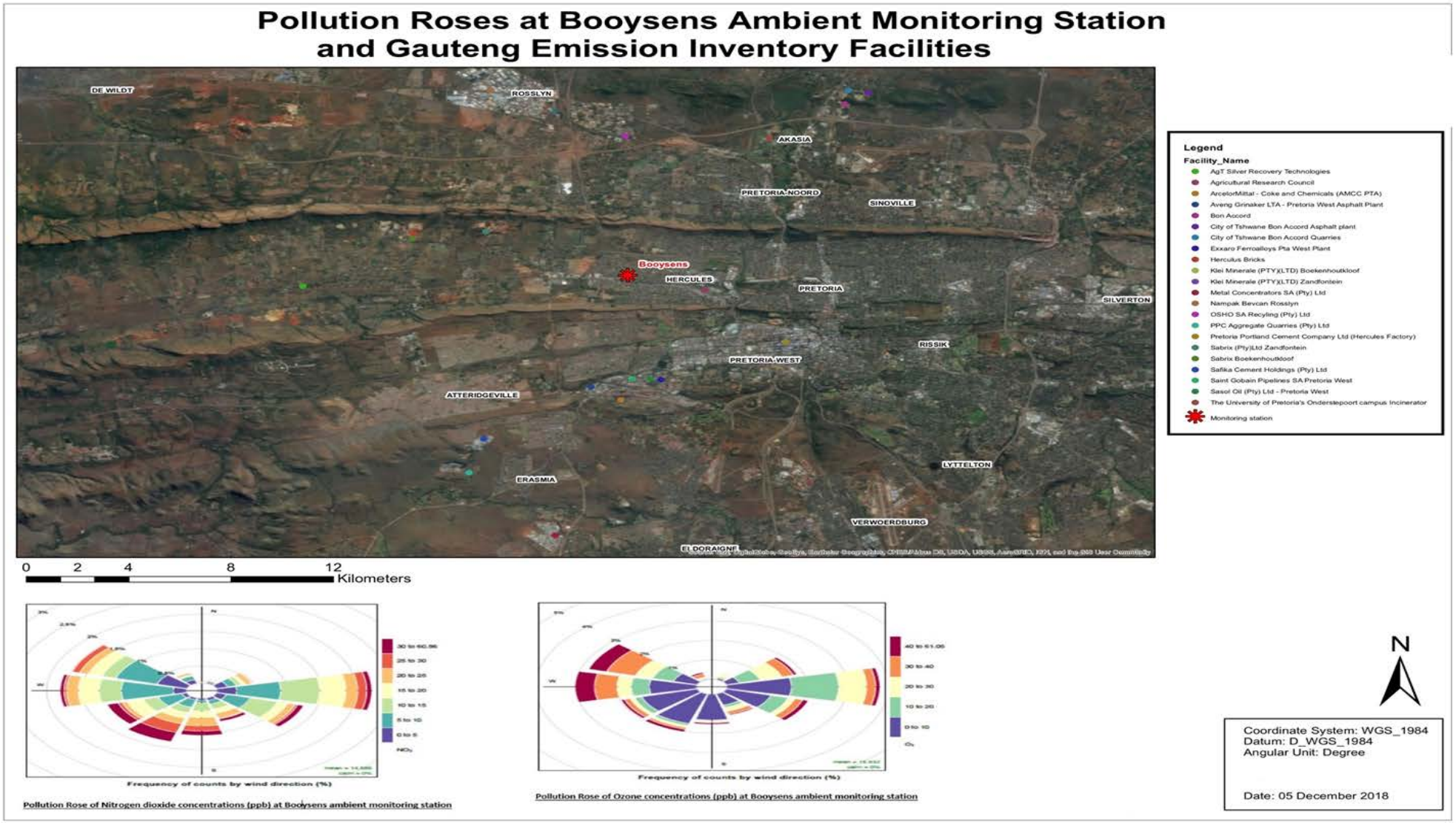

Figure 4.35: Pollution Roses at the Booysens Ambient Monitoring Station and Gauteng Emission Inventory Facilities

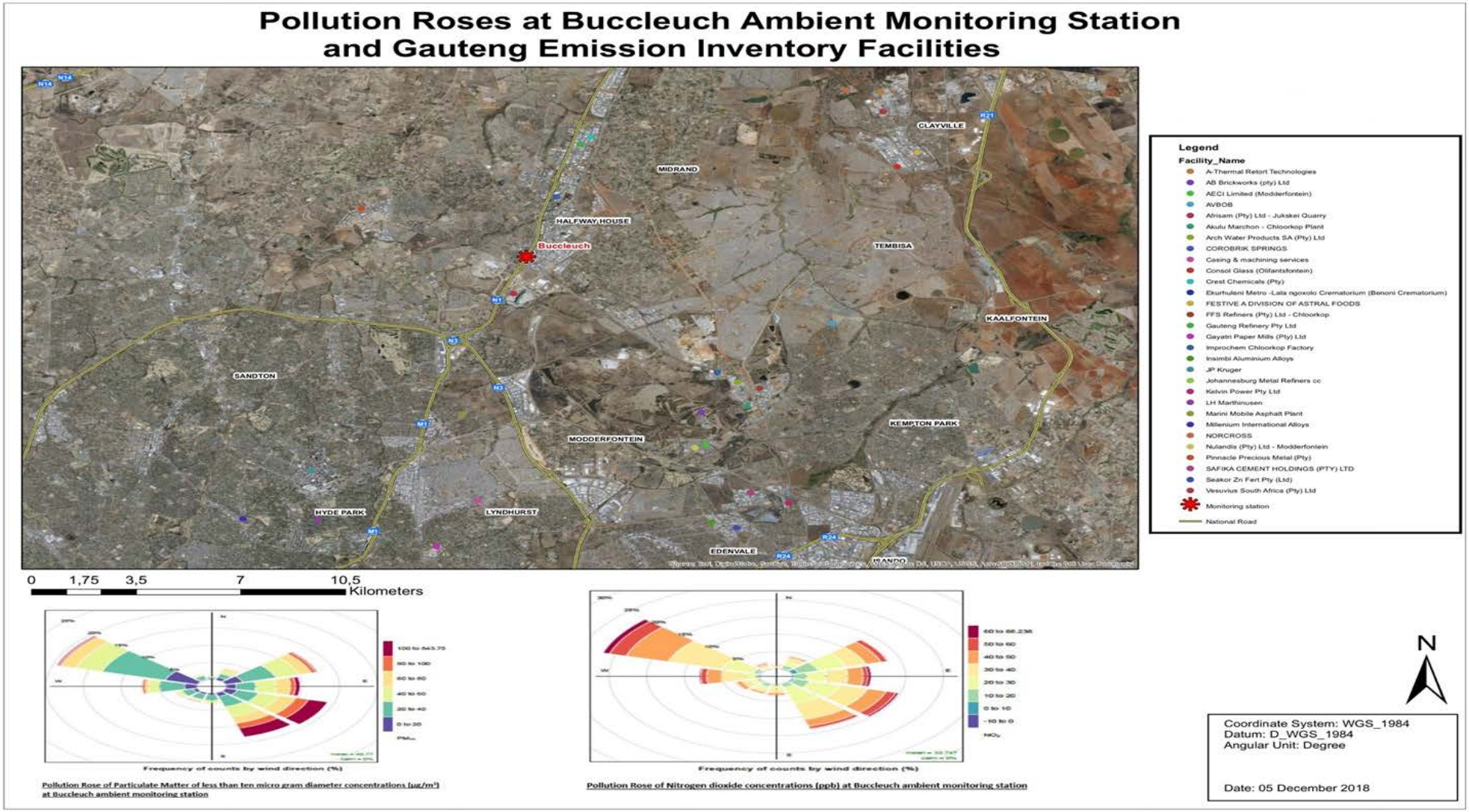

Figure 4.36: Pollution Roses at the Buccleuch Ambient Monitoring Station and Gauteng Emission Inventory Facilities

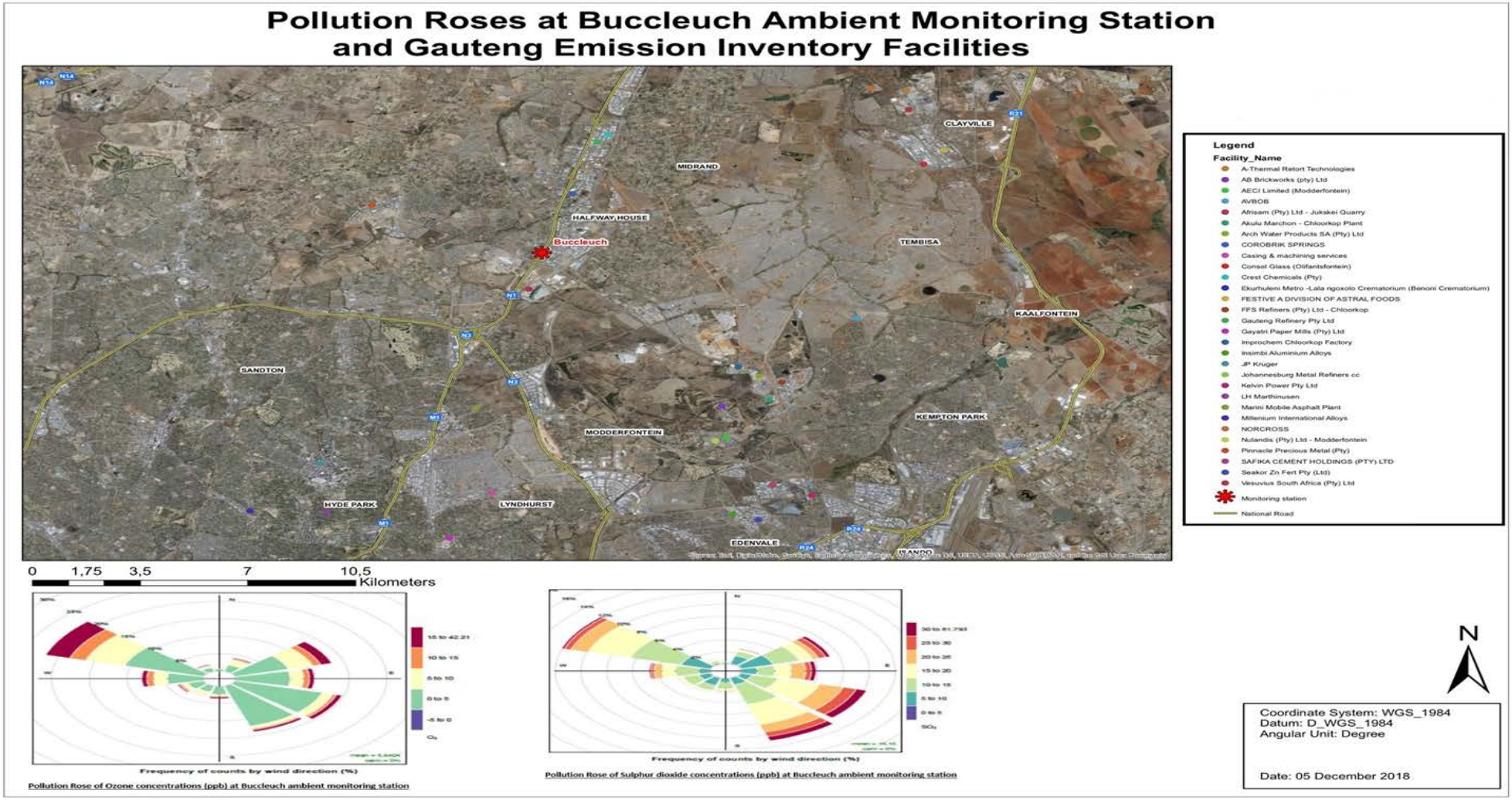

Figure 4.37: Pollution Roses at the Buccleuch Ambient Monitoring Station and Gauteng Emission Inventory Facilities

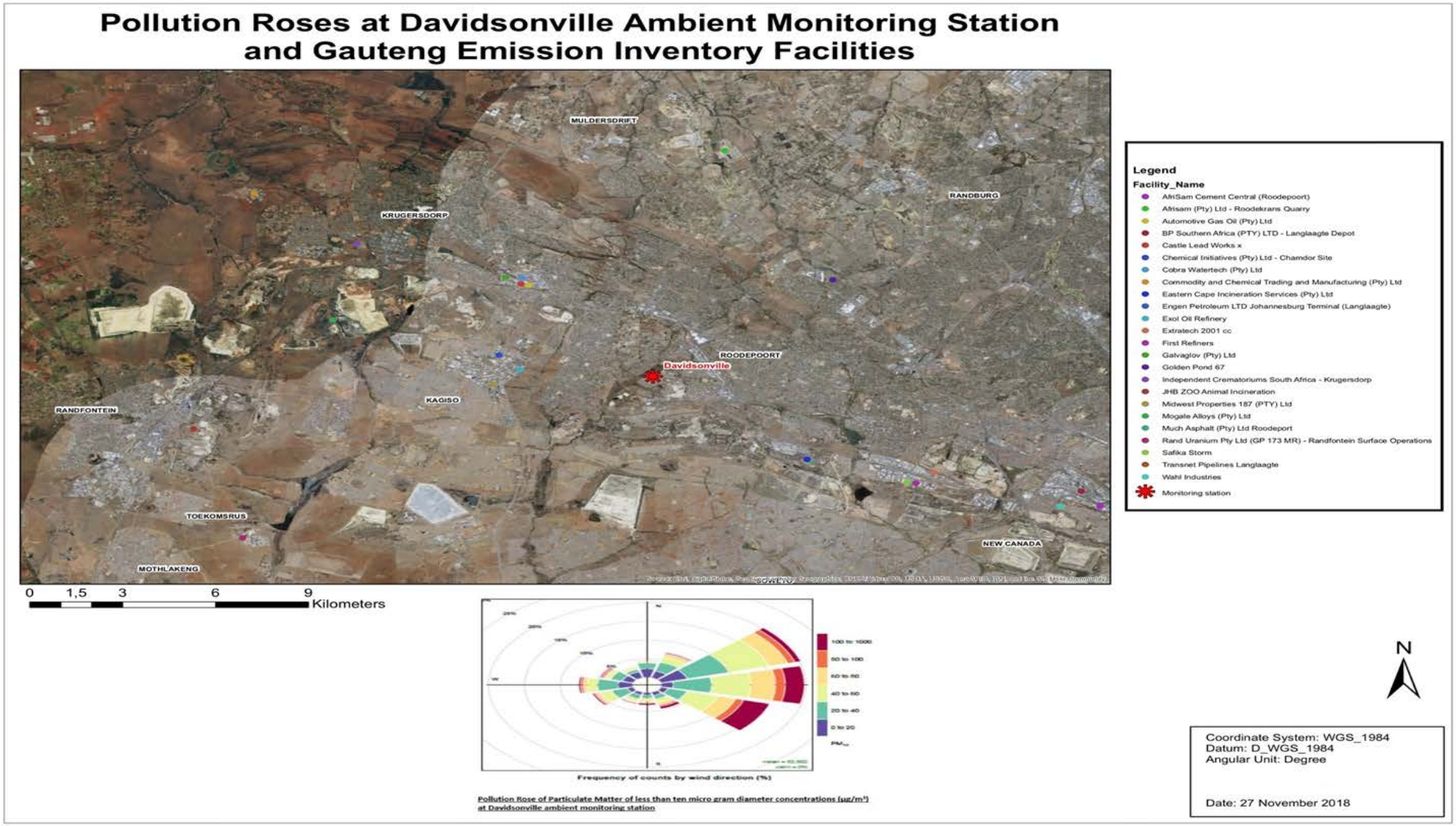

Figure 4.38: Pollution Roses at the Davidsonville Ambient Monitoring Station and Gauteng Emission Inventory Facilities

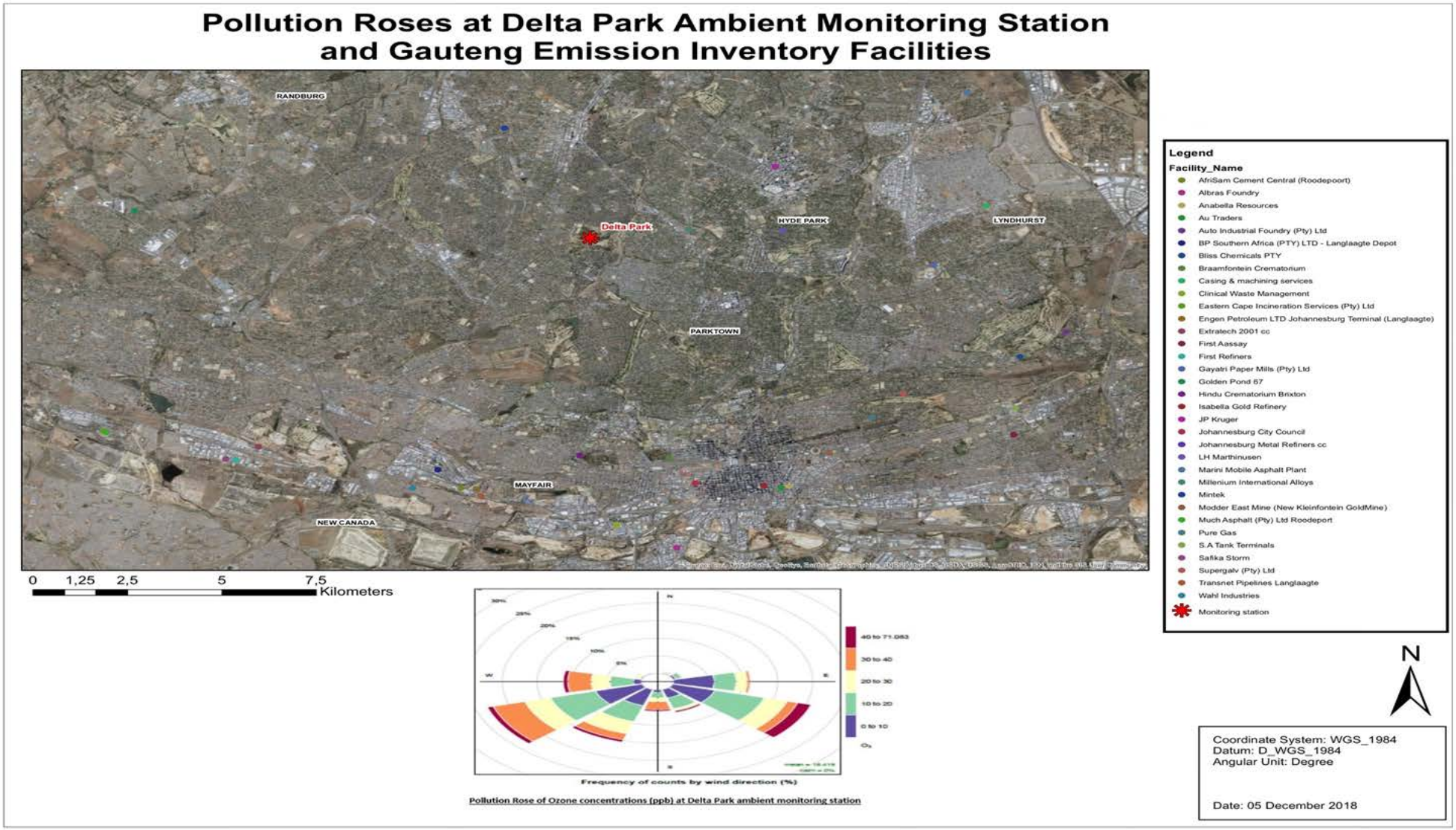

Figure 4.39: Pollution Roses at the Delta Ambient Monitoring Station and Gauteng Emission Inventory Facilities

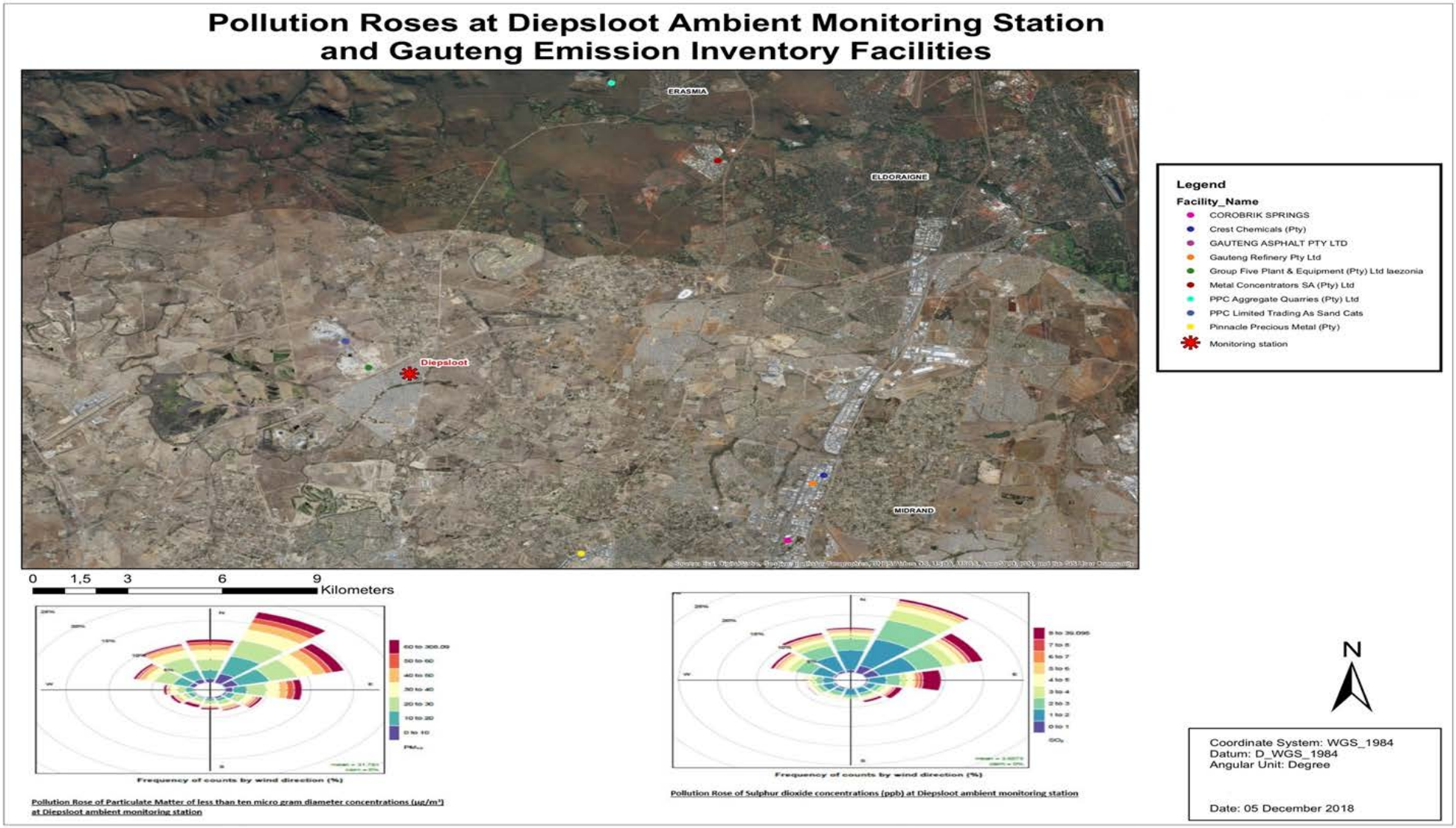

Figure 4.40: Pollution Roses at the Diepsloot Ambient Monitoring Station and Gauteng Emission Inventory Facilities

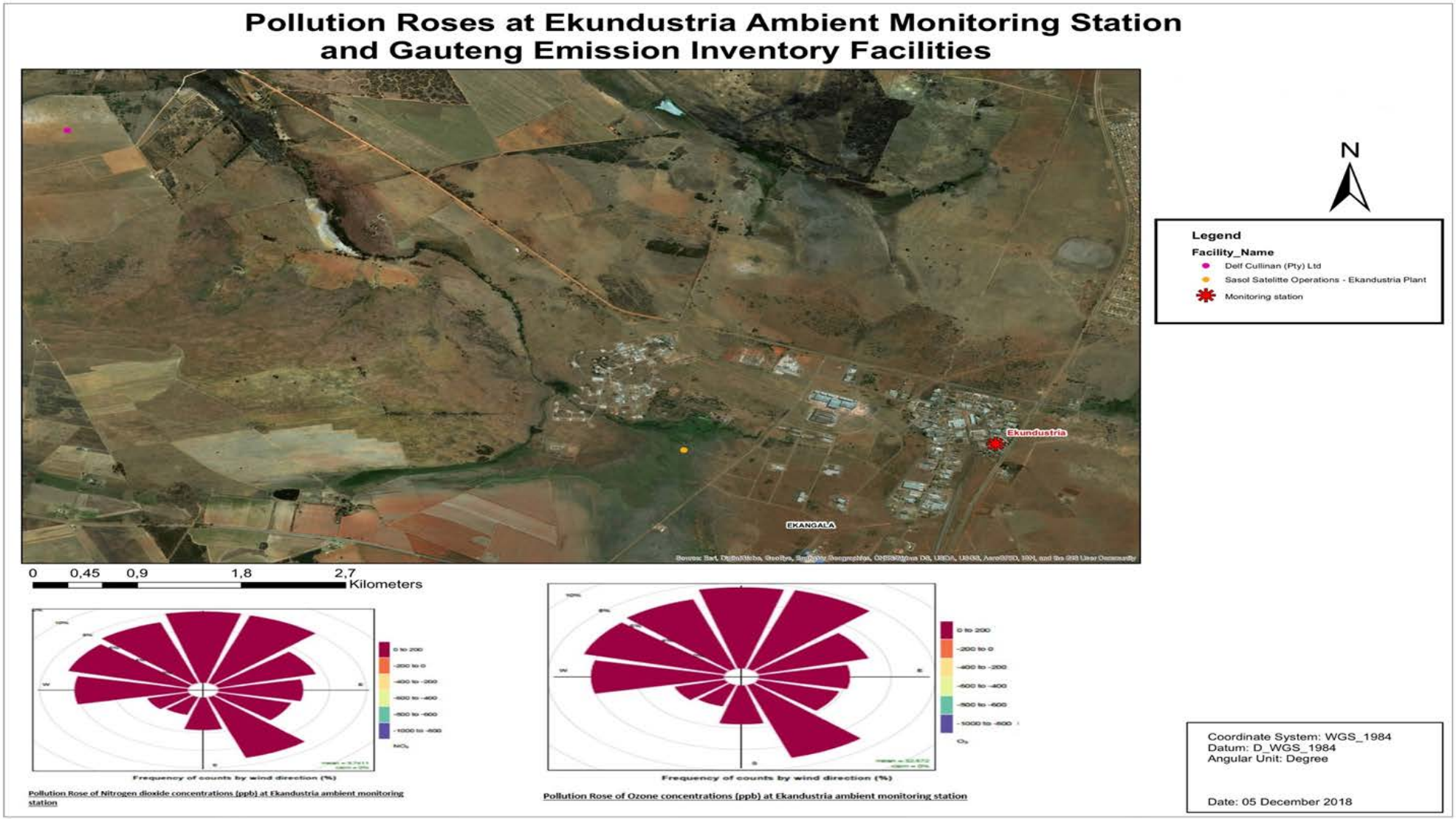

Figure 4.41: Pollution Roses at the Ekandustria Ambient Monitoring Station and Gauteng Emission Inventory Facilities

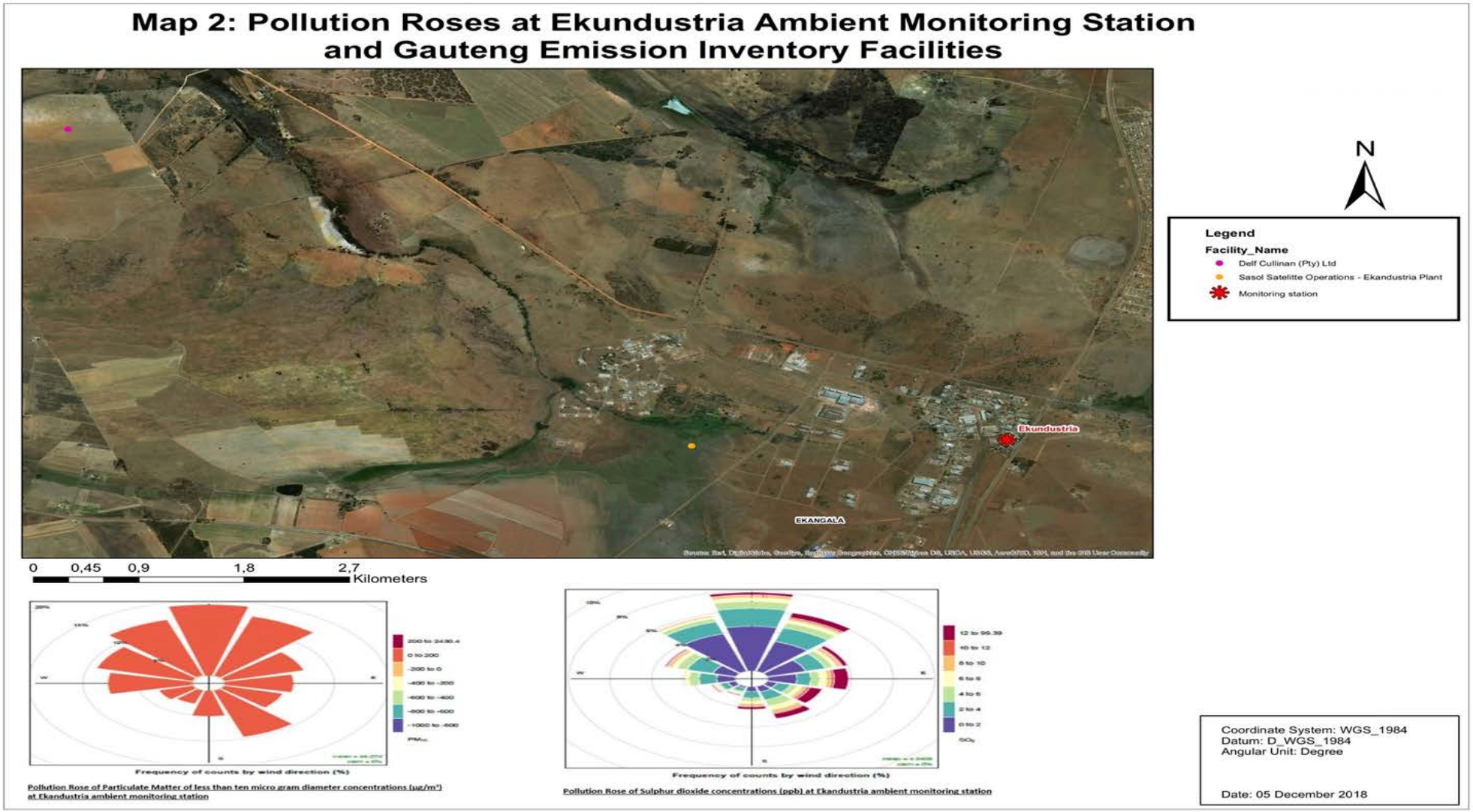

Figure 4.42: Pollution Roses at the Ekandustria Ambient Monitoring Station and Gauteng Emission Inventory Facilities

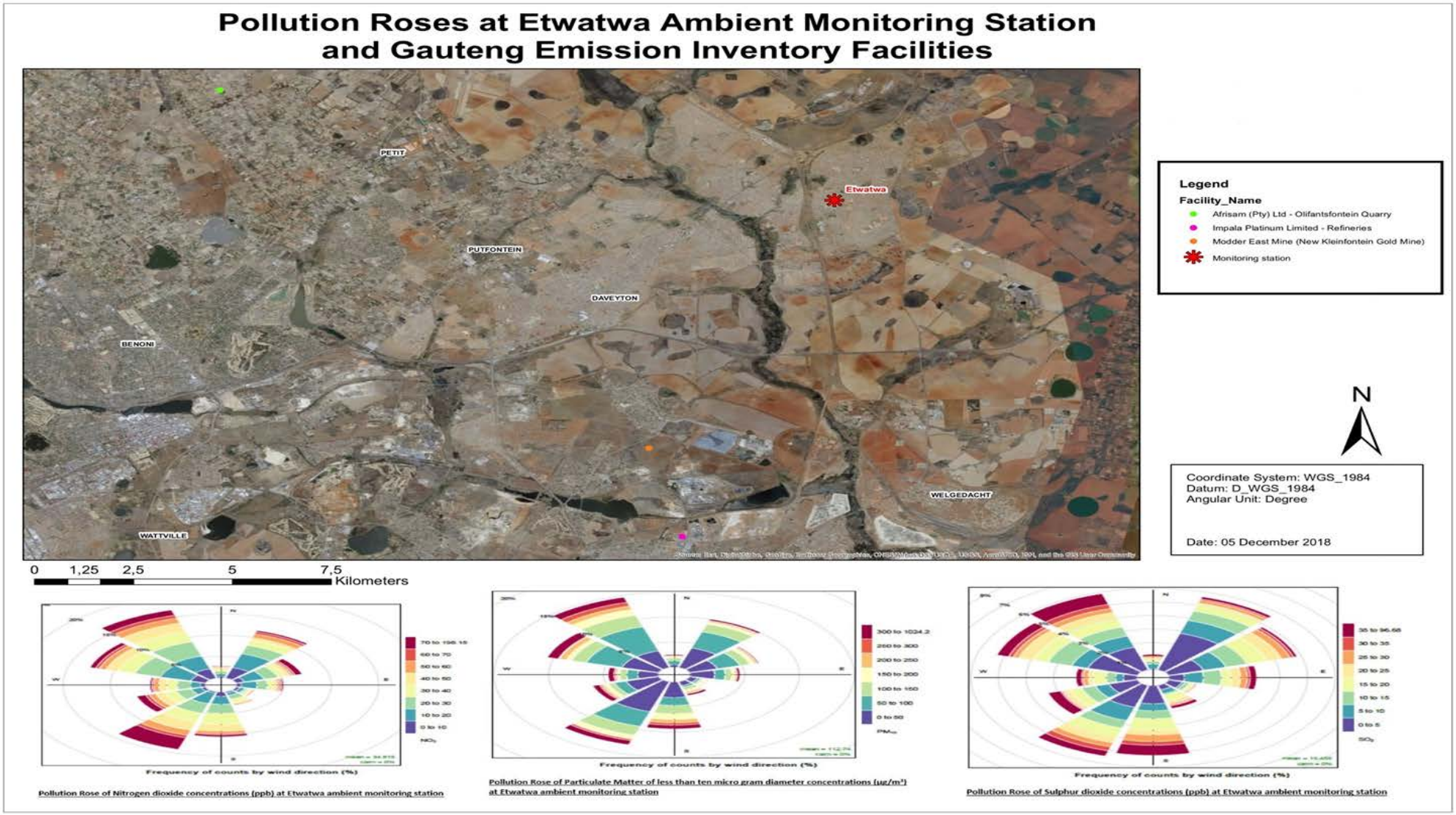

Figure 4.43: Pollution Roses at the Etwatwa Ambient Monitoring Station and Gauteng Emission Inventory Facilities

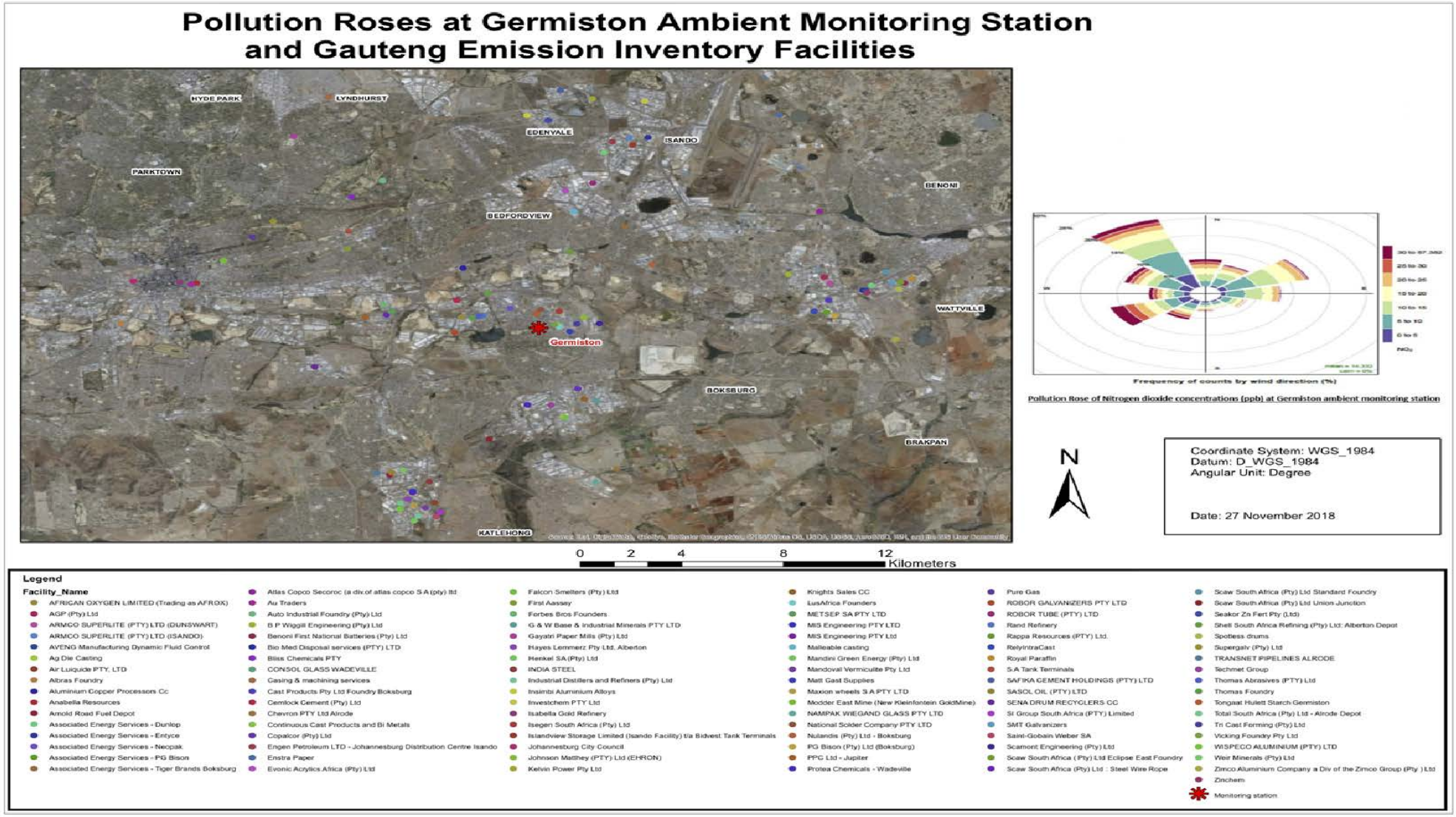

Figure 4.44: Pollution Roses at the Germiston Ambient Monitoring Station and Gauteng Emission Inventory Facilities

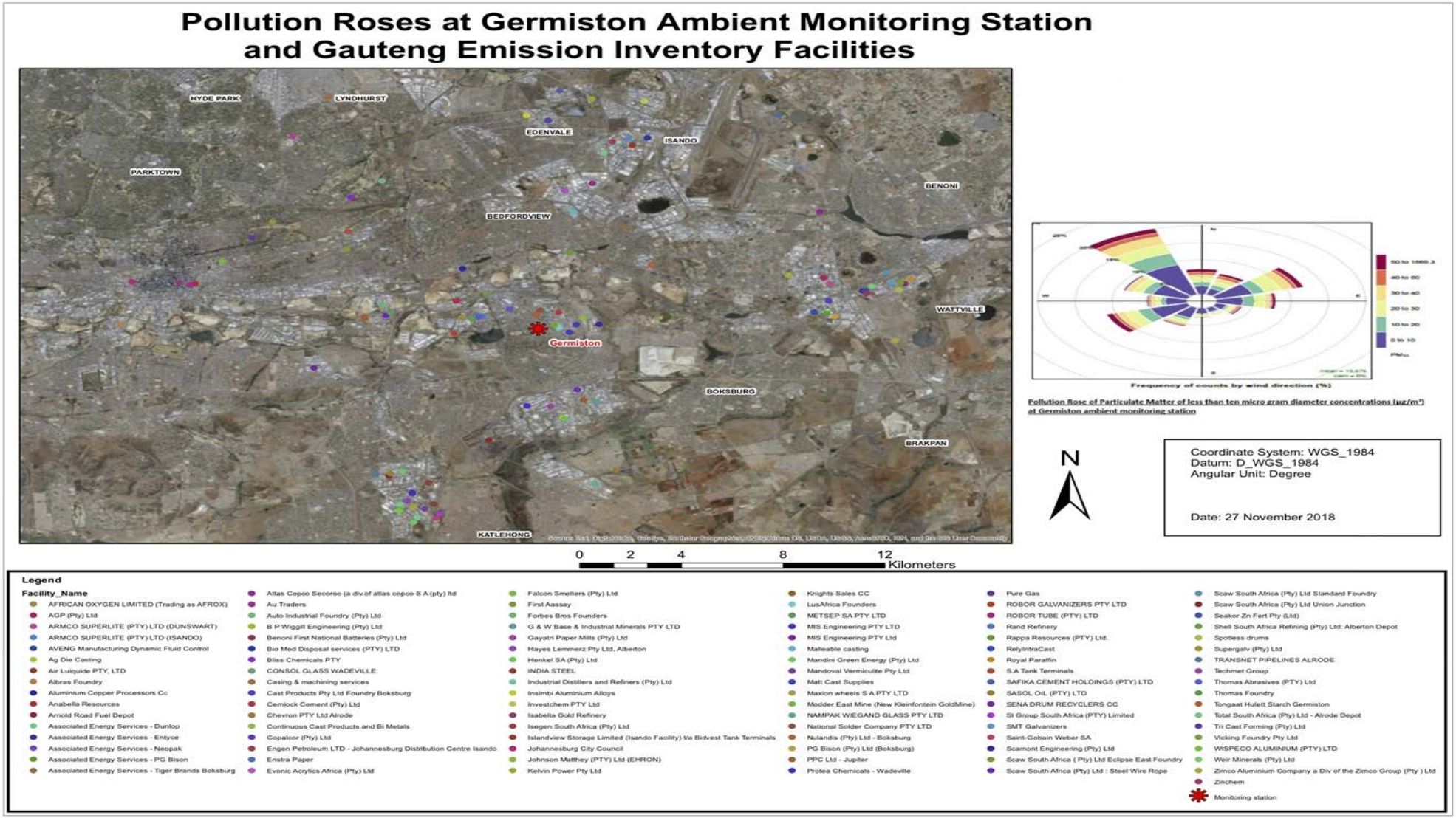

Figure 4.45: Pollution Roses at the Germiston Ambient Monitoring Station and Gauteng Emission Inventory Facilities

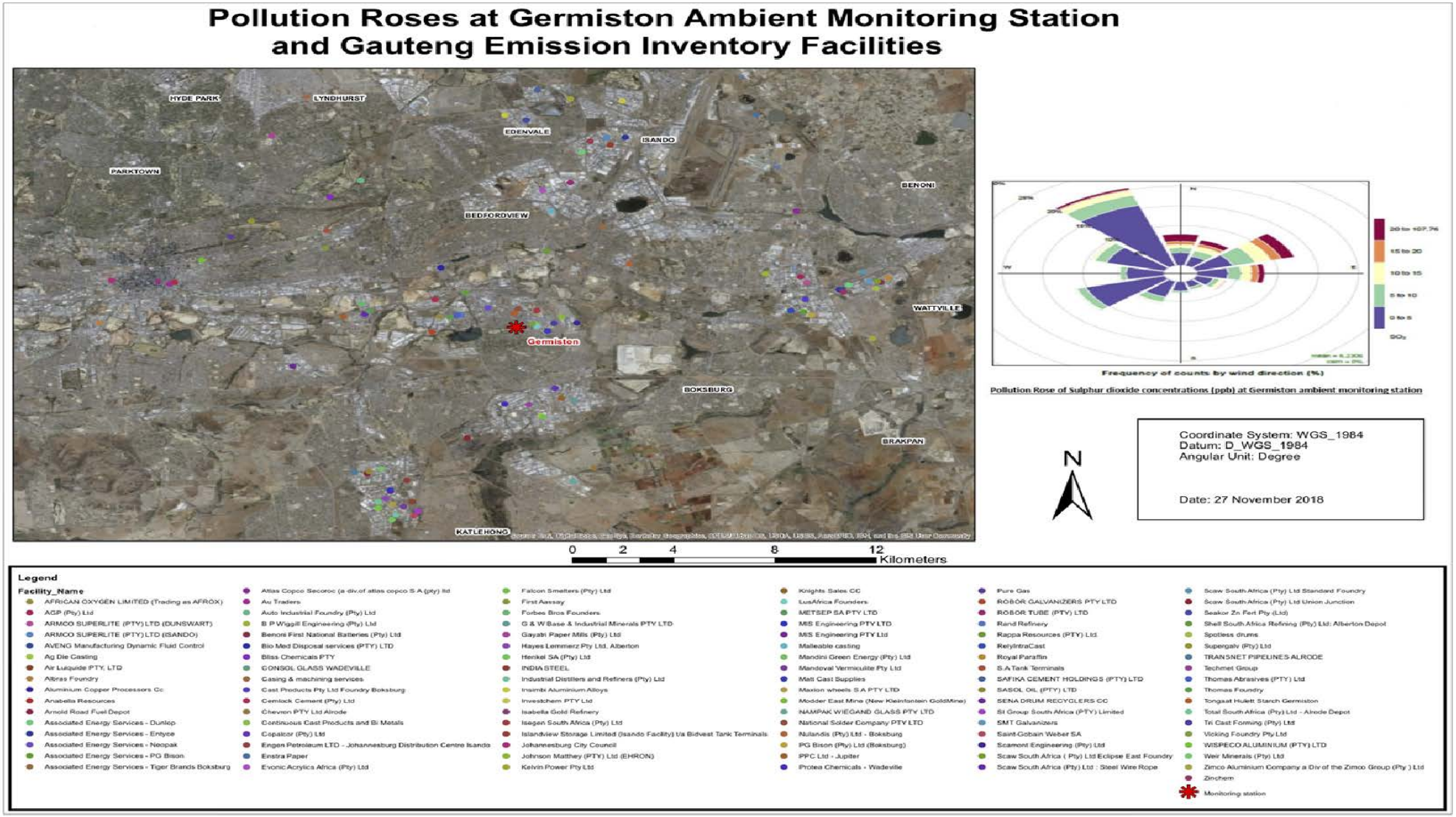

Figure 4.46: Pollution Roses at the Germiston Ambient Monitoring Station and Gauteng Emission Inventory Facilities

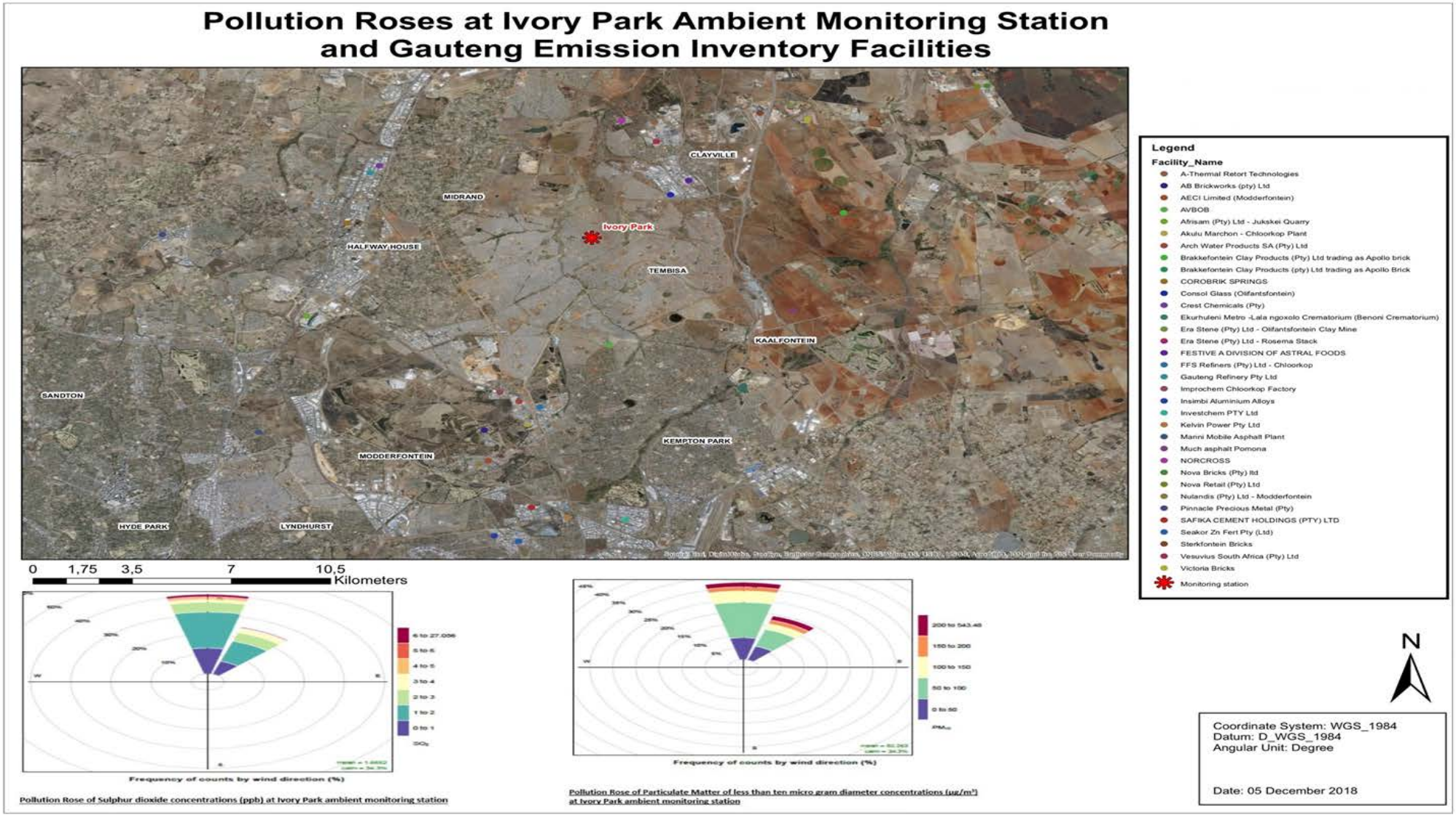

Figure 4.47: Pollution Roses at the Ivory Park ambient Monitoring Station and Gauteng Emission Inventory Facilities

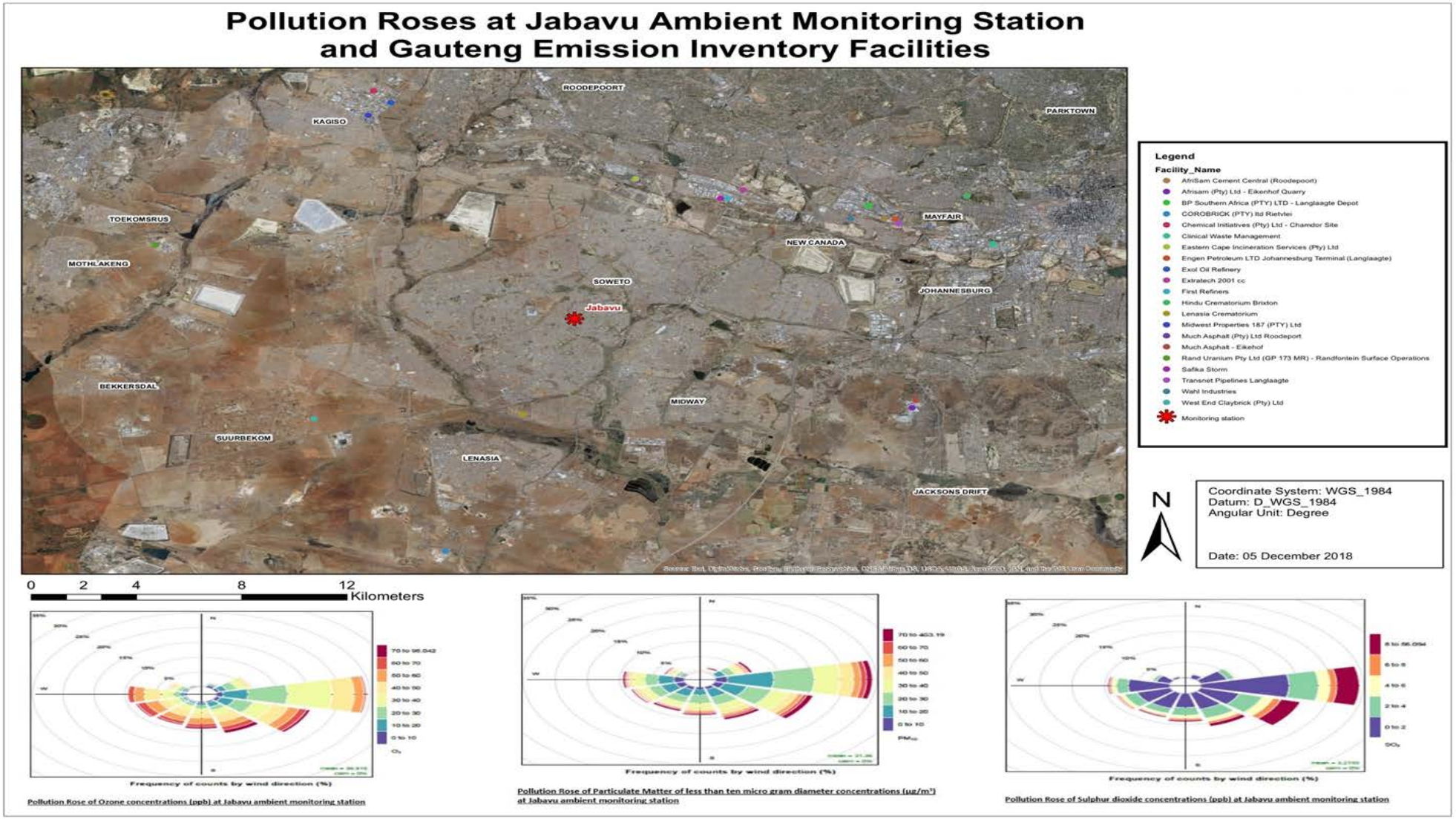

Figure 4.48: Pollution Roses at the Jabavu Ambient Monitoring Station and Gauteng Emission Inventory Facilities

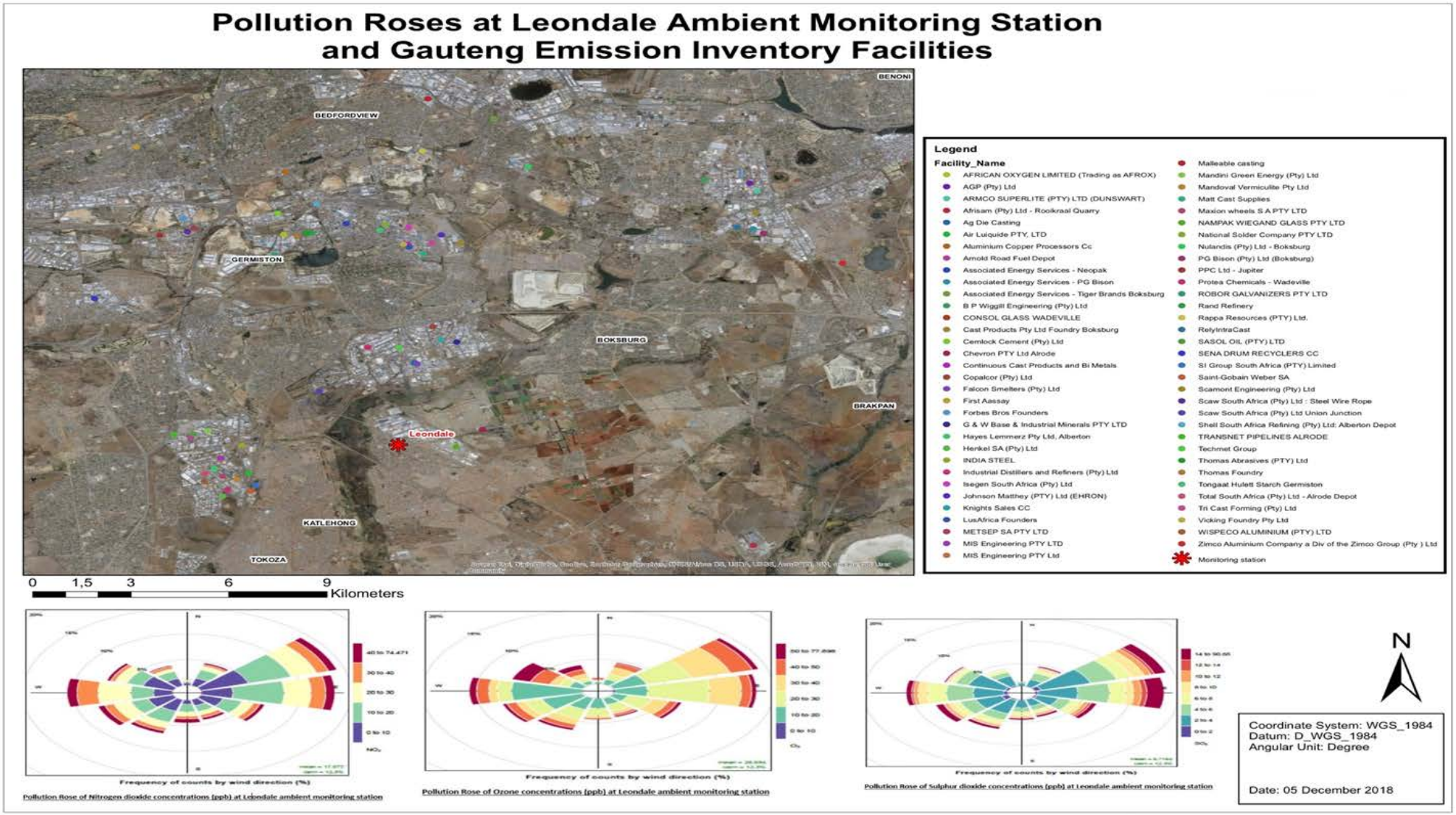

Figure 4.49: Pollution Roses at the Leondale Ambient Monitoring Station and Gauteng Emission Inventory Facilities

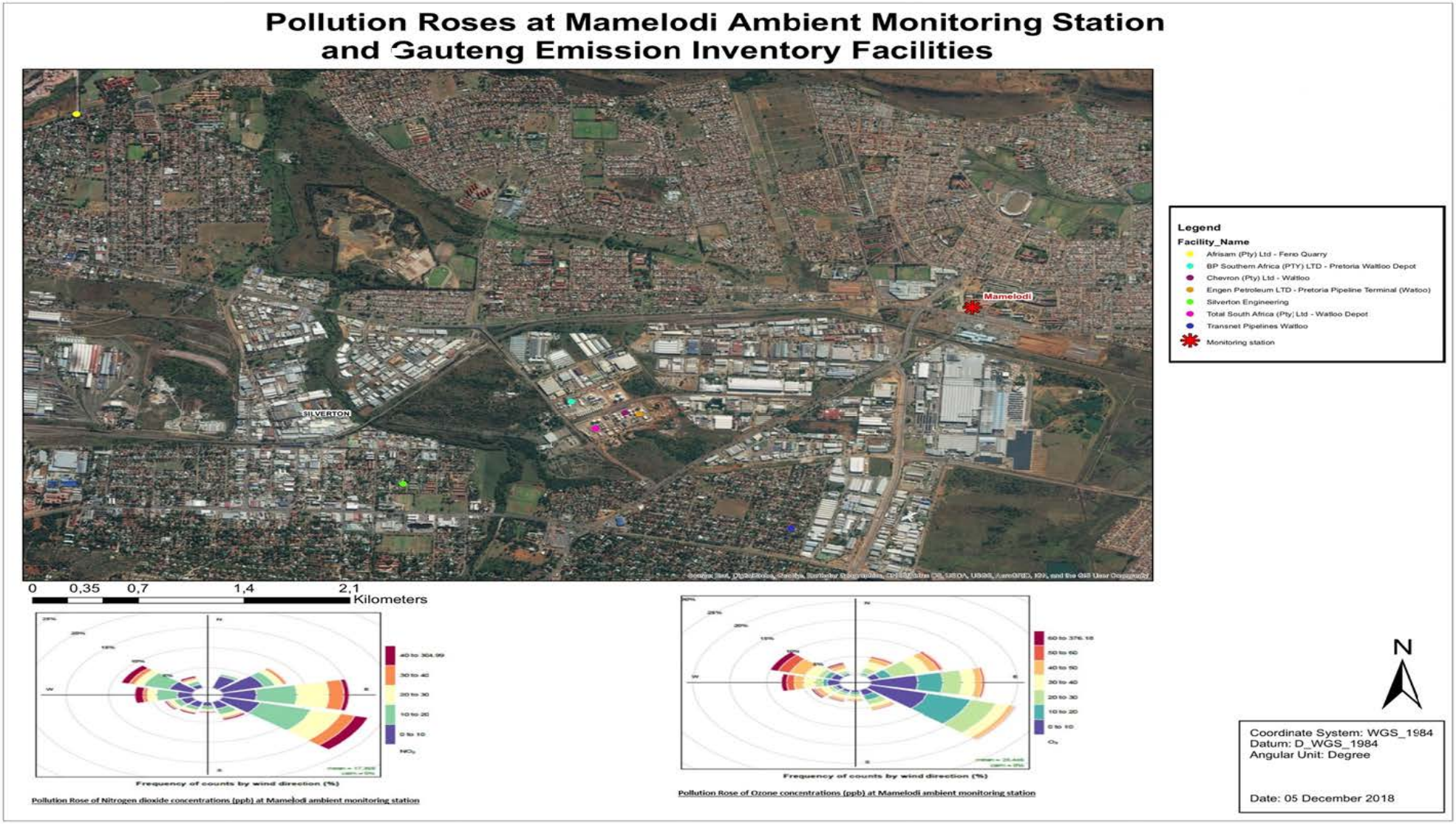

Figure 4.50: Pollution Roses at the Mamelodi Ambient Monitoring Station and Gauteng Emission Inventory Facilities

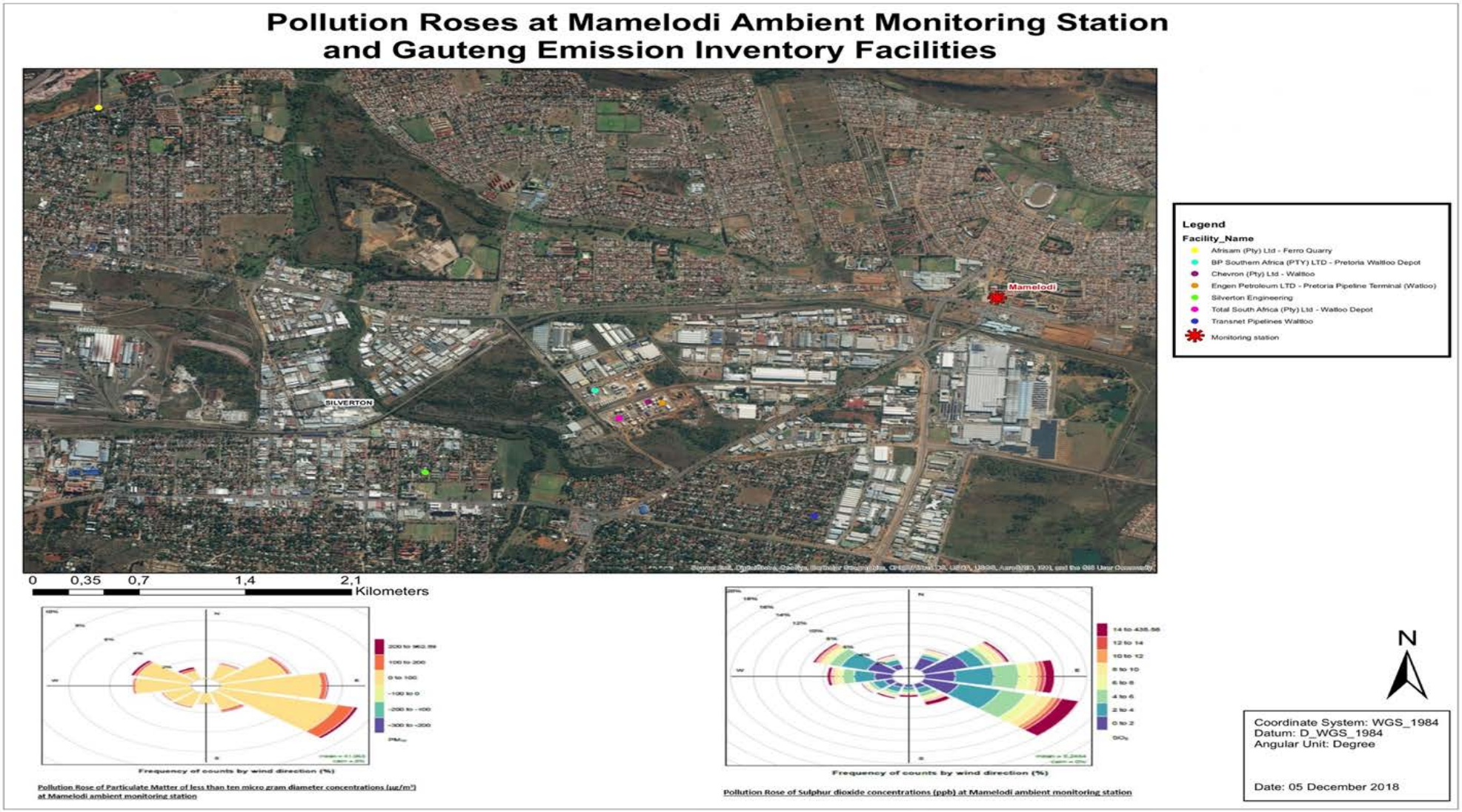

Figure 4.51: Pollution Roses at the Mamelodi Ambient Monitoring Station and Gauteng Emission Inventory Facilities

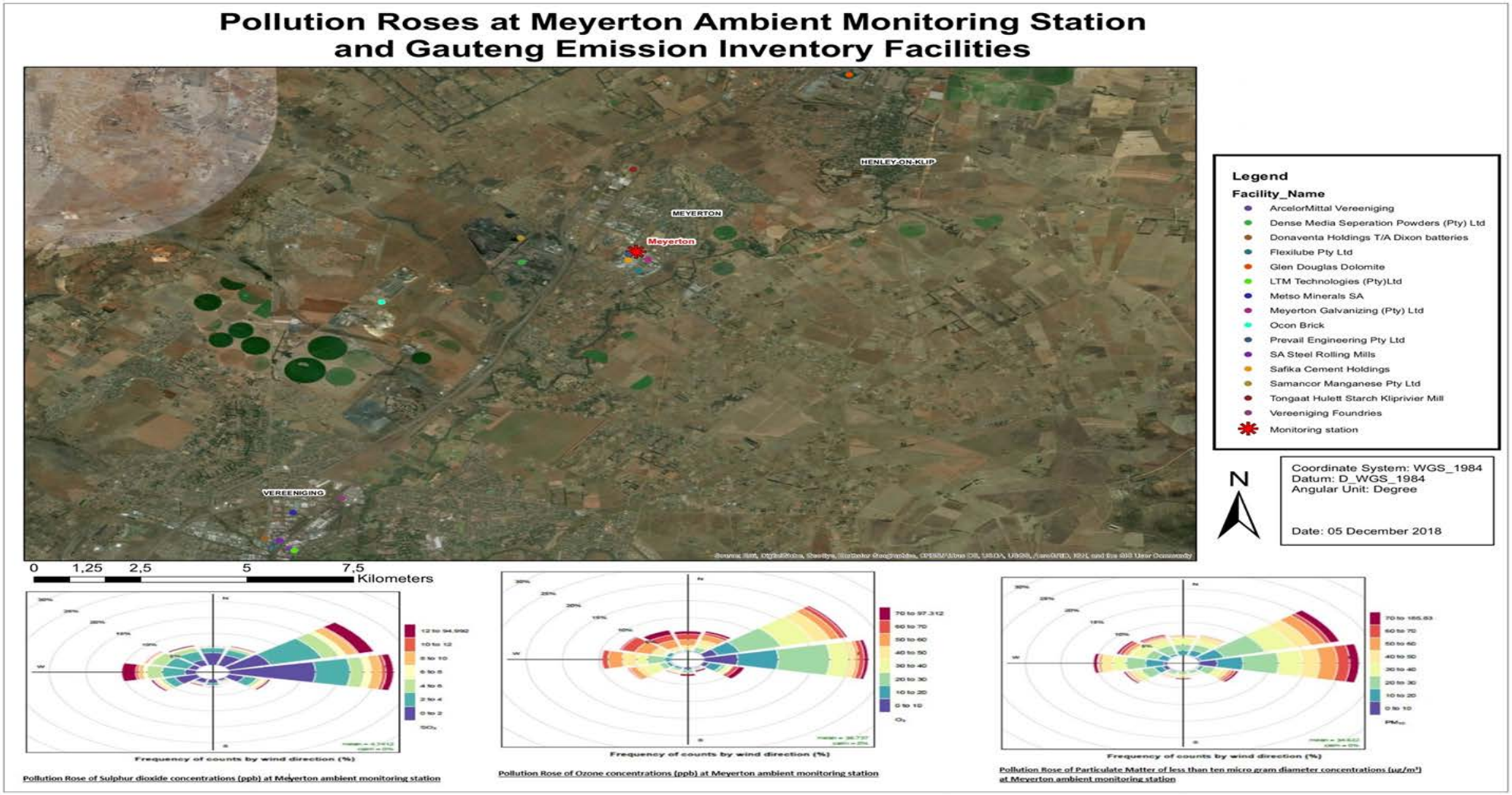

Figure 4.52: Pollution Roses at the Meyerton Ambient Monitoring Station and Gauteng Emission Inventory Facilities

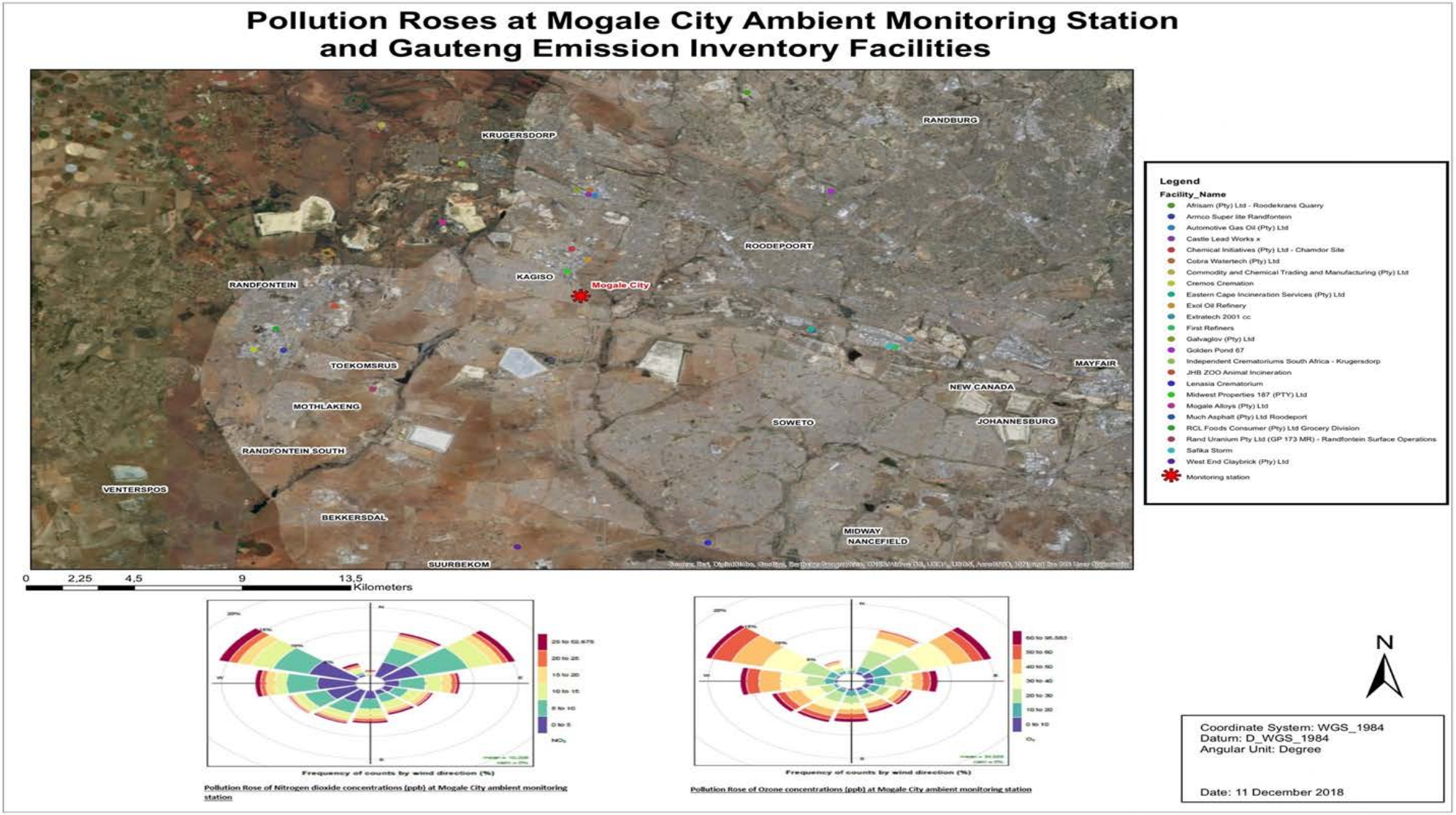

Figure 4.53: Pollution Roses at the Mogale City Ambient Monitoring Station and Gauteng Emission Inventory Facilities

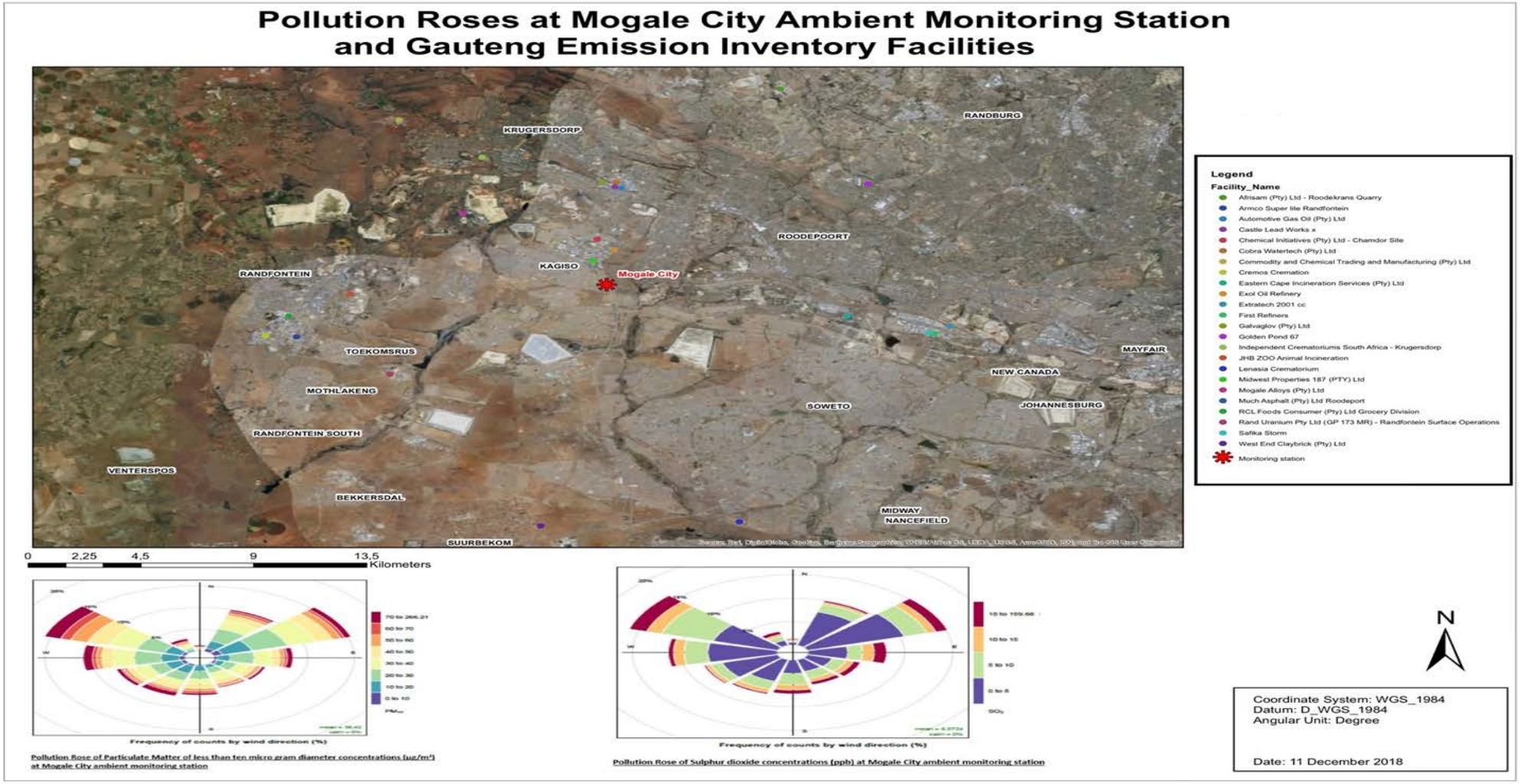

Figure 4.54: Pollution Roses at the Mogale City Ambient Monitoring Station and Gauteng

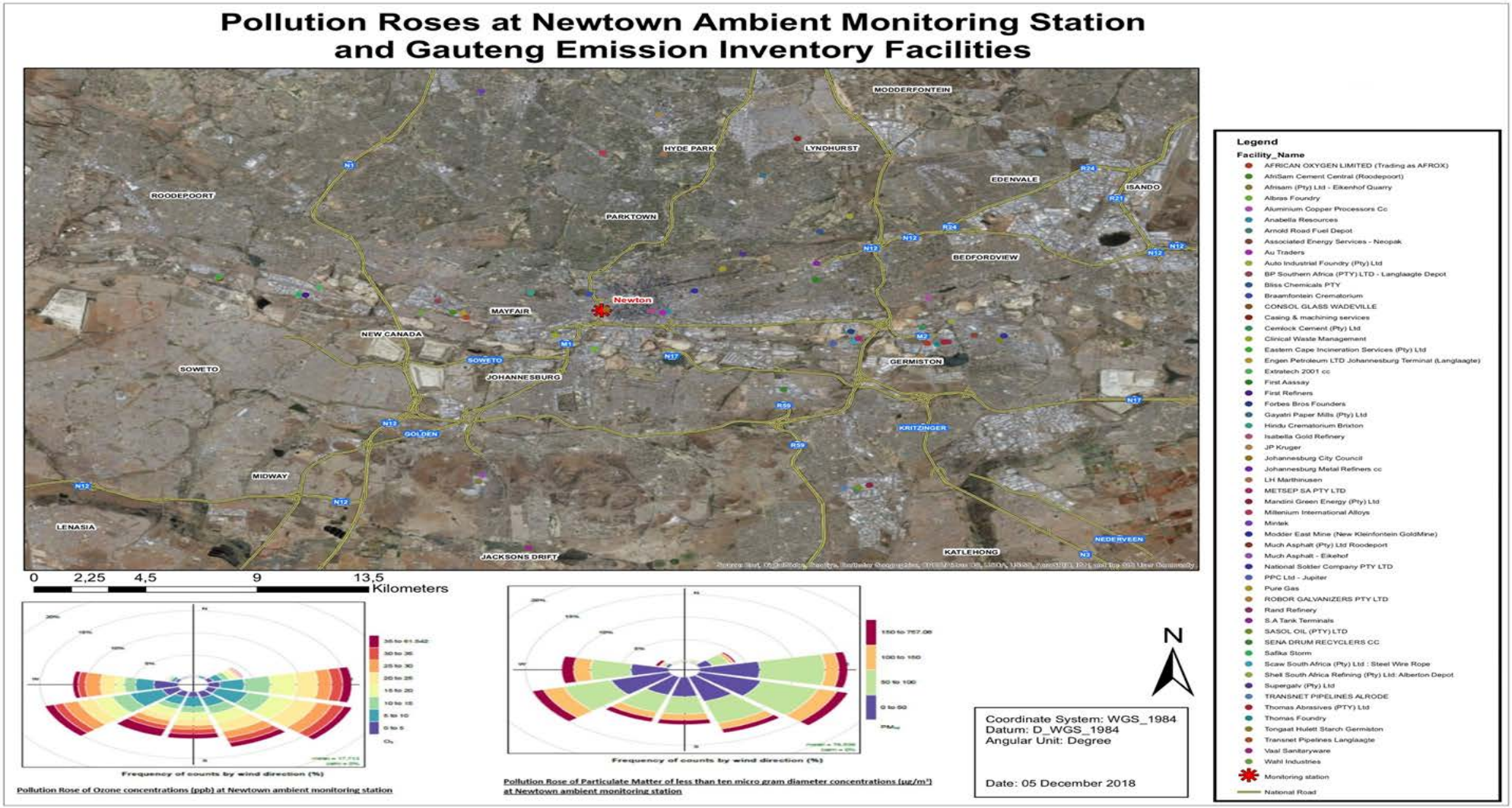

Figure 4.55: Pollution Roses at the Newtown Ambient Monitoring Station and Gauteng Emission Inventory Facilities

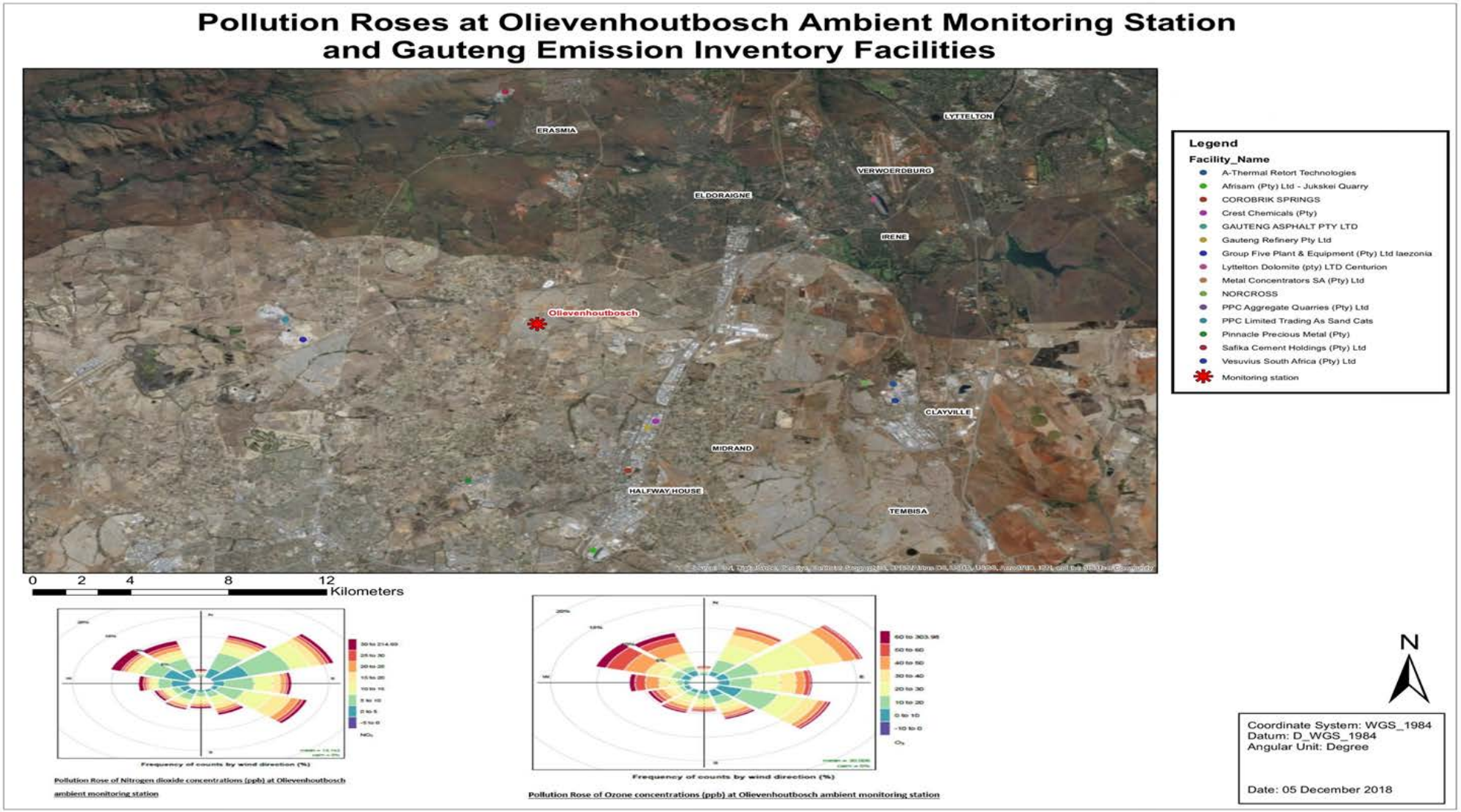

Figure 4.56: Pollution Roses at the Olievenhoutbosch Ambient Monitoring Station and Gauteng Emission Inventory Facilities

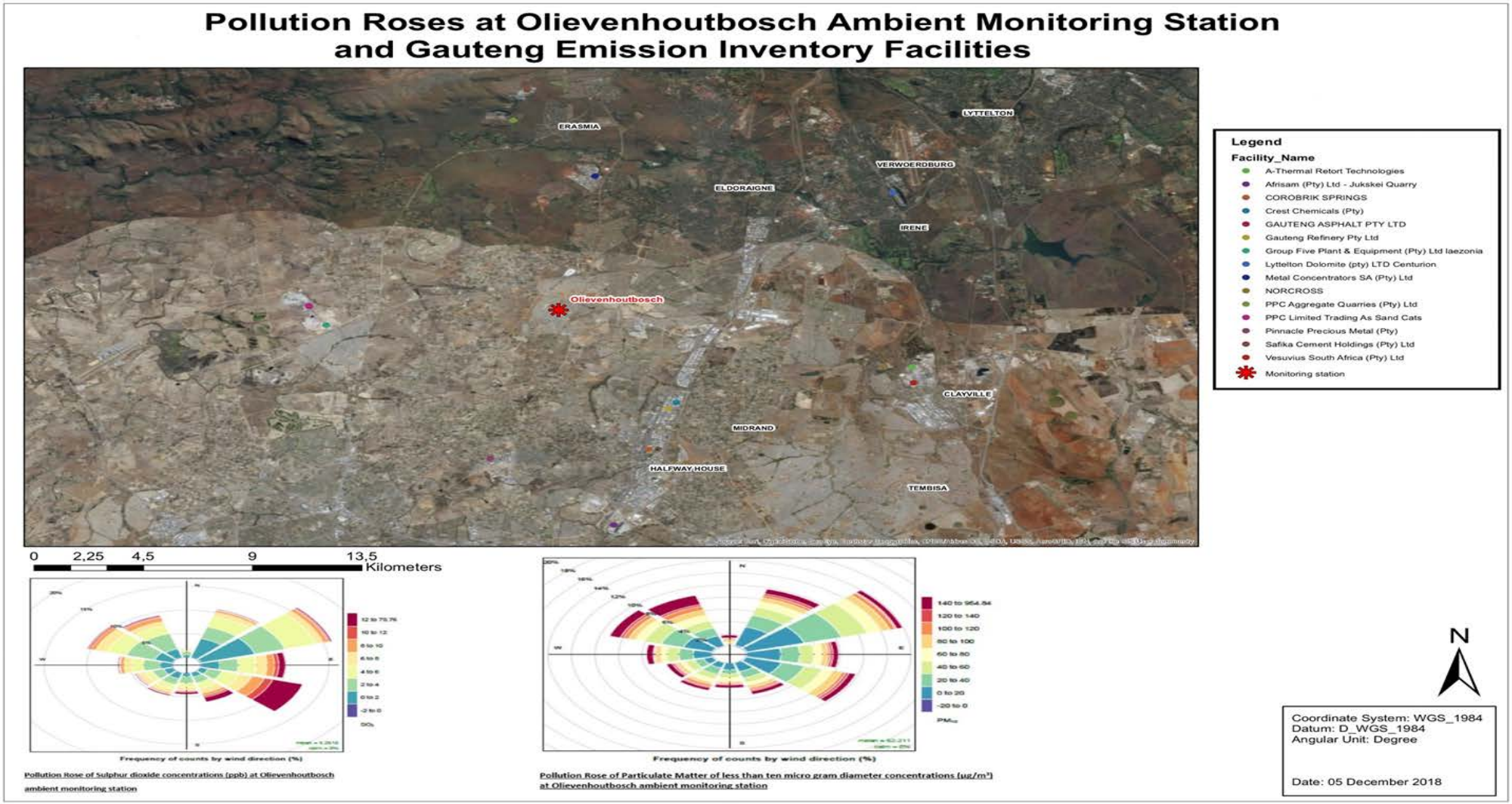

Figure 4.57: Pollution Roses at the Olievenhoutbosch Ambient Monitoring Station and Gauteng Emission Inventory Facilities

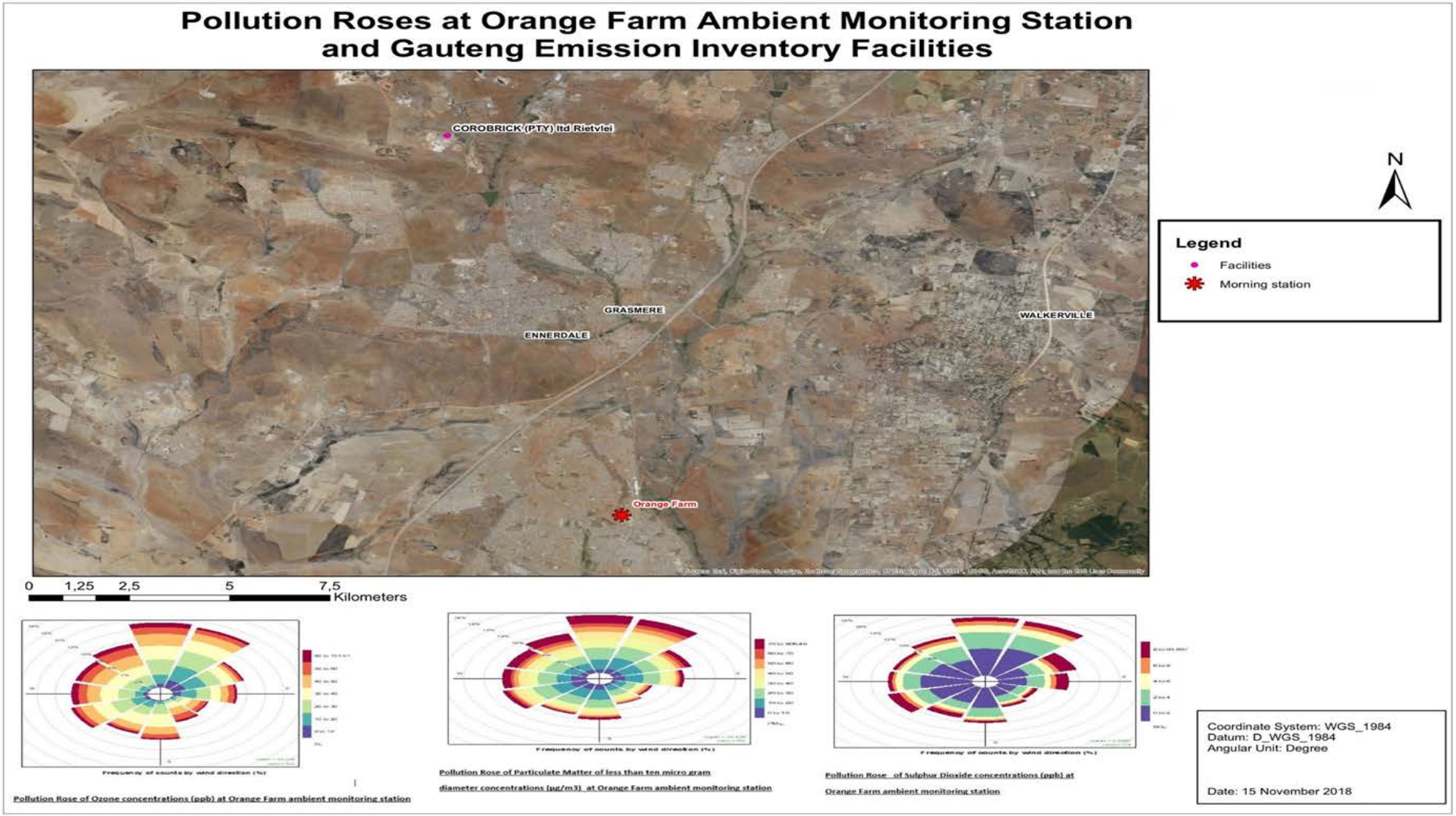

Figure 4.58: Pollution Roses at the Orange Farm Ambient Monitoring Station and Gauteng Emission Inventory Facilities

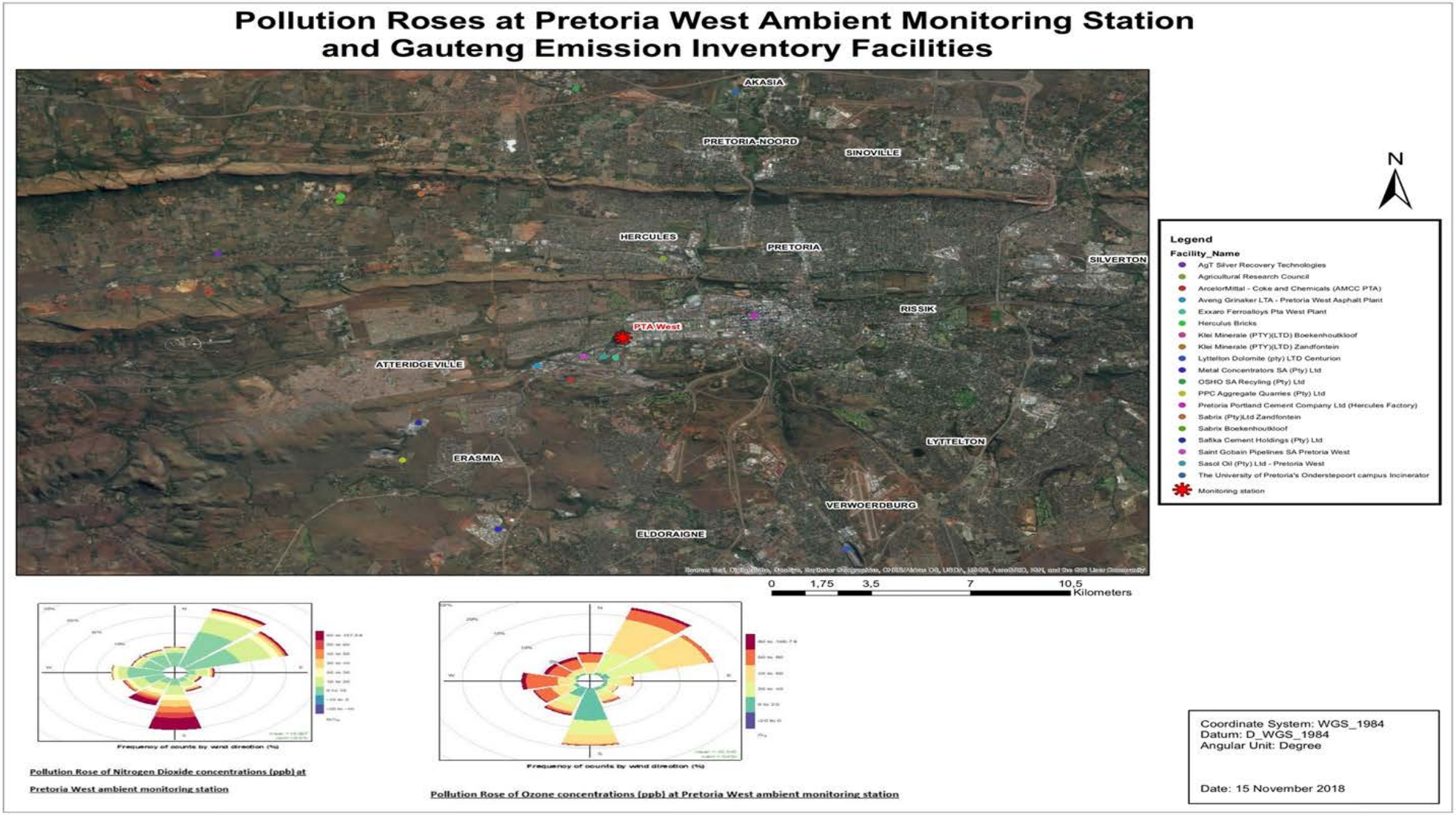

Figure 4.59: Pollution Roses at the Pretoria West Ambient Monitoring Station and Gauteng Emission Inventory Facilities

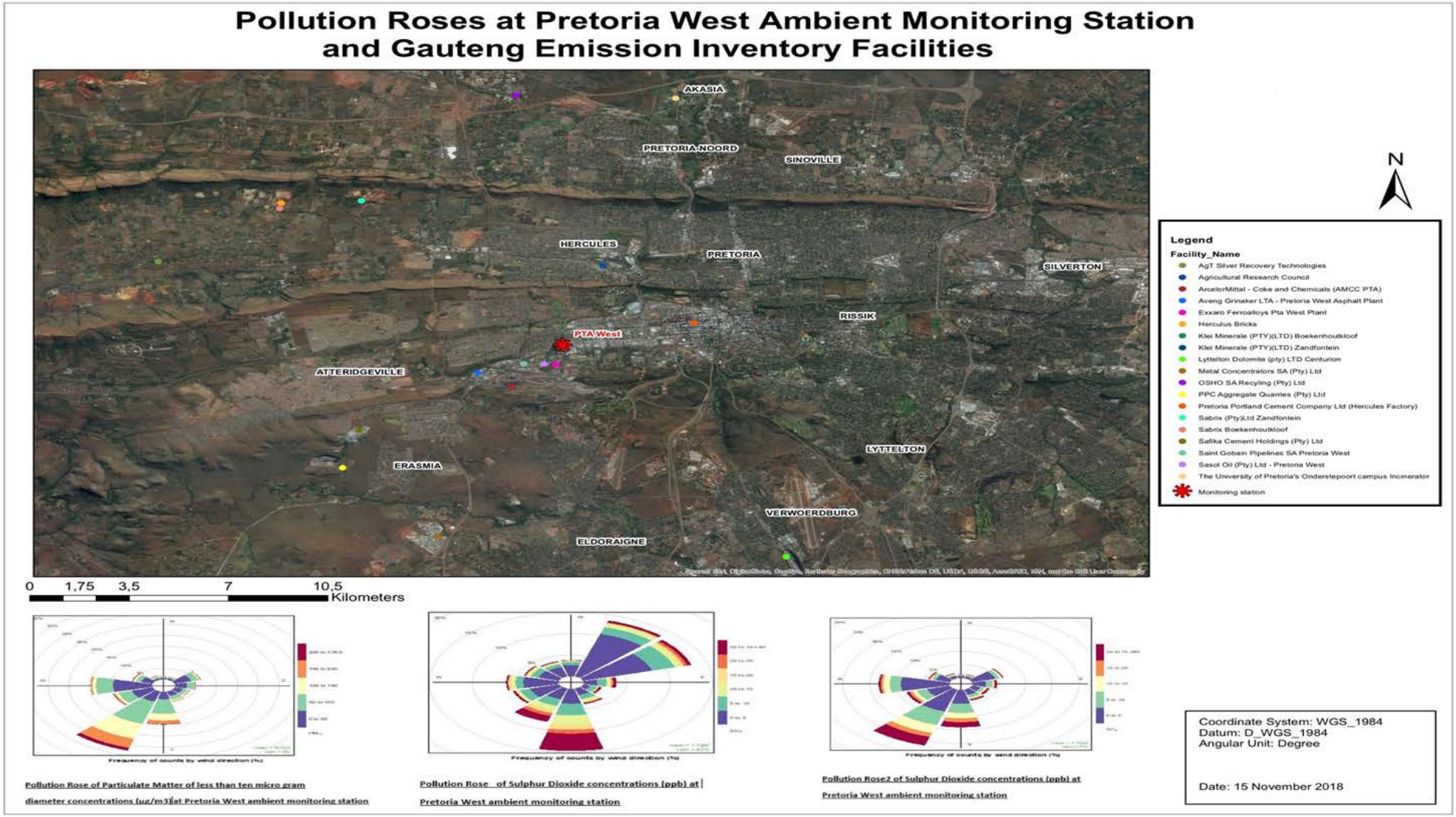

Figure 4.60: Pollution Roses at the Pretoria West Ambient Monitoring Station and Gauteng Emission Inventory Facilities

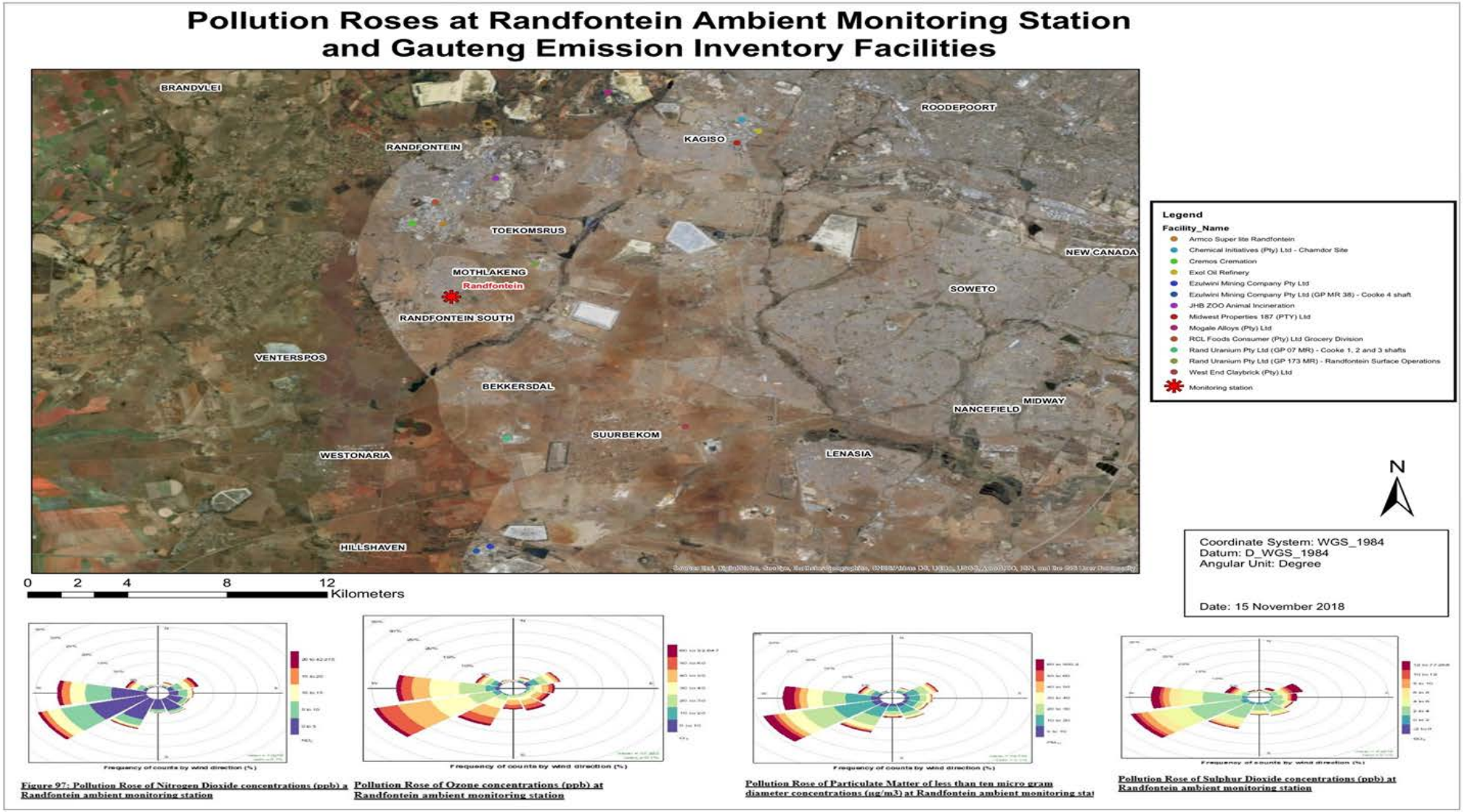

Figure 4.61: Pollution Roses at the Randfontein Ambient Monitoring Station and Gauteng Emission Inventory Facilities

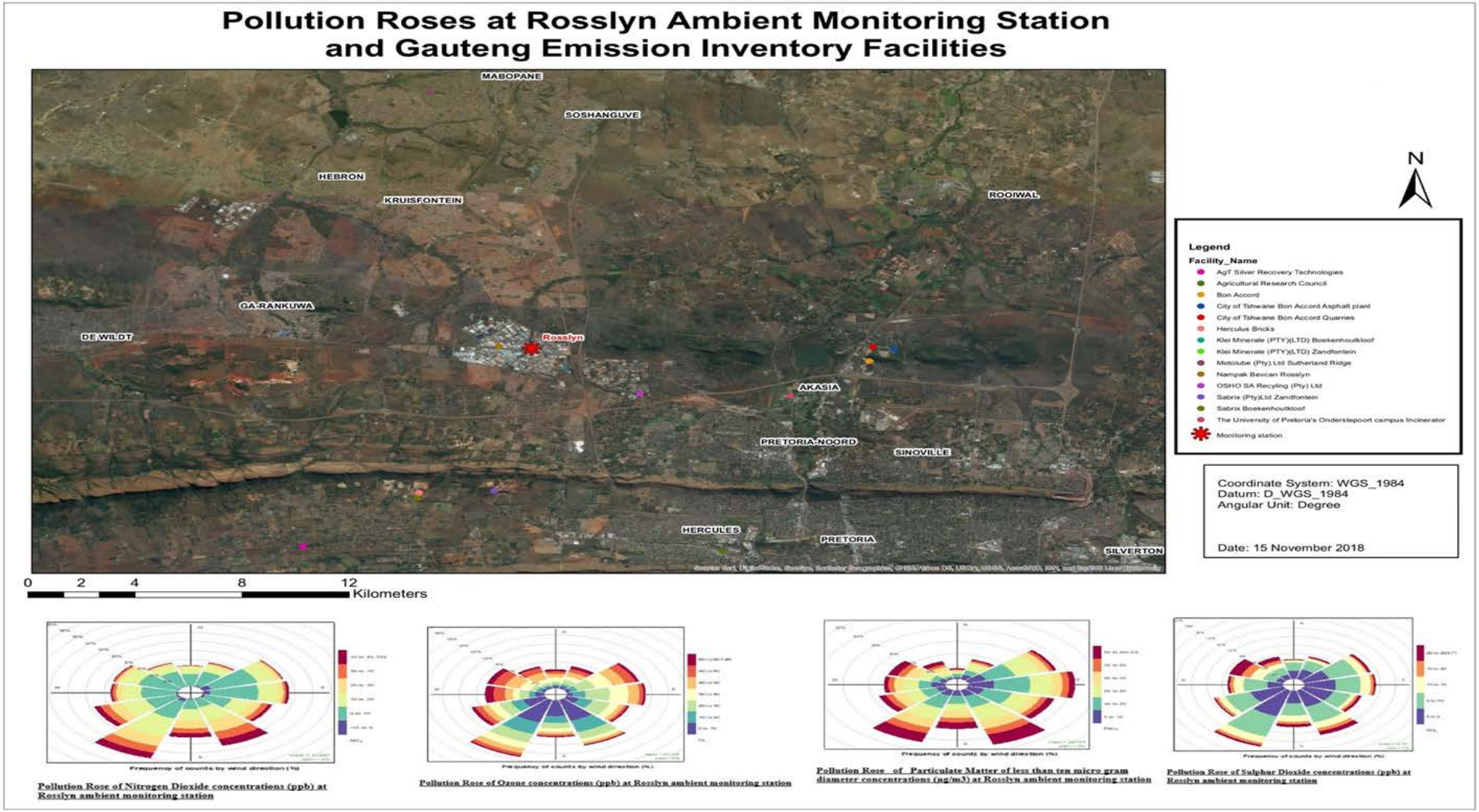

Figure 4.62: Pollution Roses at the Rosslyn Ambient Monitoring Station and Gauteng Emission Inventory Facilities

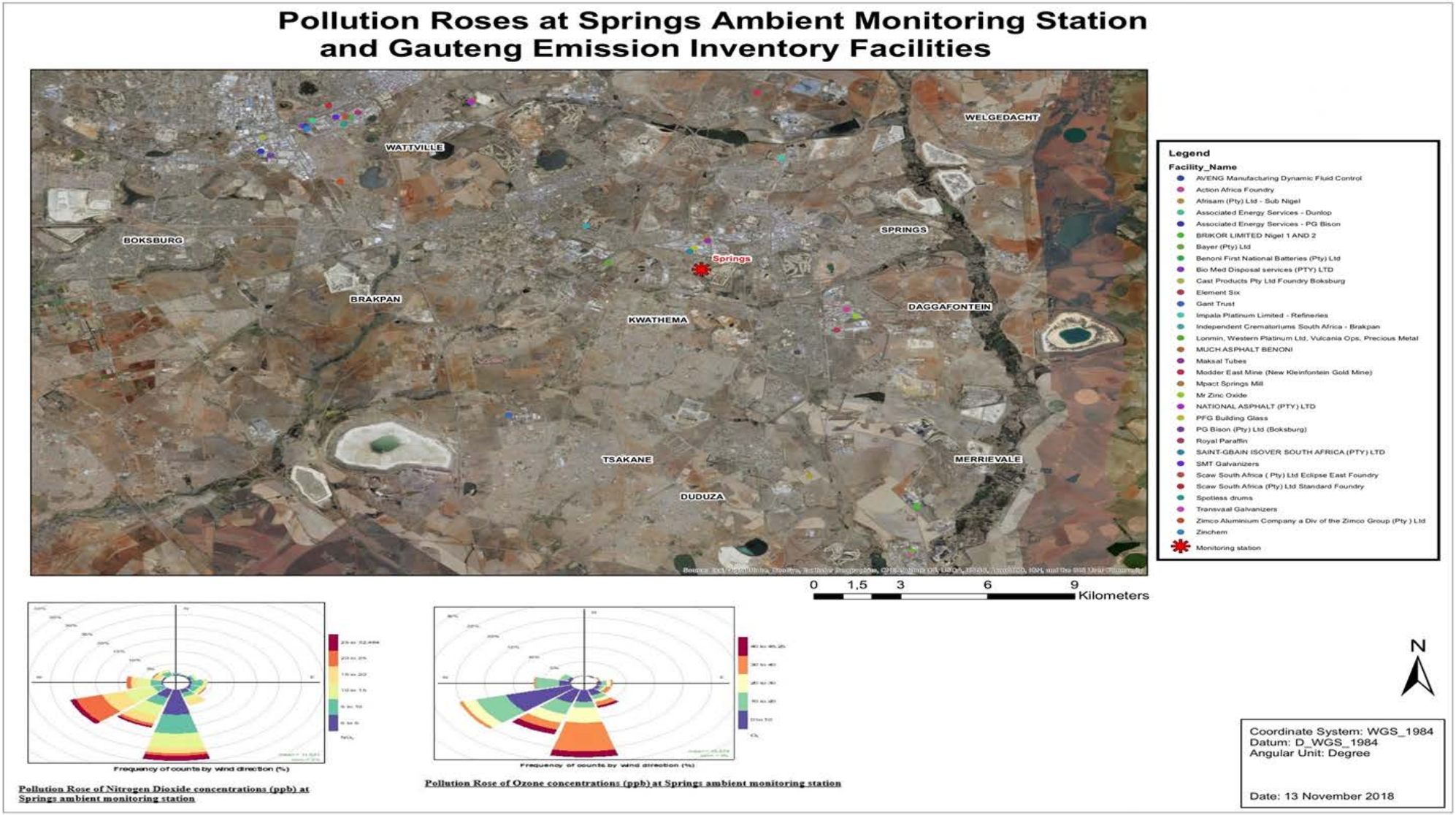

Figure 4.63: Pollution Roses at the Springs Ambient Monitoring Station and Gauteng Emission Inventory Facilities

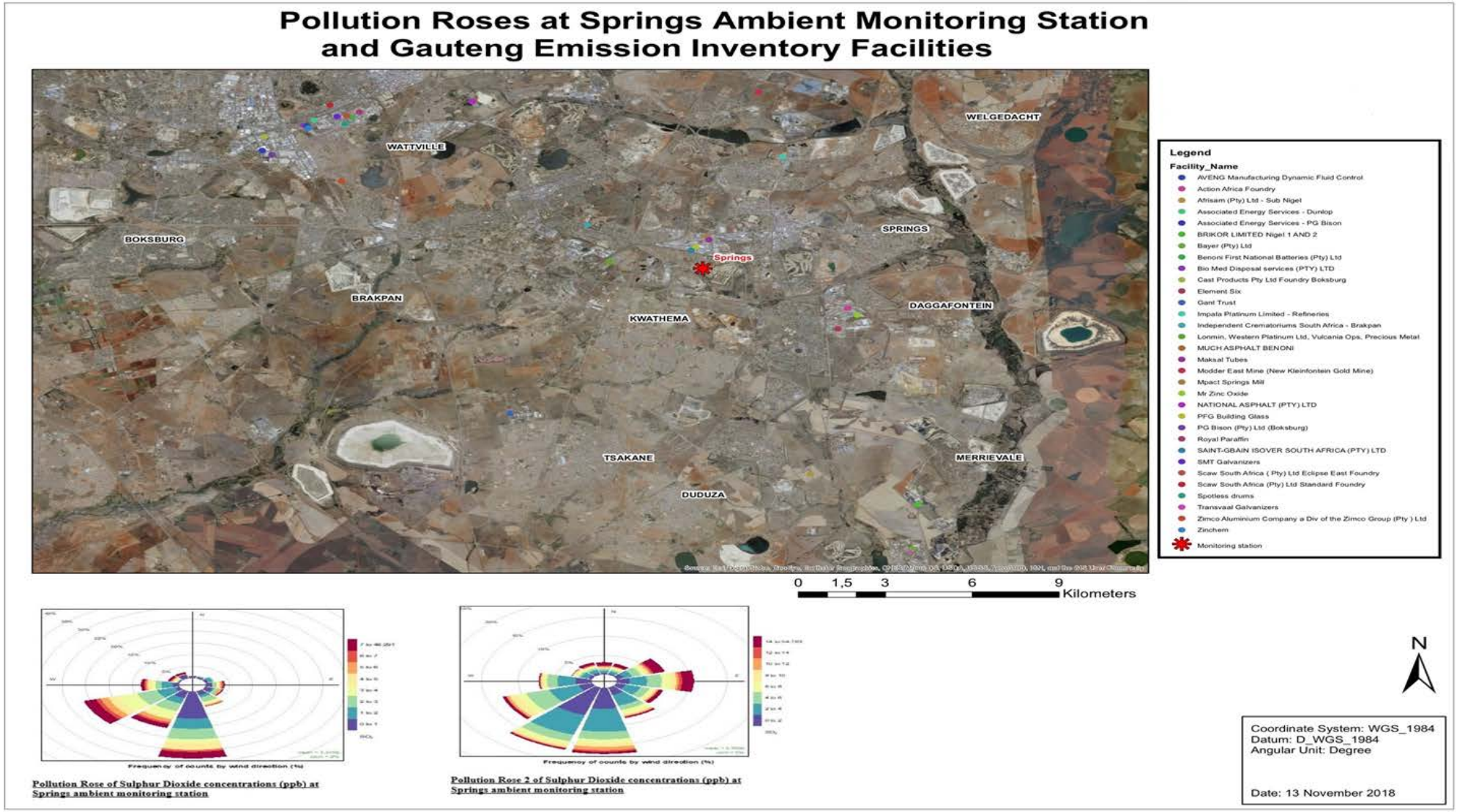

Figure 4.64: Pollution Roses at the Springs Ambient Monitoring Station and Gauteng Emission Inventory Facilities

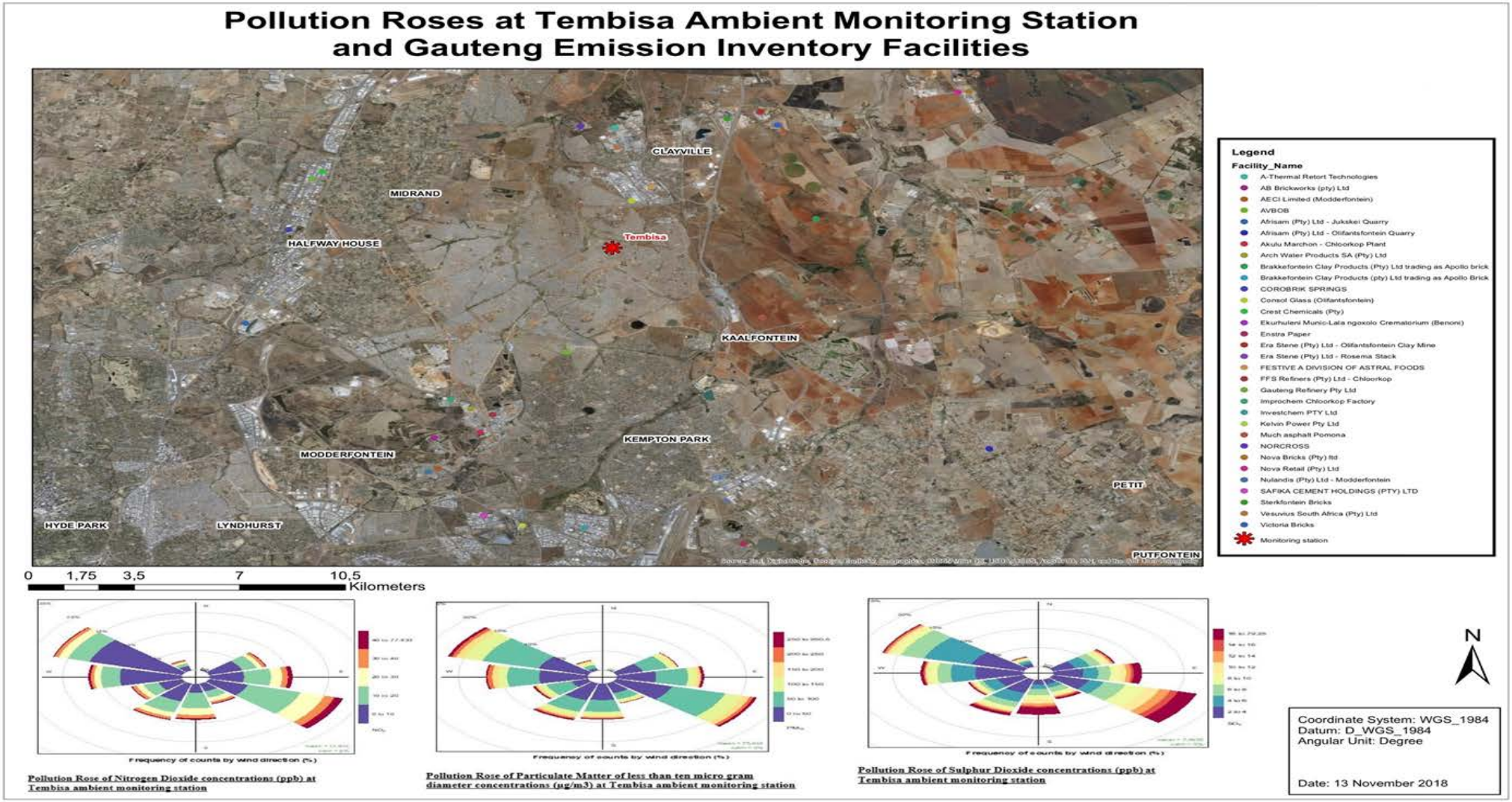

Figure 4.65: Pollution Roses at the Tembisa Ambient Monitoring Station and Gauteng Emission Inventory Facilities

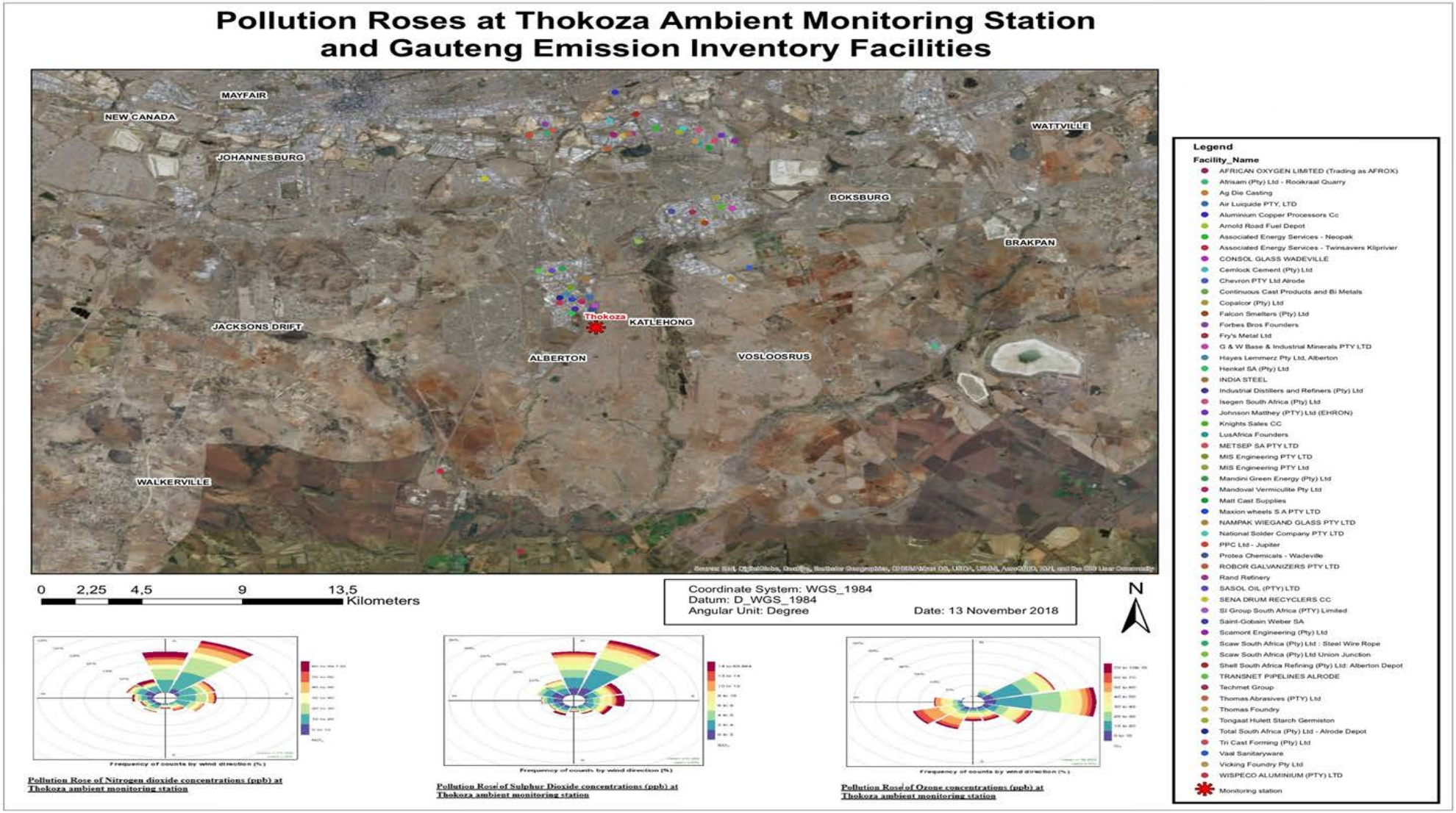

Figure 4.66: Pollution Roses at the Thokoza Ambient Monitoring Station and Gauteng Emission Inventory Facilities

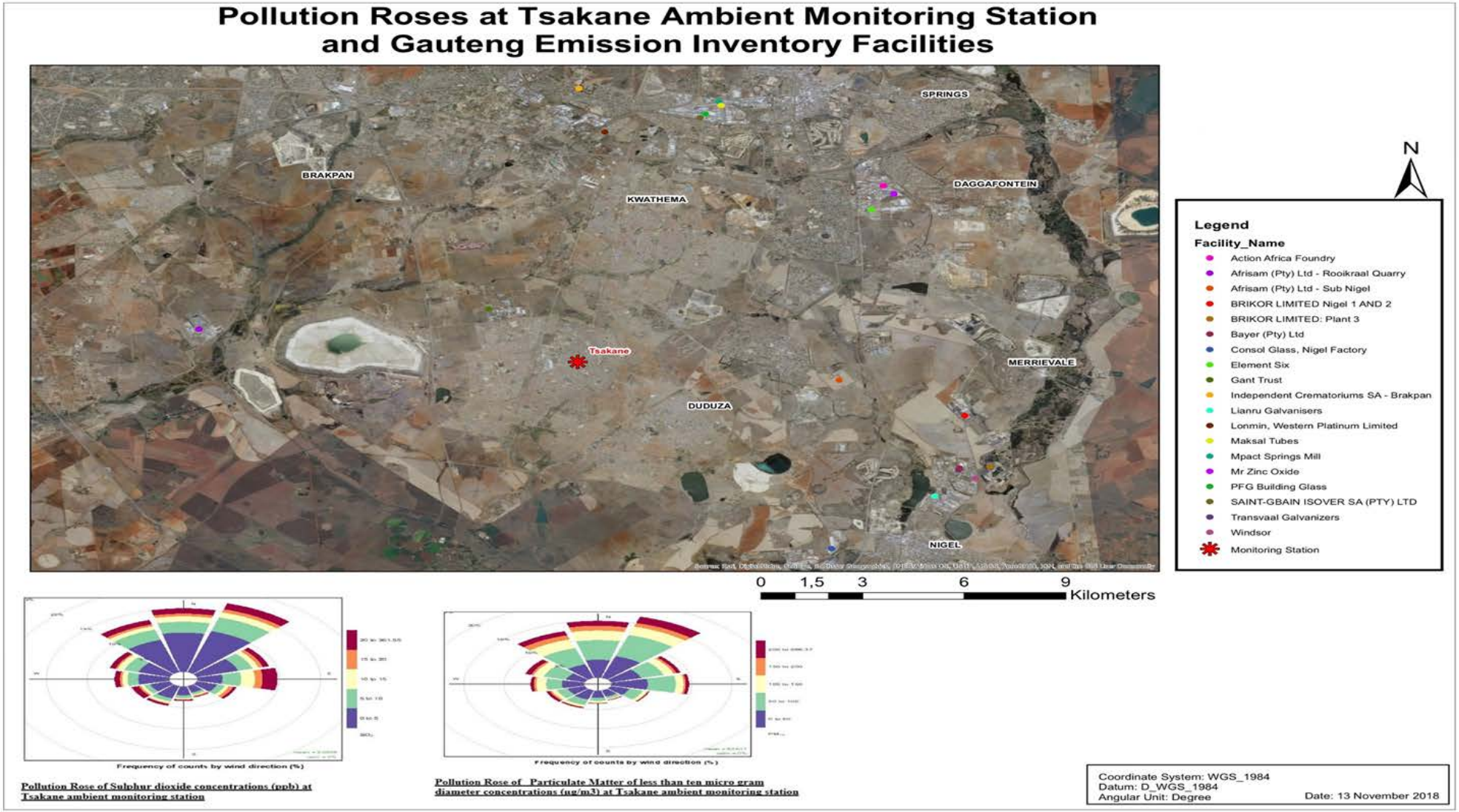

Figure 4.67: Pollution Roses at the Tsakane Ambient Monitoring Station and Gauteng Emission Inventory Facilities



Figure 4.68: Pollution Roses at the Tsakane Ambient Monitoring Station and Gauteng Emission Inventory Facilities

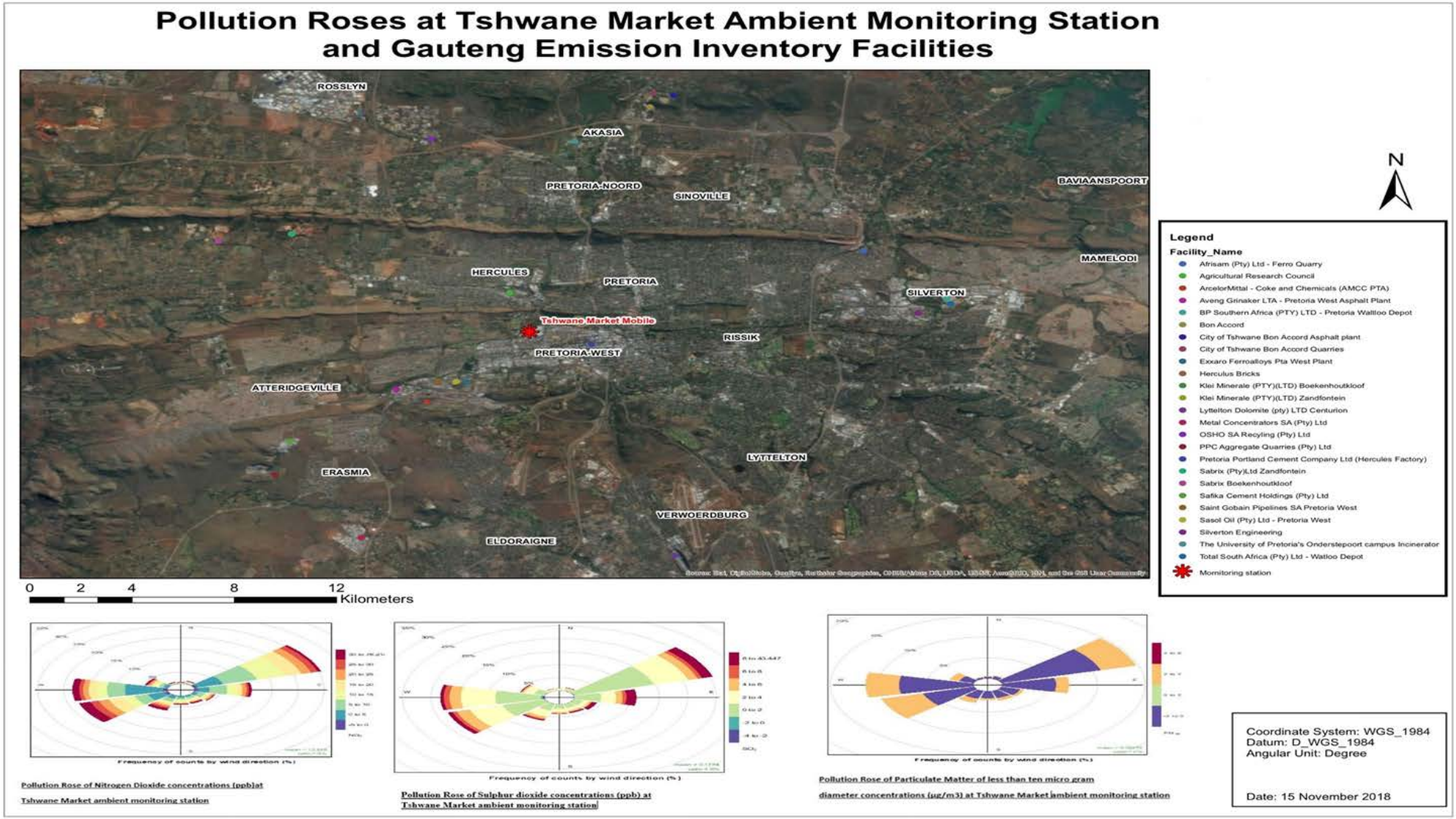

Figure 4.69: Pollution Roses at the Tshwane Market Ambient Monitoring Station and Gauteng Emission Inventory Facilities

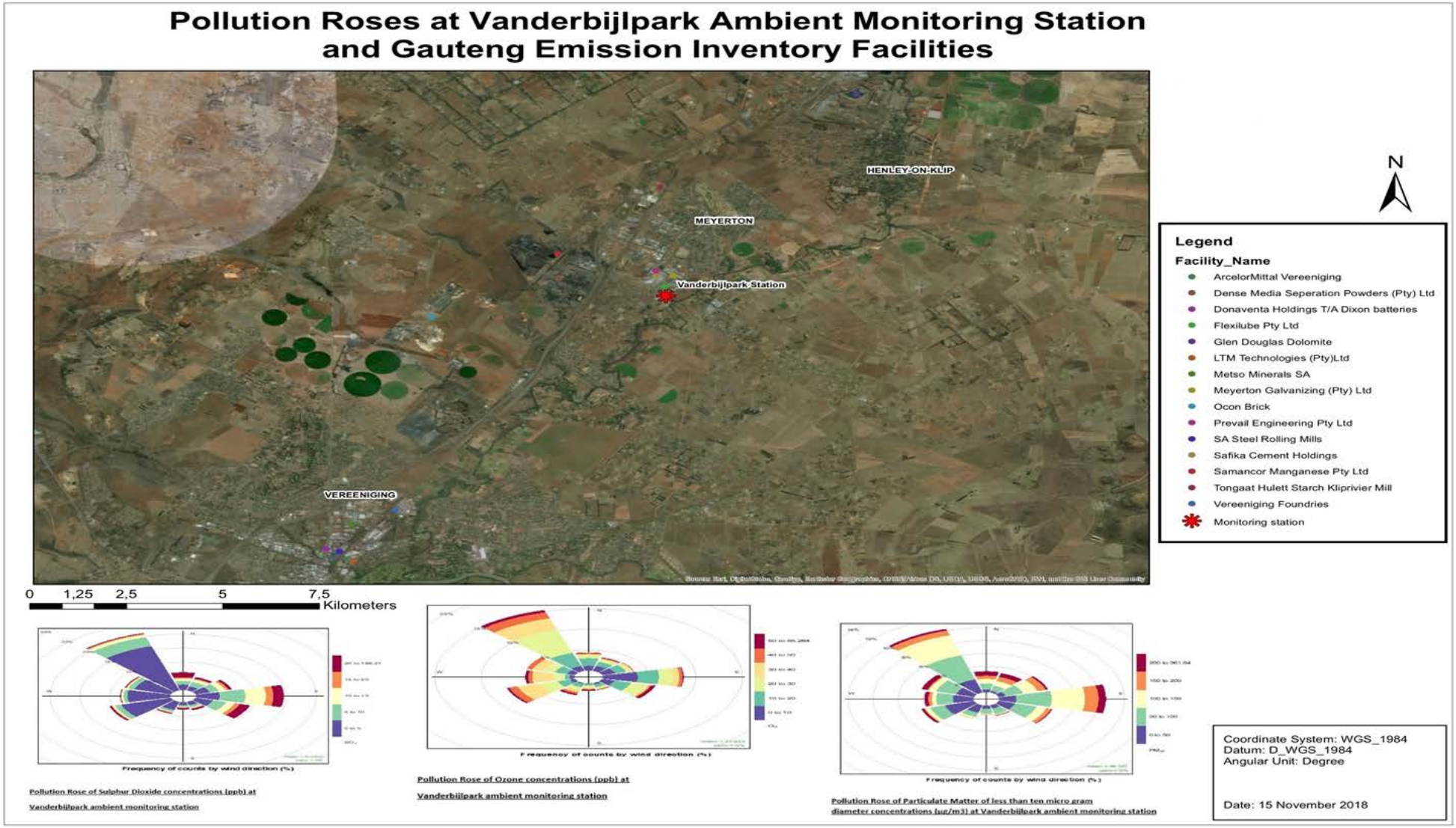

Figure 4.70: Pollution Roses at the Vanderbijlpark Ambient Monitoring Station and Gauteng Emission Inventory Facilities

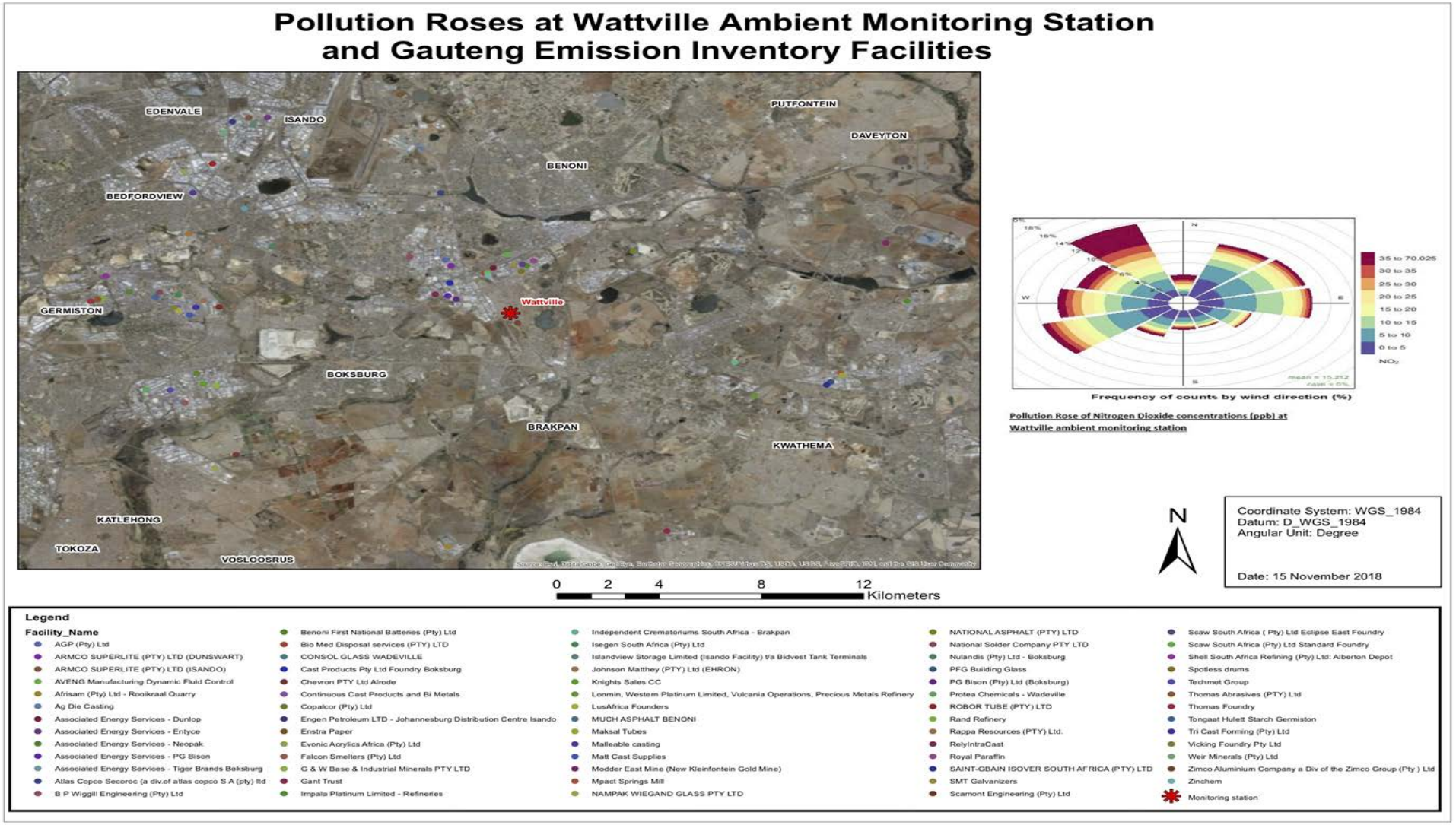

Figure 4.71: Pollution Roses at the Wattville Ambient Monitoring Station and Gauteng Emission Inventory Facilities

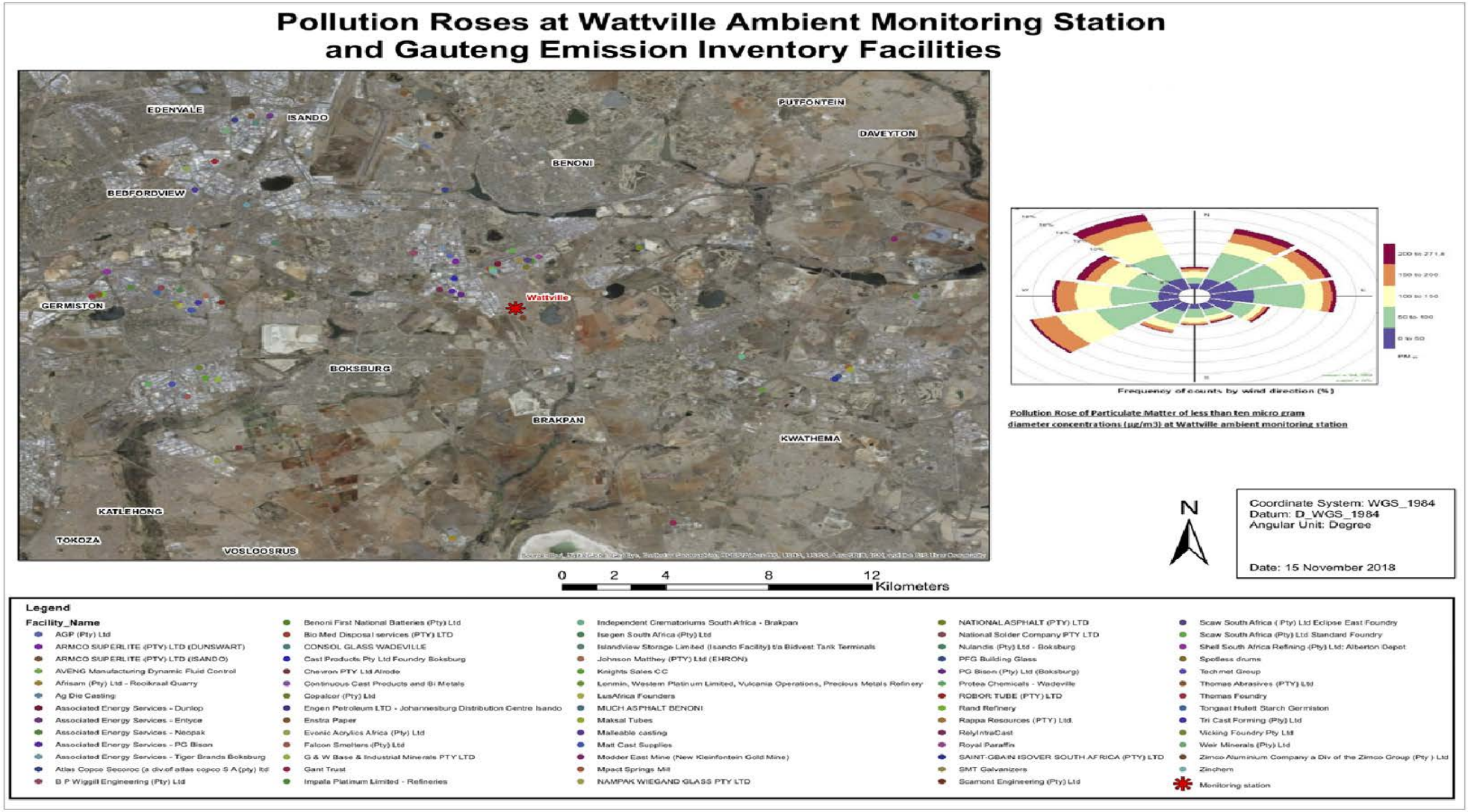

Figure 4.72: Pollution Roses at the Wattville Ambient Monitoring Station and Gauteng Emission Inventory Facilities

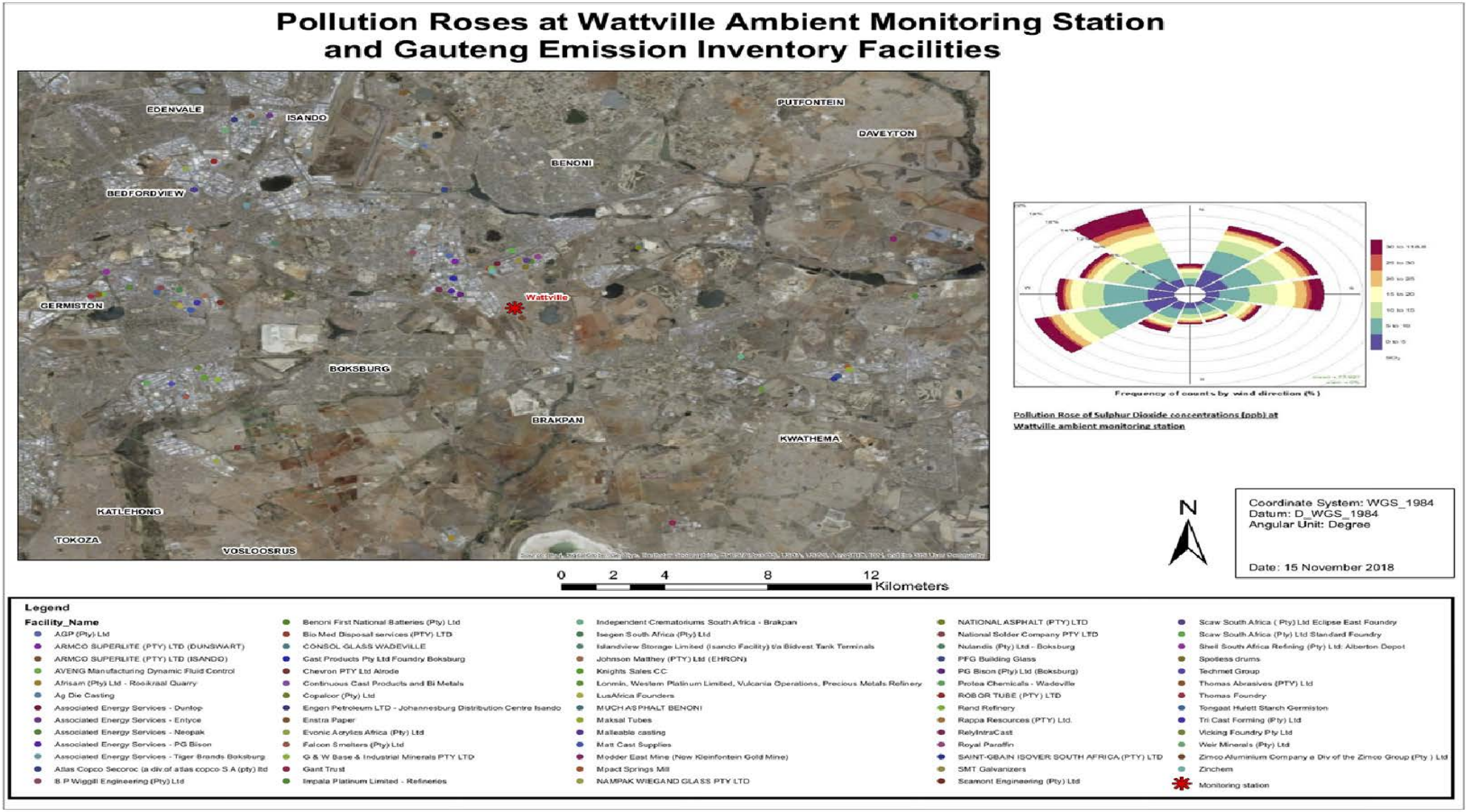

Figure 4.73: Pollution Roses at the Wattville Ambient Monitoring Station and Gauteng Emission Inventory Facilities

.

In Figure 4.32, Bedfordview ozone pollution rose indicated 0 to 10 parts per billion at 6.2% count level in the South-East and South. West and East had a median concentration of 6%. Higher concentrations were observed in the North and North-West of the atmospheric monitoring station, with 8 to 10 and 5 to 6 percentage points respectively.

Bodibeng emissions increased in the North-East direction with atmospheric concentrations averaging 15% of counts in the North-East direction, suggesting a greater frequency of counts in the wind direction. Figure 4.33 indicated that 10% of counts in North, West, North-West, South-East or South-West were below count. Southern areas had a higher atmospheric concentration of 35 to 210.12 parts per billion, accounting for 8 to 12% of the counts in the Southern regions of the ambient monitoring station. The largest bins were in the North-East. Medium bins were situated in either the South or the North-East. The short bin was situated in the Eastern direction and stayed less than 10%.

PM_{10} emissions increased at the Bodibeng ambient monitoring station, showing results in Figure 4.33 of the longest bin with 0 to hundred counts at 18, 11 or 9% at the North-East, upper North-East or East. North and North-west had fewer than 5% frequency of wind counts. Higher concentrations of PM_{10} were found to be between 11 and 12 ambient concentrations of 200 to 573.9 $\mu g/m^3$.

In Figure 4.33, sulfur dioxide at the Bodibeng ambient monitoring station indicated fewer than 10% of the frequency bin counts to the North, west, northwest, South-East and Southwest of the ambient monitoring station. The longest bin in the North-East was down to 20 %. There seemed to be a level of bin count between 10 and 15% in the North-East and over 10% in 2 to 4 atmospheric concentrations of sulfur dioxide in the South. There was 11% in the East, with 7% of the ambient concentration of 2 to 4 parts per billion.

In Figure 4.34, PM_{10} showed the longest range at 20% in the West, followed by 14% in the lower North-East at Booysens. 11% of the count rate was actually higher in the West and South-East. Between 5 10% of the frequency counts were to the North-East higher, to the North-West lower, to the South-East lower and higher, to the South as well as to the South-West lower. Maximum and mean ambient concentrations for PM_{10} at the Booysens ambient monitoring station were 570.77 and 39.543 μg/m3 respectively. 0 to 20 atmospheric

concentrations were between 5 and 10% of the frequency count by West and North-West. All bins below the ambient concentration of 0 to 20 µg/m3 were fewer than 5% count.

In Figure 4.34, sulfur dioxide pollution showed an increased pollution with the longest bins at 4% frequency of counts in the Eastern direction of Booysens. Around 3 and 4% of the counts in the Northern, Western and North-west bins were smaller. Between 2 and 3% of the frequency were North-East lower, North-west higher, Southerly and South-East lower. Ambient concentrations of 0 to 2 parts per billion probably showed the longest bin in the Northern regions, which was between 2 and 3% of the frequency counts. The Eastern field count had a 2% level of counts. Around one and 2% frequency counts were found in the South, southwest, higher and lower, North-East, lower and higher South-East, South, West, southwest, higher and lower, northwest, higher and lower, and South-East, higher and North-East. The smallest range from South-East to South and lower, which was less than one or equal to one% of the count frequency.

In Figure 4.35, ozone pollution increased from 0 to 5 parts per billion, with 10 to 15% counts per North-East lower, South-East for both higher and lower areas. Ozone pollution at the Booysens ambient monitoring station showed the longest bin up to 2.7% of 10 to 20 parts per billion ambient concentrations. The smallest bins with all ambient concentration ranges were situated in North-East, South, South-West below, North-West, North-East, or the North below 2% count frequency. 0 to 10 ambient concentration ranged from South-West to lower, South-East and East to higher, South and southwest to South, Southwest and West to one to 2% frequency ranges. Between 0 and 1 % of the frequency counts from the smallest range to the North, North-East, South-East and North-west.

In Figure 4.36, PM_{10} at the Buccleuch ambient monitoring station indicated probably the longest range of 15 to 20% at the lower northwest, followed by a range of 10 to 15% at the North-East, the higher South-East and the lower South-East. Total and mean atmospheric concentrations for PM_{10} at the Buccleuch ambient monitoring station were 843.75 and 48.77 $\mu g/m^3$ respectively. 0 to 20 atmospheric concentrations indicated 15 to 20% to the North-west below and 10 to 15% to the South-East below and to the South-East below. All bins below the ambient concentration of 0 to 20 µg/m3 were below 5% count.

Figure 4.36 showed the Buccleuch atmospheric monitoring station at 10 to 20 parts per billion of nitrogen dioxide, with the longest bin below 5% of the count at the North-East lower,

followed by the South-East higher and the lower, respectively. The lowest bin of nitrogen dioxide was in the North, Northwest and Southwest respectively. The prevailing direction was North-west lower, with the tendency to decrease the sizes to the South-East lower and higher, to the North-East lower and to the East. The smallest bin was situated to the North, to the northwest higher, to the southwest lower and higher, to the North-East and South below 5%.

In Figure 4.37, the increased ozone pollution at the Buccleuch the highest frequency count of 22 % at the lower North-west range. Between 10 and 15% of the result direction is shown to the South-East higher and lower, to the North-East lower and to the East. The smallest bin was situated in the North, the North-West higher, the southwest lower and higher, the South and the North-East higher at less than 5%. 0 to 5 parts per billion are shown as South-East higher and lower, North-East lower or Easterly between 10 and 15 counts. Concentrations had a strong positive correlation with wind direction. Between 10 and 15 count frequencies were South-East higher and lower and North-West lower. The smallest bin for ozone concentrations was found at less than 5% on the North and the East.

In Figure 4.37, sulfur dioxide pollution at the Buccleuch indicated that the longest bin from the North-West was lower at 12%. Between 10 and 12% there were 2 bins on the South-East higher and lower areas. Between 4 and 6 % on the East and West areas. Between 2 and 4 % on the lower North-East areas, South, South higher and lower. Correlation of ambient concentration of 10 to 15 parts per billion had a tendency of increasing with the concentration range. The highest correlation concentrations were at 6.1% followed by South-East lower and North-East lower. Between 2 and 4 % of SO_2 concentrations at North-East, East, South-East and West, fewer than 2% at the North-west and North higher.

In Figure 4.38, PM_{10} pollution at the Davidsonville indicated frequency counts by lower North-East between 15 and 20 % at the East and South-East higher of the station. Between 5 and 10% indicated North-East higher, higher and west-south-west areas. Fewer than 5% frequency on the lower South-East, South, lower South-West, North-West higher and North and lower areas. There was a correlation of ambient concentration considering 0 to 20 $\mu g/m^3$ PM_{10} and wind direction. PM_{10} ambient concentrations of 20 to 40 $\mu g/m^3$ correlated to wind direction between 5 and 10% on the Lower and Eastern North-East. Fewer than 5% was proportional to half scale with respect to the length of the bin.

In Figure 4.39, Ozone pollutants in Delta Park indicated longest bins between 20 and 25 % on the higher South-West and higher South-East areas. Between 15 and 20 % on the lower South-West. Between 5 and 10% there were 2 bins on the South-East and South areas. Fewer than 5% displayed on the North-west, North and North-East. At 0 to 10 parts per billion displayed longest range on the South-East and South-West areas between 10 and 15%.

In Figure 4.40, Diepsloot PM_{10} pollution indicated prevailing direction on the North-East higher and lower, North and North-West higher and lower pollution rose. Fewer than 5% was found on the South-East higher and lower, South and South-East higher and lower. Higher ambient concentration for North-East higher and lower between 10 and 20 per frequency of counts.

In Figure 4.40, sulfur dioxide pollutants in Diepsloot indicated strong winds and similar pattern prevailing on the North-East higher and lower which was actually between 15 and 20 %. Strong pollution between 10 and 15% situated on the North-west and North. At the area between 5 and 10% there were 2 bins on the lower North-West and Western Area. Areas from West, South-West higher and lower, South and South-East was below 5%.

In Figure 4.41, nitrogen dioxide pollution at the Ekandustria showed direct relationship of ambient concentrations and directional bins of 0 to 200 parts per billion. NO_2 pollution was prevalent from North and North-East higher at 8%. At 6 to 8 % display at the North-west higher and lower, West and South-East lower. At 4 to 6% display on the South-East higher, East and North-East lower. Fewer than 2% on the South, South-West higher and lower.

In Figure 4.41, ozone pollution at the Ekandustria indicated predominant directions on North, North-East higher and South-East lower at 7.5%. At 7% ozone pollution dominated on the North-West higher and lower. At 6% frequency of count ozone pollution dominated on the West. Below 2% ozone pollution indicated smallest to highest bins from South-West high and lower, South and South-East higher.

In Figure 4.42, PM_{10} pollution at the Ekandustria indicated higher wind direction at North, North-west higher and North-East higher at 10 to 15%. At 5 and 10% results showed that at the North-west, West, South-East lower and higher and North-East lower areas. South-west lower and higher were actually less than 5%.

In Figure 4.42, sulfur dioxide pollution indicated ambient concentrations of up to 99.39 parts per billion at the Ekandustria. Pollution displayed wind direction that was strong on the

North, North-West and North-East. At 2 to 4% sulfur dioxide pollution displayed bins from North-East lower, East, South-East higher and lower, South, West and North-West lower. On the South-West high and lower were under 2%. At the range of 0 to 2 parts per billion sulfur dioxide pollution displayed North, North-West higher and North-East higher at 8 and 6 % respectively.

In Figure 4.43, nitrogen dioxide pollution at the Etwatwa indicated maximum of 198.15 parts per billion ambient concentration. The North-West higher and lower showed predominant direction followed by South-West lower and North-East higher. The highest bin was found at North-West higher between 15 and 20 %. At South-East, South-West, North-East higher, bins were between 10 and 15%. The smallest bins were on the South-East lower and higher followed at North which was found below 5%. At 5 and 10% East, North-East, West and South-West higher. At 0 to 10 parts per billion ambient nitrogen dioxide concentrations counted from smallest bin South-East higher and lower, South-West higher and lower, West and East.

Figure 4.43 indicated PM_{10} pollution rose from North-West higher and lower as most wind direction followed by South and North-East. At the frequency counts of 10 and 15% results displayed North-West higher and lower, South-West lower and North-East higher. The bins were arranged from the smallest range at below 5% which were put on the South-East lower and higher, West and North. The longest bin of 0 to 50 $\mu g/m^3$ PM_{10} was on the South-West lower followed by North-East higher, North-West higher, and lower and South-West higher.

Sulfur dioxide pollution at the Etwatwa indicated high predominance from North-West between 5 and 6 % in Figure 4.43. Followed by the direction on the South-West to North-East at frequency counts of between 5 and 6 %. The bins were actually in order from probably the smallest bins at South-East higher, North, South-East lower and West. At concentrations of 0 to 5 parts per billion, longest bins were arranged in order from North-East, North-West lower and higher and South-West. Low ambient concentration of 0 to 5 parts per billion North is actually found on the South-East lower, West, South-East higher and East of less than 1%.

In Figure 4.44, pollution of nitrogen dioxide at the Germiston displayed shortest bins in order South-East lower, South, and South-East higher within 5%. Between 5 and 10 of the frequency counts in the following order from probably the smallest bin on the East, South-

West lower, North-East higher, North, East and North-West lower. There were bins situated at less than 5%. At 5 to 10 ambient concentrations parts per billion longest bins were 11% in order from the North-West higher. The longest bins were in under 5% in order from probably the highest at South-East higher, South and South-East lower.

Pollution of PM_{10} at Germiston was illustrated in Figure 4.45 with probably the highest concentrations at 1869.3 $\mu g/m^3$. The longest bins of concentrations 0 to 10 $\mu g/m^3$ at 9% North-West higher. There were 3 0 to 10 $\mu g/m^3$ at 5% which is situated at North-East lower, South-West higher and North-West wind directions. The order of bins was from probably the smallest to the biggest range at South-East lower, South and South-East higher were less than 5%.

In Figure 4.46, Pollution of sulfur dioxide concentrations in parts per billion at the Germiston station displayed longest bins on the North-West higher at 20% and followed by the 10 to 15% on the North-East lower and South-West higher. At 0 to 5 parts per billion ambient concentrations highest directional representative was found at 16%. Within the range of 5 to 10% results indicated smallest bins from South-East lower, South, North-East higher, North, East, South-West lower, West and North-East.

In Figure 4.47, sulfur dioxide pollution at the Ivory Park station showed North wind direction at 40% and North-East between 20 and 30%. At the ambient concentration of one part per billion probably the longest bin was situated on the North direction whereas probably the smallest bin of ambient concentration of one to 2 parts per billion frequency counts at 20-5%. Highest ambient Sulfur dioxide concentration recorded at 27.056 parts per billion.

Figure 4.48 indicated PM_{10} pollution rose from North at 33% and North-East higher at 20%. The longest range of 50 to 100 $\mu g/m^3$ PM_{10} was on the North followed by North-East higher with the longest range of similar concentrations.

In Figure 4.48, PM_{10} at the Ivory Park station displayed pattern that was similar as sulfur dioxide sources. The longest bin was found on the Northern direction at 30 to 35%. The smallest bin with the ambient concentrations of 0 to 50 $\mu g/m^3$ had highest areas of coverage bins at 8 and 6% respectively.

In Figure 4.48, ozone pollution at the Jabavu station showed strong sources on the East bin at 24% on the South-East higher and higher, South-West lower, West, South, and lower respectively. The maximum ambient concentration recorded were 96.042 of ozone parts per billion. At the ambient concentration of 20 to 30 parts per billion highest bins found were on

the East, South-East highest and lower, South, West, South-West lower and higher, North-East lower, North-West lower and higher and North respectively.

In Figure 4.48, PM_{10} at the Jabavu station displayed pattern that was similar as ozone pollution sources. High sources were found on the East direction between 20 and 25 %. At 16 and 11% sources were determined from second-longest and thirds ranges respectively. Fewer than 10% displayed bins on probably the West, South, South h8 and lower, North-East lower, North lower and North-East. The highest recorded PM_{10} ambient concentrations were 403.19 $\mu g/m^3$.

In Figure 4.48, sulfur dioxide pollution at the Jabavu recorded highest value of ambient concentration as 56.094 parts per billion. Pattern displayed for the ozone and PM_{10} sources at the Jabavu station showed similar directional distributions. At 0 to 2 ambient concentrations displayed longest bins from Eastern, South-East higher, West, South-West higher lower and South. Fewer than 5% from smallest to probably the highest as per 0 to 2 ambient concentrations of Sulfur dioxide is actually found on North, North-West higher, North-East higher and North-West lower.

Nitrogen dioxide pollution at the Leondale displayed high sources on the North-East lower, West and East direction (Figure 4.49). Fewer than 5% from smallest to highest bin start with North, South-East lower, South, North-West higher and North-East at the Leondale. Between 5 and 10% ranges from small bins on the North, North-West, South-East lower, South and North-East higher. At 0 to 10 parts per billion ambient concentration displayed sequence from large at North-East lower, North-East lower, East, South-West higher, and lower and South-East higher. Fewer than 5% from small bin North, South-East lower, North-West higher, South and North-East. On the South and North were easy for high pollutant sources to reach the Leondale due to less buffer of 0 to 10 parts per billion ambient concentrations. The highest recorded ambient concentration was74.471 parts per billion.

Ozone ambient concentration displayed in Figure 4.49 indicated high sources from North-East lower, West and East at the Leondale. Smallest bin ranges in order from North, North-West higher, South-East lower, and North-East higher and South. The small bin was proportional to the ambient concentration of 10 to 20 parts per billion. At ranges between 5 and 10% from the smallest South-East higher, North-West lower and South-West higher. The highest recorded ambient concentration was 77.898 parts per billion.

Sulfur dioxide pollution at the Leondale station displayed strong sources prevailing on the North-East lower, East and West of frequency of counts (Figure 4.49). Fewer than 5% frequency counts from smallest North, South-East lower, North-East higher, South and North-West higher. 2 to 4 ambient concentrations displayed longer range at North-East and small buffer and North-West is actually found on the South and North respectively.

Nitrogen dioxide pollution in Figure 4.50 at the Mamelodi displayed strong sources from direction on the South-East higher and East at 18 and 15%. Fewer than 5% from smallest ambient concentrations between 0 and 10 parts per billion were situated on the North, South, North-West higher, South-West lower and higher, South-East lower and North-East higher. At the range of 5 to 10% with the ambient concentrations of 0 to 10 parts per billion frequency counts displayed East, North-West lower and North-East lower. The highest ambient nitrogen dioxide recorded was 304.99 parts per billion.

Pollution at the Mamelodi station for PM_{10} displayed ambient concentrations of 0 to 100 µg/m3 covering 8%. Figure 4.51 indicated that the longest prevailing bin was found on the South-East higher at 7% on the East at 5% and North-East lower at 3.7%. Fewer than 2% from smallest bin North, South, North-West higher, South-West lower, and North-East. At the ranges of between 2 and 4% strong wind direction were actually recorded on East and North-West lower. The highest ambient concentration recorded at the Mamelodi was 962.89 µg/m3.

In Figure 4.51, Mamelodi Pollution of sulfur dioxide concentrations in parts per billion indicated strong sources of sulfur dioxide from South-East higher between 6 and 8 %, on the East between 4 and 6 % and North-East lower between 4 and 6%. The maximum and mean ambient concentrations for sulfur dioxide at the Mamelodi were 435.58 and 5.2454 parts per billion respectively. The results displayed weak pollution sources in order from South, South-East lower and South-West lower and North. At the ambient concentrations of 0 to 2, PM_{10} showed strong pollution sources from South-West higher and North-East higher fewer than 4%.

In Figure 4.52, Sulfur dioxide pollution at the Meyerton station displayed strong sources on the East and North-East lower at 23 and 21 % respectively. At range between 0 and 10% at 0 to 2 parts per billion ambient concentration from smallest South-East lower, South, South-West lower, East, North-West higher and lower, South-East higher, South-West higher,

North-East higher and North. The highest ambient concentration recorded was 94.992 parts per billion.

Ozone pollution at the Meyerton station indicated strong sources on the East and North-East lower at 23 and 21 % respectively. The highest Ozone ambient concentration recorded in Figure 4.52 at the Meyerton was 97.312 parts per billion. At less than 5% from probably the smallest which were South-East lower, South-West lower and South. At the range between 5 and 10% from probably the highest bin on the Western, South-West higher, North-West lower and higher, South-East higher, North-West higher and North.

PM_{10} pollution at the Meyerton showed strong wind direction prevailed from East and North-East lower at 23 and 21% respectively in Figure 4.52. The highest PM_{10} ambient concentrations recorded was found at 185.83 $\mu g/m^3$. Fewer than 5% from smallest at South-East higher, South-West lower and South. Ambient concentration of 10 to 20 $\mu g/m^3$ indicated sources from large at West, North-West lower, South-West higher, North-West higher, North-East higher and North.

Nitrogen dioxide pollution at the Mogale displayed strong sources on the North-West lower at 16% and North-East lower at 15% in Figure 4.53. In Figure seventy-one probably the highest recorded ambient concentration of nitrogen dioxide was at 52.675 parts per billion. At less than 5% there were 2 smallest bins from North and North-West higher. At 12 and 10% results indicated prevailing wind direction at West and North-East respectively. At 5 and 10% frequency of counts they were different bin sizes from probably the largest West, South-West higher, South-West lower, South and South-East higher, and lower. Nitrogen dioxide ambient of concentrations of 0 to 5 parts per billion at the Mogale displayed bins according to the sizes of theirs from smallest at North, North-West higher, South-East lower and higher, East, South-East lower, North-East higher, North-East lower, South-West higher and West.

Ozone pollution at the Mogale City indicated pattern that was similar as nitrogen dioxide displayed in Figure 4.53. The results displayed bins from probably the highest at North-West lower, North-East lower than West and North-East higher respectively. Fewer than 5% displayed from the smallest bin at North and North-West. At the range of 10 to 20 parts per billion highest concentration bins occurred from North-East lower, East, North-East higher, South-East higher and lower, South, West and North-West lower. At the above-mentioned

ambient concentrations counting from probably the smallest range at North, South-West higher, North-West higher and South-West lower.

PM_{10} concentration at the Mogale displayed two highest bins in order from North-West lower at 16% and North-East lower at 15%. In Figure 4.54, there were 2 smallest bins at North and North-West higher situated at 5%. The majority of the sources at the Mogale are actually situated between 5 and 10%. The highest pollution sources were actually between 5 and 10% and situated on the North, East, South, South-West lower and higher, South and South-East lower and higher. At the ambient concentrations of 10 to 20 $\mu g/m^3$ PM_{10}, results displayed higher and fewer sources at less than 5%. On the above-mentioned ambient concentrations North-East lower was probably the highest sources followed by West, North-West lower, South-West higher and lower, South and East. The smallest source identified on the 10 to 20 ambient concentrations from North, North-West higher, South-East lower and higher.

Pollution of Sulfur dioxide in Figure 4.54 at the Mogale City displayed similar pattern of PM_{10} and ozone concentrations. On the North-West and North higher displayed smallest sources respectively, which were counted less than 5%. On the North-West lower and North-East lower showed 16 to 15% respectively. The majority of the pollution sources were between 5 and 10%. At 11 and 10% of frequency one could find pollution sources which were actually situated higher in the North-East and West directions. At the ambient concentrations of 0 to 5 parts per billion probably the highest sources on the North-East lower and higher, West and North-West lower. At the above-mentioned ambient concentrations there were smallest sources from North and North-West higher respectively.

In Figure 4.55, pollution rose of ozone concentrations at the Newtown displayed strong sources on the South-East, East and South-West at 17, 16 and 15% respectively. The smallest sources were found at North, North-East higher, North-West higher and lower and North-East lower which are actually situated less than 5%. Northern part of Newtown indicated fewer sources compared to Southern areas. West and East were actually dominated much more than South and North, however, East had strong sources compared to West of the Newtown.

Pollution of PM_{10} at the Newtown displayed southerly sources than Northern areas in Figure 4.55. Western and Eastern dominated South and North wind, however, East sources dominated Western at the Newtown. The largest sources in sequence namely at South-East

higher at 17%, East at 16%, South-West higher at 15% and South-East lower at 13%. The smallest sources were actually presented in order from North, North-West higher, North-East higher, North-West lower and North-East lower which were actually all under 5%. At 0 to 50 $\mu g/m^3$ PM_{10} displayed higher dispersion from probably the highest shading at South-West higher, South-East higher, West, South-East lower, South, South-West lower, West, North-East lower and North-West lower.

Pollution rose of nitrogen dioxide concentrations at the Olievenhoutbosch ambient monitoring station in Figure 4.56 displayed high wind domination at North-East lower followed by South-East higher, North-East higher and North-West. The smallest bins were presented in order North, South, South-West higher and South-West which were at 5%and lower frequency of counts. At the range of ambient concentrations of 0 to 5 parts per billion displayed large shade from North-East lower, North-West lower, West, North-West higher and North-East higher. At the 0 to 5 parts per billion also displayed smallest shades from North, South, South-East lower and higher.

Pollution of ozone concentrations in Figure 4.57 at the Olievenhoutbosch indicated strong sources on the Eastern areas. Results displayed highest sources in order from North-East lower at 17%, South-East higher at 13%, North-East higher at 11%, North-West lower at 11% and East at 10%. At less than 5% sources were displayed from the smallest at North, West, South-West lower and higher. At 0 to 10 parts per billion concentrations shaded from the largest at South-East higher and lower, East, North-East lower, North-East higher, North-West lower and higher which were less compared to 5%.

Pollution of sulfur dioxide concentrations at the Olievenhoutbosch recorded maximum ambient concentrations of 75.76 parts per billion in Figure 4.57. The results displayed strong sources from North-East lower at 17%, South-East higher at 13%, North-East higher at 11%, North-West at 11% and East at 10%. The results also displayed weak pollution sources from the smallest at North, South, South-West higher and South-West lower. Ambient concentrations of sulfur dioxide of 0 to 2 parts per billion displayed strong concentration dispersion from the largest area at North-East lower and higher, East, North-West lower and higher. At the same mentioned ambient concentration above displayed smallest dispersed areas in order from North, South, South-East lower and higher.

In Figure 4.57, PM_{10} pollution at the Olievenhoutbosch station displayed weak pollutant dispersion at lower, South-West higher, South, and North, West and South-East lower. The results showed strong pollution sources in order from North-East lower, South-East higher, North-West lower and higher. At the ambient concentrations of 0 to 20 $\mu g/m^3$ PM_{10} displayed strong dispersion from North-East lower, North-East higher, East, South-East higher and North-West lower. The maximum recorded PM_{10} concentration was 954.84 $\mu g/m^3$ at the Olievenhoutbosch.

In Figure 4.58, pollution of ozone concentrations at the Orange Farm displayed strong pollution sources on the North-East and North between 12 and 11%. Weak pollution sources were displayed at the South-East lower and higher. The maximum ambient concentration recorded at the Orange Farm was at 101.51 parts per billion of ozone. At the ambient concentrations of 10 to 20 parts per billion results displayed higher areas concentration dispersion at North-East higher, North-East lower, North, East and South-West higher. The results showed low area coverage close to the station starting from the smallest at South-East higher and South-East lower, North-West higher, South, South-West lower and North-West lower.

Pollution of PM_{10} at the Orange Farm displayed strong pollutant dispersion at North and North-East higher between 12 and 14%. In Figure 4.58, the results displayed weak pollution dispersion at South-East higher and South-East lower between 4 and 6 %. The maximum ambient concentration recorded at the Orange Farm was 908.45 $\mu g/m^3$ of PM_{10}. At the ambient concentrations of 20 to thirty $\mu g/m^3$ PM_{10} displayed lowest frequency of counts on the South-East higher and South-East lower. Strong dispersion of the above-mentioned ambient concentrations was found at North-East higher, North-East lower, North, South-West higher and South.

In Figure 4.58, pollution of sulfur dioxide concentrations at the Orange Farm displayed strong pollutant dispersion at North and North-East higher between 12 and 14%. The maximum ambient concentration of sulfur dioxide recorded at the Orange Farm was 93.897 parts per billion. The results displayed weakest pollution sources on the South-East higher and South-East lower at less than 6%. At the ambient concentration of 0 to 2 parts per billion the strong pollution sources at North, North-East higher and South. At the ambient concentration

displayed weak pollution sources at South-East lower, South-East higher, East and North-East lower.

Pollution of nitrogen dioxide concentrations in the Pretoria West displayed strong pollution sources from North-East higher at 18%, North-East lower at 16% and South at 15%. In Figure 4.59 results indicated weak pollution sources from South-East, East, South-East at less than 5%. The maximum ambient concentration at the Pretoria West was 157.58 parts per billion. At the ambient concentrations of 10 to 20 parts per billion strong pollution sources at North-East higher at 18%, North-East lower at 16% and South at 15%. The results displayed weak pollution sources from South-East higher, South-East lower and East below 5%.

In Figure 4.59, pollution of ozone concentrations at the Pretoria West displayed strong pollution sources on the North-East higher at 18%, North-East lower at 15% and South at 14%. The maximum ambient concentration for ozone was 100.79 parts per billion. The results displayed Ed weak pollution sources from smallest at South-East higher, South-East lower, East, North-West higher and North-West lower at less than 5%. At the ambient concentrations of 0 to 20 parts per billion displayed strong pollution at South, South-West lower, North-East lower and South-East lower. The results displayed weak pollution sources from North and West that were below 5%.

Pollution of PM_{10} at the Pretoria West station displayed strong pollutant sources at South-West lower at 20-8%, West and South both were at 15%. In Figure 4.60, the results displayed weak pollution sources at North, North-East higher, North-West higher and South-East higher which are less compared to 5%. The maximum ambient concentration at the Pretoria West was 316.5 $\mu g/m^3$ of PM_{10}. At the ambient concentrations of 0 to 50 $\mu g/m^3$ of PM_{10} results indicated strong pollution sources at West, South-West higher, South-West lower and North-East lower. The results displayed weak pollution sources from North, North-East higher and North-West higher.

In Figure 4.60, pollution of sulfur dioxide concentrations measured in parts per billion at the Pretoria West displayed strong pollution sources on the South followed by the North-East higher and North-East lower bins which were between 10 and 15%. The maximum ambient concentration at the Pretoria West was 104.94 parts per billion. The results displayed weakest pollution source on the South-East higher, South-East lower, East, North, North-West higher, North-West lower fewer than 5%. At the ambient concentrations of 0 to 5 parts per

billion strong pollution as displayed at North-East higher, North-East lower, West and South-West higher. At above given concentrations results indicated weak pollution sources at the South-East higher, South-East lower, East, North, North-West higher and North-West lower fewer than 5%.

In terms of Figure 4.61, pollution of nitrogen pollution sources on the South-West higher between 25 and 30 %, East at 20%, South-West lower between 10 and 15%. The maximum and mean ambient concentrations for nitrogen dioxide at the Randfontein were 42.216 and 7.021 parts per billion respectively. The results displayed weak pollution sources from North, North-West higher, North-East higher. At the ambient concentrations of 0 to 5 parts per billion showed strong pollution sources on the South-West higher, East and South-West lower.

Pollution of ozone concentrations at the Randfontein indicated strong pollution sources on the South-West higher, West and South-West lower. Figure 4.61, results displayed weak pollution sources at the above-mentioned ambient concentrations from North, North-West higher, North-East and South. The maximum ambient concentrations at the Randfontein were 92.647 parts per billion. At the ambient concentration of 10 to 20 parts per billion displayed strong pollution sources on the West, North-East lower, North-West lower and South-West higher.

Pollution of PM_{10} at the Randfontein station displayed strong pollutant sources at South-West higher at 24%, South-West and West lower at 14 and 8 % respectively. In Figure 4.61, the results displayed weak pollution sources from North, North-West higher, North-East lower and North-West lower. The maximum ambient concentrations at the Randfontein station were 500.2 parts per billion.

In Figure 4.61, Pollution of sulfur dioxide ambient concentration at the Randfontein displayed strong pollution sources on the South-West higher, West, South-West lower and North-East lower. The results indicated weak pollution sources on the North, North-West higher, North-East higher in order. The maximum ambient concentrations at the Randfontein were 77.258 parts per billion. Pollution of nitrogen dioxide concentration at the Rosslyn indicated strong pollution sources on the South-West at 14%, South-East at 11 and 8 % and probably the strongest at South-West higher, East, North-East lower, South and South-East higher. In Figure 4.62, the maximum ambient concentration recorded at the Rosslyn was

92.722 parts per billion. At the ambient concentrations of nitrogen dioxide of 0 to 10 parts per billion strong pollution sources were on the East, North-East lower, South-West lower and North-West lower. At the above-mentioned ambient concentrations weak pollution sources were on the South-East higher, South, North, South-East higher, North-West higher and North-East higher.

Pollution of ozone concentrations at the Rosslyn displayed strong pollution sources on the South-West between 12 and 14%, South-East lower between 10 and 12%, at 8 and 10% on the East, South-West lower and North-East lower. In Figure 4.62 results displayed weak pollution sources from North, North-West higher and North-East higher in under 6%. The maximum ambient concentration for ozone at the Rosslyn was 601.48 parts per billion. At the ambient concentrations of 0 to 10 parts per billion strong pollution sources indicated South-West lower, South-East lower, South, South-West higher and South-East higher. At the above-mentioned ambient concentration results displayed weak pollution sources on the North-West higher, North, North-East higher, North-East lower and North-West lower.

In Figure 4.60, pollution of PM_{10} at the Rosslyn displayed strong pollutant sources at South-West lower, South-West lower and East between 8 and 10%. The results in Figure 4.62 also displayed weak pollution sources from North, North-West higher and North-East higher. The maximum ambient concentration for PM_{10} recorded at the Rosslyn was 204.06 $\mu g/m^3$.

In Figure 4.62, pollution of sulfur dioxide at the Rosslyn displayed strong pollution sources in from South-West lower between 12 and 14%, South-East lower between 10 and 12%, South-West higher between 8 and 10%, East between 8 and 10% and North-East higher between 8 and 10%. The maximum ambient concentration for ozone at the Rosslyn was 253.71 parts per billion. The results displayed weak pollution sources from North, North-West higher and North-East higher at 4 and 6 %. At the ambient concentrations of 0 to 5 parts per billion displayed weak pollution sources from North-East higher, North-East lower, East, West, North-East higher and South. At the above-mentioned ambient concentration results displayed Ed strong pollution sources from South-West lower, South-West higher, South-East lower, South-East higher and East.

Pollution rose of nitrogen dioxide concentrations at the Springs in Figure 4.63 displayed strong pollution sources on the South between 5 and 30 %, South-West higher between 20 and 25 % and South-West lower between 15 and 20 %. The maximum ambient

concentration for nitrogen dioxide recorded at the Springs was 32.484 parts per billion. The results indicated weak pollution sources from North-East higher, North, North-East lower, North-West higher, North-West lower, East and South-East higher. At the ambient concentration of 5 to 10 parts per billion strong pollution sources from South, South-West lower, South-East lower, East, West, South-West higher and South-East higher. At the above-mentioned ambient concentration results displayed weak pollution sources from South-West higher, North-West higher, North, North-East higher, West and North-West lower

Pollution of ozone concentrations at the Springs displayed strong pollution sources in from South between 20 and 25 %, South-West higher at 20%, South-West lower between 15 and 20 %, South-East lower between 5 and 10% and West between 5%. In Figure 4.63, the maximum ambient concentration for ozone recorded at the Springs was 45.25 parts per billion. The results displayed weak pollution sources from North, North-West higher, North-East higher, North-West lower, West and South-East higher. At the 0 to 10 parts per billion strong pollution sources from South-West higher, South-West lower, South, South-East lower and West.

In Figure 4.64, pollution of sulfur dioxide concentrations at the Springs results displayed strong sources on the South between 15 and 20%, South-West lower between 15 and 20 %, South-West higher between 10 and 15%, South-East and West lower between 5 and 10%. The maximum ambient concentration for sulfur dioxide recorded at the Springs was 51.163 parts per billion. The results displayed weak pollution sources from North-East lower, North, North-East lower, North-West lower which were all below 5%.

In Figure 4.65, Pollution of nitrogen dioxide concentrations at the Tembisa indicated pollution sources on the South-East higher between 15 and 20 %, North-West lower between 15 and 20%, West 10 to 15% and East at 10%. The maximum ambient concentration for sulfur dioxide recorded at the Tembisa was 77.833 parts per billion. The results displayed weak pollution sources from probably the smallest on the North, North-East higher and North-West at less than 5%. At the ambient concentrations of 0 to 10 parts per billion displayed strong pollution sources from North-West lower, West, South-West lower, South East higher, East and North East lower. At the same given ambient concentrations displayed weak pollution sources from smallest at North, North East higher and North West higher.

Pollution of PM_{10} at the Tembisa displayed strong pollutant sources on the South East higher between fifteen and 20%, North West lower higher between 15 and 20% as well as on the West between 10 and 15%. Figure 4.65 recorded maximum ambient concentrations for sulfur dioxide at the Tembisa at 950.5 $\mu g/m^3$ of PM_{10}. The results displayed weak pollution sources from probably the smallest at North, North East higher and North West higher at less than 5%. At the ambient concentrations of 0 to 50 $\mu g/m^3$ of PM_{10} displayed strong pollution sources from South East higher, North West lower, West. The results indicated concentration on the North, North East higher and North East higher.

Pollution in Figure 4.65 display sulfur dioxide concentrations at the Tembisa with strong sources on the South between 15 and 20 %, South West lower between 15 and 20 %, South West higher between 10 and 15%, South-East and West lower between 5 and 10%. The maximum ambient concentration for sulfur dioxide at the Tembisa was 79.25 parts per billion. The results displayed weak pollution sources from North, North East higher and North West higher which were all below 5%. At the ambient concentrations of 2 to 4 parts per billion results displayed strong pollution sources from North West lower, West, South East higher and East.

Pollution of nitrogen dioxide concentrations at the Thokoza station in Figure 4.66 indicated strong pollution sources from North East higher at 20%, North between 15 and 20 %, North East lower between 5 and 10% and East between 5 and 10%. The maximum ambient concentration for sulfur dioxide recorded at the Thokoza station was 99.735 parts per billion. The results displayed weak pollution sources in order from South, South West higher, South East lower and South West lower. At the ambient concentrations of 10 to 20 parts per billion displayed strong pollution sources at North East higher, North, North East lower and East. The results displayed smallest pollution sources from South, South East lower and South West higher which are less compared to 5%.

Pollution of ozone concentrations at the Thokoza station displayed strong pollution sources from East between 20 and 30%, North East lower between 15 and 20%, South West higher between 10 and 15% and South East between 10 and 15%. In Figure 4.66 maximum ambient concentration for sulfur dioxide at the Thokoza was 108.19 parts per billion. The results displayed weak pollution sources from North West lower, North West higher, North and North East which were all below 5%.

Pollution rose of PM_{10} at the Tsakane station displayed strong pollution sources from North East higher between 15 and 20 %, North at 15% and North West higher between 10 and 15% in terms of Figure 4.67. The maximum ambient concentration for sulfur dioxide recorded at the Tsakane was 966.37 $\mu g/m^3$ of PM_{10}. At the ambient concentrations of 0 to 50 $\mu g/m^3$ of PM_{10} displayed strong pollution sources at North East higher, East, North and North West. The results at the same above concentrations displayed weak pollution rose from South East, South, South West lower, South West higher and South East higher.

In Figure 4.67, pollution of sulfur dioxide at the Tsakane displayed strong sources from the East between 15 and 20 %, South East lower at 10 to 15% and North at 10%. The maximum ambient concentration for sulfur dioxide at the Tsakane was 53.845 parts per billion. The results displayed weak pollution sources from South West higher, South and South West lower which were under 5%. At the ambient concentration of 0 to 5 parts per billion displayed strongest pollution rose in order from South East higher, North, East, North East higher and North East lower. The results displayed weak sources from North West lower, North West higher and South West higher.

In Figure 4.68 Pollution of Nitrogen dioxide at the Tsakane displayed strong sources from North East higher at 14%, North between 12 and 14%, North West higher between 10 and 12%. In Figure 86 maximum ambient concentration for nitrogen dioxide at the Tsakane was 88.622 parts per billion. The results displayed weak pollution sources from South East lower, South, South East, South West lower and South West higher. At the ambient concentrations of 0 to 10 parts per billion strong pollution sources from North East higher, East-North-West higher, North, South West lower and South West higher which were below 4%. The results also displayed weak pollution sources in order from South East lower, South, South West lower and South West higher.

In Figure 4.69, pollution of nitrogen dioxide at the Tshwane Market indicated strong sources from North East lower at 25%, West and West were between 15 and 20 %. The maximum ambient concentration for sulfur dioxide recorded at the Tshwane Market was 76.214 parts per billion. The results displayed weak sources on the North, North West higher, North East higher, South, South East lower and South East higher.

Pollution of PM_{10} at the Tshwane Market displayed strong sources from North East lower situated at 14%, South-West and West higher between 10 and 15%. In Figure 4.69 the

maximum ambient concentration for sulfur dioxide at the Tshwane Market was 6 $\mu g/m^3$. The results displayed weak pollution from North West higher, North, North East higher.

Pollution of sulfur dioxide concentrations at the Tshwane Market displayed strong sources from North East lower at 25%, South-West and West higher were between 15 and 25%. The maximum ambient concentrations for sulfur dioxide at the Tshwane Market were 43.447 parts per billion. In Figure 4.67 results indicated weak pollution on the North, North West lower and North East higher.

In Figure 4.70, pollution of sulfur dioxide concentrations at the Vanderbijlpark indicated strong sulfur dioxide sources from North West higher between 20 and 25 %, East at 14%, South West higher at 11%, South East higher at 9%. The maximum ambient concentration for sulfur dioxide at the Vanderbijlpark was 188.21 parts per billion. The results displayed weak pollution from South, South East lower and South West lower and North East higher. At the ambient concentrations of 0 to 5 parts per billion showed strong pollution rose from North West higher between 15 and 25%, South West higher between 5 and 10%, East between 5 and 10% and North West higher.

In Figure 4.70, Pollution of ozone concentrations at the Vanderbijlpark displayed strong sources from North West higher between 15 and 20 %, East at 5 and 10%, South West higher between 5 and 10%, South East higher between 5 and 10%. In Figure 88 maximum and mean ambient concentrations for sulfur dioxide at the Vanderbijlpark were 85.264 and 22.963 parts per billion respectively. The results indicated weak pollution roses in order from South, South East lower and South West lower and North East higher. At the ambient concentrations of 0 to 10 parts per billion showed strong pollution rose from East, South East, North East and North West higher which were under 5%.

In Figure 4.70, pollution of PM_{10} at the Vanderbijlpark indicated strong sources from North West higher between 10 and 12%, East at 8 and 10%, South West higher between 4 and 6 %, South East higher between 4 and 6 %. The maximum and mean ambient concentrations for sulfur dioxide at the Vanderbijlpark were 961.64 and 94.321 $\mu g/m^3$ PM_{10} respectively. The results displayed weak pollution in order from South, South East lower and South West lower and North East higher. At the ambient concentrations of 0 to 50 $\mu g/m^3$ PM_{10} showed strong pollution from South West higher, West, North West higher and North West lower between 4 and 6 %.

In Figure 4.71, pollution of nitrogen dioxide of parts per billion concentrations at the Wattville indicated strong nitrogen dioxide sources from North West higher between 12 and 14%, East at 8 and 10%, South West higher between 4 and 6 %, South West higher at 12%, West, East, North East higher and North East lower. The maximum and mean ambient concentrations for sulfur dioxide at the Wattville were 70.025 and 15.212 parts per billion respectively. The results displayed weak pollution roses from South, South East lower and South West lower and North. At the ambient concentrations of 0 to 5 parts per billion showed strong pollution rose from South West higher and North East higher less than 4%.

Pollution rose of PM_{10} at the Wattville indicated strong PM_{10} sources from North West higher between 12 and 14%, South West higher between 12 and 14%, South East higher between 4 and 6 %. Figure 4.72 maximum and mean ambient concentrations for sulfur dioxide at the Wattville were 271.8 and 94.389 $\mu g/m^3$ respectively. The results displayed weak pollution roses in order from South, North, South East lower and South West lower. At the ambient concentrations of 0 to 50 $\mu g/m^3$ showed strong pollution rose from South West higher, East, North West higher and North West lower less than 2%.

Figure 4.73, Pollution of sulfur dioxide of parts per billion concentrations at the Wattville displayed strong sources from North West higher between 12 and 14%, on the East at between 12 and 14%, East, North East lower, North East higher and West between 10 and 12%. The maximum and mean ambient concentrations for sulfur dioxide at the Wattville were 118.8 and 13.927 parts per billion respectively. The results displayed weak pollution from South, South East lower and South West lower and North. At the ambient concentrations of 0 to 5 parts per billion showed strong pollution rose from South West higher and North East higher less than 4%.

4.3 Bivariate Polar Plot at receptor and Emission Inventory Facilities within Gauteng Province.

Further evaluations were carried out using the bivariate polar function which is found in open-air' R' package. The technique indicates how pollution concentrations vary with the wind speed and wind direction. The ambient monitoring station location is symbolized by the graph starting point at the midpoint of the plot. The plot has 4 quadrants which resemble wind direction based on the origin of the source. The distance from the midpoint to the exterior of

the plot indicates wind speed in meters per seconds. The origin of the plot indicates less wind speed whereas higher wind speed occurs when moving out from the midpoint of the plot. Calm conditions appear closer to the origin of the receptor whereas unstable condition indicate far sources. The results are presented in Figure 4.74 to Figure 4.135 below.

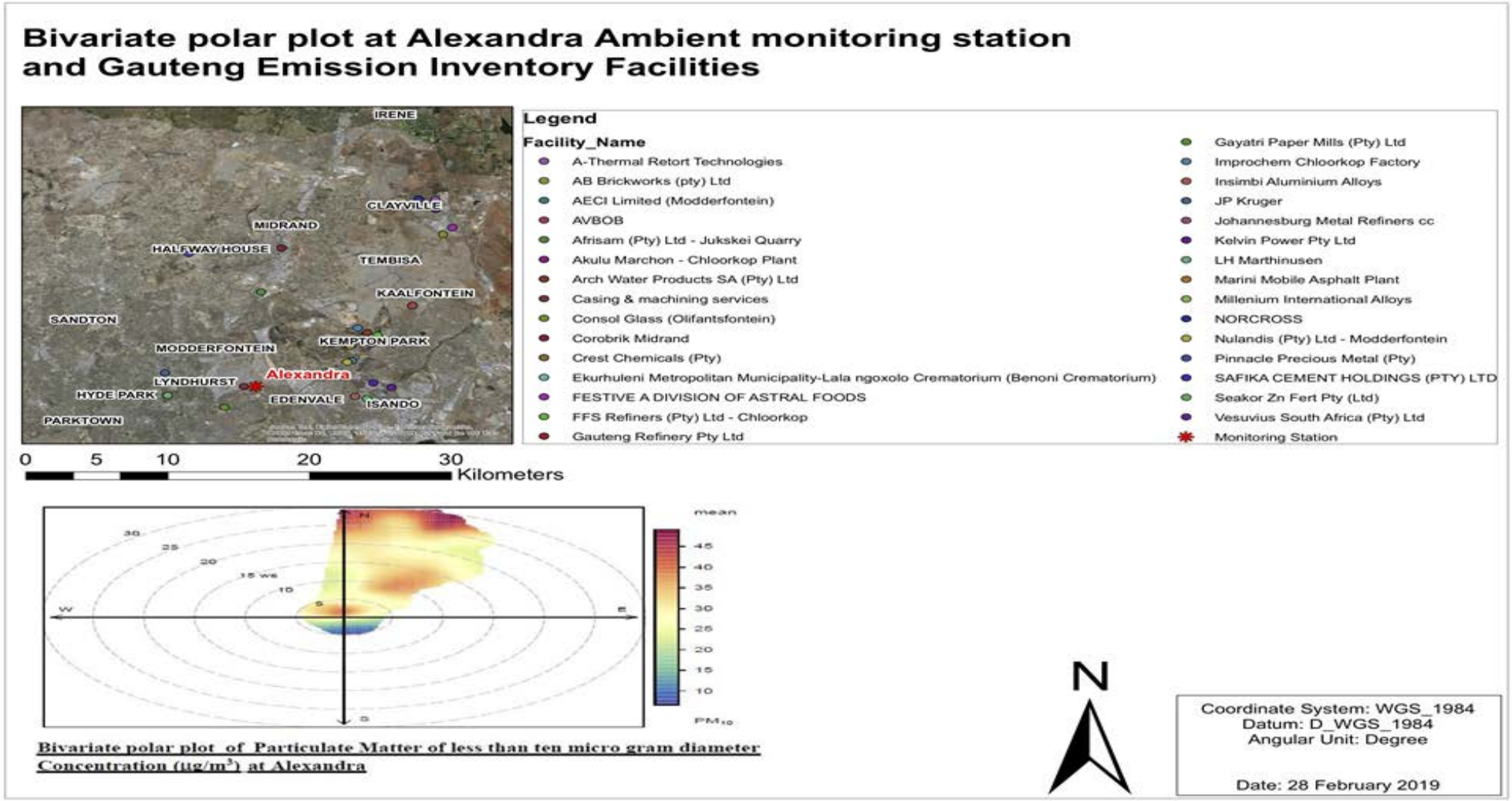

Figure 4.74: Bivariate polar plot at the Alexandra Ambient Monitoring Stations and Emission Inventory Facilities in Gauteng Province

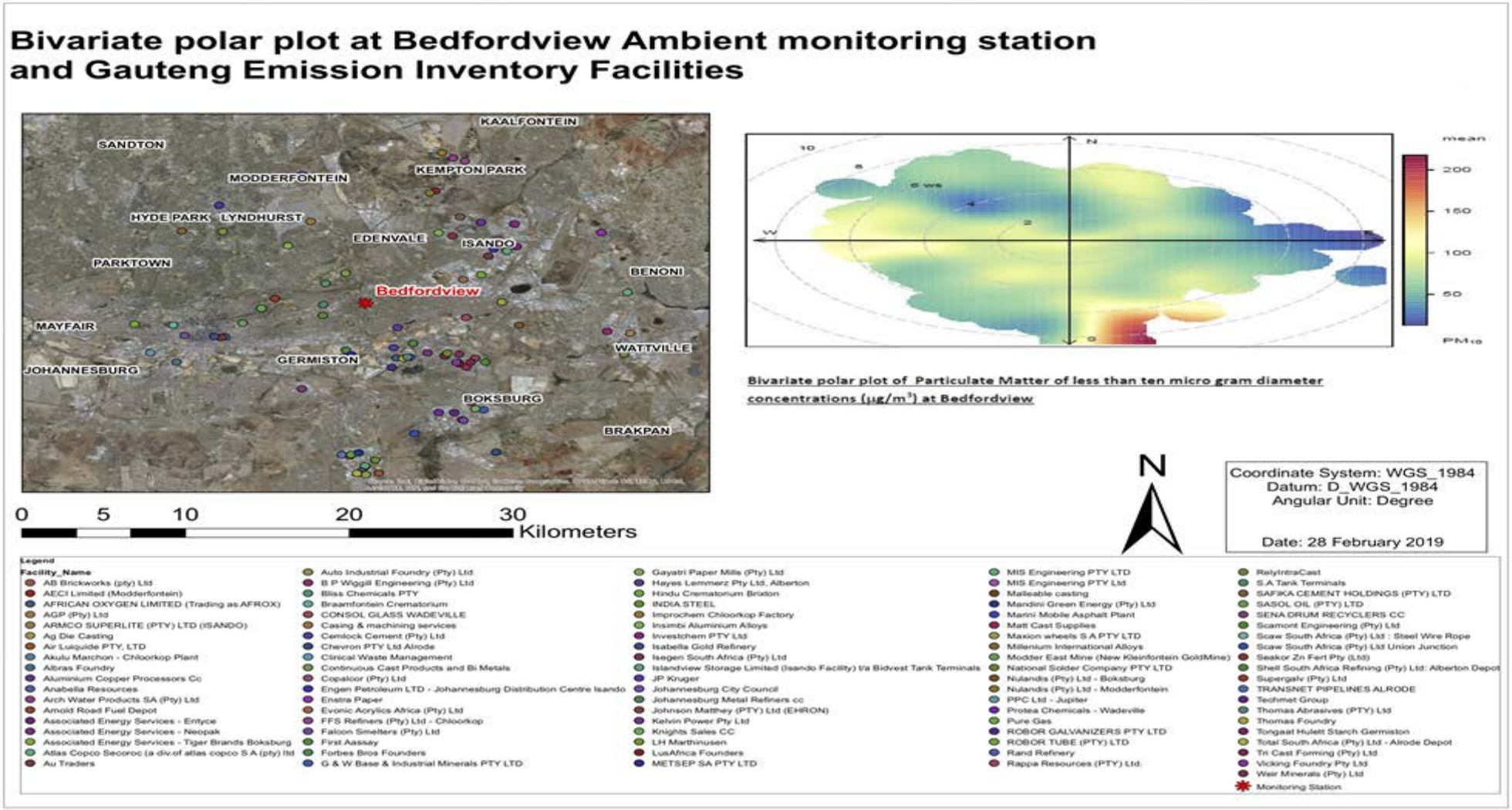

Figure 4.75: Bivariate polar plot at the Bedfordview Ambient Monitoring Stations and Emission Inventory Facilities in Gauteng Province

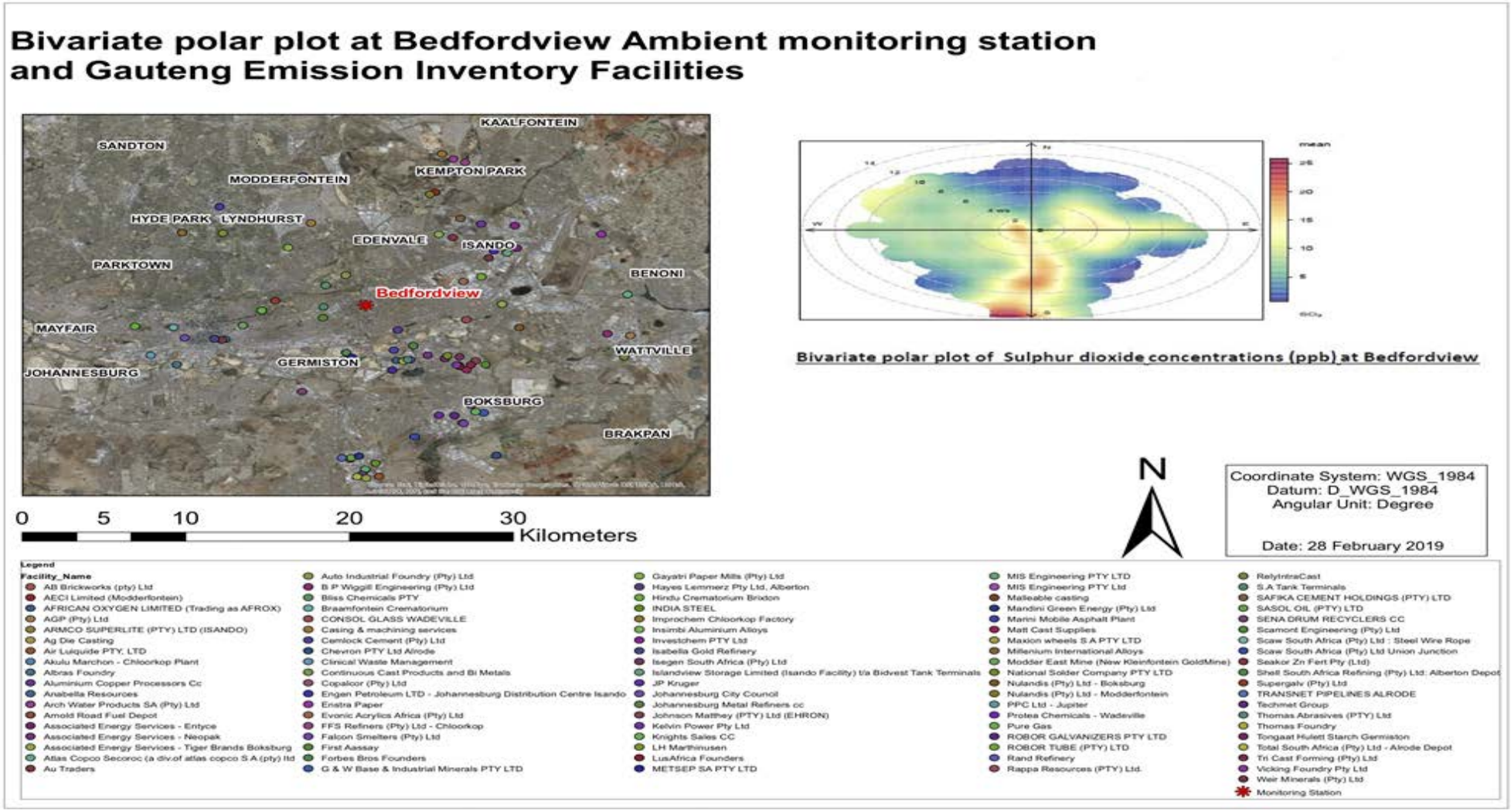

Figure 4.76: Bivariate polar plot at the Bedfordview Ambient Monitoring Stations and Emission Inventory Facilities in Gauteng Province

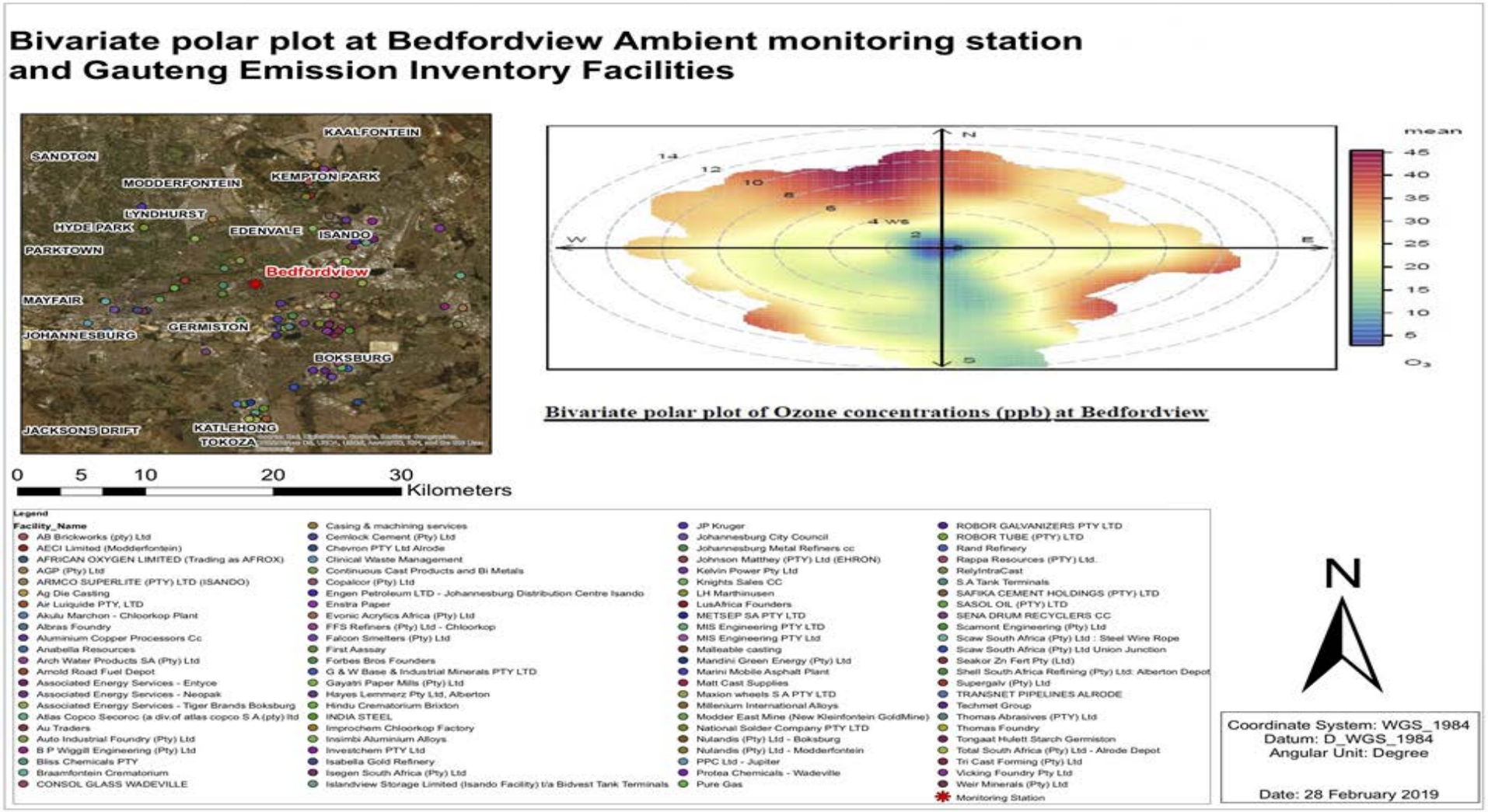

Figure 4.77: Bivariate polar plot at the Bedfordview Ambient Monitoring Stations and Emission Inventory Facilities in Gauteng Province

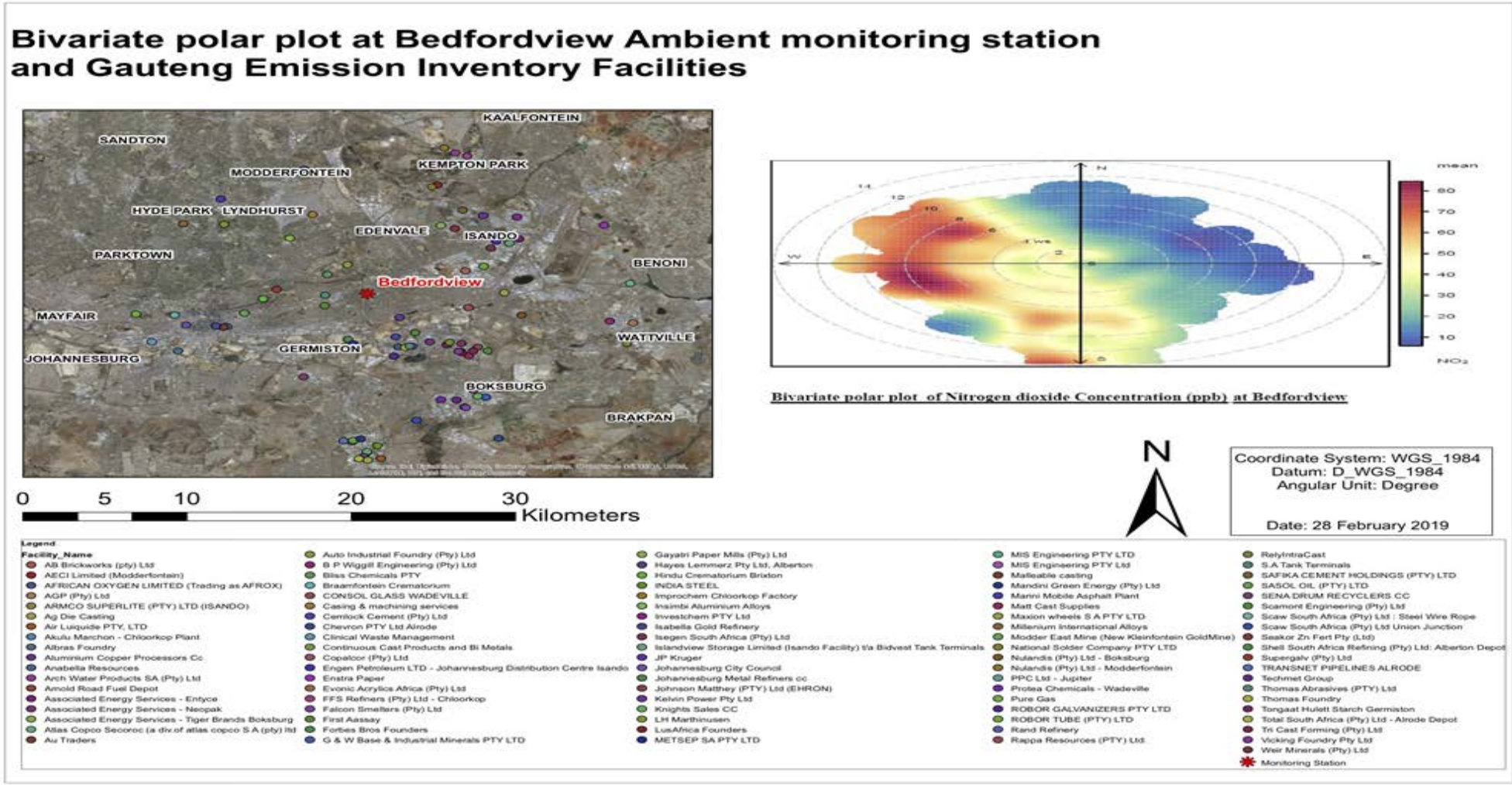

Figure 4.78: Bivariate polar plot at the Bedfordview Ambient Monitoring Stations and Emission Inventory Facilities in Gauteng Province

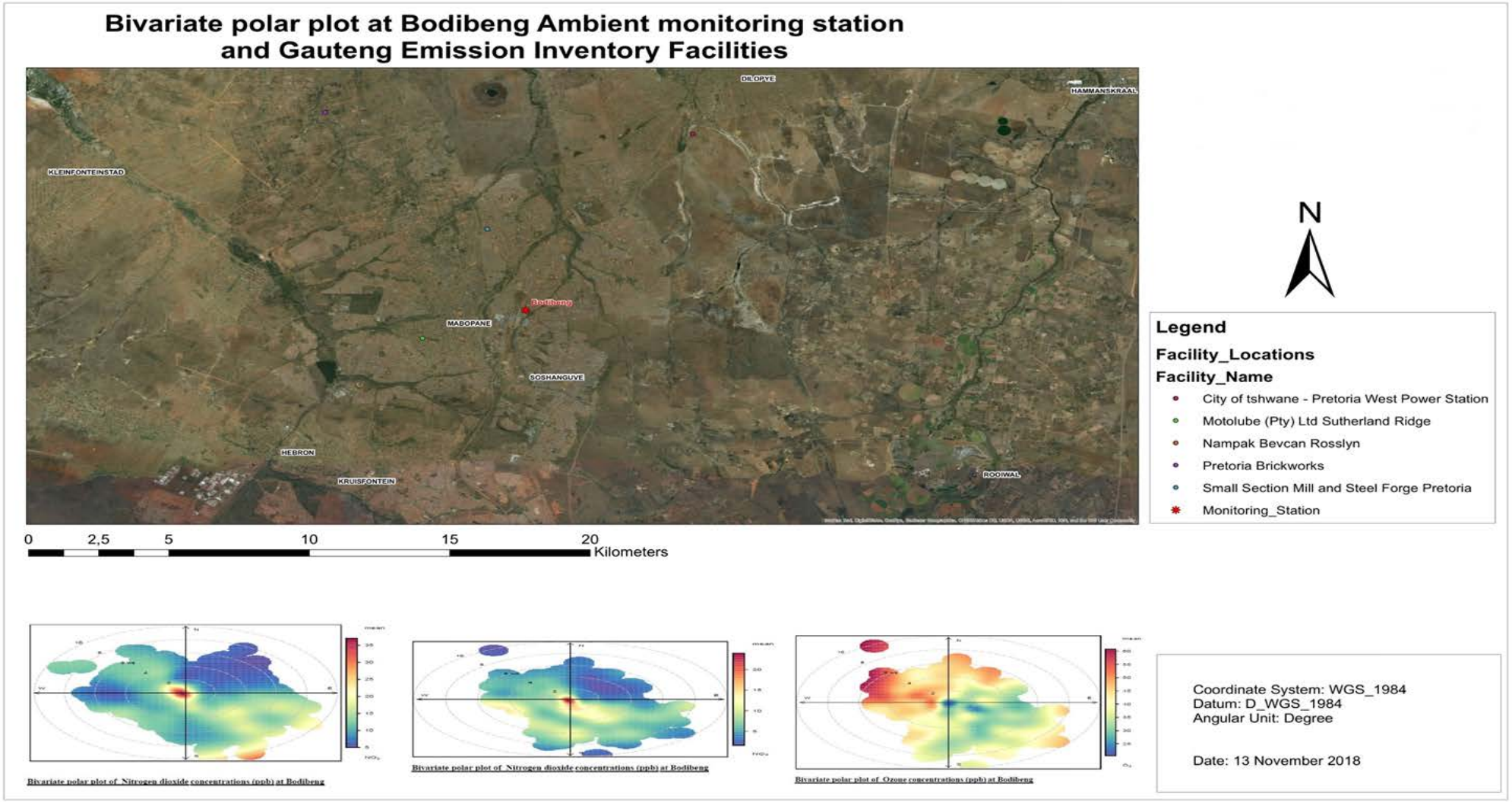

Figure 4.79: Bivariate polar plot at the Bodibeng Ambient Monitoring Stations and Emission Inventory Facilities in Gauteng Province

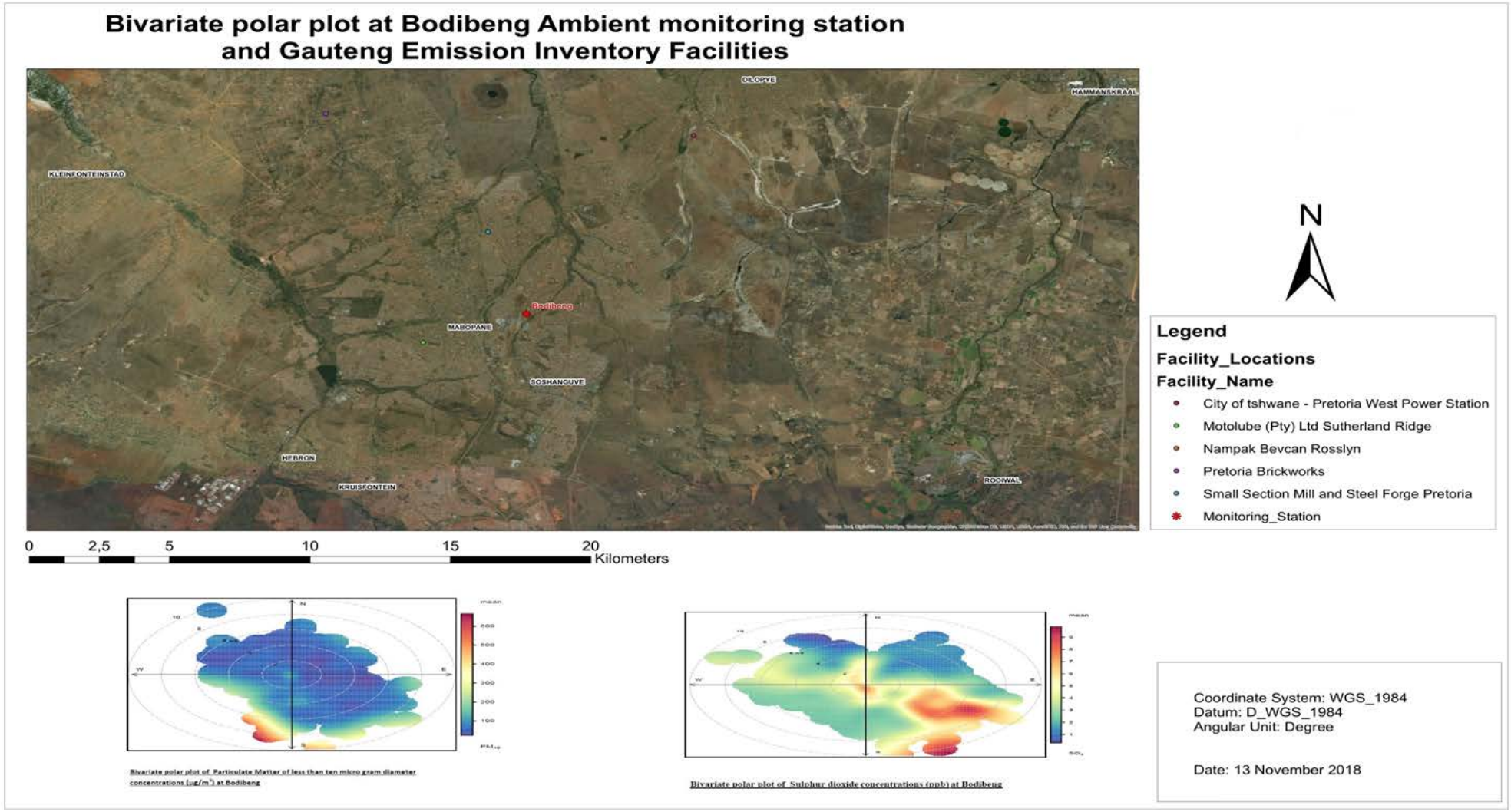

Figure 4.80: Bivariate polar plot at the Bodibeng Ambient Monitoring Stations and Emission Inventory Facilities in Gauteng Province

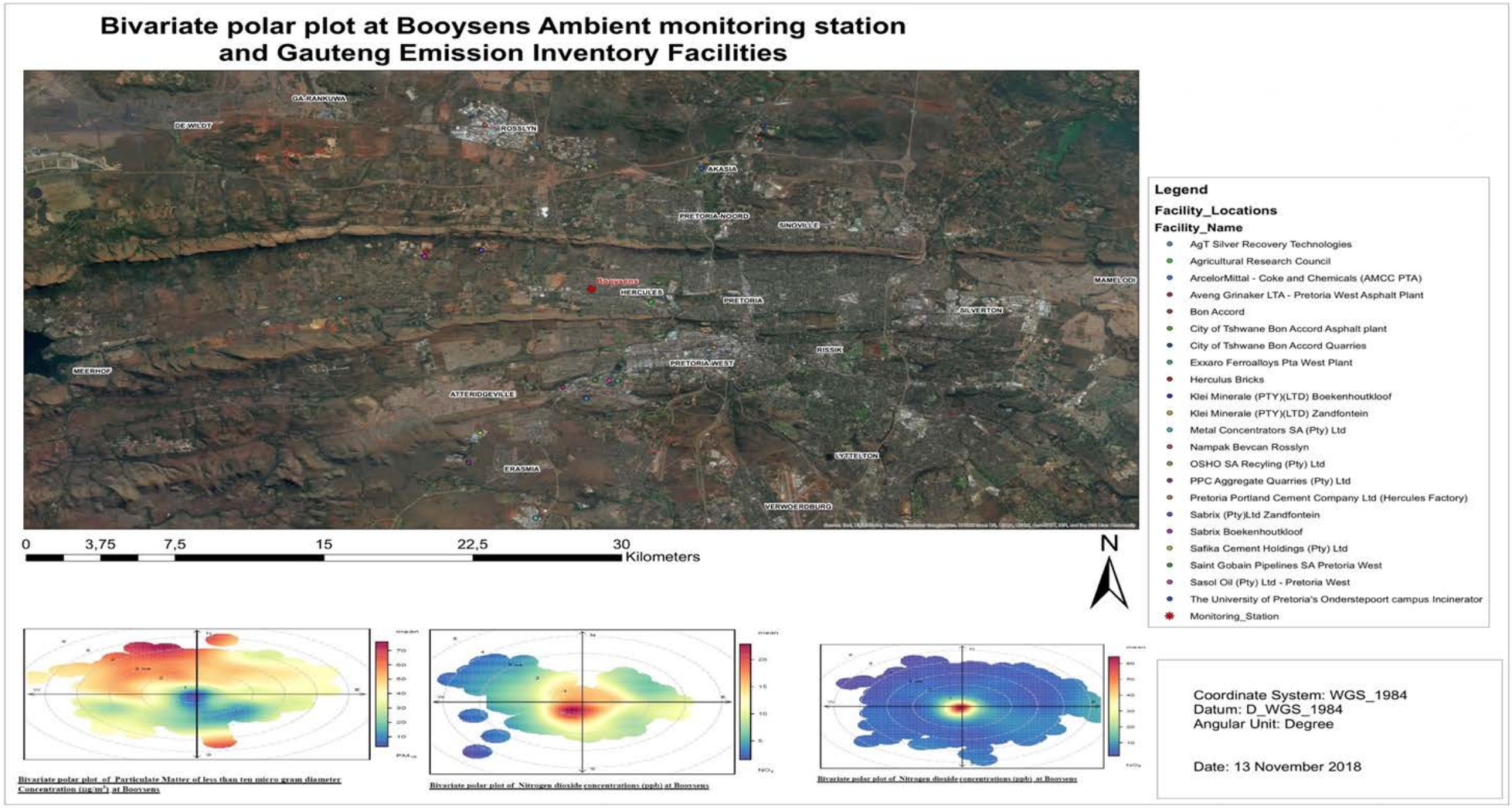

Figure 4.81 : Bivariate polar plot at the Booysens Ambient Monitoring Stations and Emission Inventory Facilities in Gauteng Province

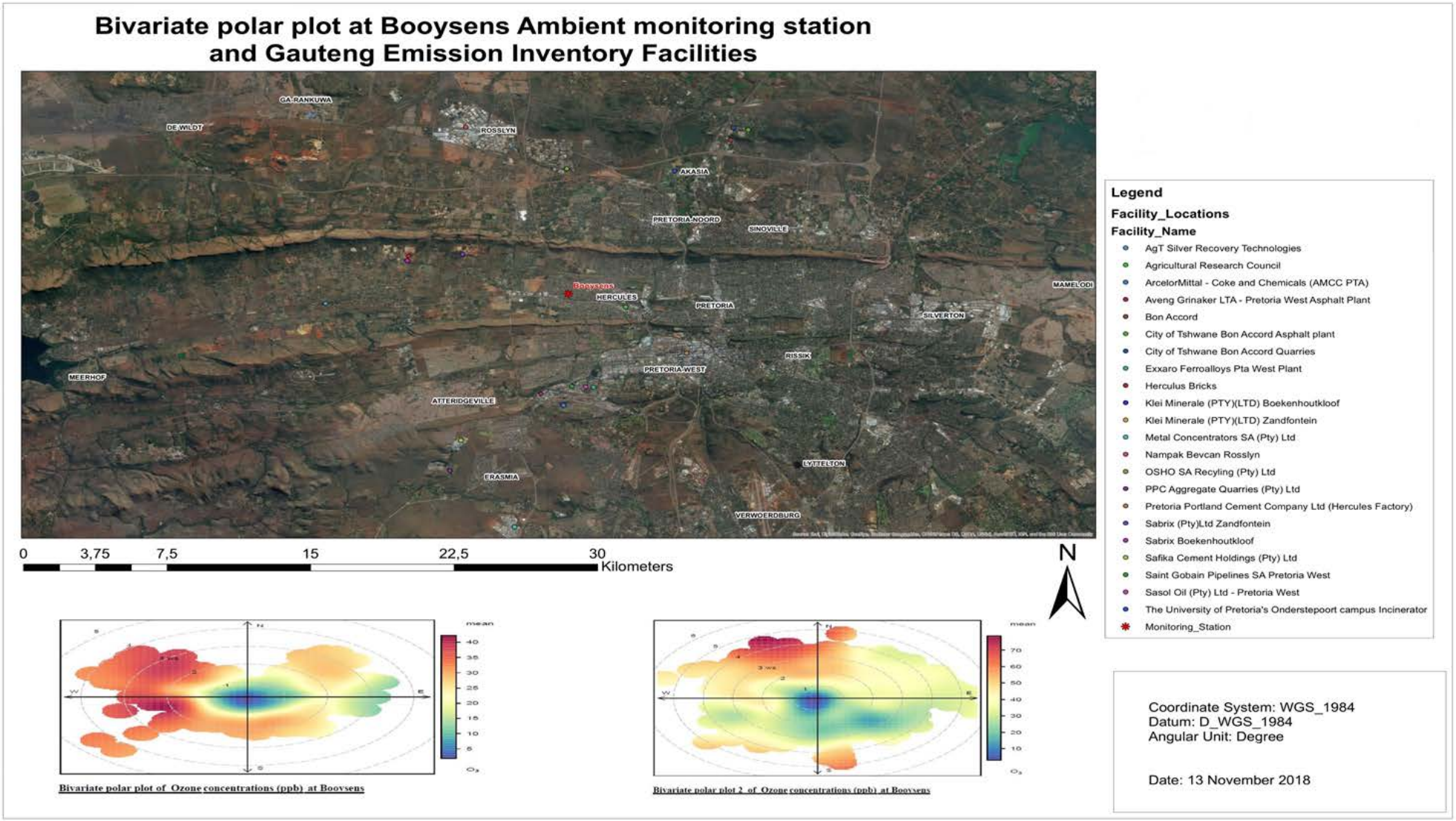

Figure 4.82: Bivariate polar plot at the Booysens Ambient Monitoring Stations and Emission Inventory Facilities in Gauteng Province

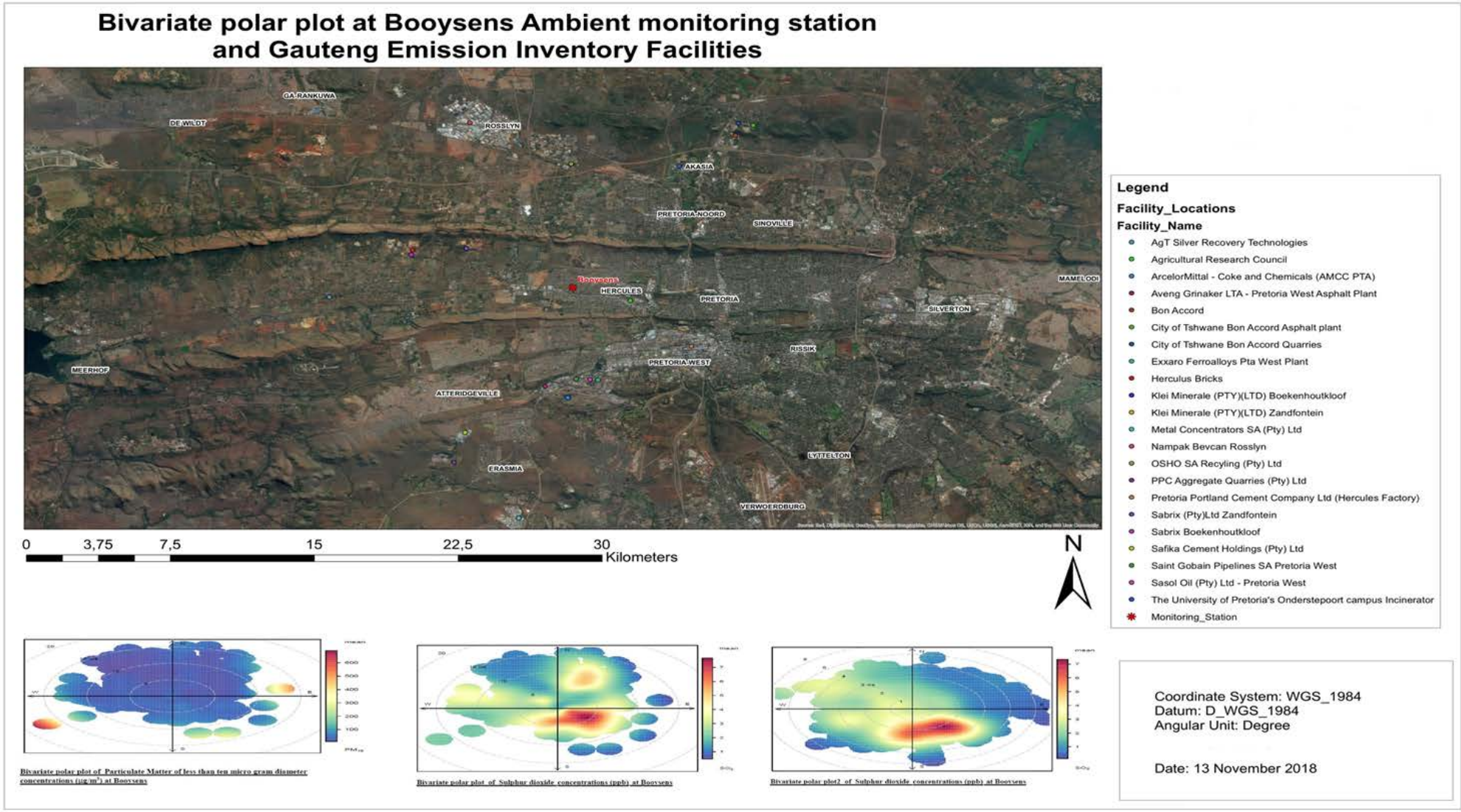

Figure 4.83: Bivariate polar plot at the Booysens Ambient Monitoring Stations and Emission Inventory Facilities in Gauteng Province

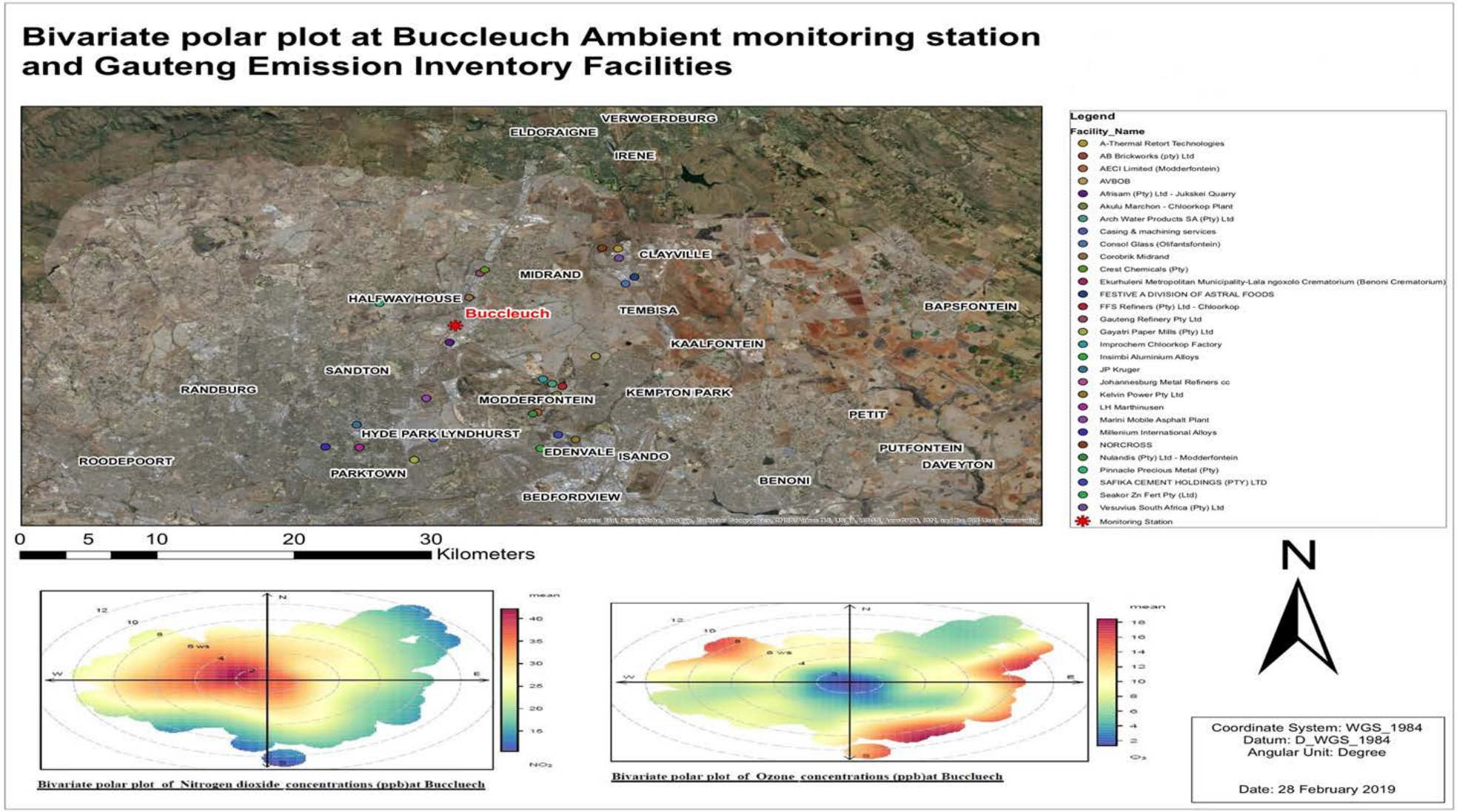

Figure 4.84: Bivariate polar plot at Buccluech Ambient Monitoring Stations and Emission Inventory Facilities in Gauteng Province

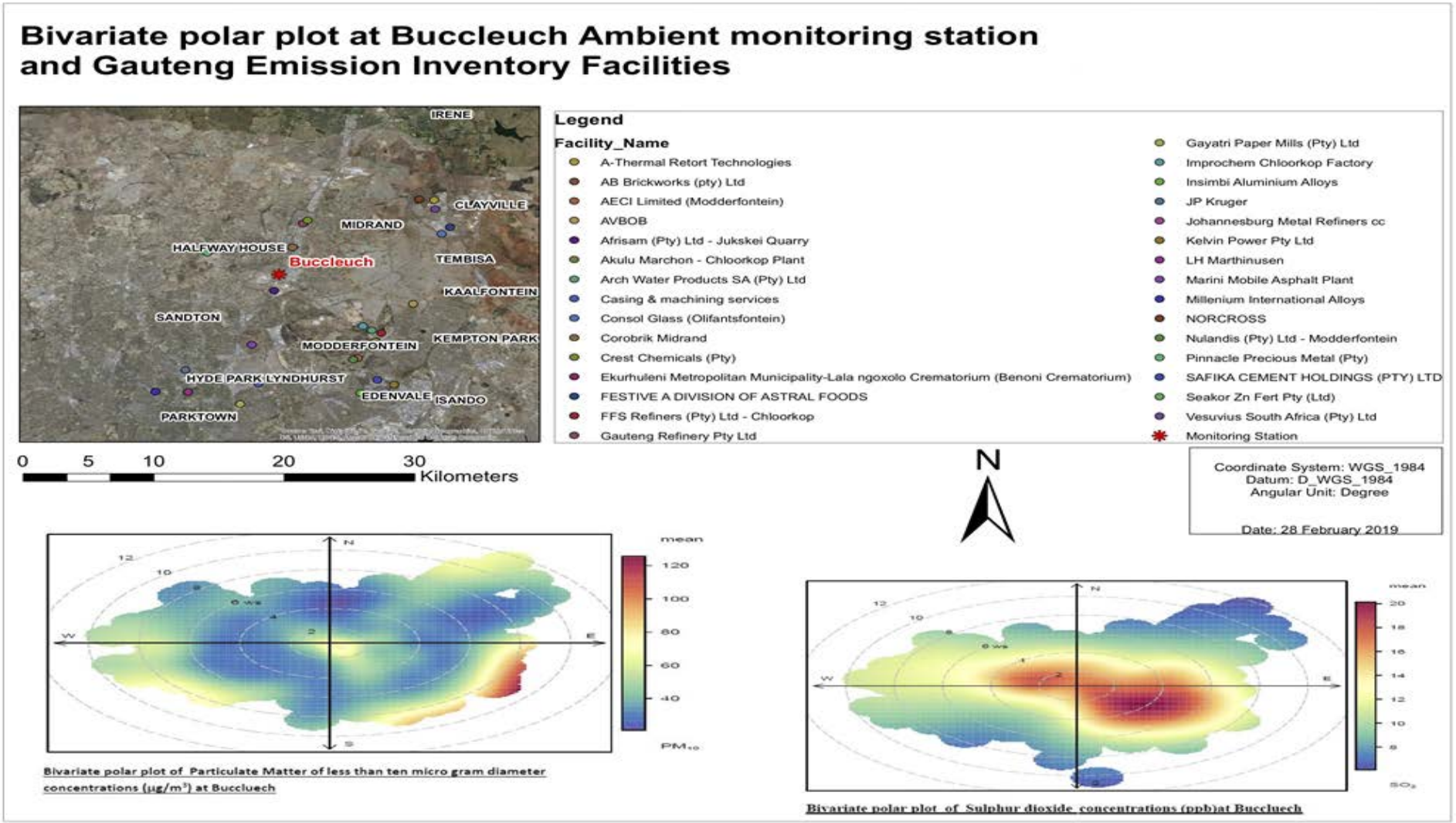

Figure 4.85: Bivariate polar plot at Buccluech Ambient Monitoring Stations and Emission Inventory Facilities in Gauteng Province

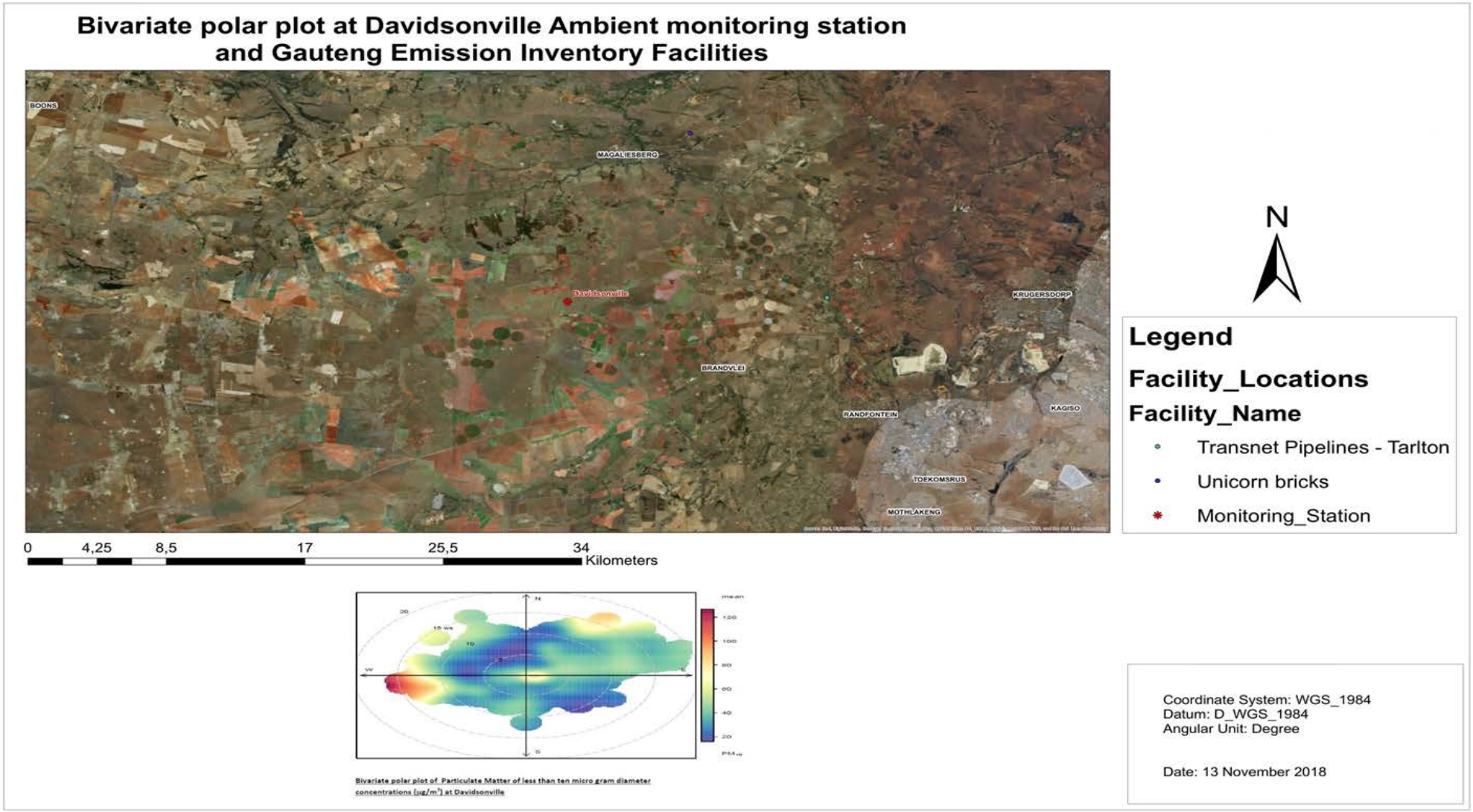

Figure 4.86: Bivariate polar plot at the Davidsonville Ambient Monitoring Stations and Emission Inventory Facilities in Gauteng Province

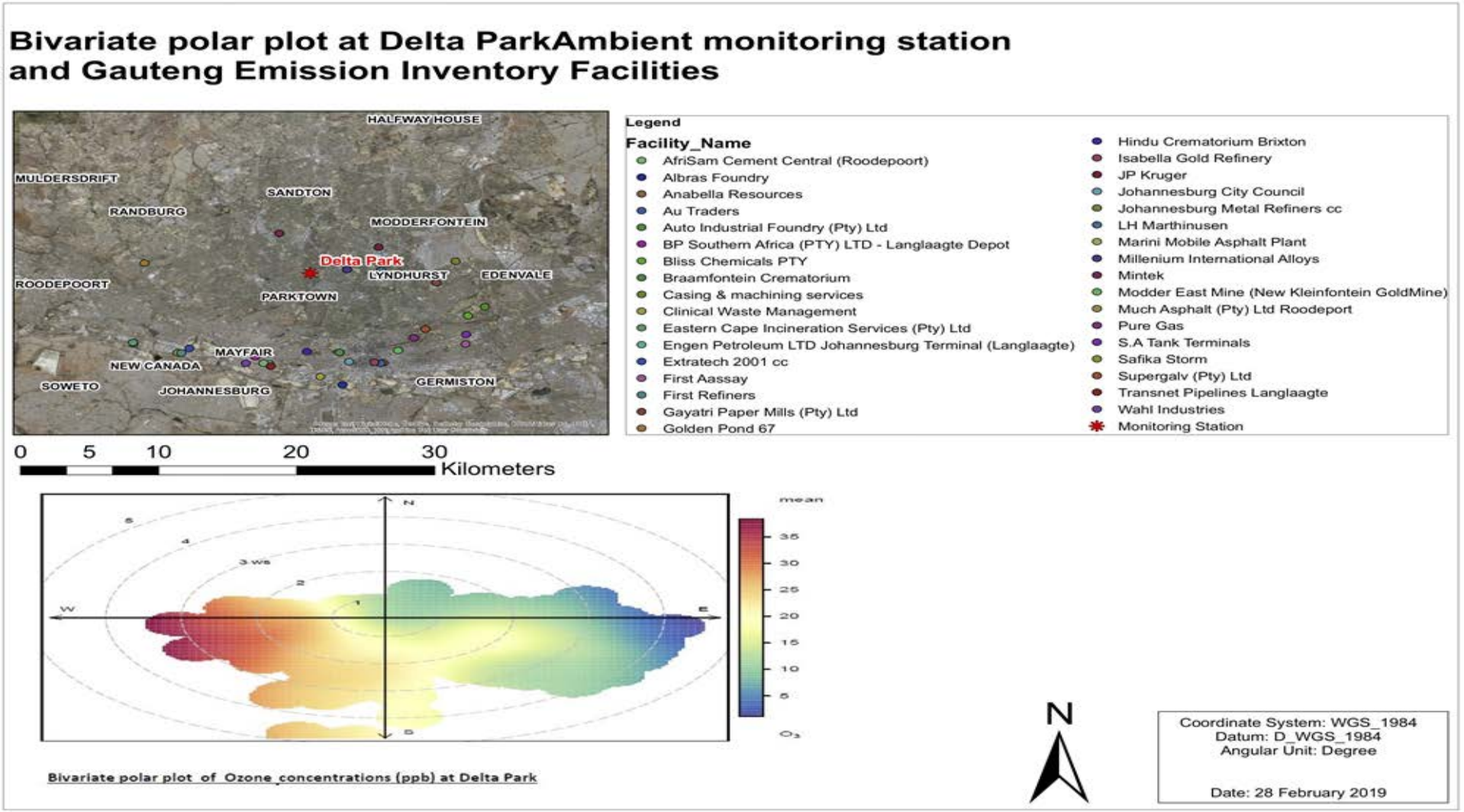

Figure 4.87: Bivariate polar plot at the Delta Park ambient Monitoring Stations and Emission Inventory Facilities in Gauteng Province

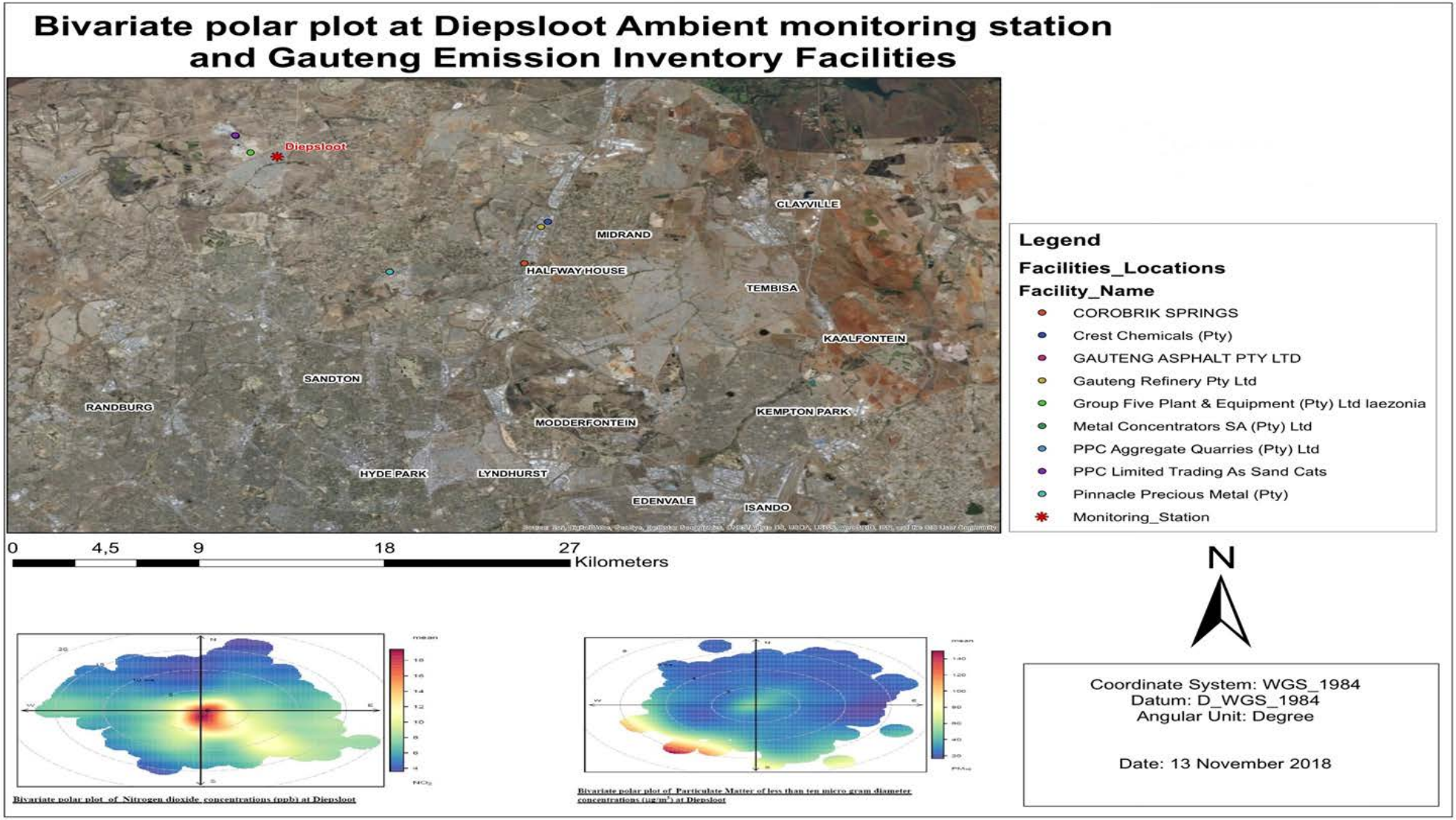

Figure 4.88: Bivariate polar plot at the Diepsloot Ambient Monitoring Stations and Emission Inventory Facilities in Gauteng Province

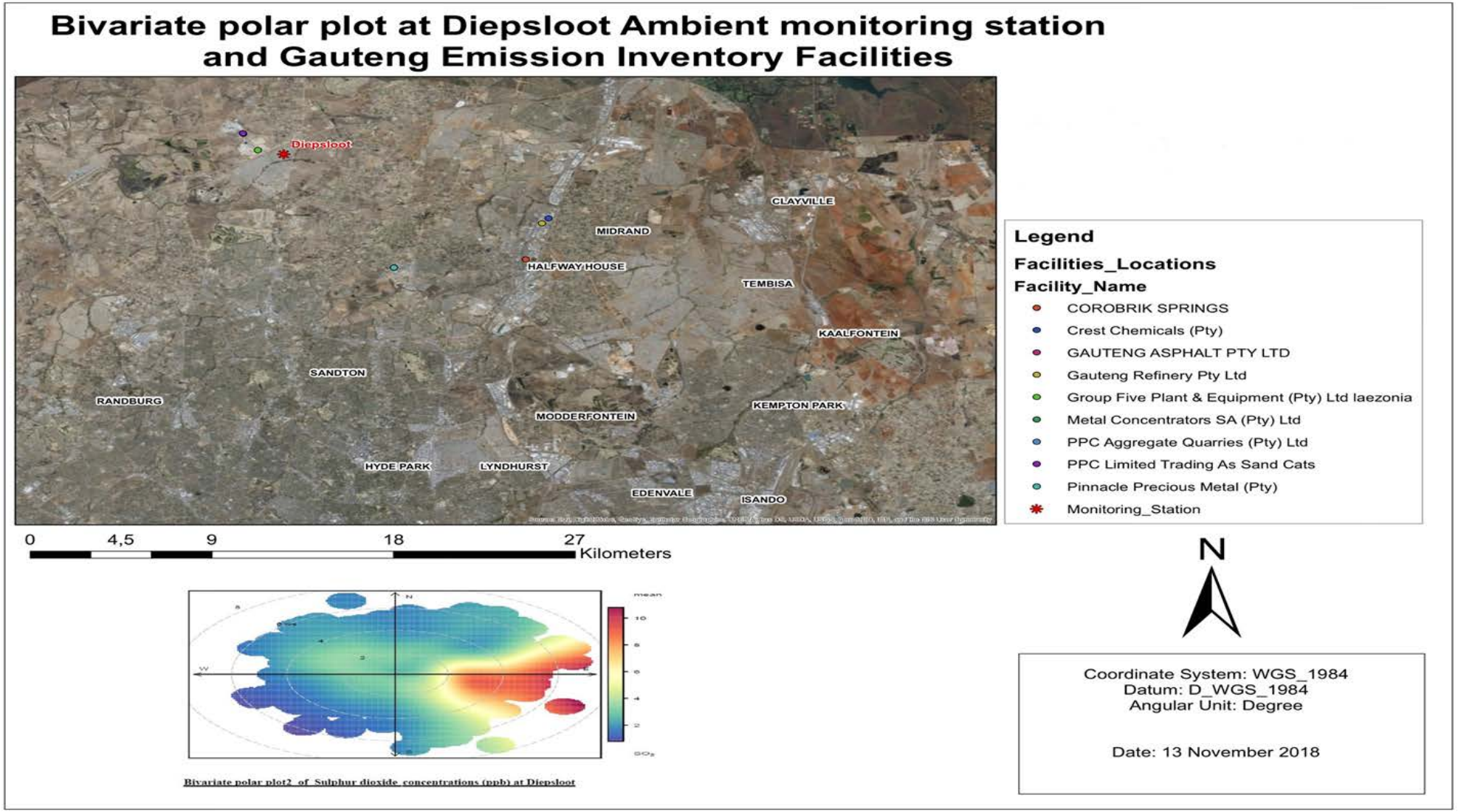

Figure 4.89: Bivariate polar plot at the Diepsloot Ambient Monitoring Stations and Emission Inventory Facilities in Gauteng Province

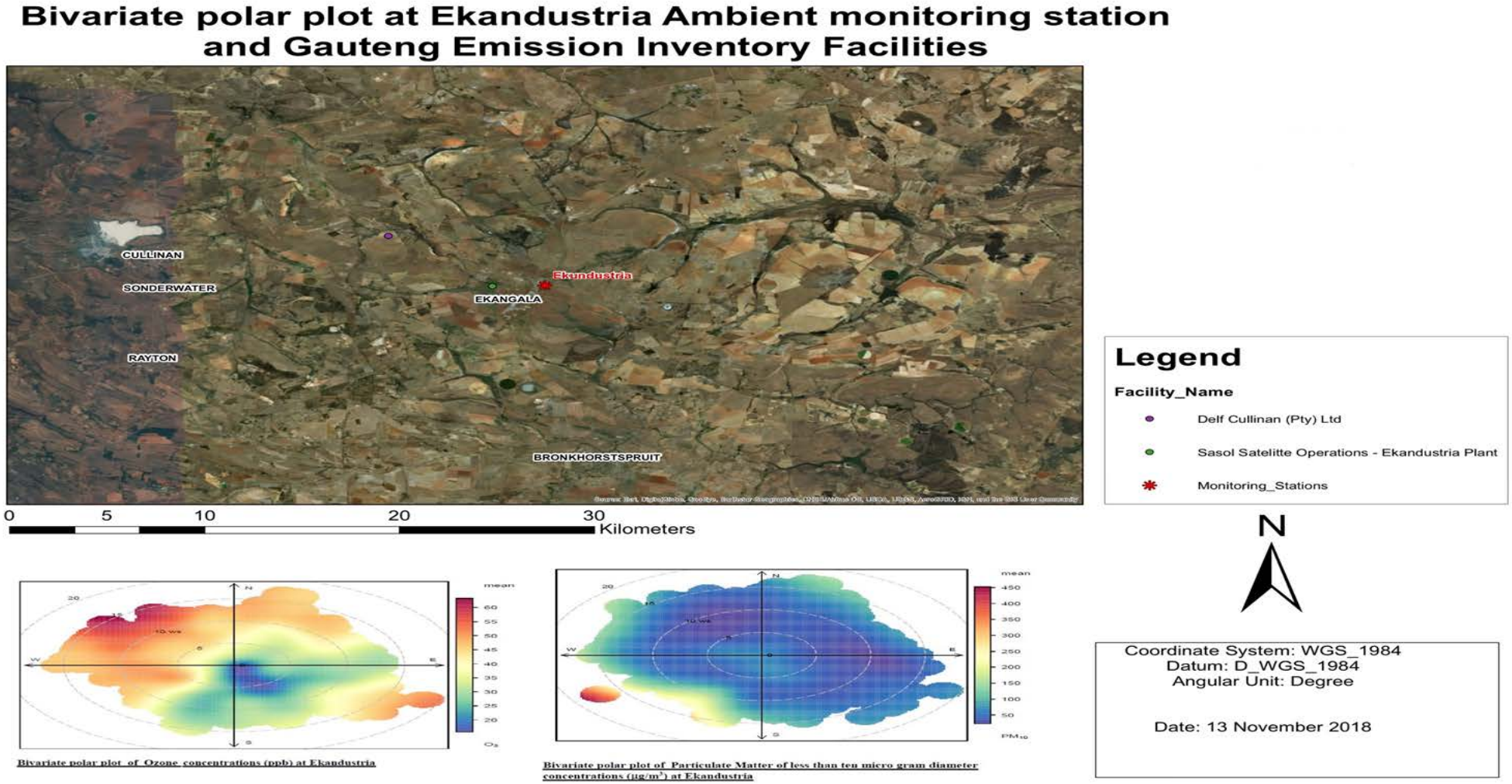

Figure 4.90: Bivariate polar plot at the Ekandustria Ambient Monitoring Stations and Emission Inventory Facilities in Gauteng Province

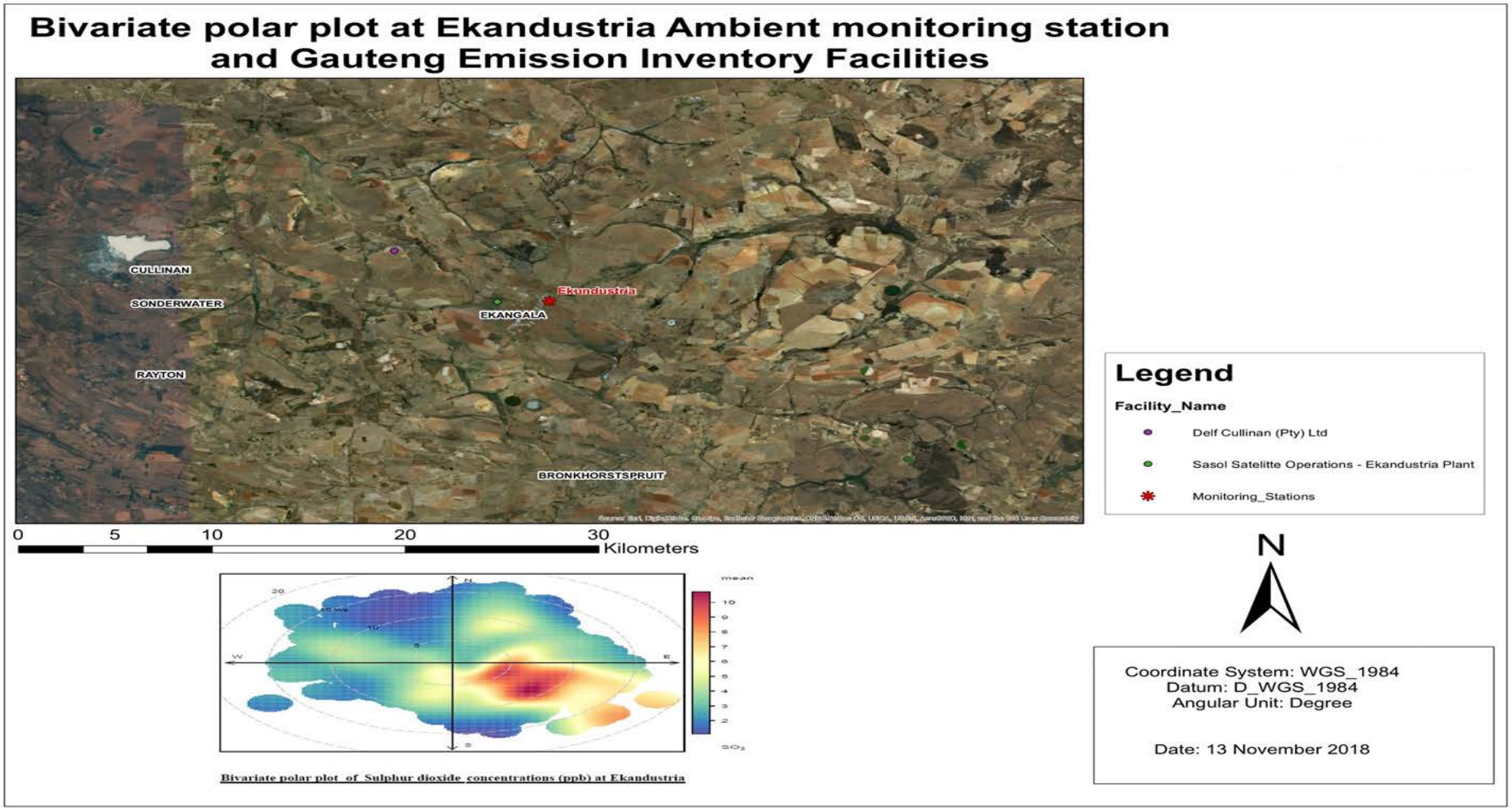

Figure 4.91: Bivariate polar plot at the Ekandustria Ambient Monitoring Stations and Emission Inventory Facilities in Gauteng Province

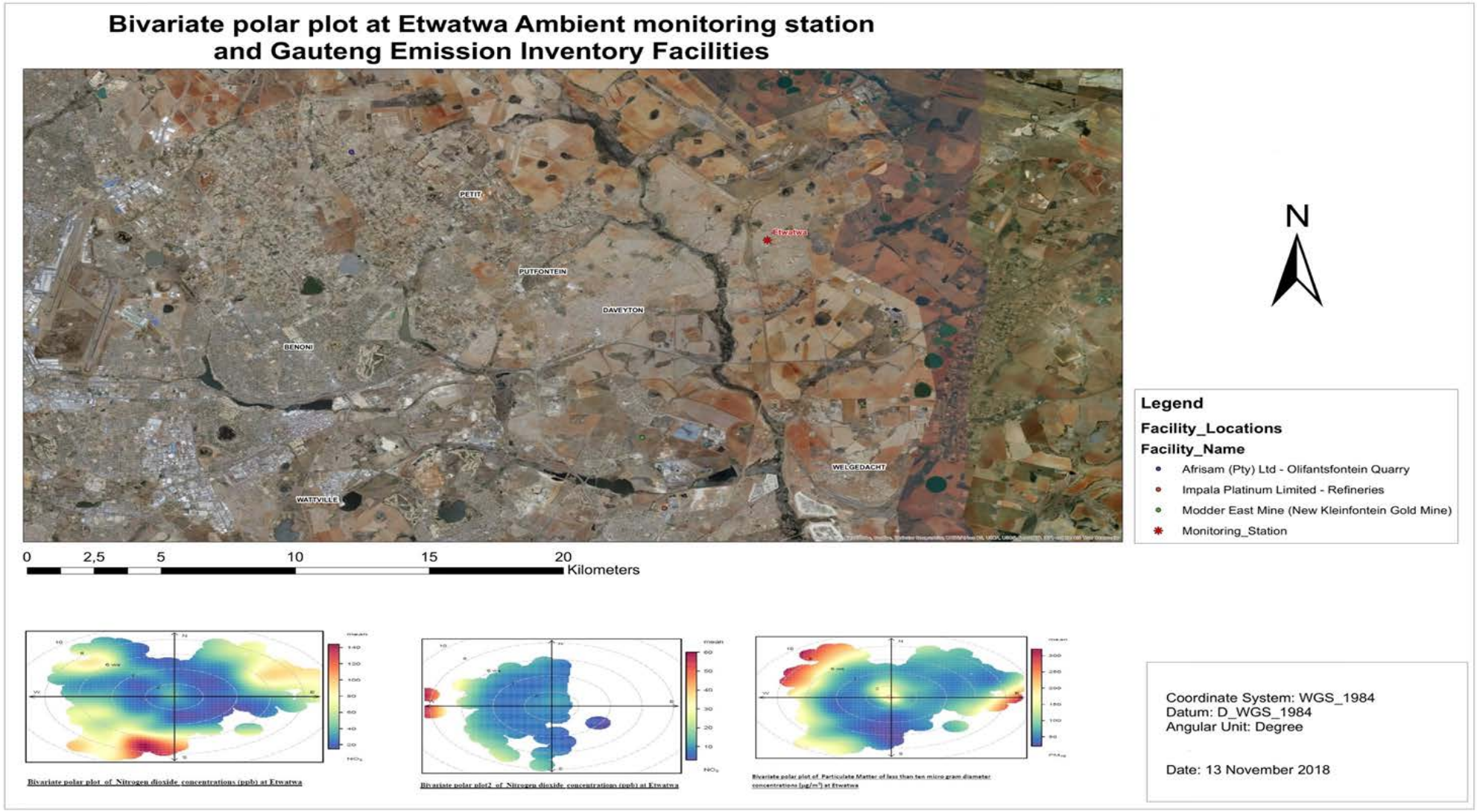

Figure 4.92: Bivariate polar plot at the Etwatwa Ambient Monitoring Stations and Emission Inventory Facilities in Gauteng Province

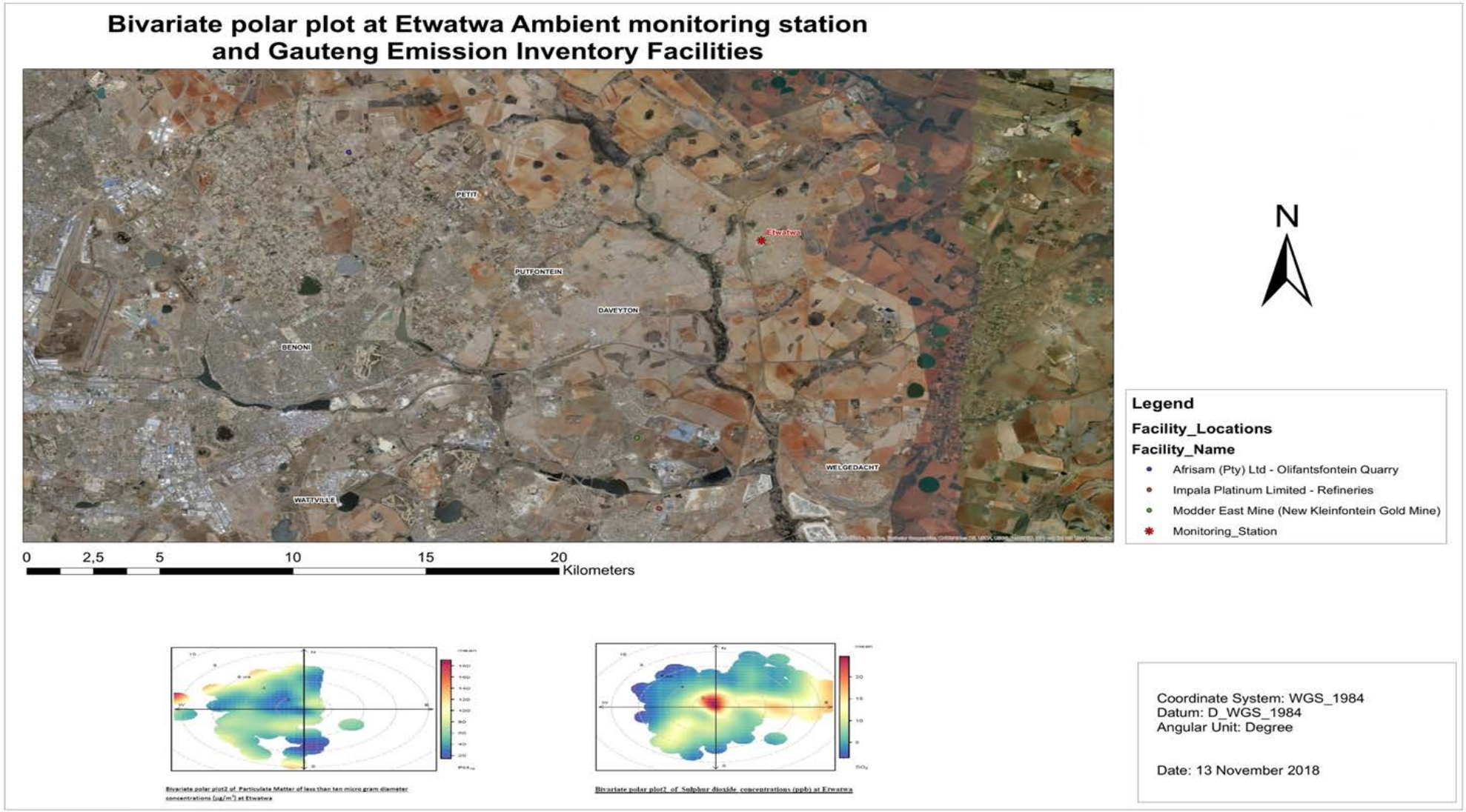

Figure 4.93: Bivariate polar plot at the Etwatwa Ambient Monitoring Stations and Emission Inventory Facilities in Gauteng Province

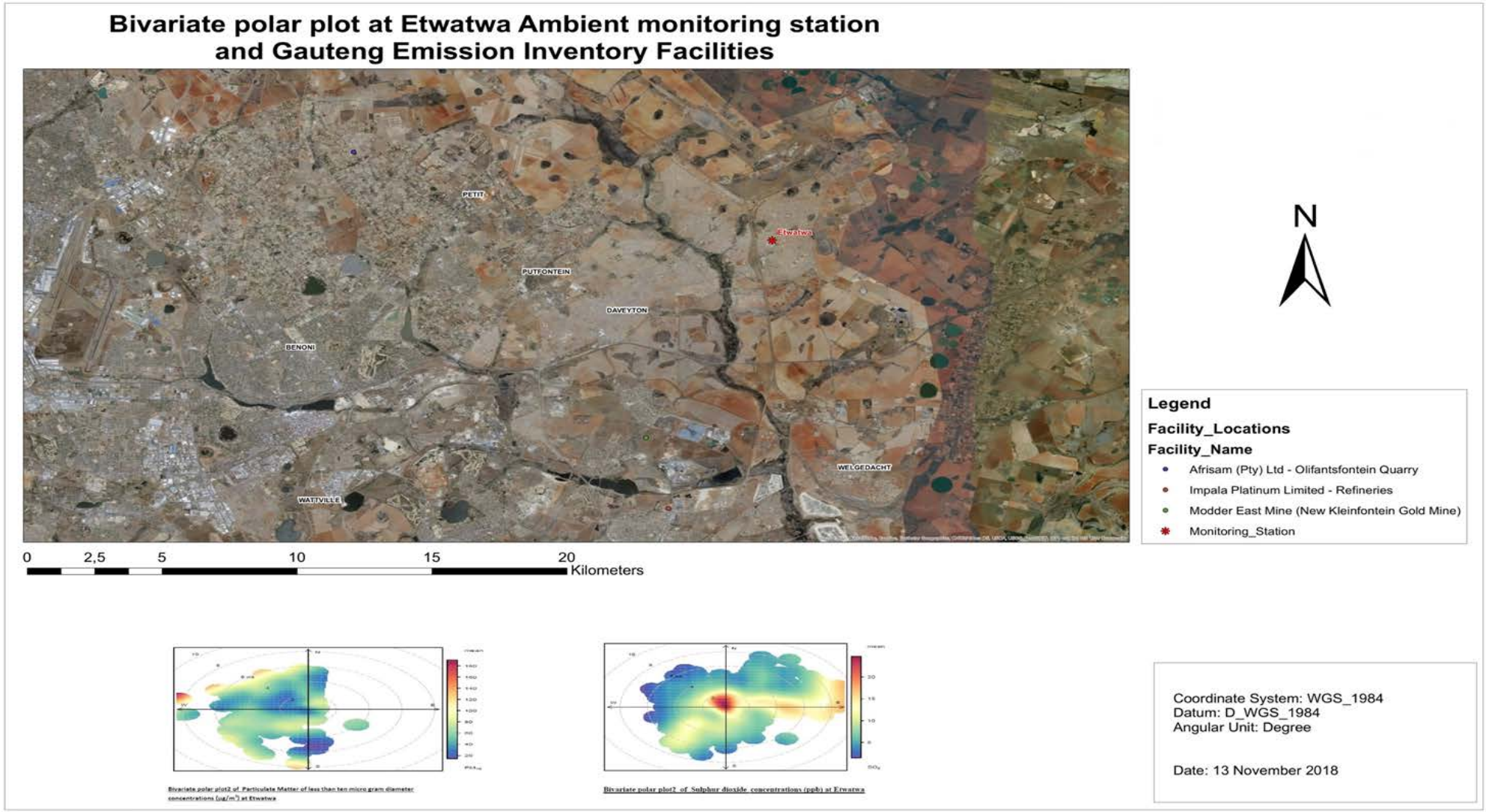

Figure 4.94: Bivariate polar plot at the Germiston Ambient Monitoring Stations and Emission Inventory Facilities in Gauteng Province

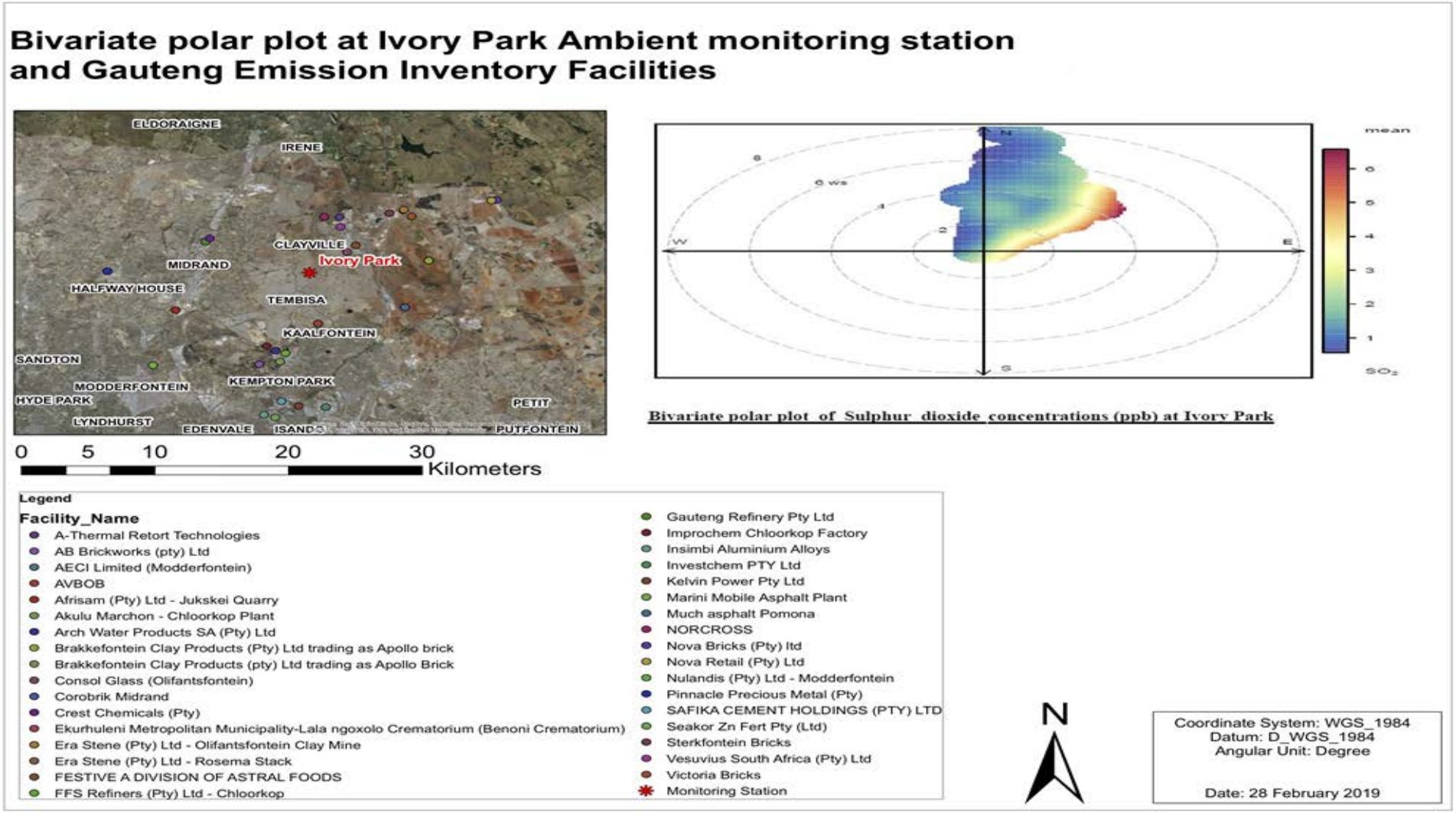

Figure 4.95: Bivariate polar plot at the Ivory Park Ambient Monitoring Stations and Emission Inventory Facilities in Gauteng Province

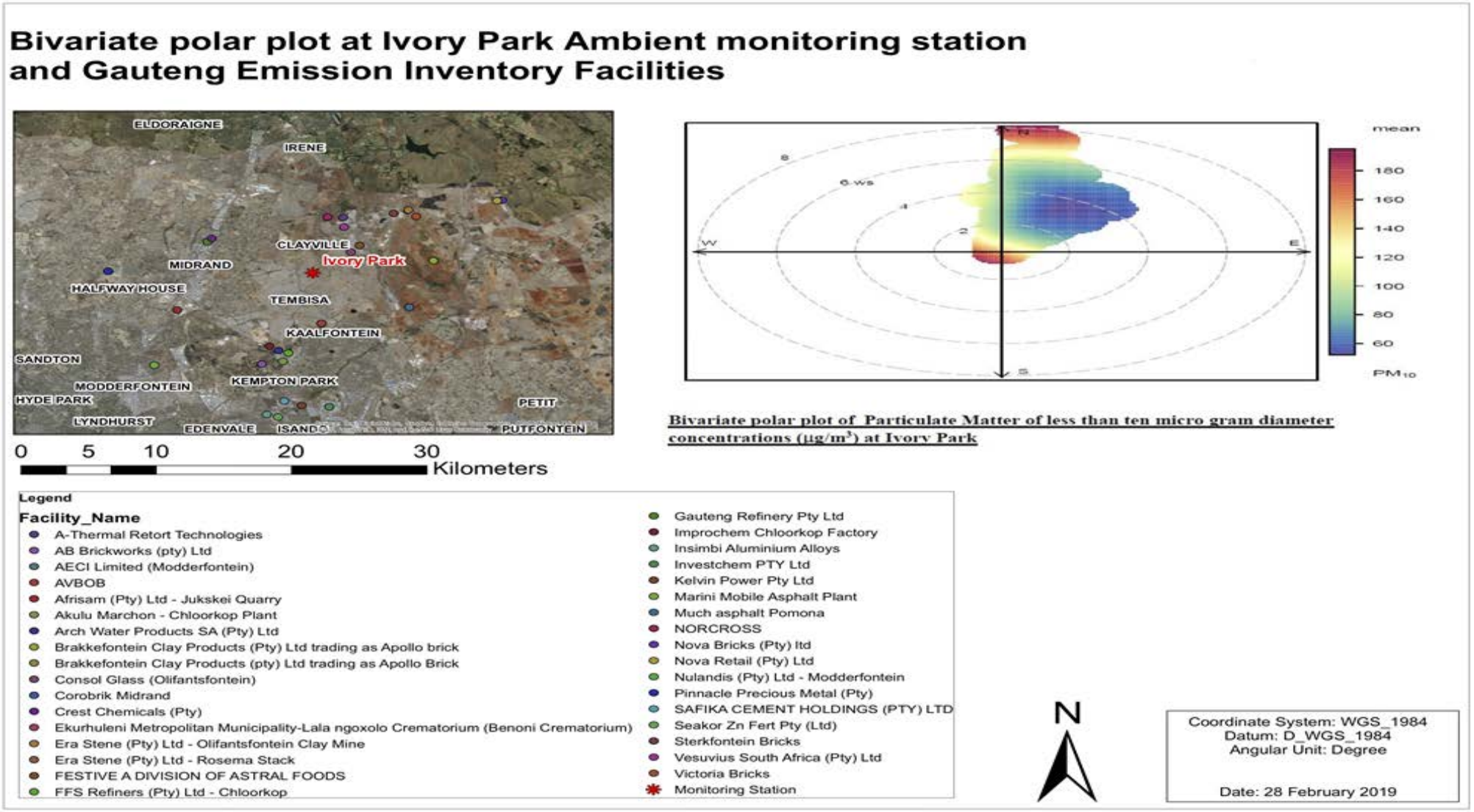

Figure 4.96: Bivariate polar plot at the Ivory Park Ambient Monitoring Stations and Emission Inventory Facilities in Gauteng Province

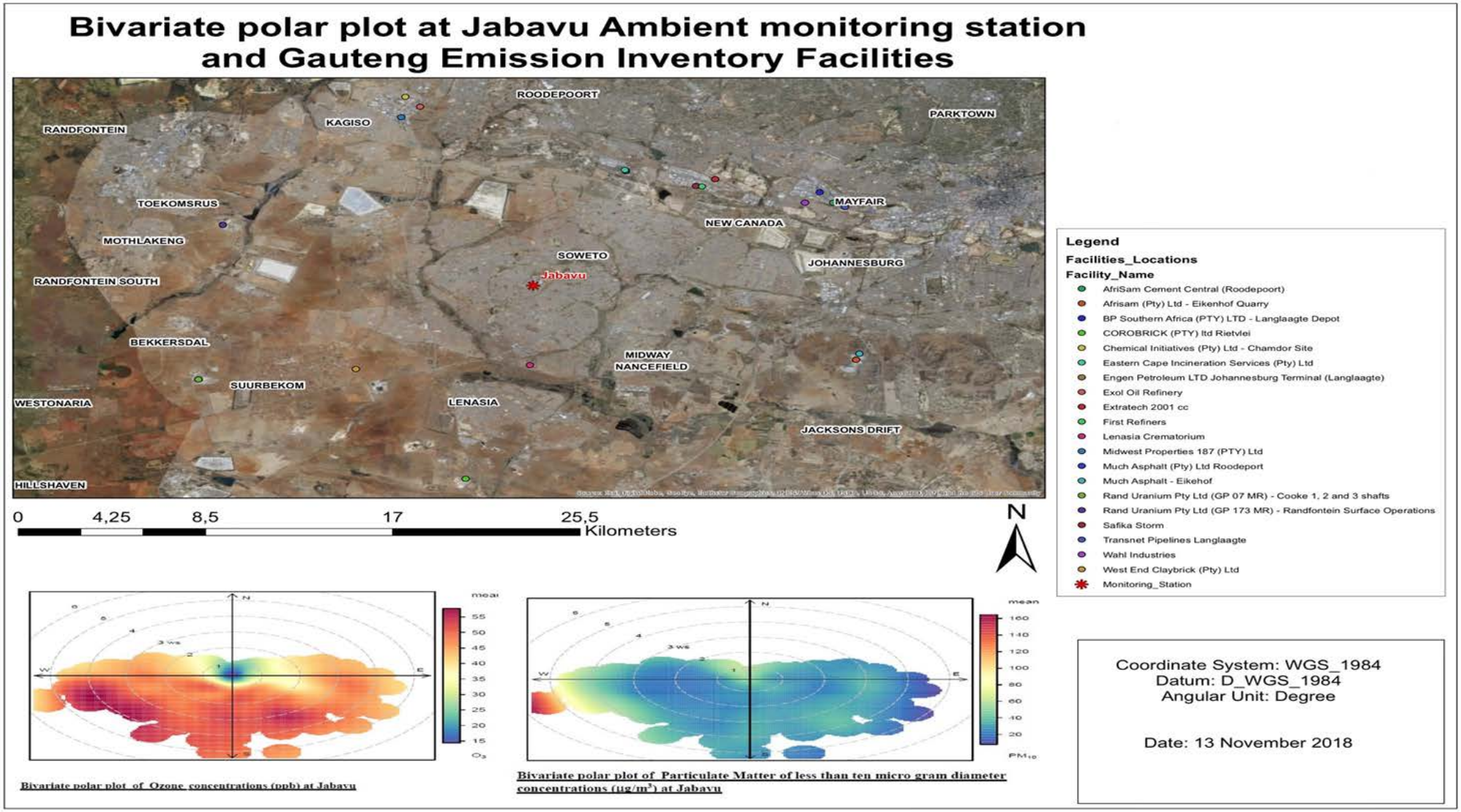

Figure 4.97: Bivariate polar plot at the Jabavu Ambient Monitoring Stations and Emission Inventory Facilities in Gauteng Province

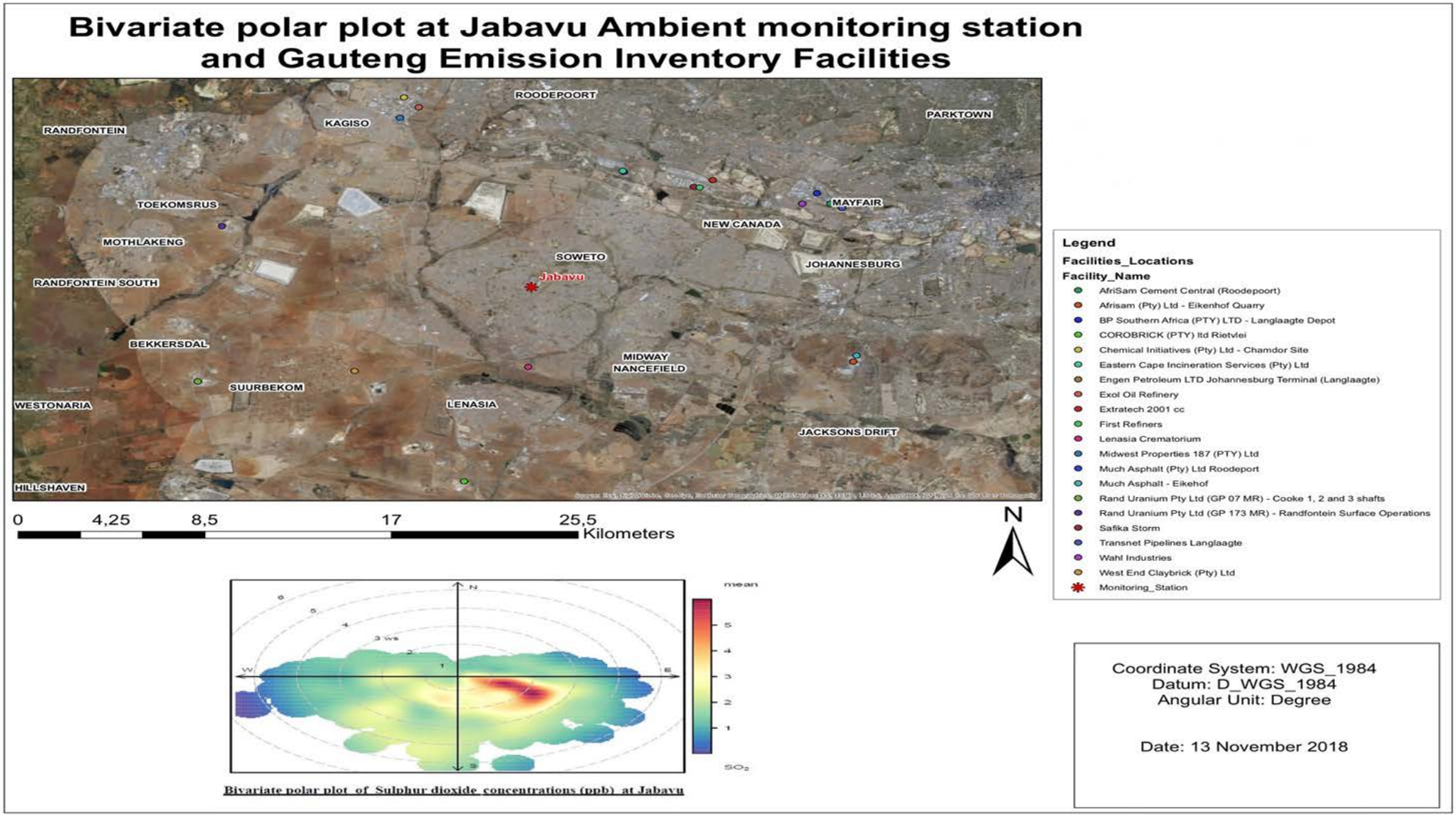

Figure 4.98: Bivariate polar plot at the Jabavu Ambient Monitoring Stations and Emission Inventory Facilities in Gauteng Province

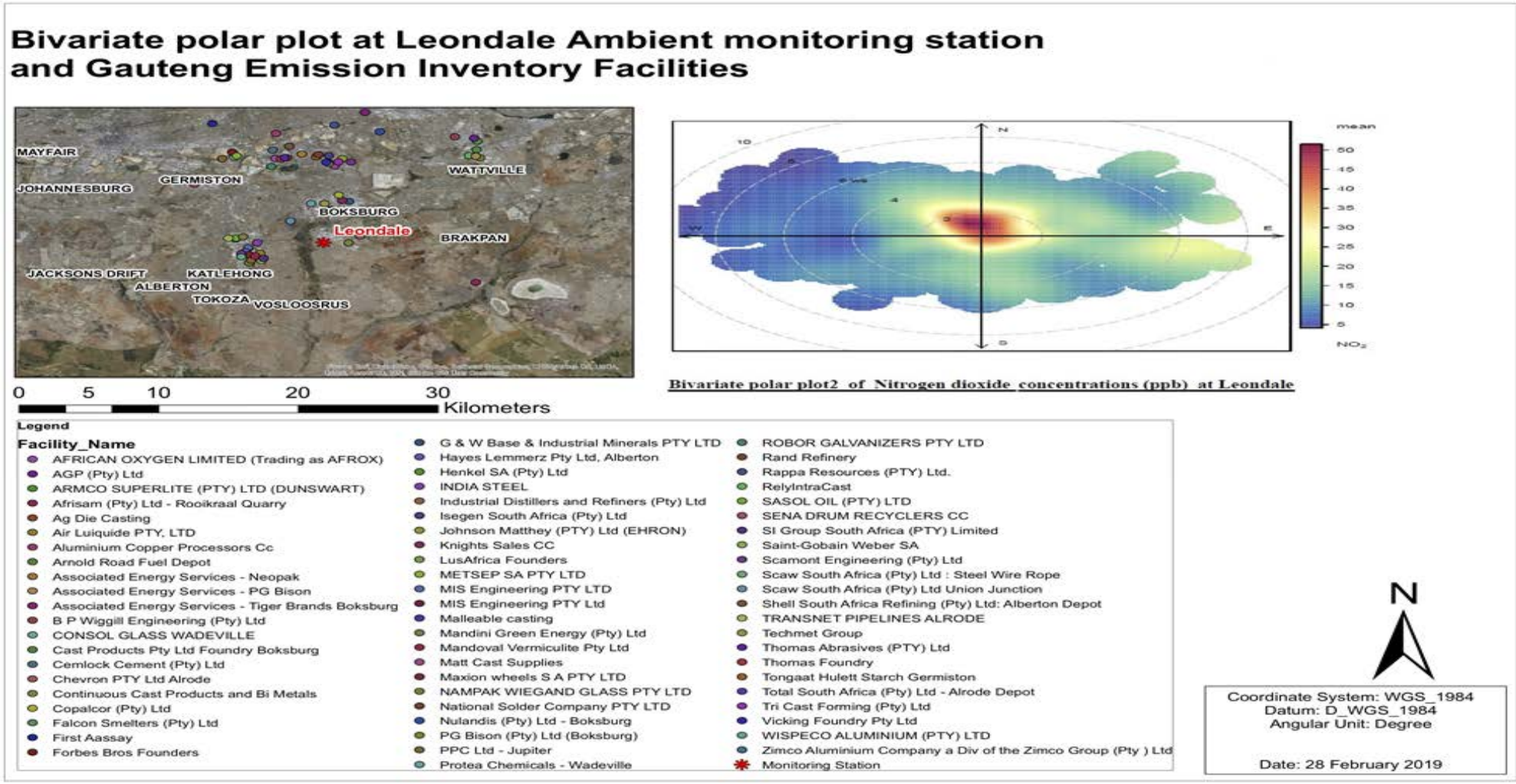

Figure 4.99: Bivariate polar plot at the Leondale Ambient Monitoring Stations and Emission Inventory Facilities in Gauteng Province

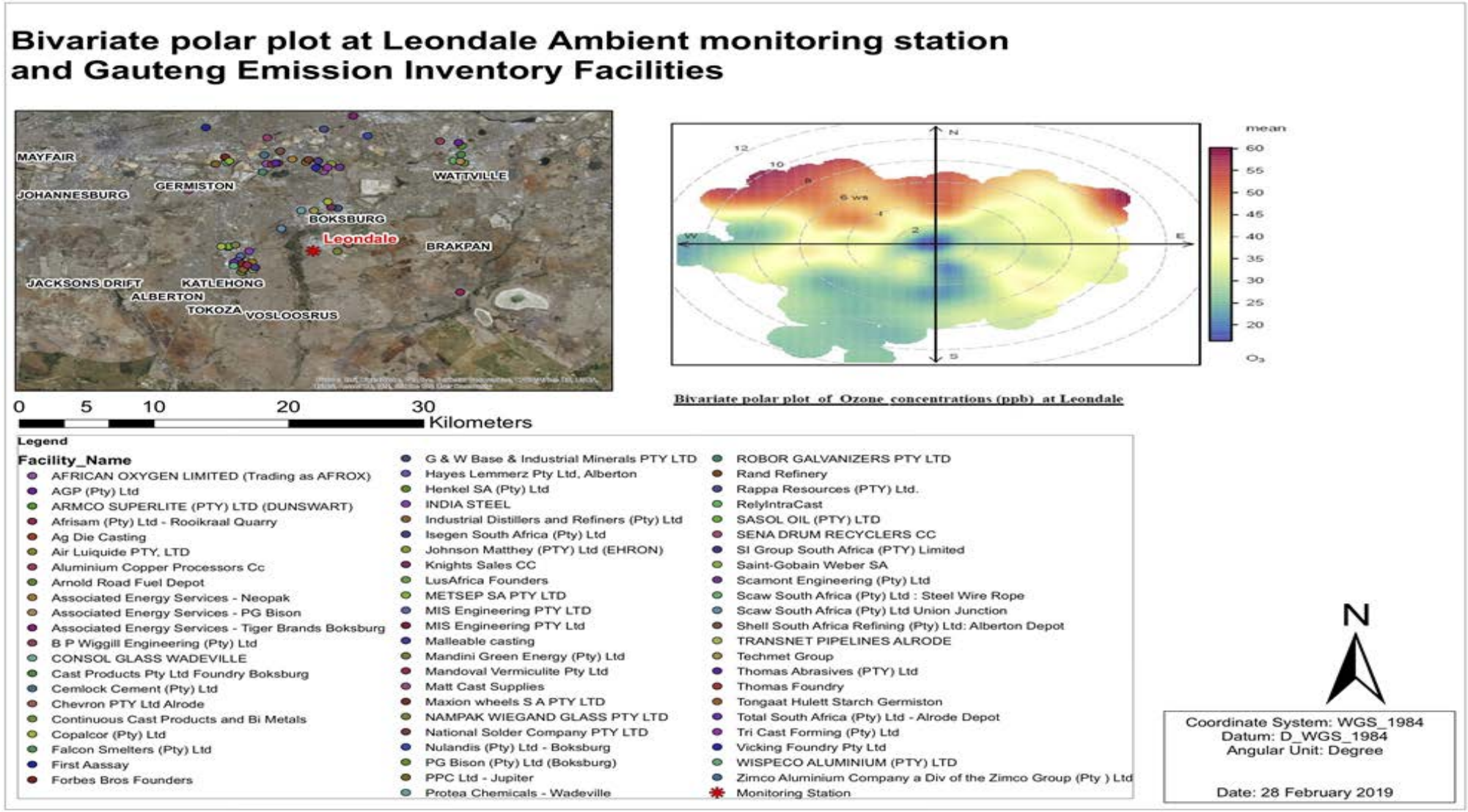

Figure 4.100: Bivariate polar plot at the Leondale Ambient Monitoring Stations and Emission Inventory Facilities in Gauteng Province

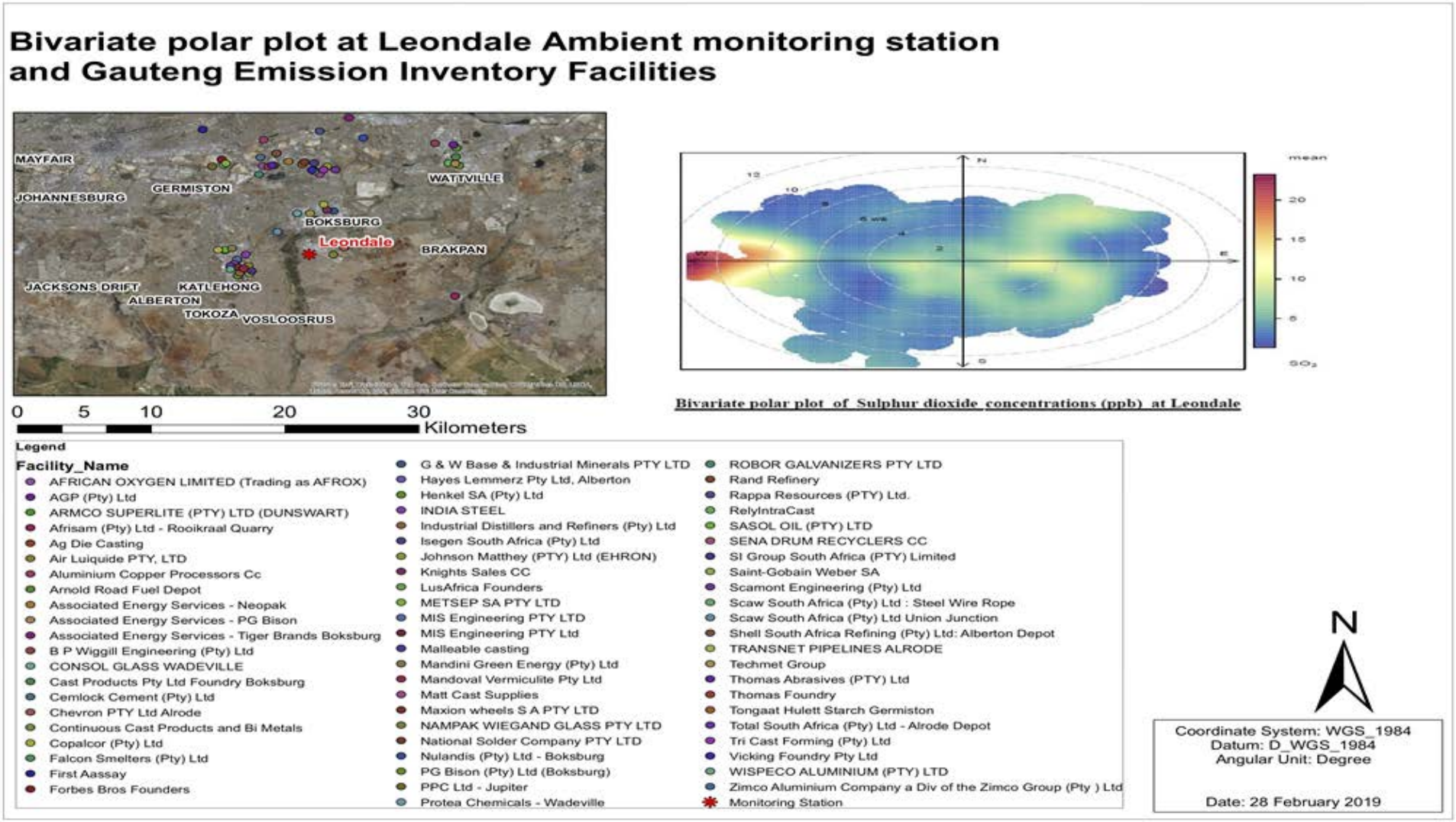

Figure 4.101: Bivariate polar plot at the Leondale Ambient Monitoring Stations and Emission Inventory Facilities in Gauteng Province

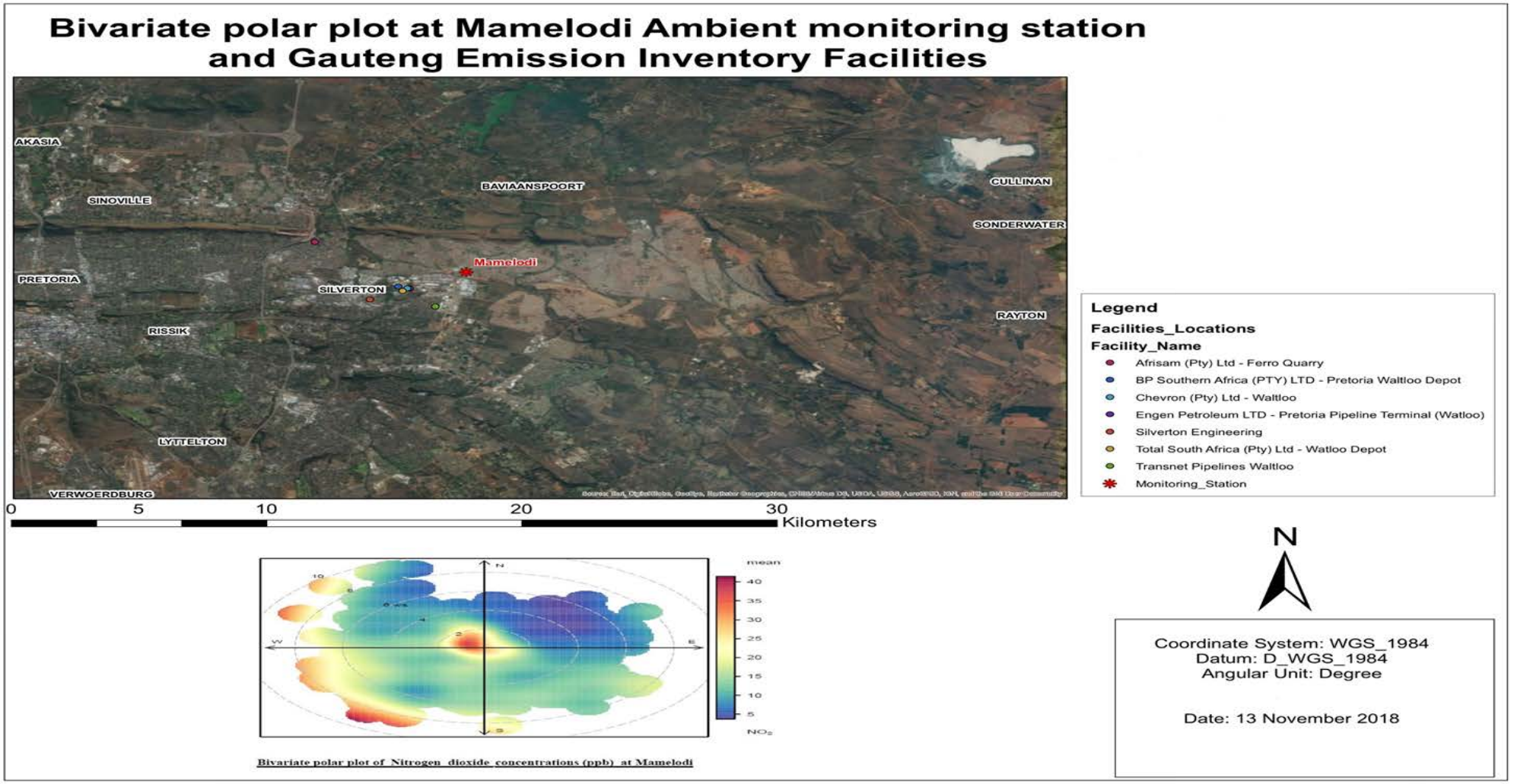

Figure 4.102: Bivariate polar plot at the Mamelodi Ambient Monitoring Stations and Emission Inventory Facilities in Gauteng Province

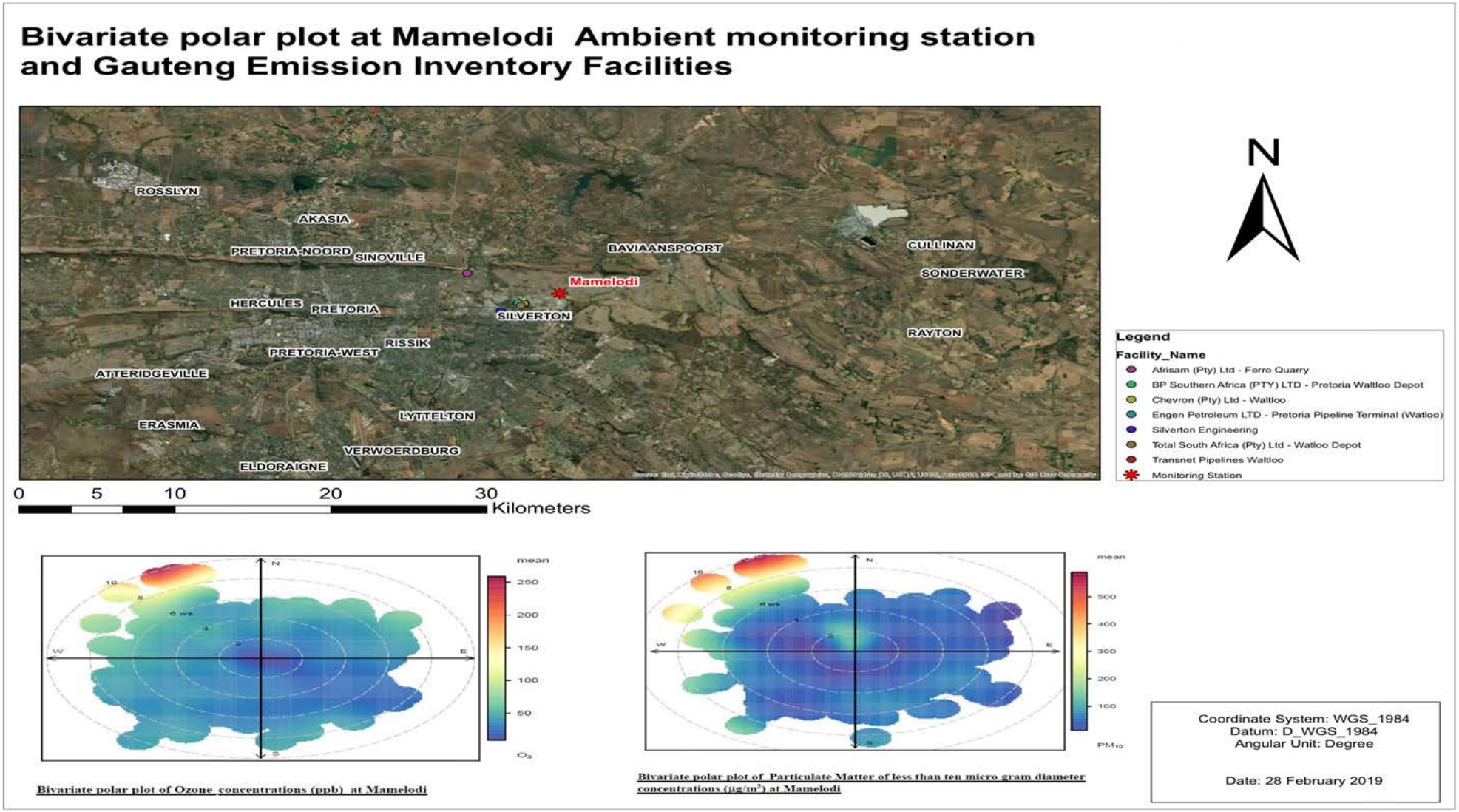

Figure 4.103: Bivariate polar plot at the Mamelodi Ambient Monitoring Stations and Emission Inventory Facilities in Gauteng Province

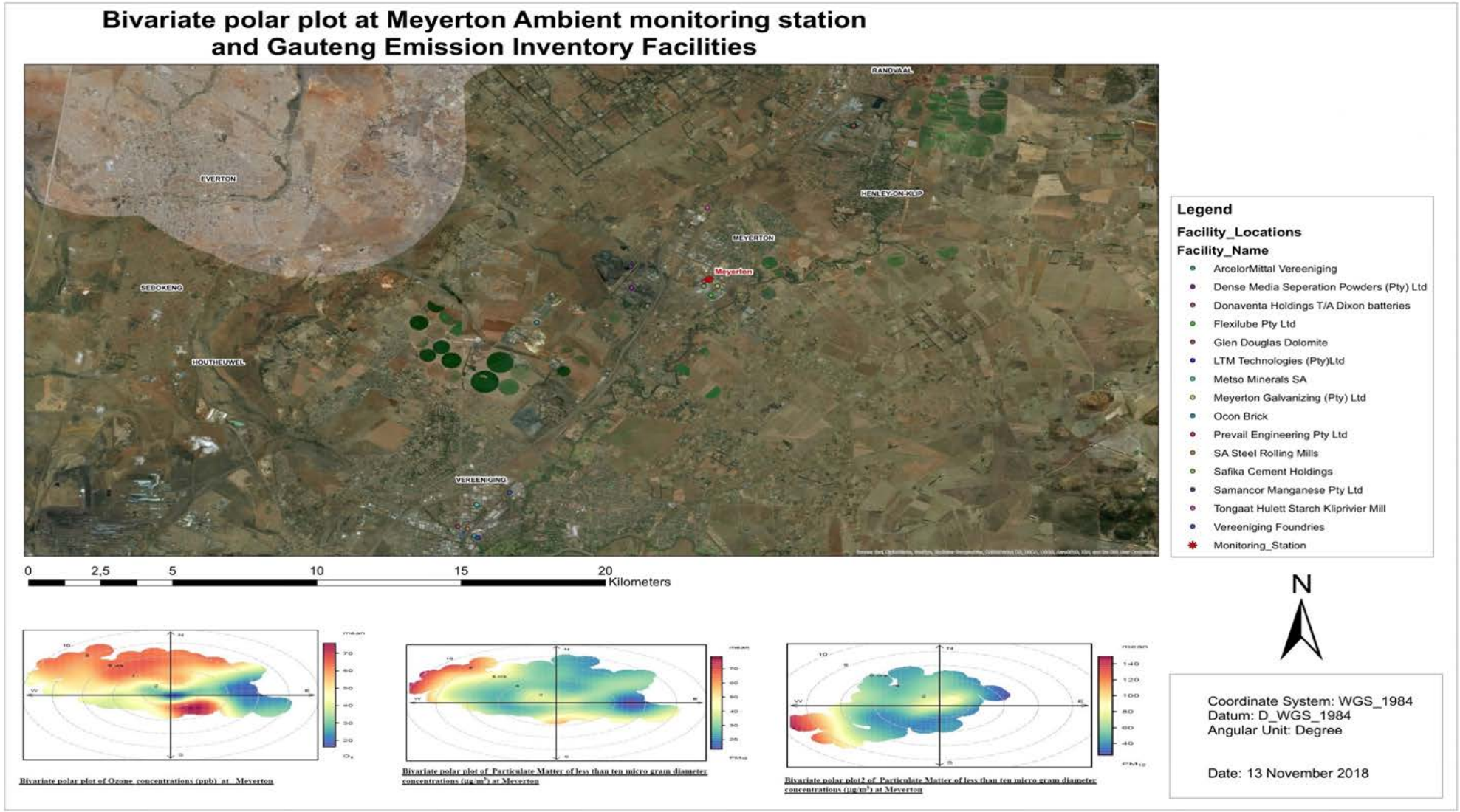

Figure 4.104: Bivariate polar plot at the Meyerton Ambient Monitoring Stations and Emission Inventory Facilities in Gauteng Province

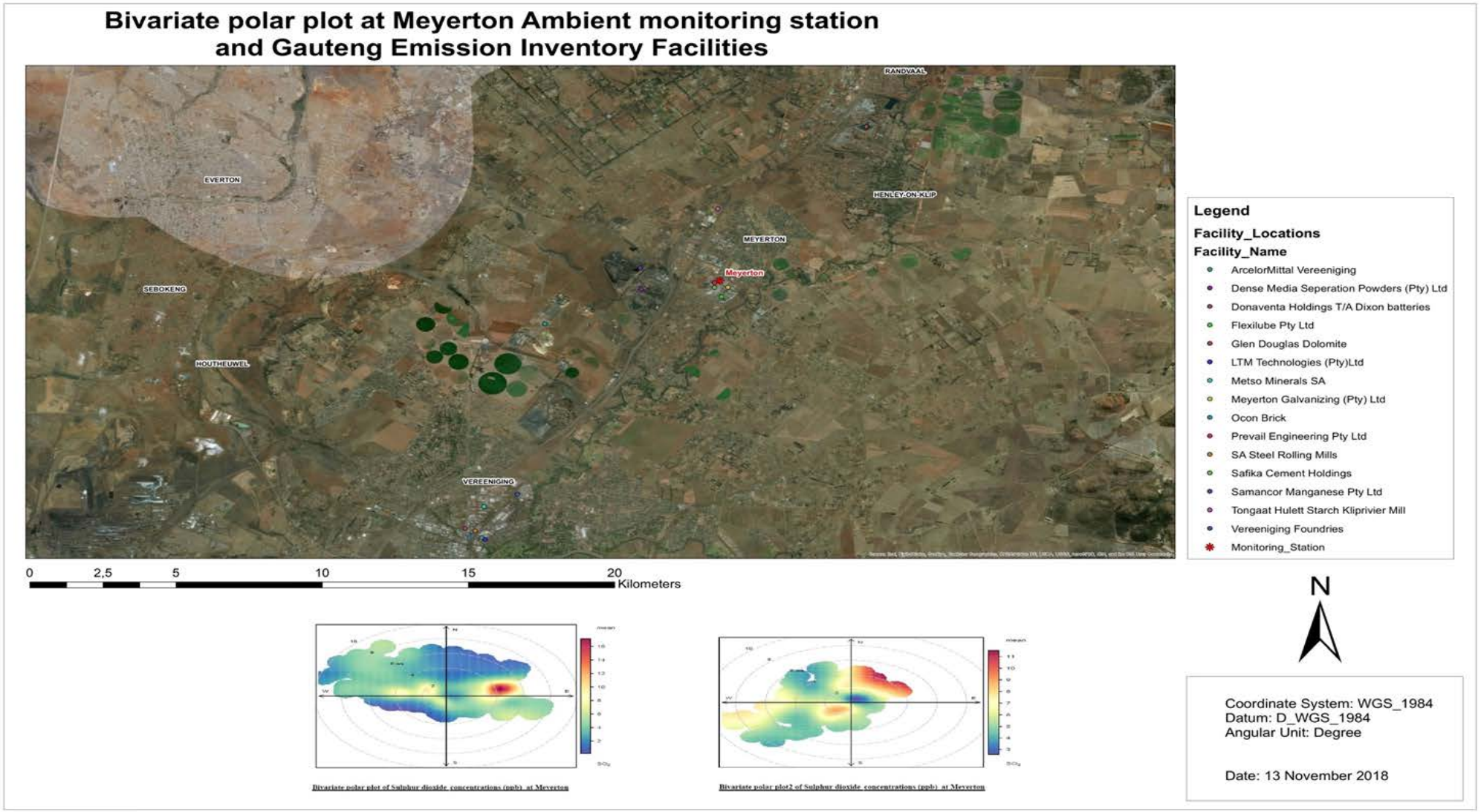

Figure 4.105: Bivariate polar plot at the Meyerton Ambient Monitoring Stations and Emission Inventory Facilities in Gauteng Province

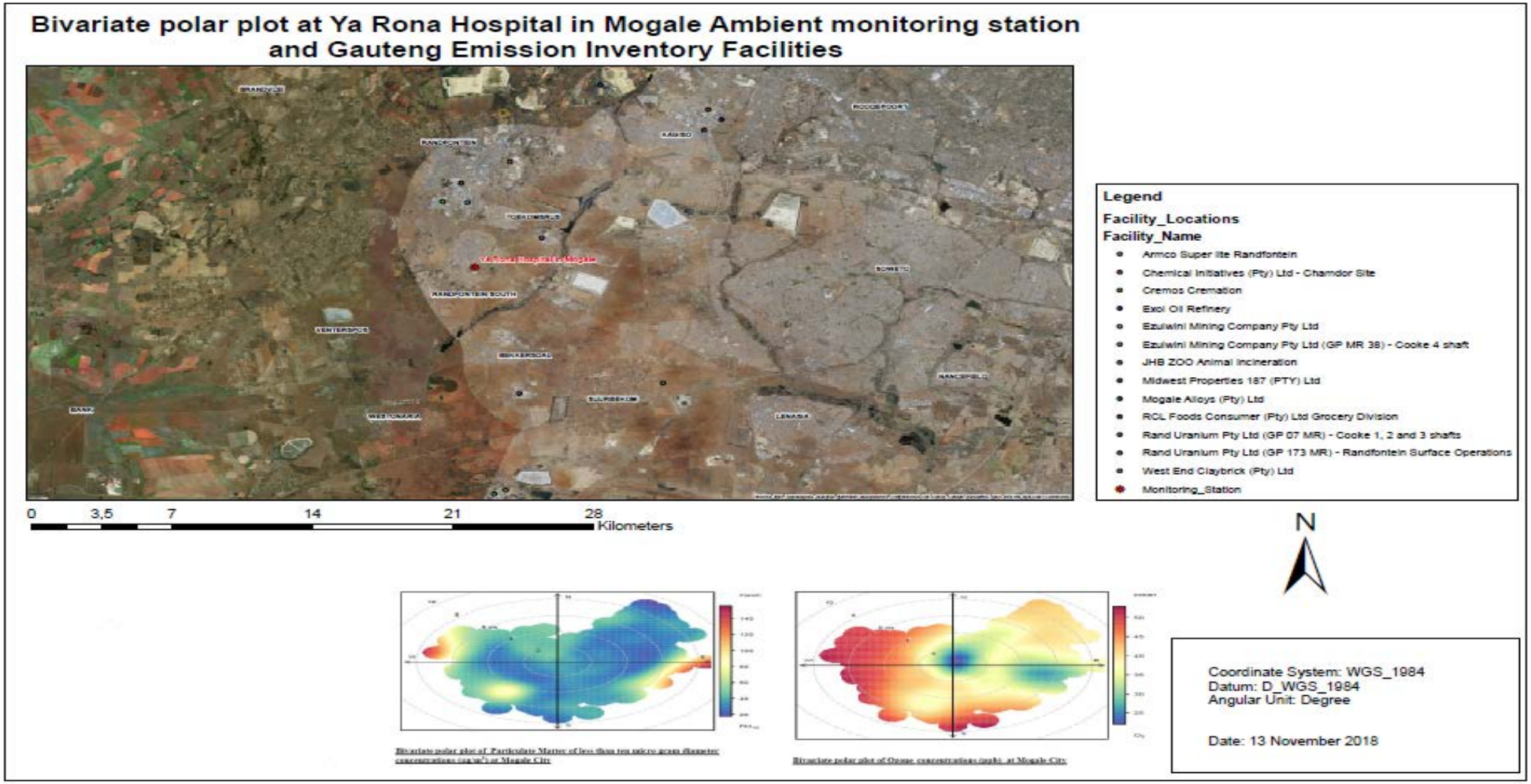

Figure 4.106: Bivariate polar plot at the Mogale City Ambient Monitoring Stations and Emission Inventory Facilities in Gauteng Province

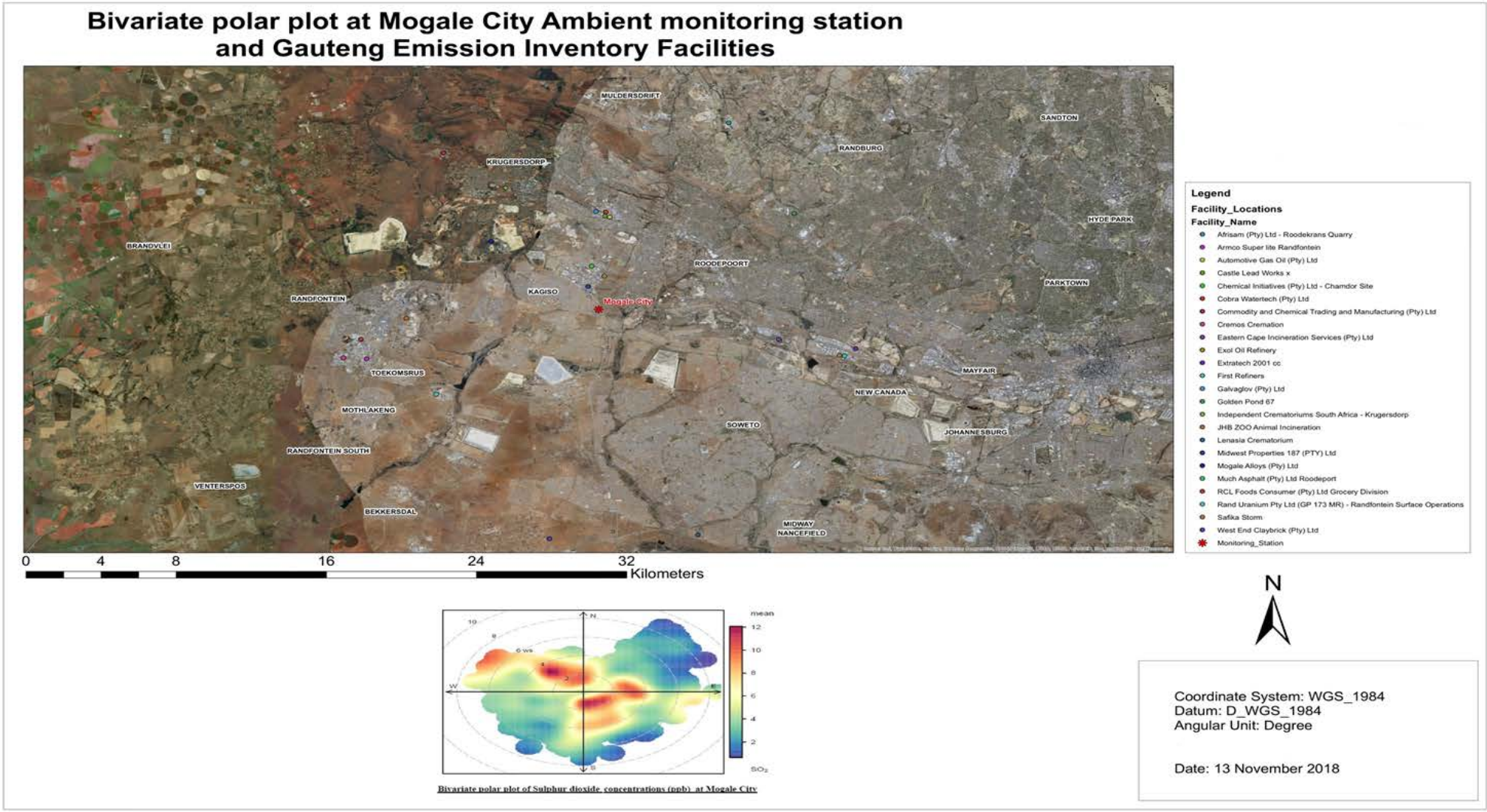

Bivariate polar plot of Sulphur dioxide concentrations (ppb) at Mogale City

Figure 4.107: Bivariate polar plot at the Mogale City Ambient Monitoring Stations and Emission Inventory Facilities in Gauteng Province

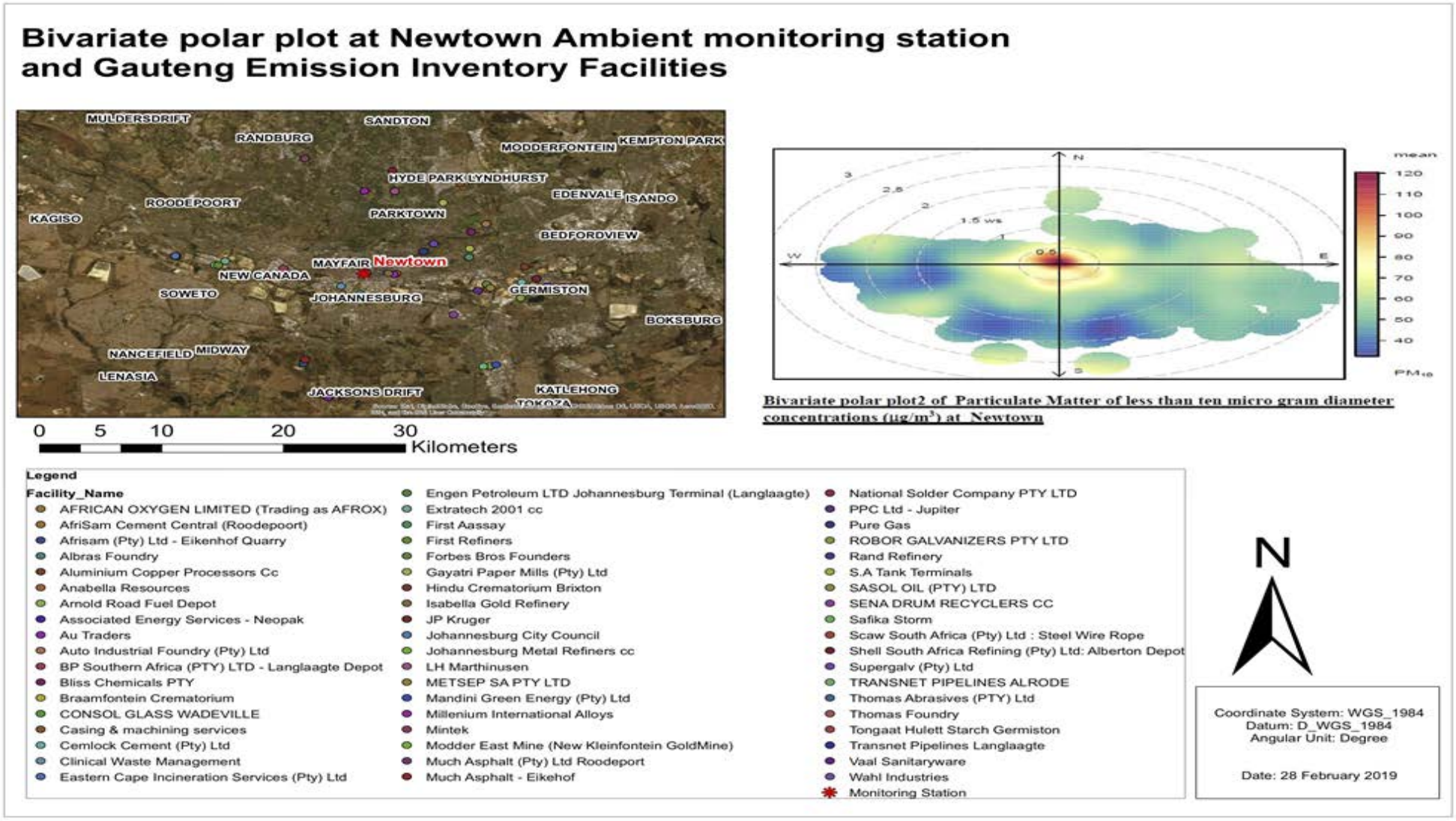

Figure 4.108: Bivariate polar plot at the Newtown Ambient Monitoring Stations and Emission Inventory Facilities in Gauteng Province

Bivariate polar plot at Newtown Ambient monitoring station and Gauteng Emission Inventory Facilities



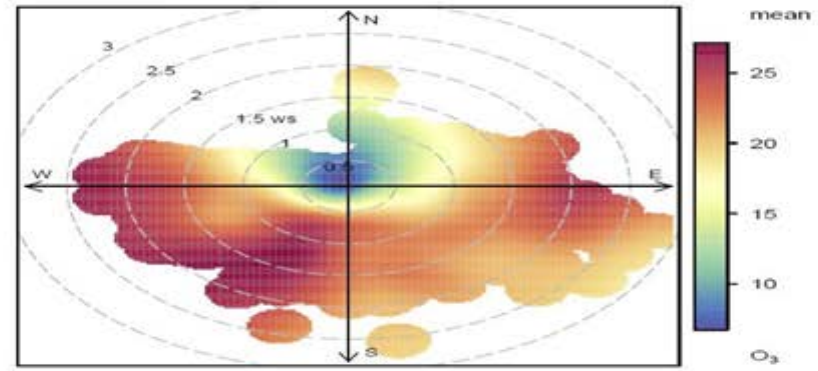

Bivariate polar plot of Ozone concentrations (ppb) at Newtown

Legend

Facility_Name

- AFRICAN OXYGEN LIMITED (Trading as AFROX)
- AfriSam Cement Central (Roodepoort)
- Afrisam (Pty) Ltd - Eikenhof Quarry
- Albras Foundry
- Aluminium Copper Processors Cc
- Anabella Resources
- Arnold Road Fuel Depot
- Associated Energy Services - Neopak
- Au Traders
- Auto Industrial Foundry (Pty) Ltd
- BP Southern Africa (PTY) LTD - Langlaagte Depot
- Bliss Chemicals PTY
- Braamfontein Crematorium
- CONSOL GLASS WADEVILLE
- Casing & machining services
- Cemlock Cement (Pty) Ltd
- Clinical Waste Management
- Eastern Cape Incineration Services (Pty) Ltd
- Engen Petroleum LTD Johannesburg Terminal (Langlaagte)
- Extratech 2001 cc
- First Aassay
- First Refiners
- Forbes Bros Founders
- Gayatri Paper Mills (Pty) Ltd
- Hindu Crematorium Brixton
- Isabella Gold Refinery
- JP Kruger
- Johannesburg City Council
- Johannesburg Metal Refiners cc
- LH Marthinusen
- METSEP SA PTY LTD
- Mandini Green Energy (Pty) Ltd
- Millenium International Alloys
- Mintek
- Modder East Mine (New Kleinfontein GoldMine)
- Much Asphalt (Pty) Ltd Roodeport
- Much Asphalt - Eikehof
- National Solder Company PTY LTD
- PPC Ltd - Jupiter
- Pure Gas
- ROBOR GALVANIZERS PTY LTD
- Rand Refinery
- S.A Tank Terminals
- SASOL OIL (PTY) LTD
- SENA DRUM RECYCLERS CC
- Safika Storm
- Scaw South Africa (Pty) Ltd : Steel Wire Rope
- Shell South Africa Refining (Pty) Ltd: Alberton Depot
- Supergalv (Pty) Ltd
- TRANSNET PIPELINES ALRODE
- Thomas Abrasives (PTY) Ltd
- Thomas Foundry
- Tongaat Hulett Starch Germiston
- Transnet Pipelines Langlaagte
- Vaal Sanitaryware
- Wahl Industries
- Monitoring Station

N

Coordinate System: WGS_1984
Datum: D_WGS_1984
Angular Unit: Degree

Date: 28 February 2019

Figure 4.109: Bivariate polar plot at the Newtown Ambient Monitoring Stations and Emission Inventory Facilities in Gauteng Province

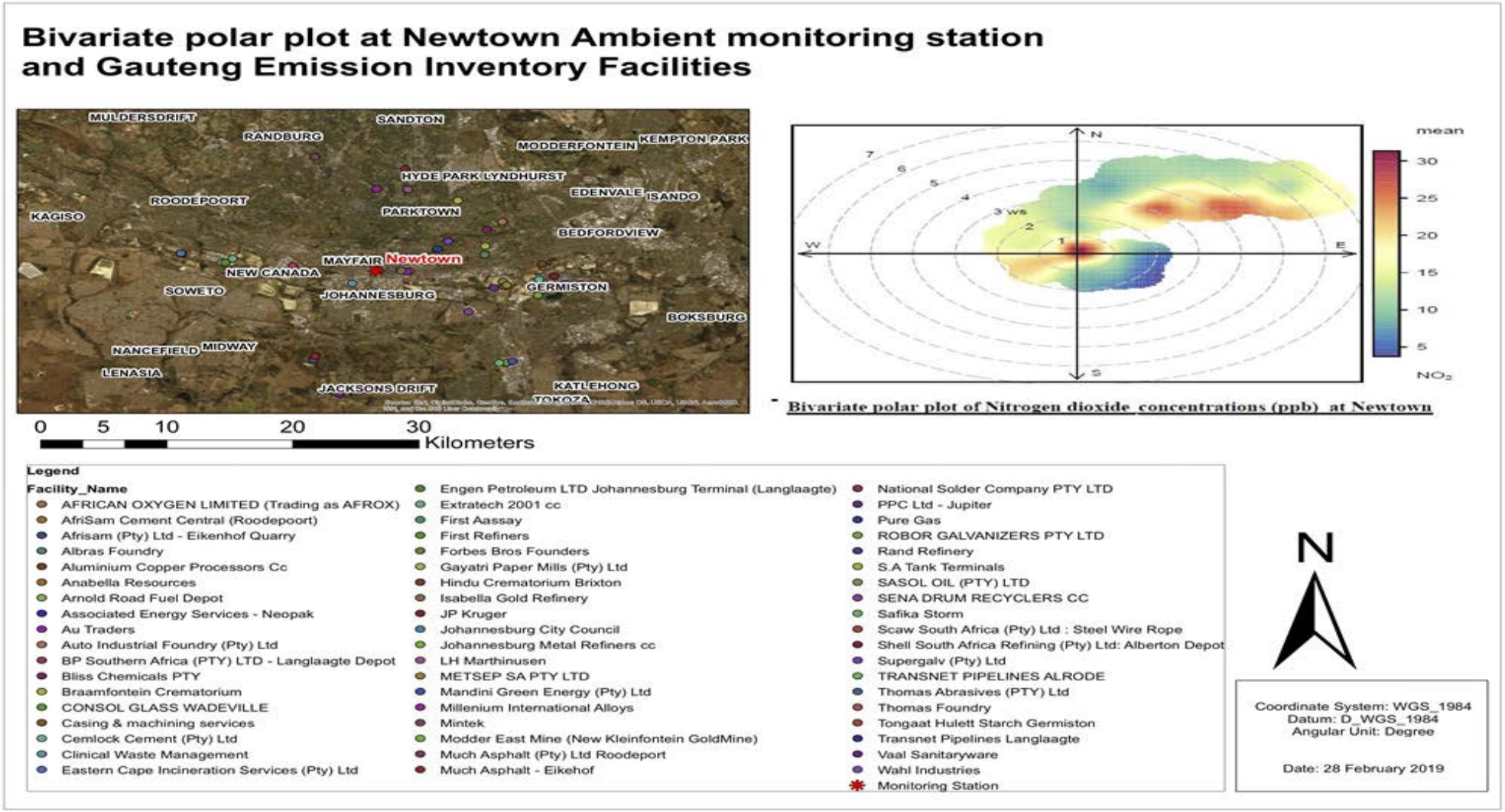

Figure 4.110: Bivariate polar plot at the Newtown Ambient Monitoring Stations and Emission Inventory Facilities in Gauteng Province

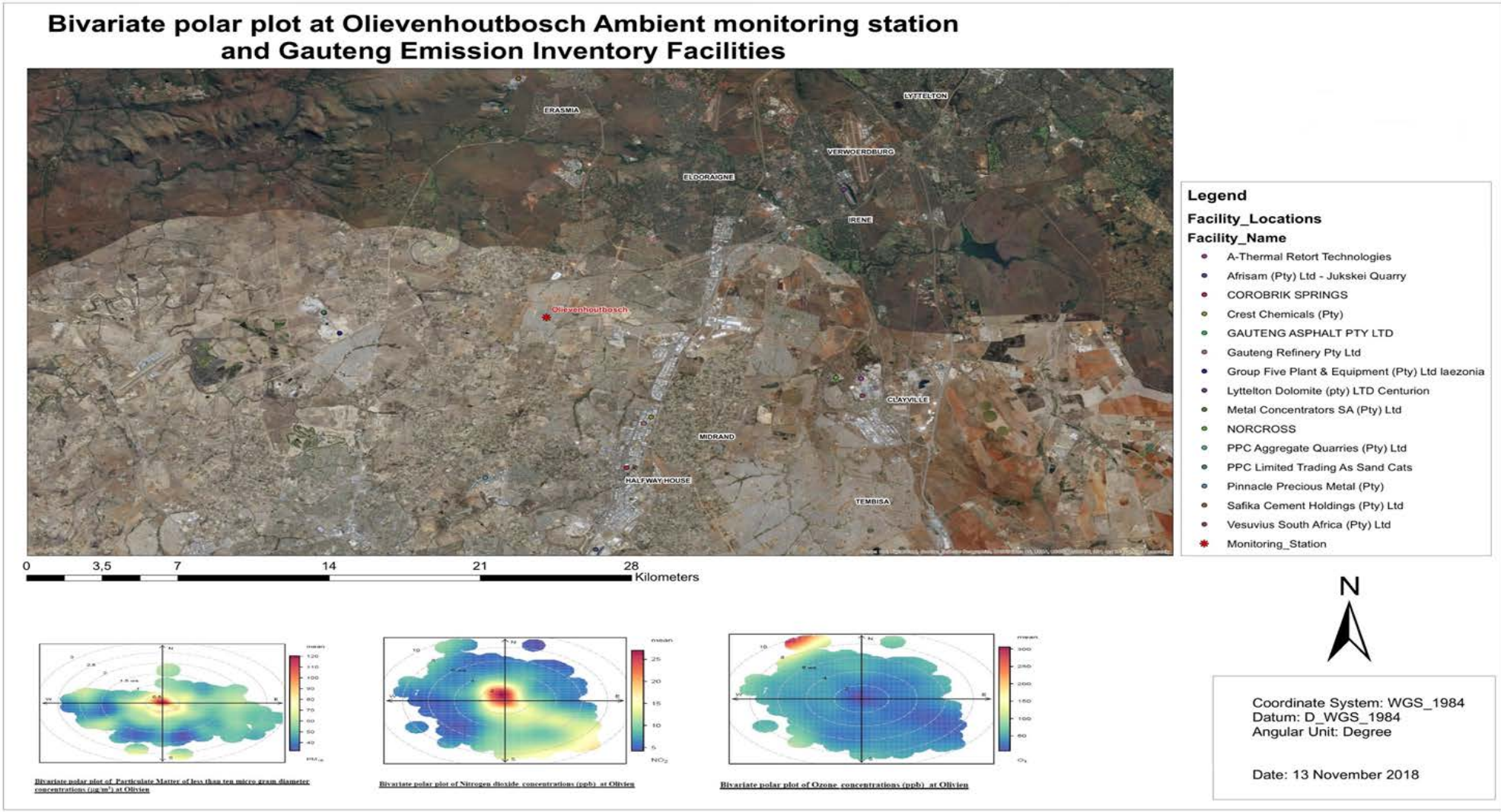

Figure 4.111: Bivariate polar plot at the Olievenhoutbosch Ambient Monitoring Stations and Emission Inventory Facilities in Gauteng Province

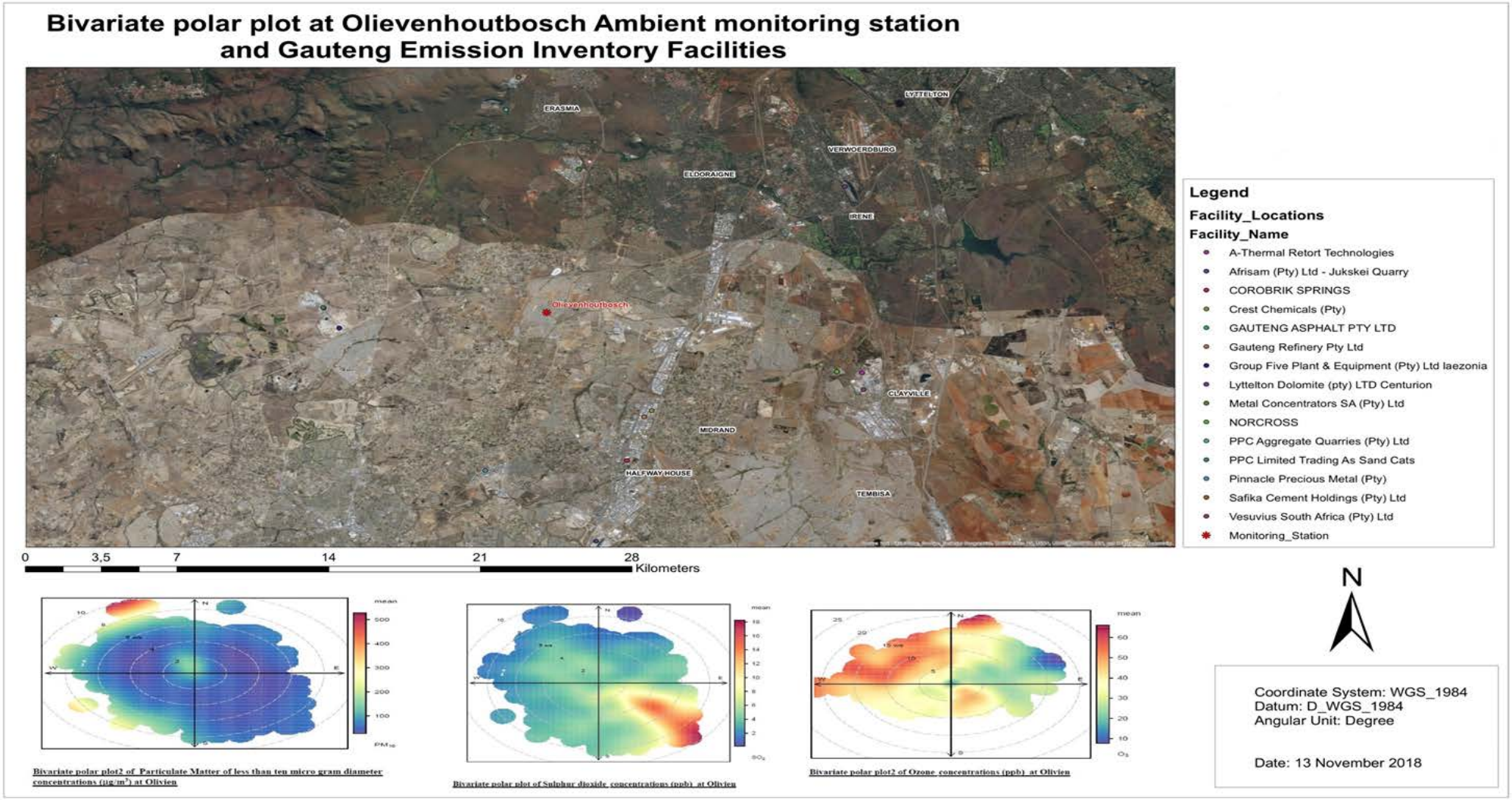

Figure 4.112: Bivariate polar plot at the Olievenhoutbosch Ambient Monitoring Stations and Emission Inventory Facilities in Gauteng Province

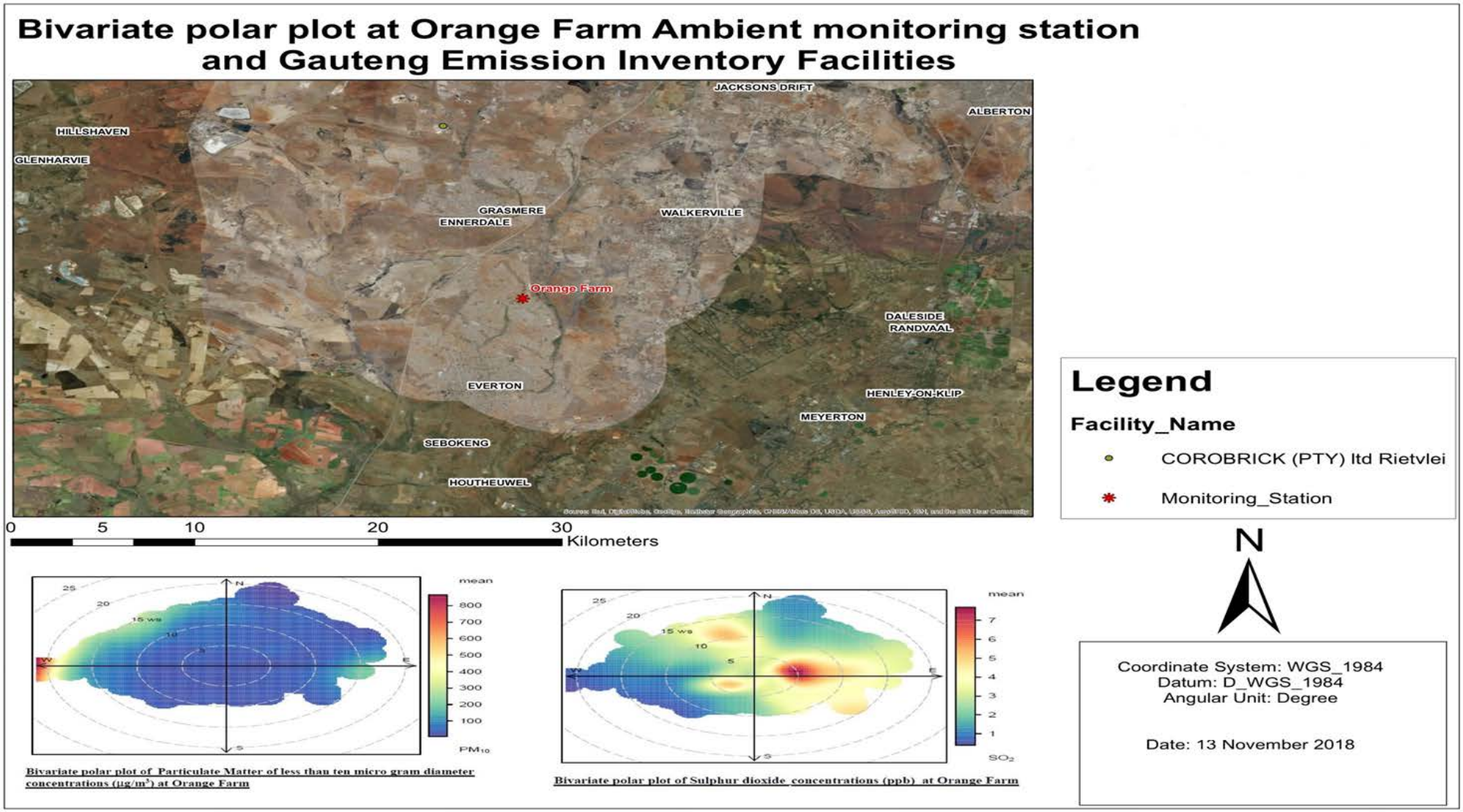

Figure 4.113: Bivariate polar plot at the Orange Farm Ambient Monitoring Stations and Emission Inventory Facilities in Gauteng Province

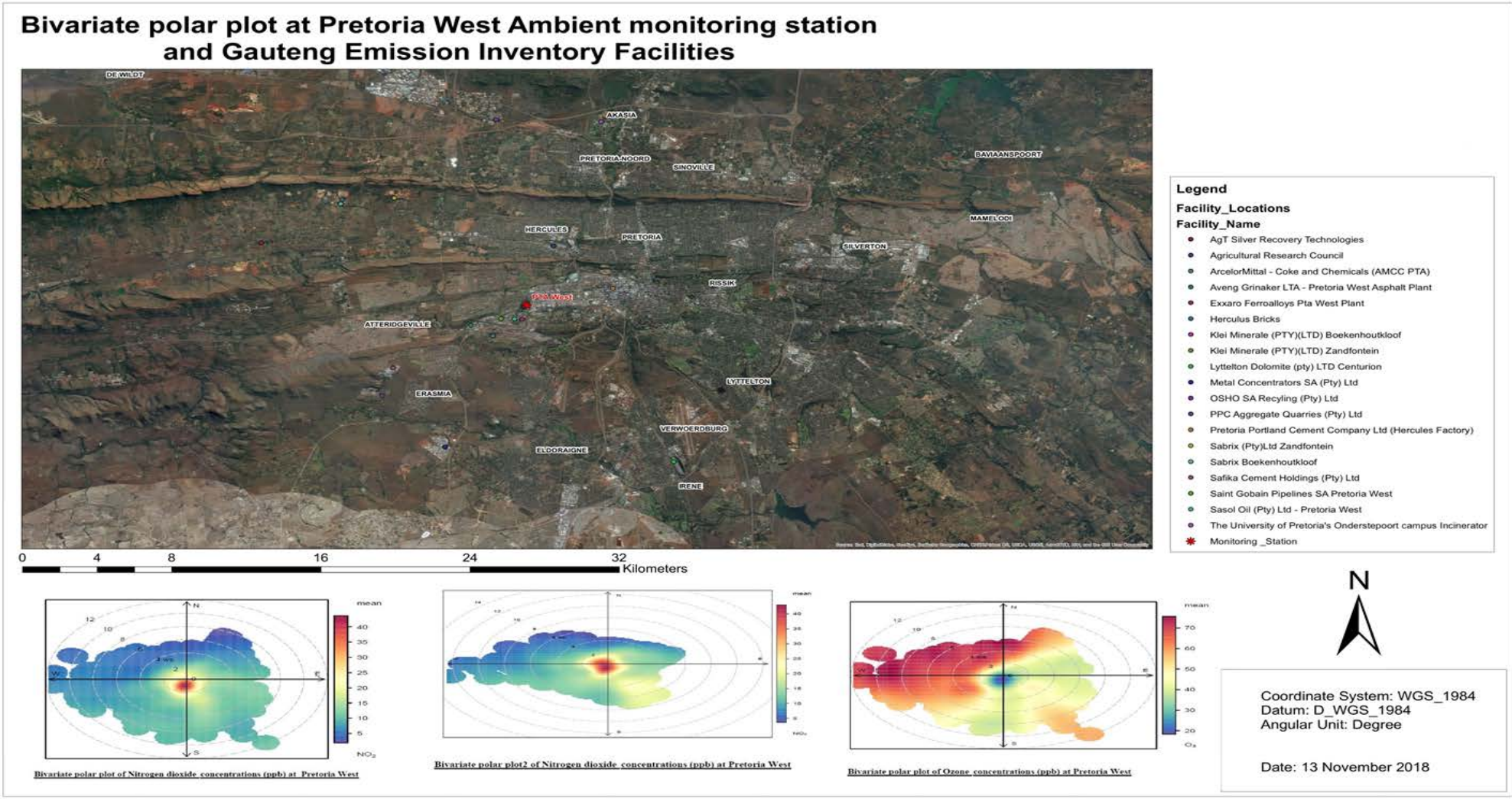

Figure 4.114: Bivariate polar plot at the Pretoria West Ambient Monitoring Stations and Emission Inventory Facilities in Gauteng Province

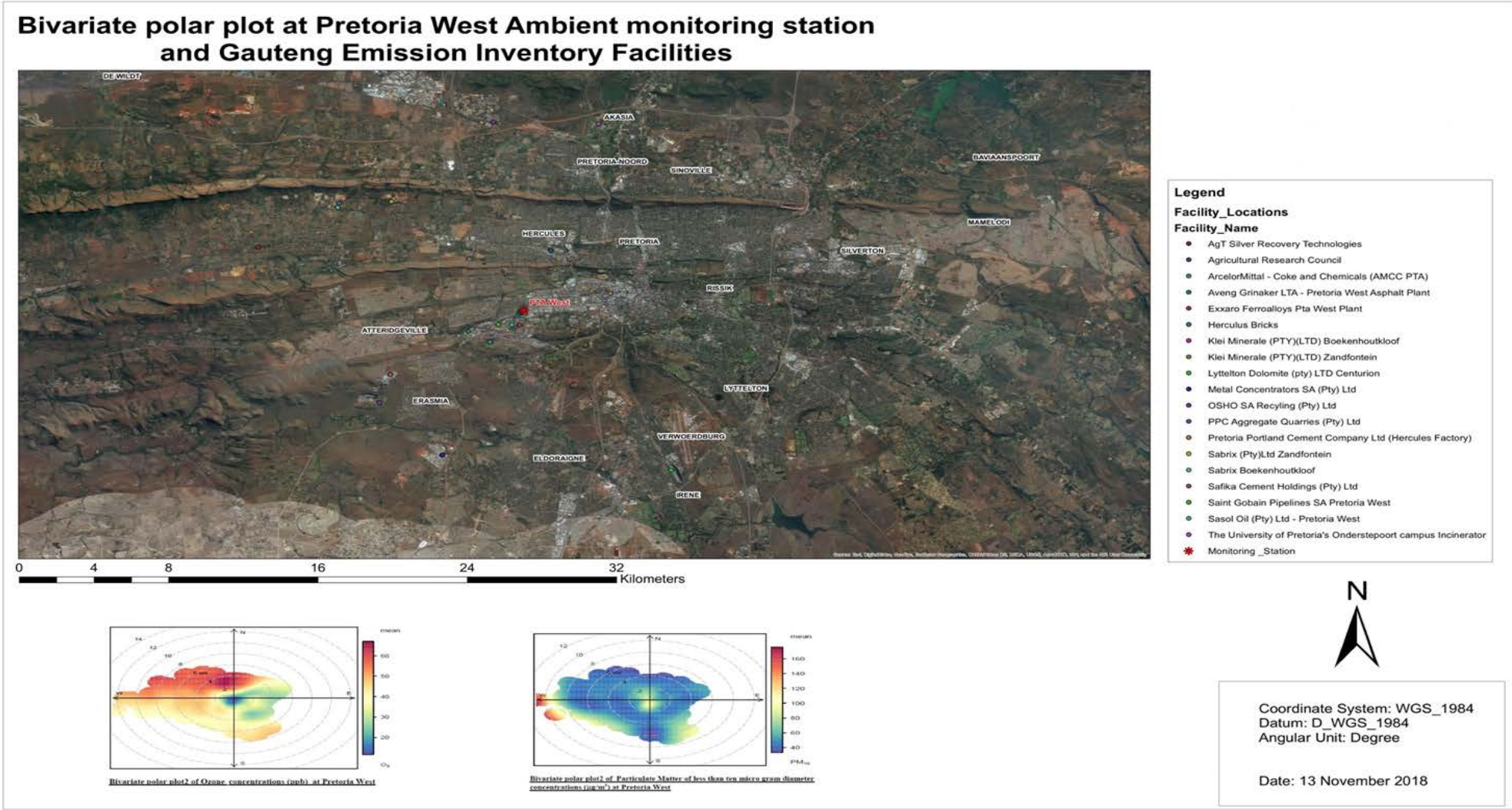

Figure 4.115: Bivariate polar plot at the Pretoria West Ambient Monitoring Stations and Emission Inventory Facilities in Gauteng Province

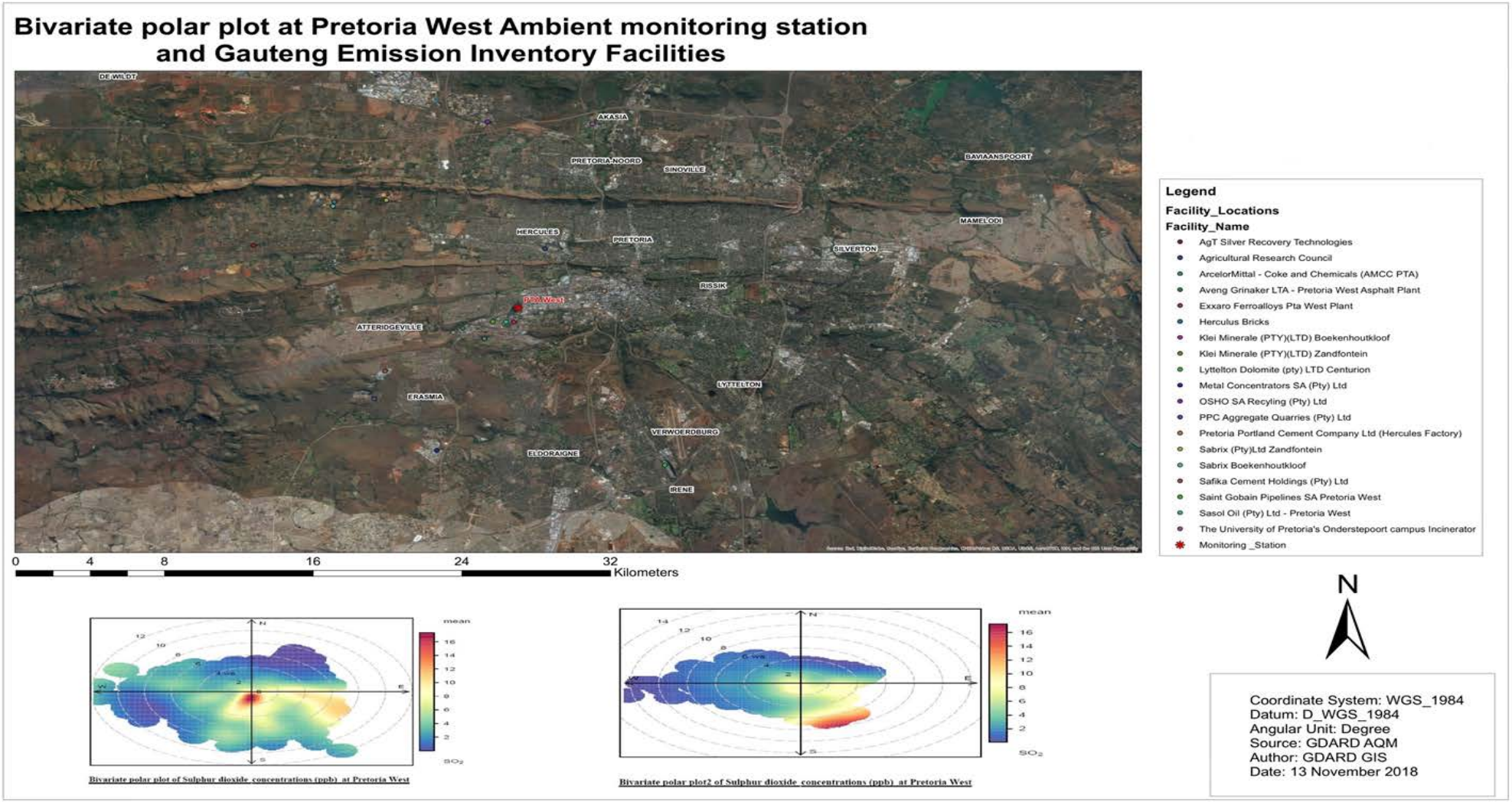

Figure 4.116: Bivariate polar plot at the Pretoria West Ambient Monitoring Stations and Emission Inventory Facilities in Gauteng Province

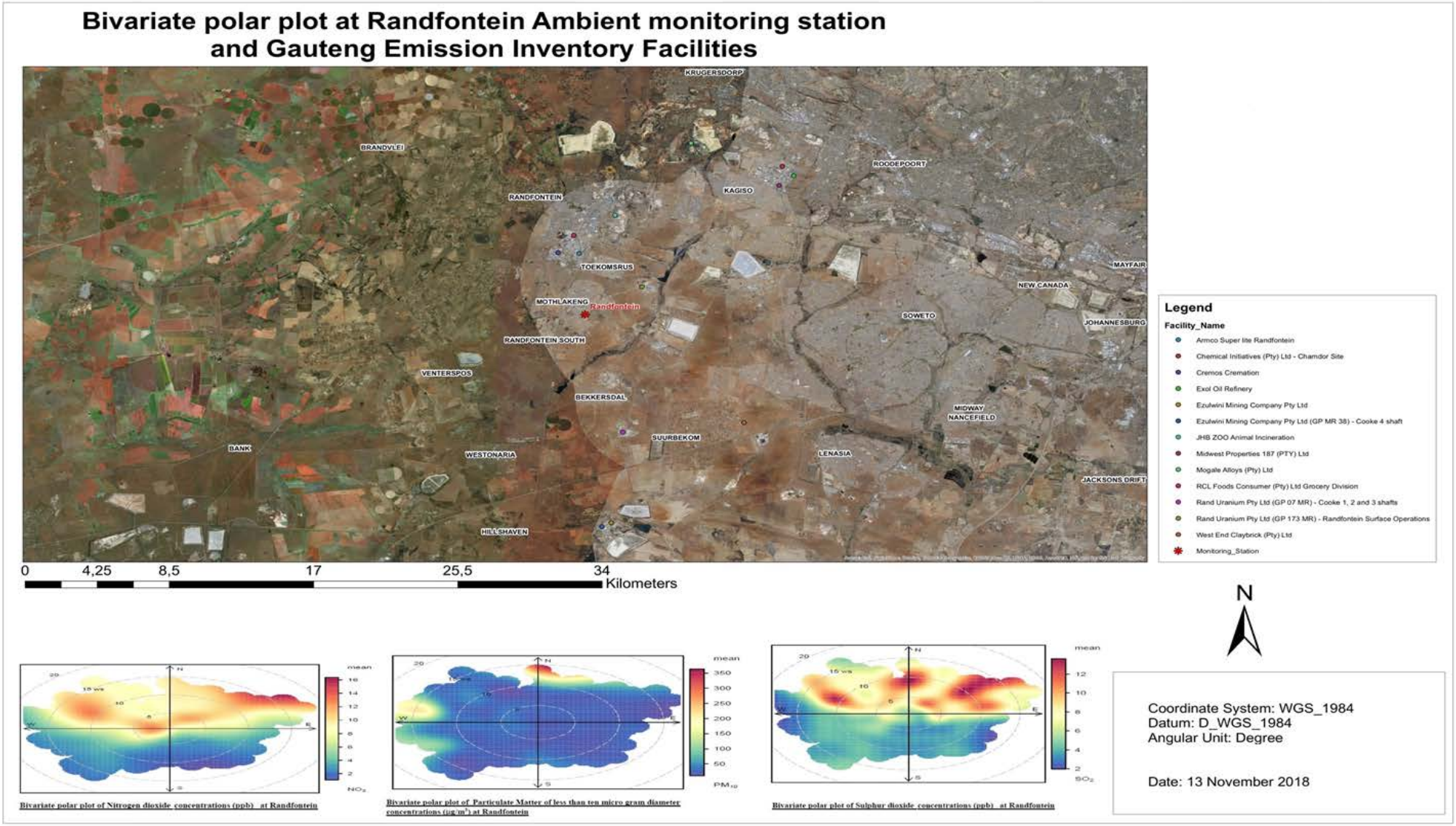

Figure 4.117: Bivariate polar plot at the Randfontein Ambient Monitoring Stations and Emission Inventory Facilities in Gauteng Province

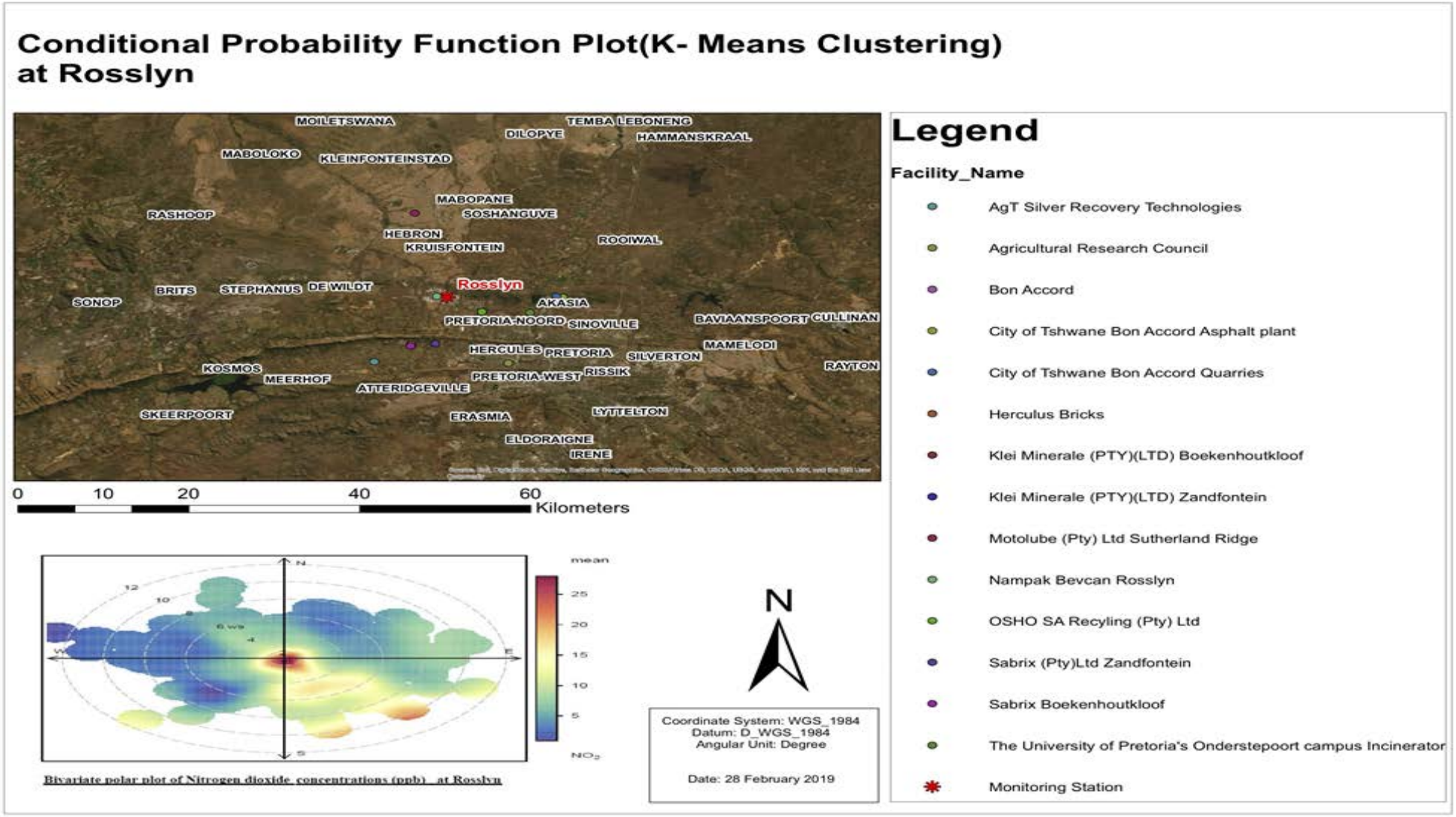

Bivariate polar plot of Nitrogen dioxide concentrations (ppb) at Rosslyn

Figure 4.118: Bivariate polar plot at the Rosslyn Ambient Monitoring Stations and Emission Inventory Facilities in Gauteng Province

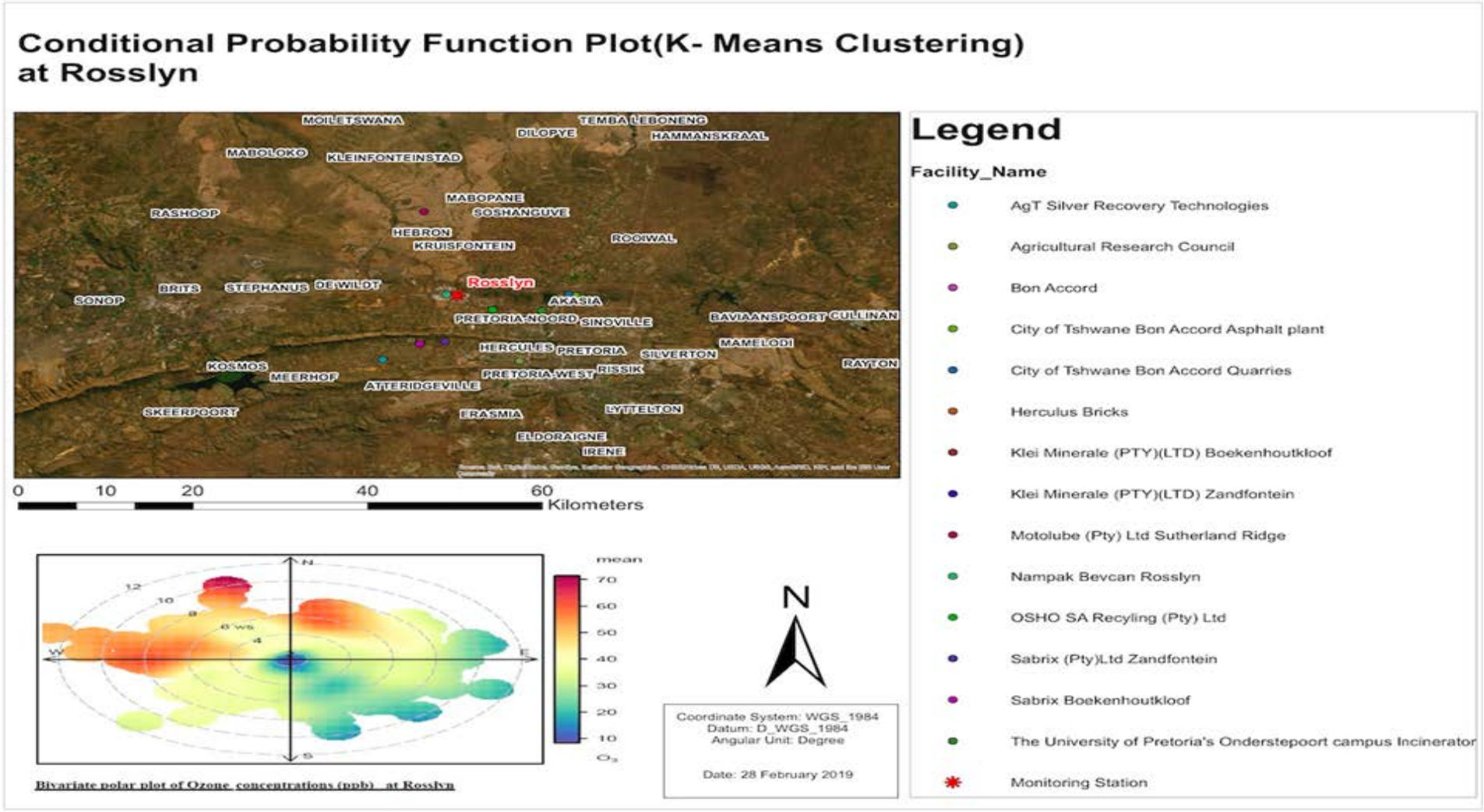

Figure 4.119: Bivariate polar plot at the Rosslyn Ambient Monitoring Stations and Emission Inventory Facilities in Gauteng Province

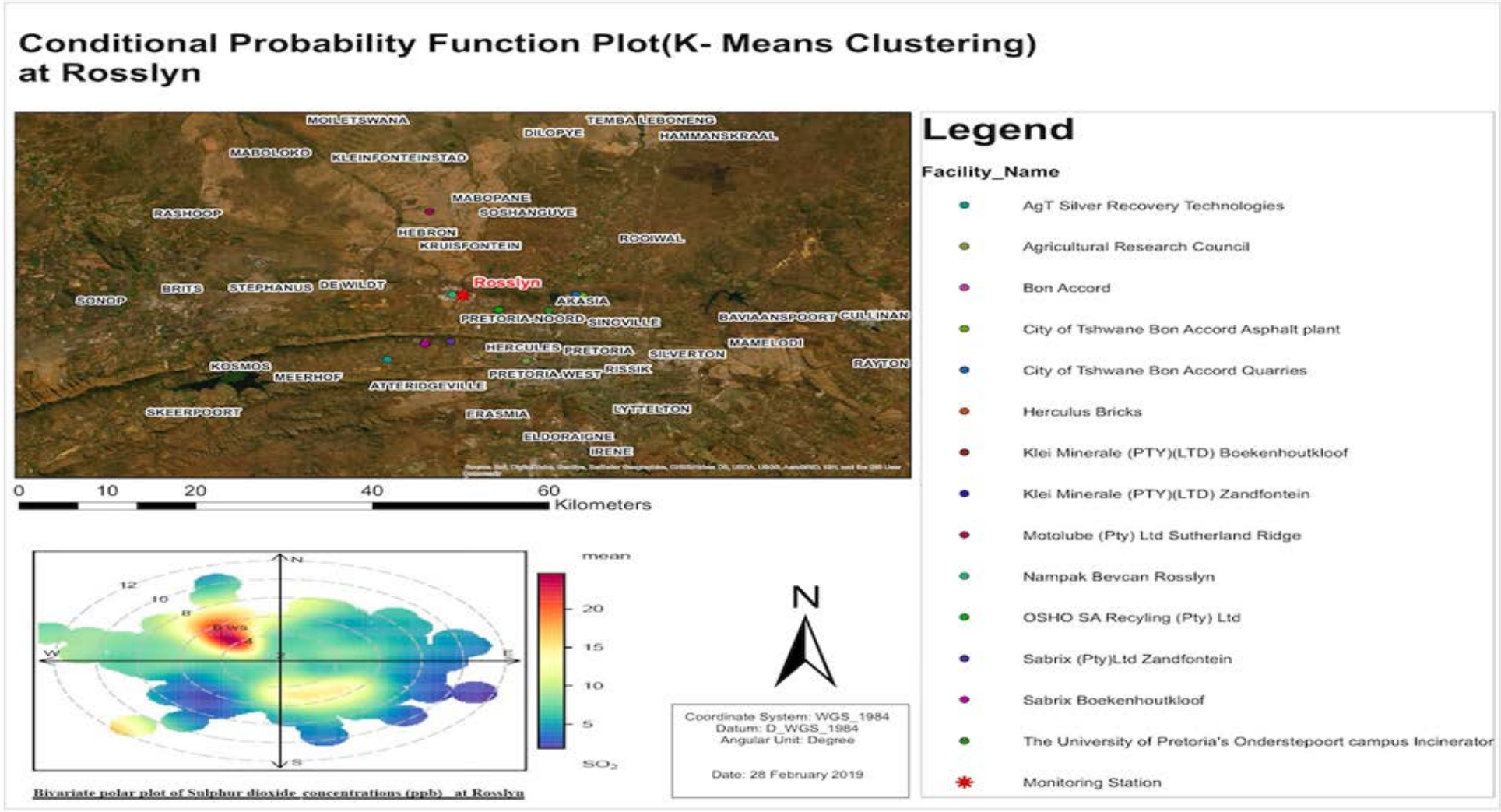

Figure 4.120: Bivariate polar plot at the Rosslyn Ambient Monitoring Stations and Emission Inventory Facilities in Gauteng Province

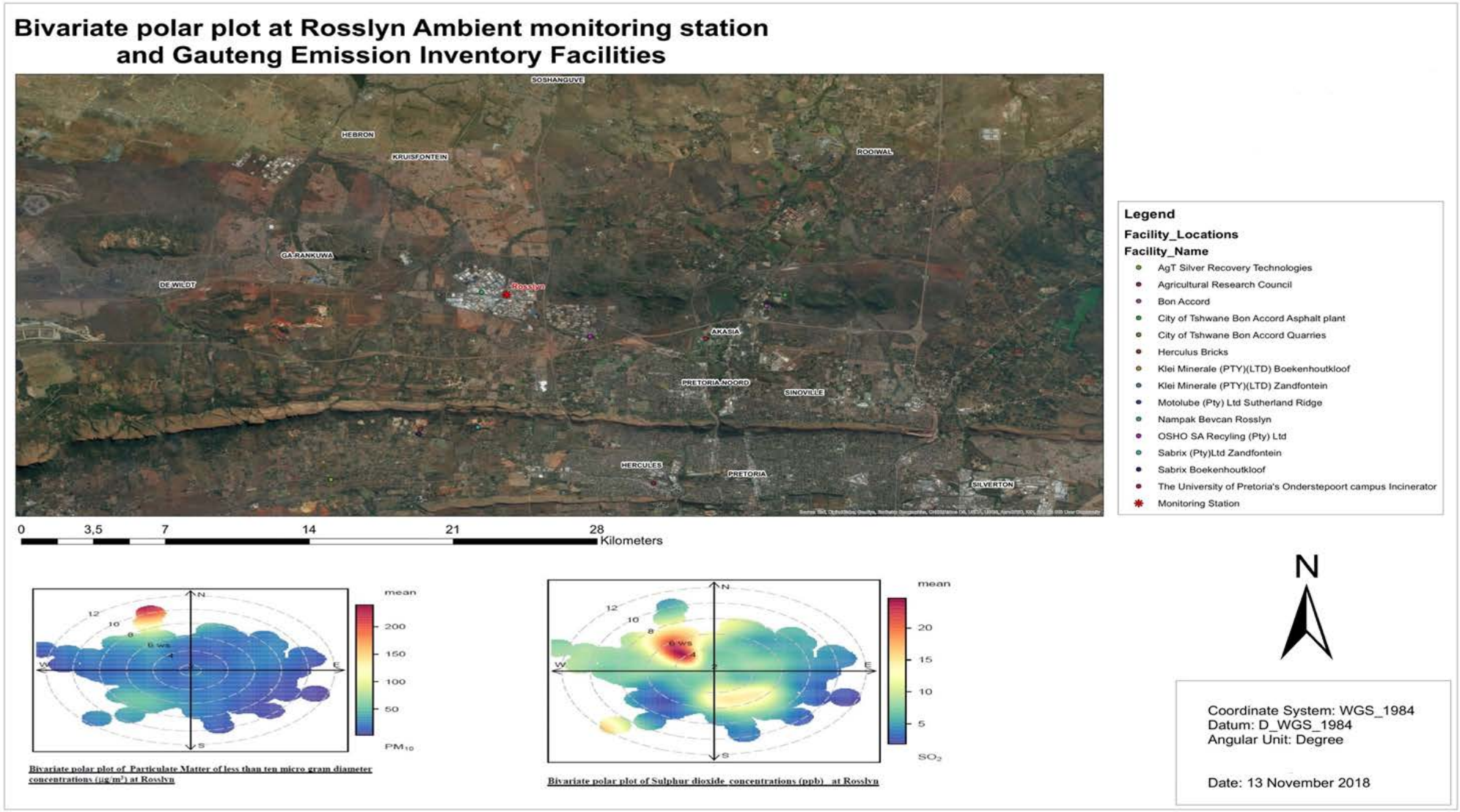

Figure 4.121: Bivariate polar plot at the Rosslyn Ambient Monitoring Stations and Emission Inventory Facilities in Gauteng Province

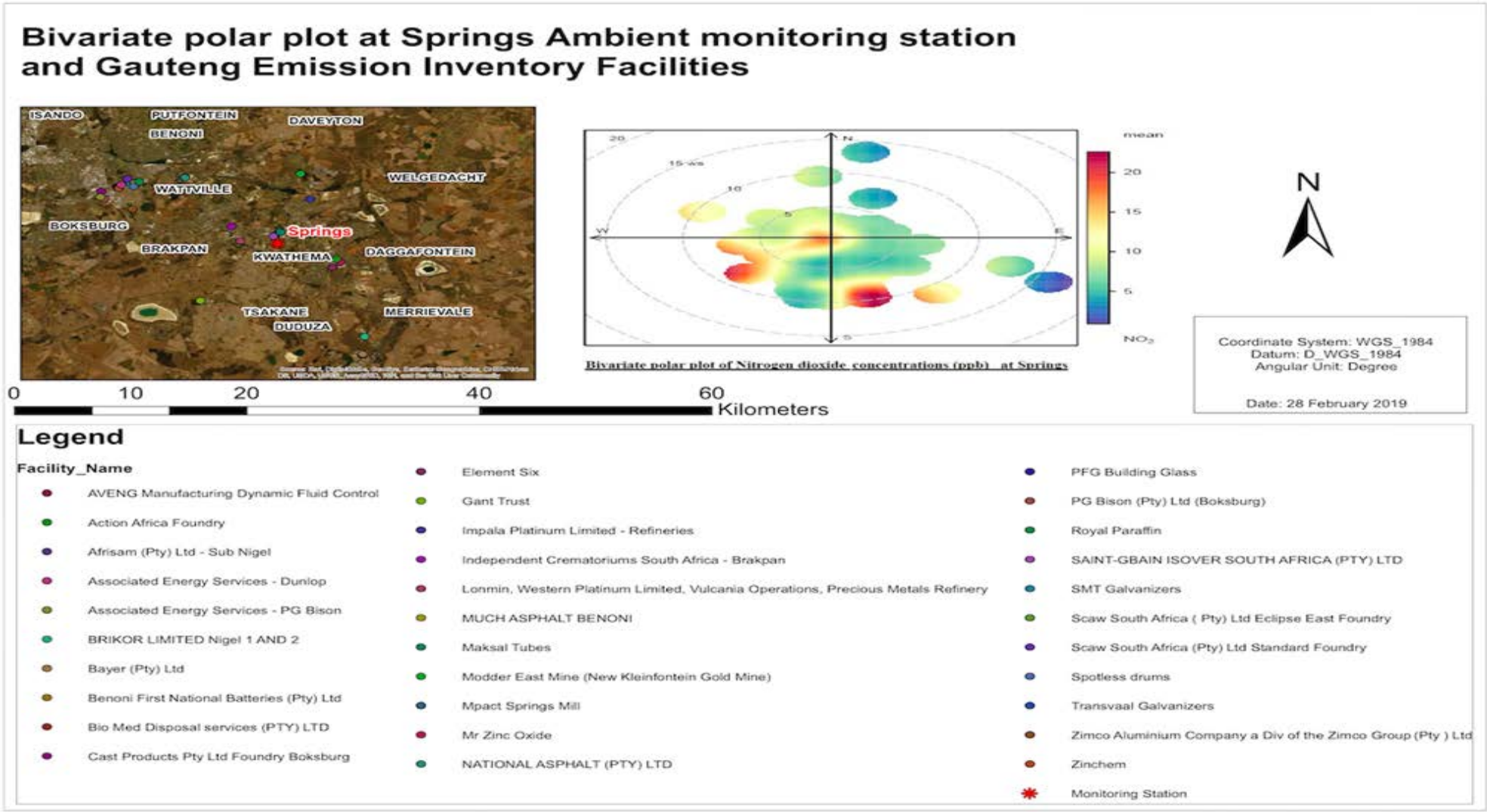

Figure 4.122: Bivariate polar plot at the Springs Ambient Monitoring Stations and Emission Inventory Facilities in Gauteng Province

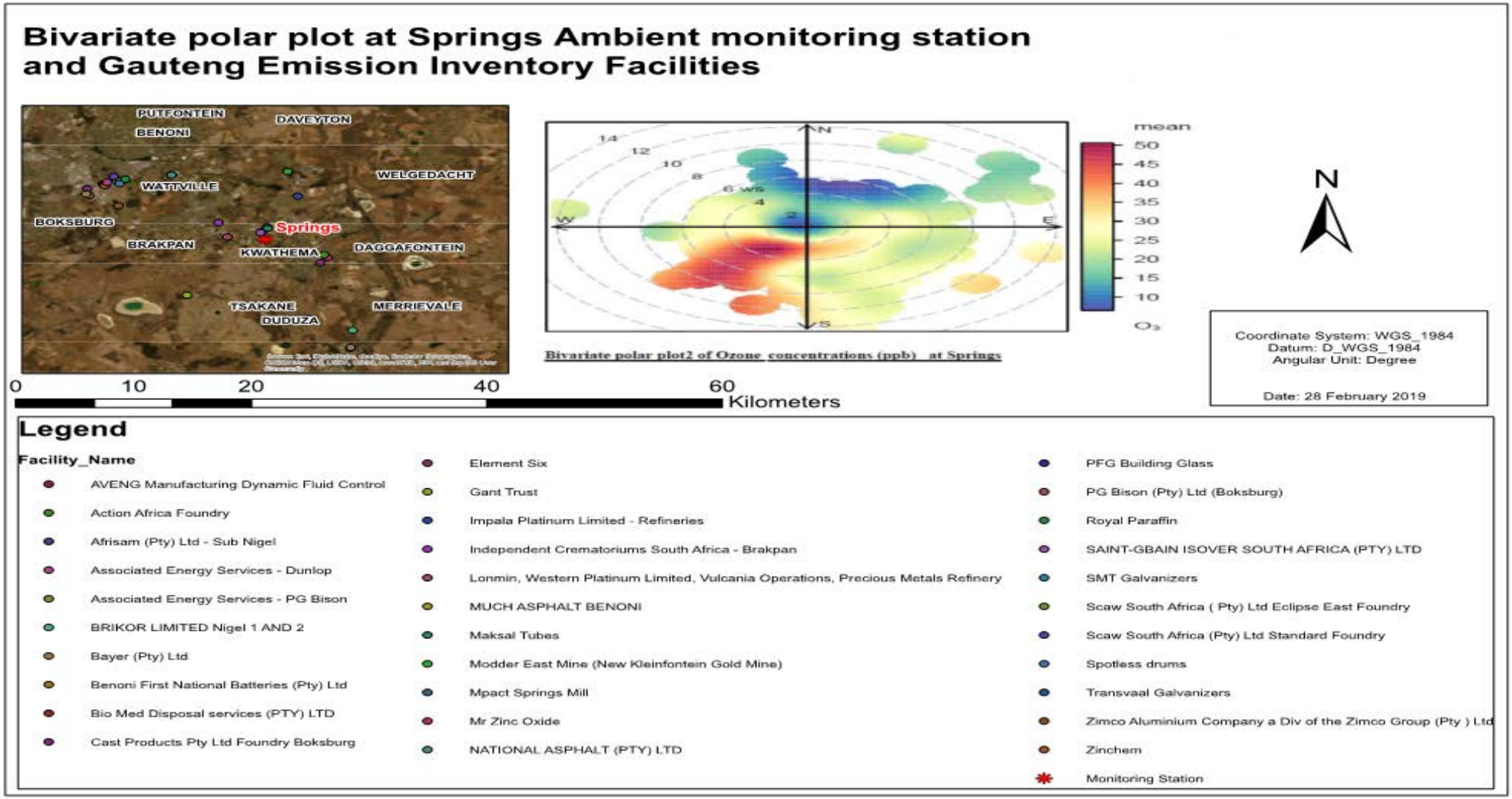

Figure 4.123: Bivariate polar plot at the Springs Ambient Monitoring Stations and Emission Inventory Facilities in Gauteng Province

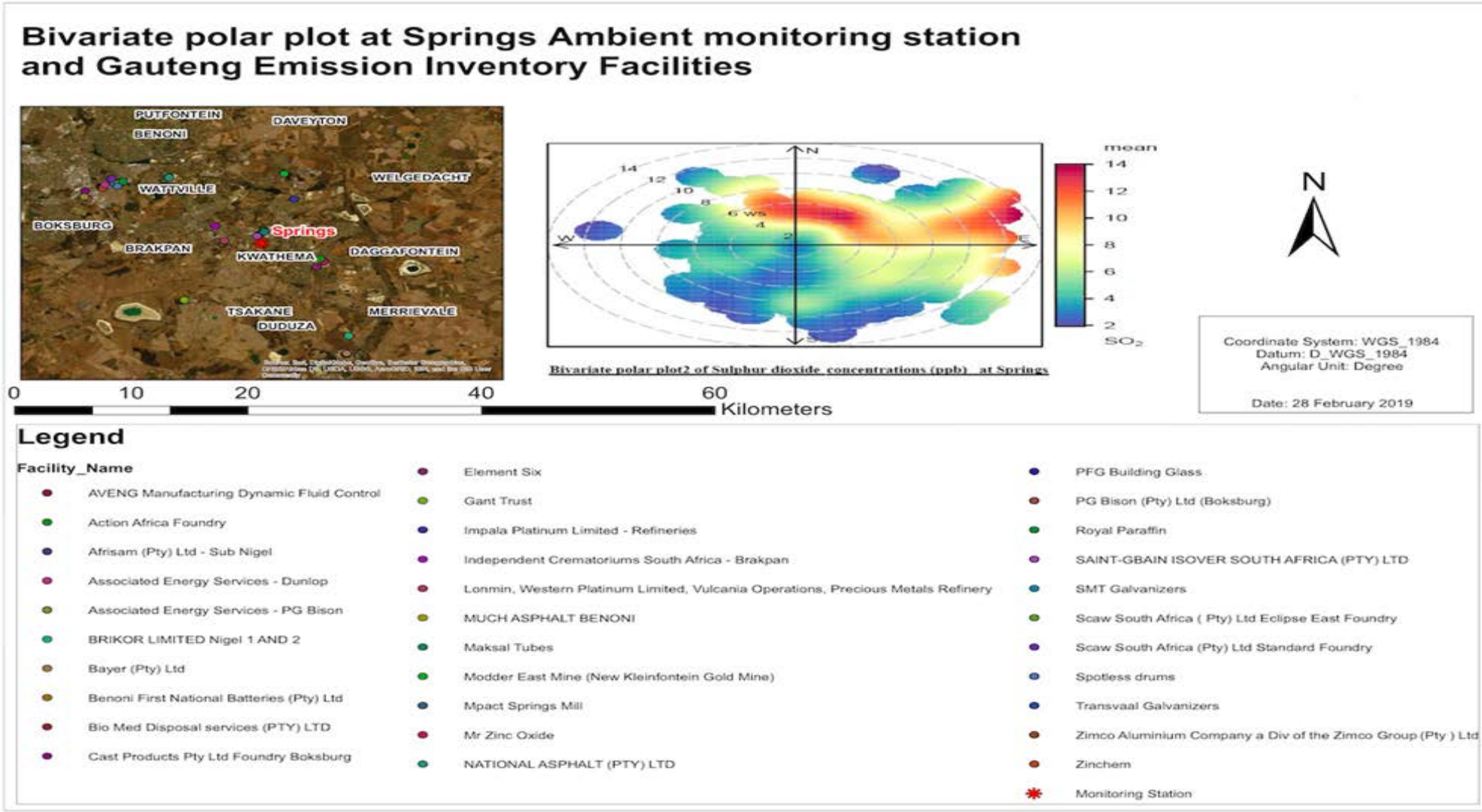

Figure 4.124: Bivariate polar plot at the Springs Ambient Monitoring Stations and Emission Inventory Facilities in Gauteng Province

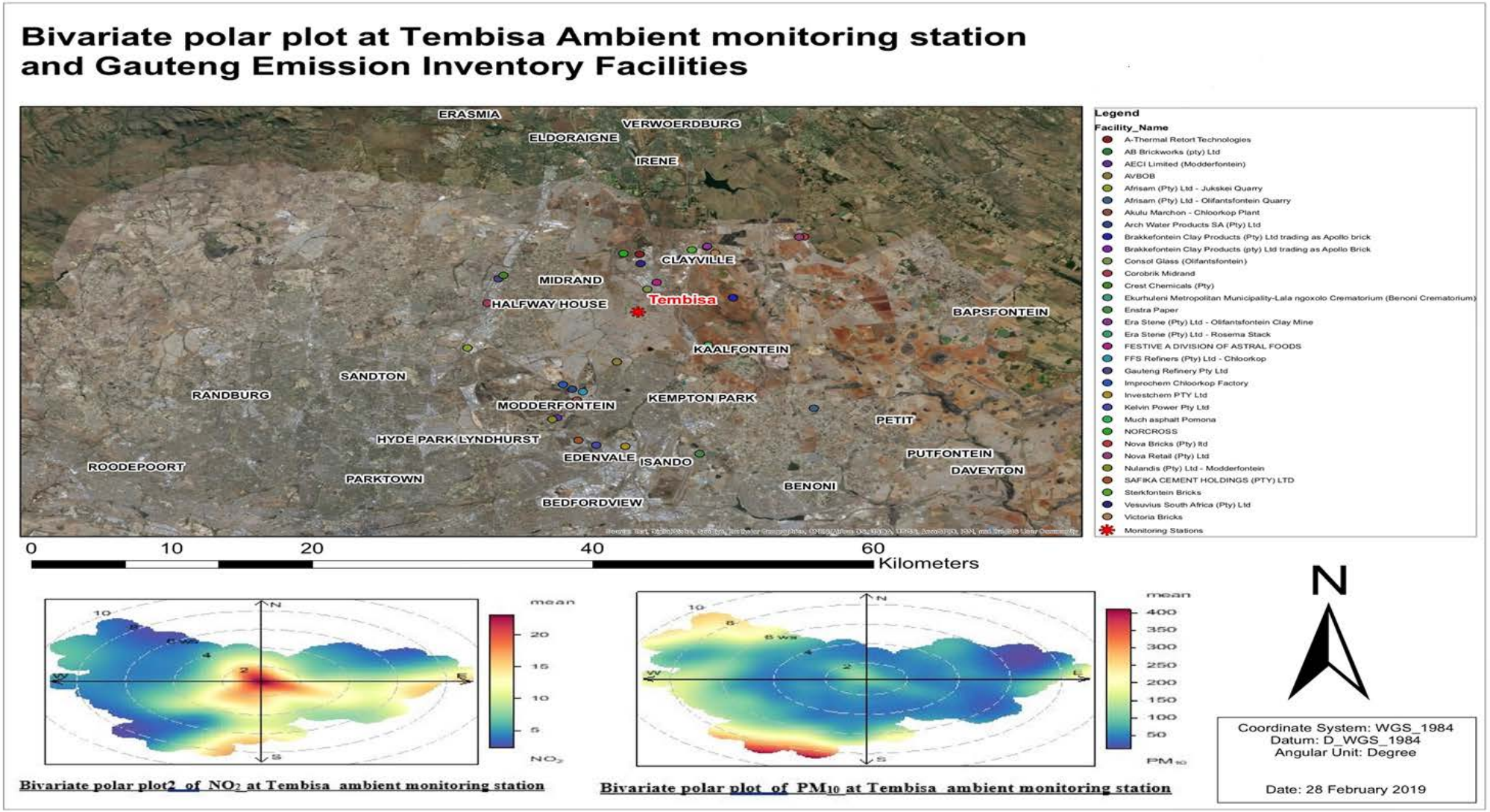

Figure 4.125: Bivariate polar plot at the Tembisa Ambient Monitoring Stations and Emission Inventory Facilities in Gauteng Province

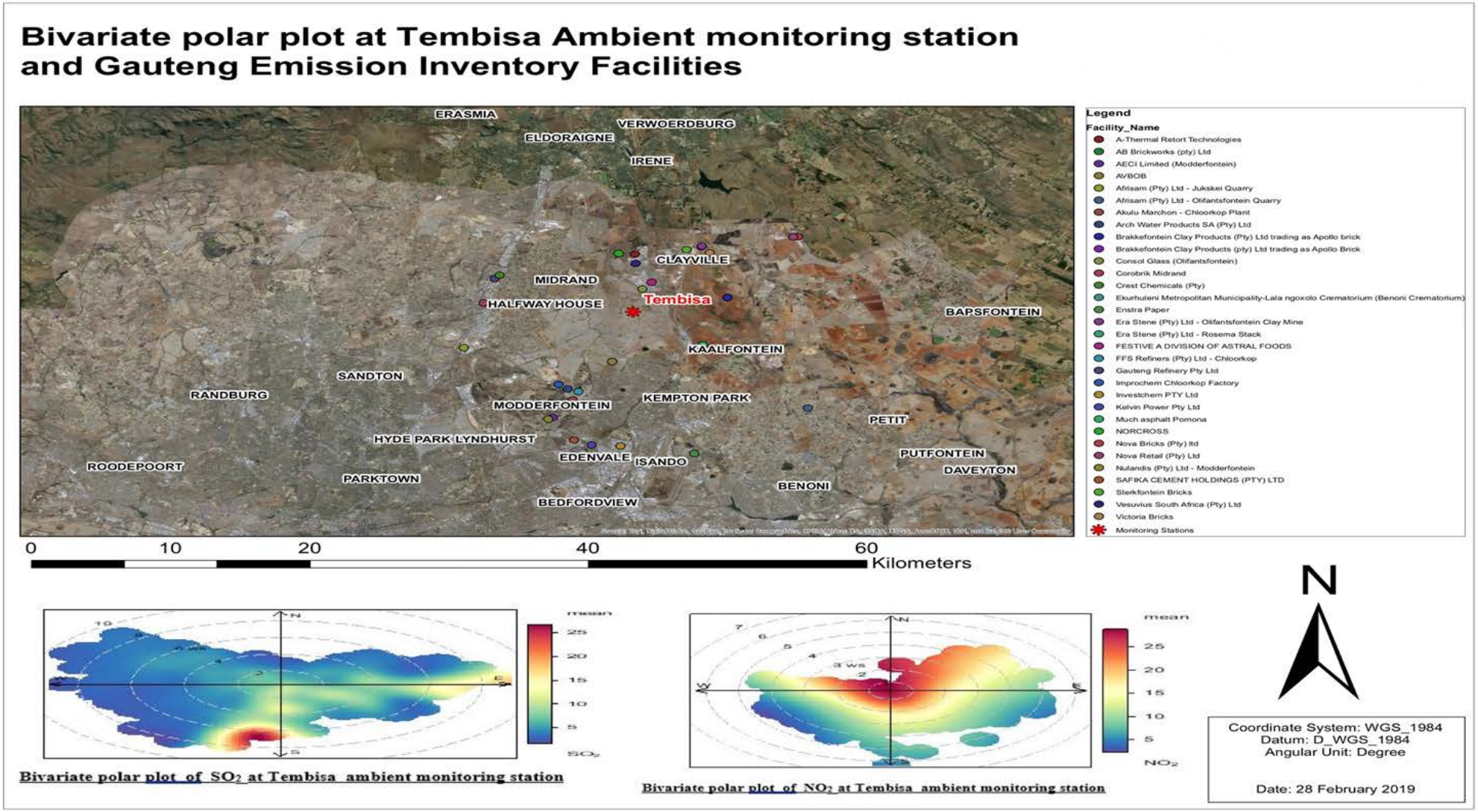

Figure 4.126: Bivariate polar plot at the Tembisa Ambient Monitoring Stations and Emission Inventory Facilities in Gauteng Province

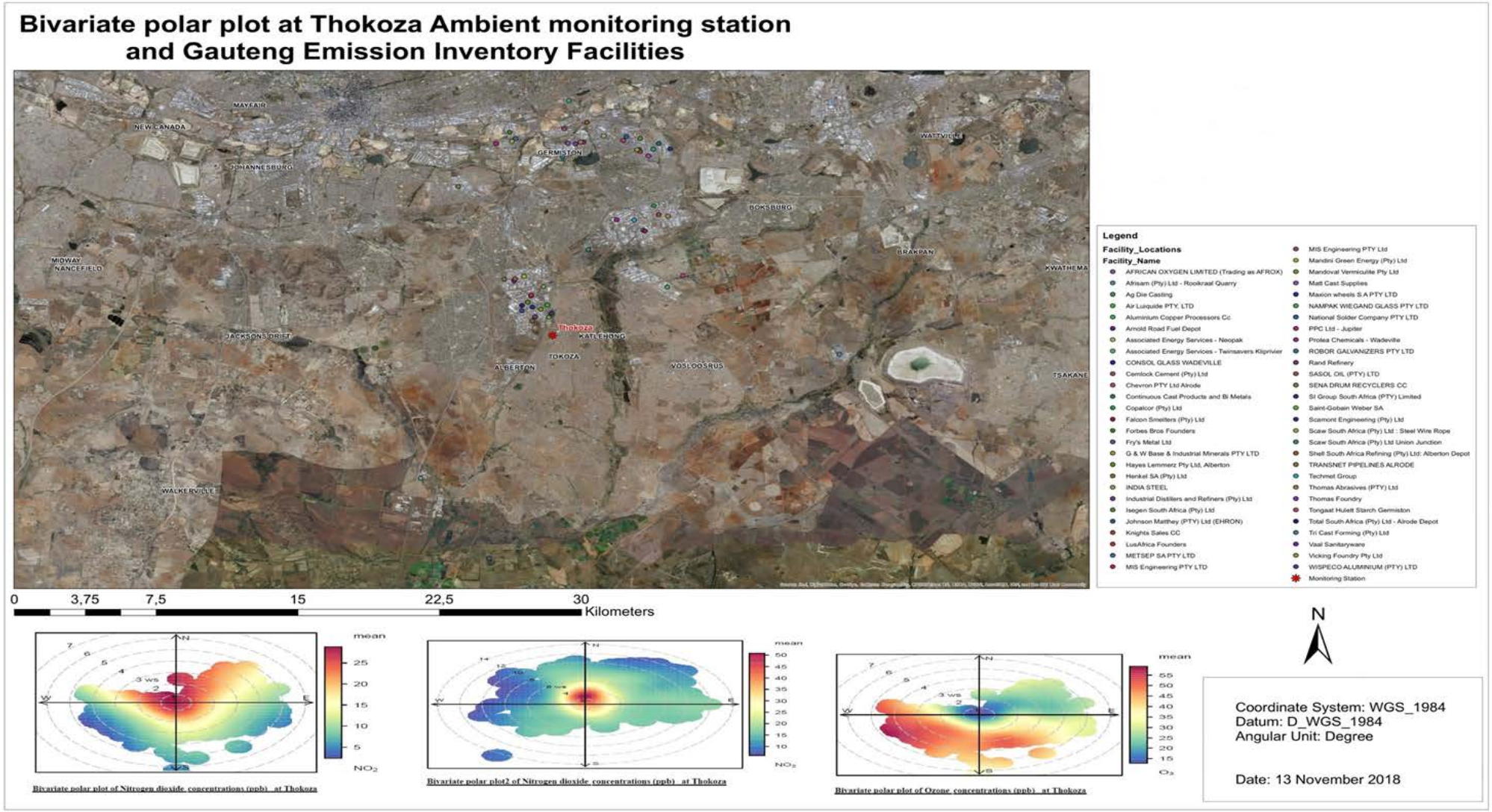

Figure 4.127: Bivariate polar plot at the Thokoza Ambient Monitoring Stations and Emission Inventory Facilities in Gauteng Province

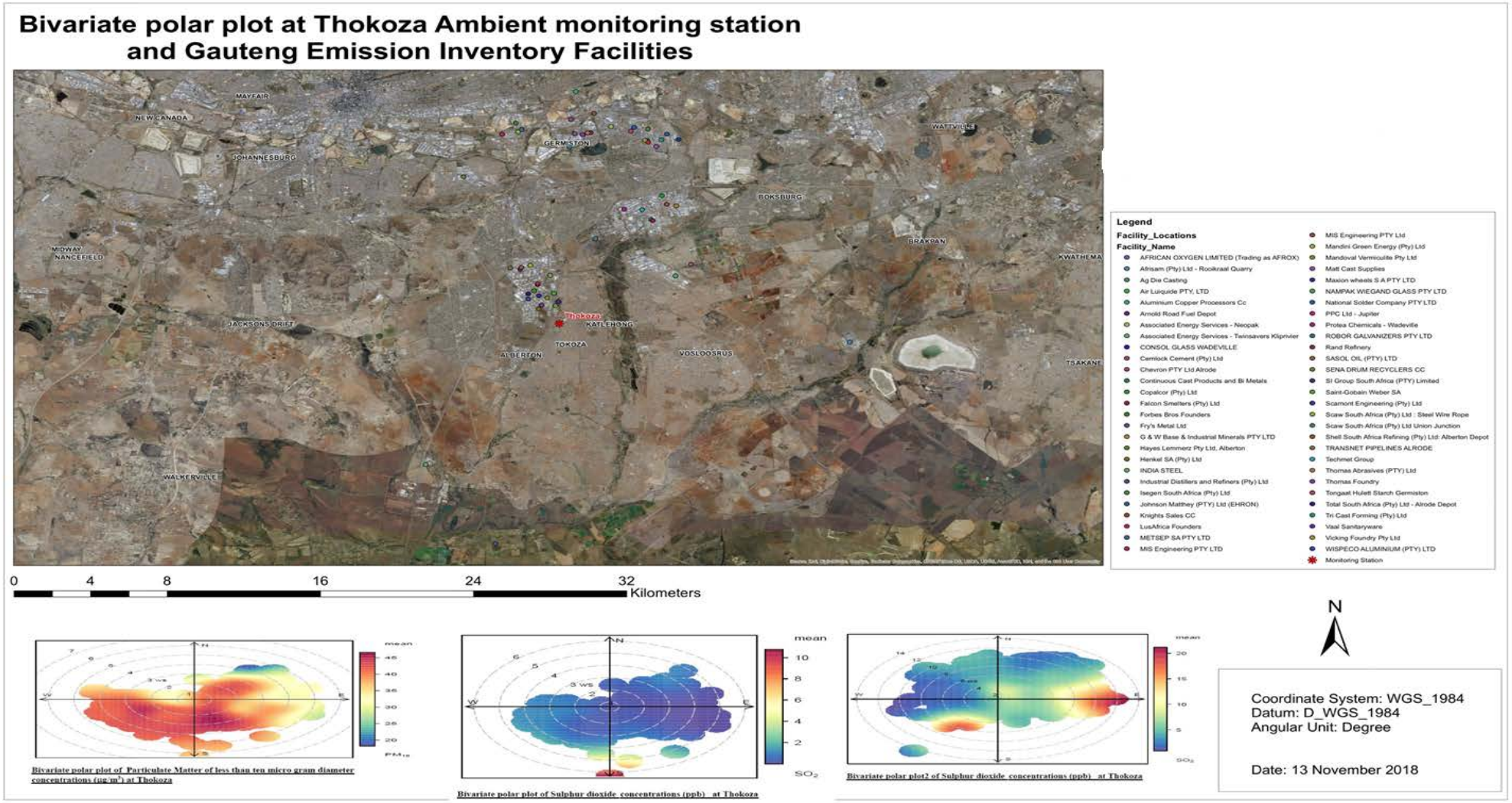

Figure 4.128: Bivariate polar plot at the Thokoza Ambient Monitoring Stations and Emission Inventory Facilities in Gauteng Province

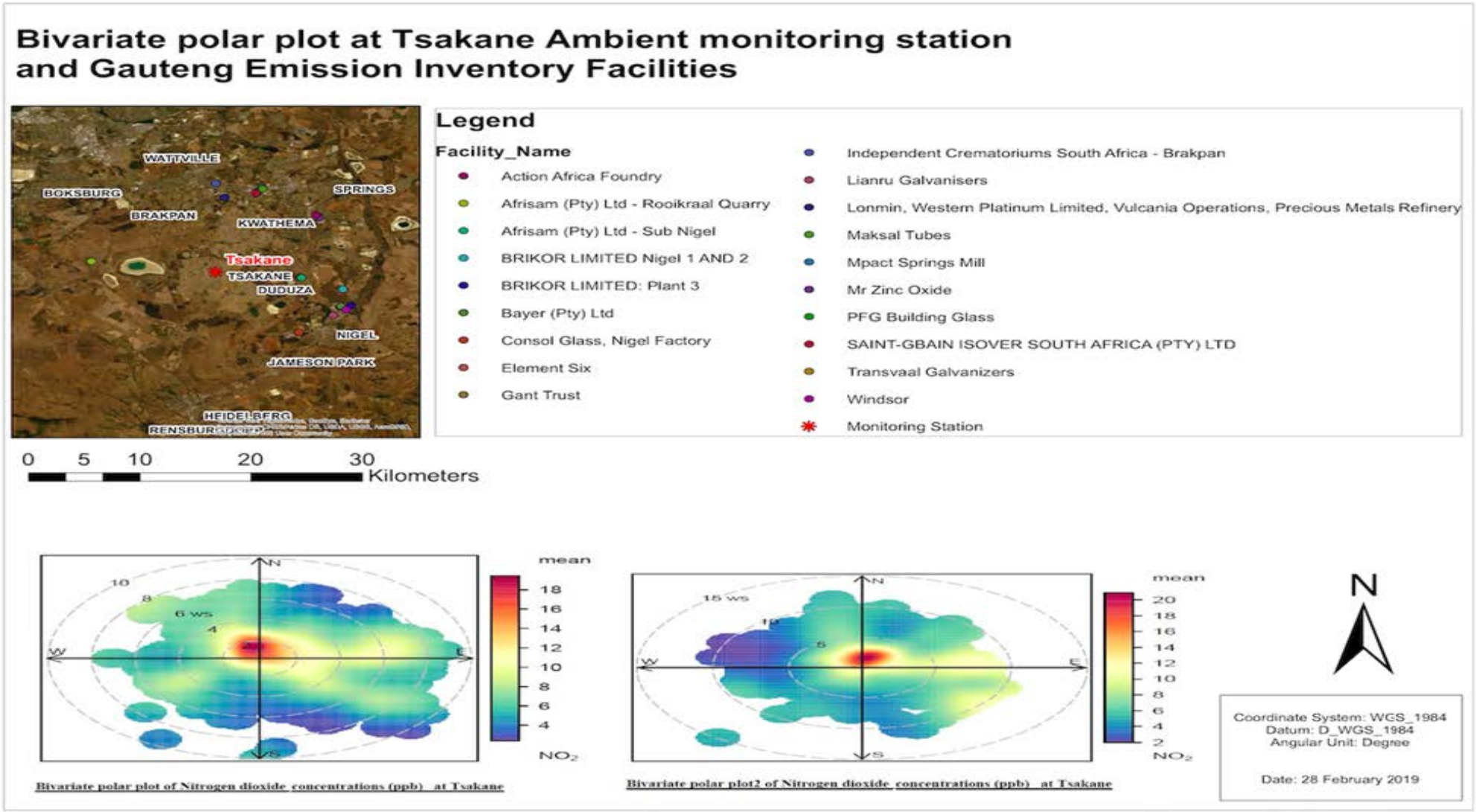

Figure 4.129: Bivariate polar plot at the Tsakane Ambient Monitoring Stations and Emission Inventory Facilities in Gauteng Province

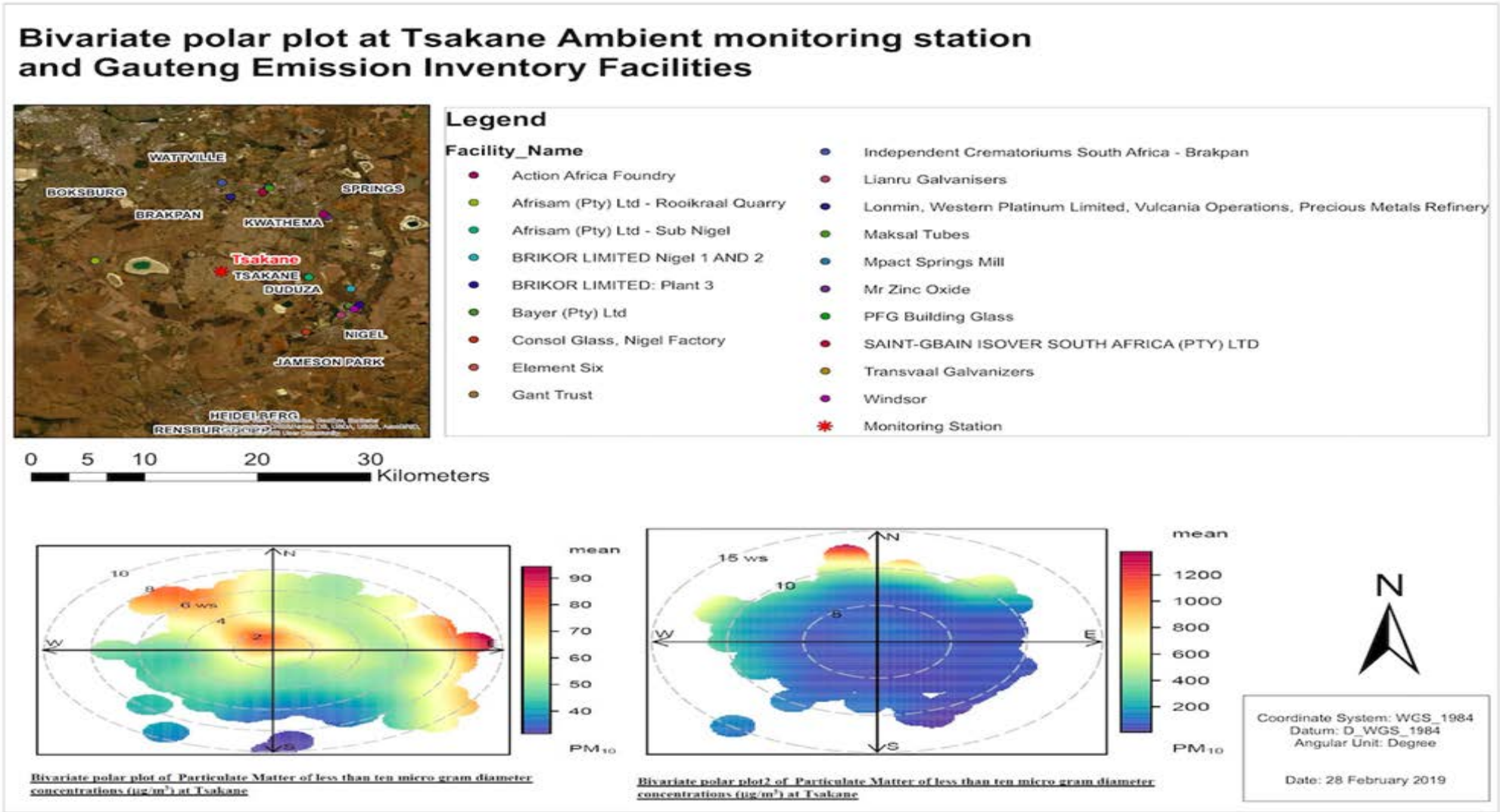

Figure 4.130: Bivariate polar plot at the Tsakane Ambient Monitoring Stations and Emission Inventory Facilities in Gauteng Province

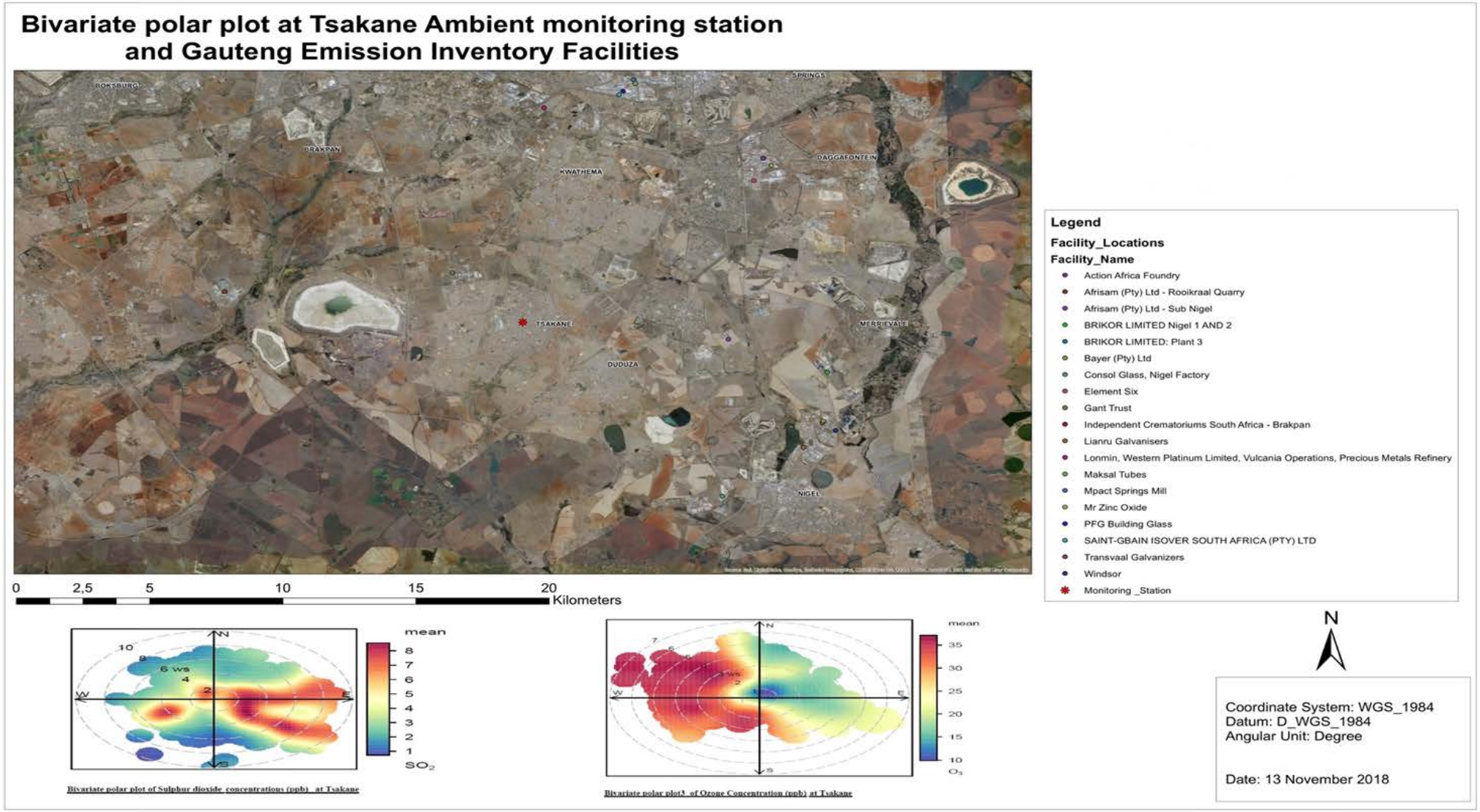

Figure 4.131: Bivariate polar plot at the Tsakane Ambient Monitoring Stations and Emission Inventory Facilities in Gauteng Province

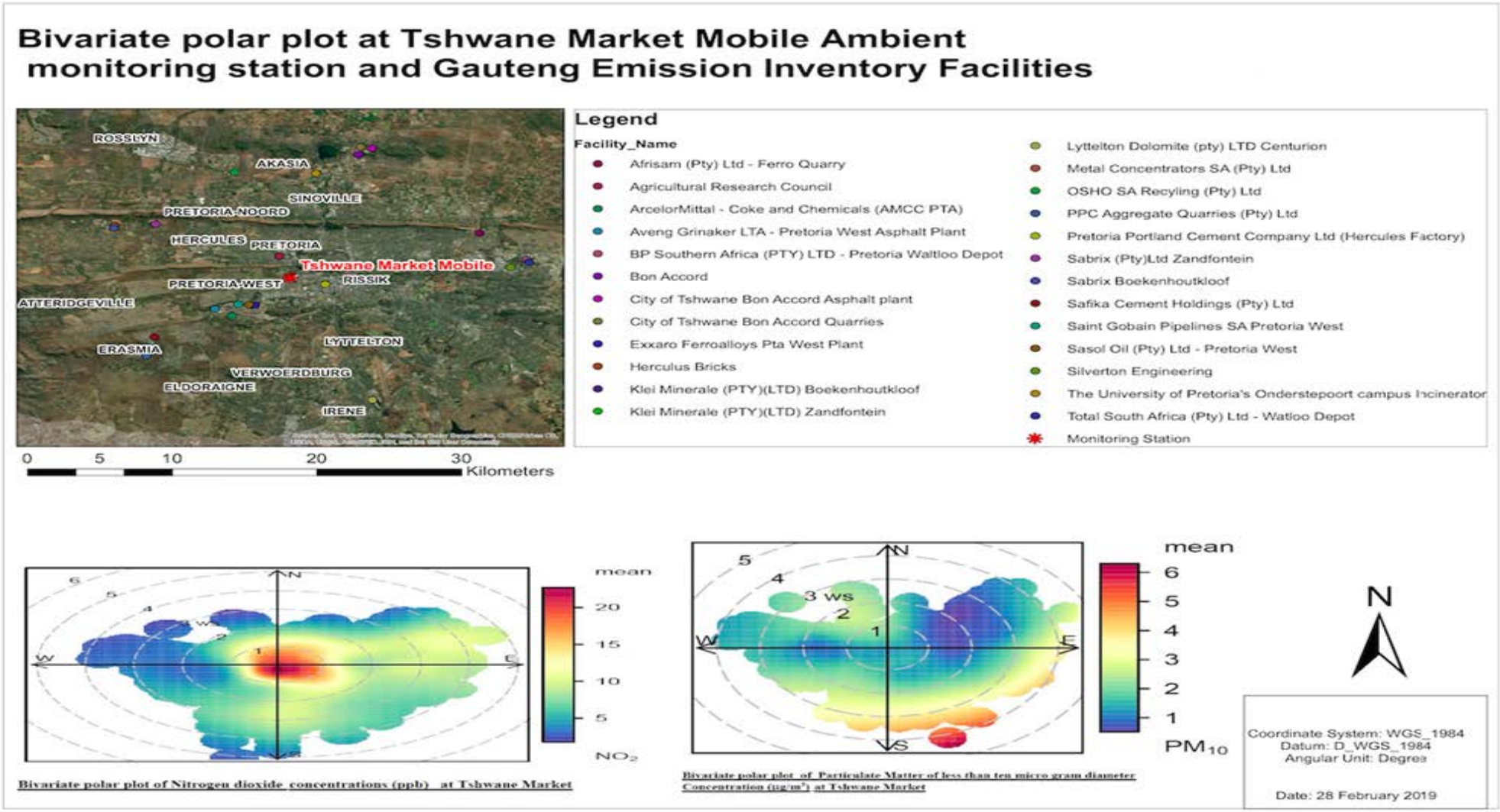

Figure 4.132: Bivariate polar plot at the Tshwane Market Mobile Ambient Monitoring Stations and Emission Inventory Facilities in Gauteng Province

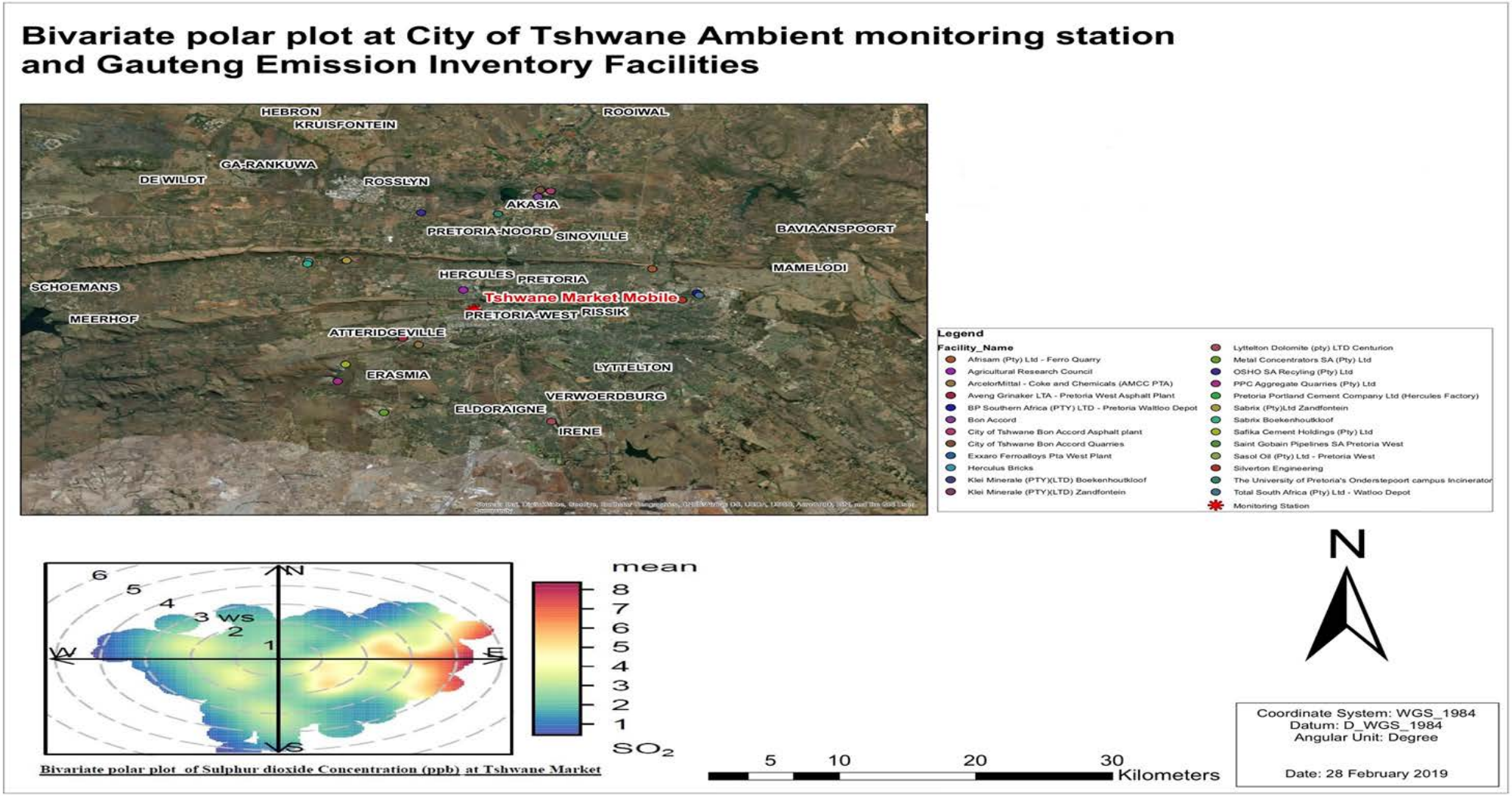

Figure 4.133: Bivariate polar plot at the Tshwane Market Mobile Ambient Monitoring Stations and Emission Inventory Facilities in Gauteng Province

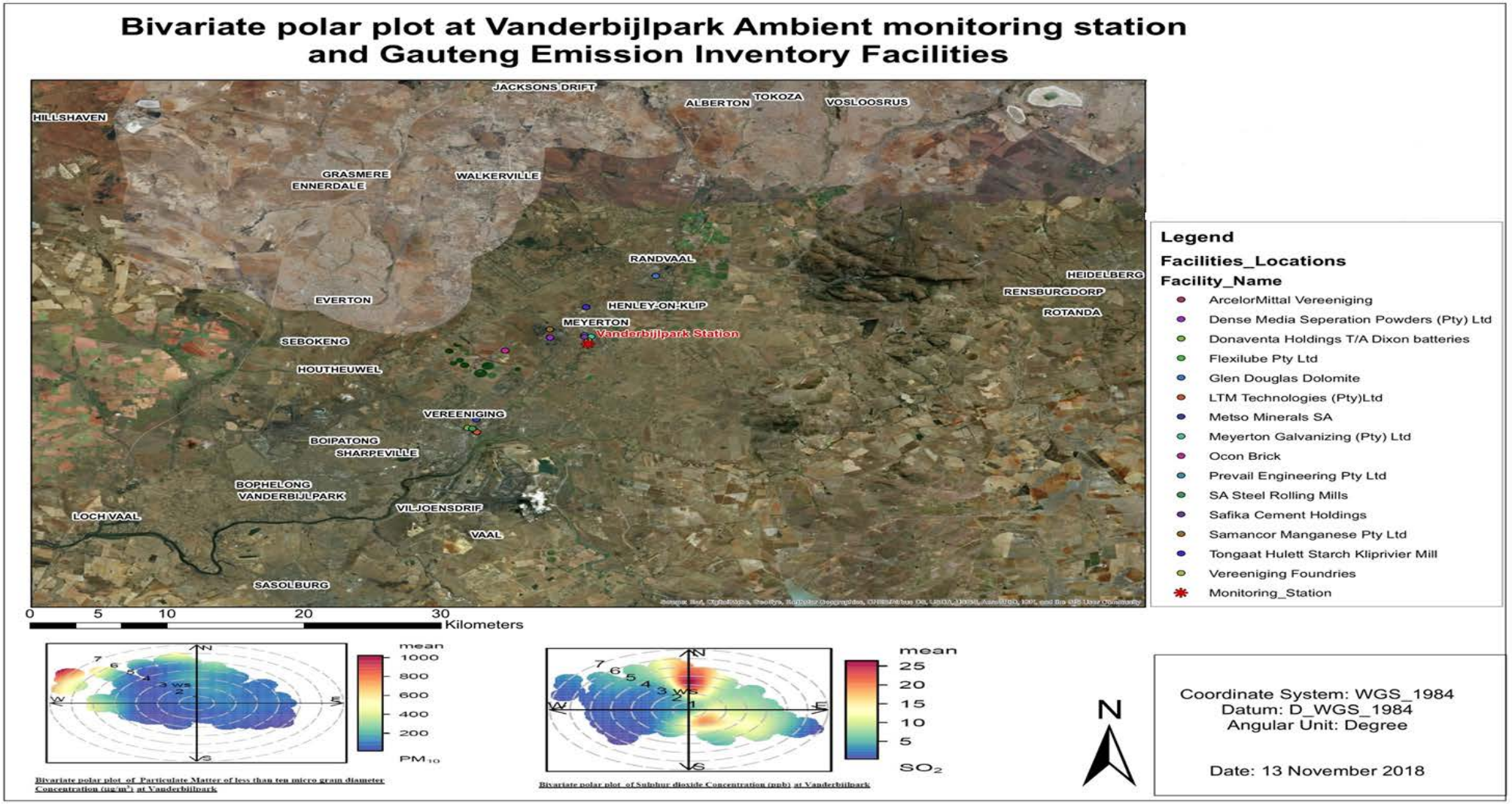

Figure 4.134: Bivariate polar plot at the Vanderbijlpark Ambient Monitoring Stations and Emission Inventory Facilities in Gauteng Province

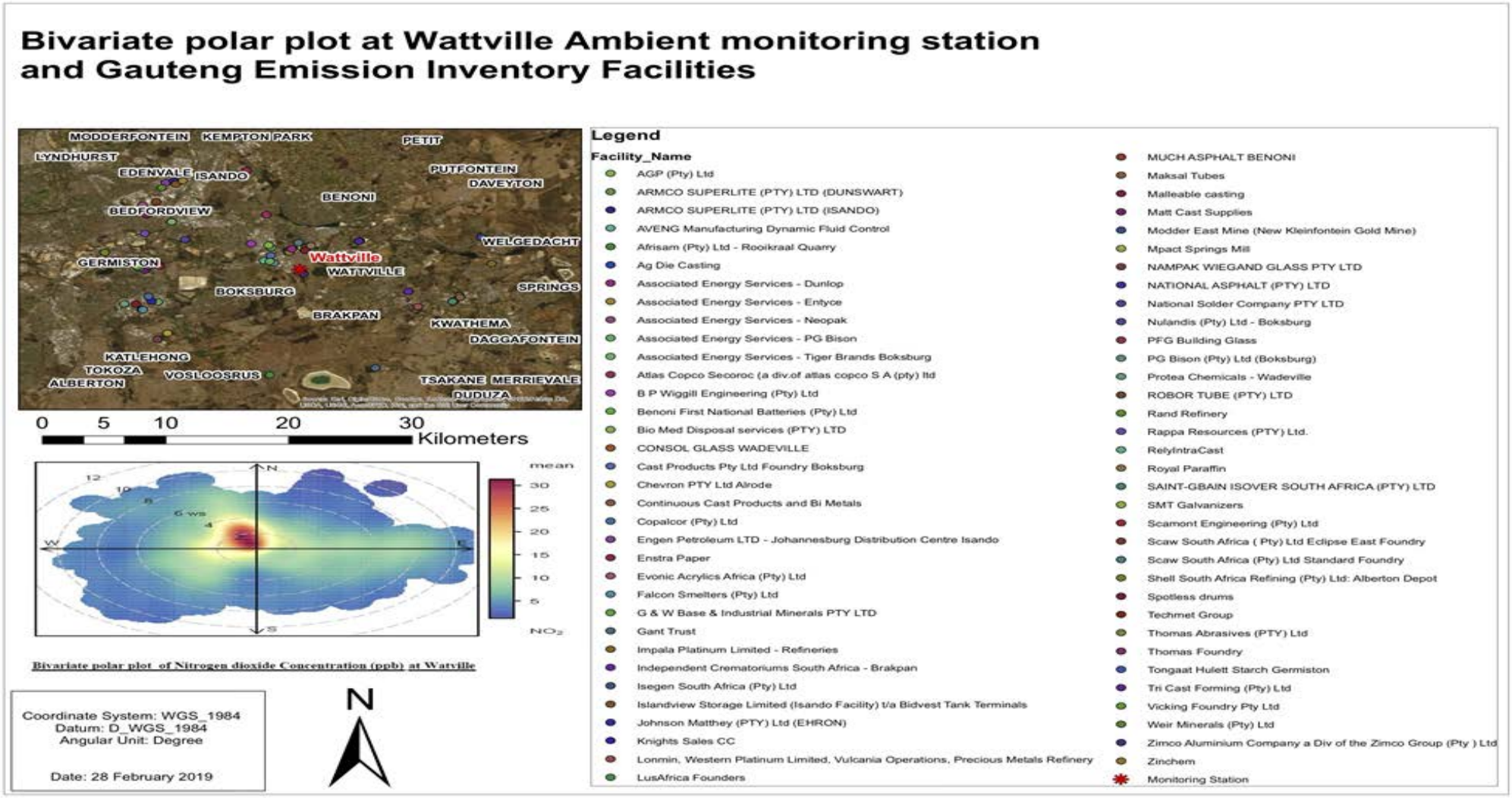

Figure 4.135: Bivariate polar plot at the Wattville Ambient Monitoring Stations and Emission Inventory Facilities in Gauteng Province

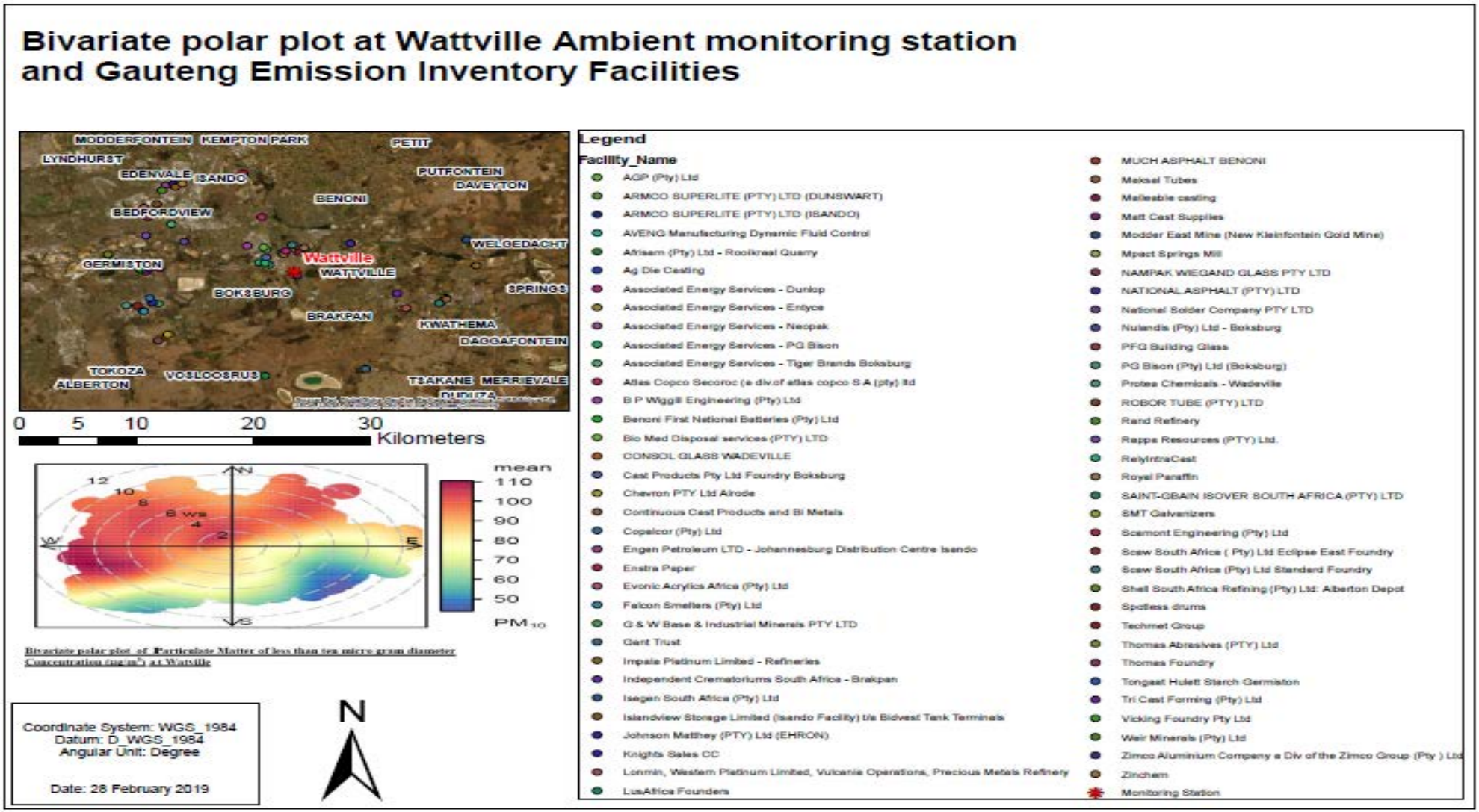

Figure 4.136: Bivariate polar plot at the Wattville Ambient Monitoring Stations and Emission Inventory Facilities in Gauteng Province

In Figure 4.74, Alexandra Environmental Monitoring Station is likely to record 29 facilities within a 15-kilometer buffer zone. This monitoring station is situated in the residential area with the aim of quantifying domestic fuel combustion. The bivariate polar plot of particulate matter had a concentration of only 10 µg/m3 for data collected over the past 6 years and was predominant in the North to East quadrants. The map indicated under 5 meters per second wind speed in the West-South and East-South zones, with sources releasing less than 15 µg/m3 concentrations of PM_{10}. The plot suggested a local source at a wind speed of under 5 meters per second with an atmospheric concentration of around 20 to 40 µg/m3 PM_{10}. When the direction of the wind prevailed in the North East with wind speeds of approximately 8 to 17 meters per second, the cause of the cluster was shown. The plot showed a higher concentration of PM_{10} at a high wind speed of about 20 and above in the North to the North-East of the ambient station. There are chemical industries such as AEL Mining Service Limited in under 10 kilometers North East of the Alexandra Ambient Station. The N3 road is situated on the North-East side of the ambient station less than 4 kilometers away.

Figure 4.75 showed a high number of pollution installations recorded within the Germiston and Island industrial areas situated in the North-East and South direction of the Bedfordview ambient monitoring station. The City of Ekurhuleni has probably the highest number of manufacturing industries relative to any other municipality in the Republic of South Africa. The Bedfordview Environmental Monitoring Station is situated much less than a kilometer South of the N3 East Bypass of the Gillooly Interchange, built on the old farm and the R24 and Tambo Airport Intersection, probably the busiest interchange in South Africa. Geldenhys Interchange is situated at the station's Southern site, less than 4 kilometers away from the Bedfordview ambient monitoring station. The main purpose of this monitoring station is mainly traffic emissions.

PM_{10} at the Bedfordview ambient air quality monitoring, displayed probability distribution of approximately 8 to one hundred and 40 from South to South East clockwise direction around the monitoring station at 0 to 8 meters per second. This meant that one could find sources closer and far to the station. Figure 4.75 displayed high probability of PM_{10} concentration of about 120 $\mu g/m^3$ at Eastern site of the station at wind speed of 4 to 7 meters per seconds. The plot also displayed other source of PM_{10} concentrations of approximately 8

to 130 $\mu g/m^3$ at Gillooly's interchange. The plot displayed high probability sources of PM_{10} from Germiston industrial area of up to 220 $\mu g/m^3$ at the wind speed from 6 meters and higher per second. Greater concentration of PM_{10} at the Bedfordview ambient monitoring is mostly due to the industrial sector situated in the South-Eastern Region (Germiston industrial area) than the transport sector as one would expect.

The sulfur dioxide concentration showed higher probability at the Southern side of the Bedfordview ambient monitoring station and displacement patterns towards Southern direction showing close and far sources towards the Geldenhys interchange which is within the Germiston industrial area. Figure 4.76 confirmed that high source of SO_2 is found at the Southern direction of Bedfordview ambient monitoring station than at Gillooly's as expected by the purpose of the station. At the Eastern side of the station there was a high chance of closer sources to the station with concentration of approximately 15 to 20 parts per billion when wind speed is 2 to 6 meters per second. At the North Eastern to South-West anticlockwise direction of ambient monitoring station there was sulfur dioxide concentration of about 10 to 15 parts per billion which was read at any given wind speed.

The plot showed high ozone concentrations in the North direction of the station situated at Gillooly's interchange (Figure 4.77). The ozone pollutant is formed from the reaction between volatile organic compounds and nitrogen oxides in the presence of sunlight. This means that at higher wind speed of less than 2 meters per second pollution sources are visible to direction and plot indicated 10 parts per billion of concentration and less. At Bedfordview station plot showed that closer sources wind speed increases from North-West to North-East. High concentration was shown at higher than 30 parts per billion at the Bedfordview. On the Southern site of the station at the Geldenhys interchange less ozone formation was noticed. This was probably due to better traffic flow at Geldenhys Interchange than at Gillooly's interchange which may have resulted in less nitrogen oxide from automobile engines and less fuel (volatile organic compounds) evaporation from vehicles. When wind speed increased to 2 meters per second and higher there was a higher probability formation of ozone concentration at top areas of South East of the station. At South-East direction site (Germiston) there's a higher number of chemical and metallurgical industries registered in the Gauteng Emission inventory system portal. When wind speed reached 10 meters per second, there was a high probability formation of ozone concentration at the South-East direction.

In Figure 4.78, Bedfordview indicated sources of nitrogen oxide from North to South anticlockwise direction at less than 2 meters per second. Unlike ozone pollutants from North-West to South West clockwise direction, results indicated no source closer and far off the station. At North-West to South-East clockwise direction there was a high probability of nitrogen oxide at any wind speed. Plot showed high clustered sources of nitrogen oxide between North-East to South West at sources that are far and closer sources, particularly when wind speed reached 6 meters per second. There was a high probability of nitrogen dioxide concentration at wind speed of 8 meters per second at the Southern site of the station. There was high likelihood of nitrogen dioxide concentration at the wind speed of 12 and more meters per second on the Southern site situated at Geldenhys Interchange. This meant that there were far sources of nitrogen dioxide at the Southern site of Bedfordview.

In Figure 4.79 Bodibeng station is situated near domestic residential areas such as Mabopane and Soshanguve. The primary objective of the station is usually to measure domestic fuel burning. The plot displayed s high probability of nitrogen dioxide concentrations when wind speed was less than 2 meters per second. This meant that there were nitrogen dioxide sources closer to Bodibeng ambient monitoring station situated on the Western direction. The results displayed concentration of approximately 15 to 30 nitrogen dioxide parts per billion on the South-East (Soshanguve) of the ambient station. When wind speed travelled at 2 to 8 meters per second on the South East of the station reading of nitrogen dioxide concentration of under 20.5 parts per billion was recorded. At the wind exceeding 8 meters per second there was a higher probability of nitrogen dioxide on the South-East direction. The results showed local source and far source at Soshanguve residential areas. The results displayed sources of nitrogen dioxide concentration of fewer than 20 parts per billion at wind speed of more than 2 meters per second at North to South anticlockwise movement direction (Mabopane, Hebron and Kruisfontein residential areas).

High probability ozone concentration was displayed at the Bodibeng station at different wind speed on the West to North-East clockwise movement direction of the station. As the wind speed reached 4 meters per second on the North-West areas. In Figure 4.79, results indicated less probability of ozone concentration when the wind speed is much less than 1 meter per second. Eastern to Southern areas clockwise direction displayed less ozone

concentration at the wind speed of less than 6 meters per second. High ozone formation is linked to high sunlight, nitrogen dioxide and volatile compounds.

The bivariate polar plot displayed less probability of PM_{10} at a local source of about fewer than 300 µg/m^3 at wind speed of less than 1 meter per second. Figure 4.80 had high probability of concentration displayed on the Southern areas of the Bodibeng at Mabopane and Soshanguwe areas. When wind speed picked to 6 meters per second on the South West higher concentrations of up to 700 µg/m3 was shown. In general, most of the PM_{10} sources are situated on the East to West clockwise movement direction.

Sulfur dioxide probability bivariate polar plot displayed local sources when the wind speed was at less than 2 meters per second. Figure 4.80 had higher concentration of sulfur dioxide of up to 8 parts per billion mostly on the Southern and North-West of the station at less than 2 meters per second of speed wind. When the wind speed was between 2 and 4 meters per second, there was a higher probability of sulfur dioxide source around Bodibeng ambient monitoring stations. When wind speed increases to 3 meters per second and higher, there was a high probability of sulfur sources up to 10 parts per billion on the South East (Soshanguve) of the station. On the North-West of the Bodibeng ambient monitoring station there were high chances of scattered sources of sulfur dioxide at any wind speed recorded on the plot of 2 to 6 parts per billion. South-West quadrant (Klipfontein, Hebron, Mabopane and Soshanguve) displayed exact same levels of sulfur dioxide concentrations of less than 4 parts per billion from 1 to 8 meters per second wind speed.

22 facilities were recorded within 15-kilometer radius from Booysens ambient air quality monitoring station. In Figure 4.81, when the wind speed was much less than 1 meter per second the probability plot indicated less concentration of PM_{10} at local sources that are affected. As the wind speed passed 1 meter per second upwards, PM_{10} concentration increase gradually at North West (Rosslyn industrial area) which was in quadrant 4 of Booysens bivariate polar results of PM_{10} with maximum concentration of up to 80 µg/m^3. The results showed local and far sources from the station. The results also displayed high probability of PM10 concentration from areas such as Akasia, Sinoville and Pretoria-North. The results displayed close and far sources of PM_{10} concentration at thirty to 55 µg/m^3 at areas such as Pretoria and Silverton. The study further showed PM_{10} sources at far South sources i.e. Pretoria West industrial area, which was visible at the wind speed of 4 to 5 meters per second. The

study displayed probability of PM_{10} concentrations of about 40 µg/m^3 at Atteridgeville and Erasmia. There was high visibility of PM_{10} sources at the wind speed of 3 meters per seconds and above.

The results displayed high probability of nitrogen dioxide concentration at the local sources in Figure 4.81. At the wind speed of less than 2 meters per second nitrogen dioxide concentrations of up to 55 parts per billion was recorded. Higher probability concentration of nitrogen dioxide results displayed local sources at the South West of the ambient station around Hercules area. There was also probability of far sources at the Eastern parts of the station with ambient concentration of up to 14 parts per billion at Hercules and Pretoria central business district, as the wind speed picked of up to 3 meters per second.

The results showed high probability of ozone around Booysens at the wind speed of 1 meter per above and second. In Figure 4.82 results displayed high sunlight with volatile organic compounds and oxides of nitrogen resulting in high formation of ozone. The results displayed less probability of ozone at the Eastern areas at wind speed picked at 1.5 meters per second and above.

The bivariate polar plot results displayed high probability of sulfur dioxide concentration at South East (Pretoria West industrial area to Atteridgeville residential area) of the Booysens. The sulfur dioxide concentration results displayed wind speed of 1 to 9 meters per second. In Figure 4.83 results displayed high probability of sulfur dioxide sources at North-East (Pretoria-North and Akasia) direction at wind speed of 5 to 14 meters per second. North-West of the Booysens there was a higher probability sources of sulfur dioxide sources of 4 parts per billion. However, there were close and far sources displayed on the bivariate polar plot results at the areas of Ga Rankuwa and Rosslyn.

In Figure 4.84, Buccleuch is within the City of Johannesburg. The Buccluech interchange and monitoring station was designed to monitor traffic emissions. There were high chances of nitrogen dioxide concentrations sources at the North-West up to 40 parts per billion, especially when the wind speed was between 1 and 6 meters per second. Results displayed high probability at local sources at the less wind speed condition. Furthermore, results displayed less probability of nitrogen dioxide concentration at North East at calm wind condition. As the wind speed increases from Buccluech to North-East direction (Midrand and Halfway House) less concentration of nitrogen dioxide is visible of up to thirty parts per billion.

At the South East of the ambient monitoring station higher nitrogen dioxide concentration was recorded at the local source. This showed that nitrogen dioxide measured from Buccluech ambient monitoring station emanated from local source which were at Buccluech Interchange. There were high chances of nitrogen dioxide at the Eastern side of the ambient station at busiest areas of the inter-exchange.

The bivariate polar results of displayed far sources than local sources in Figure 4.84. When the wind speed was much less than two meters per second, less ozone concentrations were found around Buccleuch ambient monitoring stations. Higher ozone probability concentration was recorded at the wind speed of two meters per second and above. The bivariate plot results displayed high probability concentrations at the South-East to North East for wind speed of 6 meters per second and higher. There was a higher probability concentration of ozone at North-West at wind speed of 6 meters per second and higher. Higher temperature in the presence of volatile organic compound and oxide of nitrogen resulted in higher ozone concentrations.

The bivariate polar plot results displayed PM_{10} concentrations at local sources next to the Buccluech ambient monitoring stations. Figure 4.85 showed local sources at the wind speed of less than 2 meters per second. The source of PM_{10} displayed high probability sources at traffic interchange. The bivariate plot results displayed high probability of PM_{10} concentrations at Buccluech at the wind speed of 6 meters per second and higher. The results displayed higher probability of PM_{10} concentrations in the South East areas at the facilities in Modderfontein industrial area. The results also displayed probability of PM_{10} concentrations at the North East at the wind speed of 10 meters per second at 70 to 80 $\mu g/m^3$. Higher likelihood of PM_{10} concentrations on the South West (Modderfontein, Kempton and Kaalfontein Park) to Western Area (Tembisa) at the wind speed of 8 meters per second and higher.

The bivariate polar plot results of sulfur dioxide concentrations in Figure 4.85 displayed high probability at regional and far sources. At the wind speed of 2 and less meters per second there was a higher probability of SO_2 concentration of up to 18 parts per billion. When the wind speed increased to 4 meters per second less concentrations were displayed on the South-West direction. When wind speed blew from South East of the station, results displayed higher SO_2 probability of 20 parts per billion.

Davidsonville ambient monitoring station was designed to monitor pollutants from domestic fuel burning and other areas close to the station within the City of Johannesburg. Figure 4.86 indicated that two facilities around the area of mining activities were reported to the Gauteng Atmospheric Emission Inventory system within 15 kilometers radius. Because of the nature of the facility (mining activities) there is high likelihood of PM_{10} concentrations. As the wind was on calm conditions of less than 5 meters per second, the plot displayed local source situated on the Eastern side at the station. The bivariate polar plot showed 3 major sources at far West, Far North East and local East direction. The source close to the station displayed PM_{10} concentration of the range of 60 to 80 $\mu g/m^3$. The primary source at far West were recorded when wind speed was at 10 meters per second and higher with the concentration of up to 125 $\mu g/m^3$. The plot showed major source at North East, which effect could be experienced at the station at the wind speed of thirteen meters per second and above. However, there were other minor sources which were visible at the North East, South East and North West-South West at any given wind speed.

Delta Park ambient monitoring station was designed to monitor pollutants from domestic fuel burning. In Figure 4.87, there are 34 registered within Gauteng Emission inventory activities within 15 kilometers radius of Delta Park ambient monitoring station. The bivariate polar plot of ozone concentrations showed major sources on the West, North West, South East and South West of the ambient monitoring station. At calm conditions of less than 1 meter per second, results displayed probability of ozone concentration on the South West with the ambient concentration of 20 parts per billion. When the wind speed exceeded one meter per second and above on the North West, West, South and South-East showed ozone pollutants. High likelihood of ozone concentration at South East was apparent at the wind speed of two meters per second. Delta Park ambient monitoring station did not monitor nitrogen oxide and sulfur dioxide pollutants.

Diepsloot ambient monitoring station is situated in the City of Johannesburg and the station was created to monitor domestic fuel burning as per Figure 4.88. The bivariate polar plot results showed nitrogen dioxide with high probability sources at the nearby area. High concentration of nitrogen dioxide up to 20 parts per billion was recorded at calm conditions. When the wind speed was under 5 meters per second, high probability concentration was recorded at near the Diepsloot ambient monitoring station. The other source was recorded as

the wind speed increases from 5 meters per second to 15 meters per second on the South East of the station with the ambient concentration of 12 meters per second. However, there were other minor sources on the Eastern regions of the station that were visible at the wind speed of 5 meters per second and above. Results indicated sources on Eastern regions and the South of the station at any given wind speed.

The bivariate polar plot of PM_{10} at the Diepsloot showed far major sources than local sources. In Figure 4.88 results showed that during calm weather conditions minor sources emitted PM_{10} of approximately 60 $\mu g/m^3$. The results also showed higher probability of PM_{10} sources as the wind speed increased to 4 meters per second. When the wind speed reached 8 meters per second far sources are shown on the South East of the station.

The bivariate polar plot results for sulfur dioxide at the Diepsloot showed high likelihood of the sources on the Eastern side of the station, especially when wind speed blew at 2 meters per second and above. In Figure 4.89, the concentration of identified major sources on the Eastern direction of the above-mentioned station accounted to an amount of eleven parts per billion. Besides major source on the Eastern direction there were other sources of 4 to 6 parts per billion concentrations of sulfur dioxide.

Ekandustria ambient monitoring station is situated at the Ekandustria industrial area in the City of Tshwane and the station was designed to monitor pollutants from industrial activities as per Figure 4.89. The plot showed high probability of ozone concentration on the West, North West, North and North East closer and far to the station. Far sources on the North West had high concentration of up to 65 parts per billion. When the wind speed was on calm condition of 14 meters per second on the South East, the concentration was much less than 25 parts per billion. On the same South-East direction, the plot displayed s other major sources of higher concentration to 55 parts per billion.

In Figure 4.90, bivariate polar plot of PM_{10} showed far major sources on the South West, North East and North West at wind speed of 10 meters per second and above at higher concentrations of 450 $\mu g/m^3$. The results displayed sources of PM_{10} at the wind speed of less than 10 meters per second. North-East and North-West sources at the wind speed of fifteen meters per second displayed probability of PM_{10} concentration of approximately 150 to 200 $\mu g/m^3$. Sources which are situated on the South West of ambient concentrations of 450 $\mu g/m^3$ at the wind speed between 15 and 20 meters per second.

In Figure 4.91, the bivariate polar plot results indicated sulfur dioxide concentrations at the Ekandustria on the South East minor area of South West of the ambient station at wind speed of 3 meters per second and above. Other sources were found on the North East at the wind speed of 10 meters per second with concentration of 6 parts per billion. The plot also revealed other pollution sources on the North West at calm wind speed conditions and sulfur concentration up to 5 parts per billion.

Etwatwa ambient monitoring station is situated in the City of Ekurhuleni and the station is designed to monitor pollutants from domestic fuel burning activities. The results displayed in Figure 4.92 bivariate polar plot of nitrogen dioxide indicated major sources on the North East, North West and South West. When the wind speed was much less than two meters per second, less than 60 parts per billion was recognized at the nearby areas to the station. When the wind speed picked to 4 meters per second, the plot showed sources on the North-West and South-West. When the wind speed reached 6 meters per second and above the plot revealed high probability of nitrogen dioxide concentration of approximately 140 parts per billion at Southern areas of the ambient station. The results showed major source on the North East of the ambient station, when the wind speed picked to 6 up to 10 meters per second with the high likelihood of nitrogen dioxide concentration to 100 parts per billion. The plot also revealed major sources on the North West as the wind speed picked from 6 to 8 meters per second.

The bivariate polar plot results indicated PM_{10} concentration at the Etwatwa local and far sources from the ambient station in Figure 4.92. The plot showed local sources at the wind speed of less than two meters per second. The bivariate polar plot results displayed high probability concentration of PM_{10} of 200 µg/m3. When the wind speed picked to 4 meters per second, the ambient station had higher chances of recording less PM_{10} concentrations. When the wind speed picked at 6 meters per second, there was a higher likelihood of PM_{10} concentration from North to South anti clockwise movement direction. The results showed far sources on the Eastern areas at the wind speed of 6 meters per second and higher.

In Figure 4.93, the bivariate polar plot results displayed sulfur dioxide at the Etwatwa ambient monitoring station with higher likelihood of the major local and far sources on the Eastern regions of the ambient station. When the wind speed was much less than 2 meters per second the plot displayed higher probability of sulfur dioxide concentrations up to 30 parts per billion. When the wind speed was at two to 4 meters per second there was a probability of

sources on the Eastern areas as well as on the South West of the station. When the wind speed picked from 4 to 6 meters per second there were other major sources on the South West of the ambient station. One could find other minor sources on the North East, South East and North West of the ambient monitoring station with the concentrations of up to 10 parts per billion. When wind speed reached 6 meters per second and above on the Eastern side of the Etwatwa concentration reached 18 parts per billion. On the South West of the ambient station, the concentrations reached thirteen parts per billion.

Germiston ambient monitoring station is situated at the Germiston in the City of Ekurhuleni and the station is designed to monitor pollutants from domestic fuel burning activities. Figure 4.94 bivariate polar plot results indicated nitrogen dioxide concentrations at the high likelihood of significant sources near the station, when the wind speed was much less than two meters per second. Local sources showed highest concentrations around the ambient monitoring station. As the wind speed picked to two meters per second and above, two major sources were shown on the North areas and Eastern regions of the ambient monitoring station. When the wind speed exceeded 2 meters per second minor pollution sources were visible around the station with 14 parts per billion ambient nitrogen dioxide concentrations. The bivariate polar plot results displayed two major sources areas with the ambient sulfur dioxide concentrations of 14.5 parts per billion. At the Northern area of the Germiston station high concentrated source was detected of 14.5 parts per billion when the wind speed exceeded 1 to 3 meters per second.

Figure 4.95, Ivory Park bivariate polar plot results indicated sulfur dioxide major sources on the North East to East and the ambient concentration estimated to 6.5 parts per billion. When wind speed picked at one to 8 meters per second results showed an ambient concentration of 1.5 parts per billion from North East to North-West direction.

The Ivory Park Environmental Control Station is currently situated within the City of Johannesburg and is primarily designed to monitor emissions from domestic fuel burning operations. In Figure 4.96, bivariate polar plot showed local PM_{10} emissions when the wind speed was currently slightly less than one meter per second with an atmospheric concentration with 100 and 80 $\mu g/m^3$. When the wind speed was within the range of 1 to 6 meters per second in the direction of the North East, the atmospheric concentration was 60 $\mu g/m^3$. As the wind

speed picked from 1 to 6 meters per second, the atmospheric concentration was typically measured at 100 and 200 μg/m3.

The Jabavu Environmental Monitoring Station is currently situated within the City of Johannesburg and is specifically designed to track emissions from domestic fuel burning. Figure 4.97 displayed the bivariate polar ozone concentration. The findings revealed a lower probability of local sources at calm conditions at less than 0.5 meters per second, which is currently less than 20 parts per billion atmospheric concentrations. As the wind speed reached 0.5 meters per second, the plot displayed a high reading of up to 57 parts per billion atmospheric concentrations.

In Figure 4.97 bivariate PM_{10} polar plot findings revealed far-reaching origins when the wind speed was 4.8 meters per second in the western regions of Jabavu. However, there were still small sources in calm conditions at the 60 $\mu g/m^3$ concentration. When the wind speed was 3 meters per second on the south-east to the south-west, the ambient concentration was 70 $\mu g/m^3$.

The bivariate polar plot results of sulfur dioxide at Jabavu revealed a high likelihood of the major sources when the wind speed was less than 3 meters per second. In Figure 4.98, the main source showed a high likelihood of 5.5 parts per billion sulfur dioxide concentrations in the South East. At 2 to 3 meters per second on the south west of the atmospheric station, a large source of sulfur dioxide ambient concentrations was detected. There were other small outlets when the wind speed was at any given wind speed of up to 5 meters per second except on the south side when the wind speed was at 6 meters per second with the same atmospheric concentration of 2 parts per billion.

Results in Figure 4.99 are shown by the Leondale Environmental monitoring station located in the city of Ekurhuleni and built to track contaminants from Ekurhuleni domestic fuel burning activities. The results displayed major nitrogen dioxide sources in the local area when wind speed was less than 2 meters per second and the ambient concentration of 28 parts per billion. When the wind speed was between 2 and 4 meters per second there was a source which was visible on Southern and South East of Leondale ambient monitoring station. The results also displayed minor sources around the ambient station. The minor sources ambient concentration was predicted to the amount of 15 parts per billion.

The bivariate polar map of the Leondale atmospheric concentration of ozone revealed significant sources both on the northern and southern sides of the experimental station. Figure 4.100 indicated the wind speed at one meter per second but less than two meters per second at an average concentration of 30 parts per billion. Once the wind speed was between 2 and 11 meters per second from the North East to the North West of the station. The atmospheric concentration of ozone in the above-mentioned areas is currently measured at 60 parts per billion. In the South East, as wind speeds rose from 4 to 8 meters per second, the plot revealed a significant source with an atmospheric concentration of up to 40 parts per billion. The map revealed another big source in the southwest of the atmospheric station when the wind speed was between 3 and 8 meters per second with an average of 43 parts per billion ozone atmospheric concentrations.

The bivariate triangular map of Sulfur dioxide at the Leondale had large sources of 10 and more parts per billion in the South West, North East and South East. When the wind speed was less than two meters per second, the plot showed local sources, particularly North East and South West and South East. There were manor sources in the North West at up to 6 parts per billion atmospheric concentrations. The primary source in North East was 10 parts per billion of sulfur dioxide at the Leondale atmospheric station facility, as seen in Figure 4.101.

Mamelodi ambient monitoring station is represented by Figure 4.102 and situated within the City of Tshwane and the station was designed to monitor pollutants from domestic fuel burning activities. The bivariate polar plot displayed both major local and far sources for the ambient concentration of 40 parts per billion. When the wind speed was less than two meters per second, local major source was shown with the estimated Nitrogen dioxide ambient concentrations of 40 parts per billion. When the wind speed was between 2 and 6 meters per second, 20 parts per billion ambient concentration was estimated on the South East, North West and South West of the Mamelodi. When the wind speed was between 2 and 8 meters per second results showed ambient concentration of under 10 parts per billion on the North to East of Mamelodi.

In Figure 4.103 results displayed high probability of ozone ambient concentration around the ambient station except North East, East and South East. When the wind speed was at one meter per second there was less than 20 parts per billion. When wind speed picked to 5

meters per second higher probability ozone at North West and South East, West and North at ambient concentrations of 40 parts per billion.

In Figure 4.103, results displayed high likelihood of significant sources of PM_{10} of 550 ambient concentration on the North of North West, West and North-West of North West areas for wind speed higher than 6 meters per second. When the wind speed was much less than 4 meters per second, local sources of fewer than 200 $\mu g/m^3$ of PM_{10} were detected on the North West, North of Northern areas and North-West of Mamelodi. On the South West of the ambient monitoring station. Sources were detected with the ambient concentration of 150 $\mu g/m^3$ of PM_{10} when the wind speed exceeded 6 meters per second. Most of sources detected at the Mamelodi exceeded the national ambient air quality standards of 75 $\mu g/m^3$ PM_{10} with exceedance of up to 4 times in one day.

Meyerton ambient monitoring station is within the Sedibeng District Municipality and was created to monitor pollutants from industrial burning activities. In Figure 4.104, bivariate polar plot results of ozone ambient concentration which were around the Meyerton except on the Eastern side of the station where the value was at less than 30 parts per billion. When the wind speed picked at two meters per second, higher chances of ambient concentration was recorded on Southern areas and the North parts of the station. When the wind speed reaches 10 meters per second on the North East, North and South East indicated more than 70 parts per billion of the ambient concentrations.

The bivariate polar plot results of PM_{10} at the Meyerton showed sources close and far to the station. In Figure 4.104, when wind speed picked at seven meters per second there were sources predicted at Eastern areas and North West respectively of the station with the ambient concentrations of 50 µg/m3.

The bivariate polar plot of sulfur dioxide results at the Meyerton displayed various sources far and close from the ambient station in Figure 4.104. When the wind speed picked at two meters per second there were sources detected on the South West of the ambient station with concentration of up to 8 parts per billion.

In Figure 4.106, Mogale City Ambient monitoring station is situated at Krugersdorp within the West Rand District Municipality and was designed to monitor background activities. The bivariate polar plot results of PM_{10} indicated both major local and far sources with the ambient concentration of 150 µg/m3. When the wind speed was less than two meters per

second, major local sources were recorded on the North and North-West of the ambient monitoring station. When the wind speed reached 4 to 6 meters per second, ozone sources were recorded on the South West of 150 µg/m3.

The bivariate polar plot of ozone concentrations at the Mogale City predicted higher ozone concentrations of maximum of 54 parts per billion. In Figure 4.106, when wind speed was less than two meters per second there was a low probability of ozone ambient concentration around the ambient monitoring station. When wind speed exceeded two to 4 meters per second, there was a high probability of ozone formation around the ambient station.

The bivariate polar plot of sulfur dioxide at the Mogale displayed various sources far and close from the ambient station. The results in Figure 4.107 showed local and far sources around the ambient station. When the wind speed was less than two meters per second there was a local source on the North, North West, East and south areas. When the wind speed picked at two meters per second there was a source detected on the North-West and South-East of the ambient station with the ambient concentration of up to 12 parts per billion.

The bivariate polar plot of PM_{10} at the Newtown ambient monitoring station showed sources locally and far to the station. In Figure 4.108, when the wind speed was less than one meter per second, results indicated local sources which spread out when wind speed increases on the Western, North West and South West areas with the ambient concentrations of 45 $\mu g/m^3$.

The bivariate polar plot in Figure 4.109 displayed ozone concentrations at the Newtown with high sources of ozone concentrations around the station except North-West direction. When the wind speed exceeded 0.5 to 3 meters per second there was a high probability of ozone ambient concentrations. The plot of ozone pollutants showed higher ambient concentration of 27 parts per billion.

In Figure 4.110, at the Newtown station there were similarities relationship between PM_{10} and nitrogen dioxide of the main sources' location. A plot showed that when wind speed picked from calm to 6 meters per second along South West and North East with ambient concentrations of 32 µg/m3.

The bivariate polar plot of nitrogen dioxide at the Olievenhoutbosch Clinic displayed probability of major local source and minor far source. In Figure 4.111 when wind speed was less than two meters per second, more major sources were detected next to the ambient station with concentrations of 27 parts per billion. When the wind speed exceeded two to 10 meters

per second there were minor pollution sources on the South-East and South of the ambient concentration of fifteen parts per billion.

The bivariate polar plot of O_3 at the Olievenhoutbosch Clinic indicated local and far sources in Figure 4.111. When wind speed was much less than two meters per second there was less probability of O_3 close to the station of ambient concentration of under 60 parts per billion. When the wind speed exceeded 8 meters per second on the North West, highest probability was observed of 300 parts per billion which exceeded national ambient air quality standards of ozone of 61 parts per billion during an average period of 8 hours.

The bivariate polar plot of PM_{10} at the Olievenhoutbosch Clinic indicated local and far sources in Figure 4.112. When wind speed was much less than two meters per second there was a higher probability of PM_{10} close to the station of up to 208 µg/m3. When the wind speed was between 2 and 6 meters per second there was no source detected around the ambient station.

The bivariate polar plot of sulfur dioxide at the Olievenhoutbosch Clinic showed major sources on the South East of the ambient station (Figure 4.112). When the wind speed exceeded two to 10 meters per second major sources were shown on the South East with predicted sulfur dioxide ambient concentrations of up to 8een parts per billion. Other directions except South East revealed minor sources of 7 parts per billion.

In Figure 4.113, results displayed Orange Farm ambient monitoring station which is situated within the City of Johannesburg and was designed to monitor pollutants from domestic fuel burning activities. The bivariate polar plot of sulfur dioxide displayed different sulfur dioxide local and far sources from the ambient station. When the wind speed picked to 5 meters per second two areas were visible which were on the Eastern side of the station with the ambient concentrations of 7.5 parts per billion.

In Figure 4.113 bivariate polar plot of PM_{10} at the Orange Farm displayed far sources from the Orange Farm ambient station. When the wind speed picked from 0 to 10 meters per second there was no PM_{10} sources detected around the ambient station.

In Figure 4.114, Pretoria West ambient monitoring station is situated at the Pretoria West in the City of Tshwane and was designed to monitor pollutants from industrial domestic activities. The bivariate polar plot of nitrogen dioxide for Pretoria West displayed South major

local sources when the wind speed was less than two meters per second with ambient concentrations of 45 parts per billion.

The bivariate polar plot of ozone concentrations at the Pretoria West predicted higher ozone concentrations on the North East, North, North West, South West and West of the ambient station. In Figure 4.115 wind speed picked to 2 meters per second there was high ozone ambient concentration on the North West, South West and West of the ambient station with the ambient concentrations of 55 parts per billion.

The bivariate polar Plot of PM_{10} at the Pretoria West displayed different pollution sources around the ambient monitoring station in Figure 4.115. When the wind speed was less than 10 meters per second there was higher chances of PM_{10} sources on the Southern regions of the ambient station with ambient concentrations of 110 $\mu g/m^3$.

In Figure 4.116, bivariate polar plot of sulfur dioxide at the Pretoria West ambient monitoring station displayed local and far sulfur dioxide sources. When the wind speed was less than 2 meters per second there was a high probability of sulfur dioxide local source on the Southern side of the ambient monitoring station with the ambient concentrations of fifteen parts per billion.

Randfontein ambient monitoring station is situated at the Randfontein in the West Rand District Municipality and was designed to monitor pollutants for background info. In Figure 4.117, the bivariate polar plot of nitrogen dioxide at the Randfontein showed local and far sources. When the wind speed was less than 5 meters per second there were sources on the Eastern side as well as on the North East of the ambient station with the ambient concentration of up to 14 parts per billion.

The bivariate polar plot of PM_{10} at the Randfontein display far sources on the North, South-West and West areas of the ambient monitoring station. In Figure 4.117, when wind speed picked to 10 meters per second there were no sources detected around the ambient monitoring station. When wind speed was between 10 and 15 meters per second there was a major PM_{10} sources detected on the Northern Region of the ambient monitoring station with the ambient concentration of 350 $\mu g/m^3$.

Rosslyn ambient monitoring station is situated within the City of Tshwane and was designed to monitor pollutants from industrial domestic activities. The bivariate polar plot of nitrogen dioxide at the Rosslyn displayed local and far sources from the ambient monitoring

station. When wind speed was between 2 to 4 meters per second there was a local source next to ambient monitoring station with the ambient concentrations of 27 parts per billion. In Figure 4.118 when wind speed was between 4 and 6 meters per second there was nitrogen dioxide sources on the South East of the ambient monitoring station with the ambient concentration of 16 parts per billion.

The bivariate polar plot of ozone pollutants at the Rosslyn displayed major sources of ozone ambient concentrations predominated on the North East, North, North West, South West and West. In Figure 4.119, when the wind speed was between 4 and 8 meters per second there were ozone sources detected. When the wind speed was between seven and eleven meters per second the ambient ozone concentrations was 70 parts per billion.

Figure 4.120 showed the bivariate polar plot of sulfur dioxide for ambient concentrations at the Rosslyn station. When the wind speed was actually between 4 and 6 meters per second, the ambient concentration was fifteen parts per billion. When wind speed was between 10 and 12 meters per second, the ambient concentrations of 15 parts per billion.

In Figure 4.121, the bivariate polar plot of PM_{10} at the Rosslyn station displayed far major source on the North West area of the ambient monitoring station with the ambient concentration of 240 µg/m3.

Springs ambient monitoring station is actually situated within the City of Ekurhuleni and was designed to monitor pollutants from domestic fuel burning activities. The bivariate polar plot of nitrogen dioxide ambient concentration in Figure 4.122 at the Springs station displayed display different sources around Springs ambient monitoring station. When the wind speed was under 5 meters per second the plot showed local nitrogen sources next to the station and towards South West with the ambient concentrations of 18 parts per billion. When the wind speed was actually between 5 and 10 meters per second there were actually several nitrogen dioxide sources on the North West of the ambient station with the estimated ambient concentrations of 20 parts per billion.

The bivariate polar plot of ozone ambient concentrations at the Springs station showed high probability of ozone pollutants on North-East, East, South-East, South, and the South-West of the station. In Figure 4.123, when the wind speed was actually between 2 and 8 meters per second there was a higher probability of ozone concentration on North-East, East, South-East, South, and South-West of the ambient monitoring station with the concentrations of 35

parts per billion. When the wind speed was between 8 and 12 meters per second there was a high probability on the South West of the station with the ambient concentrations of 34 parts per billion.

Figure 4.124 showed bivariate polar plot of sulfur dioxide at the Springs indicating high major sources on the North West, North, North East, East and South East of the ambient station. There were also minor sulfur dioxide sources on the South East, South, North West and South West of the ambient station. Sources ambient concentration of 14 parts per billion were actually situated on the North West, North, North East and East when wind speed was actually between 2 and 8 meters per second.

Tembisa ambient monitoring station is actually situated at the Tembisa in the City of Ekurhuleni and was designed to monitor pollutants from domestic fuel burning activities. Figure 4.125 results displayed local and far sources. When the wind speed was under two meters per second there was a higher probability of nitrogen dioxide sources at local location. When wind speed exceeded two but less than 4 meters per second there was a higher probability of nitrogen dioxide sources on the South West, South and South East of the ambient station with the ambient concentrations of 20 parts per billion.

The bivariate polar plot of PM_{10} showed that there were major and minor sources around Tembisa ambient station. In Figure 4.125, when the wind speed was under two meters per second there was high PM_{10} at the nearby areas with ambient concentrations of 200 $\mu g/m^3$. When wind speed picked at 6 to 10 meters per second there was PM_{10} ambient concentrations 250 $\mu g/m^3$. On the Western and eastern regions of the ambient station there was a source of PM_{10} with the ambient concentration of 220 $\mu g/m^3$. There was also higher PM_{10} probability on the South and South-West of the ambient station.

In Figure 4.126, the bivariate polar plot of sulfur dioxide at the Tembisa ambient monitoring station displayed both local and far sources.

In Figure 4.127, the Thokoza ambient monitoring station is actually situated in the City of Ekurhuleni and was actually designed to monitor pollutants from domestic fuel burning activities. The bivariate polar plot of nitrogen dioxide displayed strong probability when the wing speed was under 4 meters per second with the ambient concentrations of 50 parts per billion. Figure 4.28 results displayed ambient pollutants on the entire areas on the plot except

at the North East when the wind speed was at 2 to 5.2 meters per second with the ambient PM_{10} concentrations of 20 $\mu g/m^3$.

The bivariate polar plot for sulfur dioxide at the Thokoza ambient monitoring station showed 3 major areas with higher ambient concentrations. In Figure 4.128, wind speed in the ranges 2 to 4 meters per second showed high probability of sulfur dioxide ambient concentrations of 10 parts per billion. The ambient concentrations of 20 parts per billion. When the wind speed is between 6 and 10 meters per second resulted on the ambient concentration of 20 parts per billion.

Tsakane ambient monitoring station is situated within the City of Ekurhuleni and was designed to monitor pollutants from domestic fuel burning activities. In Figure 4.129, the wind speed was less than 2 meters per second and there was higher concentrated ambient air quality of 18 parts per billion on the Northern areas of the station. When the wind speed was between two and 4 meters per second the ambient concentrations of 11 parts per billion at the North-West, North, North-East, East and South-East. When the wind speed was between 4 and 10 meters per second there was visible nitrogen dioxide sources on the East, South-East, South-West and North-West of the Tsakane ambient station with probability of ambient concentration of 10 parts per billion.

In Figure 4.130 the bivariate polar plot of PM_{10} at the Tsakane ambient monitoring station displayed local and far sources around the station. When the wind speed was less than 4 meters per second there was a high probability of local sources on the North-West of the station with the ambient concentration of 85 $\mu g/m^3$ of PM_{10}.

In Figure 4.131, the bivariate polar plot of O_3 at the Tsakane ambient monitoring station displayed local and far sources around the station. When the wind speed was less than 2 meters per second there was a high probability of local sources on the North-West of the station with the ambient concentration of 35 parts per billion of O_3.

The bivariate polar plot of sulfur dioxide concentrations at the Tsakane ambient monitoring station displayed local and far sources. In Figure 4.131 when the wind speed was less than two meters per second there were two main hot spots displayed on the North-West and Eastern areas of the ambient station with the ambient concentrations of 8 parts per billion. When the wind speed was between two and 6 meters per second there was a higher probability of sulfur

dioxide sources on the South-West, East and South-East of the ambient station with concentration of 8 parts per billion.

In Figure 4.132, the Tshwane Market Mobile ambient monitoring station is situated at the Tshwane Market in the City of Tshwane and was designed to monitor pollutants from traffic activities. The bivariate polar plot of nitrogen dioxide at the Tshwane Market displayed local and far sources. When wind speed was less than two meters per second there was a source at the local area with the ambient concentrations of 22 parts per billion. When wind speed exceeded two to 6 meters per second nitrogen dioxide sources were visible sources on the North-East, East and South with ambient concentration of 13 parts per billion.

Figure 4.132 bivariate polar plot of PM_{10} at the Tshwane Market displayed major sources at the wind speed of 3 meters per second. When wind speed is between one and 3 meters per second there were PM_{10} sources on the North-West of the ambient station with the concentration of 3 $\mu g/m^3$ of PM_{10}.

The bivariate polar plot of sulfur dioxide ambient concentration at the Tshwane Market indicated different major sources on the Eastern area and minor sources on the Western areas of the ambient station. In Figure 4.132 for wind speed between one to 3 meters per second there were major sources on the East and South-East of ambient concentrations of 6 parts per billion.

Vanderbijlpark ambient monitoring station is situated at the Vanderbijlpark in the City of Ekurhuleni and was designed to monitor pollutants from industrial activities. Figure 4.134 results displayed PM_{10} sources that were visible at the Western Area of the ambient concentrations of 1000 $\mu g/m^3$ of PM_{10} when the wind speed was at 6 to 8 meters per second. When the wind speed was between 5 and seven meters per second results showed 3 major sources which were situated on North-West of the ambient concentrations of 600 $\mu g/m^3$ of PM_{10}.

The bivariate polar plot of sulfur dioxide at the Vanderbijlpark displayed two major areas in Figure 4.134.When the wind speed was between one and two meters per second there was a source recorded on the South-East with ambient concentration of 20 parts per billion. When the wind speed was between two and seven meters per second there was a major area on the North of the ambient concentrations of 20-25 parts per billion.

Wattville ambient monitoring station is situated within the City of Ekurhuleni and was designed to monitor pollutants from industrial activities. In Figure 4.135, the bivariate polar plot of nitrogen dioxide at the Wattville showed major sources next to ambient monitoring station

when wind speed was between one and 4 meters per second with the ambient concentrations of thirty parts per billion. There was other minor nitrogen dioxide at the Eastern area of the ambient station with high probability of ambient concentration of 15 parts per billion.

In Figure 4.136, 50% of bivariate polar plot of PM_{10} at the Wattville showed high concentrated area 110 $\mu g/m^3$ of PM_{10}. When the wind speed was between 0 and 4 meters per second there was a major PM_{10} source on the North-West with 110 $\mu g/m^3$ of PM_{10}.

4.4 Conditional Probability Function Plot (K-Means Clustering) at Gauteng Province.

The Clustering algorithm has the ability to identify a data set with identical characteristics. Clustering helps one to detect and classify related relationships within the data set. In this analysis, k-means clustering techniques have been applied to bivariate polar plots to classify and group related characteristics. Bivariate polar plots have been used to locate unknown factors impacting the atmospheric monitoring station. The study-related bivariate polar plot and k-means for further analysis of specific source features. The findings of the study are reported in Figures 4.137 to 4.193 below.

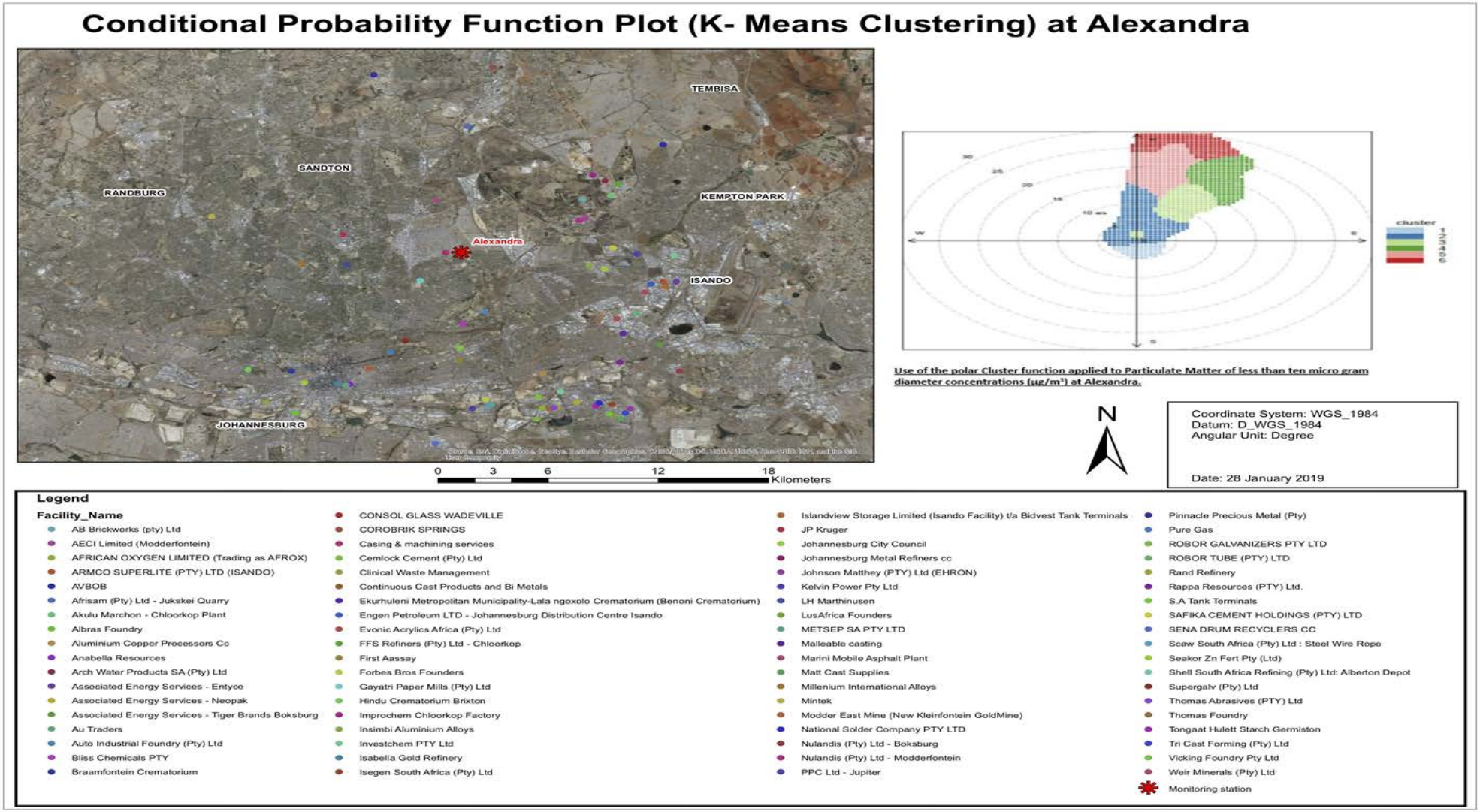

Figure 4.137: Conditional Probability Function Plot (K-Means Clustering) at the Alexandra

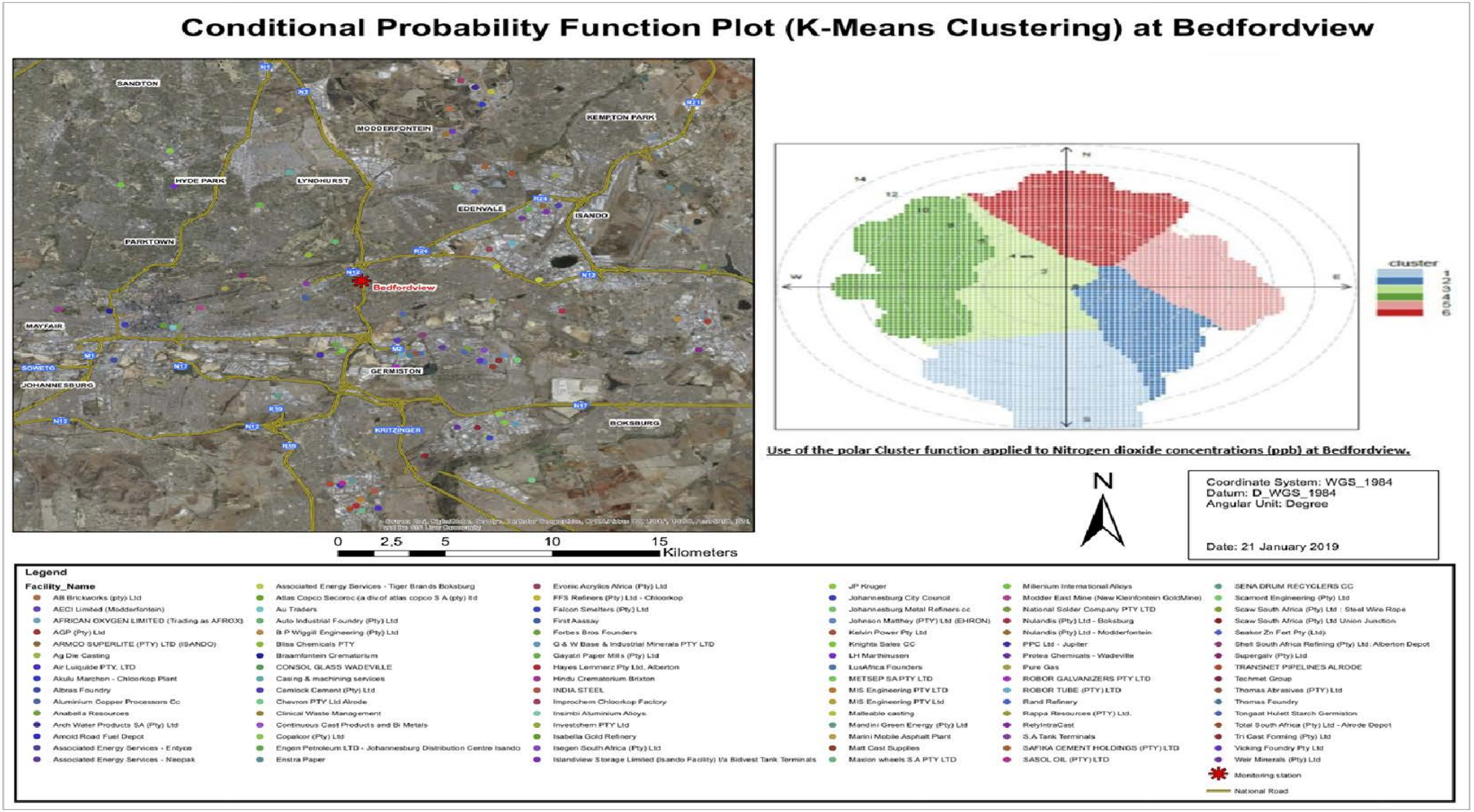

Figure 4.138: Conditional Probability Function Plot (K-Means Clustering) at the Bedfordview

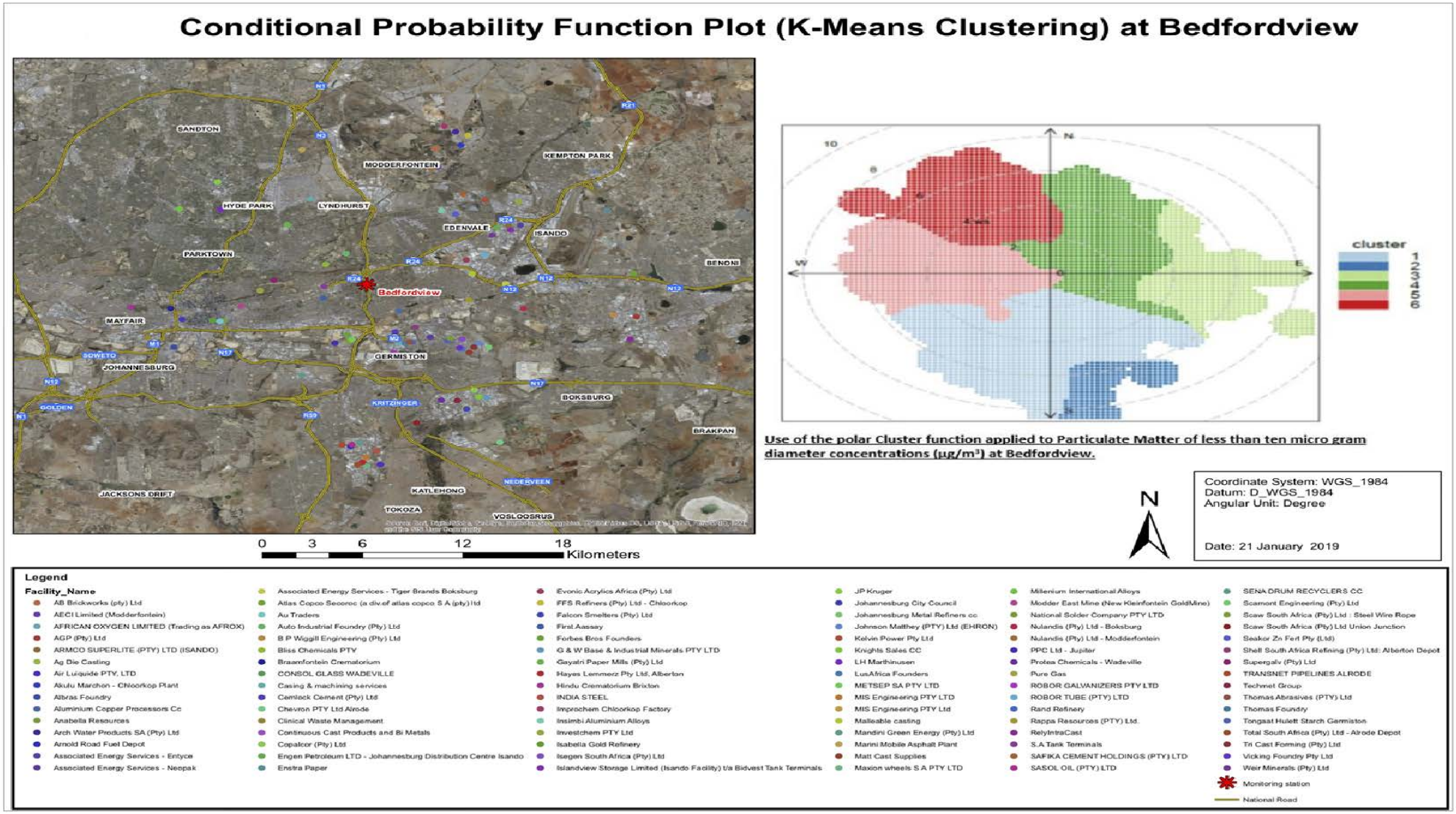

Figure 4.139: Conditional Probability Function Plot (K-Means Clustering) at the Bedfordview

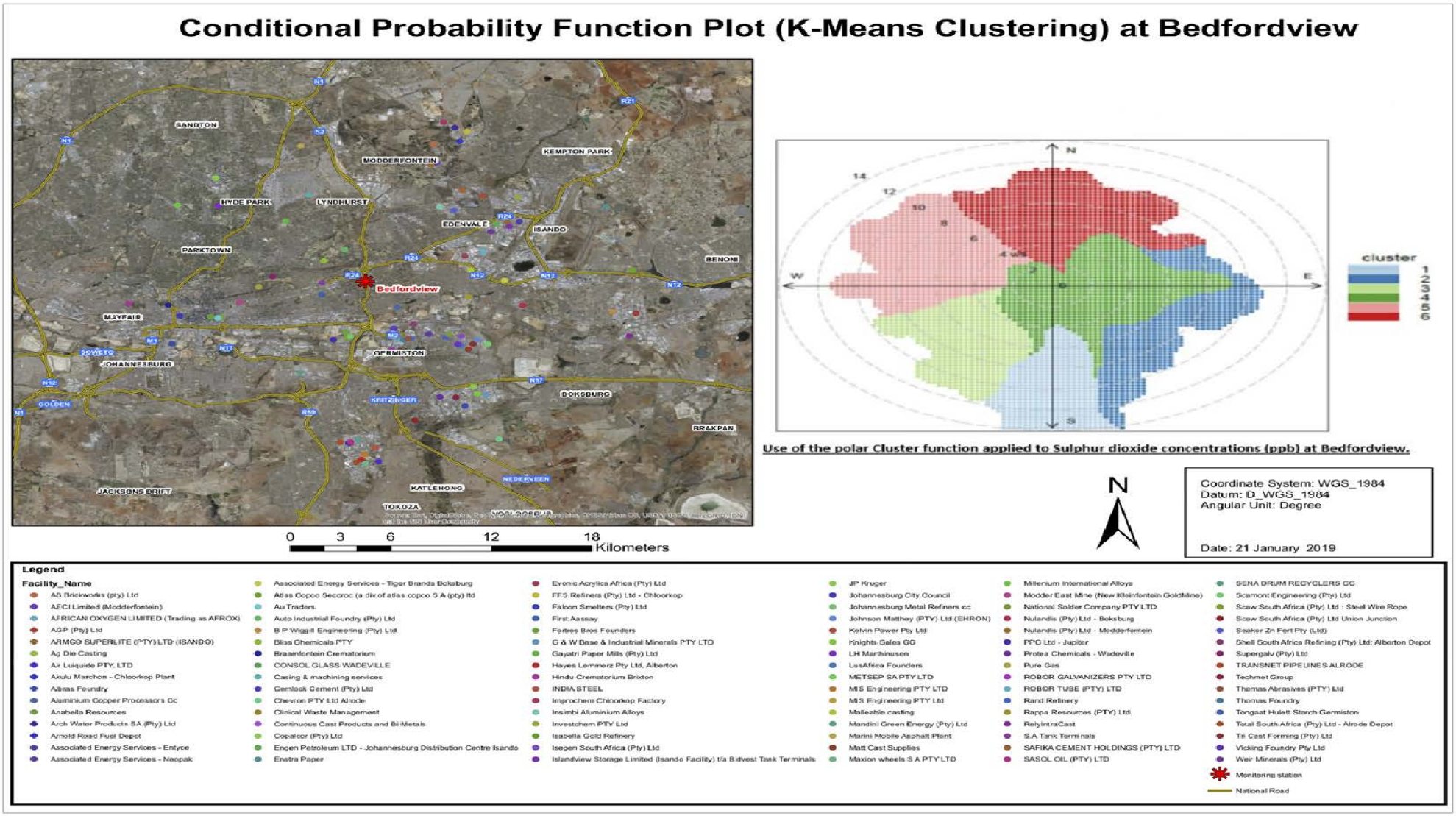

Figure 4.140: Conditional Probability Function Plot (K-Means Clustering) at the Bedfordview

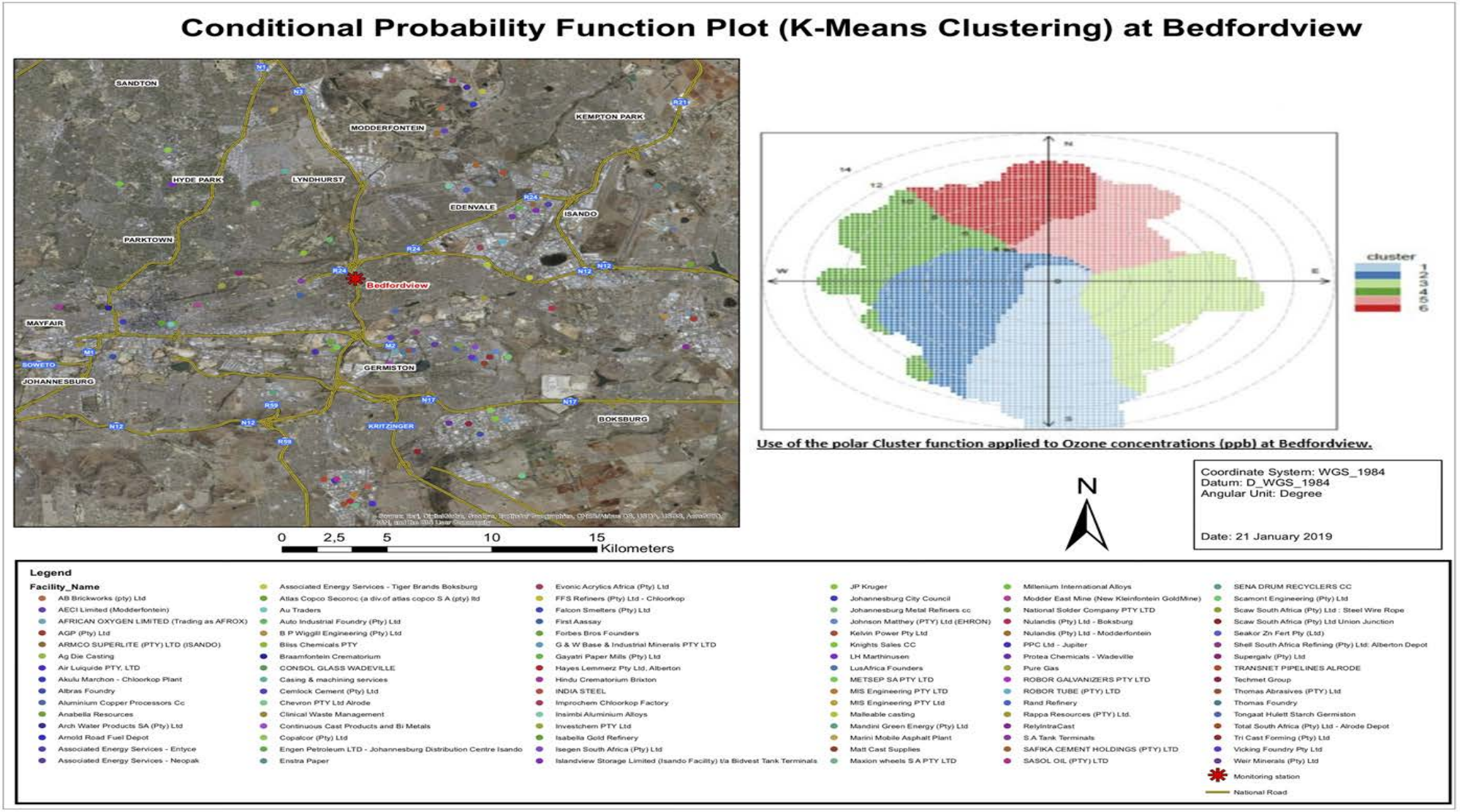

Figure 4.141: Conditional Probability Function Plot (K-Means Clustering) at the Bedfordview

Conditional Probability Function Plot (K-Means Clustering) at the Bodibeng

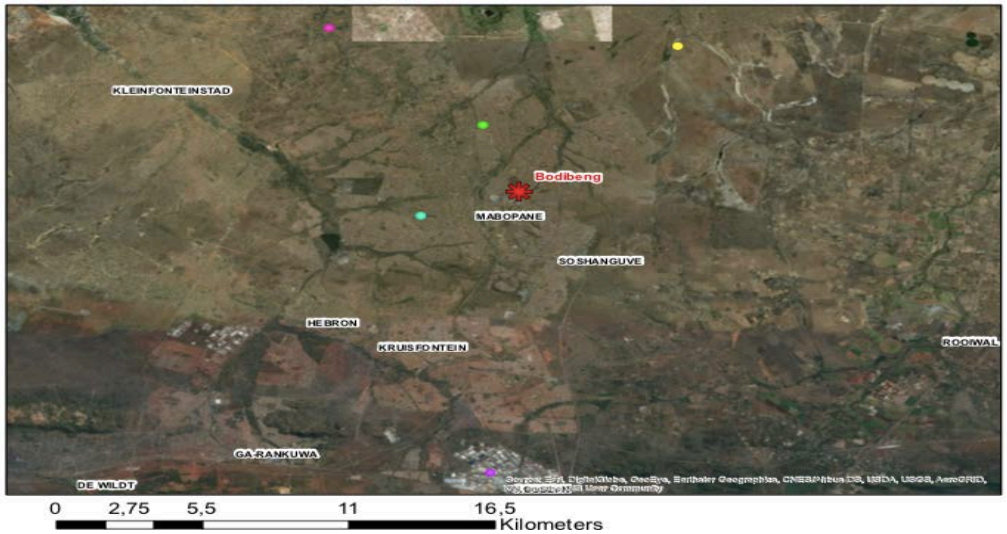

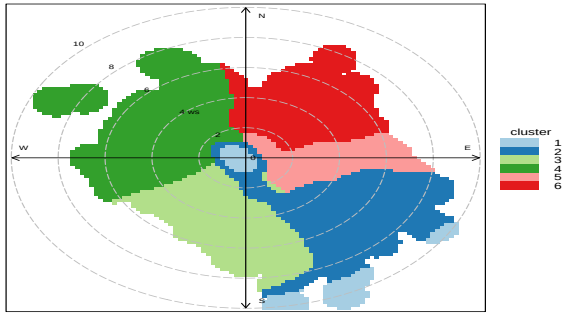

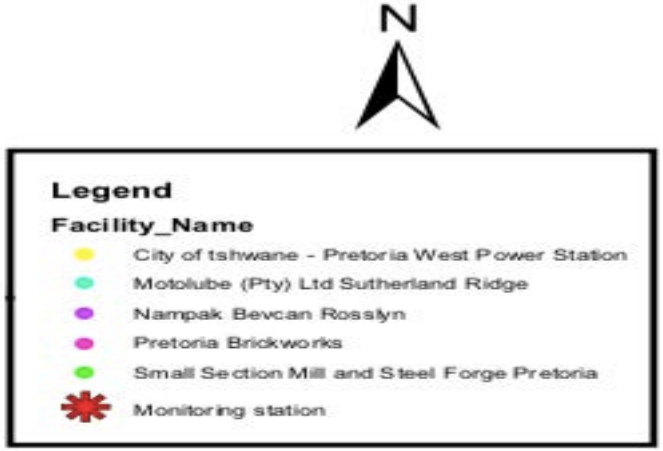

Figure 4.142: Conditional Probability Function Plot (K-Means Clustering) at the Bodibeng

Conditional Probability Function Plot (K-Means Clustering) at the Bodibeng

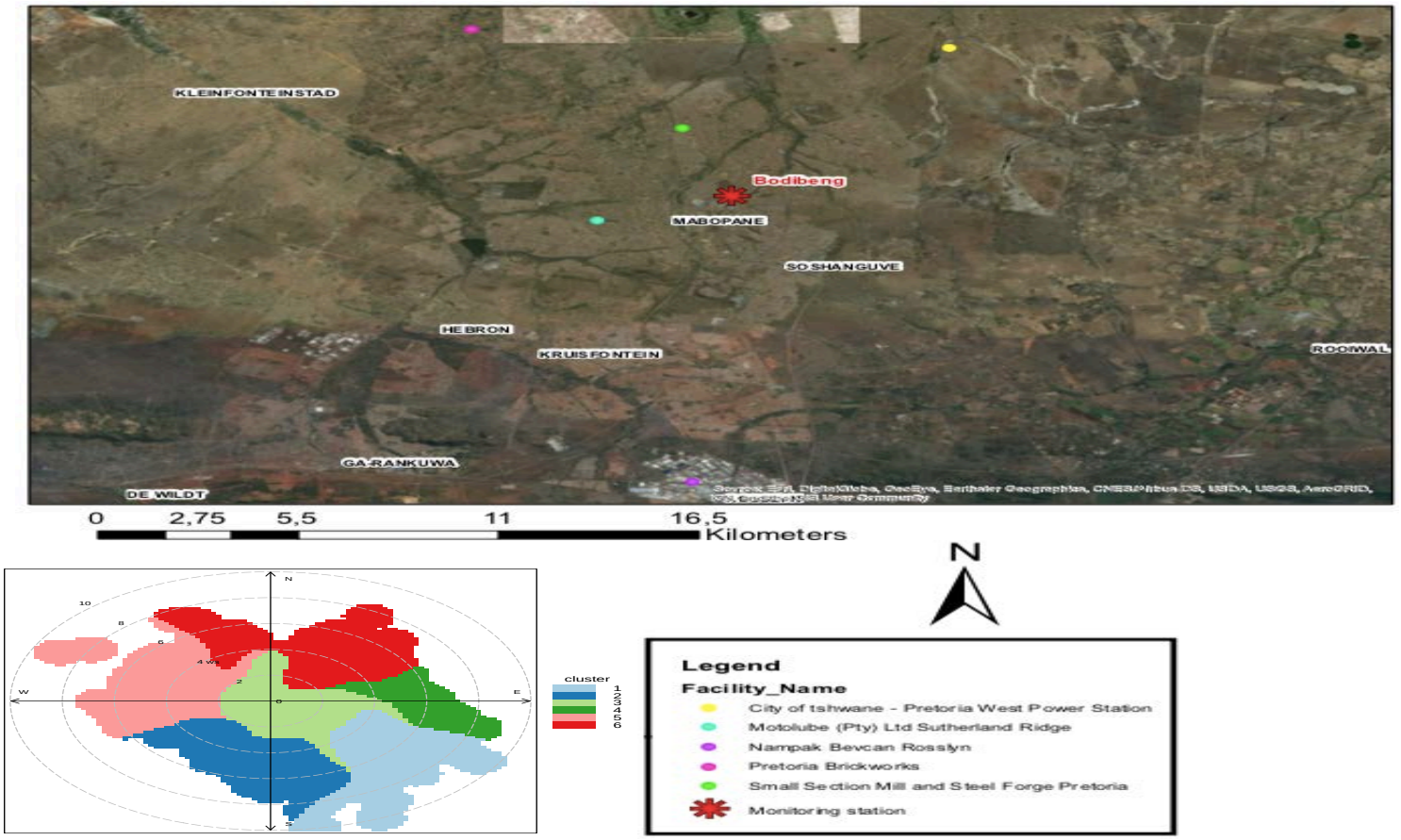

Figure 4.143: Conditional Probability Function Plot (K-Means Clustering) at the Bodibeng

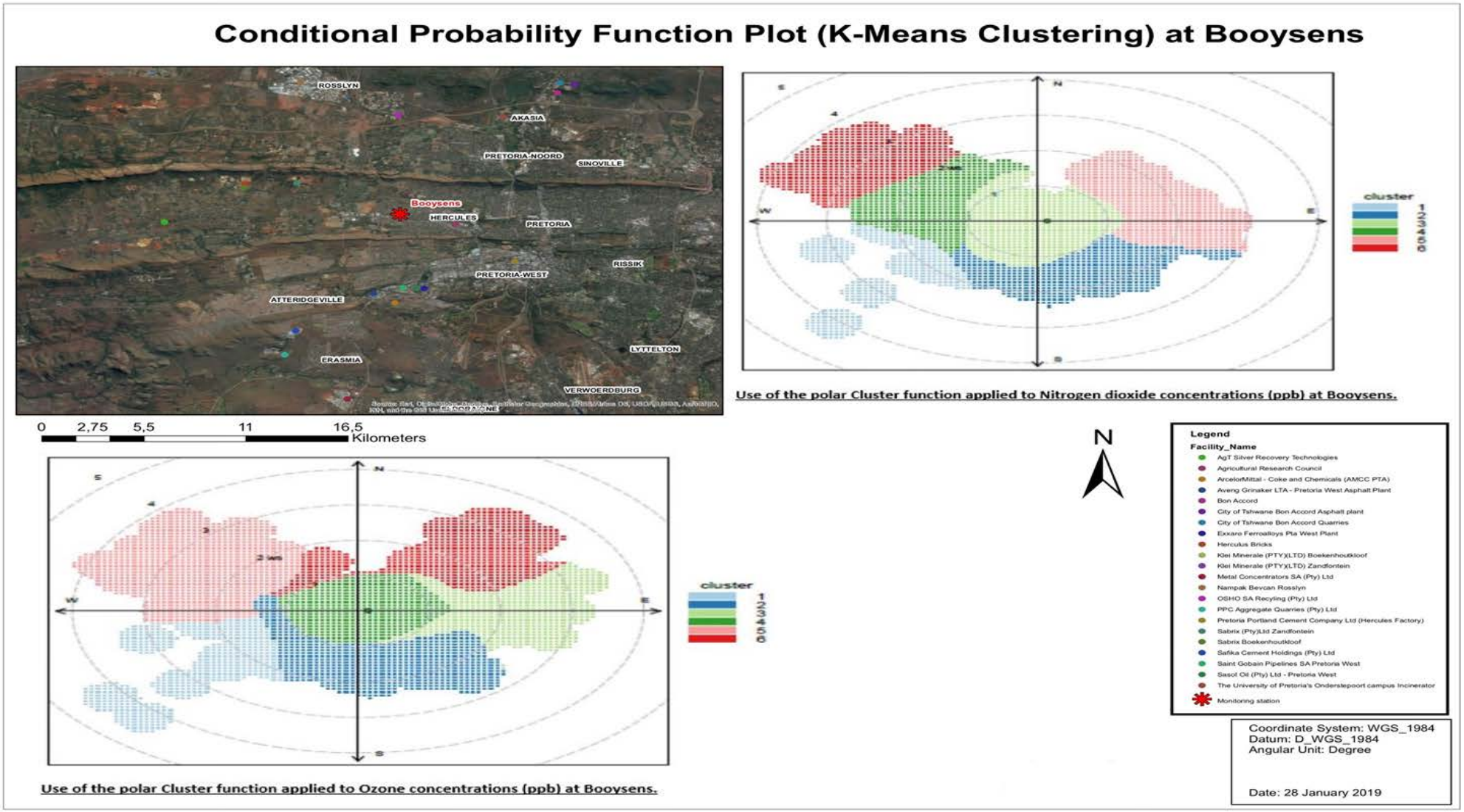

Figure 4.144: Conditional Probability Function Plot (K-Means Clustering) at the Booysens

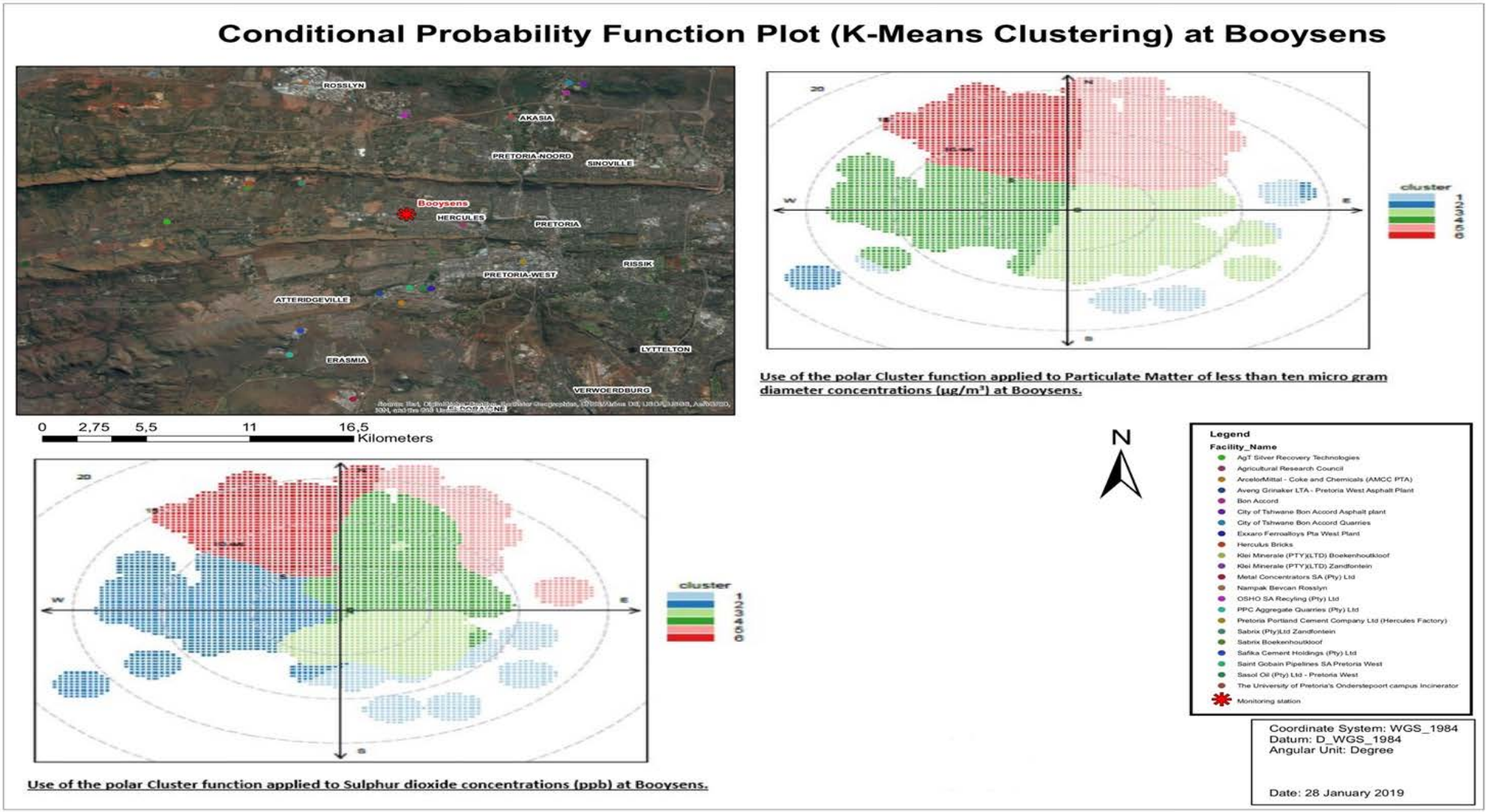

Figure 4.145: Conditional Probability Function Plot (K-Means Clustering) at the Booysens

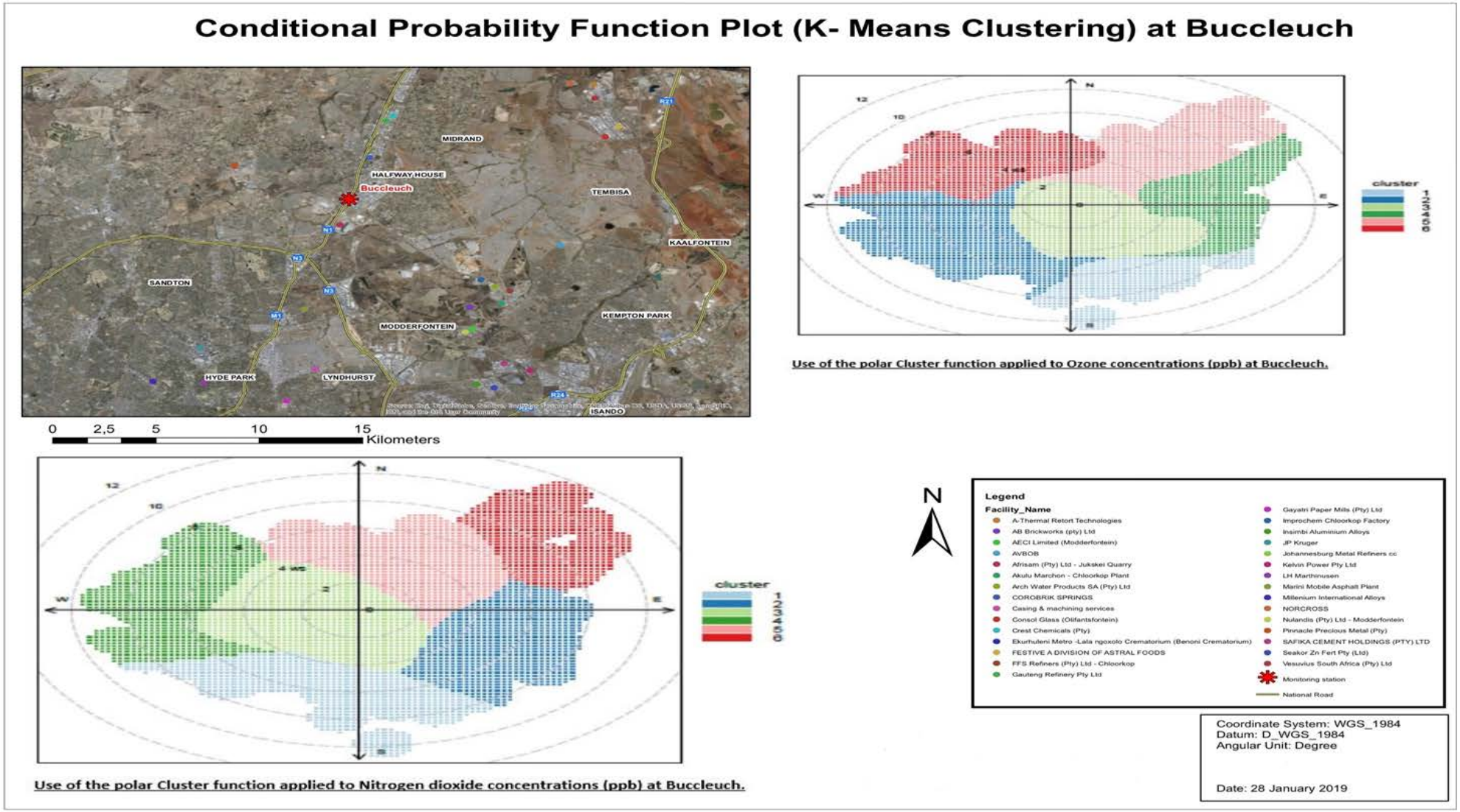

Figure 4.146: Conditional Probability Function Plot (K-Means Clustering) at the Buccleuch

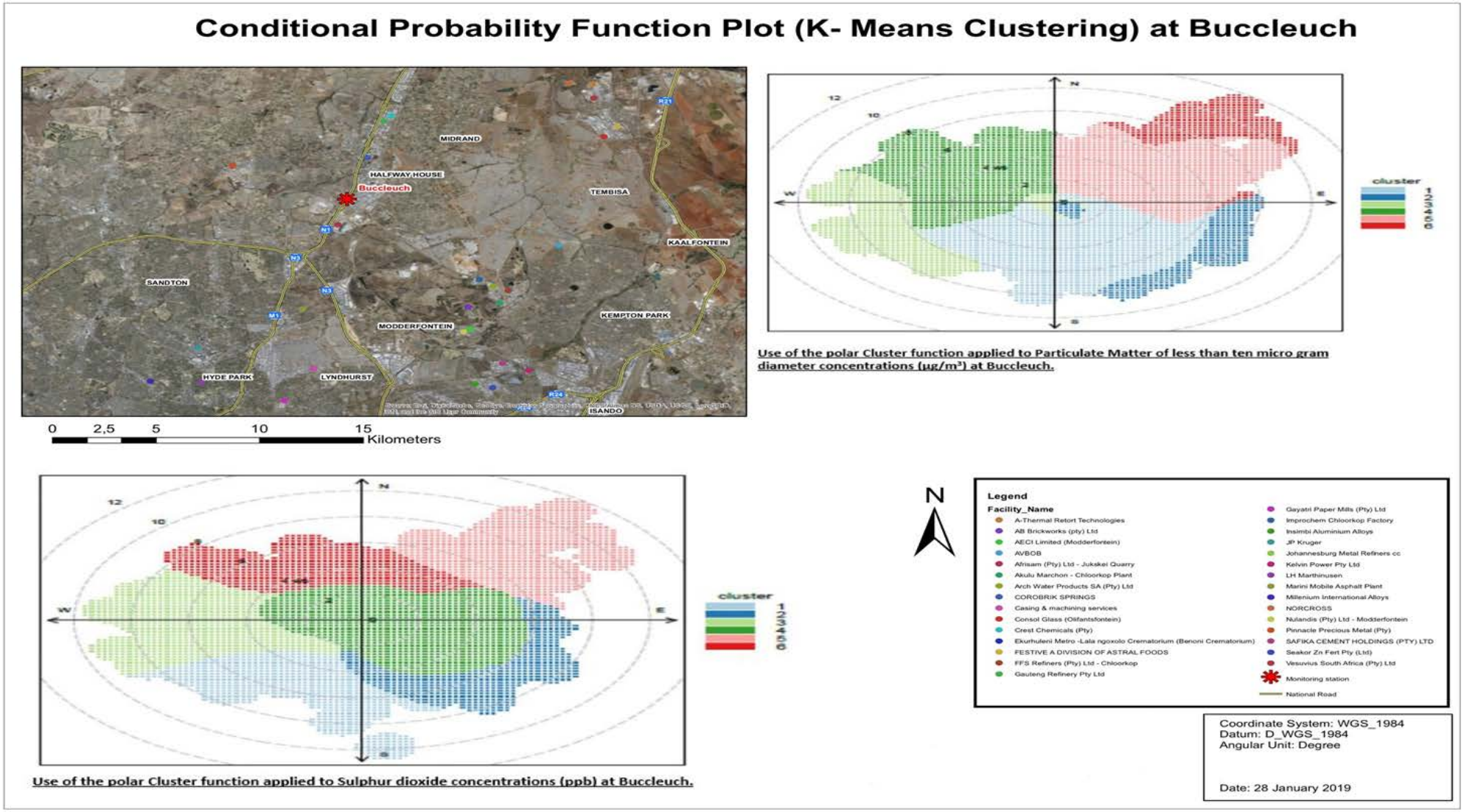

Figure 4.147: Conditional Probability Function Plot (K-Means Clustering) at the Buccleuch

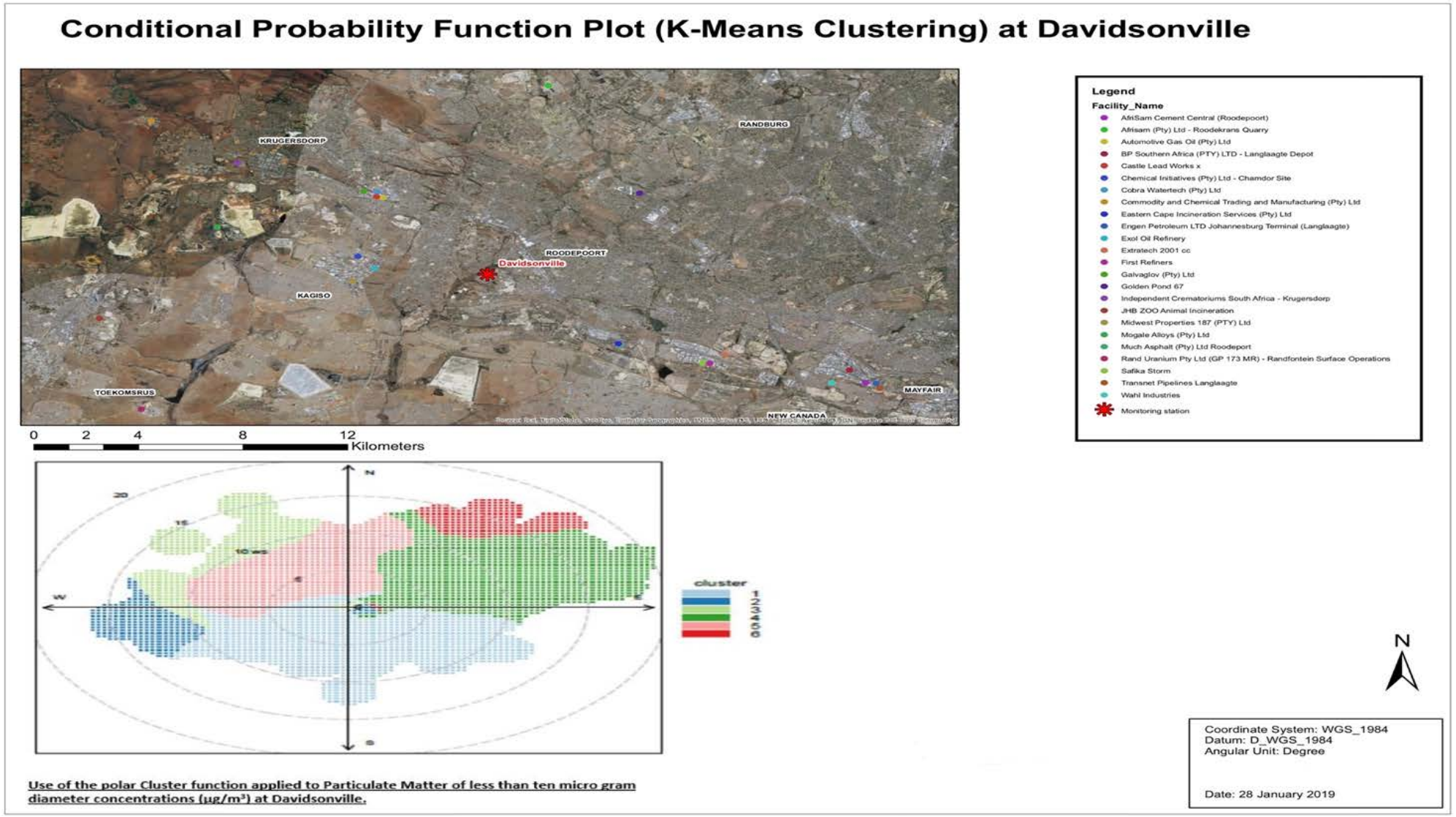

Figure 4.148: Conditional Probability Function Plot (K-Means Clustering) at the Davidsonville

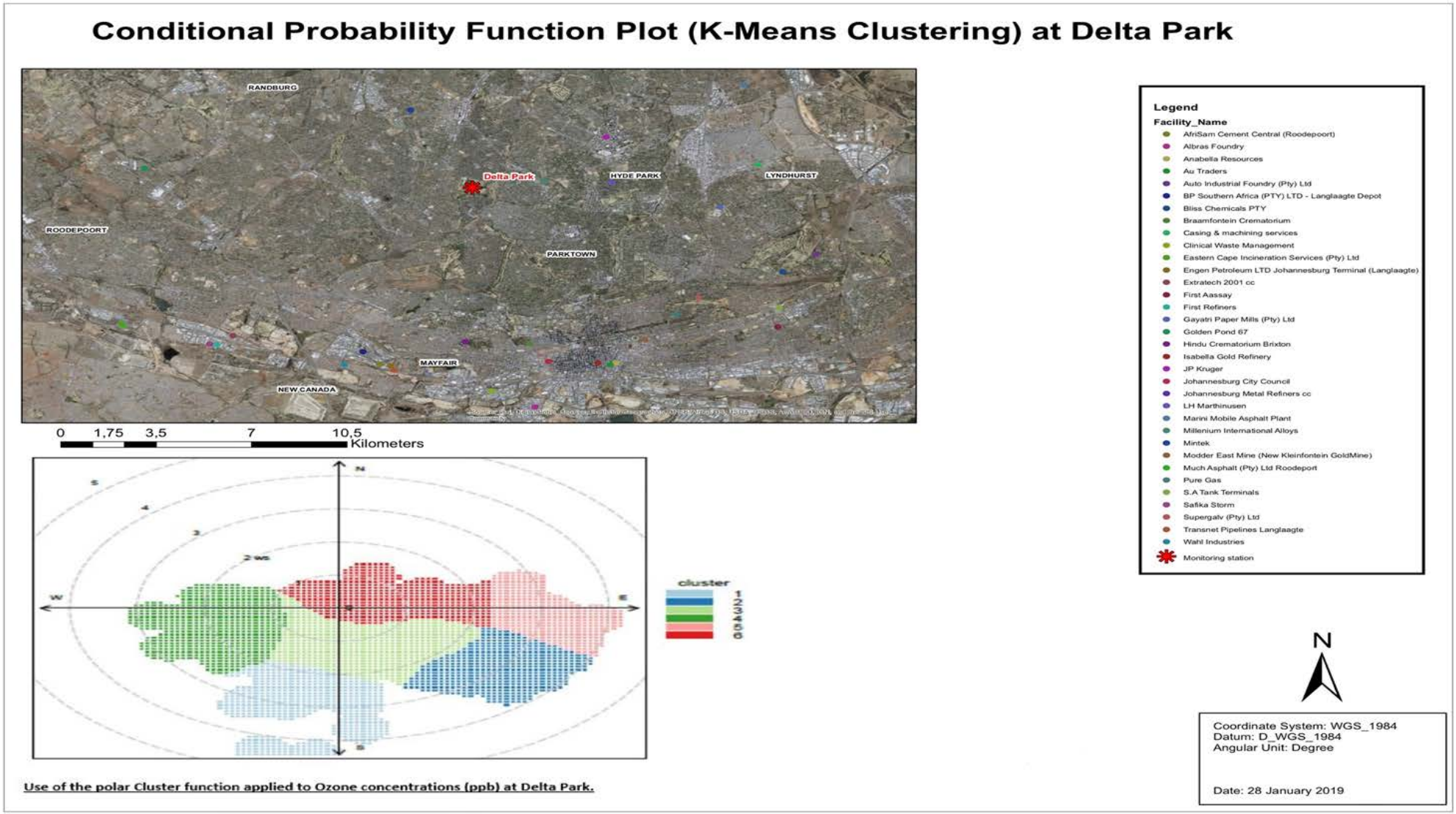

Figure 4.149: Conditional Probability Function Plot (K-Means Clustering) at the Delta Park

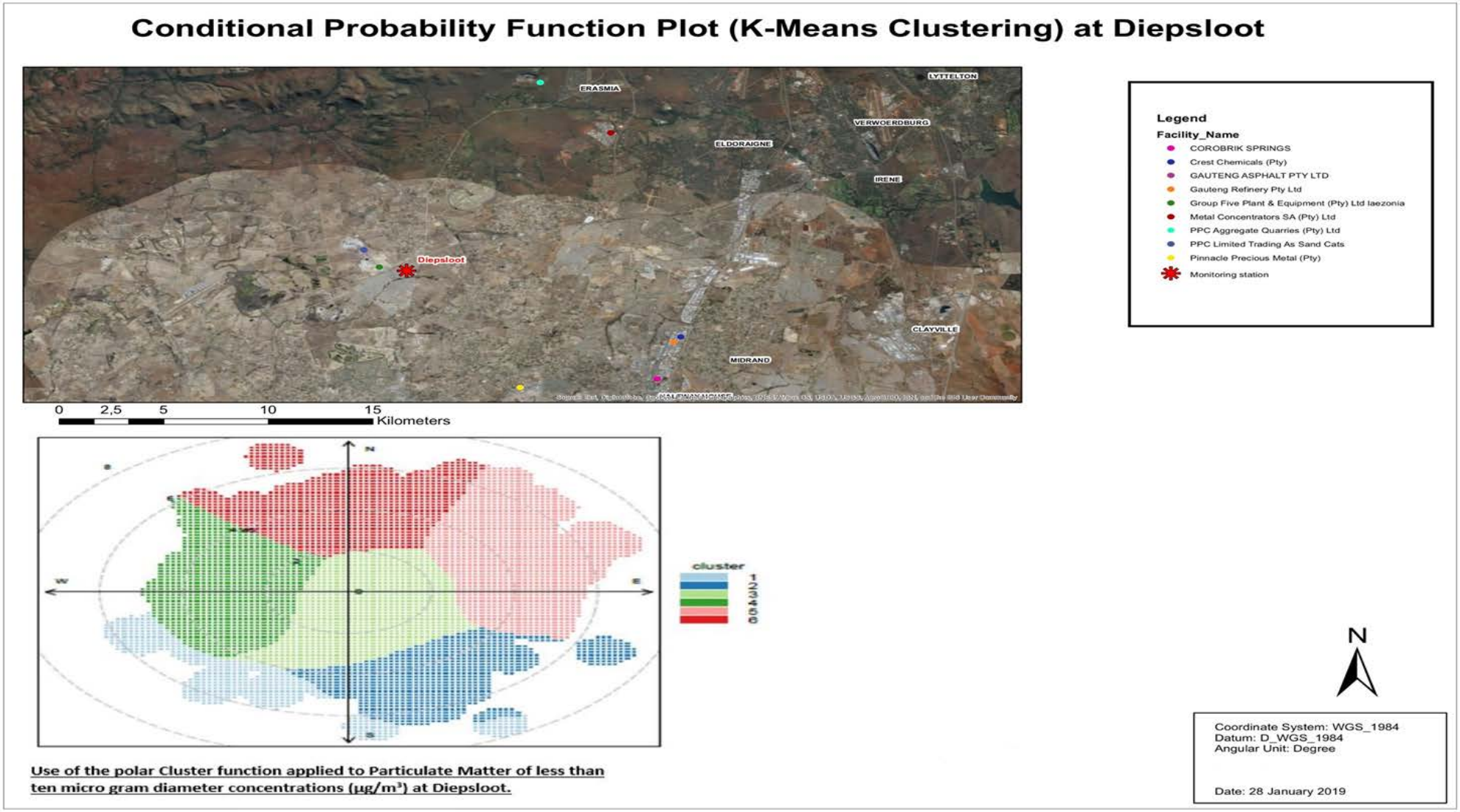

Figure 4.150: Conditional Probability Function Plot (K-Means Clustering) at the Diepsloot

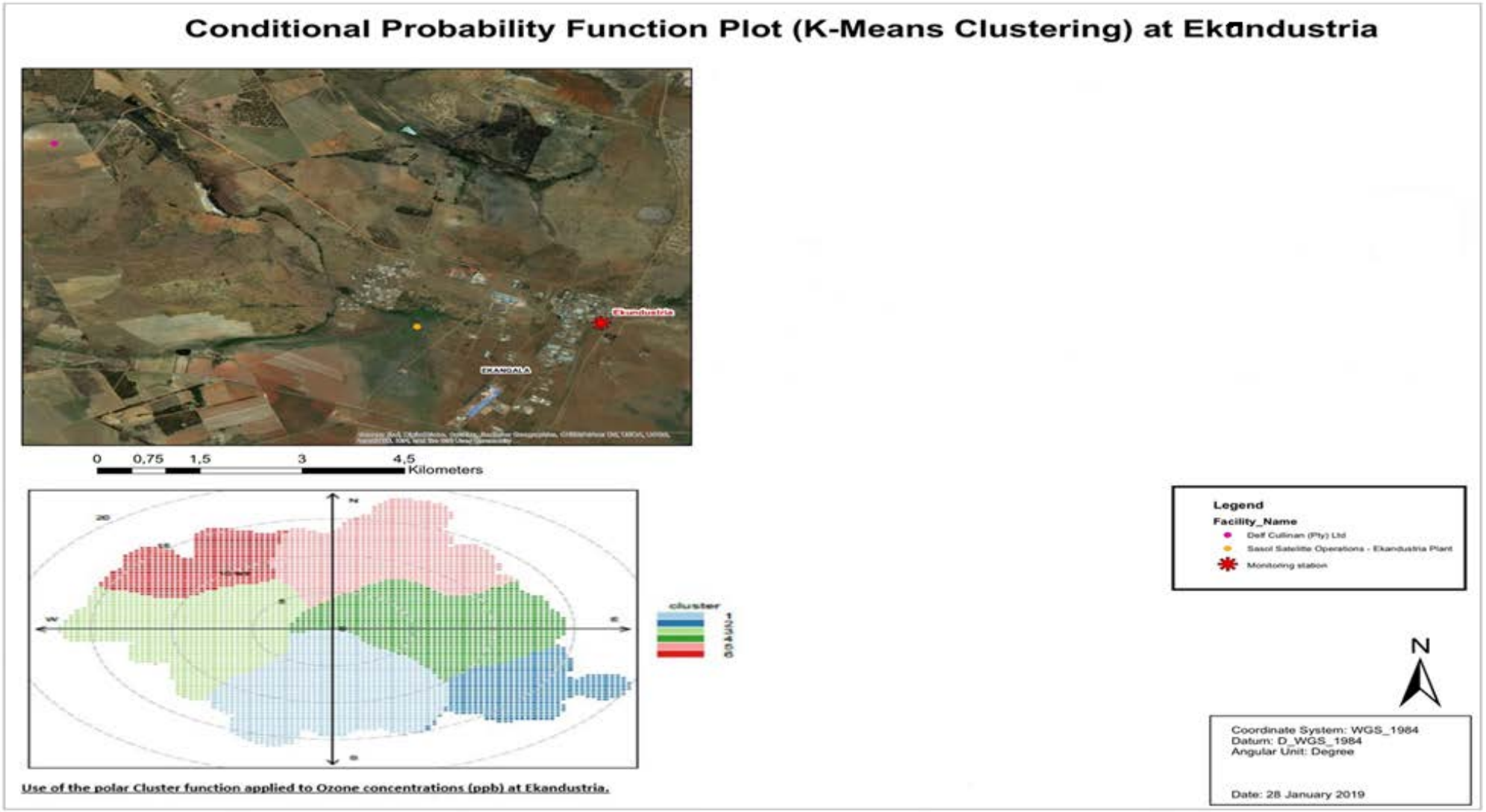

Figure 4.151: Conditional Probability Function Plot (K-Means Clustering) at the Ekandustria

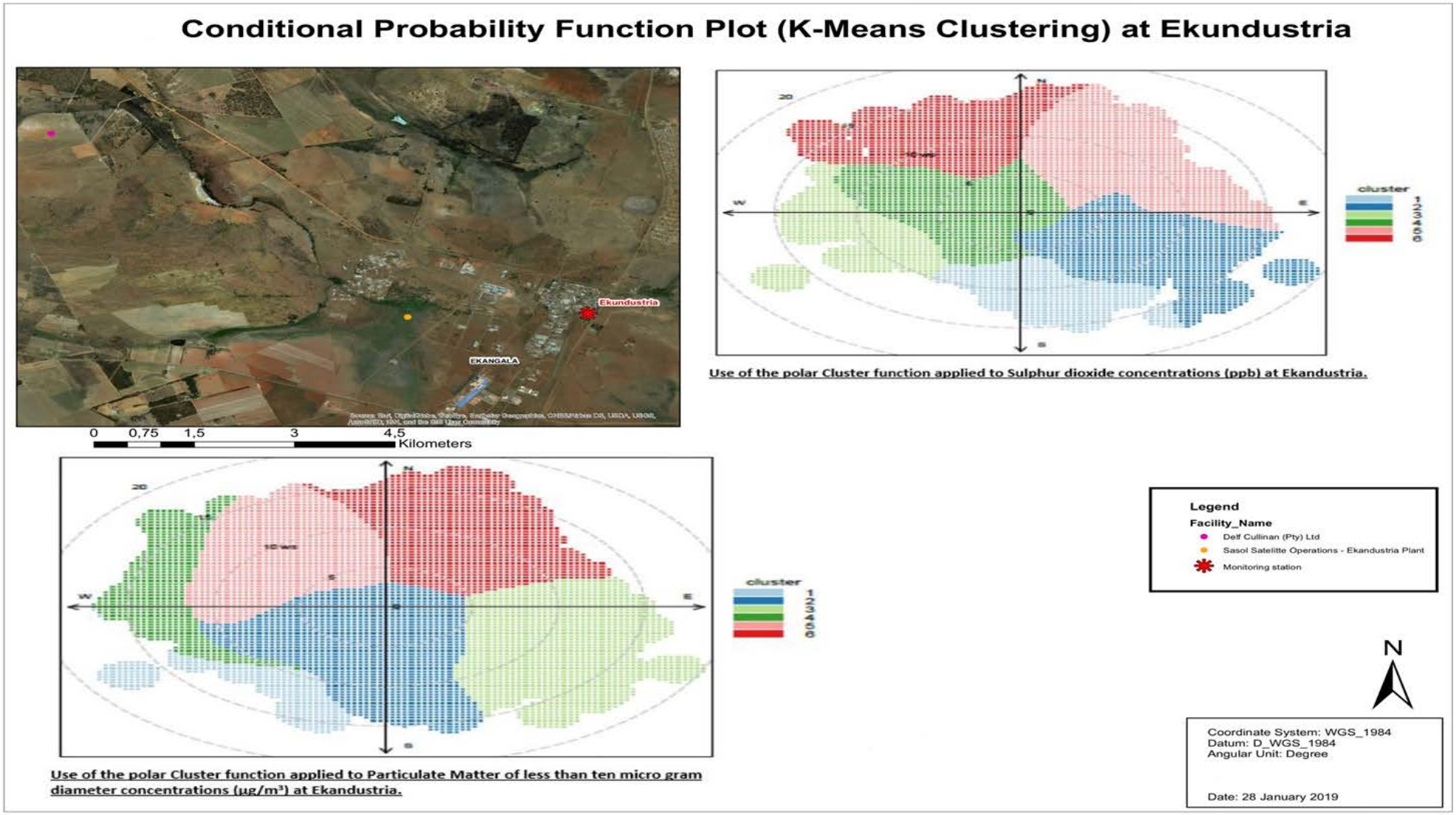

Figure 4.152: Conditional Probability Function Plot (K-Means Clustering) at the Ekandustria

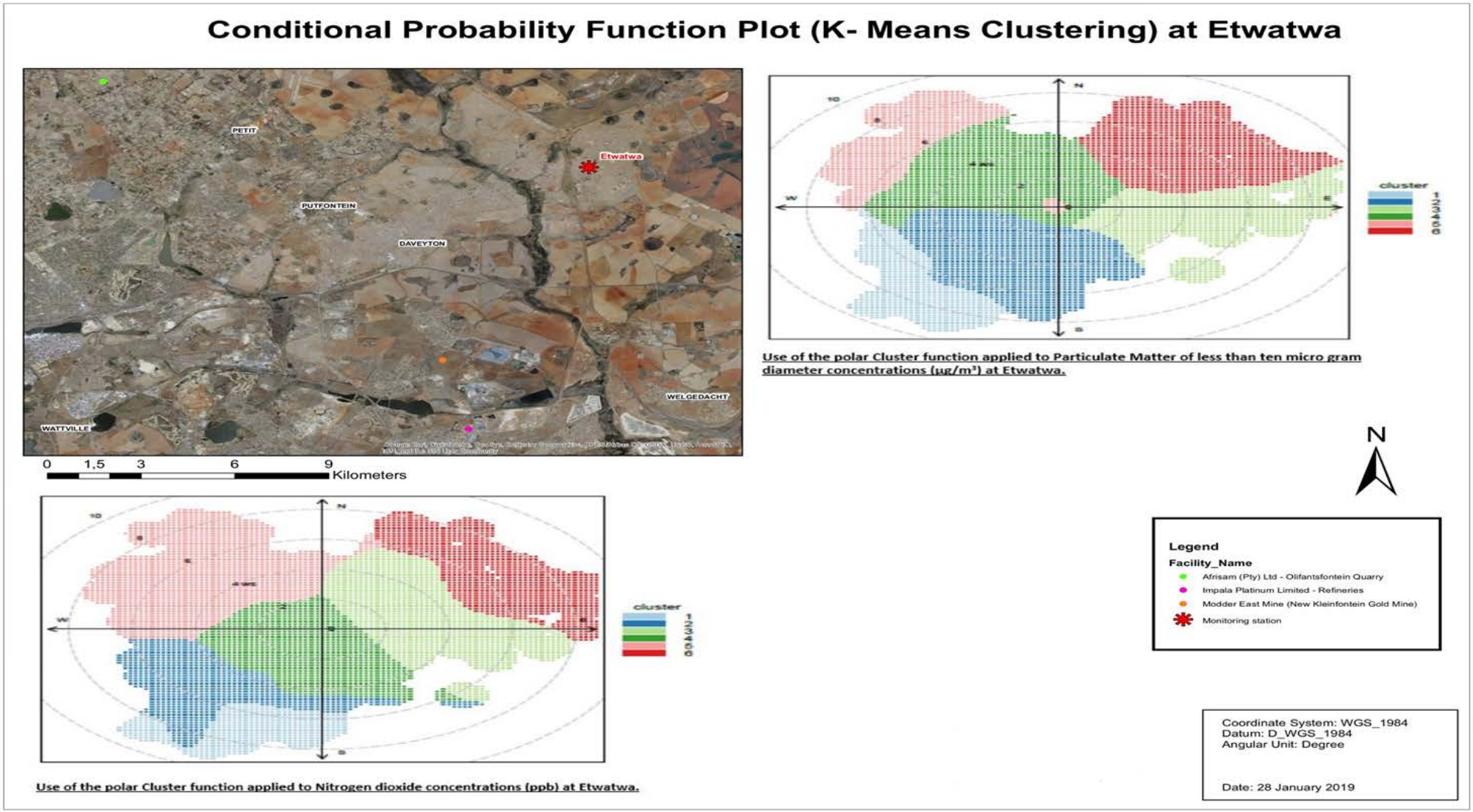

Figure 4.153: Conditional Probability Function Plot (K-Means Clustering) at the Etwatwa

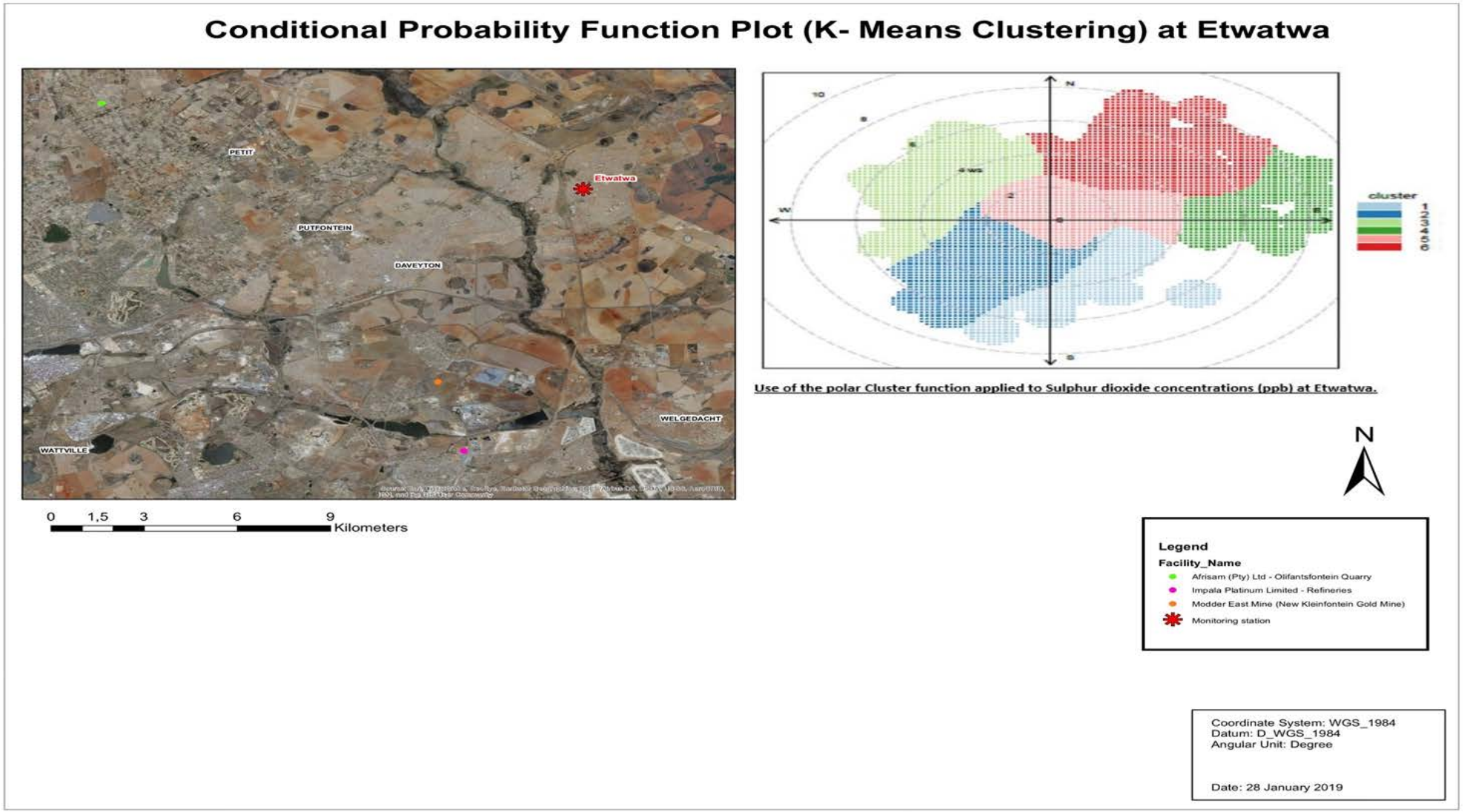

Figure 4.154: Conditional Probability Function Plot (K-Means Clustering) at the Etwatwa

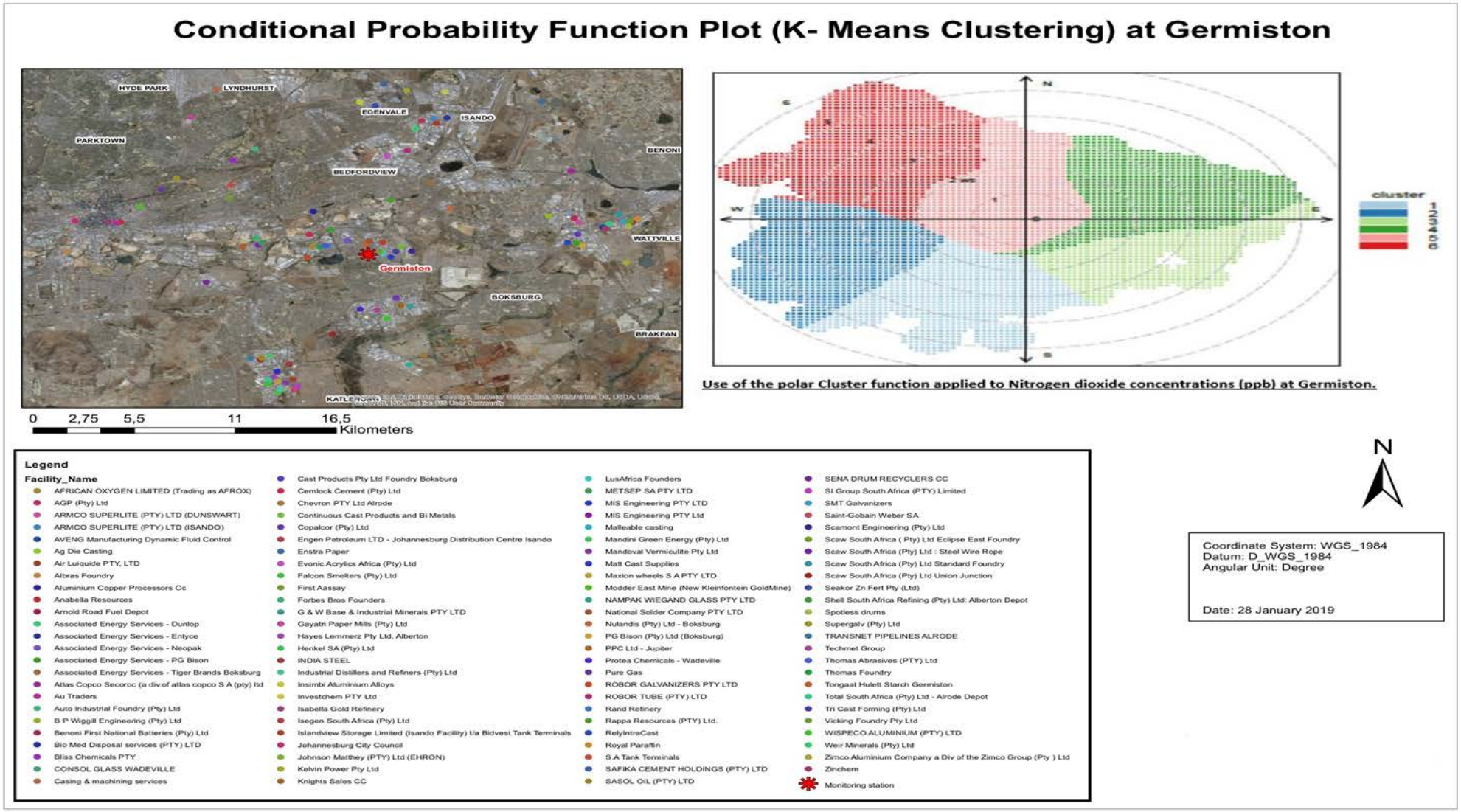

Figure 4.155: Conditional Probability Function Plot (K-Means Clustering) at the Germiston

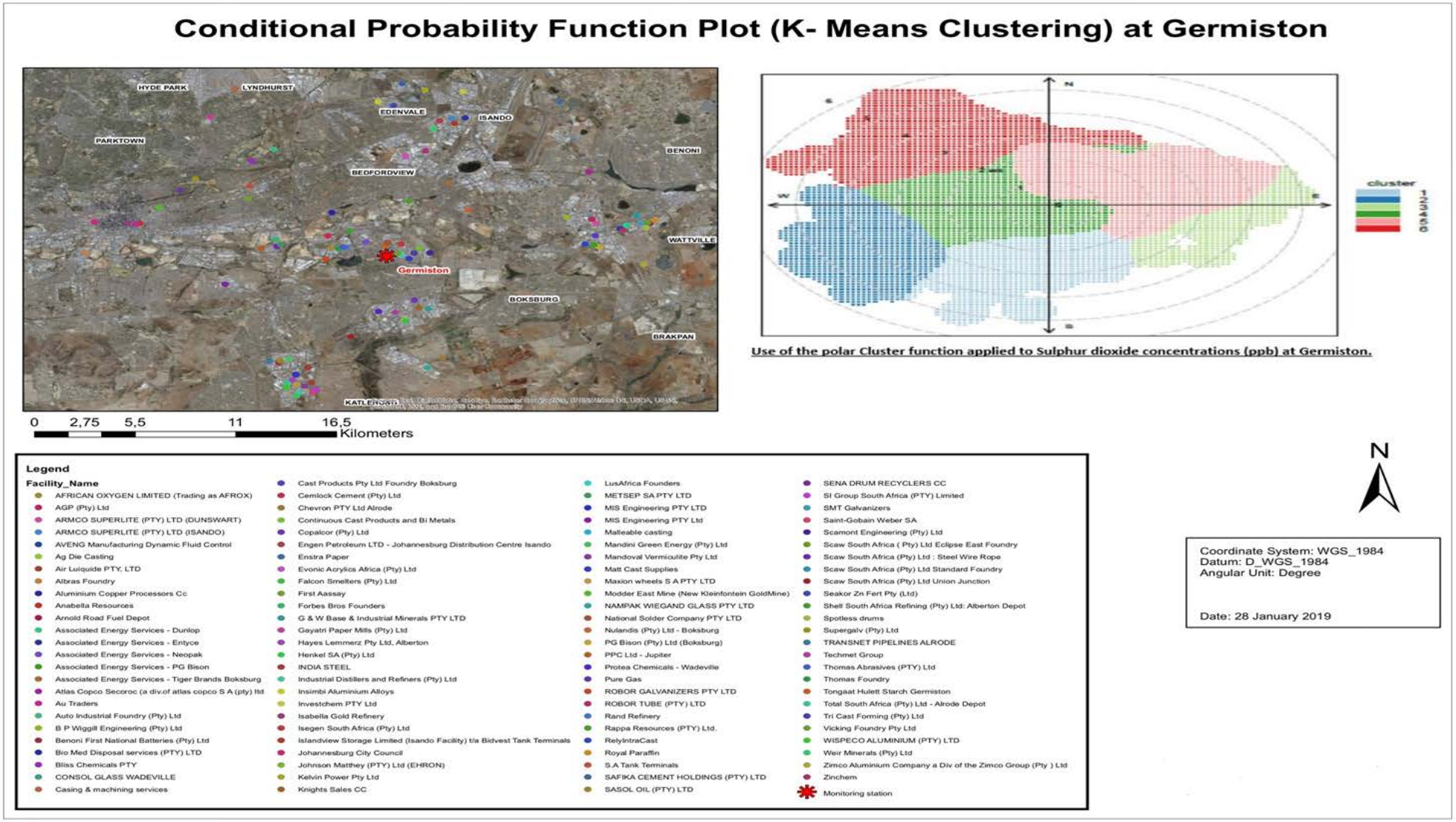

Figure 4.156: Conditional Probability Function Plot (K-Means Clustering) at the Germiston

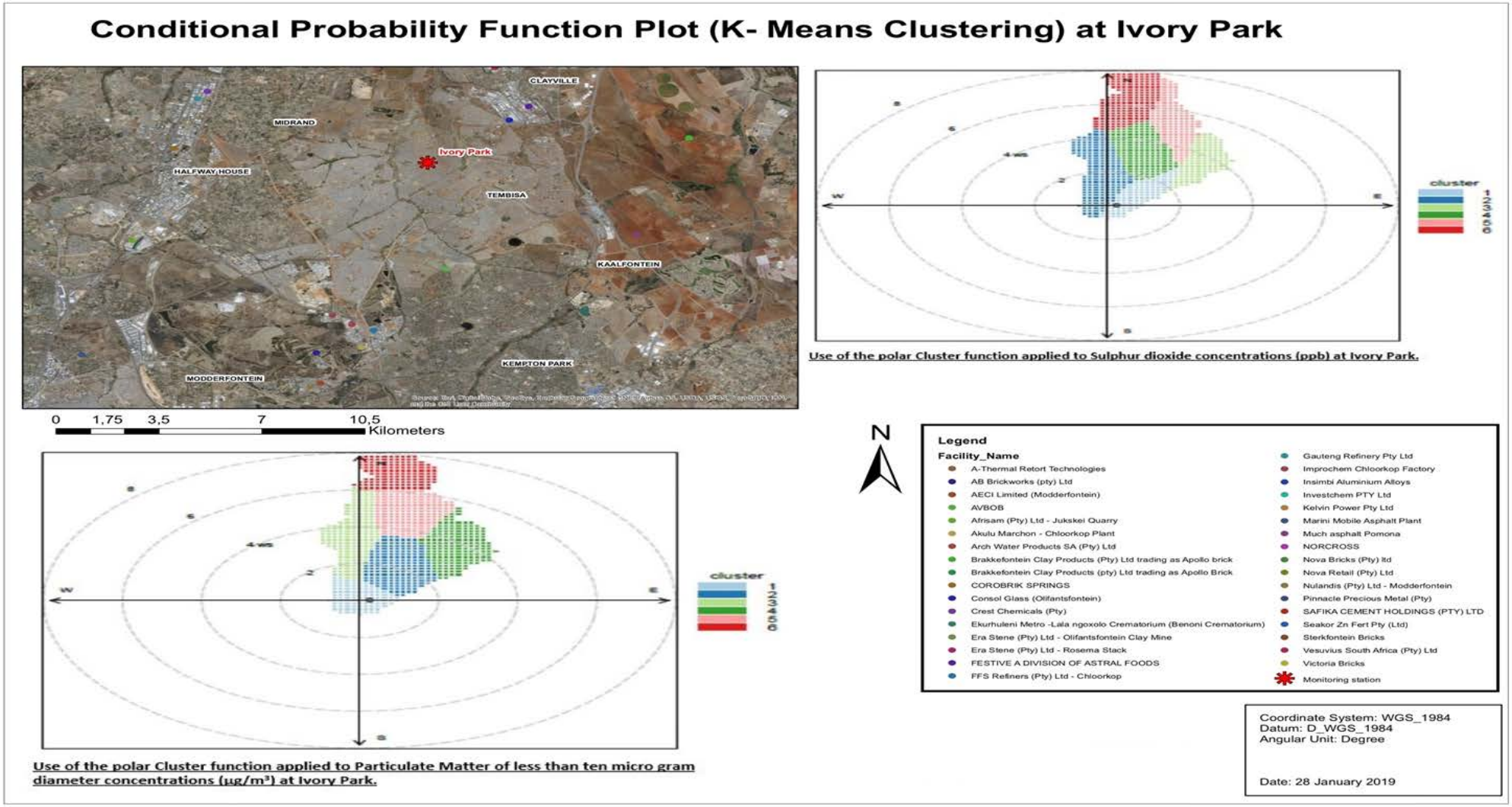

Figure 4.157: Conditional Probability Function Plot (K-Means Clustering) at Ivory

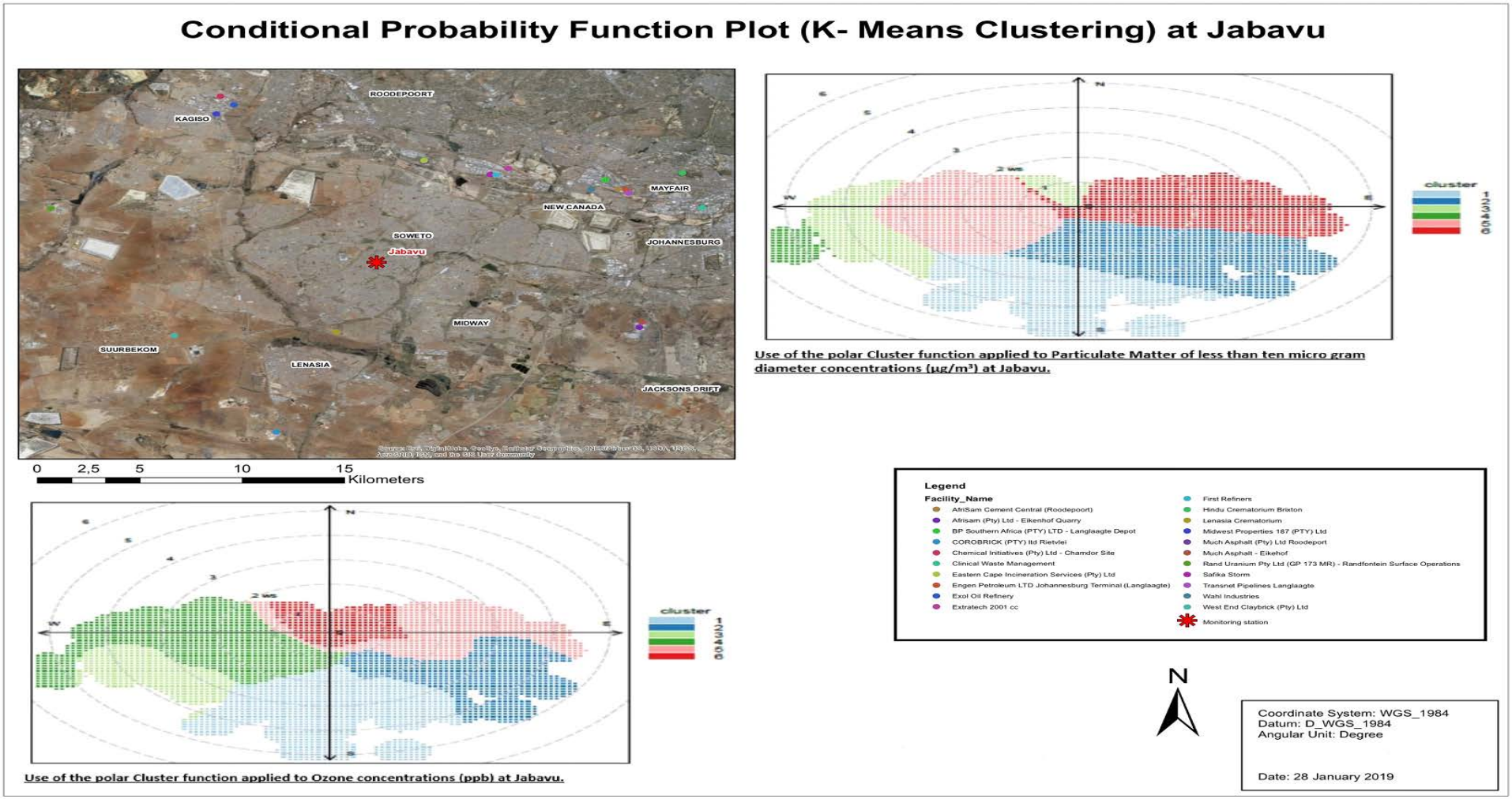

Figure 4.158: Conditional Probability Function Plot (K-Means Clustering) at the Jabavu

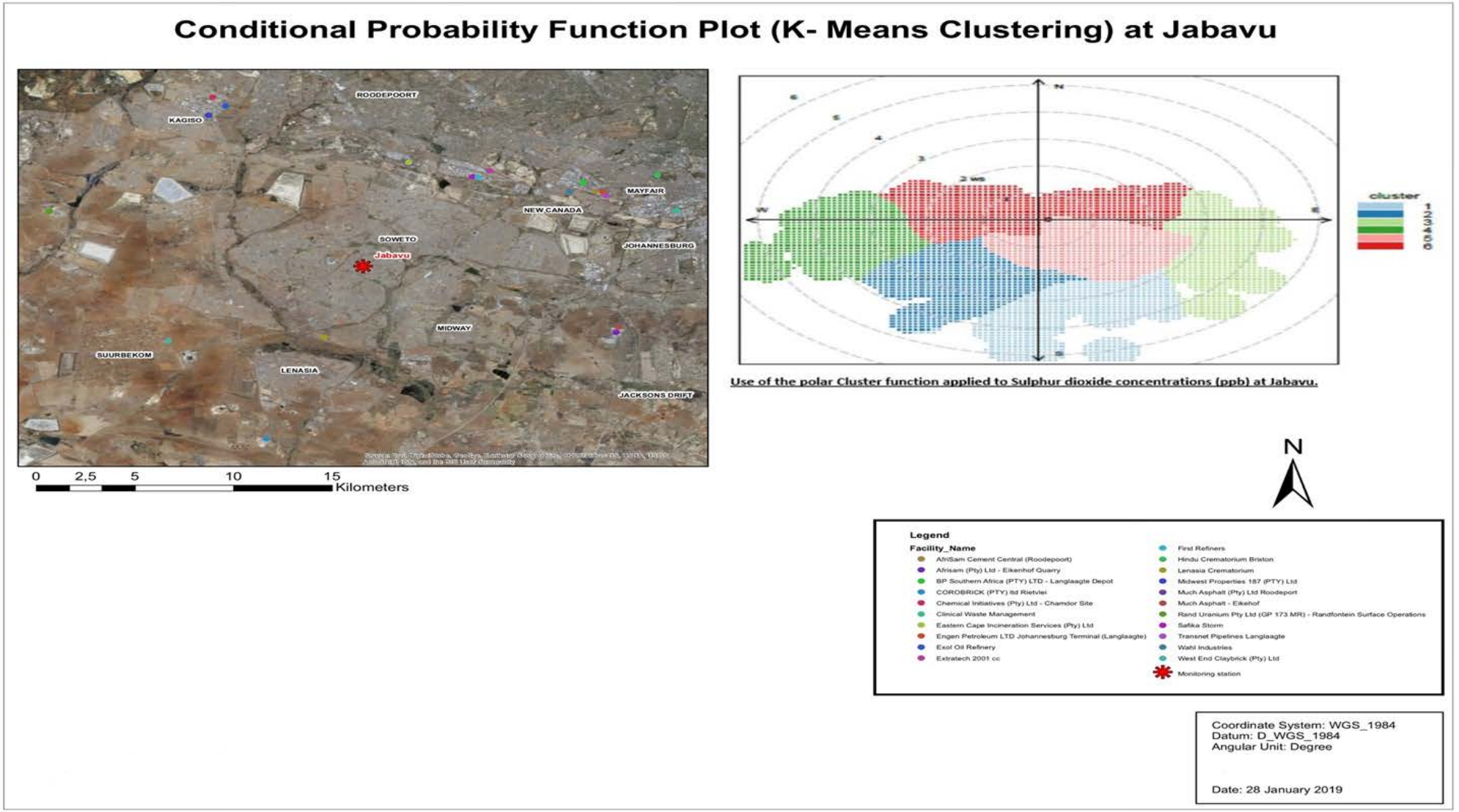

Figure 4.159: Conditional Probability Function Plot (K-Means Clustering) at the Jabavu

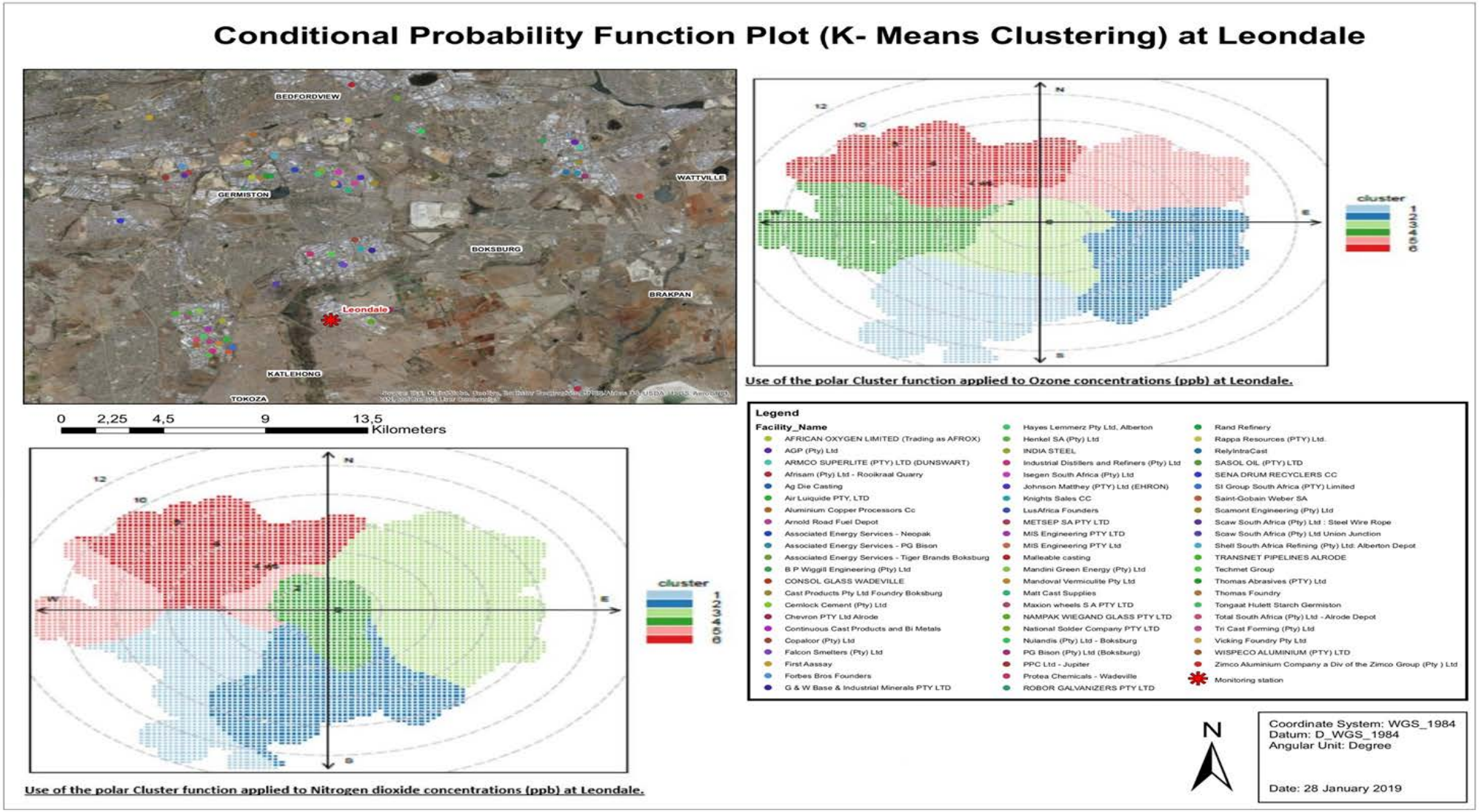

Figure 4.160: Conditional Probability Function Plot (K-Means Clustering) at the Leondale

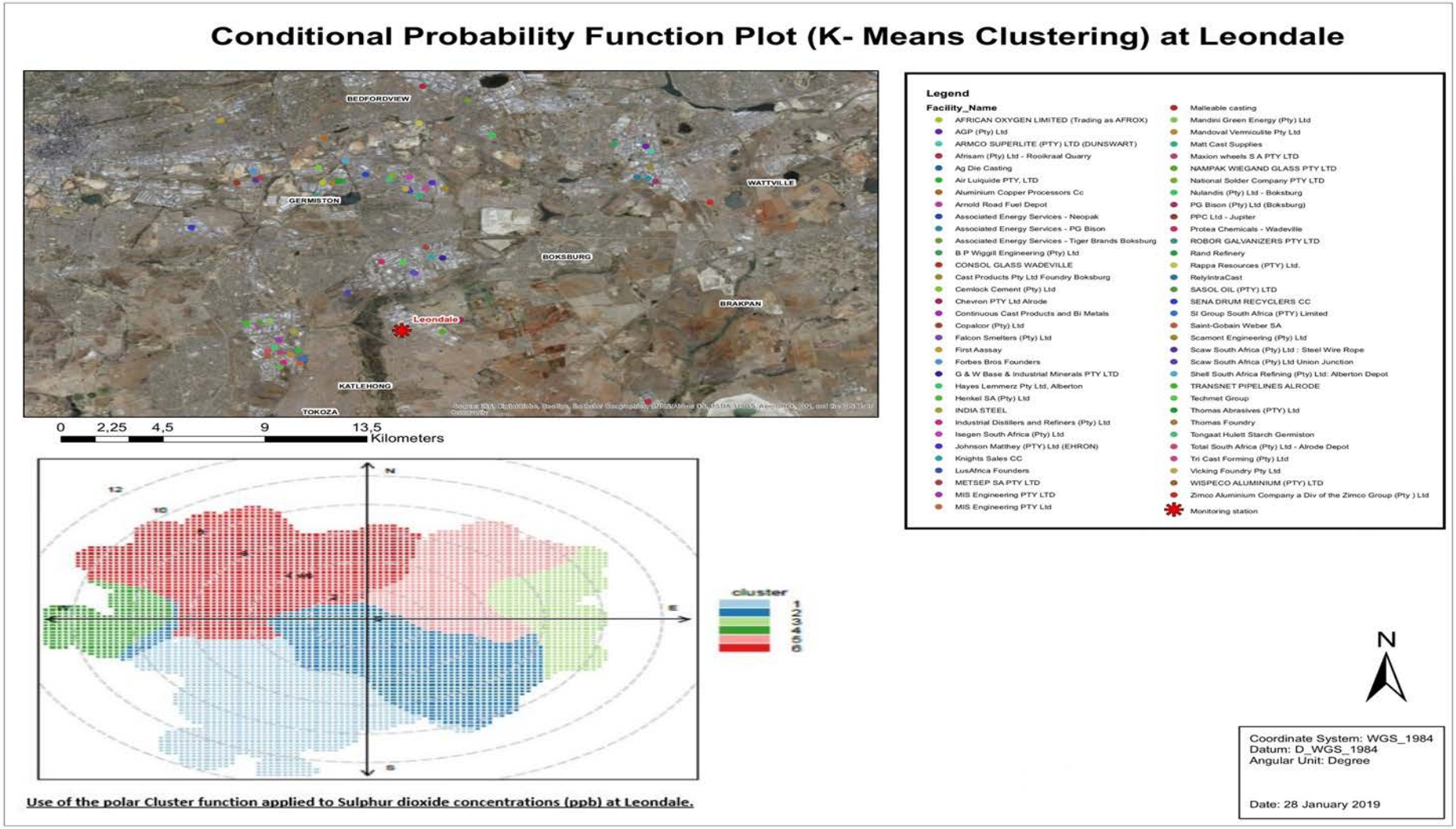

Figure 4.161: Conditional Probability Function Plot (K-Means Clustering) at the Leondale

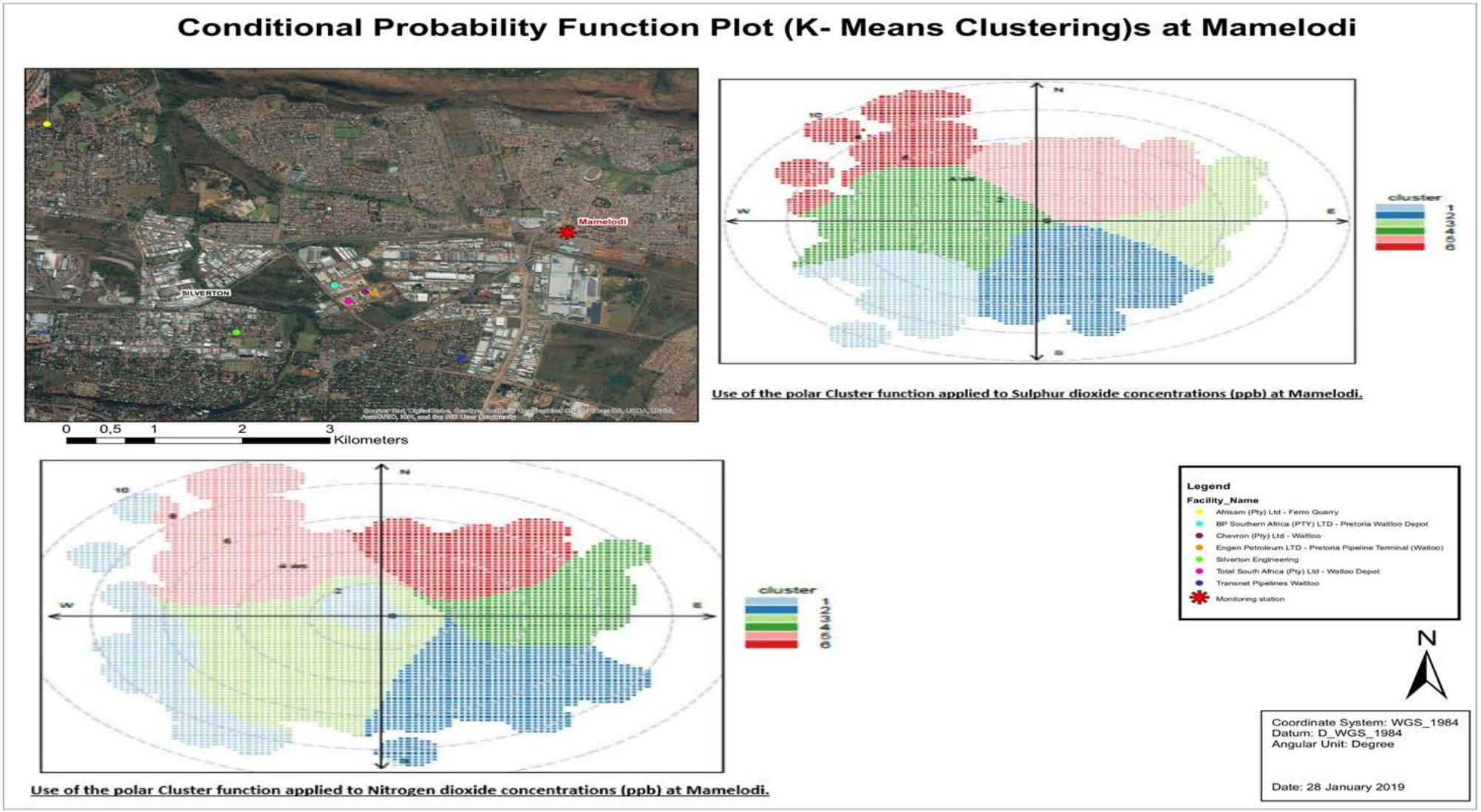

Figure 4.162: Conditional Probability Function Plot (K-Means Clustering) at the Mamelodi

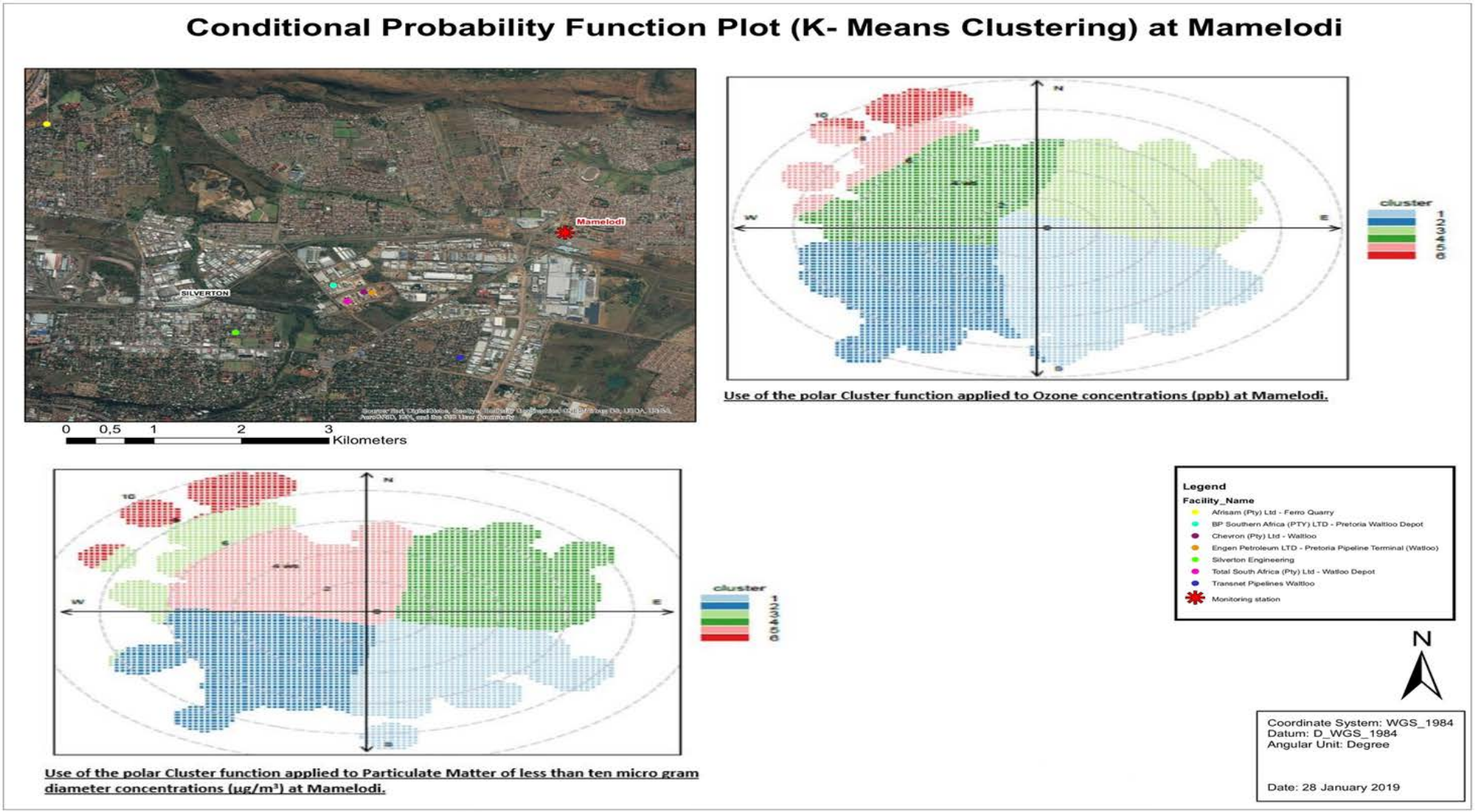

Figure 4.163: Conditional Probability Function Plot (K-Means Clustering) at the Mamelodi

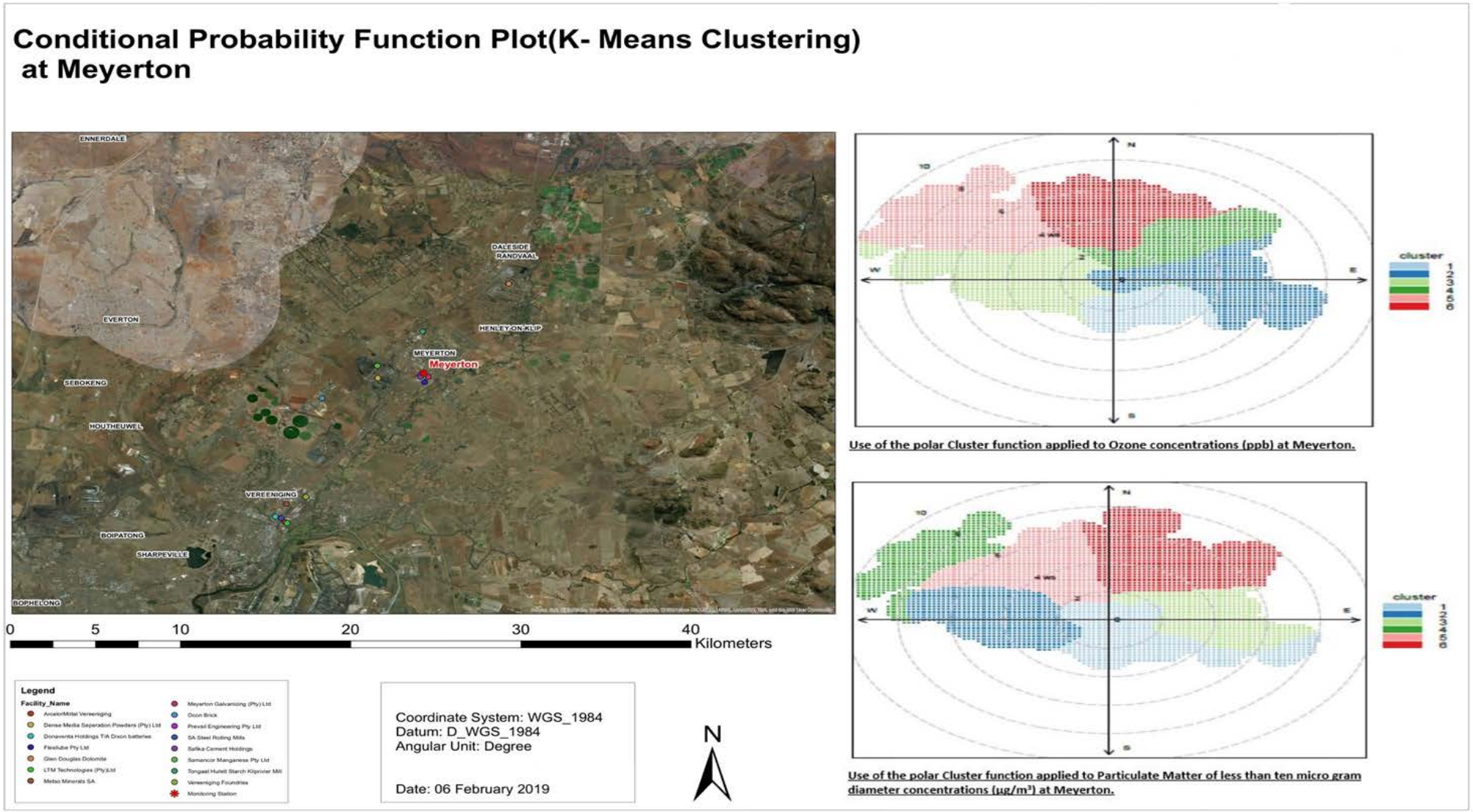

Figure 4.164: Conditional Probability Function Plot (K-Means Clustering) at the Meyerton

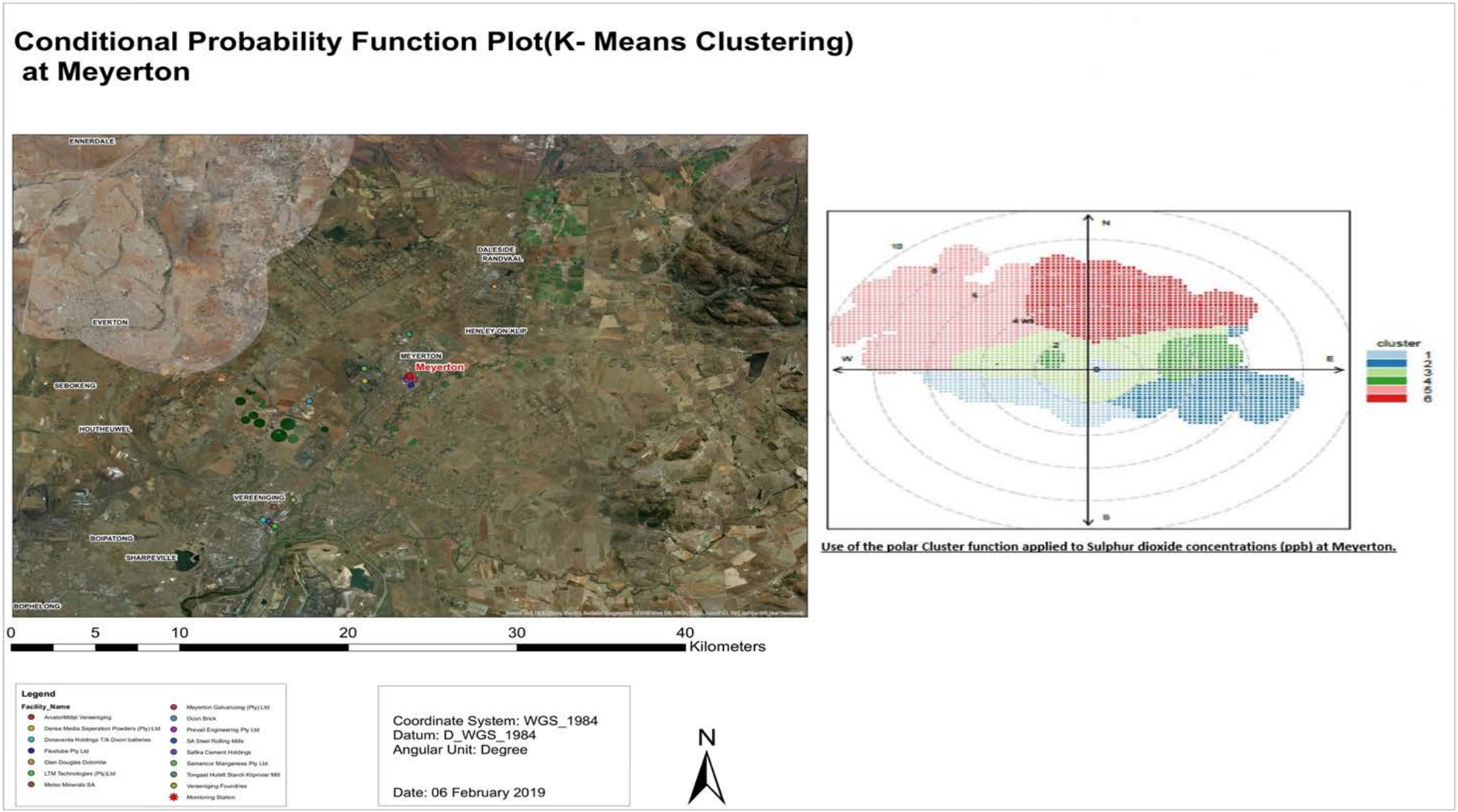

Use of the polar Cluster function applied to Sulphur dioxide concentrations (ppb) at Meyerton.

Figure 4.165: Conditional Probability Function Plot (K-Means Clustering) at the Meyerton

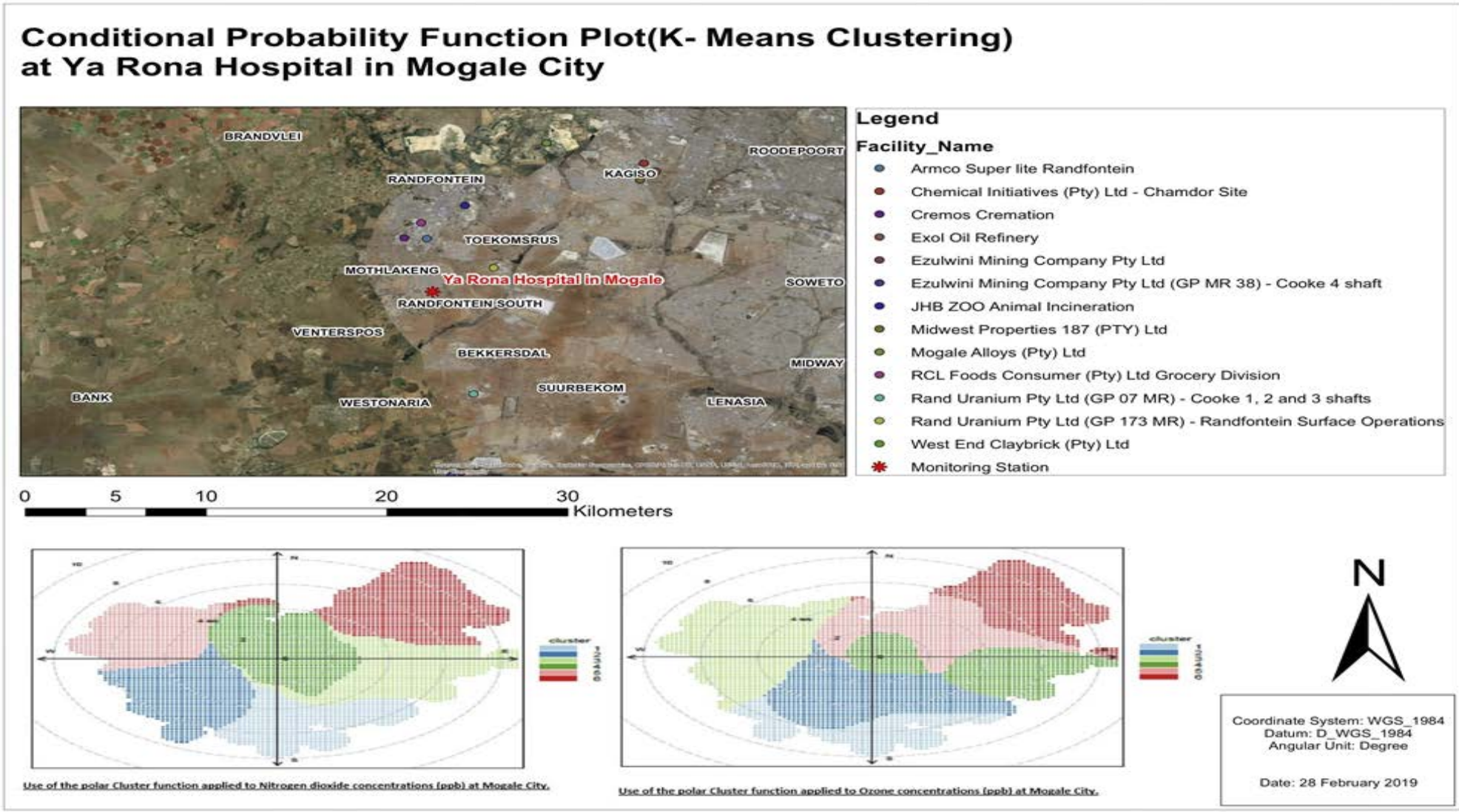

Figure 4.166: Conditional Probability Function Plot (K-Means Clustering) at the Mogale City

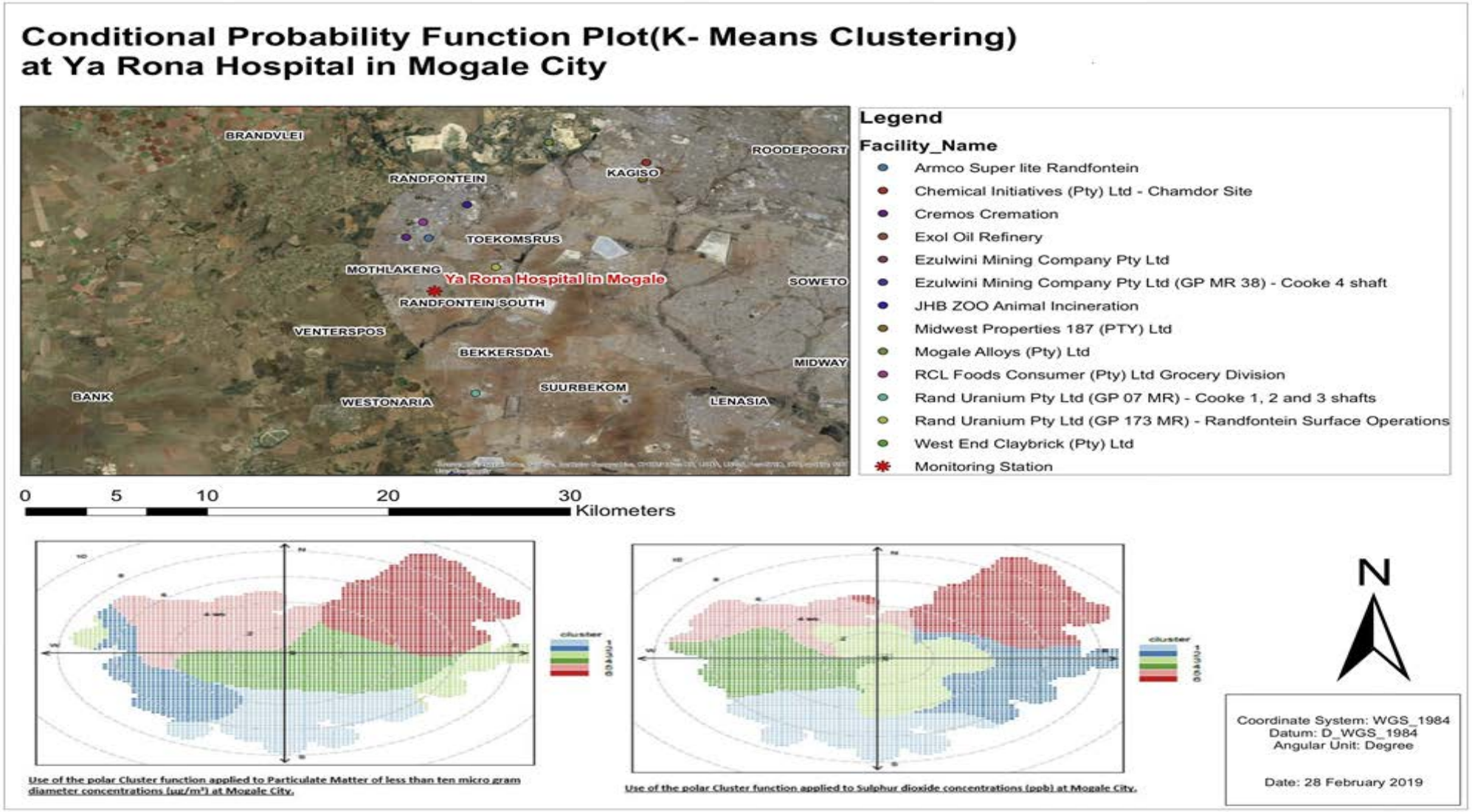

Figure 4.167: Conditional Probability Function Plot (K-Means Clustering) at the Mogale City

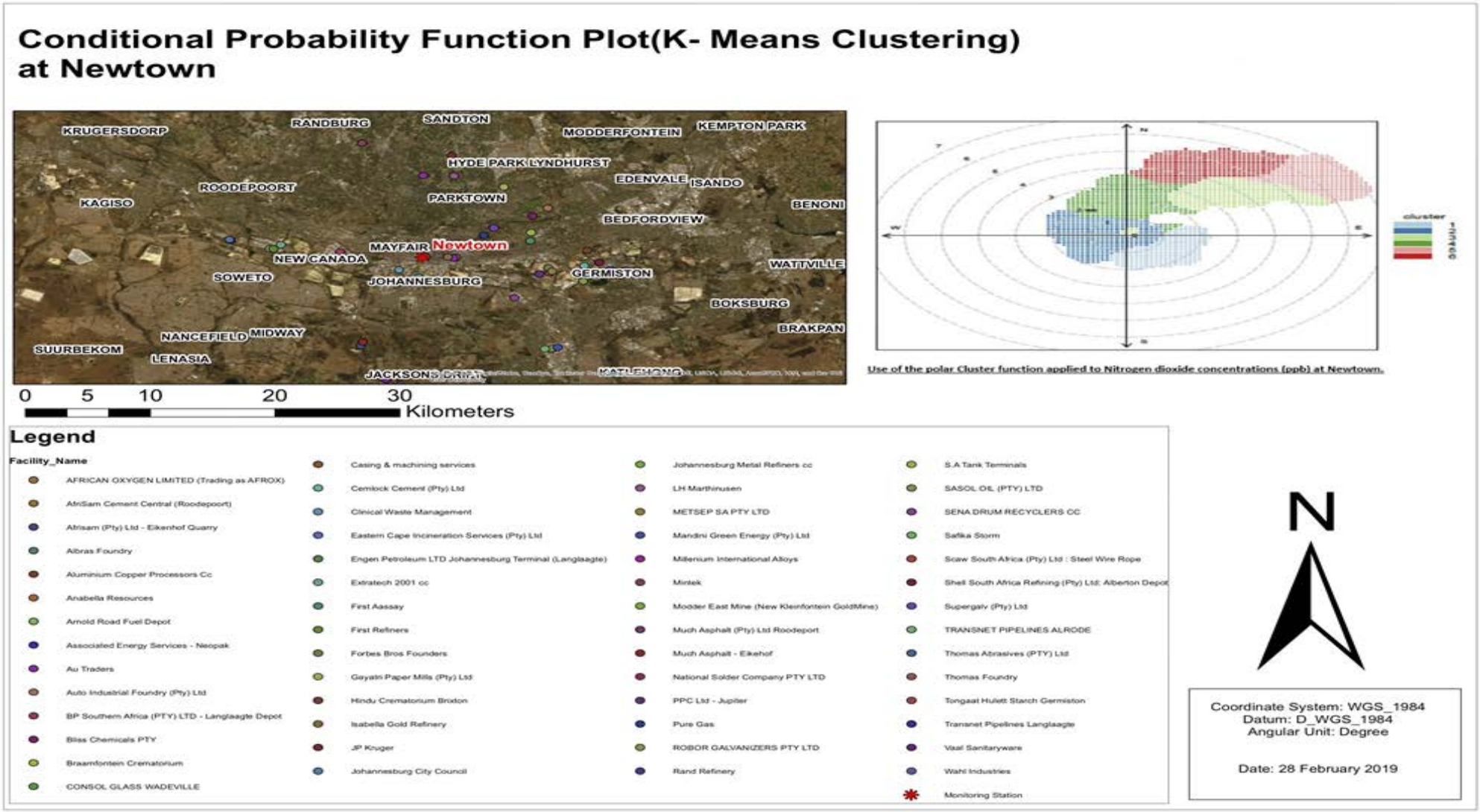

Figure 4.168: Conditional Probability Function Plot (K-Means Clustering) at the Newtown

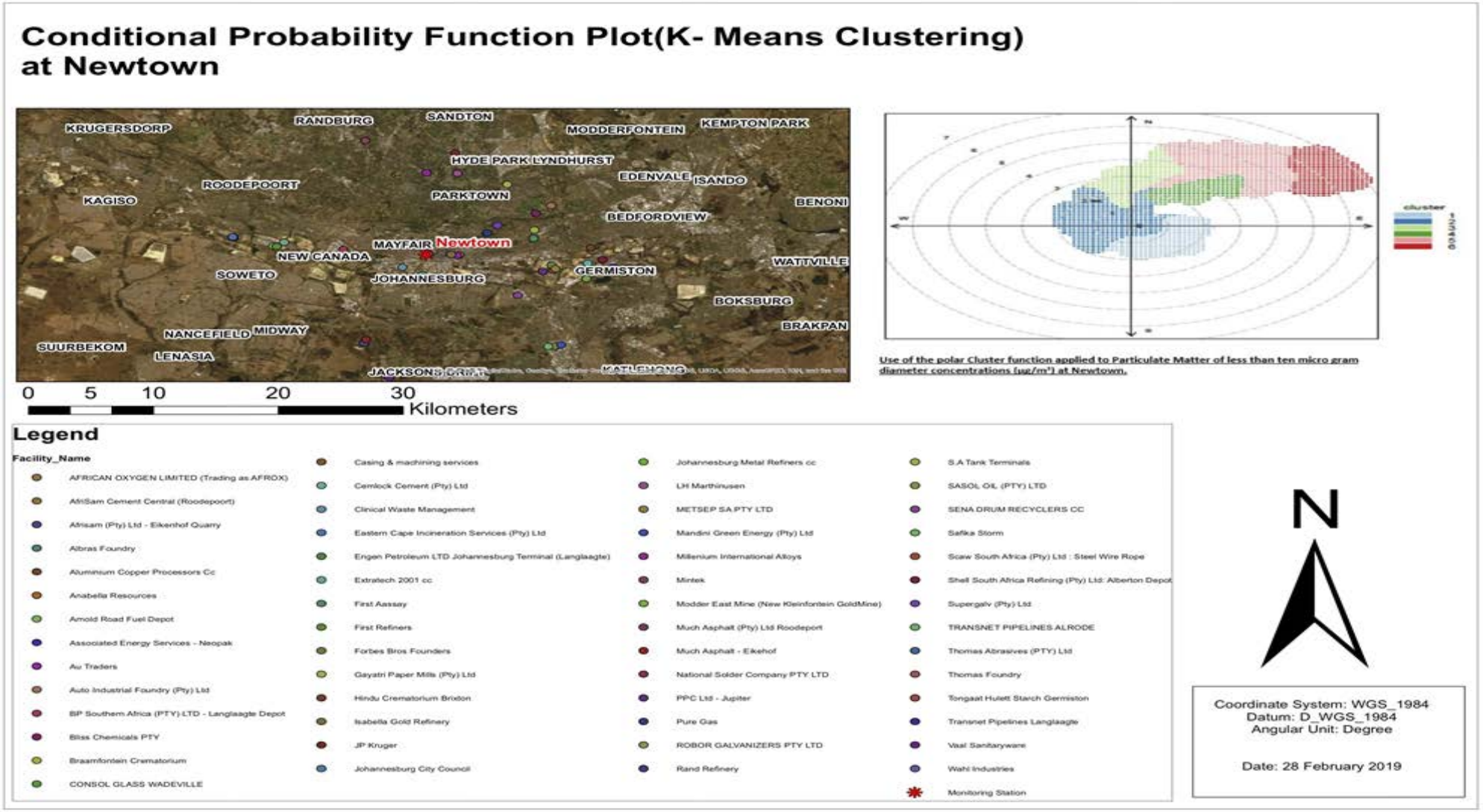

Figure 4.169: Conditional Probability Function Plot (K-Means Clustering) at the Newtown

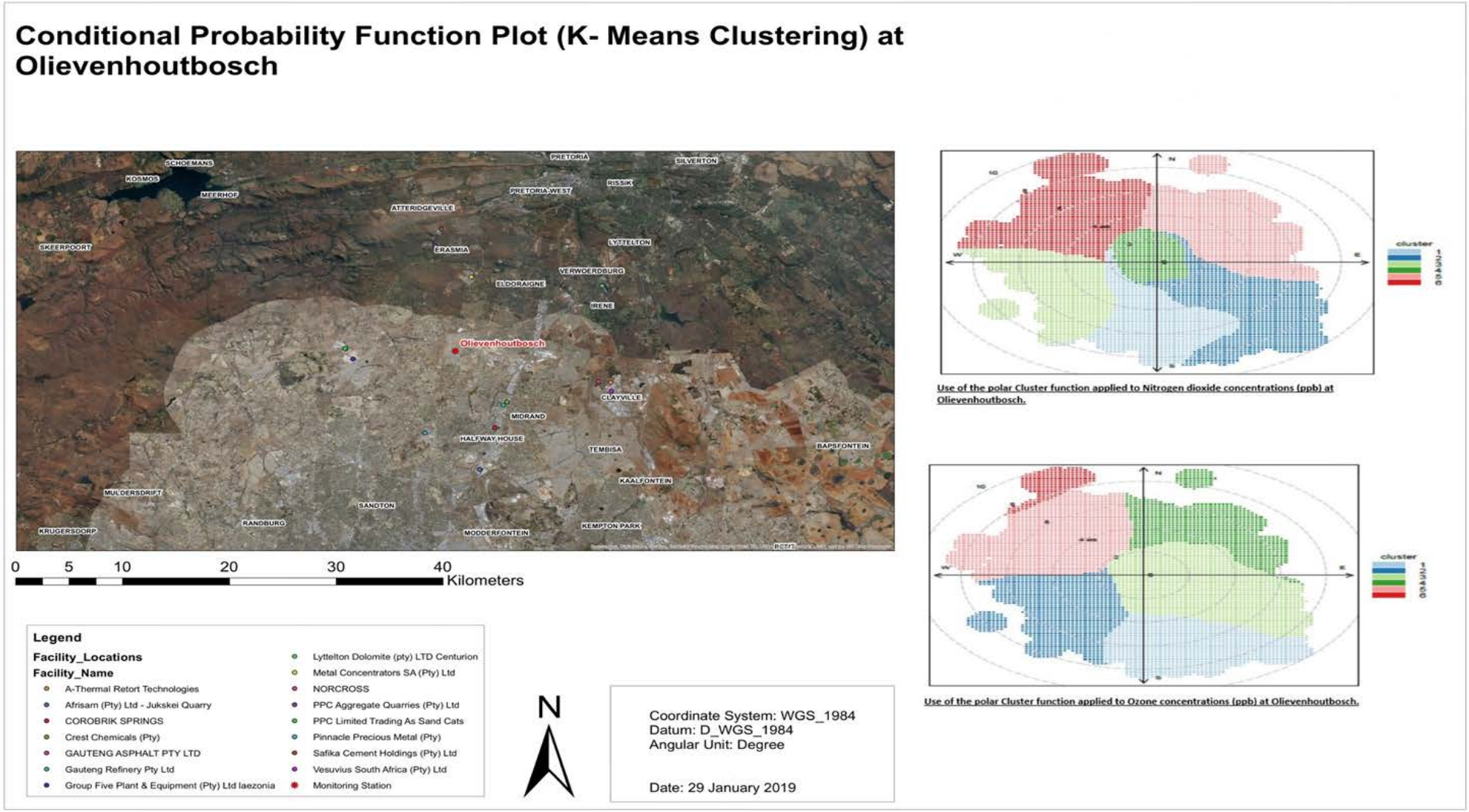

Figure 4.170: Conditional Probability Function Plot (K-Means Clustering) at the Olievenhoutbosch

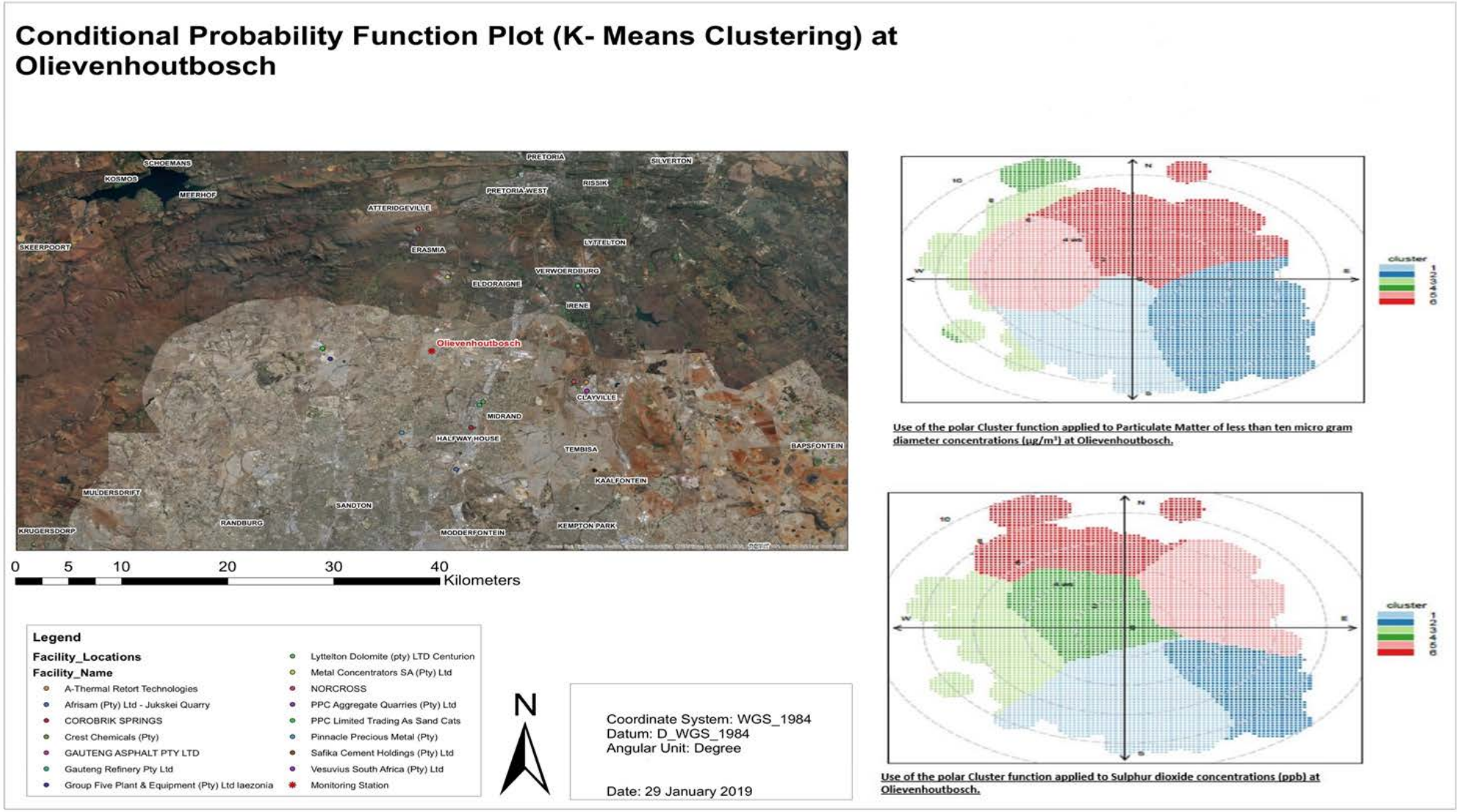

Figure 4.171: Conditional Probability Function Plot (K-Means Clustering) at the Olievenhoutbosch

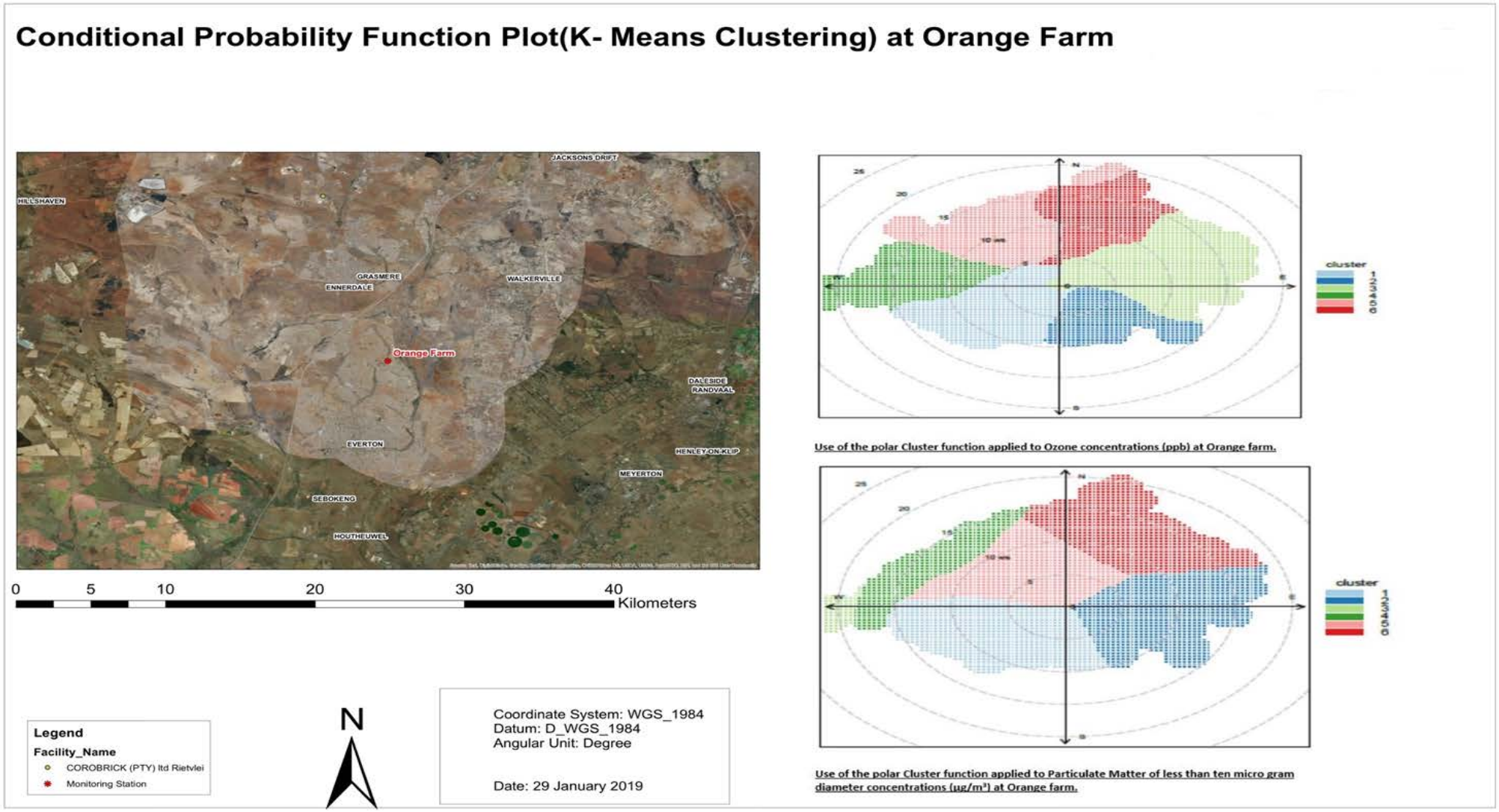

Figure 4.172: Conditional Probability Function Plot (K-Means Clustering) at the Orange Farm

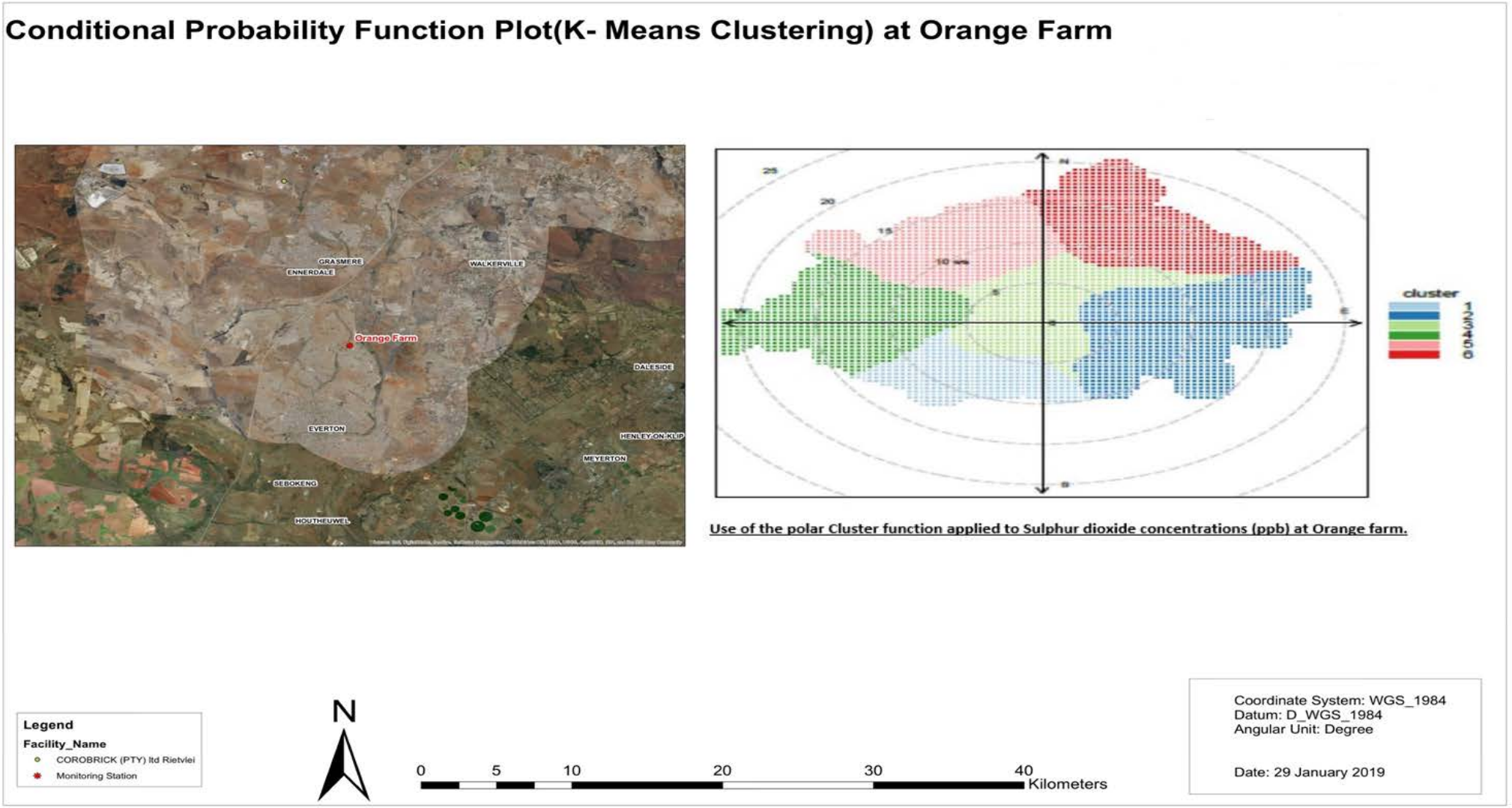

Figure 4.173: Conditional Probability Function Plot (K-Means Clustering) at the Orange Farm

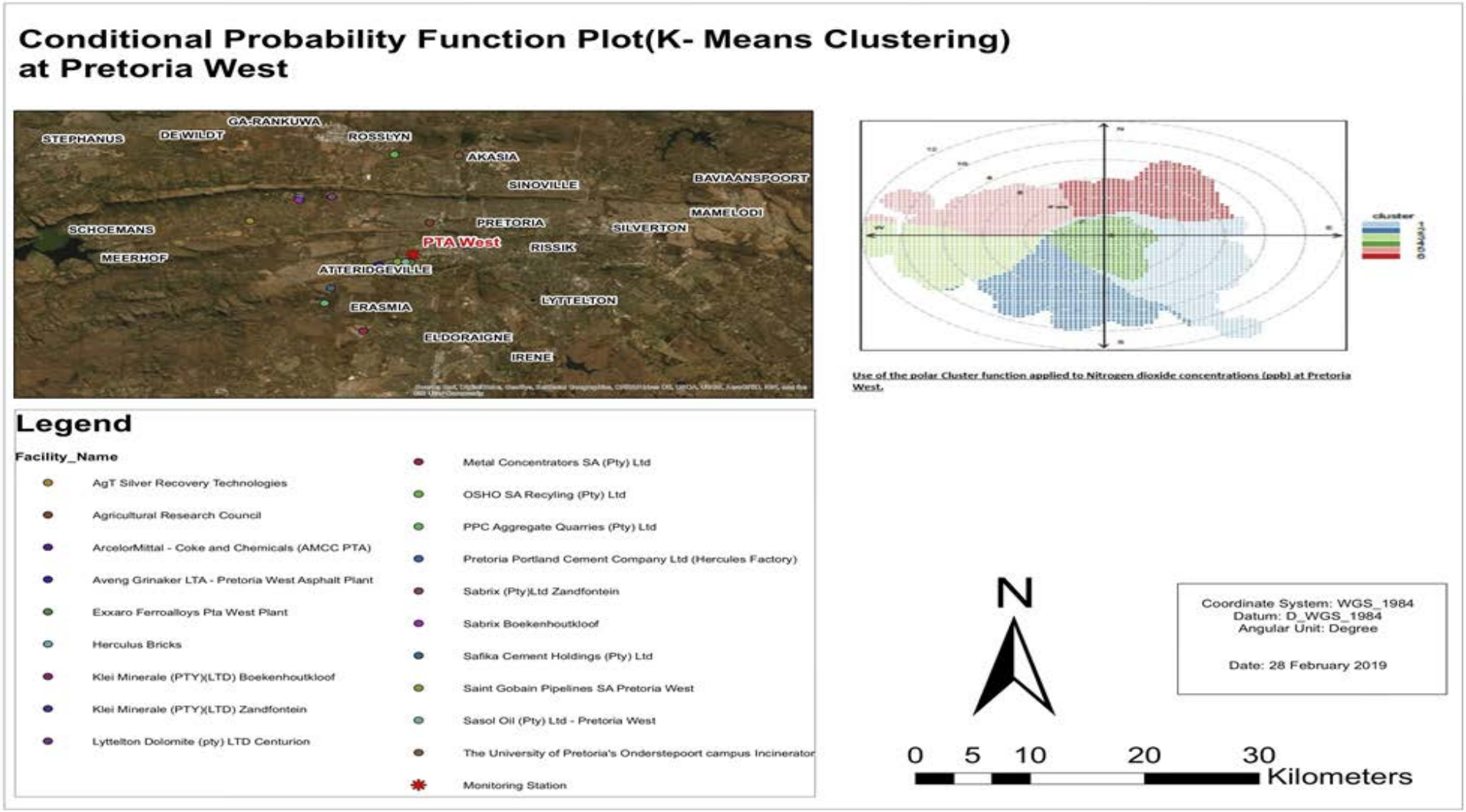

Figure 4.174: Conditional Probability Function Plot (K-Means Clustering) at the Pretoria West

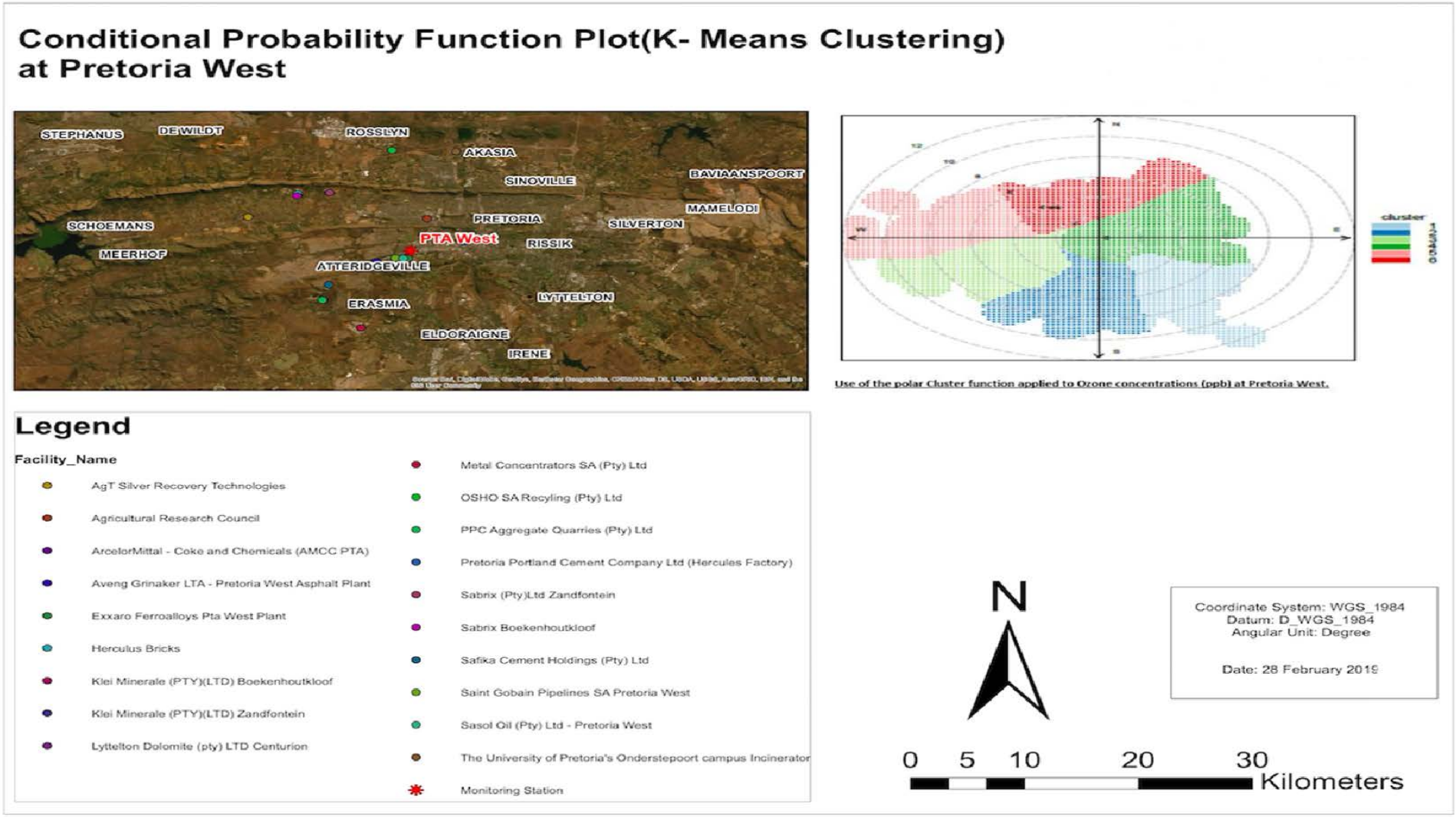

Figure 4.175: Conditional Probability Function Plot (K-Means Clustering) at the Pretoria West

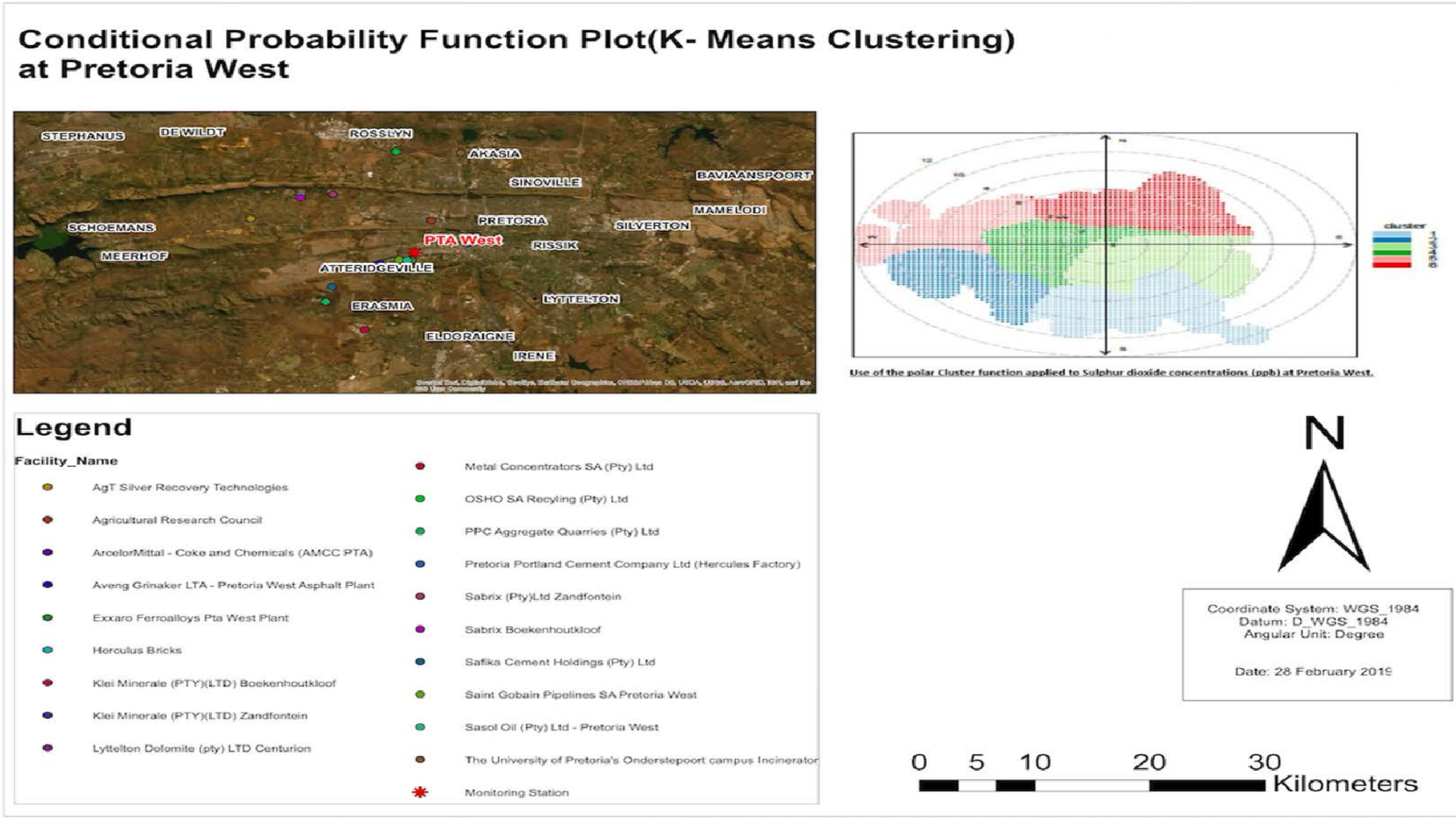

Figure 4.176: Conditional Probability Function Plot (K-Means Clustering) at the Pretoria West

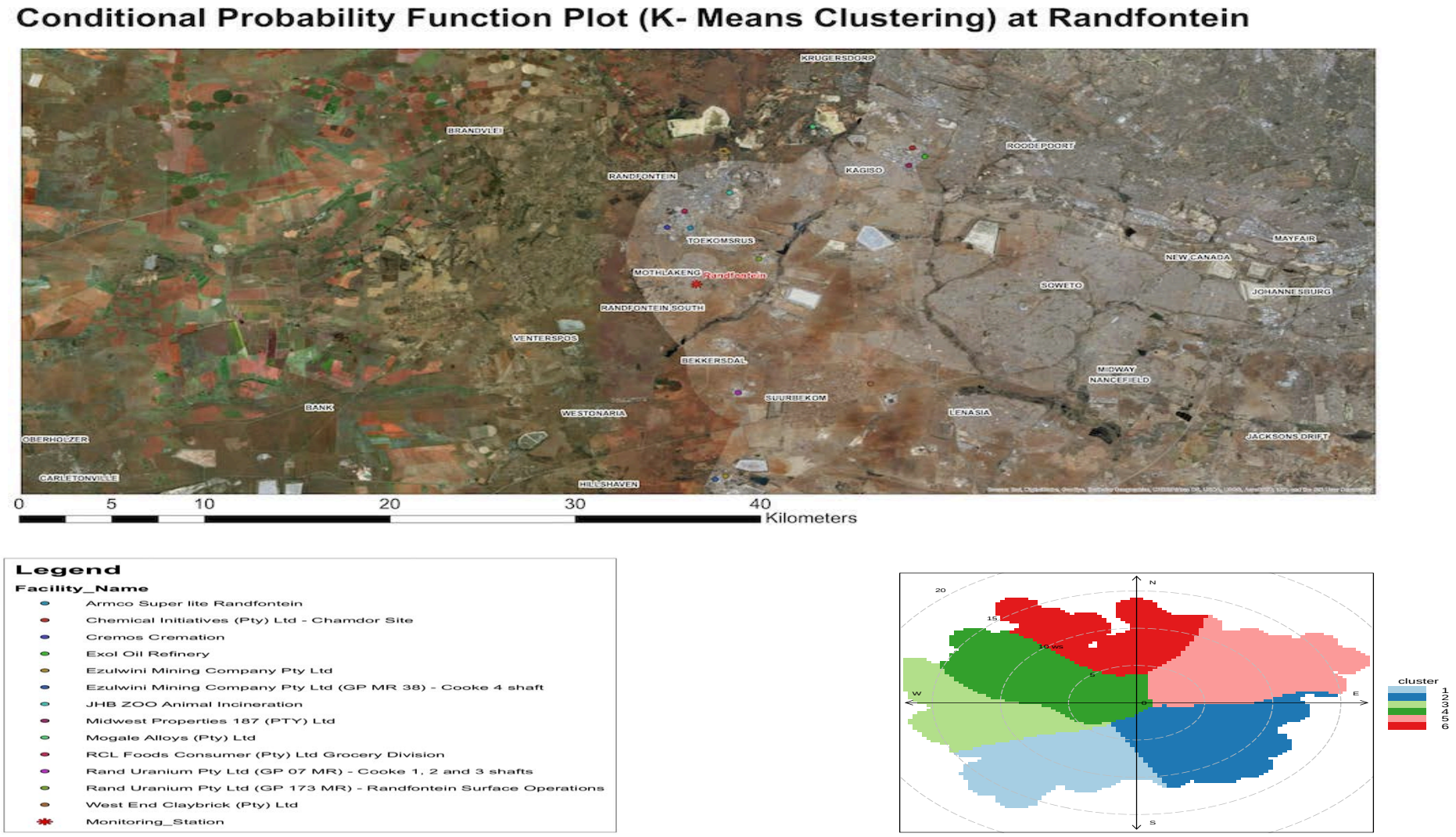

Figure 4.177: Conditional Probability Function Plot (K-Means Clustering) at the Randfontein

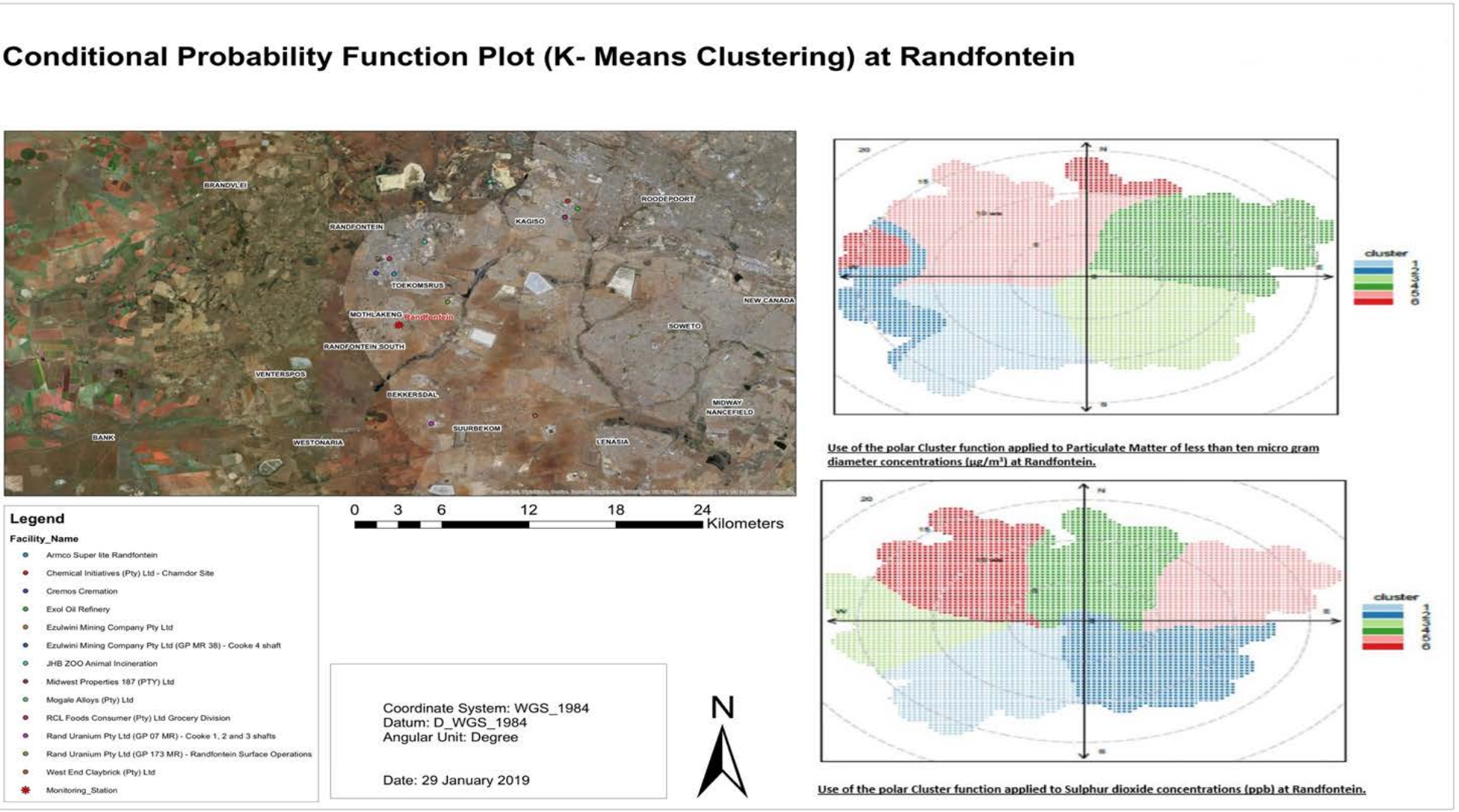

Figure 4.178: Conditional Probability Function Plot (K-Means Clustering) at the Randfontein

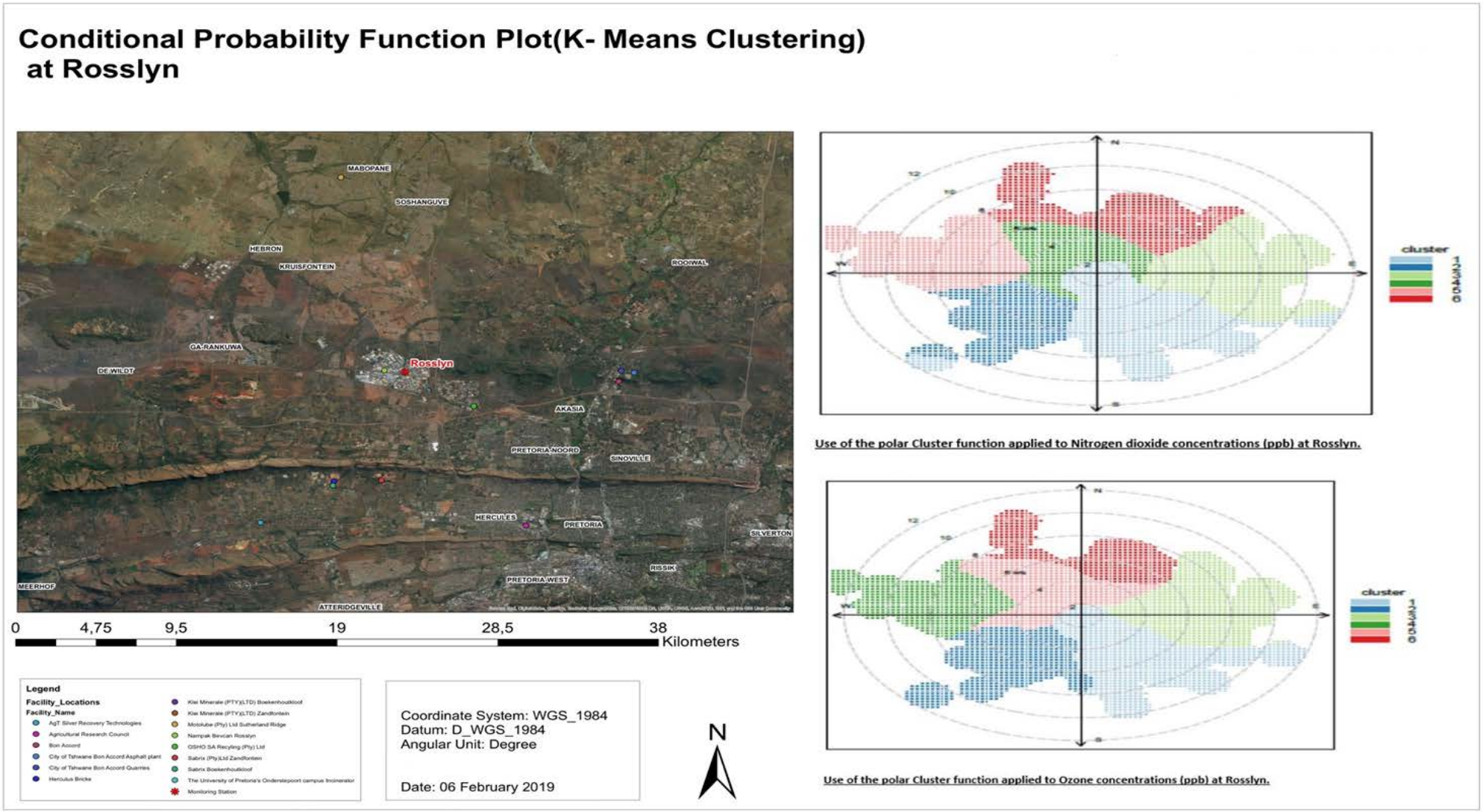

Figure 4.179: Conditional Probability Function Plot (K-Means Clustering) at the Rosslyn

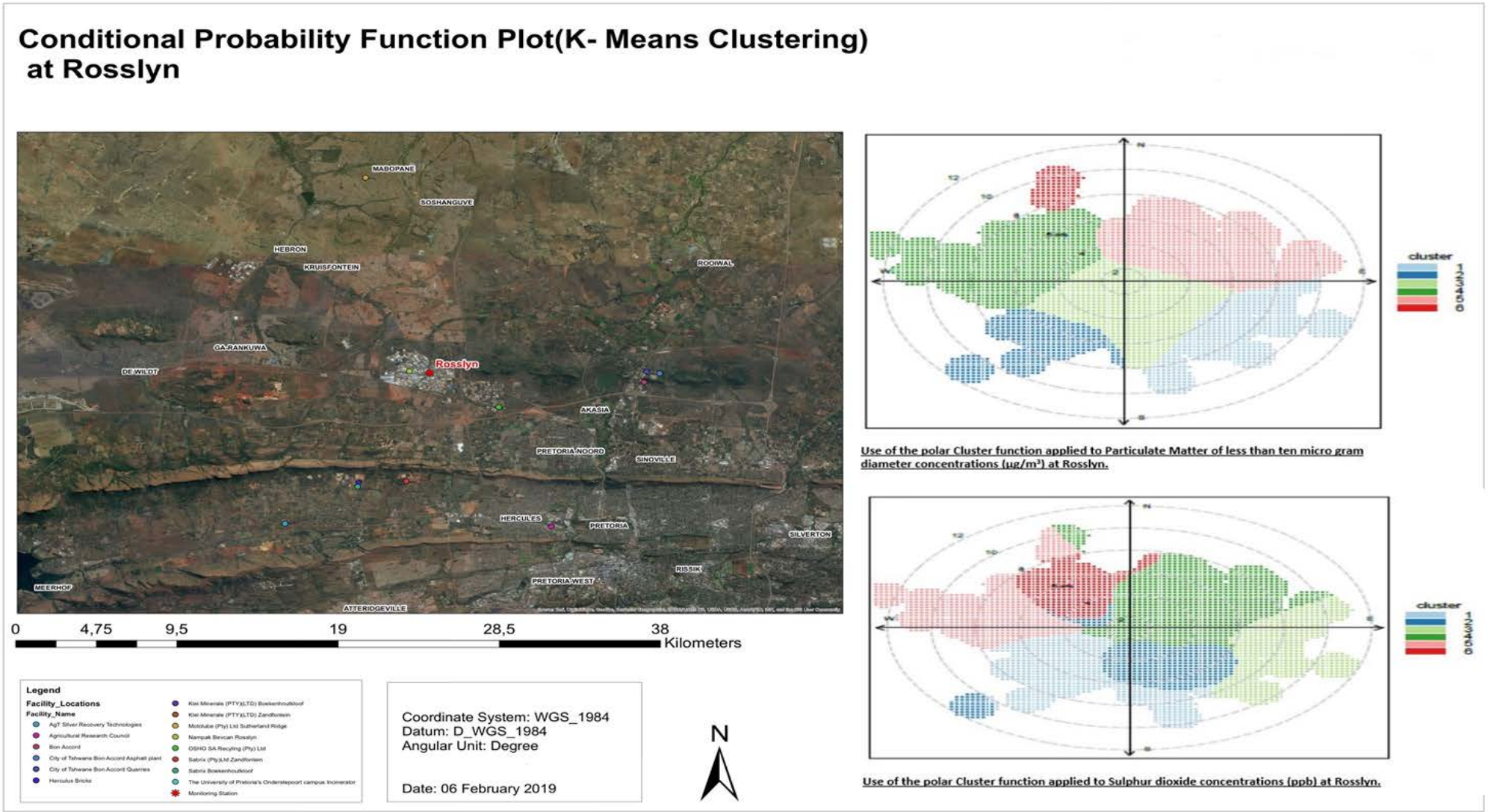

Figure 4.180: Conditional Probability Function Plot (K-Means Clustering) at the Rosslyn

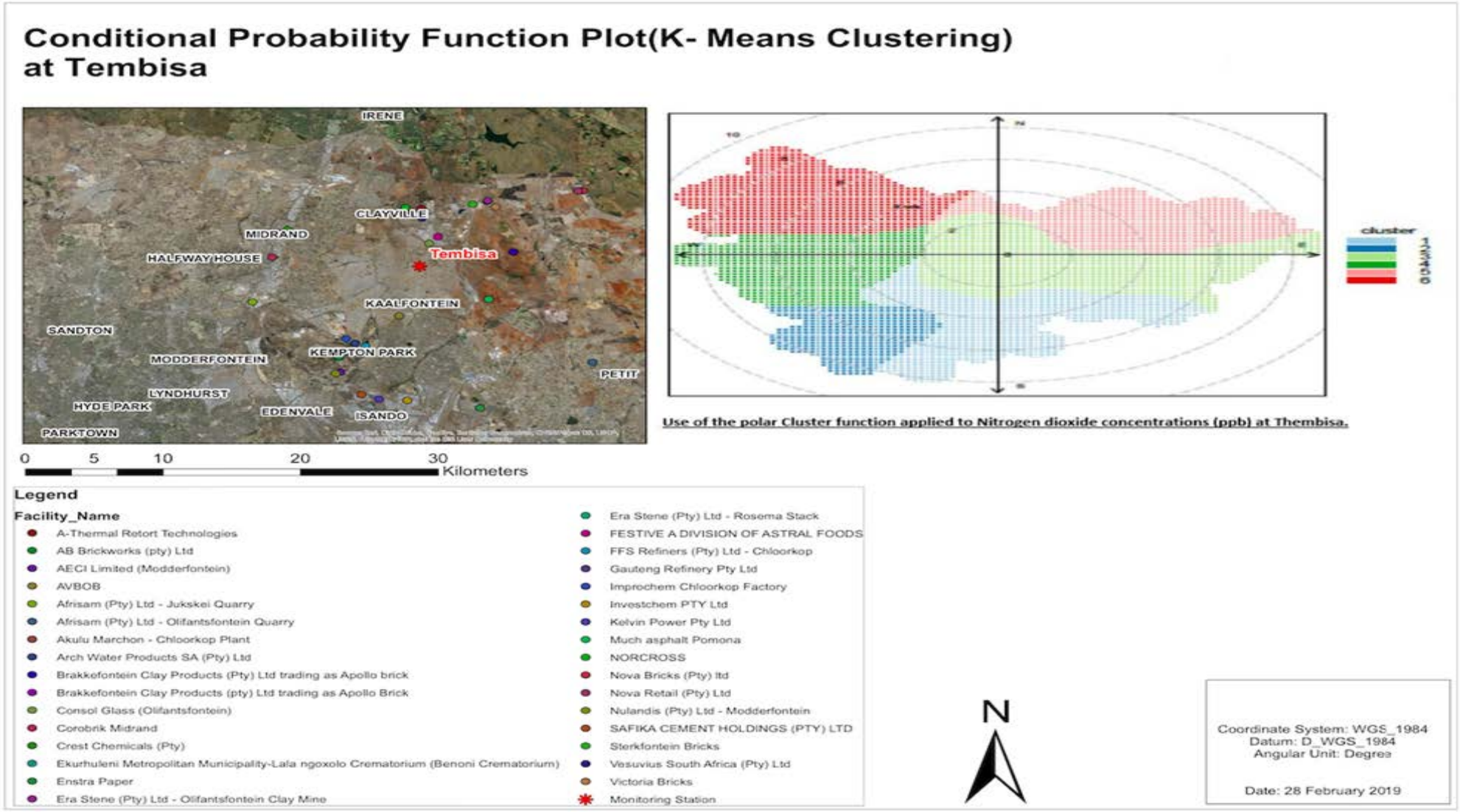

Figure 4.181: Conditional Probability Function Plot (K-Means Clustering) at the Tembisa

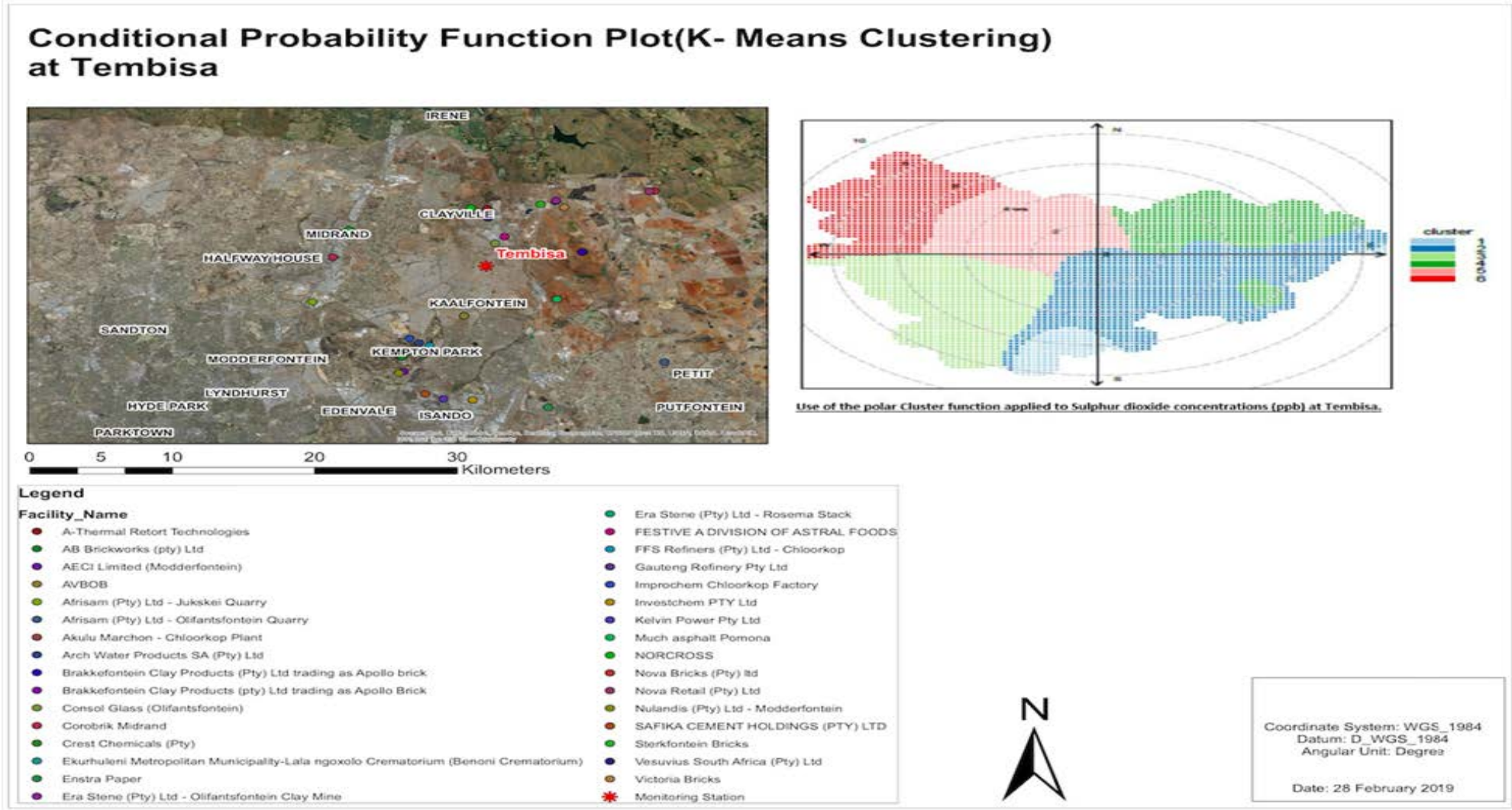

Figure 4.182: Conditional Probability Function Plot (K-Means Clustering) at the Tembisa

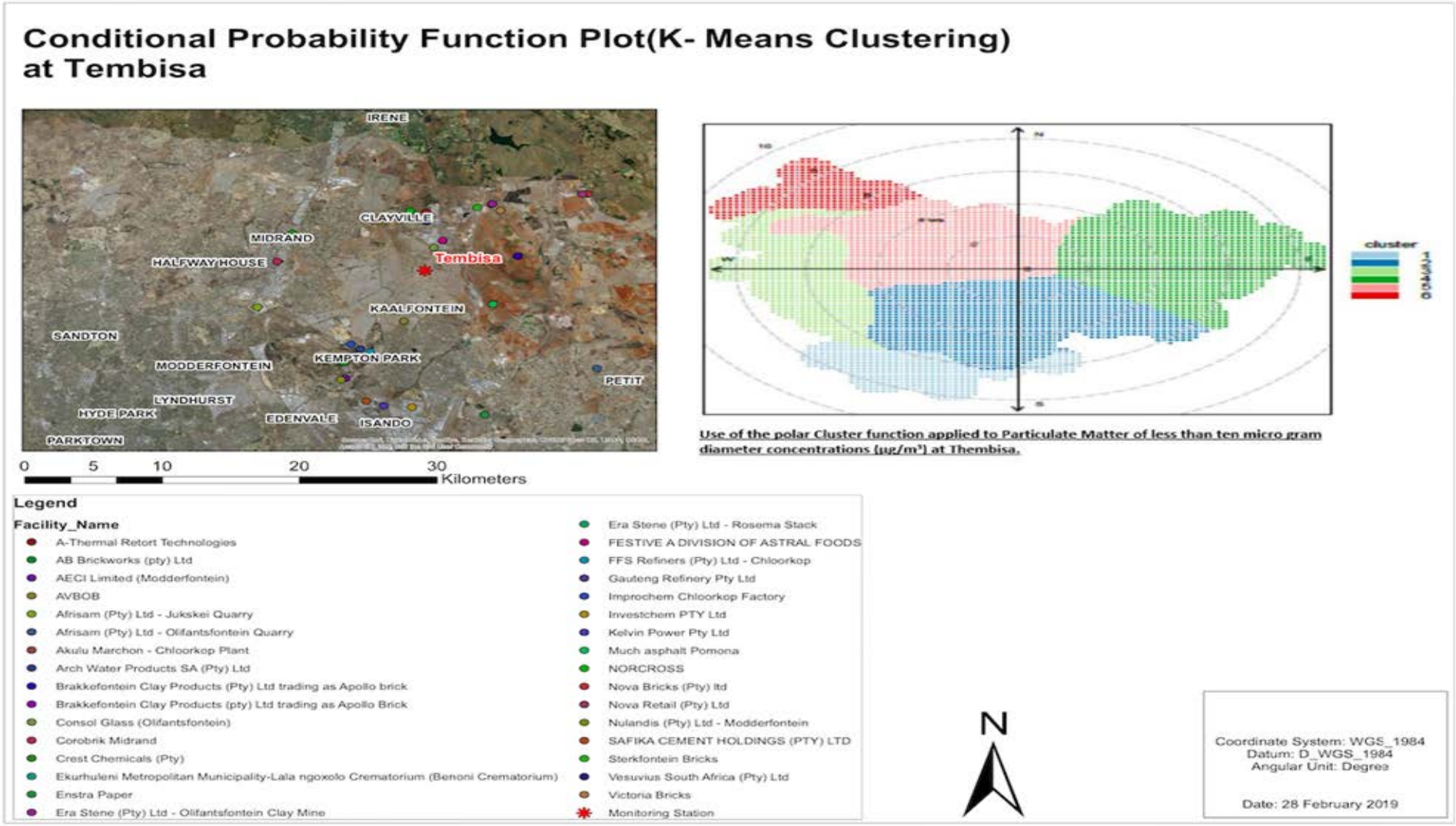

Figure 4.183: Conditional Probability Function Plot (K-Means Clustering) at the Tembisa

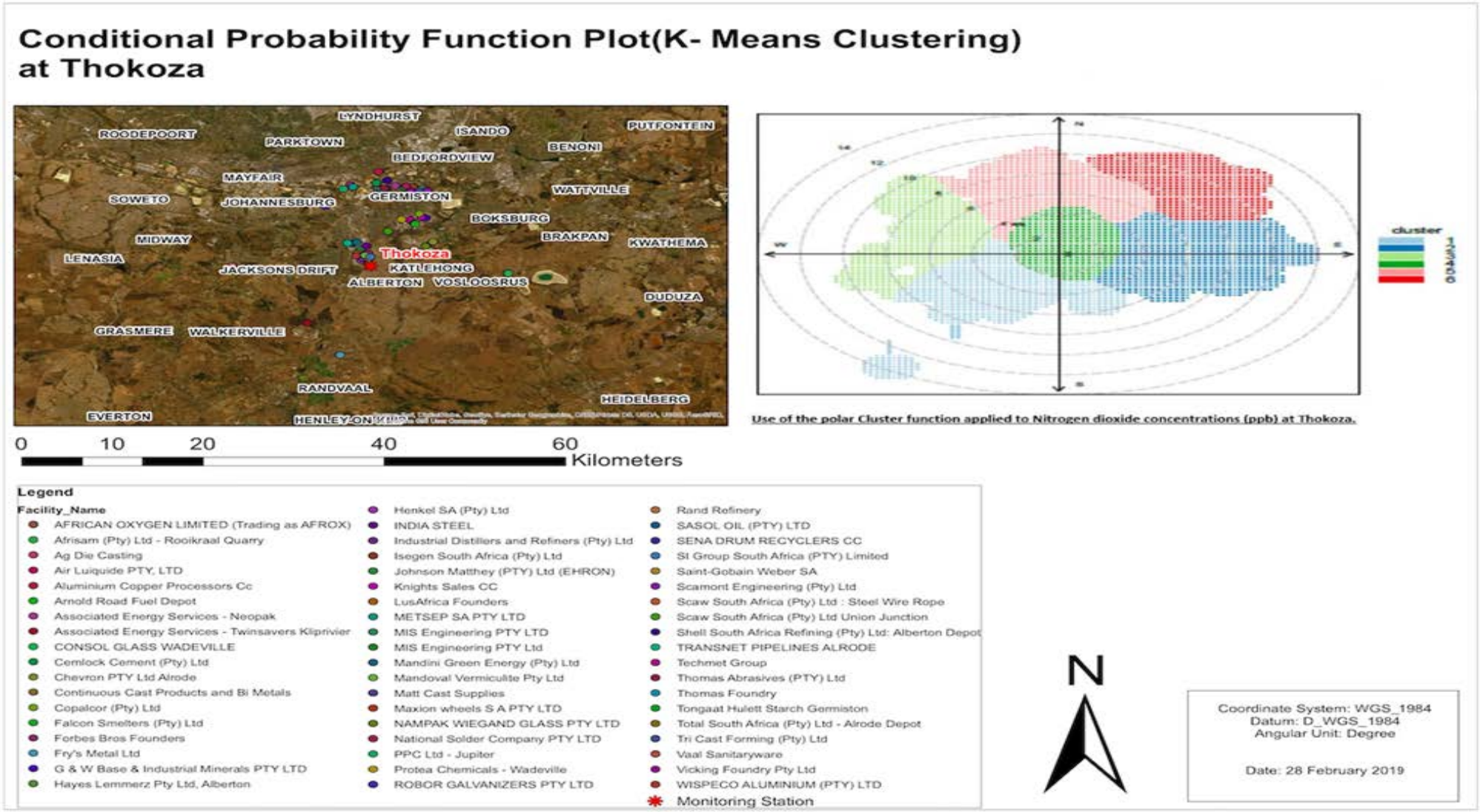

Figure 4.184: Conditional Probability Function Plot (K-Means Clustering) at the Thokoza

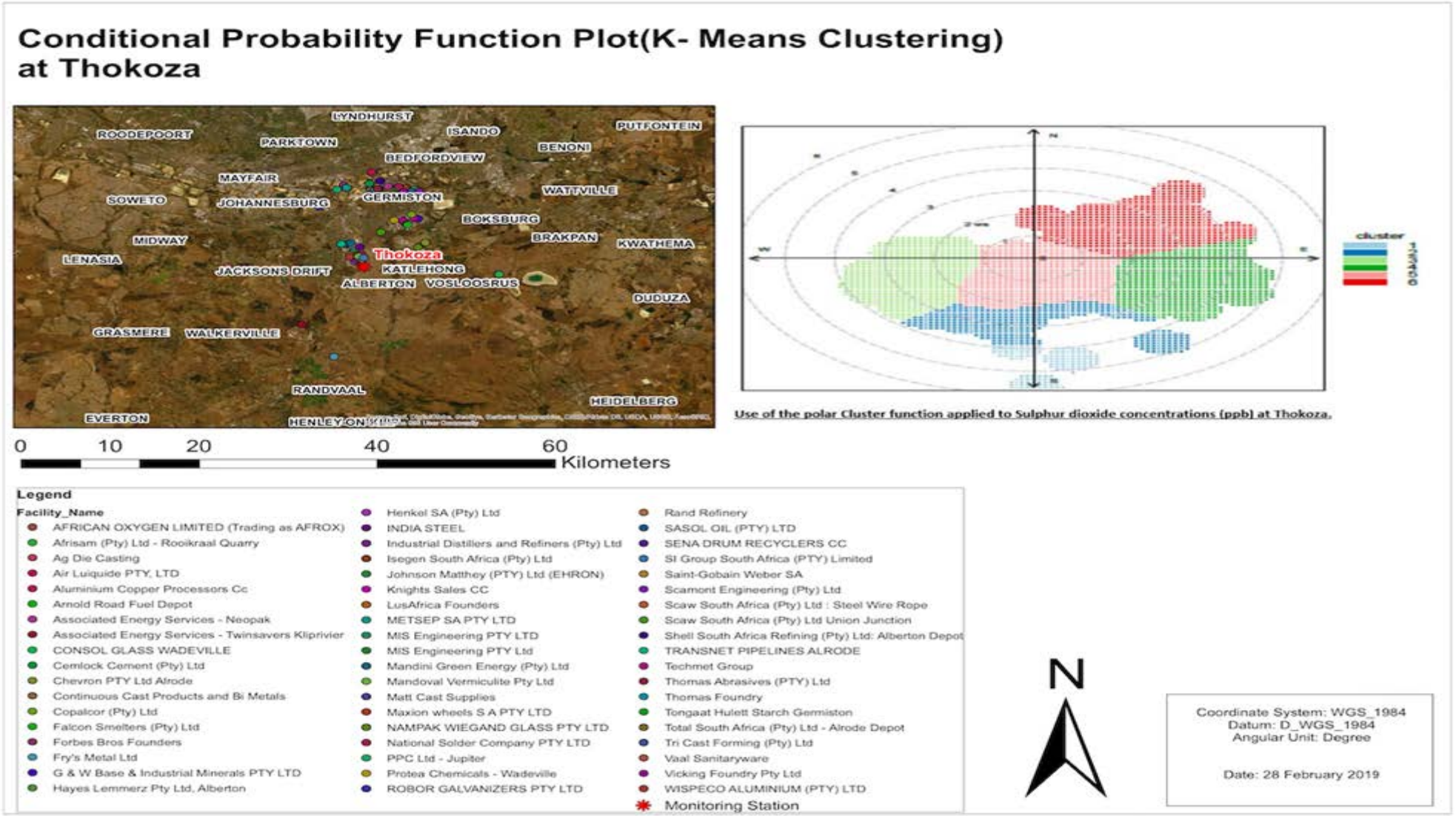

Figure 4.185: Conditional Probability Function Plot (K-Means Clustering) at the Thokoza

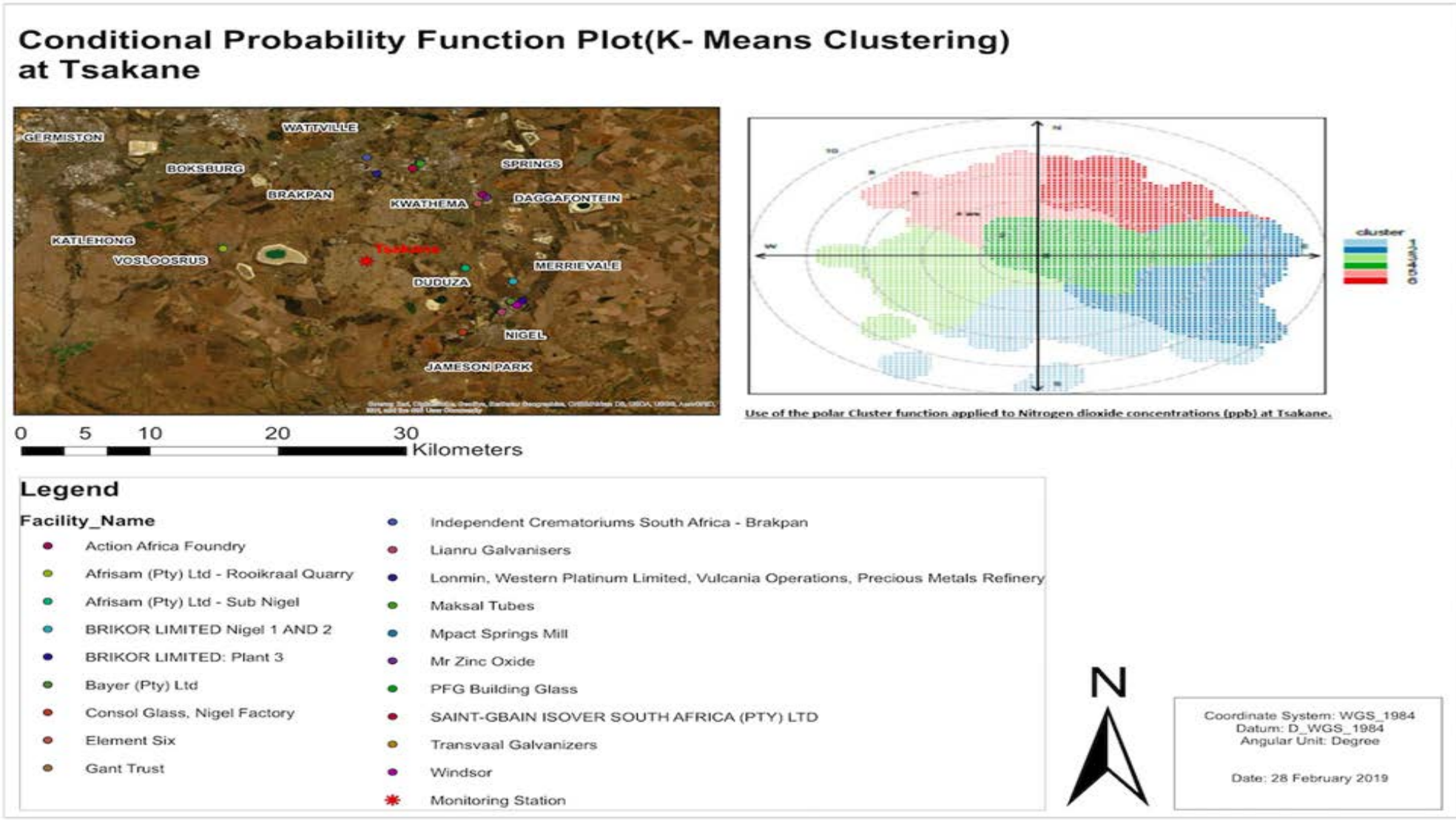

Figure 4.186: Conditional Probability Function Plot (K-Means Clustering) at the Tsakane

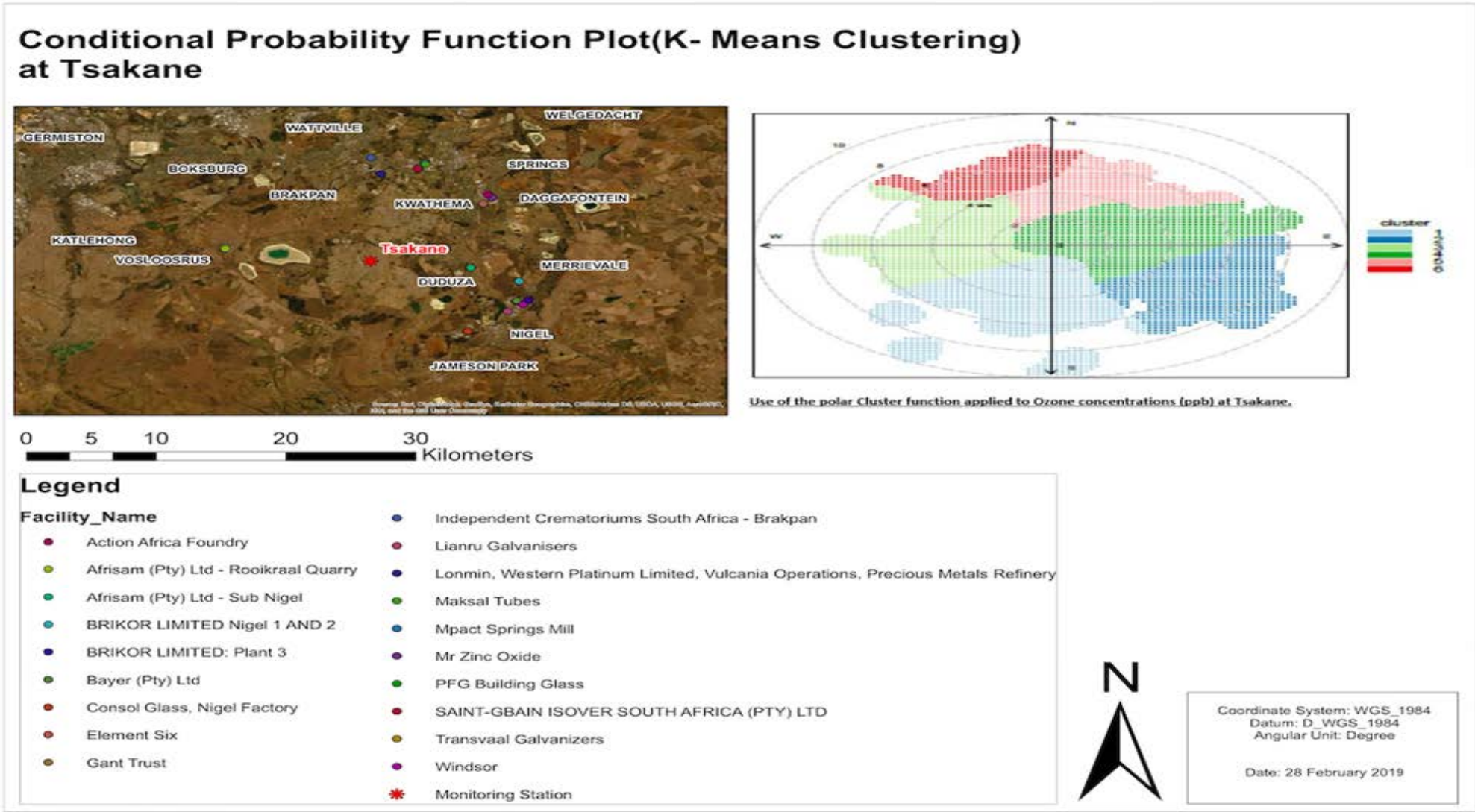

Figure 4.187: Conditional Probability Function Plot (K-Means Clustering) at the Tsakane

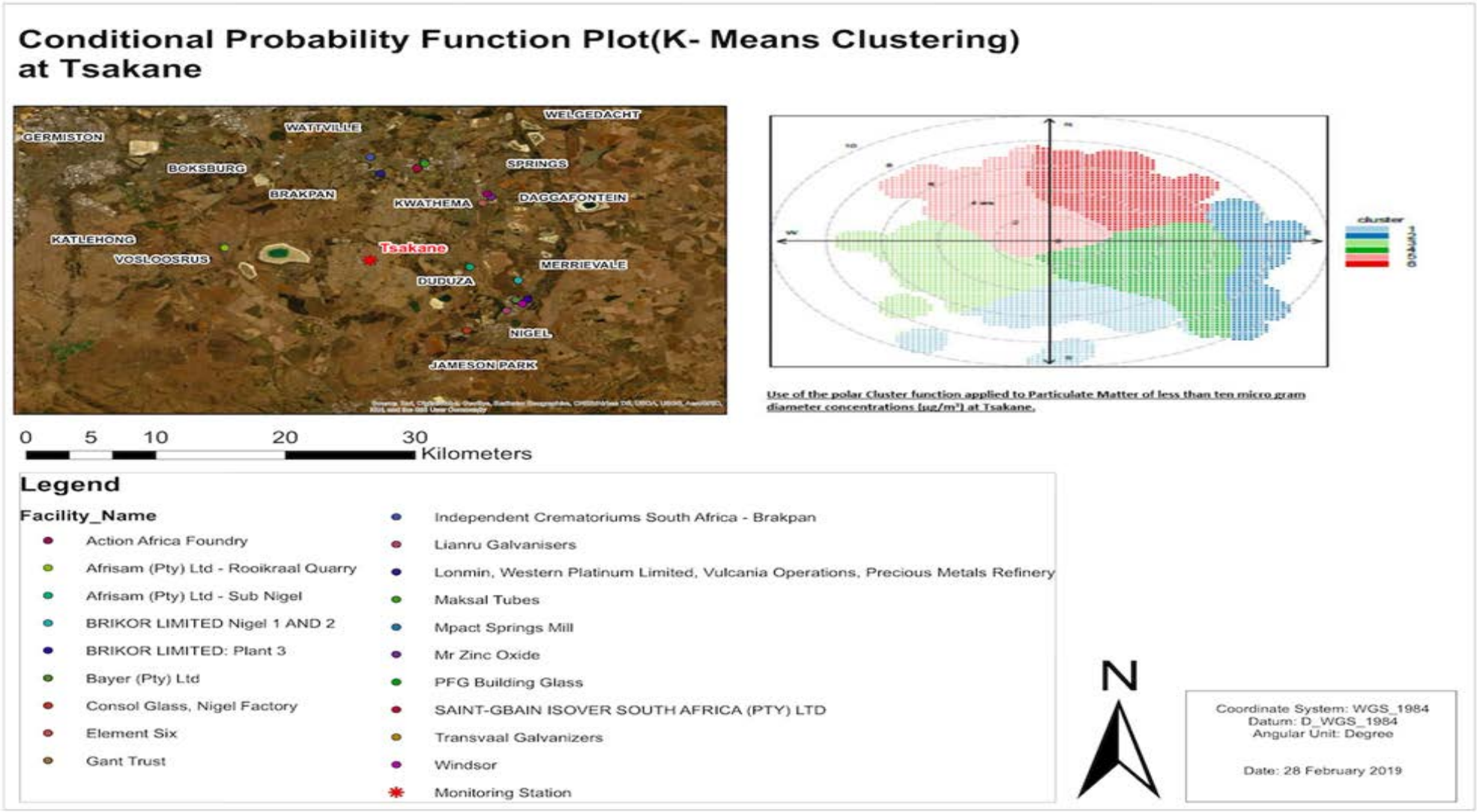

Figure 4.188: Conditional Probability Function Plot (K-Means Clustering) at the Tsakane

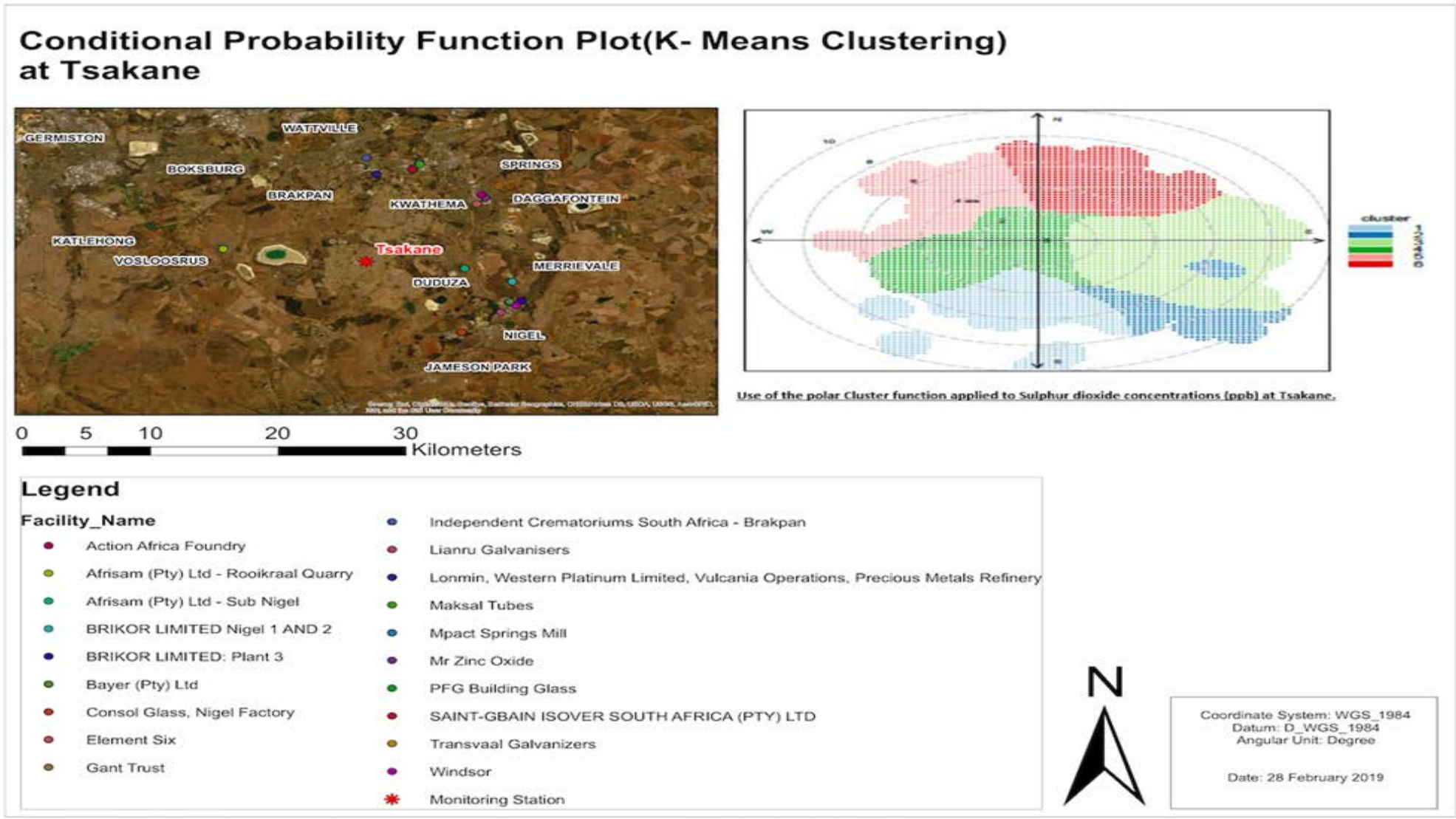

Figure 4.189: Conditional Probability Function Plot (K-Means Clustering) at the Tsakane

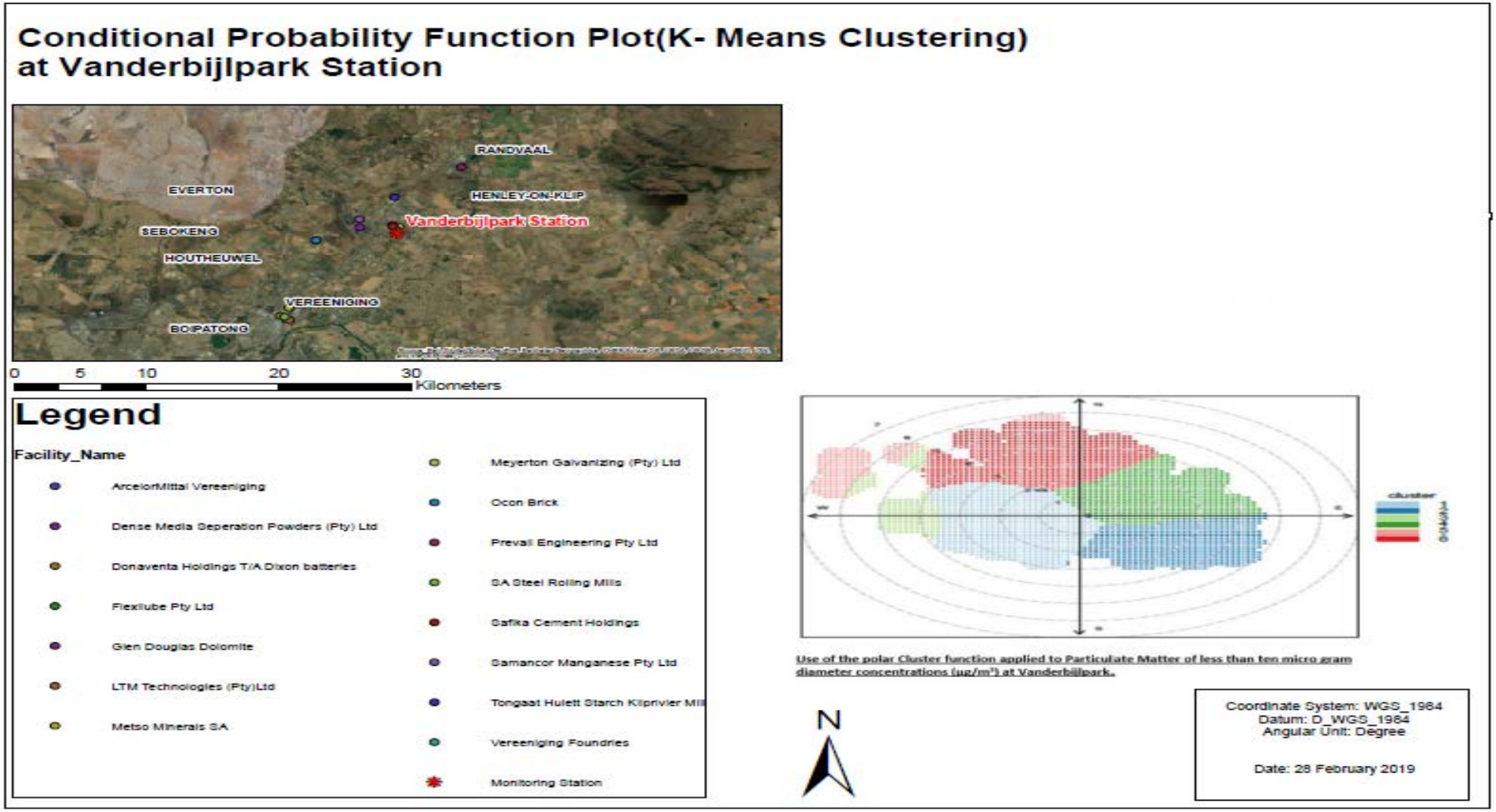

Figure 4.190: Conditional Probability Function Plot (K-Means Clustering) at the Vanderbijlpark

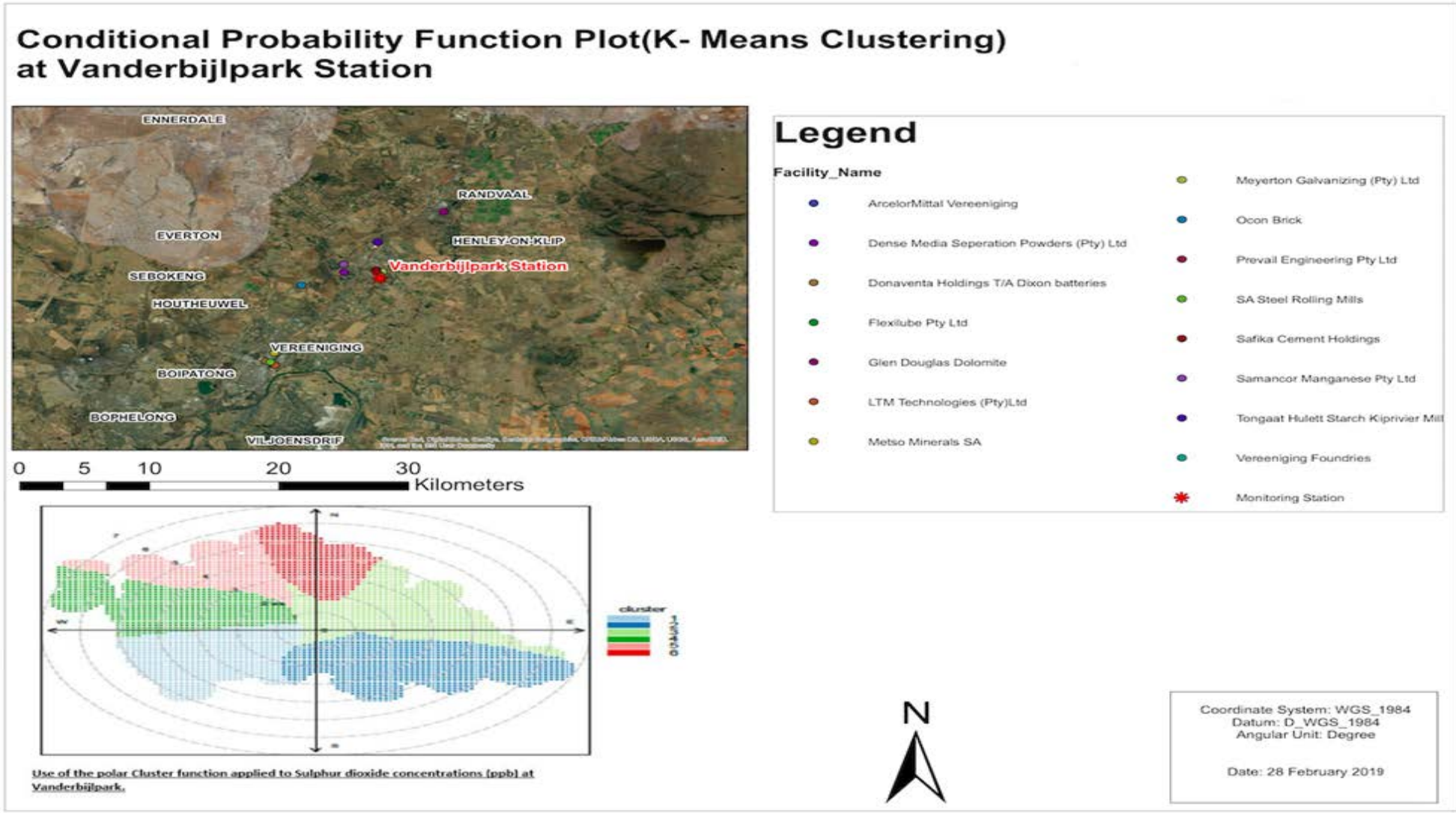

Figure 4.191: Conditional Probability Function Plot (K-Means Clustering) at the Vanderbijlpark

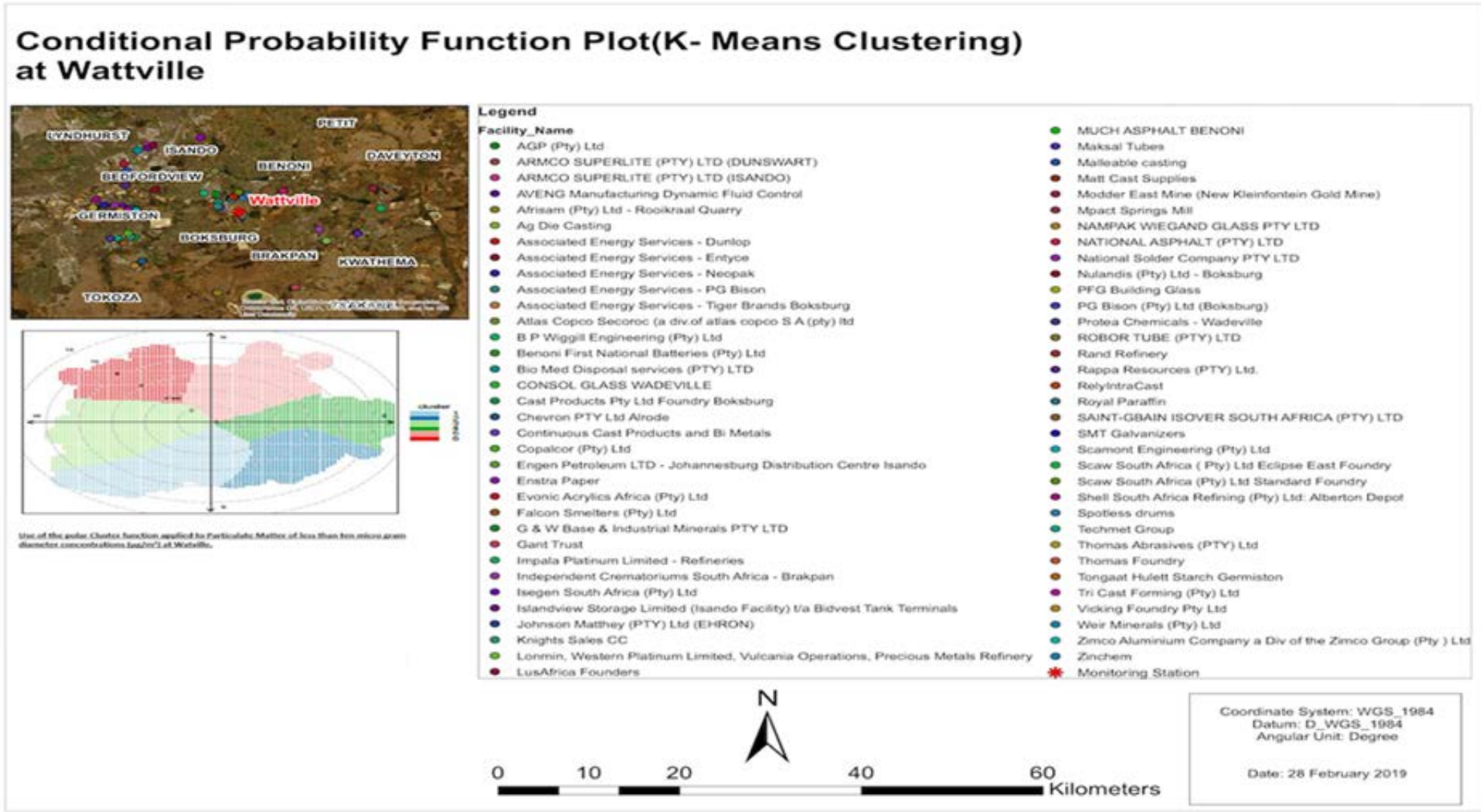

Figure 4.192: Conditional Probability Function Plot (K-Means Clustering) at the Wattville

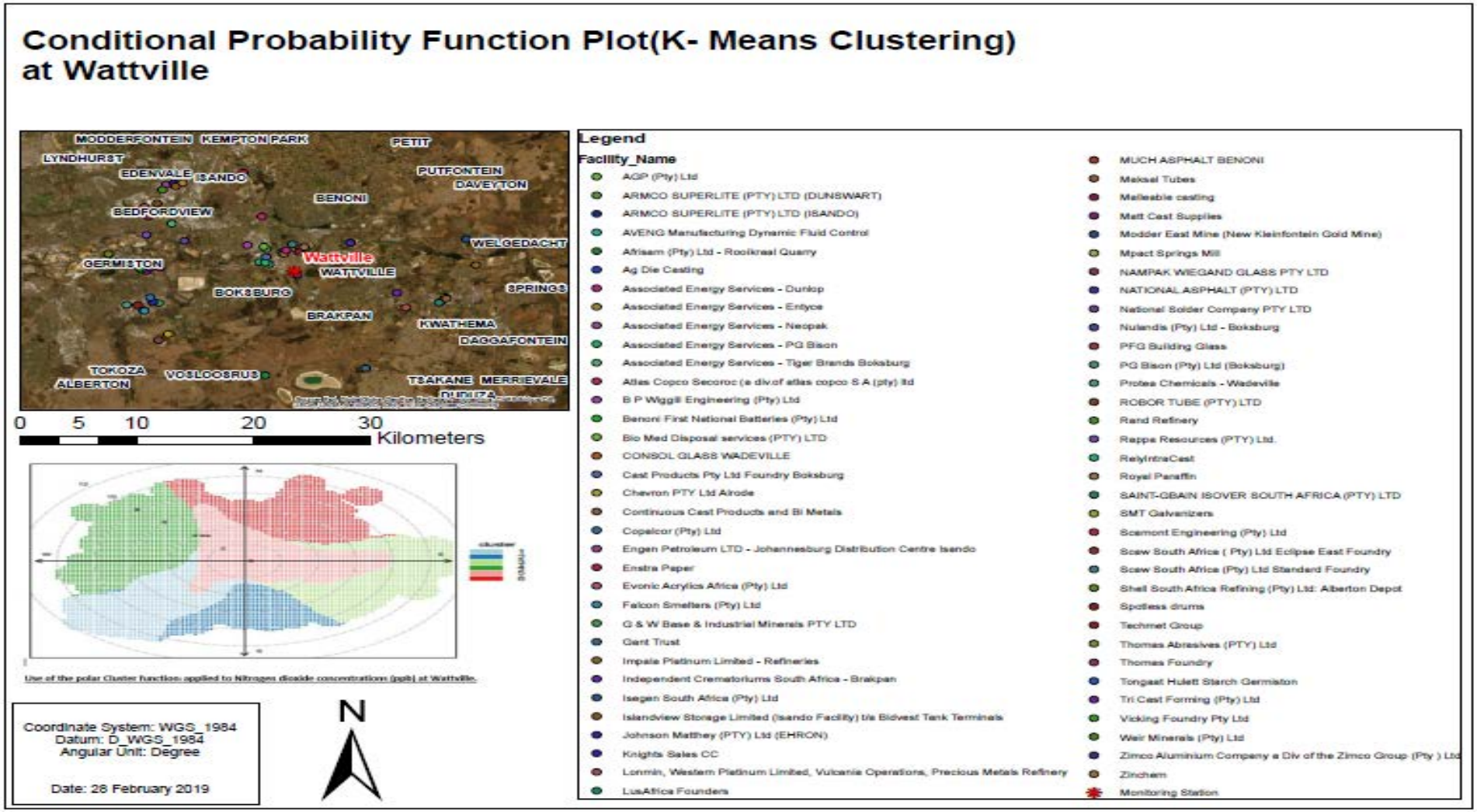

Figure 4.193: Conditional Probability Function Plot (K-Means Clustering) at the Wattville

The Alexandra k-means clustering algorithm in Figure 4.137 was used to classify groups and source detection of PM_{10}. Cluster 6 had a maximum PM_{10} concentration of 48 µg/m^3. Cluster 3 showed the PM_{10} atmospheric concentration cluster near the station at a wind speed of 10 to 15 meters per second in the North-East of the ambient station. Cluster one had a classification of less than 15 µg/m^3, which was centred in the South at less than 5 meters per second. Clusters two and 4 showed ambient concentration groups of 25 µg/m^3.

In Figure 4.138, Bedfordview ambient monitoring station within the City of Johannesburg displayed higher probability of nitrogen dioxide concentrations of 8 parts per billion on the far North-West, West and South-West areas of the ambient station. The maximum ambient concentration of 8 parts per billion was less than the national ambient air quality standard for nitrogen dioxide of 106 parts per billion in average hourly running period at 88 frequency of exceedance. Cluster 4 displayed highest average ambient concentration of fewer than 8 parts per billion. Cluster 5 displayed lowest average ambient concentration of less than 10 parts per billion.

K-means tests at the Bedfordview station indicated a hot spot of PM_{10} in Figure 4.139 on the South-East when the wind speed is more than 6 meters per second. The source emitted an excessive PM_{10} volumes of up to 220 µg/m^3_which exceeded the National Environmental Air Quality Standards for particulate matter of 75 µg/m^3. Figure 4.140 showed the sources for the Western Region of the atmospheric monitoring station with ambient concentrations of up to one hundred and 20 µg/m^3_which still meet the National Environmental Air Quality Requirements for PM_{10}. The results showed that cluster 3 could be the only region to illustrate PM_{10} compliance relative to other clusters.

Figure 4.140 showed that cluster 1 for SO_2 at Bedfordview displayed atmospheric concentrations of up to 25 parts per billion. The highest recorded value for cluster 1 is less than 134 ppb, which is within the National Environmental Air Quality Standard in South Africa. Cluster 4 showed a SO_2 ambient concentration grouping of up to 15 parts per billion, which covered the local East of the Bedfordview ambient monitoring station. Ambient concentrations of less than 5 parts per billion were detected in clusters 2 and 6, respectively. Cluster 5 situated on the centroids of less than 15 parts per billion ambient concentration levels.

In this report, the k-means cluster analysis for Bedfordview showed high concentrations of ozone in cluster 6 in Figure 4.141. This cluster indicated that there is a cluster with less atmospheric concentrations next to the ambient monitoring station. Cluster 1 showed less ambient concentrations of less than 15 parts per billion. Clusters 4 and 5 were situated on the edge of the ozone hot spot on the East and West of the cluster 6. The results showed that the area with higher concentrations of ozone turned out to be the area of lower sulfur dioxide in Bedfordview. This showed that there was no interaction between sulfur dioxide and ozone in terms of the Bedfordview source. This means that the North Wind affected the concentration of ambient ozone at the Bedfordview monitoring station.

The tests of nitrogen dioxide in Figure 4.142 of the Bodibeng Environmental Monitoring Station in the City of Tshwane showed a higher likelihood of nitrogen dioxide concentrations of 38 parts per billion in the Southern Eastern regions. Total atmospheric concentration of 154 parts per billion which was less than the National Environmental Air Quality Standard for nitrogen dioxide of 106 parts per billion in an average hourly running time. Cluster 6 showed the lowest average ambient concentration of less than 10 parts per billion.

In Figure 4.143, the sulfur dioxide results presented by cluster one in the far South-East have the highest ambient concentration cluster with an ambient concentration of less than 10 parts per billion within the City of Tshwane. The maximum ambient concentrations of 10 parts per billion, which were less than 134 parts per billion of the national ambient air quality. Cluster 6 showed similar characteristics with the lowest atmospheric concentrations of less than two parts per billion in the Northern areas of the experimental station.

Booysens bivariate k-means clusters 3 displayed highest probability of nitrogen dioxide concentrations of 23 parts per billion at less than two meters per second of wind speed. Figure 4.144 displayed maximum ambient concentration of 23 parts per billion was less than 106 of national ambient air quality standard for nitrogen dioxide at 88 frequency of exceedance. Cluster 1 and 6 displayed similar characteristics with ambient concentration of fewer than 5 parts per billion.

K-means results at the Booysens ambient monitoring station for ozone pollutants displayed similar characteristics on the cluster 1, 2 and 5 with the highest ambient concentration of 40-two parts per billion. In Figure 4.144 highest ambient concentrations value of ozone were 42 parts per billion which were not exceeding the national ambient air quality standard of 61 parts per billion

in the 8 hours running averaging period at 11 frequency of exceedance. Cluster 4 displayed lowest ambient concentration at the local sources when the wind speed was less than one meter per second.

The k-means clustering algorithm study shows clusters two as the maximum atmospheric PM_{10} concentrations at the Booysens environmental monitoring station in the City of Tshwane. In Figure 4.145, cluster 1 represented an atmospheric concentration of 200 to 400 $\mu g/m^3$ PM_{10}. The highest ambient concentration value of PM_{10} was 650 $\mu g/m^3$ which exceeded the national ambient air quality standard of 75 $\mu g/m^3$ in the daily average period. Clusters 3, 4, 5 and 6 had similar characteristics in the data set. The above-mentioned cluster had an atmospheric concentration of fewer than 80 $\mu g/m^3$ PM_{10}.

K-means results showed a large cluster of sulfur dioxide in the South-West of the Booysens ambient station situated in the City of Tshwane. The results in Figure 4.145 showed the highest ambient concentration recorded in cluster 3 was 7 parts per billion. The maximum atmospheric concentration of sulfur dioxide was 7 parts per billion, which is less than the national ambient air quality standard of 134 parts per billion in the hourly average. Clusters 1, 5 and 6 have similar characteristics in the data collected.

Booysens bivariate k-means cluster 3 has the highest likelihood of nitrogen dioxide concentrations of 23 parts per billion at less than 2 meters per second. Figure 4.146 showed a maximum ambient concentration of 23 parts per billion fewer than 106 of the National Environmental Air Quality Standard for nitrogen dioxide at a frequency of 88. Clusters 1 and 6 had similar characteristics with an ambient concentration of fewer than 5 parts per billion.

K-means findings at Buccluech ambient ozone pollutants monitoring station showed similar characteristics in clusters 1, 2 and 5 with the maximum atmospheric concentration of 42 parts per billion. In Figure 4.146, the maximum atmospheric concentrations of ozone were 42 parts per billion, which did not exceed the national ambient air quality standard of 61 parts per billion in the 8-hour average of the 11 frequencies overrun season. Cluster 4 showed the lowest ambient concentration at local sources when the wind speed was less than one meter per second.

Figure 4.147 showed clusters two as the highest ambient PM_{10}. Cluster 1 displayed average atmospheric concentrations of 125 $\mu g/m^3$ PM_{10}. Clusters 3, 4 and 5 had similar characteristics of ambient air concentrations of fewer than 50 $\mu g/m^3$ PM_{10}. The tests of the sulfur dioxide atmospheric pollutant at the Buccleuch ambient monitoring station in the City of Johannesburg

showed a high ambient value of cluster 4 with an ambient concentration of 20 parts per billion. Figure 4.147 showed the highest ambient concentrations of sulfur dioxide of 20 parts per billion, which was less than the national ambient air quality standard of 125 parts per billion in the hour-long average. Clusters 1 and 5 had the lowest atmospheric concentration value of less than 10 parts per billion.

The K-means clustering algorithm analysis showed that cluster 2 as the highest ambient concentrations of 120 $\mu g/m^3$ PM_{10} at the Davidsonville ambient monitoring station within the City of Johannesburg. Cluster 2 displayed maximum ambient concentrations of 125 $\mu g/m^3$ of PM_{10}. Figure 4.148 showed the highest ambient concentrations value of particulate matter 125 $\mu g/m^3$ of PM_{10} which was exceeding the national ambient air quality standard of 75$\mu g/m^3$ in the daily averaging period at 4 frequency of exceedance. Cluster 1 and 5 displayed similar characteristics of the ambient air concentrations of less than 50 $\mu g/m^3$ of PM_{10}.

The results of Ozone pollutants at the Delta Park ambient monitoring station within the City of Johannesburg displayed clusters 1 and 4 as the highest ambient concentration clusters at 38 parts per billion in Figure 4.149. The highest ambient concentrations value of Ozone were 38 parts per billion which were less than the national ambient air quality standard of 61 parts per billion in the 8 hours running averaging period at 11 frequency of exceedance. Cluster 5 displayed lowest ambient concentration area when the wind speed was more than 2 meters per second situated on the Eastern areas.

Results of K-means clustering algorithm analysis further revealed that cluster one as the highest ambient concentrations of 150 $\mu g/m^3$ of PM_{10} at the Diepsloot ambient monitoring station within the City of Johannesburg designed to monitor domestic fuel burning pollution. Cluster one displayed maximum ambient concentrations of 150 $\mu g/m^3$ of PM_{10}. Figure 4.150 displayed the highest ambient concentrations value of PM_{10} of 1504 $\mu g/m^3$ which was exceeding the national ambient air quality standard of 75 $\mu g/m^3$ in the daily averaging period at 4 frequency of exceedance. Cluster 4, 5 and 6 displayed similar characteristics of the ambient air concentrations of fewer than 50 $\mu g/m^3$.

Figure 4.151 showed the results of Ozone pollutants at the Ekandustria ambient monitoring station within the City of Tshwane and displayed clusters two, 3, 5 and 6 as the highest ambient concentration clusters at 63 parts per billion. The highest ambient concentrations value of Ozone were 63 parts per billion which exceeded the national ambient air quality standard of 61 parts per

billion in the 8 hours running averaging period at 11 frequency of exceedance. Cluster 1 and 4 displayed lowest ambient concentration area of less than 40 parts per billion.

The results of Sulfur dioxide ambient pollutants at the Ekandustria ambient monitoring station within the City of Tshwane displayed high cluster of Sulfur dioxide ambient value at cluster two with the ambient concentration value of 10 parts per billion. In Figure 4.152, the highest ambient concentrations value of Sulfur dioxide were 10 parts per billion which were less than the national ambient air quality standard of 134 parts per billion in the hourly run average period at 88 frequency of exceedance. Cluster 6 displayed lowest ambient concentration value of less than 3 parts per billion.

The K-means clustering algorithm analysis showed that cluster two as the highest ambient concentrations of 120 $\mu g/m^3$ of PM_{10} as described in Figure 4.152 from Ekandustria ambient monitoring station. Cluster 2 displayed maximum ambient concentrations of 450 $\mu g/m^3$ of PM_{10}. The highest ambient concentrations value of PM_{10} of 450 $\mu g/m^3$ which was exceeding the national ambient air quality standard of 75 $\mu g/m^3$ in the daily averaging period at 4 frequency of exceedance. Cluster 3 and 5 displayed similar characteristics of the ambient air concentrations of fewer than 50 $\mu g/m^3$.

In Figure 4.153, K-means clustering algorithm analysis showed that cluster two as the highest ambient concentrations of 320 $\mu g/m^3$ of PM_{10} at the Etwatwa ambient monitoring station within the City of Ekurhuleni designed to monitor domestic fuel burning activities. Cluster 3 and 5 displayed maximum ambient concentrations of 320 $\mu g/m^3$ of PM_{10}. The highest ambient concentrations value of 320 $\mu g/m^3$ of PM_{10} exceeded the national ambient air quality standard of 75 $\mu g/m^3$ of PM_{10} in the daily averaging period at 4 frequency of exceedance. Cluster 2 displayed lowest ambient concentrations of fewer than 50 $\mu g/m^3$ of PM_{10}.

The results of nitrogen dioxide at the Etwatwa ambient monitoring station within the City of Ekurhuleni displayed higher probability of nitrogen dioxide concentrations on the Southern areas when the wind speed reached 6 meters per second of one hundred and 40 parts per billion at less than 2 meters per second. The maximum ambient concentration was one hundred and 40 parts per billion in Figure 4.153 which exceeded the national ambient air quality standard for nitrogen dioxide at 88 frequency of exceedance. Clusters 3 and 4 displayed similar characteristics with ambient concentration of fewer than 40 parts per billion.

The results of Sulfur dioxide ambient pollutants in Figure 4.154 at the Etwatwa ambient monitoring station within the City of Ekurhuleni displayed high cluster of sulfur dioxide ambient value at cluster 5 with the ambient concentration value of 28 parts per billion. The highest ambient concentrations value of Sulfur dioxide were 28 parts per billion which were less than the national ambient air quality standard of 134 parts per billion in the hourly run average period at 88 frequency of exceedance. Cluster 3 displayed lowest ambient concentration value of less than 10 parts per billion.

In Figure 4.155, the results at the Germiston ambient monitoring station of nitrogen dioxide pollutants at cluster 5 within the City of Ekurhuleni displayed higher probability of nitrogen dioxide concentrations at the local area. The maximum ambient concentration of 24 parts per billion which were less than the national ambient air quality standard for nitrogen dioxide of 106 parts per billion at 88 frequency of exceedance. Cluster 2 and 3 displayed lowest ambient concentration of fewer than 10 parts per billion.

The results of Sulfur dioxide ambient pollutants at the Germiston ambient monitoring station within the City of Ekurhuleni displayed high cluster of sulfur dioxide ambient value at cluster 5 with the ambient concentration value of 15 parts per billion as presented in Figure 4.156. The highest ambient concentrations value of Sulfur dioxide were 15 parts per billion which were less than the national ambient air quality standard of 134 parts per billion in the hourly run average period at 88 frequency of exceedance. Cluster 2, 3 and 6 displayed lowest ambient concentration value of less than 4 parts per billion.

Figure 4.157 displayed K-mean results of Sulfur dioxide ambient pollutants at the Ivory Park ambient monitoring station within the City of Johannesburg displayed high cluster of Sulfur dioxide ambient value at cluster 1 and 3 with the ambient concentration value of 6 parts per billion. The highest ambient concentrations value of Sulfur dioxide were 6 parts per billion which were less than the national ambient air quality standard of 134 parts per billion in the hourly run average period at 88 frequency of exceedance. Cluster 2, 4 and 6 displayed lowest ambient concentration value of less than 3 parts per billion.

The K-means clustering algorithm analysis showed that cluster one and 6 are the highest ambient concentrations cluster with the ambient concentration of 190 $\mu g/m^3$ of PM_{10} at the Ivory Park ambient monitoring station within the City of Johannesburg designed to monitor domestic fuel burning activities. In Figure 4.157, the maximum ambient concentrations of 190 $\mu g/m^3$ of

PM_{10} exceeded the national ambient air quality standard of 75 µg/m^3 of PM_{10} the daily averaging period at 4 frequency of exceedance. Cluster 2 and 5 displayed lowest ambient concentrations of less 50 µg/m^3 of PM_{10}. Cluster 4 displayed the lowest ambient concentrations of fewer than 60 µg/m^3 of PM_{10}.

The results of Ozone pollutants at the Jabavu ambient monitoring station within the City of Johannesburg displayed clusters one, two and 3 as the highest ambient concentration clusters at 58 parts per billion. Figure 176 the highest ambient concentrations value of Ozone was 58 parts per billion which were less than the national ambient air quality standard of 61 parts per billion in the 8 hours running averaging period at 11 frequency of exceedance. Cluster 6 displayed local area sources at lowest ambient concentrations area of less than 25 parts per billion.

Figure 4.158 the ambient results of K-means clustering algorithm techniques presented cluster 4 as the highest ambient concentrations cluster with the ambient concentration of 160 µg/m^3 of PM_{10} at the Jabavu ambient monitoring station within the City of Johannesburg designed to monitor domestic fuel burning activities. The maximum ambient concentrations of 160 µg/m^3 of PM_{10} exceeded the national ambient air quality standard of 75 µg/m^3 of PM_{10} in the daily averaging period at 4 frequency of exceedance. Cluster 5 displayed the lowest ambient concentrations of fewer than 40 µg/m^3 of PM_{10}.

The results of sulfur dioxide ambient pollutants at the Jabavu ambient monitoring station within the City of Johannesburg displayed high cluster of Sulfur dioxide ambient value at cluster 5 with the ambient concentration value of 5 parts per billion. Figure 4.159 the highest ambient concentrations value of Sulfur dioxide was 5 parts per billion which were less than the national ambient air quality standard of 134 parts per billion in the hourly run average period at 88 frequency of exceedance. Clusters 3 and 4 displayed lowest ambient concentration value of less than 2 parts per billion.

The results of Ozone pollutants at the Leondale ambient monitoring station within the City of Tshwane displayed clusters 6 as the highest ambient concentration clusters at 60 parts per billion. Figure 4.160 the highest ambient concentrations value of ozone was 60 parts per billion which were less than the national ambient air quality standard of 61 parts per billion in the 8 hours running averaging period at 11 frequency of exceedance. Cluster 1 display local area source at lowest ambient concentrations area of less than 30 parts per billion.

In Figure 4.160,the results of nitrogen dioxide at the Leondale ambient monitoring station within the City of Ekurhuleni displayed higher probability of nitrogen dioxide concentrations of 29 parts per billion when the wind speed is less than 2 meters per second around the station except on the South-East area at the wind speed of less than 4 meters per second. The maximum ambient concentration of 29 parts per billion which were less than 106 parts per billion national ambient air quality standard for nitrogen dioxide at 88 frequency of exceedance. Cluster 1 displayed similar characteristics area with ambient concentration of less than 10 parts per billion.

The results of Sulfur dioxide K-means cluster for the ambient concentrations at the Leondale ambient monitoring station within the City of Ekurhuleni displayed highest cluster 4 of sulfur dioxide ambient value with the ambient concentration value of 24 parts per billion as presented in Figure 4.161. The highest ambient concentrations value of Sulfur dioxide were 204 parts per billion which were less than the national ambient air quality standard of 134 parts per billion in the hourly run average period at 88 frequency of exceedance. Cluster 1, 3 and 6 displayed lowest ambient concentration value of less than 6 parts per billion.

In Figure 4.162 results of nitrogen dioxide at the Mamelodi ambient monitoring station within the City of Tshwane displayed higher probability of nitrogen dioxide concentrations of 40-one parts per billion represented by cluster one when the wind speed is less than two meters per second around the air quality ambient station at the local area and Far Western areas when the wind picked at 4 meters per second. The maximum ambient concentration of 41 parts per billion which were less than 106 parts per billion national ambient air quality standard for nitrogen dioxide at 88 frequency of exceedance. Clusters 4 and 6 displayed similar characteristics area with ambient concentration of fewer than 10 parts per billion.

The results of Sulfur dioxide K-means cluster for the ambient concentrations at the Mamelodi ambient monitoring station within the City of Tshwane displayed high ambient concentration value at clusters two and 5 of 10 parts per billion. Figure 4.162 displayed clusters with the lowest ambient concentrations value of less than 4 and 5 parts per billion at cluster one and 5 respectively. The highest displayed cluster two with the ambient concentration of 10 parts per billion was less than the national ambient air quality standard of 134 parts per billion in the hourly run average period at 88 frequency of exceedance. Cluster one and 5 displayed similar characteristics of lower ambient concentration areas of less than 5 parts per billion.

The results of Ozone pollutants at the Mamelodi ambient monitoring station within the City of Tshwane displayed cluster 6 as the highest ambient concentration clusters at 250 parts per billion. Figure 4.163 has the highest ambient concentrations value of Ozone were two hundred and 50 parts per billion which exceeded the national ambient air quality standard of 61 parts per billion in the 8 hours running averaging period at 11 frequency of exceedance. Cluster 1, 2, 3 and 4 display similar characteristic area sources at lowest ambient concentrations of fewer than seventy parts per billion.

In Figure 4.163 results of K-means clustering algorithm techniques presented cluster 6 as the highest ambient concentrations cluster with the ambient concentration of 580 $\mu g/m^3$ of PM_{10} at the Mamelodi ambient monitoring station within the City of Tshwane designed to monitor domestic fuel burning activities. Clusters 1 and 4 displayed similar characteristics with the lowest ambient concentrations of fewer than 100 $\mu g/m^3$ of PM_{10}. Cluster 2 and 5 displayed similar characteristics with the ambient concentrations of fewer than 200 $\mu g/m^3$ of PM_{10}.

In Figure 4.164, PM_{10} at the Meyerton within the Sedibeng District Municipality with the maximum ambient concentrations of 75 $\mu g/m^3$ of PM_{10}.The sources clustered at number 4 are emitting maximum ambient concentrations of 75 $\mu g/m^3$ of PM_{10} on the North-West and when the wind speed picked at 6 meters per second. Lowest ambient concentrations were found in cluster 3 with less than 30 parts per billion.

Figure 4.165 displayed maximum ambient concentrations of 75 parts per billion and K-means resulted on cluster one situated at South-East of the ambient monitoring station when the wind speed ranged between 2 and 4 meters per second. The highest ambient concentrations value of ozone in 8 hourly average were 75 parts per billion which exceeded the national ambient air quality standards for Ozone of 61 parts per billion for 11 frequency of exceedance. Cluster 2 displayed ambient concentration of less than 30 parts per billion.

Meyerton ambient monitoring station displayed clusters 4 on the maximum ambient concentration of 17 parts per billion Sulfur dioxide. In Figure 4.165 has the highest ambient concentrations value of Sulfur dioxide in the hourly average were 16 parts per billion which is far less of the national ambient air quality standards for Sulfur dioxide of 134 parts per billion for 88 frequency of exceedance. Cluster 1 and 6 displayed similar characteristics with ambient concentration of fewer than 4 parts per billion.

Ozone pollutants at the Mogale City displayed maximum ambient concentration clusters of 54 parts per billion. In Figure 4.166 cluster 1 and 3 displayed maximum ambient concentration at the Mogale City. The highest ambient concentrations value of ozone in 8 hourly average were 54 parts per billion which is less of the national ambient air quality standards for Ozone of 61 parts per billion for 11 frequency of exceedance. Cluster 3 displayed lowest ambient concentrations cluster of ozone which were less than 30 parts per billion.

Mogale City K-means results for Sulfur dioxide displayed clusters 3 and 5 with the maximum recorded value of 12 parts per billion. Figure 4.167 the highest ambient concentrations value of Sulfur dioxide in the hourly average was 12 parts per billion which is far less of the national ambient air quality standards for Sulfur dioxide of 134 parts per billion for 88 frequency of exceedance. Cluster 1 and 6 displayed lowest sulfur dioxide ambient concentrations of fewer than 5 parts per billion.

In Figure 4.167, PM_{10} at the Mogale City ambient monitoring displayed exceedances of 150 $\mu g/m^3$ of PM_{10}. Cluster 3 displayed maximum ambient particulate matter of 150 $\mu g/m^3$ of PM_{10}.Cluster two displayed range of 60 to 90 PM_{10} ($\mu g/m^3$). Cluster one, 6 and 4 displayed pollutants range not exceeding 60 PM_{10} ($\mu g/m^3$).

Nitrogen dioxide Newtown ambient concentrations displayed maximum ambient concentrations of 31 parts per billion which were clustered at cluster number 3. The Newtown ambient monitoring station is situated in the City of Johannesburg. Figure 4.168 had the highest ambient concentrations value of nitrogen dioxide of 32 parts per billion in an hourly average of 106 parts per billion with 88 frequency of exceedance. Cluster 1 had the lowest ambient monitoring ambient concentrations of fewer than 5 parts per billion.

In Figure 4.169, PM_{10} at the Newtown displayed highest ambient concentration cluster. The highest ambient concentrations value of 44 $\mu g/m^3$ of PM_{10} daily average period did not exceed the national ambient air quality standards of 75 ($\mu g/m^3$) at 4 frequency of exceedance. Cluster 1 and 3 displayed a minimum ambient concentration of fewer than 15 $\mu g/m^3$.

Clustering sources identification using K-means method was also conducted at the Olievenhoutbosch within the City of Tshwane. Cluster 4 revealed maximum value of 27 parts per billion. The highest reported ambient concentration which was situated at cluster 4. Figure 4.170 has the highest ambient concentrations value of nitrogen dioxide of 27 parts per billion in an hourly of 106 parts per billion and have 88 frequency of exceedance. Cluster 3, 5 and 6 displayed less

ambient concentrations compared with the areas at cluster one and two. The highest ambient concentrations value of nitrogen dioxide of 25 parts per billion average hourly period not exceeding the national ambient air quality standards of Republic of South Africa of 106 parts per billion at 88 frequency of exceedance.

Figure 4.170 has the highest ambient concentrations of Ozone pollutants of 300 parts per billion display at cluster 6 which is situated at far North-West when the wind speed counts to 8 to 10 meters per second. The station is situated at the Olievenhoutbosch within the City of Tshwane, Gauteng, South Africa. The highest ambient concentrations value of Ozone 300 parts per billion in an hourly average of not exceeding 88 frequency of exceedance. Cluster 3 displayed lowest ambient concentration fewer than 50 parts per billion.

Olievenhoutbosch ambient monitoring station is situated within the city of Tshwane and was designed to monitor pollutants from domestic fuel burning as presented in Figure 4.171. Cluster two displayed maximum sulfur dioxide ambient concentrations of 18 parts per billion. The highest ambient concentrations value of Sulfur dioxide in the average hourly period was 18 parts per billion which did not exceed the national ambient air quality standards of 134 parts per billion. Cluster 6 and 3 displayed lowest ambient concentration of fewer than 4 parts per billion.

Ambient air quality clusters 4 which was situated on the North-West at the wind speed of 8 to 10 meters per second.

In Figure 4.172, PM_{10} at the Orange Farm displayed maximum ambient concentrations of 850 $\mu g/m^3$ of PM_{10}. Orange Farm is situated at the City of Johannesburg and the ambient station was designed to monitor domestic fuel burning. The highest ambient concentrations value of PM_{10} in the average hourly period of 850 $\mu g/m^3$ which did exceed the national ambient air quality standards of 134 with 88 frequency of exceedance. Cluster 1, 5 and 6 displayed lowest ambient concentration of less than ambient standards.

Results for K-means for ozone ambient concentrations in Figure 4.172 revealed clusters 4 and 5 as the most Ozone concentrated areas which recorded a maximum of 65 parts per billion. The station is situated within the City of Johannesburg. The highest ambient concentrations value of ozone for 8 average hourly period of 65 parts per billion which was exceeding the national ambient air quality standards of Republic of South Africa of 61 parts per billion at 11 frequency of exceedance. Cluster 3 demonstrated fewer than 30 parts per billion Ozone ambient concentrations.

Figure 4.173 presented K-means of Sulfur dioxide results at the Orange Farm within the City of Johannesburg displayed maximum ambient concentrations of 7 parts per billion. Cluster 2 displayed highest concentration value of 7 parts per billion which is not exceeded the national ambient air quality standards of Republic of South Africa of 134 with 88 frequency of exceedance. Cluster 1, 4 and 6 displayed lowest ambient concentrations of fewer than 3 parts per billion.

Nitrogen dioxide at the Pretoria West ambient station amounted to 44 parts per billion which is represented by cluster number 4. In Figure 4.174, the highest ambient concentrations value of nitrogen dioxide in the hourly averaging period of 44 parts per billion did not exceed the national ambient air quality standards of Republic of South Africa of 106 parts per billion at 88 frequency of exceedance. Cluster 1 and 2 had fewer than 25 parts per billion ambient concentration. Cluster 5 and 6 showed an ambient concentration of fewer than 10 parts per billion.

Results in Figure 4.175 showed cluster 6, 5 and 3 displayed maximum Ozone ambient concentrations of 74 parts per billion which exceeded the national ambient air quality standards of Republic of South Africa of 61 parts per billion. Maximum recorded Ozone ambient concentrations were detected at wind speed of two meters per second. Cluster 1 displayed 62 parts per billion which is just above ozone national ambient air quality standards of 61 parts per billion. Clusters 2 and 4 showed lowest ambient concentration areas of fewer than 50 parts per billion.

Figure 4.176, Sulfur dioxide ambient concentrations displayed highest clusters with ambient concentration not exceeding 17 parts per billion. The highest ambient concentrations value of Sulfur dioxide in the average hourly period of 17 parts per billion did not exceed the national ambient air quality standards of Republic of South Africa of 134 with 88 frequency of exceedance. Clusters 2 and 6 had the lowest Sulfur dioxide dispersion of less than 2 meters per second.

Clustering sources identification using K-means method at the Randfontein in the West Rand District Municipality showed that cluster 5 had a maximum value of 16 parts per billion. The highest reported ambient concentration was at clusters 5 and 4 situated on the North-East and North 4 respectively. Figure 4.177 had the highest ambient concentrations value of nitrogen dioxide of 16 parts per billion in an hourly of one hundred and 6 parts per billion and 88 frequency of exceedance. Cluster one and two had the lowest ambient concentration of fewer than 4 parts per billion on cluster 1 and 2.

PM_{10} at the Randfontein displayed high exceedance with the maximum PM_{10} value of 350 parts per billion. Figure 4.178 had the highest ambient concentrations value of PM_{10} in the hourly

average at 350 parts per billion which is more than the national ambient air quality standards. Cluster 3, 1 and 4 displayed PM_{10} less than 50 $\mu g/m^3$.

Figure 4.178, Sulfur dioxide ambient concentrations displayed highest clusters with ambient concentration not exceeding 13 parts per billion. Randfontein ambient monitoring station is situated within West Rand District Municipality, Gauteng, South Africa. The highest ambient concentrations value of Sulfur dioxide was 13 parts per billion which was less than the national ambient air quality standards of Republic of South Africa of 134 with 88 frequency of exceedance. Cluster 2 and 1 had the lowest Sulfur dioxide dispersion of fewer than 6 parts per billion.

At the Rosslyn station situated in the City of Tshwane, Figure 4.179 cluster 6 situated on the Northern areas of the ambient station displayed maximum ozone ambient concentrations of up to 70 parts per billion. The highest ambient concentrations value of Ozone in the 8 hourly averaging period were 70 parts per billion which exceeded the national ambient air quality standards of Republic of South Africa for Ozone. Clusters 4 and 6 displayed some exceedance on the clustered data. Cluster 1 displayed less than 30 parts per billion ambient concentrations of Ozone pollutants.

Nitrogen dioxide pollutants recorded maximum ambient concentrations of 28 parts per billion at the Rosslyn station within the City of Tshwane. Figure 4.179 cluster one displayed highest ambient air quality reported at the Rosslyn ambient monitoring station. The highest ambient concentrations value of nitrogen dioxide in the average hourly period were 88 parts per billion which was not exceeding the national ambient air quality standards of Republic of South Africa of 106 parts per billion of nitrogen dioxide. Cluster 5 displayed nitrogen dioxide of less than ambient concentrations of 5 parts per billion.

The K-means results at the Rosslyn ambient monitoring station displayed high ambient concentrations of sulfur dioxide of 25 parts per billion at cluster 6 on the North-West areas and cluster two at 15 parts per billion at the wind speed of 4 to 8 meters per second on the Southern areas. In Figure 4.180 the highest ambient concentrations value of sulfur dioxide in the hourly average were 25 parts per billion that was far less of the national ambient air quality standards for Sulfur dioxide of 134 parts per billion for 88 frequency of exceedance. Cluster 1 and 3 displayed lowest ambient monitoring results of less than 8 parts per billion.

Daily pattern of PM_{10} at the Rosslyn station displayed 240$\mu g/m^3$ of PM_{10}. In Figure 4.180, cluster 6 showed highest clustered areas on the North-West at wind speed of 8 to 12 meters per

second. The highest ambient concentrations value of PM_{10} in the hourly average were 320 µg/m^3 of PM_{10} which was more than of the national ambient air quality standards of Republic of South Africa for 75 µg/m^3 of PM_{10}.

Figure 4.181 results at the Tembisa monitoring station which was situated the City of Ekurhuleni, nitrogen dioxide ambient concentration displayed maximum ambient concentration of nitrogen dioxide at 23 parts per billion. The maximum ambient concentrations of nitrogen dioxide of 23 parts per billion was less than 106 in hourly average of 88 frequency of exceedance. Cluster 2, 4, 5 and 6 displayed lowest nitrogen dioxide ambient concentrations of fewer than 5 parts per billion. The highest ambient concentrations value of nitrogen dioxide in the hourly average were 23 parts per billion which was far less of the national ambient air quality standards for nitrogen dioxide of 106 parts per billion.

The K-means results at the Tembisa displayed highest Sulfur dioxide concentrations in the cluster one which was found on the South when wind speed reached 6 meters per second as presented in Figure 4.182. The highest ambient concentrations value of sulfur dioxide in the hourly average were 25 parts per billion which is far less of the national ambient air quality standards for sulfur dioxide of 134 parts per billion. The second-highest cluster was number clusters 2 which amounted to less than 18 parts per billion. Cluster 3, 4 and 6 displayed less than 5 parts per billion of sulfur dioxide at the Tembisa.

Nitrogen dioxide ambient concentrations at the Thokoza station displayed highest concentrated at cluster 4 which were local area sources. Figure 4.184 has the highest nitrogen dioxide concentrations recorded of 50 parts per billion which was less than on the cluster 4. Cluster 3 and 2 displayed lowest recorded ambient concentration values of less than 50 parts per billion for nitrogen dioxide. Thokoza clusters 1 displayed highest sulfur dioxide ambient concentrations of up to 10 parts per billion for the area situated on the South and concentration can be detected for wind speed of 6 meters per second as presented in Figure 4.185. Cluster 4 and 5 indicated lowest ambient concentration for sulfur dioxide less than one part per billion. The highest ambient concentrations value of sulfur dioxide in the hourly average were 10 parts per billion which was far less of the national ambient air quality standards for sulfur dioxide of 134 parts per billion.

The results at the Tsakane displayed an interesting nitrogen dioxide pattern. Cluster one has minimum emission levels located on the Southern parts of the Tsakane ambient monitoring station and amounting to less than two parts per billion. Figure 4.186 in cluster 3 displayed highest

ambient concentrations of sulfur dioxide of fewer than 8 points 5 parts per billion. The results revealed dense high nitrogen dioxide along East and South-East. Cluster 4 revealed other sources on the South-West when the wind speed was between 3 and 6 meters per second. Tsakane ambient monitoring stations recorded acceptable value which was below the national ambient air quality standard of sulfur dioxide in an hourly average.

The k-means resulted of ozone ambient concentrations at the Tsakane displayed highest cluster number 6 at wind speed of 4 meters per second on the North and North-East areas. In Figure 4.187, cluster 6 had the highest ambient concentration of 60 parts per billion which is less than national ambient air quality standard 61 parts per billion over 8 hours running of 11 frequency of exceedance. Cluster 2 displayed an ambient concentration of fewer than 25 parts per billion. Cluster 1 and 3 displayed ambient concentrations not exceeding 45 parts per billion.

PM_{10} at the Tsakane displayed high exceedance with the maximum PM_{10} value of 90 parts per billion. Figure 4.188 had the highest ambient concentrations value of PM_{10} in the hourly average of 90 parts per billion. Cluster 2 and 5 displayed up to 90 $\mu g/m^3$ of PM_{10}. Cluster 1 displayed an ambient concentration of particulate matter of less than 10 µg/m3.

The k-means results at the Tsakane ambient monitoring station situated in the City of Johannesburg displayed high ambient concentrations of sulfur dioxide of 8 parts per billion at cluster 3 on the North-East, East and South-East areas. Cluster 4 had higher probability of 8 parts per billion on the North, North-West, West and South-West of the ambient monitoring station. Figure 4.189 displayed the highest ambient concentrations value of sulfur dioxide in the hourly average of fewer than 8 parts per billion at cluster 1 which was far less than the national ambient air quality standards for sulfur dioxide of 134 parts per billion for 88 frequency of exceedance. Cluster 1 and 6 displayed lowest ambient monitoring results of fewer than 2 parts per billion.

Figure 4.190 results displayed high value of 1000 $\mu g/m^3$ of PM_{10} at cluster 6, 3 and 5 at the Vanderbijlpark ambient monitoring stations. This area falls under Vaal Triangle Air-Shed Priority Area. When the wind speed picked at 4 meter per second on the Western Area, North-West and North displayed ambient concentration not exceeding 600 $\mu g/m^3$ of PM_{10}.

In Fig 4.191, the results of sulfur dioxide at the Vanderbijlpark ambient monitoring station displayed different clusters, however, cluster 6 was detected on the Northern area at the wind speed of 2 meters per second and above. Cluster 6 displayed maximum ambient concentration of 26 parts per billion which is fewer than 134 parts per billion. Cluster two displayed maximum ambient

concentrations of not more than 20 parts per billion. Cluster 1 and 3 had fewer than 5 parts per billion situated on the South-West and North-West respectively.

Figure 4.192 displayed maximum ambient concentration at the Wattville station of about 110 $\mu g/m^3$ of PM_{10}. Highest reported clusters are 3, 6 and 5 which were South-West clockwise movement to the Eastern side of the Wattville ambient station.

The k-means clustering 5 at the Wattville ambient monitoring station identified and characterized emission sources for nitrogen dioxide pollutants. Figure 4.193 results showed clusters 5 as the highest concentrations distribution of ambient nitrogen dioxide on the Eastern area of the ambient station when the wind speed was at 8 meters per second. The maximum ambient concentrations never exceeding the national ambient air quality standards for nitrogen dioxide of 134 parts per billion at the maximum concentration of 32 parts per billion. Another cluster displayed fewer than 15 parts per billion at cluster 6 at the Northern area, 2 at the Southern area and 4 on the Western Area of the ambient station.

4.5. Summary of the results and discussions Chapter

4.5.1 Correlations

The results displayed strong positive correlation of benzene and toluene concentration sources in most of Gauteng ambient monitoring. Springs ambient monitoring stations displayed a very strong positive correlation of relative humidity and wind speed. Wind speed and wind direction results displayed strong positive correlation. Oxides of nitrogen at displayed very strong positive correlation of either nitrogen dioxide or nitrogen monoxide. Wind speed and ozone pollutants revealed strong positive correlation at the Buccleuch ambient monitoring stations. At the Buccleuch ambient monitoring stations, Carbon monoxide concentration displayed strong positive correlation with the ambient pressure and ambient pressure displayed moderate strong positive correlation with either nitrogen monoxide, oxides of nitrogen or relative humidity. Delta Park, ozone ambient concentrations had a strong positive correlation and relative humidity, furthermore, wind direction had a strong positive correlation either relative humidity or ozone concentrations. At the Delta Park, ambient pressure had a strong positive correlation either with relative humidity, ozone pollutant or wind direction. Rain at the Delta Park had a strong positive correlation either relative humidity, ozone, wind direction or ambient pressure. The wind speed at the Delta Park had a strong positive correlation either ozone pollutant, solar radiation, rain or ambient pressure. At the Newtown ambient monitoring station there was a strong positive correlation between rain recorded and nitrogen monoxide concentration. At the Pretoria West ambient monitoring station ambient pressure displayed strong positive correlation either with wind direction or solar radiation.

Pretoria West ambient PM_{10} results had no correlation with Etwatwa ambient monitoring stations. Randfontein PM_{10} ambient results had no correlation with Mamelodi ambient monitoring stations. PM_{10} results at the Davidsonville and Etwatwa had no correlation and both ambient monitoring stations were designed to monitor domestic fuel burning activity. Most of the ambient monitoring station displayed no correlation for the rain and nitrogen monoxide results. Results at the Mogale City ambient monitoring stations showed that there was no correlation between wind direction and solar radiation data trend. PM_{10} at the Orange Farm displayed no correlation with the

solar radiation data at the Orange Farm. Tsakane ambient monitoring stations, wind speed displayed no correlation either sulfur dioxide or nitrogen monoxide. Solar radiation displayed no correlation with rain recorded at the Tsakane ambient station. Wattville, ambient temperature displayed no correlation with benzene concentration.

4.5.2 Pollution Rose

Pollution rose of PM_{10} concentration at the Alexandra ambient monitoring station displayed wind direction of North and North-East directions. The maximum and mean ambient concentrations for PM_{10} at the Bedfordview ambient monitoring stations were 499.95 and 87.154 μg/m3. PM_{10} pollution rose at the Bodibeng ambient monitoring station displayed longest bin with 0 to 100 $\mu g/m^3$ at 18, 11 or 9% counts at North-East, upper North-East or East. Bodibeng ambient monitoring stations showed that higher concentration of PM_{10} concentrations were found between 11 and 12 ambient concentrations of 200 to 573.9 $\mu g/m^3$. PM_{10} displayed longest range found at 20% at West followed by 14% at lower North-East at the Booysens station. The maximum and mean ambient concentrations for PM_{10} at the Booysens ambient monitoring station were 570.77 and 39.543 $\mu g/m^3$ respectively. PM_{10} at the Buccleuch ambient monitoring station displayed longest range between 15 and 20% at North-West lower followed by a range between 10 and 15% at North-East, South-East higher and South-East lower. The maximum and mean ambient concentrations for PM_{10} at the Buccleuch ambient monitoring station were 843.75 and 48.77 $\mu g/m^3$ respectively. Germiston ambient monitoring stations, the highest ambient concentrations found was 1869.3 $\mu g/m^3$. The longest bins of concentrations 0 to 10 $\mu g/m^3$ at 9% North-West higher. At the Jabavu station, less than 10% frequency displayed the following bins: West, South, South high and lower, North-East lower, North lower and North-East. The highest recorded PM_{10} ambient concentrations were 403.19 $\mu g/m^3$. The longest prevailing bin was found on the South-East higher at 7% frequency of counts followed by East at 5% and North-East lower at 3.7%. The highest ambient concentration recorded at the Mamelodi station was 962.89 $\mu g/m^3$. Meyerton ambient monitoring stations, had strong wind direction prevailing from East and North-East lower at 23 and 21 % respectively. The highest PM_{10} ambient concentration recorded was 185.83 $\mu g/m^3$.

The results also displayed strong pollution raised in order from North-East lower, South-East higher, North-West lower and higher. The maximum recorded PM_{10} was 954.84 μg/m^3 at the Olievenhoutbosch ambient monitoring stations. The maximum ambient concentration recorded at the Pretoria West station was 316.5 μg/m^3 of PM_{10}. Results displayed strong pollutants rose at South-West lower at 28 %, West and South both are at 15% of frequency. The Randfontein ambient monitoring station displayed strong pollution rose at the South-West higher, West and South-West lower counts. The minimum ambient concentration recorded at the Randfontein ambient monitoring station was 92.647 μg/m^3. The maximum ambient concentrations recorded at the Randfontein ambient monitoring station were 500.2 μg/m^3. The results displayed strong pollutant rose at South-West higher at 24 %, West and South-West lower at 14 and 8 % of frequency of counts respectively. The maximum ambient concentrations for PM_{10} recorded at the Rosslyn ambient monitoring station was 204.06 μg/m^3. Results displayed strong pollutants rose at South-West lower, South-West lower and East between 8 and 10 %. The maximum ambient concentrations for PM_{10} recorded at the Rosslyn ambient monitoring station was 204.06 μg/m^3 of PM_{10}. Results displayed strong pollutants rose at South-West lower, South-West lower and East between 8 and 10 %. Vanderbijlpark ambient monitoring stations displayed strong PM_{10} pollution rose from North-West higher between 10 and 12 %, East at 8 and 10 %, South-West higher between 4 and 6 %, South-East higher between 4 and 6 %. The maximum and mean ambient concentrations for sulfur dioxide at the Vanderbijlpark ambient monitoring station were 961.64 and 94.321μg/m^3 of PM_{10} respectively.

The maximum ambient concentration for particulate matter recorded at the Tembisa ambient monitoring station was 950.5 μg/m^3 of PM_{10}. Tembisa displayed strong pollutants rose at South-East higher between 15 and 20 %, North-West lower higher between 15 and 20 % and West between 10 and 15 %. Watville ambient monitoring stations displayed strong PM_{10} pollution rose from North-West higher between 12 and 14 %, South-West higher between 12 and 14 %, South-East higher between 4 and 6 %. The maximum and mean ambient concentrations for sulfur dioxide at Watville ambient monitoring stations were 271.8 and 94.389 μg/m^3 of PM_{10}.

The maximum ambient concentration for ozone recorded at the Rosslyn ambient monitoring station was 253.71 parts per billion. Results displayed strong pollution roses in order from South-West lower between 12 and 14 %, South-East lower between 10 and 12 %, South-West higher between 8 and 10 %, East between 8 and 10 % and North-East higher between 8 and

10 %. The maximum ambient concentration for ozone recorded at the Rosslyn ambient monitoring station was 253.71 parts per billion. Results displayed strong pollution roses in order from South-West lower between 12 and 14 %, South-East lower between 10 and 12 %, South-West higher between 8 and 10 %, East between 8 and 10 % and North-East higher between 8 and 10 %.

Pollution rose of NO_2 concentration at the Bedfordview displayed on the South and South-West at 12 and 11% frequency of count respectively. Bedfordview ambient monitoring stations, 4% on the South-East displayed highest ambient concentrations of 25 to 361.67 parts per billion. Nitrogen dioxide pollution rose at the Ekandustria had a direct relationship directional bins and ambient concentrations of 0 to 200 parts per billion and NO_2 pollution rose prevailed from North and North-East higher at 8% of frequency of counts. Nitrogen dioxide pollution rose at the Etwatwa displayed maximum of 198.15 parts per billion ambient concentration and the highest bin was found at North-West higher between 15 and 20 % frequency counts. The highest ambient nitrogen dioxide recorded at the Mamelodi ambient monitoring station was 304.99 parts per billion and displayed strong wind direction South-East higher and East at 18 and 15% frequency of counts. The maximum ambient concentration recorded at the Pretoria West ambient monitoring station was 157.58 parts per billion of nitrogen dioxide. Results also showed strong pollution rose from North-East higher at 18 %, North-East lower at 16% and South at 15 %.

Higher ground ozone concentration at the Bedfordview ambient monitoring stations are found on North or North-West of the ambient monitoring station with frequency of count between 8 and 10 and 5 to 6 points % respectively. Rosslyn displayed strong pollution roses on the South-West between 12 and 14 %, South-East lower between 10 and 12% between 8 and 10 %. The maximum ambient concentration for ozone recorded at the Rosslyn ambient monitoring station was 601.48 parts per billion.

Diepsloot, sulfur dioxide pollution rose displayed strong winds prevailing on the North-East higher and lower which were between 15 and 20% of frequency of counts. The maximum and mean ambient concentrations for sulfur dioxide at the Mamelodi ambient monitoring station were 435.58 and 5.2454 parts per billion respectively. The results displayed strong sulfur dioxide pollution rose from South-East higher between 6 and 8 %, East between 4 and 6 % and North-East lower between 4 and 6 %. The maximum ambient concentrations for sulfur dioxide recorded at the Tembisa ambient monitoring station were 950.5 of PM_{10}. Tembisa displayed strong pollutants rose at South-East higher between 15 and 20%, North-West lower higher between 15 and 20% and

West between 10 and 15 %. The maximum ambient concentration for sulfur dioxide recorded at the Thokoza ambient monitoring station was 108.19 parts per billion. Results displayed strong pollution rose from East between 25 and 30 %, North-East lower between 15 and 20 %, South-West higher between 10 and 15 and South-East between 10 and 15 %. Tsakane results displayed strong pollution rose from North-East higher between 15 and 20 %, North at 15% and North-West higher between 10 and 15 frequency of counts. The maximum ambient concentrations for sulfur dioxide recorded at the Tsakane ambient monitoring station was 966.37 of PM_{10}.

Ozone pollution rose at the Jabavu station displayed strong East bins at 24% of frequency of counts followed by South-East higher and lower, South, West, South-West lower and higher respectively. The maximum ambient concentration recorded was 96.042 of ozone parts per billion. Ozone ambient concentration displayed strong direction distribution from longest North-East lower, East and West Leondale ambient monitoring stations. The highest concentration recorded at the Leondale station was 77.898 parts per billion. Ozone ambient concentration pollution rose at the Mamelodi station displayed longest bins from South-East higher at 21 %, East at 16 and 11% on the North-East lower. The highest recorded ambient ozone concentrations were 376.18 parts per billion.

4.5.3 Bivariate Polar Plot at receptor and Emission Inventory Facilities within Gauteng Province.

Bivariate polar plots provided effective graphical means of source detection and characteristics. PM_{10} at the Bedfordview ambient air quality monitoring, displayed probability distribution of about 8 to 140 from South to South-East clockwise direction around the monitoring station at 0 to 8 meters per second. The results showed that plot at above-mentioned direction displayed high probability of PM_{10} concentration of about 120 $\mu g/m^3$ of PM_{10} at Eastern site of the station at wind speed of 4 to seven meters per second. The plot also displayed other sources of PM_{10} concentrations of about 8 to 130 $\mu g/m^3$ of PM_{10} at Gillooly's interchange. The plot displayed high probability sources of PM_{10} from Germiston industrial area of up to 220 $\mu g/m^3$ of PM_{10} at wind speed from 6 meters per second and higher.

The plot displayed probability of PM_{10} concentrations at the North-East of the ambient station when the wind speed is 10 meters per second of about 70 to 80 $\mu g/m^3$ of PM_{10}. Higher probability of PM_{10} concentrations on the South-West (Modderfontein, Kaalfontein and Kempton Park) to West (Tembisa) of the ambient station when wind speed travelled at 6 meters per second and higher.

The Davidsonville ambient monitoring station was designed to monitor pollutants from domestic fuel burning around Davidsonville and other areas close to the station within the City of Johannesburg. The bivariate polar plot showed 3 major sources at far West, far North-East and local East direction. The source close to the station displayed PM_{10} concentration of the range of 60 to 80 $\mu g/m^3$ of PM_{10}. The major source at far West was shown when the wind speed was at 10 meters per second and higher with the concentration of up to 125 $\mu g/m^3$ of PM_{10}.

Ekandustria ambient monitoring station is situated at the Ekandustria industrial area in the City of Tshwane and the station is designed to monitor pollutants from industrial activities. The bivariate polar plot of PM_{10} showed far major sources situated on the South-West, North-West and North-East when wind speed reached 10 meters per second and above with the higher concentrations of 450 $\mu g/m^3$ of PM_{10}. North-West and North-East sources at the wind speed of fifteen meters per second displayed probability of PM_{10} concentration of about 150 to 200 $\mu g/m^3$ of PM_{10}. Sources that are situated on the South-West the plot revealed highest probability of concentration of 450 $\mu g/m^3$ of PM_{10} at the wind speed between 15 and 20 meters per second.

4.5.4 Conditional Probability Function Plot (K-Means Clustering) at Gauteng Province.

K-means results at the Bedfordview showed K-means results at the Bedfordview station showed sources on the Western Area of the ambient monitoring station with the ambient concentrations of up to hundred and 20 $\mu g/m^3$ which is still exceeding National Ambient Air Quality Standards for PM_{10}. The results further showed that cluster 3 could be the only area that demonstrated PM_{10} compliance compared to other clusters. The K-means clustering algorithm analysis showed clusters two as the highest ambient concentrations of PM_{10} at the Booysens ambient monitoring station within the City of Tshwane. The highest ambient concentration of PM_{10} of 650 $\mu g/m^3$ which exceeded the national ambient air quality standard of 75 $\mu g/m^3$ in the daily averaging period. The K-means clustering algorithm analysis showed that cluster two as the highest ambient

concentrations of PM_{10} at the Buccleuch ambient monitoring station within the City of Johannesburg which was designed to monitor traffic pollution. The K-means clustering algorithm analysis showed that cluster two as the highest ambient concentrations of 120 $\mu g/m^3$ of PM_{10} at the Davidsonville ambient monitoring station within the City of Johannesburg designed to monitor domestic fuel burning pollution. Cluster two displayed maximum ambient concentrations of 120 $\mu g/m^3$ of PM_{10}. The highest ambient concentration value of PM_{10} was of 125 $\mu g/m^3$ which exceeded the national ambient air quality standard 75 $\mu g/m^3$ of PM_{10} in the daily averaging period at 4 frequency of exceedance.

5. CHAPTER 5: CONCLUSION AND RECOMMENDATIONS

The study has determine correlation matrix for ozone, sulphur dioxide, oxide of nitrogen and particulate matter 10 microgram diameter. Figure 4.1 displayed highest correlation at moderate level of ozone at Mogale city and Buccleuch. In figure 4.2 results has highest correlation of sulphur dioxide Jabavu and Diepsloot at moderate level. In figure 4.3 results display moderate level of oxide of nitrogen at Newtown and Olifansfontein. In figure 4.4 PM_{10} displayed highest correlation at moderate at Thokoza and Springs. Correlation matrix at the Gauteng ambient monitoring station and wind speed and wind direction has displayed strong correlations. Strong correlation was found between benzene and toluene as well as nitrogen dioxide and oxides of nitrogen and or nitrogen monoxide.

Pollution rose predominates were determined at all Gauteng ambient monitoring station for concentration level and direction of origin in figure 4.28 to 4.73. Bivariate polar plot was investigated to determine new and problematic sources within Gauteng province at figure 4.74 to 4.135. Emissions groups were determining characteristics and relation of the emissions sources in figure 4.137 to 4.193. New sources have been determined and identified according to the level of concentrations and location within Gauteng province. The main objective of the study has been achieved in emissions sources and characterized groups based on the level of concentration and sources.

It is recommended that polar annulus function be investigated to get trend hourly, day seasonal and time to all operational activities so that time of operational of that specific activity be determined in case the activity is not Licence. This will help authorities/compliance to target unknown or unlicensed emissions sources or activities at the time of operation.

6. REFERENCES

Altieri, K.E. and Keen, S.L., 2019. Public health benefits of reducing exposure to ambient fine particulate matter in South Africa. Science of The Total Environment, 684, pp.610-620.

Annegarn, H.J., Grant, M.R., Kneen, M.A. and Scorgie, Y., 1998. Direct source apportionment of particulate pollution within a township. Low-Smoke Coal Program: Draft of the final report. Report No. AER98. 117DME, Department of Minerals and Energy, Pretoria.

Uria-Tellaetxe, I. and Carslaw, D.C., 2014. Conditional bivariate probability function for source identification. Environmental modelling & software, 59, pp.1-9.

Babchishin, K.M. and Helmus, L.M., 2016. The influence of base rates on correlations: An evaluation of proposed alternative effect sizes with real world data. Behaviour research methods, 48(3), pp.1021-1031.

Bae, M.S., Schwab, J.J., Chen, W.N., Lin, C.Y., Rattigan, O.V. and Demerjian, K.L., 2011. Identifying pollutant source directions using multiple analysis methods at a rural location in New York. Atmospheric environment, 45(15), pp.2531-2540.

Canty, A. and Ripley, B., 2016. Bootstrap R (S-Plus) functions. R package version 1.3–18.
Carslaw, D.C., 2015. The open-air manual–open-source tools for analysing air pollution data. Manual for version, 1.

Carslaw, D.C. and Beevers, S.D., 2013. Characterizing and understanding emission sources using bivariate polar plots and k-means clustering. Environmental modelling & software, 40, pp.325-329.

Carslaw, D.C., Beevers, S.D., Ropkins, K. and Bell, M.C., 2006. Detecting and quantifying aircraft and other on-airport contributions to ambient nitrogen oxides in the vicinity of a large international airport. Atmospheric Environment, 40(28), pp.5424-5434.

Carslaw, D.C. and Ropkins, K., 2012. Openair—an R package for air quality data analysis. Environmental Modelling & Software, 27, pp.52-61.

CDP., 2014.City of Johannesburg. CDP Cities 2014 Report. http://c40-production-images.s3.amazonaws.com/other_uploads/images/181_CDP_Cities_2014_Johannesburg_final_(reduced).original.pdf?1424836516.

Chen X, Li F, Liu C, Yang J, Zhang J, Peng C. Monitoring, human health risk assessment and optimized management for typical pollutants in indoor air from random families of university staff, Wuhan city, China. Sustainability. 2017 Jul;9(7):1115.

Chiloane, K.E., Beukes, J.P., Van Zyl, P.G., Maritz, P., Vakkari, V., Josipovic, M., Venter, A.D., Jaars, K., Tiitta, P., Kulmala, M. and Wiedensohler, A., 2017. Spatial, temporal and source contribution assessments of black carbon over the northern interior of South Africa. Atmospheric Chemistry and Physics.

Coker, E. and Kizito, S., 2018. A narrative review on the human health effects of ambient air pollution in Sub-Saharan Africa: An urgent need for health effects studies. International journal of environmental research and public health, 15(3), p.427.

Cluster analysis.,2019.Wikipedia.Availabe at : https://en.wikipedia.org/wiki/Cluster_analysis Accessed:24 November 2019)

Cosemans, G. and Kretzschmar, J., 2002. Pollution roses for 24 h averaged pollutant concentrations by regression. In 8h International Conference on Harmonization within Atmospheric Dispersion Modelling for Regulatory Purposes (pp. 414-418).

DEA (Department of Environmental Affairs).,2013. Amendment to the 2007 National Framework for Air Quality Management in the Republic of South Africa. Government Gazette N.O 37078. Republic of South Africa.

Deat, A., 2000. White paper on integrated pollution and waste management for South Africa. A policy on pollution prevention, waste minimization, impact management and remediation. Dept. Environ. Affairs Tourism, 80, pp.274-275.

Engelbrecht, J., Mostert, J., Reddy, V. and Swanepoel, L., 1998. Aerosol monitoring and source apportionment in the Vaal Triangle.

Evans, J.D., 1996. Straightforward statistics for the behavioural sciences. Thomson Brooks/Cole Publishing Co.

Falcon-Rodriguez, C.I., Osornio-Vargas, A.R., Sada-Ovalle, I. and Segura-Medina, P., 2016. Aeroparticles, composition, and lung diseases. Frontiers in immunology, 7, p.3.

Gauteng Department of Agriculture, Conservation and Environment (GDACE).,2009. Gauteng Province Air Quality Management Plan-Final. Gauteng Provincial Government

Gauteng Department of Agriculture and Rural Development (GDARD).,2011. Gauteng State of the Environment Report 2011. Gauteng Provincial Government

Ghorani-Azam, A., Riahi-Zanjani, B. and Balali-Mood, M., 2016. Effects of air pollution on human health and practical measures for prevention in Iran. Journal of research in medical sciences: the official journal of Isfahan University of Medical Sciences, 21.

Greenslade, J., 2019. Constraining natural contributions to tropospheric ozone production over Australia and selected areas of the Southern Ocean.

Haskins, J.D., Lopez-Hilfiker, F.D., Lee, B.H., Shah, V., Wolfe, G.M., DiGangi, J., Fibiger, D., McDuffie, E.E., Veres, P., Schroder, J.C. and Campuzano-Jost, P., 2019. Anthropogenic control over wintertime oxidation of atmospheric pollutants. Geophysical Research Letters, 46(24), pp.14826-14835.

Hartigan, J.A. and Wong, M.A., 1979. Algorithm AS 136: A k-means clustering algorithm. Journal of the Royal Statistical Society. Series C (Applied Statistics), 28(1), pp.100-108.

Horváth, I., Barnes, P.J., Loukides, S., Sterk, P.J., Högman, M., Olin, A.C., Amann, A., Antus, B., Baraldi, E., Bikov, A. and Boots, A.W., 2017. A European Respiratory Society technical standard: exhaled biomarkers in lung disease. European Respiratory Journal, 49(4), p.1600965.

Henry, R., Norris, G.A., Vedantham, R. and Turner, J.R., 2009. Source region identification using kernel smoothing. Environmental science & technology, 43(11), pp.4090-4097.

http://www.saaqis.org.za/Priority%20Areas.aspx (Accessed date on 07 September 2017)

https://saaelip.environment.gov.za/SAAELIP/NAEIS_AUTHORITY/Pages/State/EIReport/MasterList.aspx (Accessed date on 11 September 2017)

ICAO (International Civil Aviation Organization)., 2011.Canada. (www.icao.int, Accessed 13 September 2017)

Inglesi-Lotz, R. and Blignaut, J.N., 2011. Estimating the price elasticity of demand for electricity by sector in South Africa. South African Journal of Economic and Management Sciences, 14(4), pp.449-465.

Joradol, A., Uthaibutra, J., Lithanatudom, P. and Saengnil, K., 2019. Induced expression of NOX and SOD by gaseous sulfur dioxide and chlorine dioxide enhances antioxidant capacity and maintains fruit quality of ‘Daw’longan fruit during storage through H2O2 signaling. Postharvest Biology and Technology, 156, p.110938.

Kalaiarasan, G., Balakrishnan, R.M., Sethunath, N.A. and Manoharan, S., 2018. Source apportionment studies on particulate matter (PM10 and PM2. 5) in ambient air of urban Mangalore, India. Journal of environmental management, 217, pp.815-824.

Kassambara, A., 2017. Practical guide to cluster analysis in R: Unsupervised machine learning (Vol. 1). Sthda.

Kim, E. and Hopke, P.K., 2004. Comparison between conditional probability function and non-parametric regression for fine particle source directions. Atmospheric Environment, 38(28), pp.4667-4673.

Lehner, R., Weder, C., Petri-Fink, A. and Rothen-Rutishauser, B., 2019. Emergence of nanoplastic in the environment and possible impact on human health. Environmental science & technology, 53(4), pp.1748-1765.

Li, Z., Ji, S., Liu, Y., Cao, X., Tian, S., Chen, Y., Niu, Z. and Li, Y., 2019. Well-defined materials for heterogeneous catalysis: from nanoparticles to isolated single-atom sites. Chemical Reviews, 120(2), pp.623-682.

Lourens, A.S., Beukes, J.P., Van Zyl, P.G., 4ie, G.D., Burger, J.W., Pienaar, J.J., Read, C.E. and Jordan, J.H., 2011. Spatial and temporal assessment of gaseous pollutants in the Highveld of South Africa. South African Journal of Science, 107(1-2), pp.1-8.

Malby, A.R., Whyatt, J.D. and Timmis, R.J., 2013. Conditional extraction of air-pollutant source signals from air-quality monitoring. Atmospheric environment, 74, pp.112-122.

Mc Naught, A.D. and Wilkinson, A., 2012. IUPAC. Compendium of Chemical Terminology, (the" Gold Book"): redox potential. 2012.
http://goldbook.iupac.org/W06679.html (http://goldbook.iupac.org/W06679.html)

Mdluli, T.N., Piketh, S.J. and Igbafe, A.I., 2005. Assessment of indoor respirable particulate matter (PM7) in township houses with coal-fired stoves at Kwaguqa (Witbank). National Electricity Regulator Quarterly Journal, 12.

Mdluli, T.N., 2007. The societal dimensions of domestic coal combustion: People's perceptions and indoor aerosol monitoring (Doctoral dissertation, University of the Witwatersrand).

Mushongera D, Zikhali P, Ngwenya P. A multidimensional poverty index for Gauteng province, South Africa: evidence from Quality of Life Survey data. Social Indicators Research. 2017 Jan 1;130(1):277-303.

Nkosi V, Wichmann J, Voyi K. Indoor and outdoor PM 10 levels at schools located near mine dumps in Gauteng and North West Provinces, South Africa. BMC public health. 2017 Dec 1;17(1):42.

Patel, C., Chandra, K., Hwang, J., Agarwal, R.A., Gupta, N., Bae, C., Gupta, T. and Agarwal, A.K., 2019. Comparative compression ignition engine performance, combustion, and emission characteristics, and trace metals in particulates from Waste cooking oil, Jatropha and Karanja oil derived biodiesels. Fuel, *236*, pp.1366-1376.

Panichev N, Mokgalaka N, Panicheva S. Assessment of air pollution by mercury in South African provinces using lichens Parmelia caperata as bioindicators. Environmental Geochemistry and Health. 2019 Oct 1;41(5):2239-50.

Retief FP, Mlangeni G, Sandham LA. The effectiveness of state of the environment reporting (SoER) at the local government sphere–a developing country's experience. Local Environment. 2011 Aug 1;16(7):619-36.

Schraufnagel, D.E., Balmes, J.R., Cowl, C.T., De Matteis, S., Jung, S.H., Mortimer, K., Perez-Padilla, R., Rice, M.B., Riojas-Rodriguez, H., Sood, A. and Thurston, G.D., 2019. Air pollution

and noncommunicable diseases: A review by the Forum of International Respiratory Societies' Environmental Committee, Part 2: Air pollution and organ systems. Chest, 155(2), pp.417-426.

Scorgie, Y., Kneen, M.A., Annegarn, H.J. and Burger, L.W., 2003. Air pollution in the Vaal Triangle-quantifying source contributions and identifying cost-effective solutions. Clean Air Journal= Tydskrif vir Skoon Lug, 13(2), pp.5-18.

SOER.,2004. Gauteng State of Environment Report 2004. Department of Agriculture, Conservation and Environment, Gauteng Provincial Government.

Statistics-eNatis.,Vehicle population statistics for October /November 2019. http://www.enatis.com/index.php/statistics/13-live-vehicle-population (Accessed date on 21 December 2019)

Strauss, T. and von Maltitz, M.J., 2017. Generalising Ward's method for use with Manhattan distances. PloS one, 12(1), p.e0168288.

Szulecka, A., Oleniacz, R. and Rzeszutek, M., 2017. Functionality of openair package in air pollution assessment and modelling—a case study of Krakow. Ochrona Srodowiska i Zasobów Naturalnych, 28(2), pp.22-27.

United States Environmental Protection Agency (USEPA).,1997. Clean Air Technology Centre, Air Emission from Scrap Tyre Combustion.

United States Environmental Protection Agency (USEPA).,2010a. Health and Environmental Impact of Ground Ozone.htt://www.epa.gov/air/ozonepollution/health.html.Accessed November 2018.

Vedantham, R., Norris, G. and Duvall, R., 2014. Receptor and Hybrid Modelling Tools. Wiley Stats Ref: Statistics Reference Online.

World Health Organization., 2006. Air Quality Guidelines: Global Update 2005. Particulate Matter, ozone, nitrogen Dioxide and sulfur Dioxide. World Health Organization.

World Health Organization.,1979b. Sulfur Oxides and Suspended particulate matter (EHC, 8). (http://www.inchem.org/documents/ehc/ehc/ehc008.htm. Accessed November 2018).

World Health Organization.,1997.Nitrogen Oxides Second Edition (EHC 188). (http://www.inchem.org/documents/ehc/ehc213.htm.Accessed November 2018).

World Health Organization, 2002. The world health report 2002: reducing risks, promoting healthy life. World Health Organization.

World Health Organization, 2013. Global tuberculosis report 2013. World Health Organization. (http://www.who.int/healthinfo/global_burden_disease/definition_regions/en/,Accessed 07 September 2017).

World Health Organization., 2016."92% of the world's population exposed to unsafe levels of air pollution." ScienceDaily. www.sciencedaily.com/releases/2016/09/160927144248.htm (accessed January 4, 2020).

Wood, S.N., 2003. Thin plate regression splines. Journal of the Royal Statistical Society: Series B (Statistical Methodology), 65(1), pp.95-114.

Wang, J. and Zhao, T., 2017. Regional energy-environmental performance and investment strategy for China's non-ferrous metals industry: a non-radial DEA based analysis. Journal of cleaner production, 163, pp.187-201.

Zheng, H., Zhao, B., Wang, S., Wang, T., Ding, D., Chang, X., Liu, K., Xing, J., Dong, Z., Aunan, K. and Liu, T., 2019. Transition in source contributions of PM2.5 exposure and associated premature mortality in China during 2005–2015. Environment international, 132, p.105111.

7. APPENDIX - Gauteng ambient air quality data summary

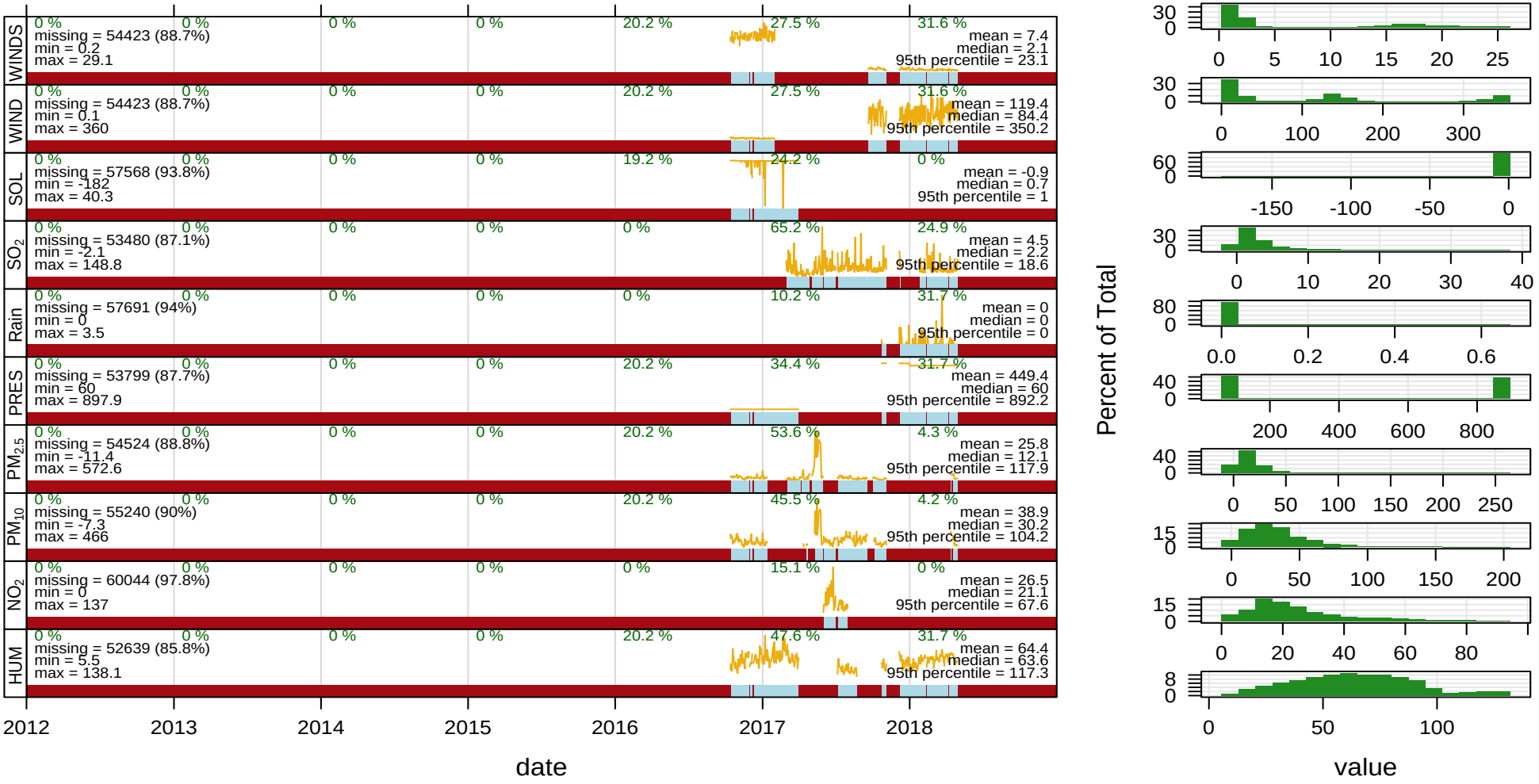

Figure 7.1: Alexandra ambient air quality data summary

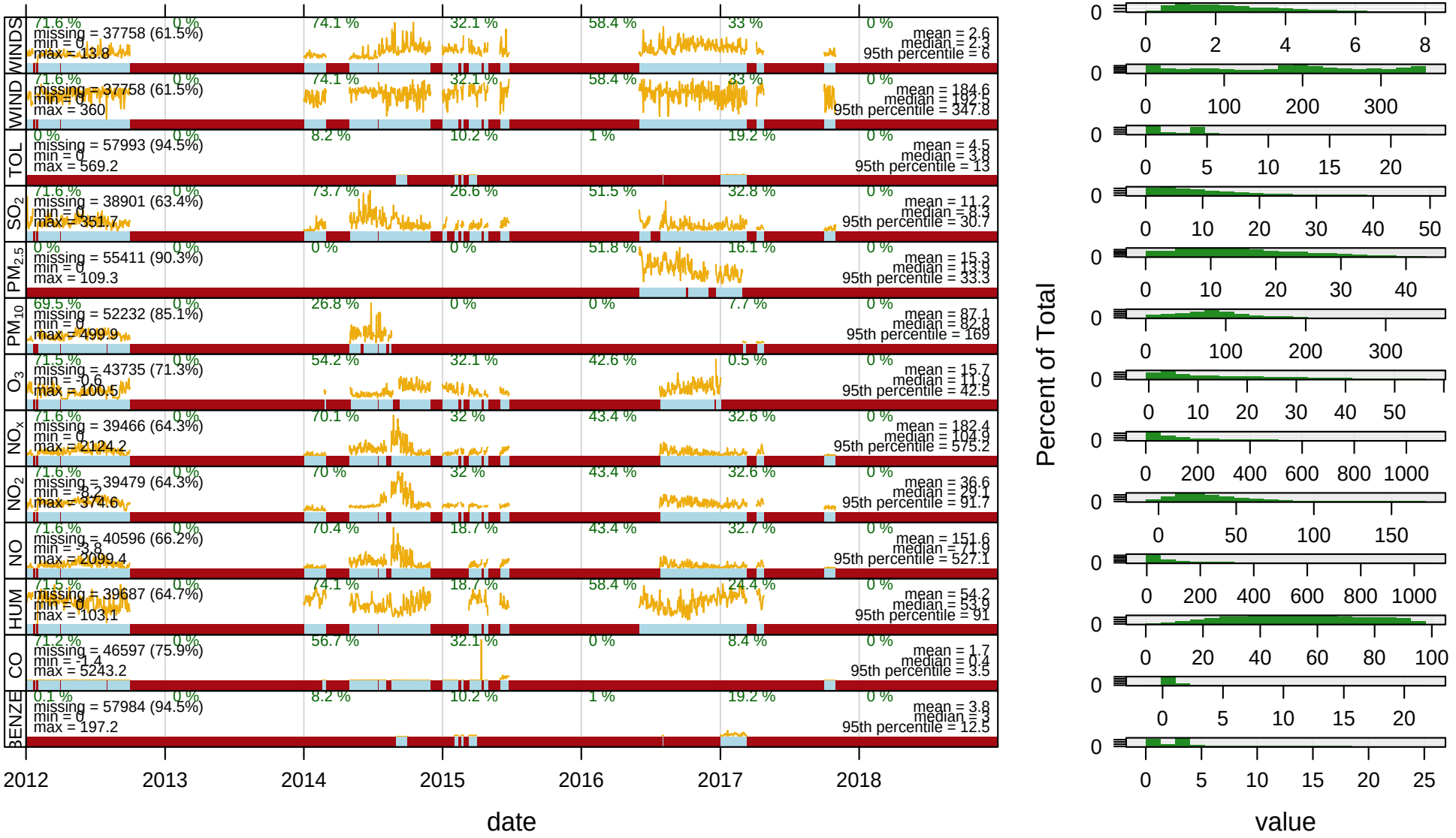

Figure 7.2: Bedfordview ambient air quality data summary

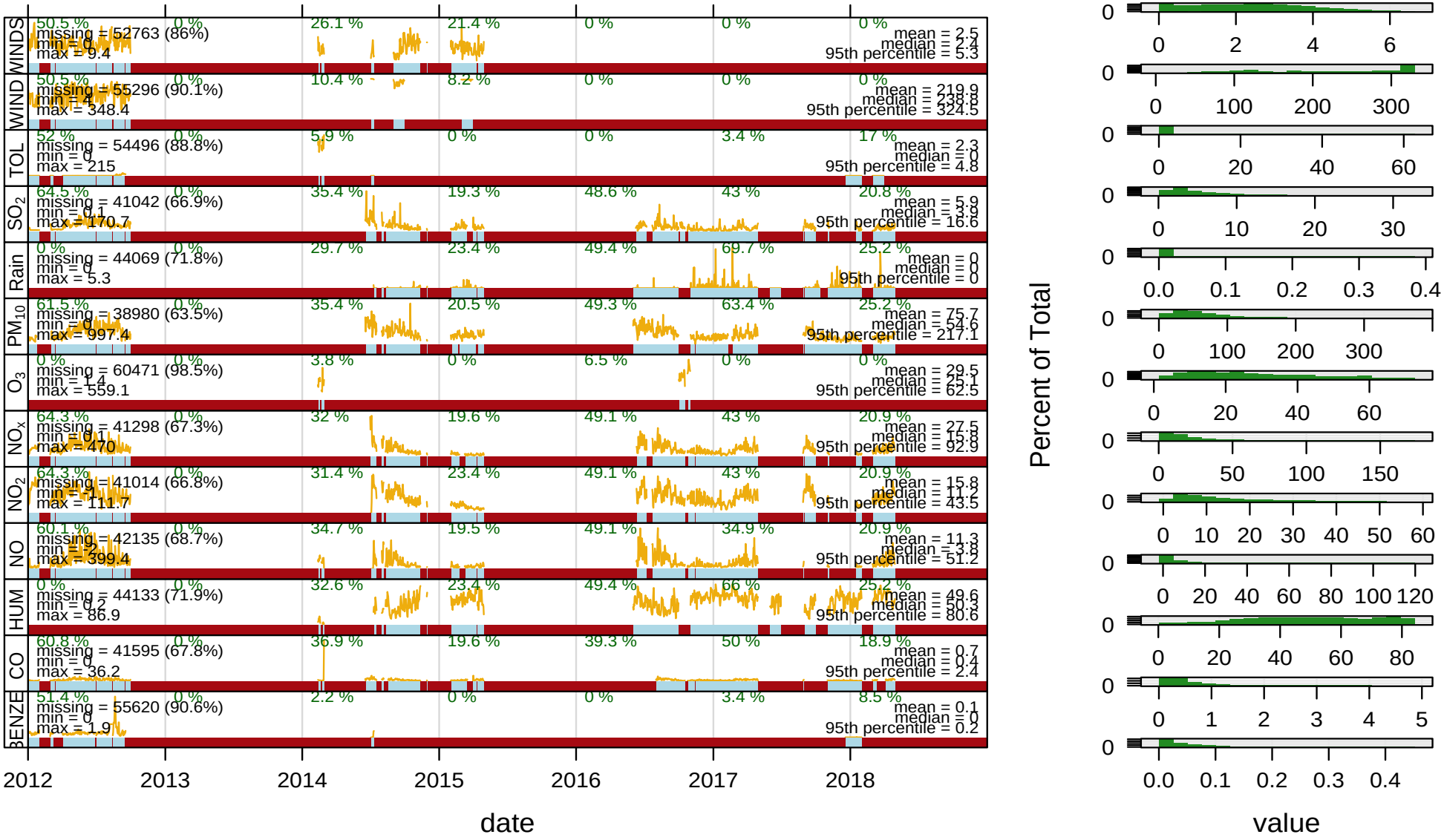

Figure 7.3: Booysens ambient air quality data summary

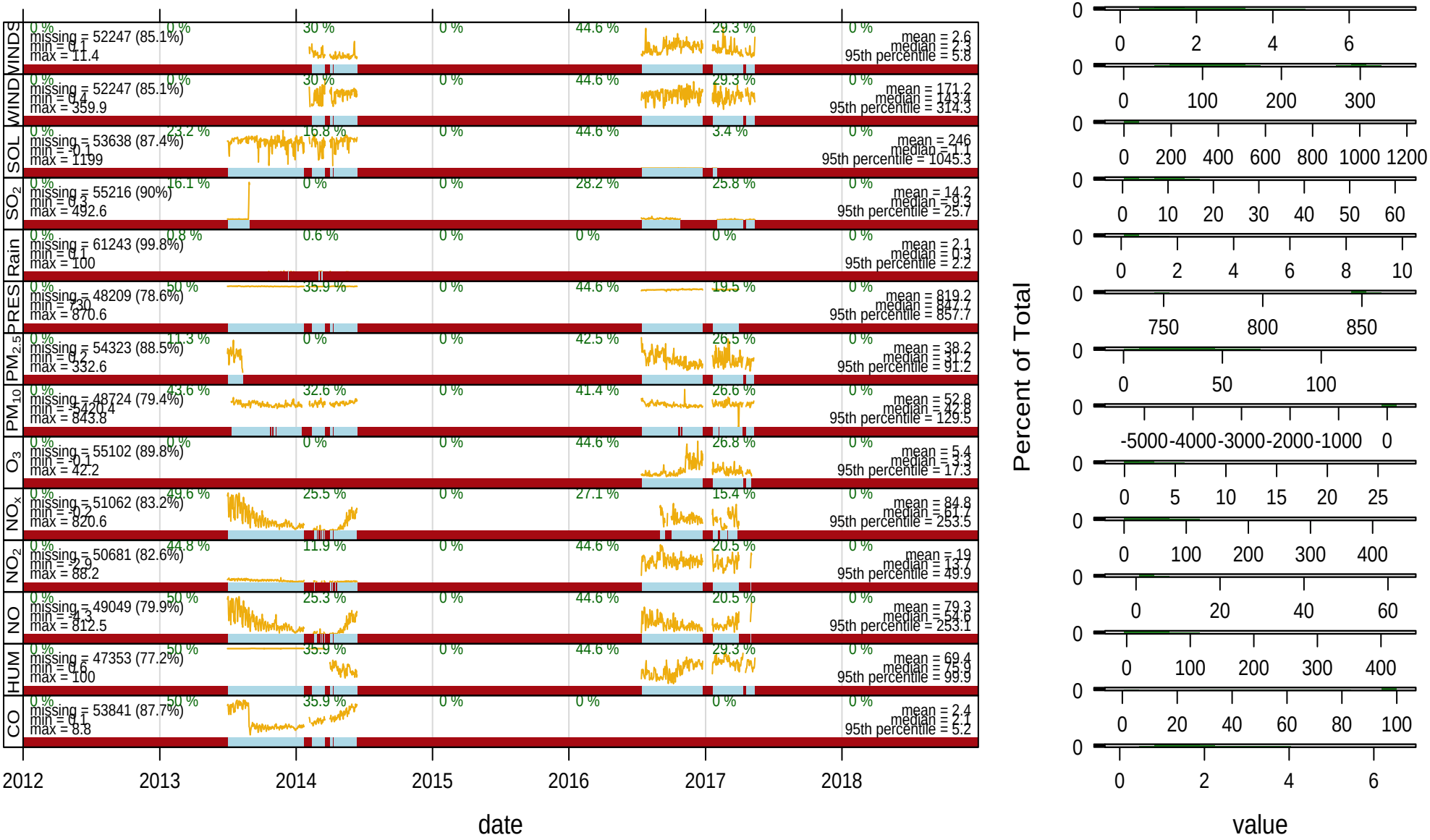

Figure 7.4: Buccleuch ambient air quality data summary

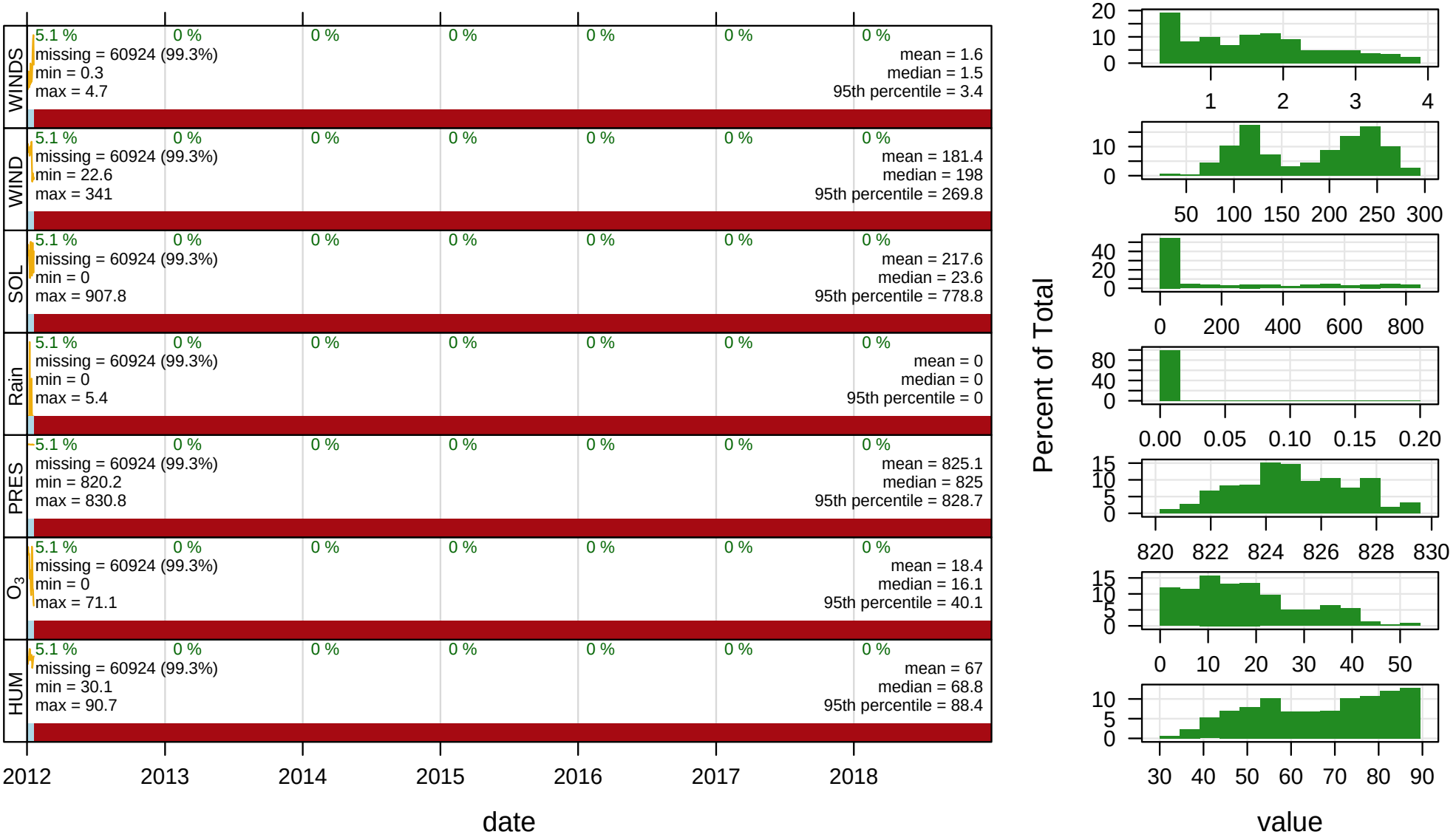

Figure 7.5: Delta Park ambient air quality data summary

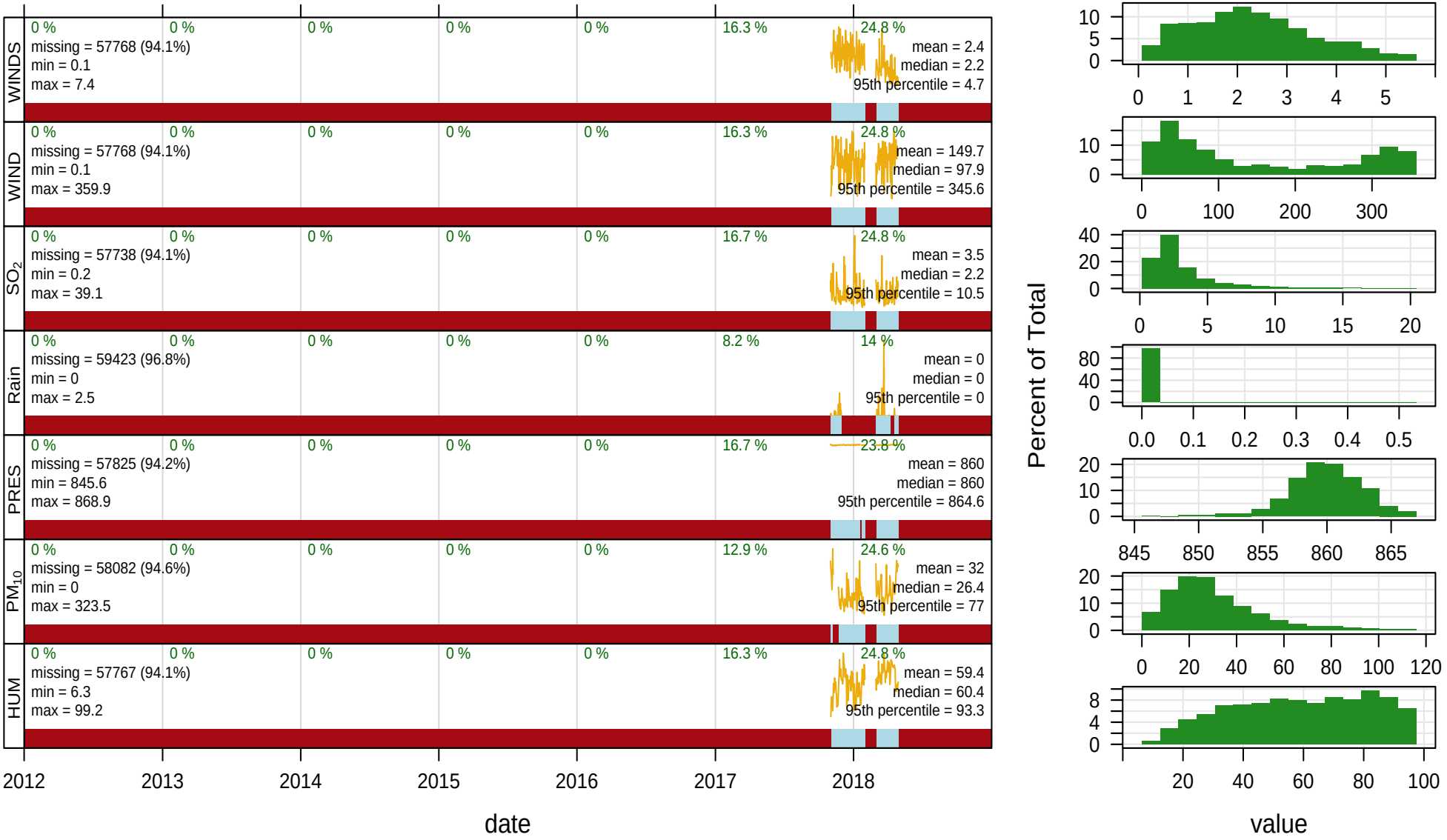

Figure 7.6: Diepsloot ambient air quality data summary

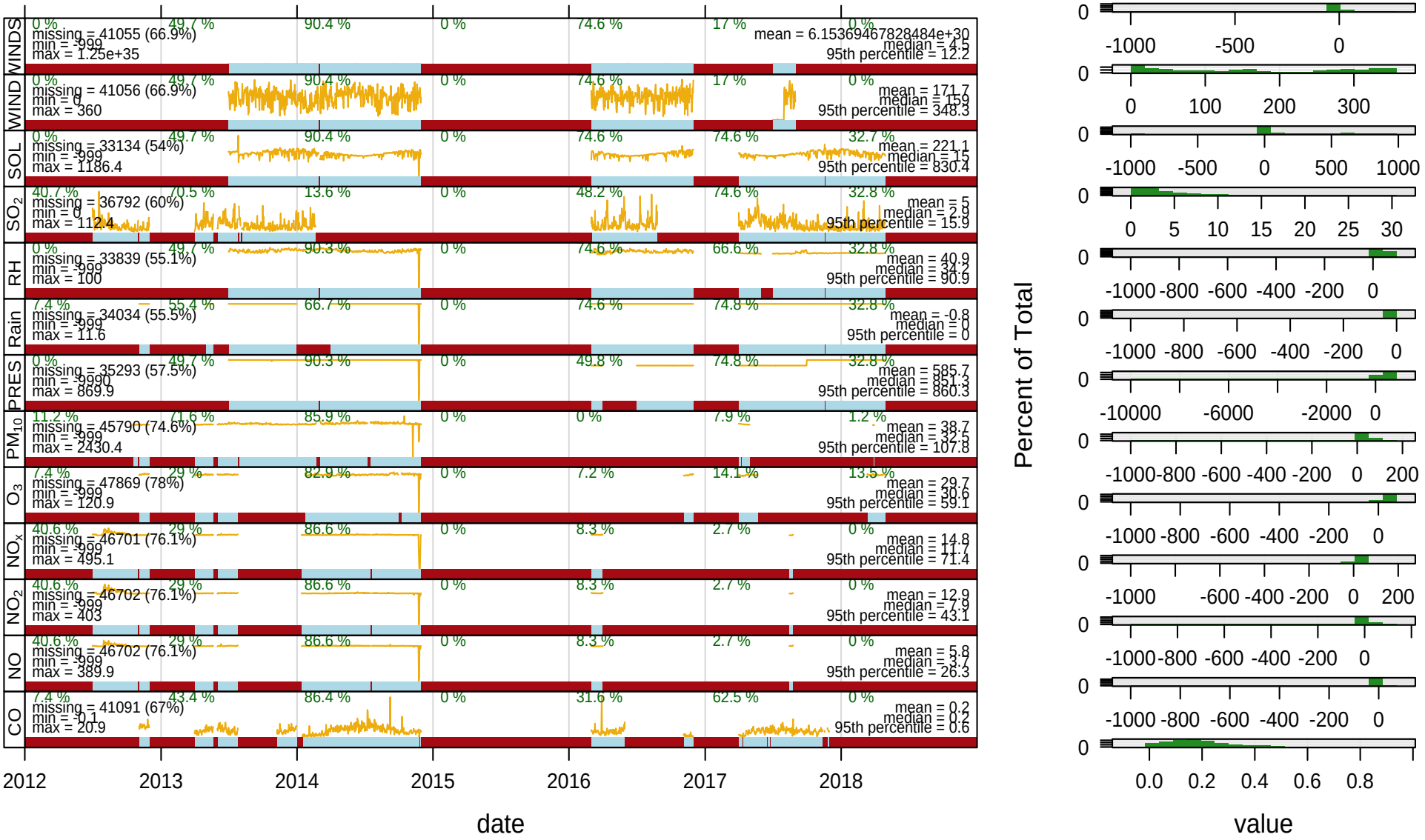

Figure 7.7: Ekandustria ambient air quality data summary

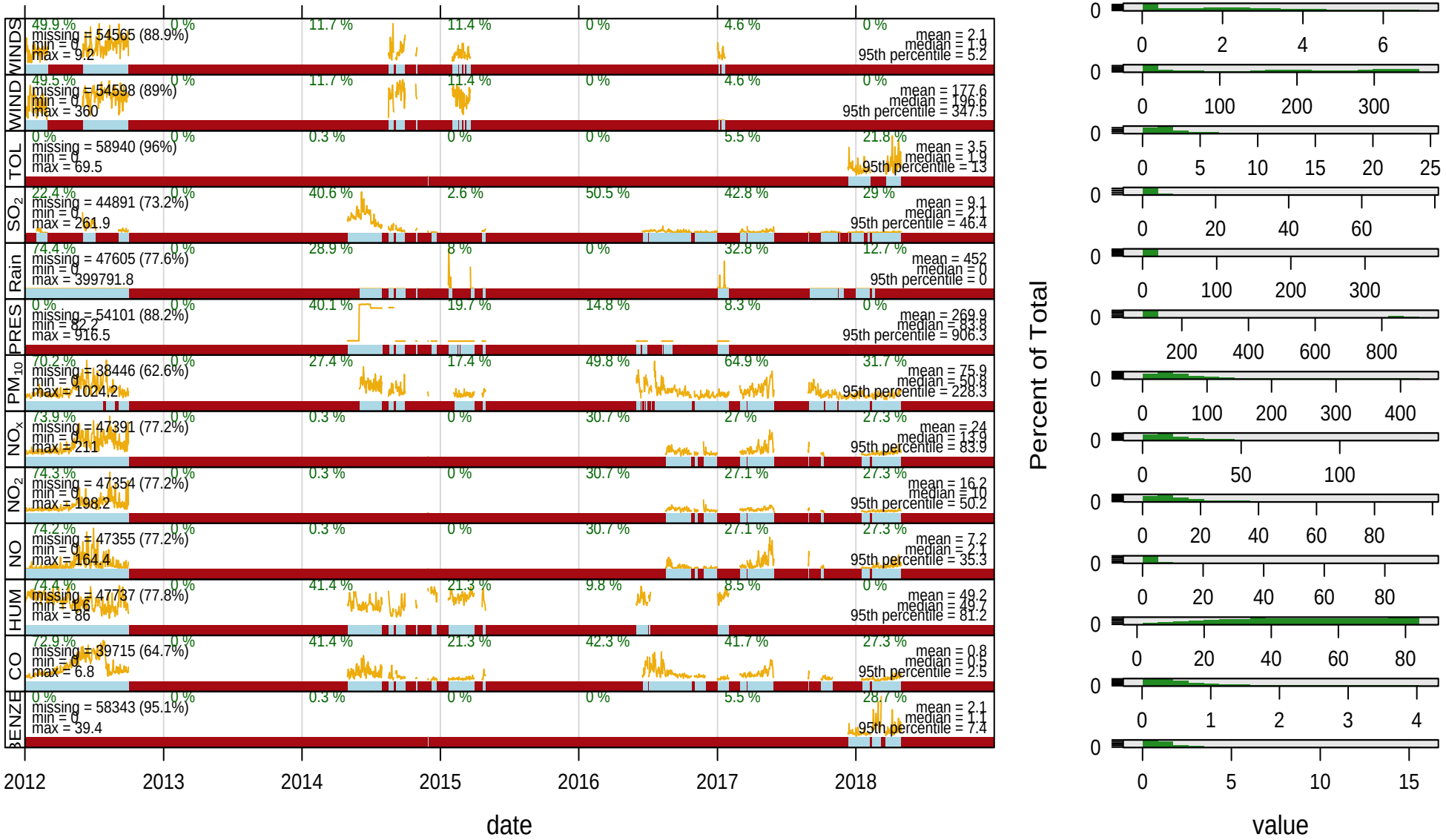

Figure 7.8: Etwatwa ambient air quality data summary



Figure 7.9: Germiston ambient air quality data summary

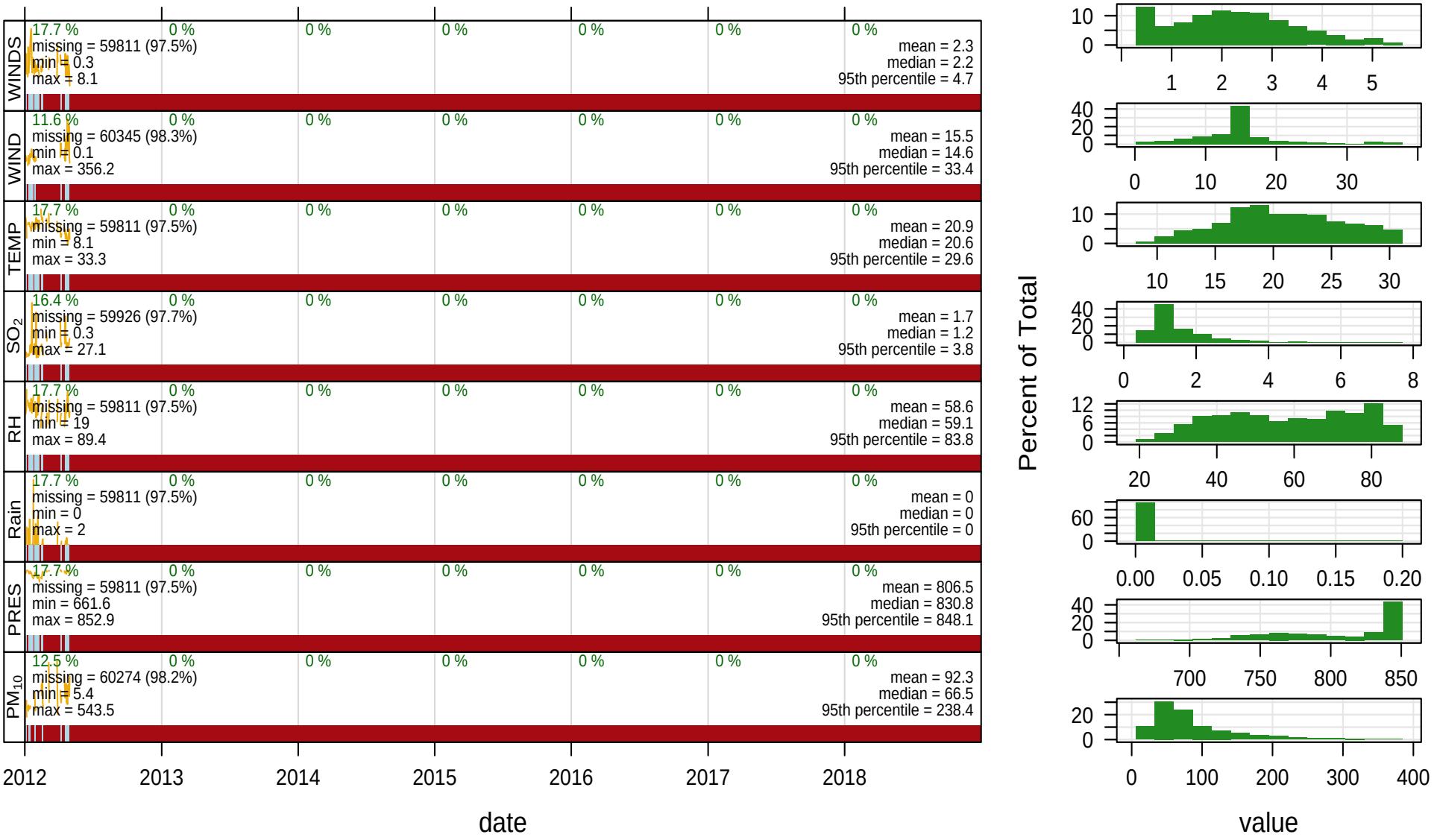

Figure 7.10: Ivory Park ambient air quality data summary

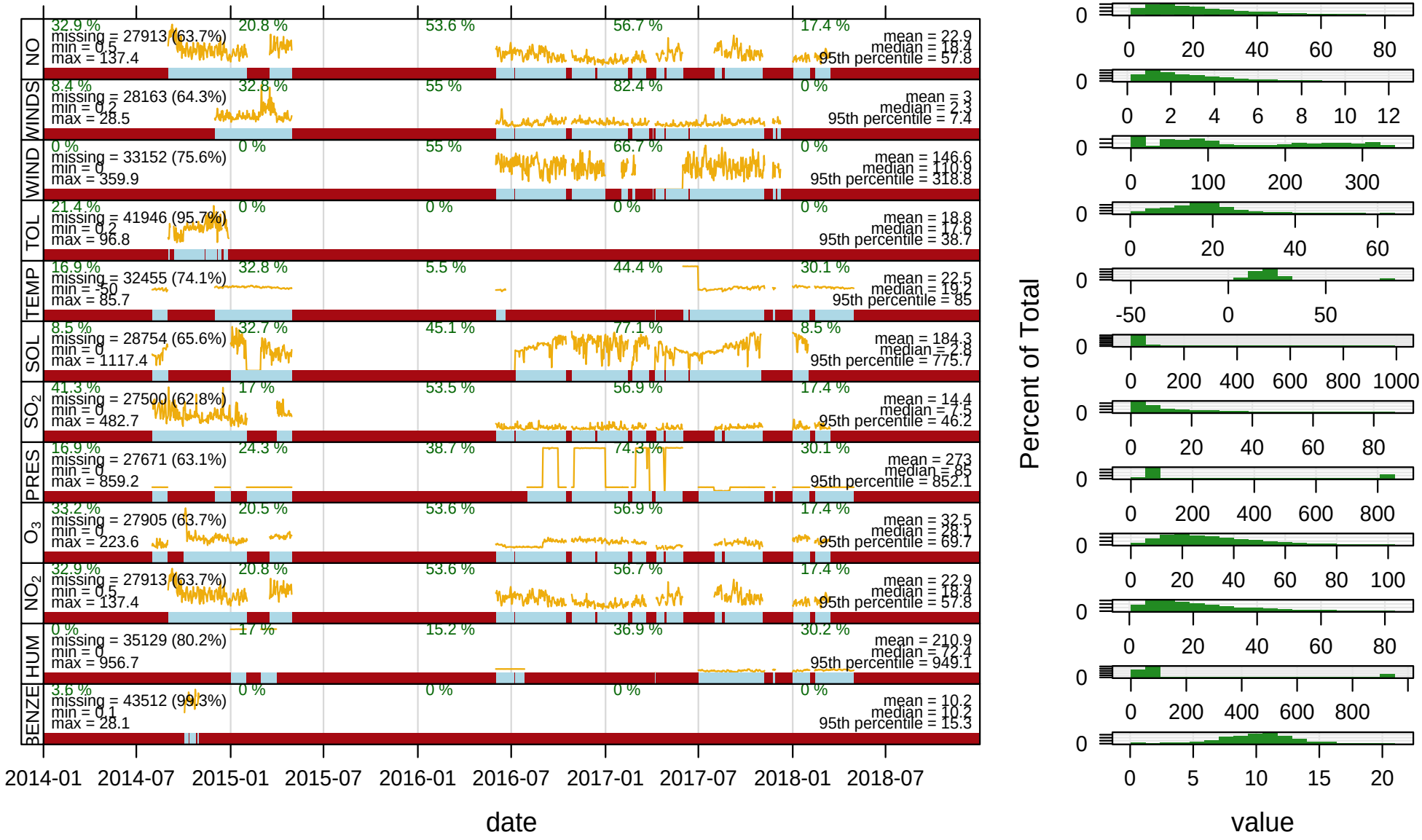

Figure 7.11: Leondale ambient air quality data summary

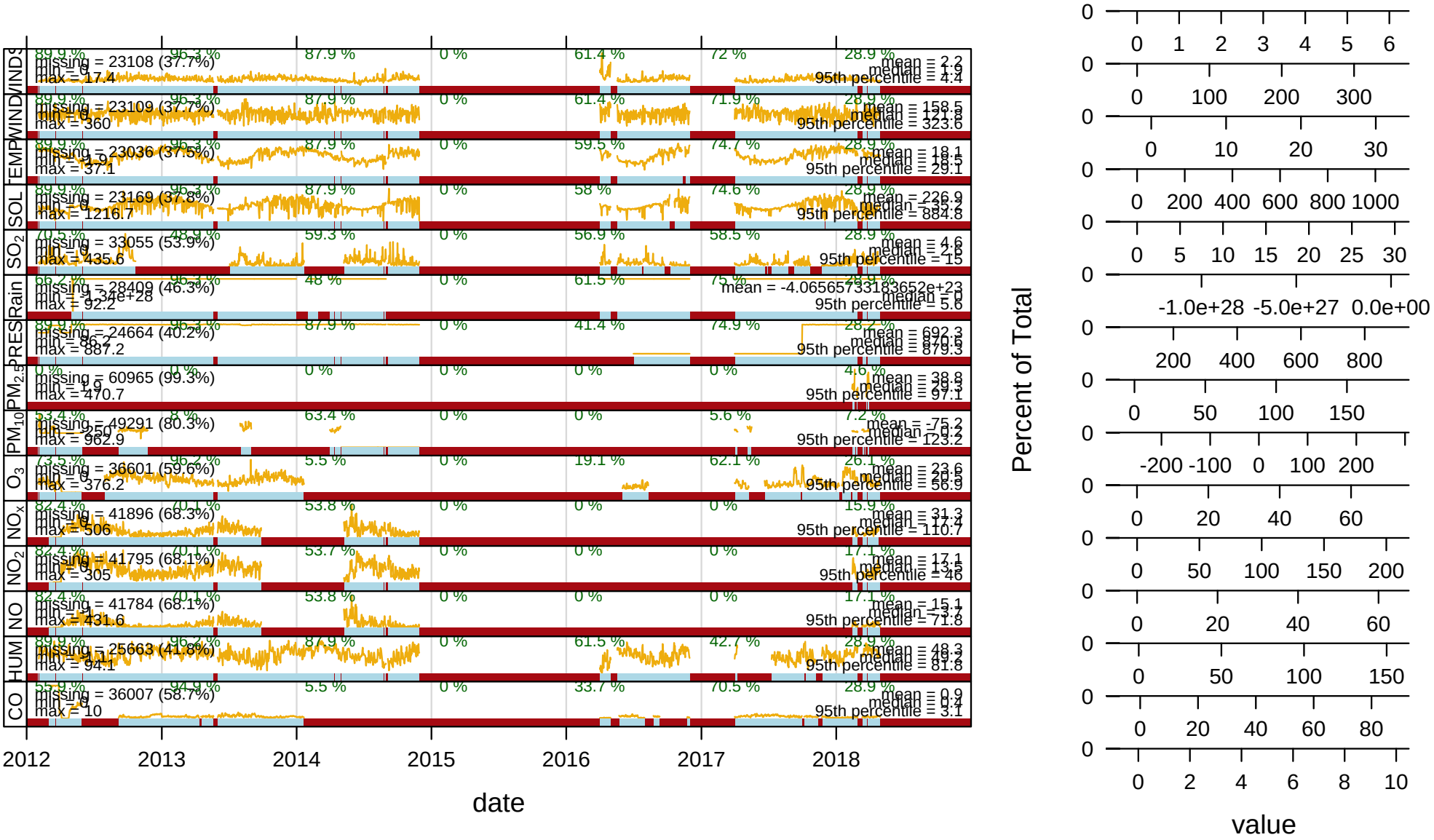

Figure 7.12: Mamelodi ambient air quality data summary

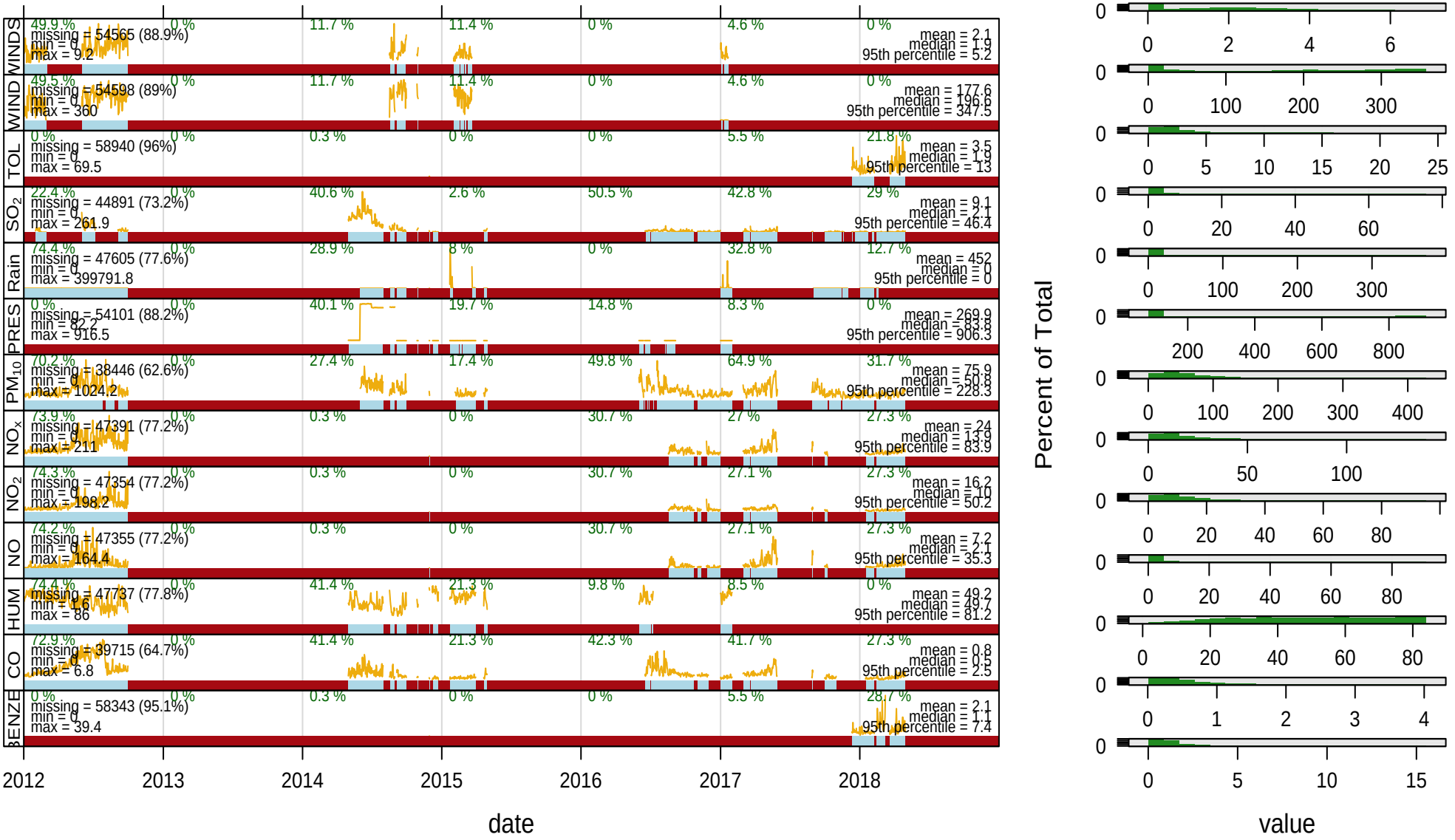

Figure 7.13: Meyerton ambient air quality data summary

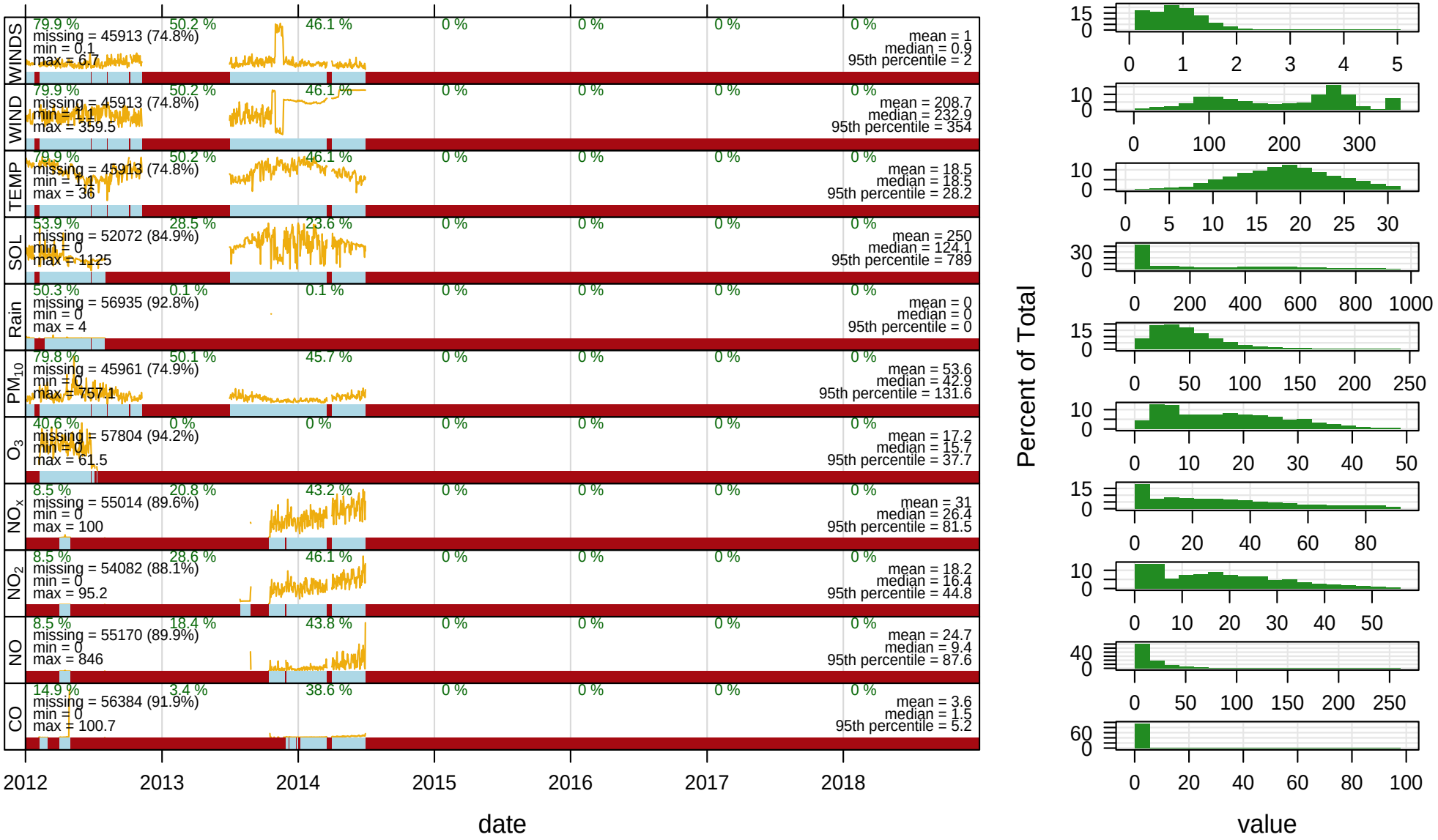

Figure 7.14: Newtown ambient air quality data summary

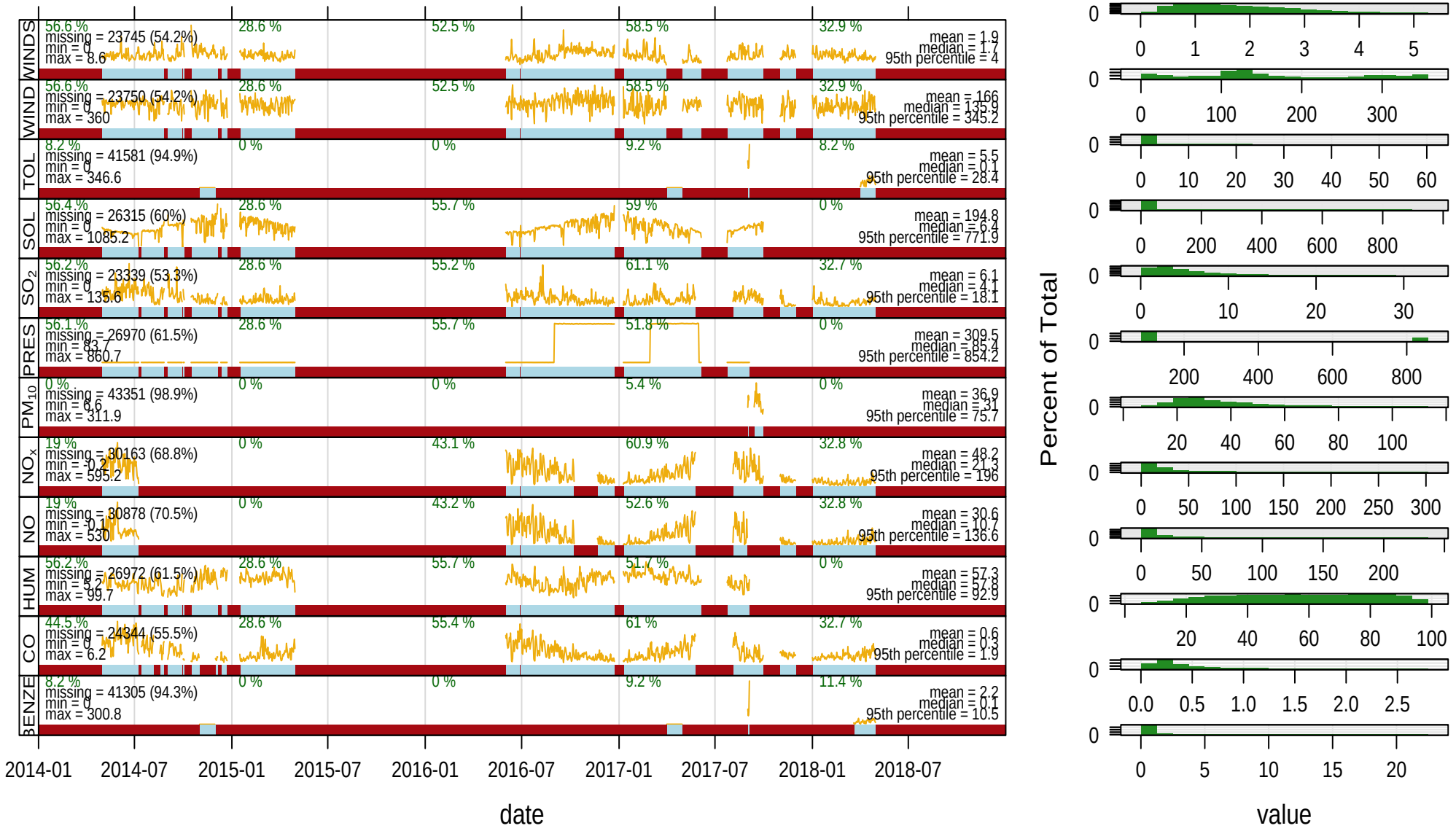

Figure 7.15: Olifansfontein ambient air quality data summary

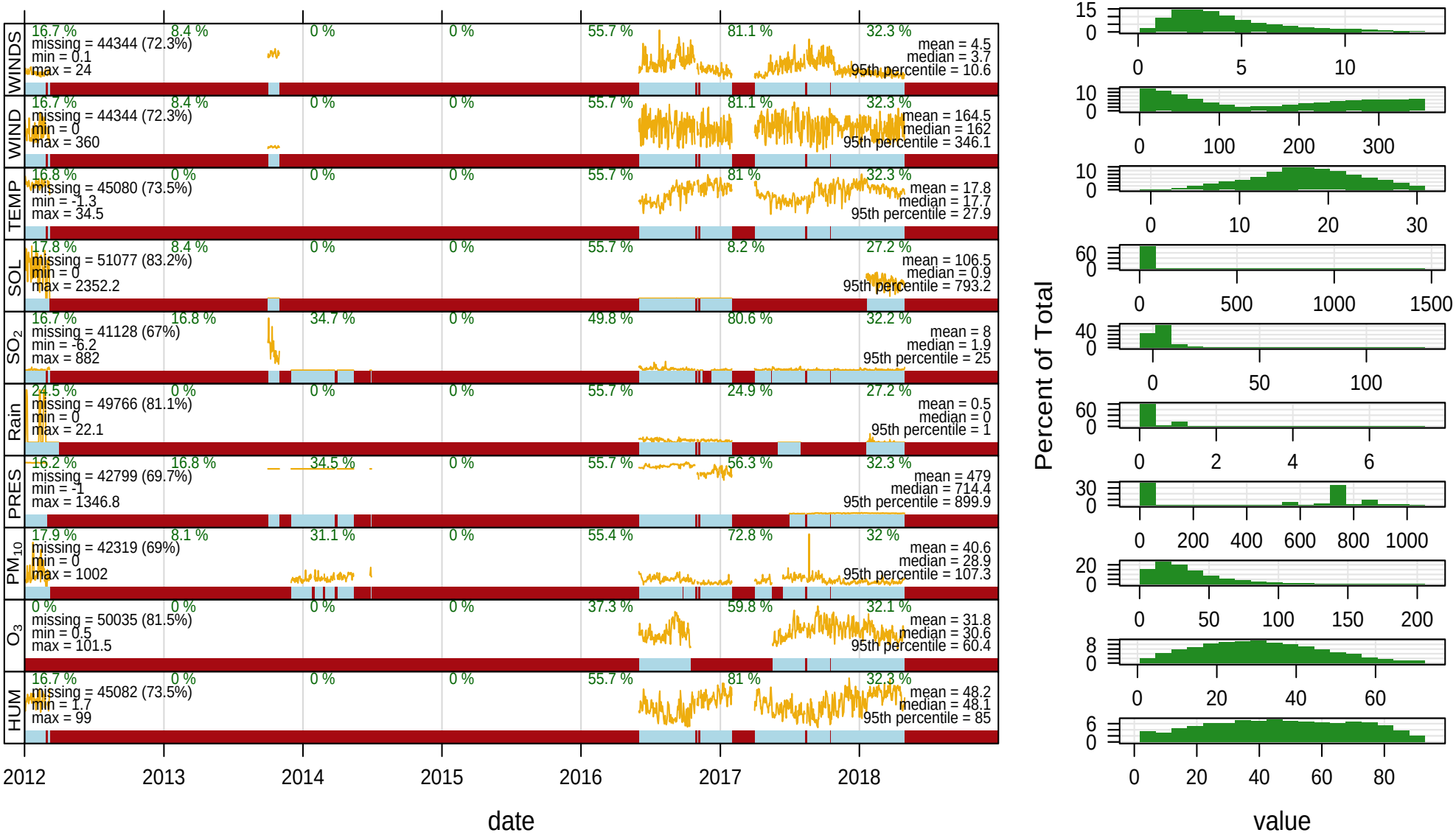

Figure 7.16: Orange Farm ambient air quality data summary

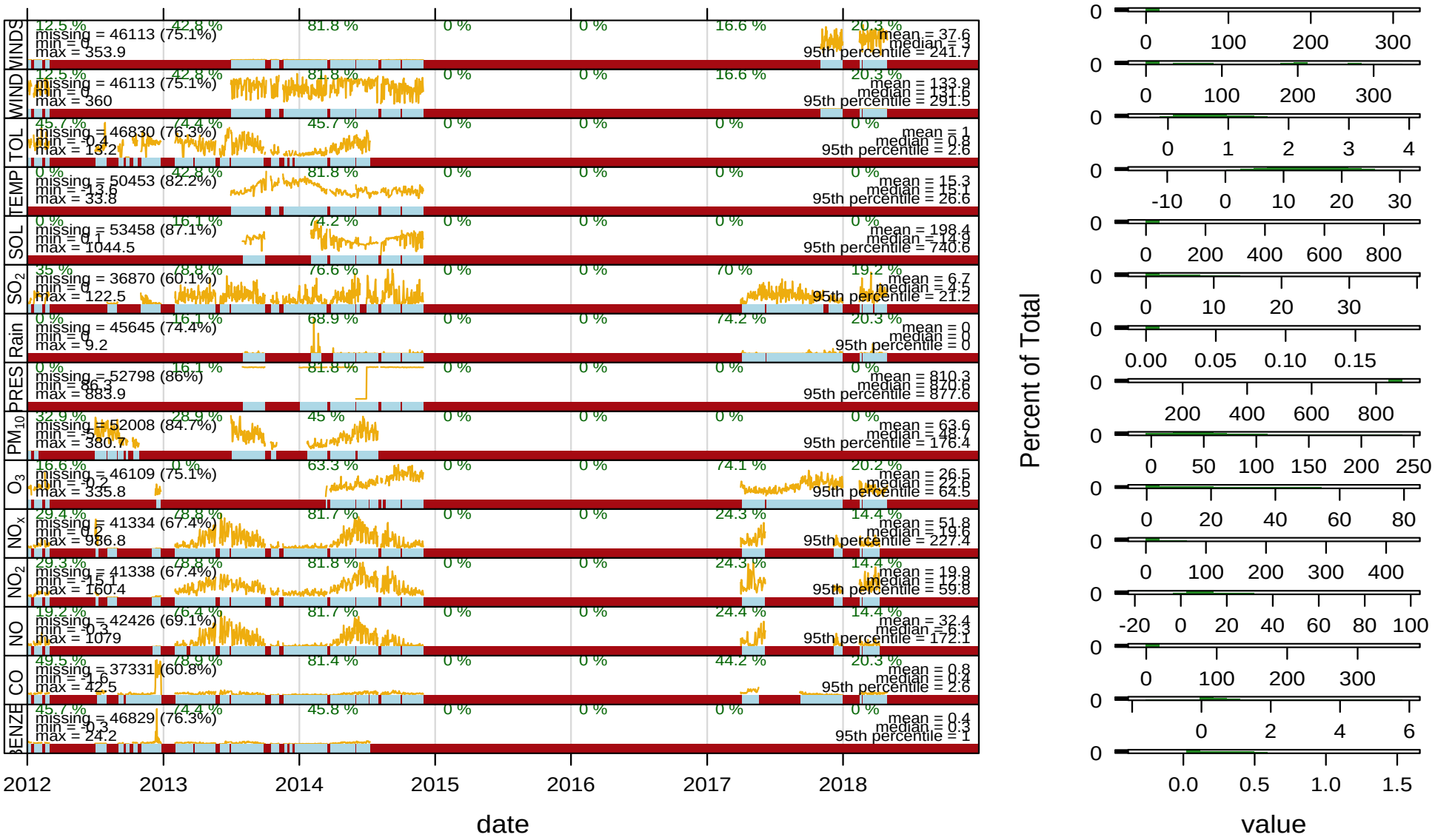

Figure 7.17: Pretoria West ambient air quality data summary

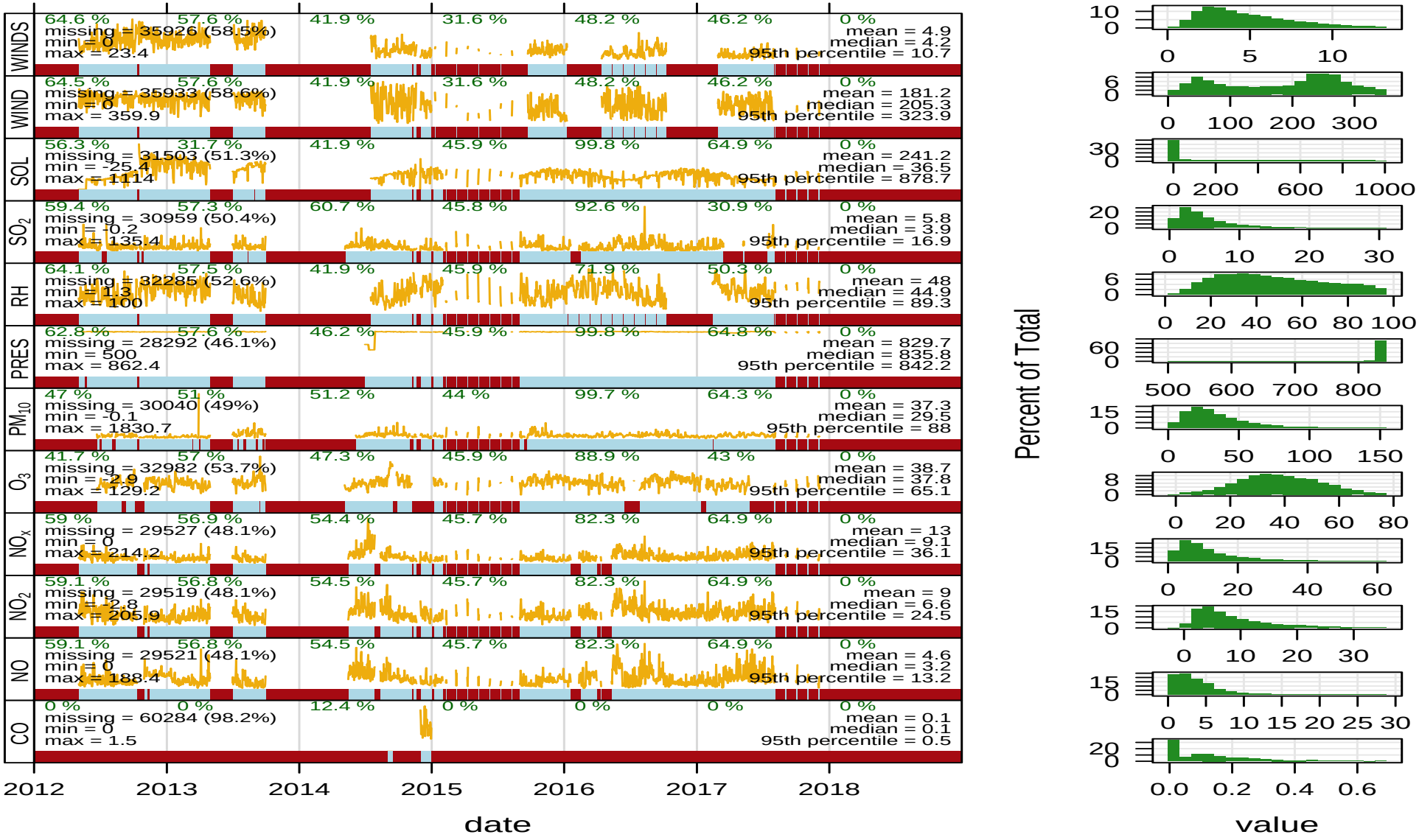

Figure 7.18: Randfontein ambient air quality data summary

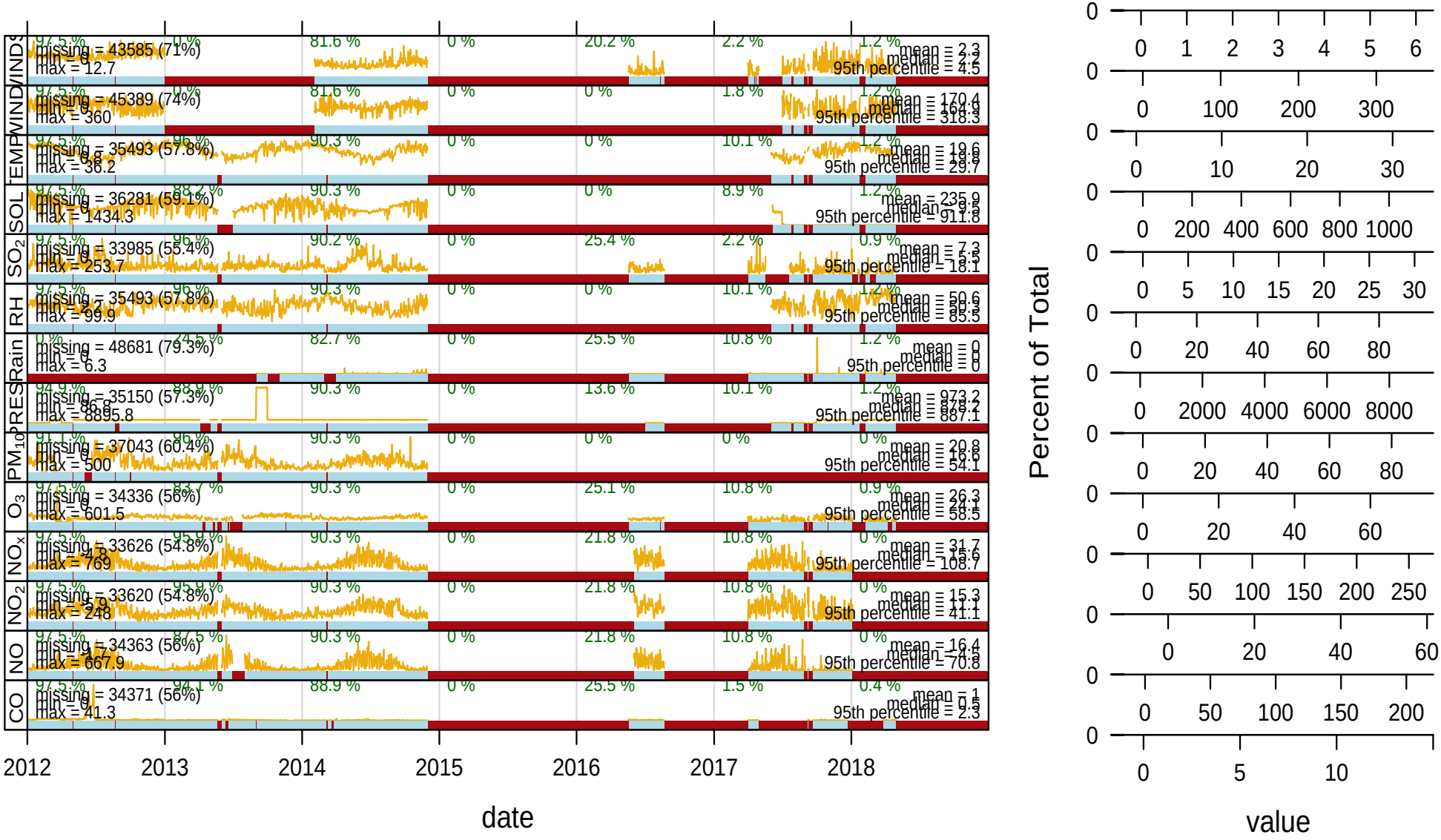

Figure 7.19: Rosslyn ambient air quality data summary

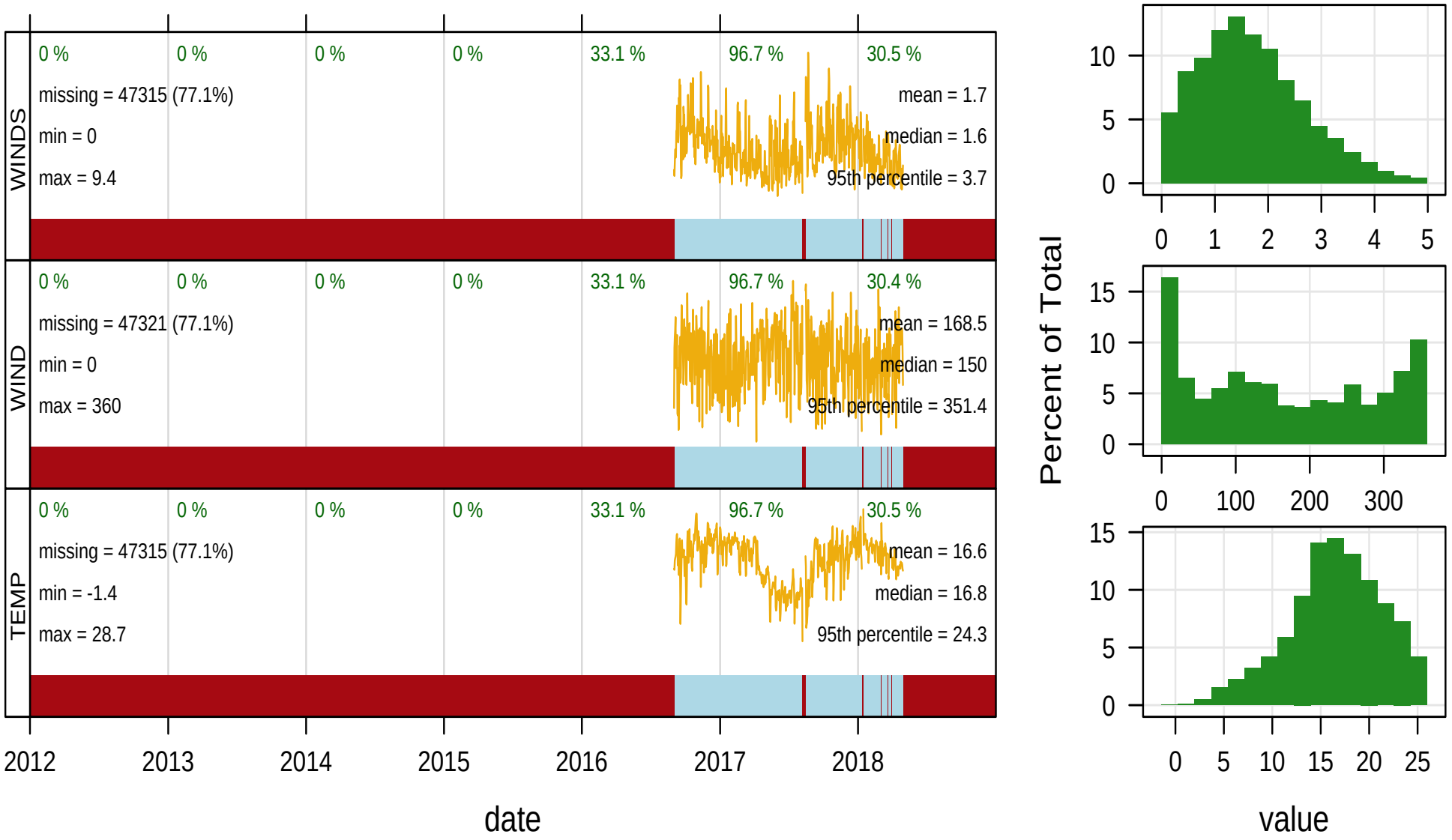

Figure 7.20: Springs ambient air quality data summary

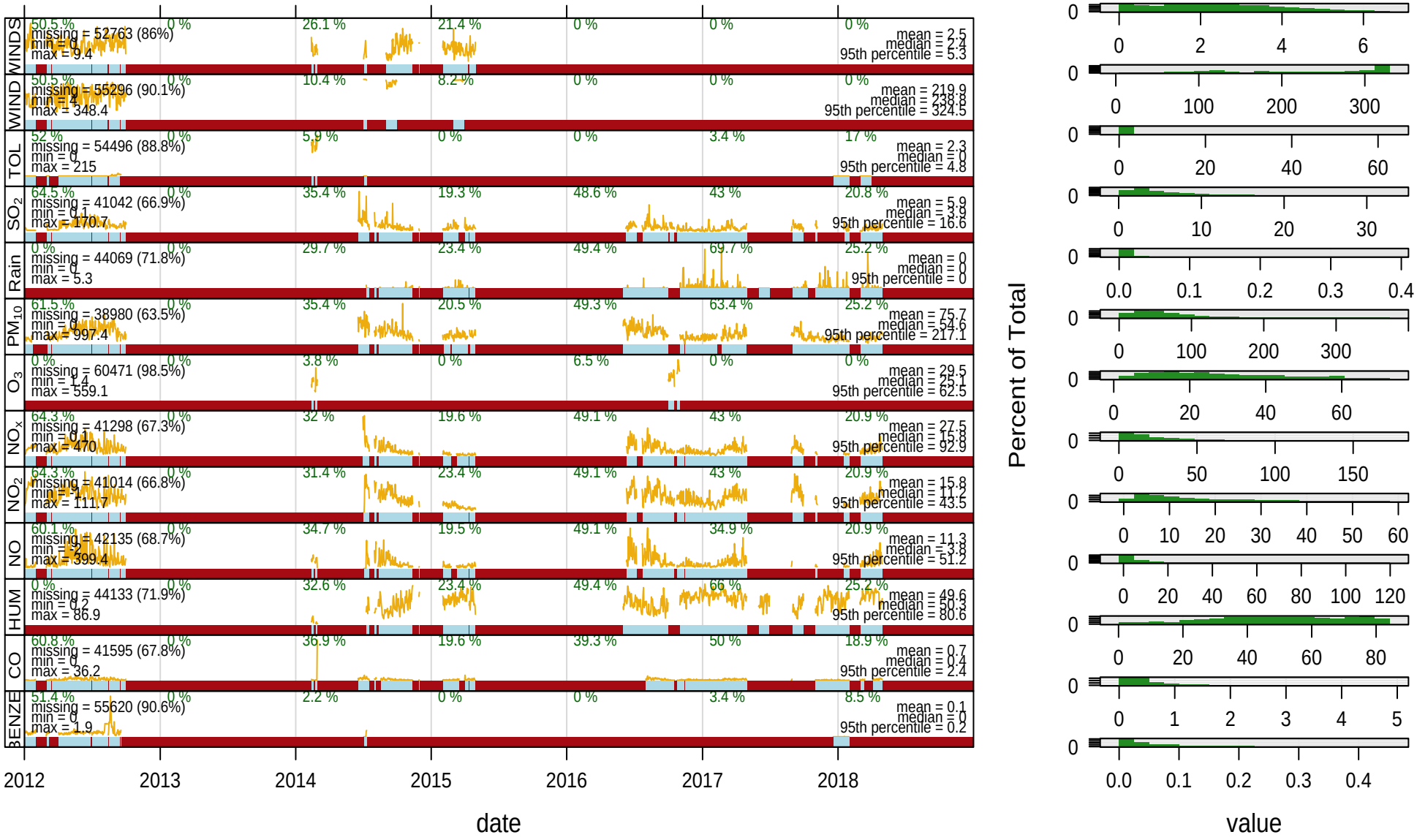

Figure 7.21: Tembisa ambient air quality data summary

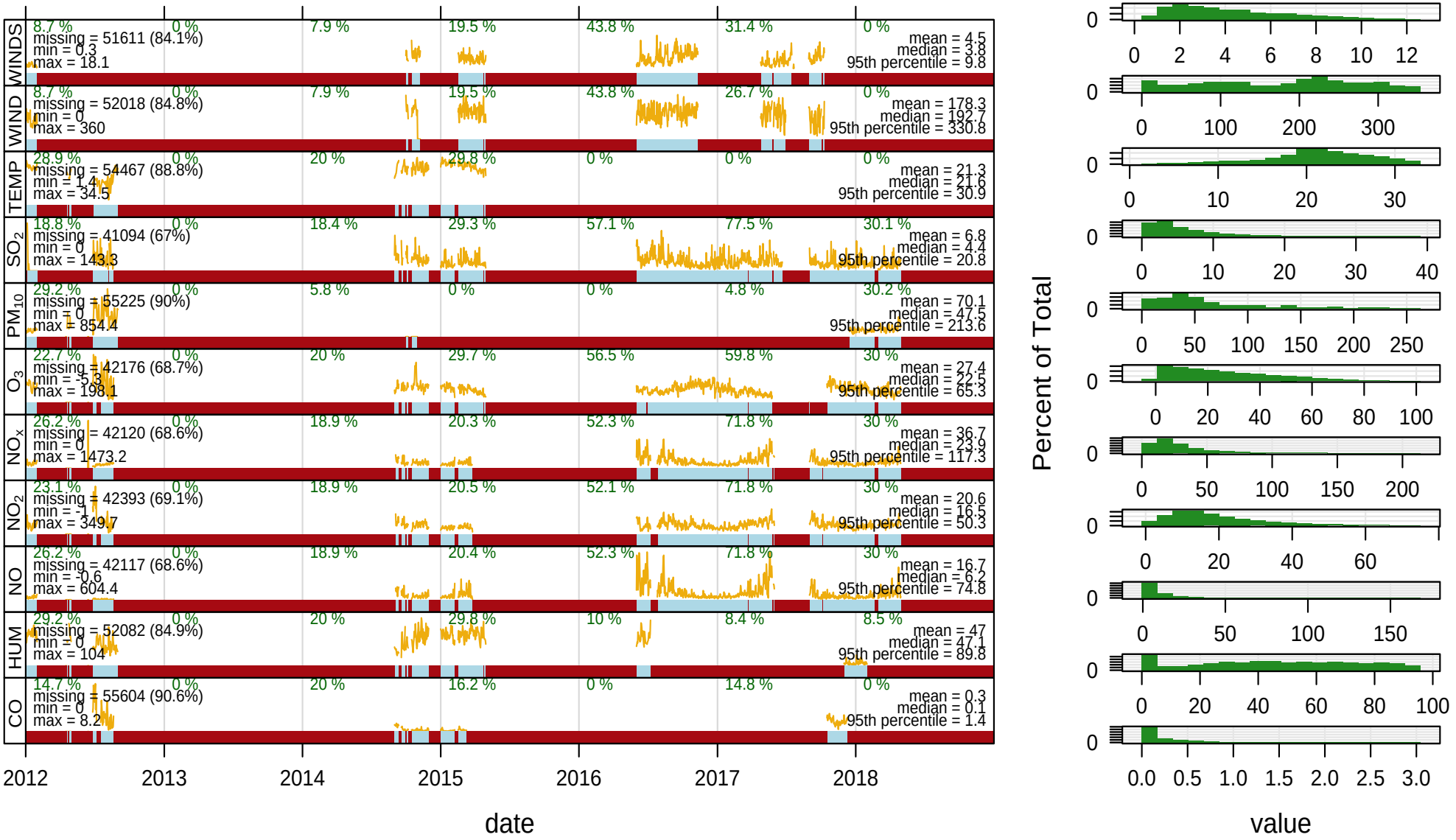

Figure 7.22: Thokoza ambient air quality data summary

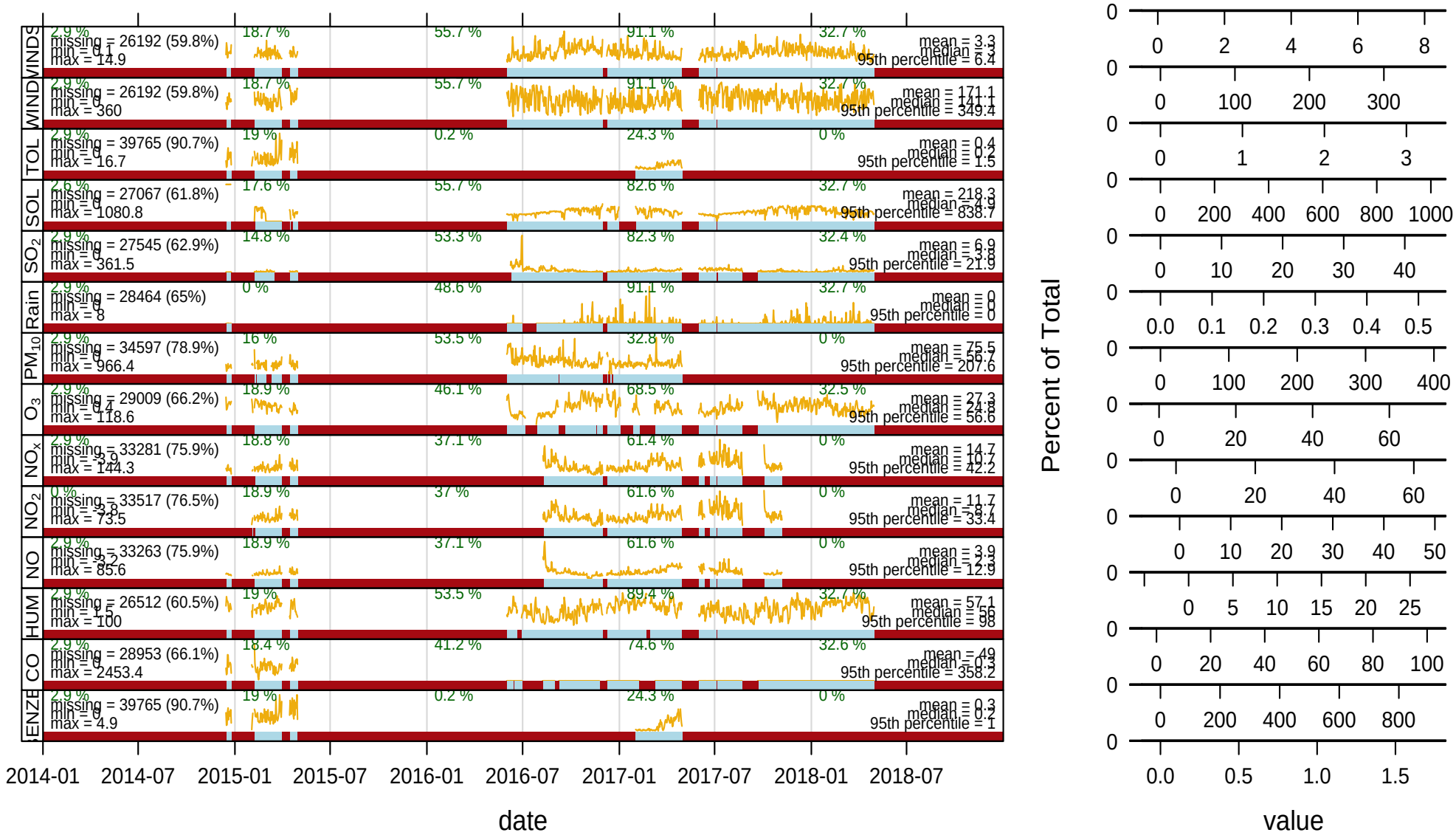

Figure 7.23: Tsakane ambient air quality data summary

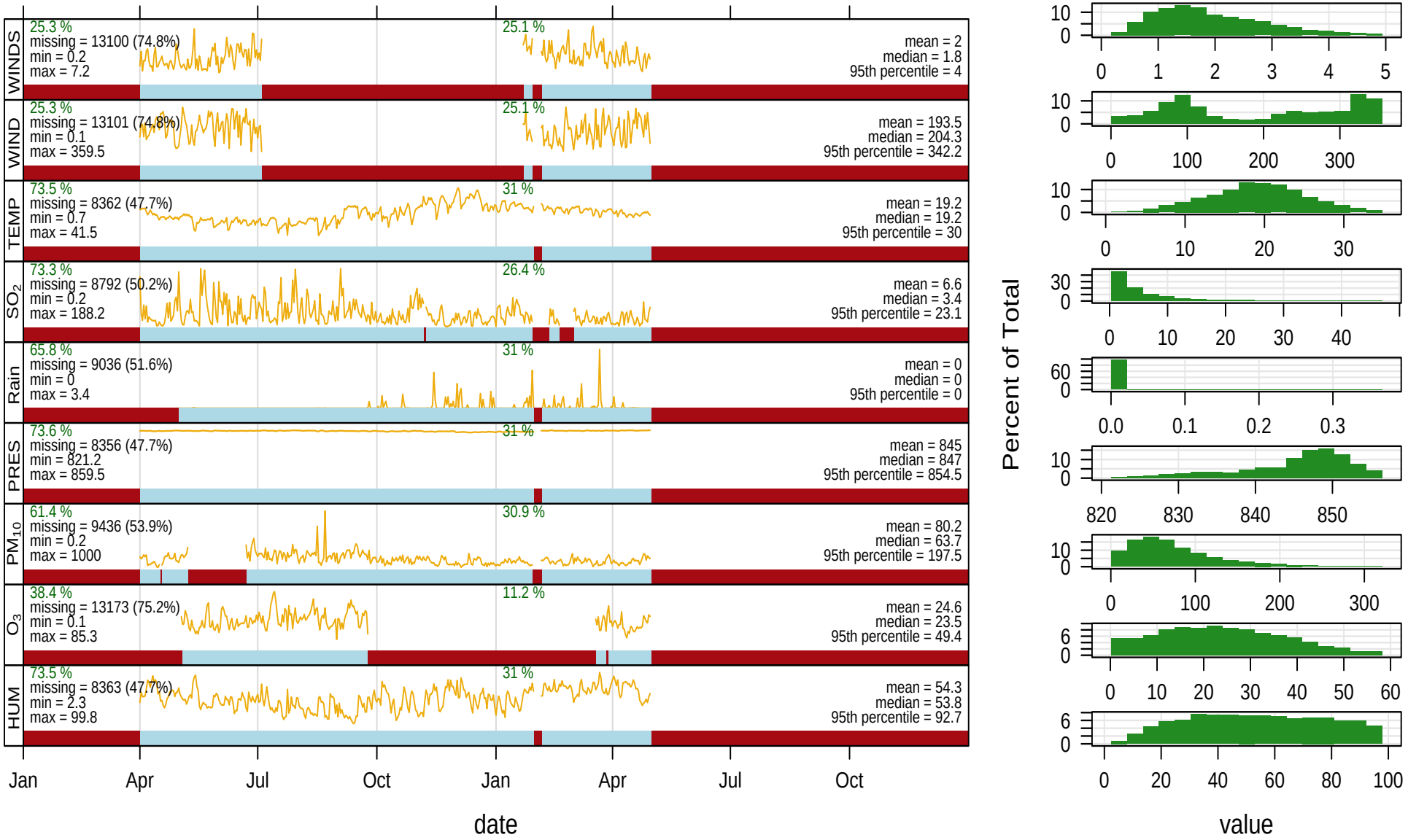

Figure 7.24: Vanderbijlpark ambient air quality data summary (2017 -2018)

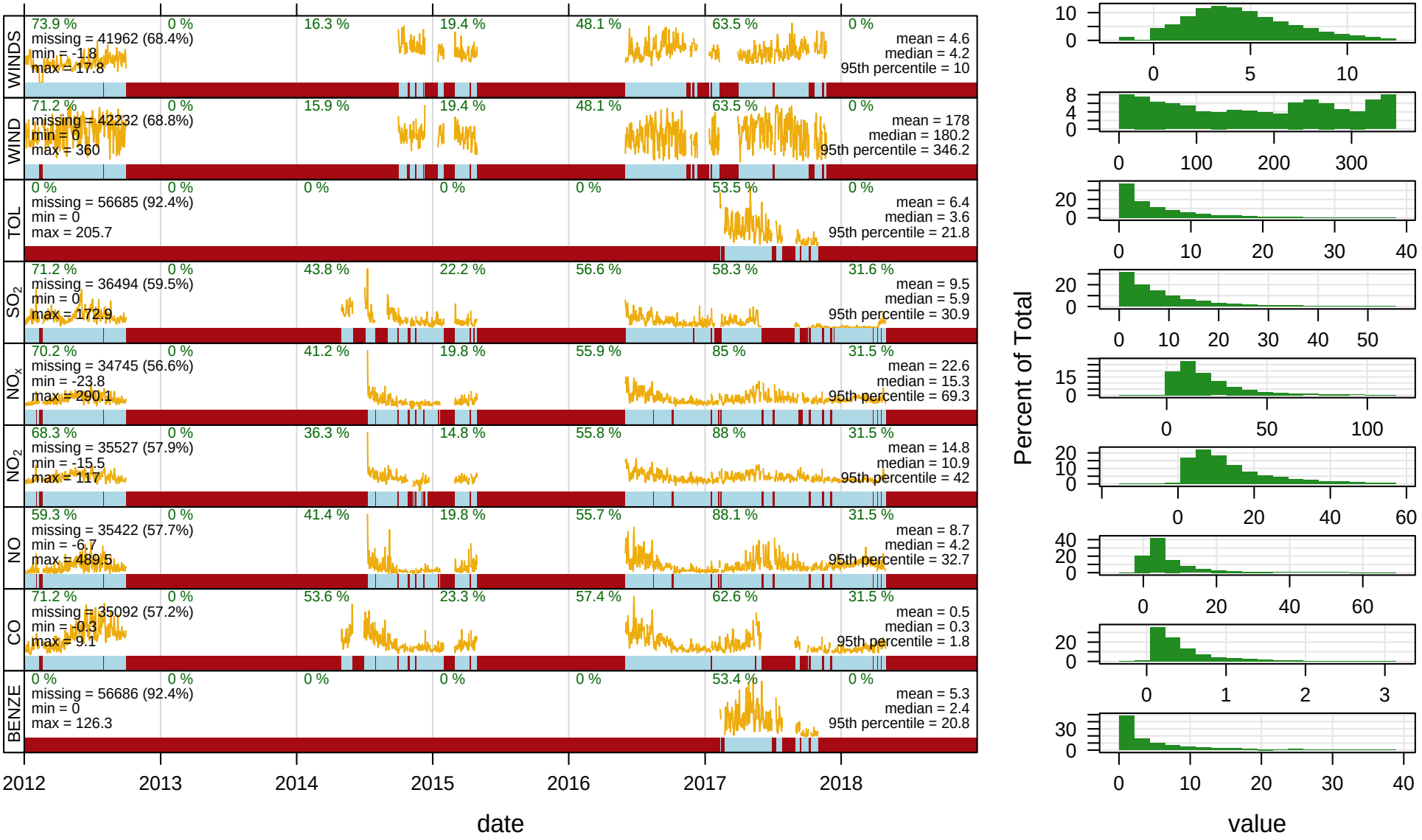

Figure 7.25: Watville ambient air quality data summary